The Geological Evolution of the Norseman Area, Western Australia

by

Matthew William Hope BSc(Hons)

Submitted in fulfilment of the requirements for the Degree of
Master of Science (Exploration Geoscience)

University of Tasmania (July, 2004)

CODES

Declaration

This thesis contains no material which has been accepted for a degree or diploma by the University or any other institution, except by way of background information and duly acknowledged in the thesis, and to the best of my knowledge and belief no material previously published or written by another person except where due acknowledgement is made in the text of the thesis

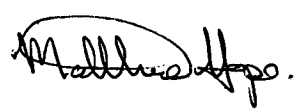

Matthew Hope

This thesis may be made available for loan and limited copying in accordance with the *Copyright Act 1968*.

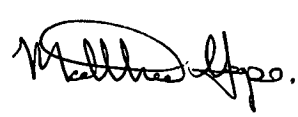

Matthew Hope

Abstract

Norseman lies 200 km south of Kalgoorlie within the most southern part of the late Archaean Eastern Goldfields Province of Western Australia. This study resolves the stratigraphy and structure of the upper Norseman Terrane and proposes tectonic models to explain the formation of the terrane and differences with the adjacent Kalgoorlie Terrane. Problems with the current understanding of the lower stratigraphy of the Norseman Terrane were identified, but not fully resolved.

Geological mapping at 1:2500-scale of the upper part of the Norseman Terrane at the Polar Bear Peninsula, revealed five Archaean facies associations:

- Mafic volcanic rocks and dolerite intrusives;
- Ultramafic rocks;
- Mafic conglomerate and sandstone;
- Fine-grained sedimentary units, dominantly pyritic black shales and thin-bedded, siltstone-shale turbidites; and
- Rhyolite lavas and both *in situ* and resedimented breccias.

The stratigraphy and geometry of the map patterns, when combined with age dating from the Eastern Goldfields, suggests that basalts overlying the Norseman komatiite are a thrust repetition of basalts from below the komatiite. This hypothesis is supported by trace element geochemistry that found all basalts above and below the komatiite have similar tholeiitic composition. They do not possess the distinctive siliceous high magnesium chemistry of the basalts that overlie the komatiite at Kambalda. Basalts from the lower Penneshaw Formation at the base of the Norseman stratigraphic succession also have a tholeiitic composition and are interpreted as another thrust repetition of the mafic greenstone package.

The uppermost stratigraphy preserved within the Norseman Terrane is rhyolite at Polar Bear. Facies analysis of rhyolite and breccias indicates the rock units represent a submarine lava dome that was emplaced upon unconsolidated black shale, generating peperite breccias. At the margins of the dome, where it pinches out of the stratigraphy, the equivalent strata are rhyolite-sediment breccias and sandstone. These represent the lower sections of gravelly and sandy high-density turbidites resulting from gravitational collapse of sections of the dome. Underlying fine-grained sediments were incorporated as rip-up clasts.

Two evolved felsic rock suites are distinguished within the Norseman Terrane. The first suite (Polar Bear rhyolite lava, intrusive Ajax rhyolite porphyry, Harlequin rhyolite porphyry dyke and the Dundas Granite) is interpreted to have been derived from fusion of a siliceous crustal basement source. The second suite (intrusive Polar Bear quartz porphyry and Harlequin granodiorite) is interpreted to have originated as magma with a high-Al Trondhjemite-Tonalite-Dacite (TTD) chemistry. Low pressure feldspar fractionation was a key process in the subsequent development of the members in both suites.

In the adjacent Coolgardie Domain of the Kalgoorlie Terrane, at an equivalent upper stratigraphic level, dacitic conglomerate, sandstone and siltstone of the Black Flag Beds (BFB) are present. These rocks represent erosional products of emergent volcanic centres, which were subsequently deposited as high density turbidites within the Kalgoorlie Basin, a depression that previous studies indicate is a rift basin developed under an extensional tectonic regime. These dacitic epiclastic rocks and other intrusive felsic porphyries have distinctive high-Al TTD suite chemistry, thought to form by melting of young, hot, subducted oceanic crust. There is no geochemical evidence within these dacites and other felsic intrusives, of low pressure feldspar fractionation.

The stratigraphic and geochemical differences between the felsic rocks within the Kalgoorlie Terrane and the Norseman Terrane are interpreted to be the result of differing degrees of extension. The Kalgoorlie Terrane formed the central axis of an island arc. The arc rifted, forming the Kalgoorlie Basin, which was filled with BFB epiclastic volcanics and sediments. The extension assisted the ready passage to the surface, of magmas generated deep in the subduction zone. The Norseman area was marginal to the Kalgoorlie Basin and did not undergo substantial extension. Efficient magma conduits were not developed so that subduction zone magmas became trapped in crustal magma chambers and underwent feldspar fractionation. Intrusion and underplating of subduction zone magmas caused melting of felsic basement forming the rhyolites.

Closure of the Kalgoorlie Basin occurred during N-S directed compression, suggested to have resulted from continental collision at the subduction zone. This compression caused large scale thrusts that throw the basaltic greenstones over the komatiite in the Norseman Terrane. It also pushed the entire Norseman area to the north, developing it as an allochthonous fault-bounded terrane, which split the former Kalgoorlie Basin and caused it to wrap around the Norseman Terrane to the east and west.

Acknowledgements

This work was made possible by the support of Central Norseman Gold Corporation.

Chris Stephens, as Manager of Geology, arranged CNGC financial support that allowed me to attend short courses at the University of Tasmania. He was also an early and ongoing supporter of the work, provided encouragement and showed interest in the findings. Chris also corrected the earliest written attempts of what ultimately evolved into the geochemistry chapters.

Chris Stephens driving across Lake Dundas.

Thanks to my former colleagues at CNGC, for patiently accepting my phone calls twice a day on weekends over a couple of years as I left to go to the mapping at Polar Bear and returned.

Thankyou to Dr Peter McGoldrick and Dr Stuart Bull, for making the long trip over to Western Australia, to visit the Norseman Area and assist with my geological interpretations.

Thankyou to the combined team of Dr Peter McGoldrick, Dr Stuart Bull and Professor Tony Crawford of the University of Tasmania, who provided corrections that improved the thesis.

And finally, thankyou to Dr Peter McGoldrick for navigating me through the administrative processes of gaining extensions and submitting the thesis.

Contents

List of Figures

List of Plates

CHAPTER ONE

Introduction

1.1 BACKGROUND TO THE PROJECT

Late Archaean mafic and ultramafic rock successions in the greenstone belt between Norseman and Menzies in the Eastern Goldfields of Western Australia have received extensive study over the past 30 years due to their proclivity as hosts for major gold and nickel ore bodies (figure 1.1). The most prolific mining centres, Kalgoorlie and Kambalda - St Ives, are the two best-studied areas, and Norseman, to the south, has also received significant study. The Dundas Goldfield at Norseman has produced over 5 million ounces of gold, the majority by Central Norseman Gold Corporation (CNGC), which operated continuously between 1935 and its sale to Croesus in 2001.

Until recently, in comparison to mafic-ultramafic rocks, relatively little study had been carried out on the felsic volcanic, volcaniclastic and associated sedimentary rocks within the Eastern Goldfields, due largely to their perceived paucity of economic mineralisation. In the 1970's, a rush of exploration was directed at felsic rocks following the discovery of Zn-Cu massive sulfide deposits at Teutonic Bore in the Eastern Goldfields, but was largely targeted at the major felsic complexes north of Kalgoorlie. Discoveries since 1990 of significant gold resources hosted by felsic rocks, most notably Kanowna Belle east of Kalgoorlie, has led to a re-evaluation of the importance of felsic and sedimentary successions. This has greatly benefited research into the origin of granite-greenstone terranes because felsic and sedimentary successions yield substantial information about the original tectonic environments.

Despite a number of previous geological studies of the Norseman area, details of the felsic and sedimentary successions in the Norseman region were little known at the commencement of the work reported herein. This can be attributed to three causes; there is extensive surficial cover over most of the area; the felsic and sedimentary outcrops lie many kilometres from the main gold producing area; and studies at Norseman have been focused on detailed investigations into one particular rock type or the gold mineralisation or have used one particular technique such as geochronology. Since the early 1970's, no previous studies have specifically evaluated the stratigraphy and integrated all the findings of the individual projects. Hence, a major aim of this thesis is documenting the felsic and sedimentary successions in the Norseman area and clarifying their relationship with the better known mafic units.

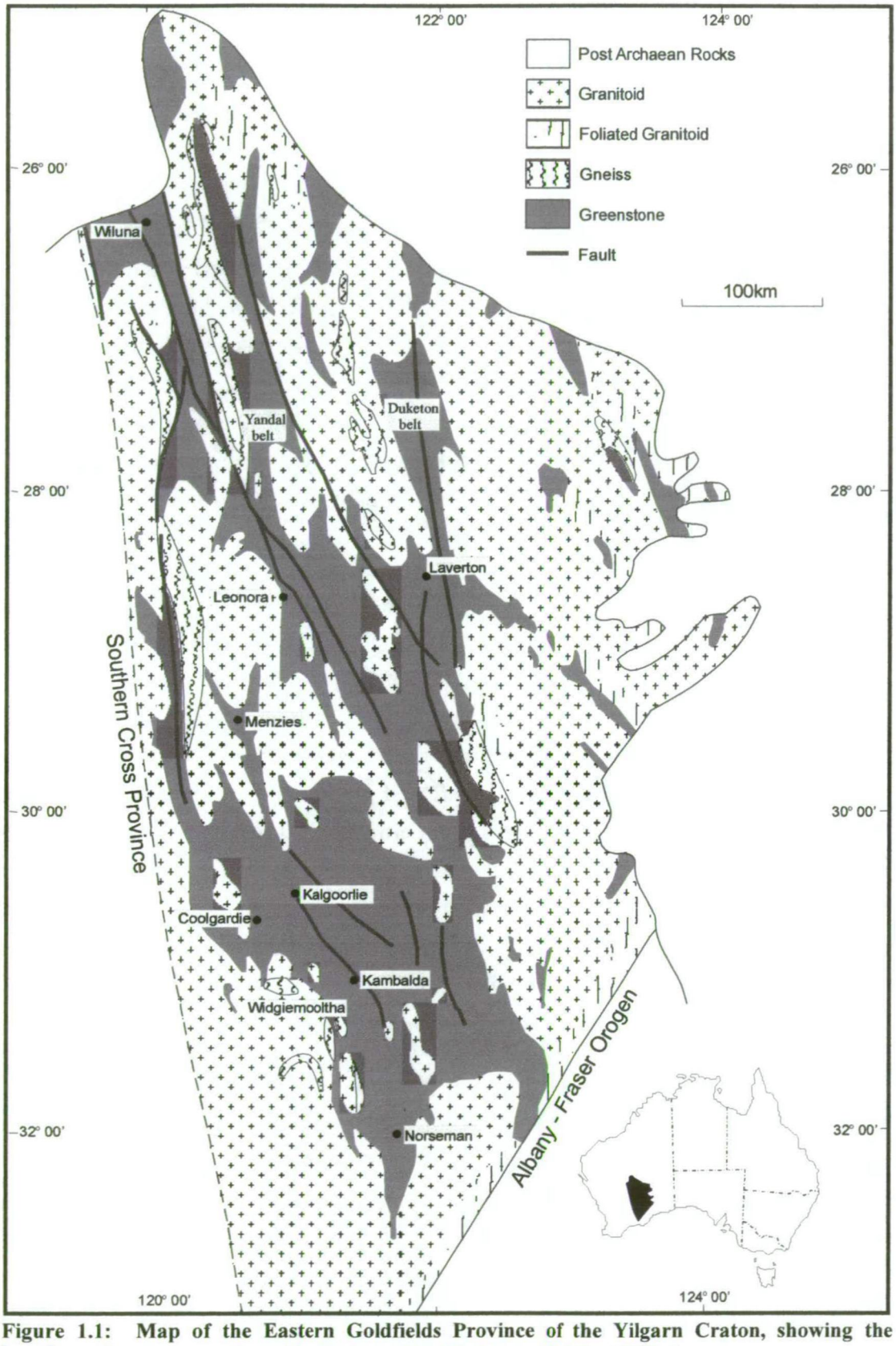

Figure 1.1: Map of the Eastern Goldfields Province of the Yilgarn Craton, showing the locations of regions mentioned in the text. Modified from Griffin (1990a).

1.2 OUTLINE OF THE PROBLEM

The regional geology of the greenstone belt between Norseman and Menzies is well documented due to the geological mapping of the 1:100,000-scale series of geology

sheets undertaken in the 1980's by the Geological Survey of Western Australia (GSWA). These fact maps, when combined with multiclient aeromagnetic data and detailed stratigraphic, geochemical and geochronological studies from the mining centres, allowed a regional stratigraphy to be erected for the Kalgoorlie to Kambalda area (figure 1.2) (Cowden & Archibald, 1989-ms; Griffin, 1990b; Swager & others, 1995). Geochronological studies demonstrated that stratigraphic repetitions have the same age and define major thrusts. In particular, it appears that there is only one komatiitic volcanic event (Nelson, 1997) so komatiite forms excellent chronostratigraphic marker that is usually visible in aeromagnetic images (figure 1.2).

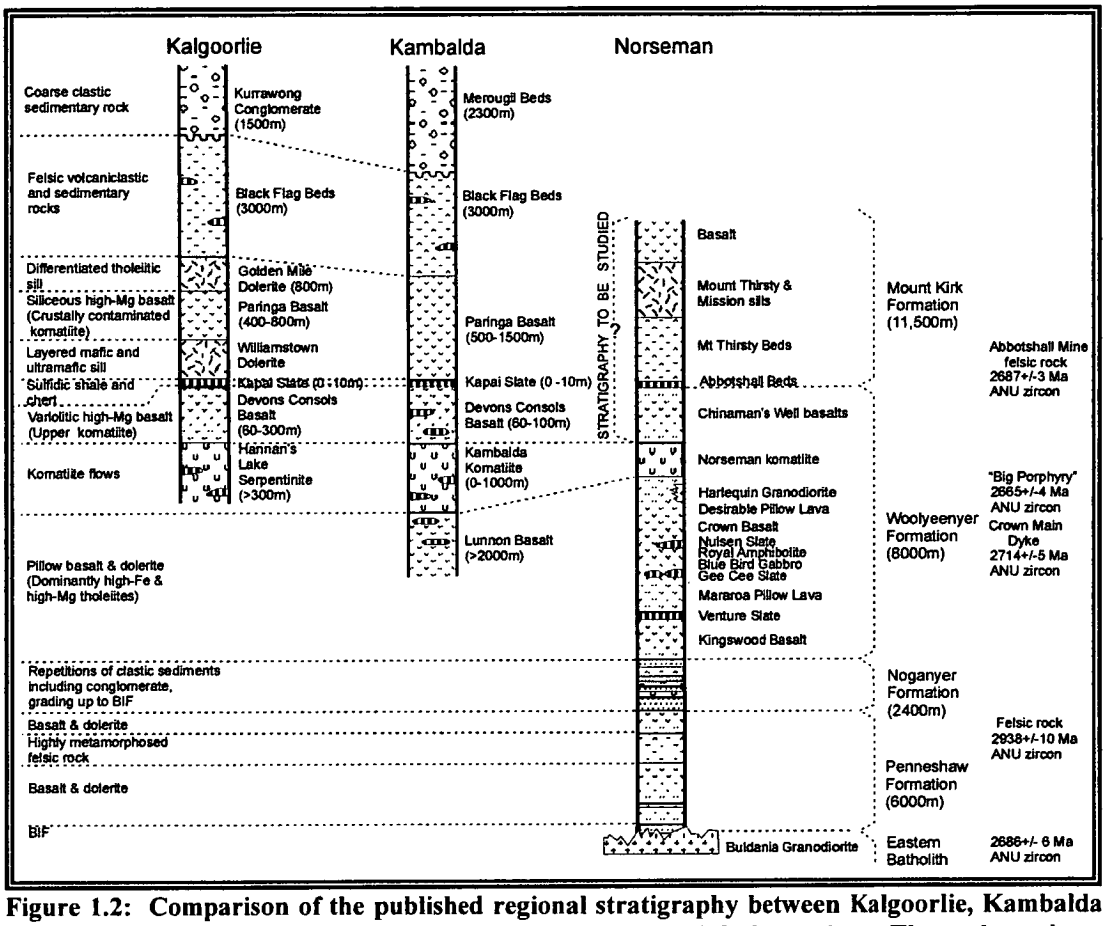

Figure 1.2: Comparison of the published regional stratigraphy between Kalgoorlie, Kambalda and Norseman using the komatiite units as a marker unit to link the sections. The geology above the komatiite at Norseman is poorly known and is the major subject of this study. The Mount Kirk Formation, shown as the uppermost Norseman stratigraphy, was defined by Doepel (1973) at a type area west of the Mission Fault (see figure 1.3). The Kalgoorlie and Kambalda stratigraphy is modified from Griffin (1990b); the Norseman stratigraphy is the synthesis of Doepel (1973), modified by former CNGC geologists L. Offe & N. Archer.

The regional stratigraphy defined for the Kalgoorlie and Kambalda region was not extrapolated by the GSWA south of the northern shore of Lake Cowan into the Norseman area. Within the Norseman area, the local stratigraphy and structural architecture remained undefined. The members of the mafic Woolyeenyer Formation that host the major gold deposits have been well described through studies of drilling results (Thomas & others, 1990; Thomas, 1991), but the drilling did not extend to the

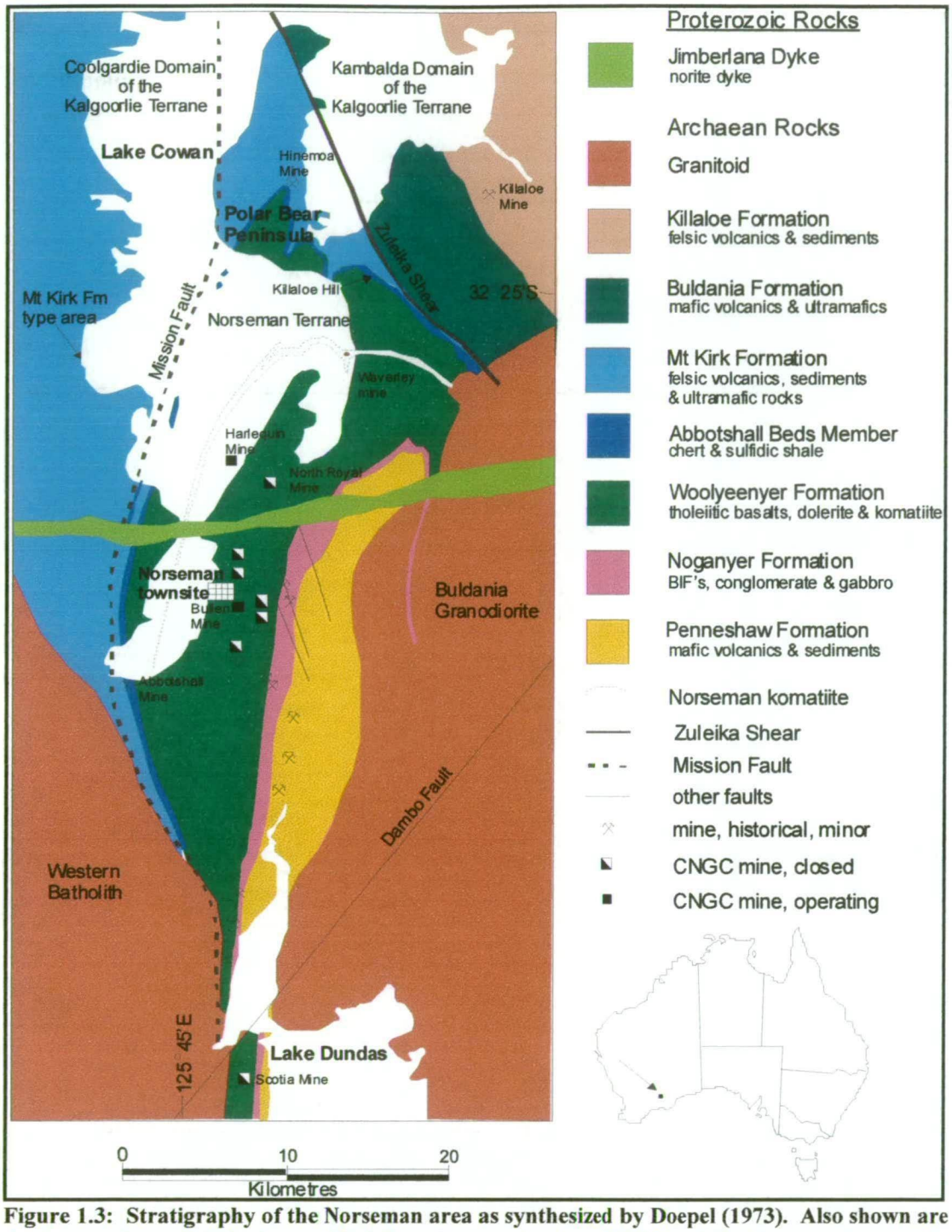

Figure 1.3: Stratigraphy of the Norseman area as synthesized by Doepel (1973). Also shown are the terrane-bounding faults modified from Swager & others (1995) and the Norseman komatiite as revealed by drilling and aeromagnetic images.

overlying units, which are largely covered by unconsolidated sediments filling Lake Cowan. Felsic and sedimentary rocks, thought to be upper sequences, occur with mafic and ultramafic sequences at Polar Bear, north of Norseman, and to the west near Mount Thirsty, but it was unclear where these exposures fit in the local stratigraphy (figure 1.3).

In essence, the conventional view of the greenstone stratigraphy at Norseman is that it consists of a number of mafic, sedimentary and mixed formations, all folded into a

north plunging antiform with the majority of the eastern limb truncated by the Buldania Granodiorite (figure 1.3).

The core of the antiform comprises the Penneshaw Formation (Doepel, 1973), a poorly exposed assemblage of basaltic and highly metamorphosed felsic rocks from which a U-Pb zircon date of *ca.* 2930 Ma has been obtained (Nelson, 1995). A major fault is thought to separate the Penneshaw Formation from the overlying sedimentary Noganyer Formation. The Noganyer Formation includes several repetitions of pebbly conglomerate and ferruginous turbiditic siltstone, the latter traditionally regarded as BIF, and is intruded by ultramafic and gabbroic sills. The mafic Woolyeenyer Formation overlies the Noganyer Formation with an apparently conformable contact and consists of upper and lower basalt successions, separated by komatiite, known informally as the Norseman komatiite. The lower Woolyeenyer Formation is 6-7 km thick and comprises basalt flows intruded by felsic porphyry and sub-volcanic dolerite dykes and sills, one of which, the Crown Main Dyke, contained a zircon dated at 2714±5 Ma (Hill & others, 1992). The characteristics of the upper Woolyeenyer Formation are not well known. The Woolyeenyer Formation in turn is overlain by the Abbotshall Beds, a poorly defined unit which includes a laterally continuous shale unit approximately 25-50 metres thick, which is commonly silicified near surface to form laminated cherty outcrops. Details of the stratigraphy above the Abbotshall Beds are poorly understood due to lack of exposure.

Doepel (1973) assigned the upper units including the Abbotshall Beds to the Mount Kirk Formation, and described it as comprising "acid lavas, pyroclastic rocks and associated waterlain deposits...also...cherts, black shales and basic volcanic rocks. Ultrabasic rocks...are present in at least two positions in the sequence. All these rocks are intruded by basic sills." The type area for the Mount Kirk Formation was described as the western shore of Lake Cowan, 18 km northwest of Norseman, where the Norseman-Coolgardie Highway skirts the lake margin (figure 1.3). Doepel considered that from the type area, the Mount Kirk Formation trended northeast across Lake Cowan to the Polar Bear Peninsula and then was folded to trend southeast through Killaloe Hill.

In 1995, Swager & others published a tectonostratigraphic terrane map of the Eastern Goldfields based upon the GSWA 1:100,000 scale mapping, which provided an alternative to the synthesis of Doepel (1973). Their terranes were defined as packages with distinct stratigraphy and deformation history, bounded by faults across which the stratigraphy cannot be correlated. From east to west, the Norseman area was divided into the Kambalda Domain of the Kalgoorlie Terrane, the Norseman Terrane and the Coolgardie Domain of the Kalgoorlie Terrane, all separated by major structures. The Coolgardie Domain and the Norseman Terrane are separated by the

Mission Fault, which lies between the Mount Kirk Formation type area and the Polar Bear Peninsula, so the felsic and sedimentary rocks at Polar Bear could not belong to the Mount Kirk Formation as proposed by Doepel (1973) (figure 1.3).

Swager and others (1995) differentiated the Norseman Terrane from the Kalgoorlie Terrane by the apparent minor volumes of komatiite, the presence of extensive BIF units of the Noganyer Formation that have not been found in the Kalgoorlie Terrane and the old age of the Penneshaw Formation. They considered that the "presence of BIF and pre-2700 Ma greenstones and the overall structural and stratigraphic setting, distinguish the Norseman Terrane from the Kalgoorlie Terrane".

The Mission Fault is clearly a major structure as it separates rock sequences with discordant strikes. Nevertheless, there is some doubt about the validity of the Swager & others (1995) reasoning that led to the proposal of the Norseman Terrane as an entity with a distinctly different stratigraphy. Firstly, Norseman is unusual in that the Norseman antiform has exposed an extensive cross-section of the stratigraphy. The "BIF" of the Noganyer Formation and the older Penneshaw Formation lie beneath 6-7 km of basalt in the lower Woolyeenyer Formation. In contrast, the deepest drill testing of the equivalent basaltic unit at Kambalda extends less than 2 km below the komatiite so the nature of the deeper stratigraphy is unknown. It is possible that "BIF" and Penneshaw Formation equivalents may exist below the Lunnon Basalt at Kambalda. Secondly, McGoldrick (1993), mapping for the Geological Survey of WA, located outcropping komatiite at a small island in Lake Cowan within the Woolyeenyer Formation. Aeromagnetics and subsequent drilling have shown that the unit is substantial and continuous around the Norseman antiform (figure 1.3). The presence of the komatiite suggests a closer relationship between the Norseman Terrane and the Kalgoorlie Terrane than was previously believed. Direct correlation with the Kalgoorlie Terrane has, however, been difficult to achieve due to uncertainties about the units overlying the Norseman komatiite (figure 1.2).

1.3 AIMS FOR THIS STUDY

This study aims to fill the gap in knowledge about the Norseman succession above the komatiite and in doing so, allow better regional comparisons of this stratigraphy. The work has implications for arguments that the Norseman area comprises a separate terrane rather than a lower order fault-bounded domain.

The main the goals of this thesis are as follows:

- Document the felsic and sedimentary stratigraphy that overlies the mafic sequences at Norseman.

- Compare this stratigraphy to better studied areas at Widgiemooltha and Kambalda in the Kalgoorlie Terrane.

- Collect geochemical data for the upper Woolyeenyer Formation and felsic rocks to assist in correlation with Kambalda and well studied felsic centres in the north of the Eastern Goldfields.

- Use the defined stratigraphy and geochemistry to recognise major structures.

- Use the stratigraphy and geochemistry to determine the tectonic environment in which the rocks were emplaced.

- Use the updated structural and stratigraphic information to propose regional controls on the gold mineralisation at Norseman and describe mineralisation styles at the Polar Bear Peninsula.

The initial aim was approached by 1:2500-scale geological mapping of the Polar Bear Peninsula. This area has the best exposures of the felsic and sedimentary stratigraphy within the Norseman Terrane. In addition, it also exposes basalt and komatiite, the latter useful as a chronostratigraphic marker. 1:2500-scale was chosen because smaller scale mapping had been previously completed and the excellent exposures required a more detailed documentation to extract the maximum information. In addition, this scale would make the maps useful for gold prospecting.

Reconnaissance mapping and field checking were completed in other areas, particularly west of Lake Cowan, broadly in the vicinity of the Mount Kirk Formation type area (figure 1.3). These areas lie within the better studied Coolgardie Domain of the Kalgoorlie Terrane and exposures of felsic and sedimentary rocks of the Mount Thirsty Beds (Doepel 1973) (figure 1.2) were compared with the felsic rocks at the Polar Bear Peninsula. For additional information between the Mount Kirk Formation type area and the Polar Bear Peninsula, extensive aircore drilling on Lake Cowan since 1991 provided data about the distribution of rock types beneath the lake cover, a dataset not available to previous researchers.

The geochemical study of the upper Woolyeenyer Formation, (above the Norseman komatiite) utilised diamond drill core that became available over the last few years following drilling of a number of gold prospects on Lake Cowan by CNGC. The upper basalts at Kambalda are geochemically distinctive, being komatiite contaminated with continental crust. A geochemical study of the upper Woolyeenyer was undertaken for comparison to the Kambalda basalts.

Recent studies (Barley & others, 1998) have described the geology and geochemistry of felsic and sedimentary successions in the Eastern Goldfields. For comparative purposes, in this study, geochemical samples were collected from the felsic rocks at the Polar Bear Peninsula and west of Lake Cowan, and also from intrusive felsic porphyries in the lower Woolyeenyer Formation at Norseman.

Finally, these results were integrated in order to reassess the structural architecture of the Norseman Terrane. Major structures became apparent and allowed an answer to the question as to whether the Archaean sequences in the Norseman area comprise a separate tectonostratigraphic terrane from the Kalgoorlie Terrane. The combination of all the studies assisted with establishing the tectonic environment in which the Norseman area was developed.

The detailed characteristics of Norseman mineralisation and local controls on gold deposition have been documented in a number of previous studies (eg. Keele, 1984, Campbell, 1990; Thomas & other, 1990; McCuaig, 1996), but regional controls on the formation of shear zone complexes, that include gold-bearing structures, have not previously been discussed. This study uses the updated stratigraphy and structural architecture to reassess the controls localising auriferous shear zone complexes, which may assist gold prospecting.

The second part of the mineralisation study documents gold mineralisation at the Polar Bear Peninsula. Although the Polar Bear Peninsula has been poorly explored for gold in the past, one structure, the Hinemoa Fault contains a gold-bearing quartz vein, which has been mined at a small scale. The detailed mapping undertaken for this study clarified the geology and structure at Polar Bear and traced the Hinemoa Fault for several kilometres. This study describes the nature of the gold mineralisation at the Hinemoa Mine and a second pair of mineralised structures that were discovered while the study was underway.

1.4 LAYOUT OF THE THESIS

The thesis is divided into 13 chapters, this introduction being the first. Chapter 2 sets the scene by describing the current understanding of the regional geology of the Yilgarn Craton. The stratigraphy within the well-known Kambalda Domain of the Kalgoorlie Terrane is described for comparison with the Norseman Terrane later in the thesis. Finally, key geological findings are summarised from AMIRA P437, a study of felsic and sedimentary successions in the Eastern Goldfields.

Chapter 3 presents the geology and stratigraphy of the upper Norseman Terrane, determined by detailed mapping and petrographic studies at the Polar Bear Peninsula. Data from the Microwave Tower area and the Harlequin prospect are also included.

The chapter includes a description and interpretation of the geology of the units mapped at Polar Bear in order of the stratigraphic succession and acts as explanatory notes for the series of detailed geological maps of the Polar Bear Peninsula (maps 1-8, Appendix 4). Geological descriptions of key areas that were important in determining aspects of the stratigraphy are presented in Appendix 1.

Chapter 4 tests a hypothesis about structural repetition of the stratigraphy in the Norseman Terrane, which was presented in the conclusions to Chapter 3. Petrographic and geochemical characteristics of basalts overlying the Norseman komatiite are evaluated, to determine whether the basalts are similar to the lower basalts or the upper basalts at Kambalda. The chapter commences with a petrographic study of the basalts, and then continues with a geochemical study for the remainder of the chapter.

Chapter 5 presents a detailed facies analysis of some unusual coarse clastic rocks located at the Polar Bear Peninsula. The characteristics of the units are discussed in detail and conclusions drawn about the origin of the units.

Reconnaissance studies were undertaken in the southern Coolgardie Domain for comparison with the Norseman Terrane. The work focussed on the felsic rocks, sedimentary rocks and mafic sills, and used reconnaissance mapping, field checks, petrography and geochemistry. The results of the field studies and petrography are described in Chapter 6.

Chapter 7 details the results of a reconnaissance study of parts of the lower stratigraphy of the Norseman Terrane. The lower stratigraphy has received more work than the upper geology of the Norseman Terrane, and was previously regarded as reasonably well constrained. The current study was intended to clarify a number of points, but instead, identified major problems with conventional ideas about the lower stratigraphy. Some conclusions are drawn, but a lack of time prevented a full investigation of the lower stratigraphy. The problems that require further studies to resolve are identified.

Chapter 8 consists of a geochemical study of the felsic rocks in the Norseman Terrane and a comparison with felsic rocks in other terranes of the Eastern Goldfields. The study includes felsic volcanic rocks, high level intrusive rocks and granitoids. The study is used to identify differences between the Norseman Terrane and other terranes, and considers the petrogenesis of the rocks, leading to conclusions about the tectonic development of the Norseman and Kalgoorlie Terranes.

Chapter 9 is a brief description and geochemical study of three komatiite samples, with the aim of evaluating whether cumulate channel facies komatiite is present at the Polar Bear Peninsula.

In Chapter 10, structural deformation events in the Norseman Terrane are reviewed and an updated classification is provided. The improved understanding of the stratigraphy and the origin of rock units developed through this study (and presented in Chapters 3 to 7), led to the recognition of major structures. These structures are fully evaluated and placed into a logical structural context. Key field areas where significant structures were identified are described.

Chapter 11 evaluates the major controls on gold mineralisation in the Norseman Terrane. This work differs from previous detailed studies of mineralisation by focussing on controls that can be identified and used for targeting rather than a detailed mineral paragenesis. Characteristics of gold mineralisation at Polar Bear are also described.

Chapter 12 integrates the results from the previous chapters to refine the understanding of the stratigraphy, structure, and geochemistry of the Norseman Terrane and its relation to surrounding terranes. The evolution of the Archaean geology at Norseman is discussed using the results of the studies.

The thesis is concluded in Chapter 13 which summarises and highlights the major findings of this study.

CHAPTER TWO

Regional Geological Setting

2.1 INTRODUCTION

The Yilgarn Craton in Western Australia has an area of 657,000 km^2 of which, 80% comprises granite-greenstone with an age of between 3.0 Ga and 2.6 Ga. The remaining 20% consists of gneiss (Trendall, 1990).

Gee & others (1981) subdivided the Yilgarn Craton into four provinces, each of which was perceived as having "a unified lithology, structural history and perhaps even stratigraphy". The four subdivisions are, the Western Gneiss Terrain; the Murchison Province; the Southern Cross Province and the Eastern Goldfields Province (figure 2.1). These names persist to the present along with the "Norseman-Wiluna Belt", a term Gee used in previous publications, which includes the majority of the greenstone belts within the Eastern Goldfields Province.

A more recent subdivision of the Yilgarn Craton (Myers, 1993) followed extensive geological mapping undertaken by the Geological Survey of Western Australia and uses terrane nomenclature. Individual tectono-stratigraphic terranes, distinct fault bounded blocks of unified stratigraphy, are grouped into four superterranes. These are the West Yilgarn, West Central Yilgarn, East Central Yilgarn and East Yilgarn Superterranes.

2.2 YILGARN CRATON REGIONAL GEOLOGY

The following description of the Yilgarn Craton geology has been summarised from the Geological Survey of Western Australia Memoir 3 (1990) unless otherwise referenced. It outlines the regional geology as a setting for the more detailed stratigraphy developed and examined in this study. The older province subdivision of Gee & others (1981) is described rather than Myers (1993) superterranes because province subdivision remains the most widely used scheme.

2.2.1 Western Gneiss Terrane

The western margin of the Yilgarn Craton comprises the loosely defined Western Gneiss Terrane, which is dominated by repeatedly deformed and metamorphosed banded gneiss, but also contains granite and greenstone. The three main components are:

- gneiss complexes older than 3.0 Ga;
- gneiss complexes younger than 3.0 Ga; and

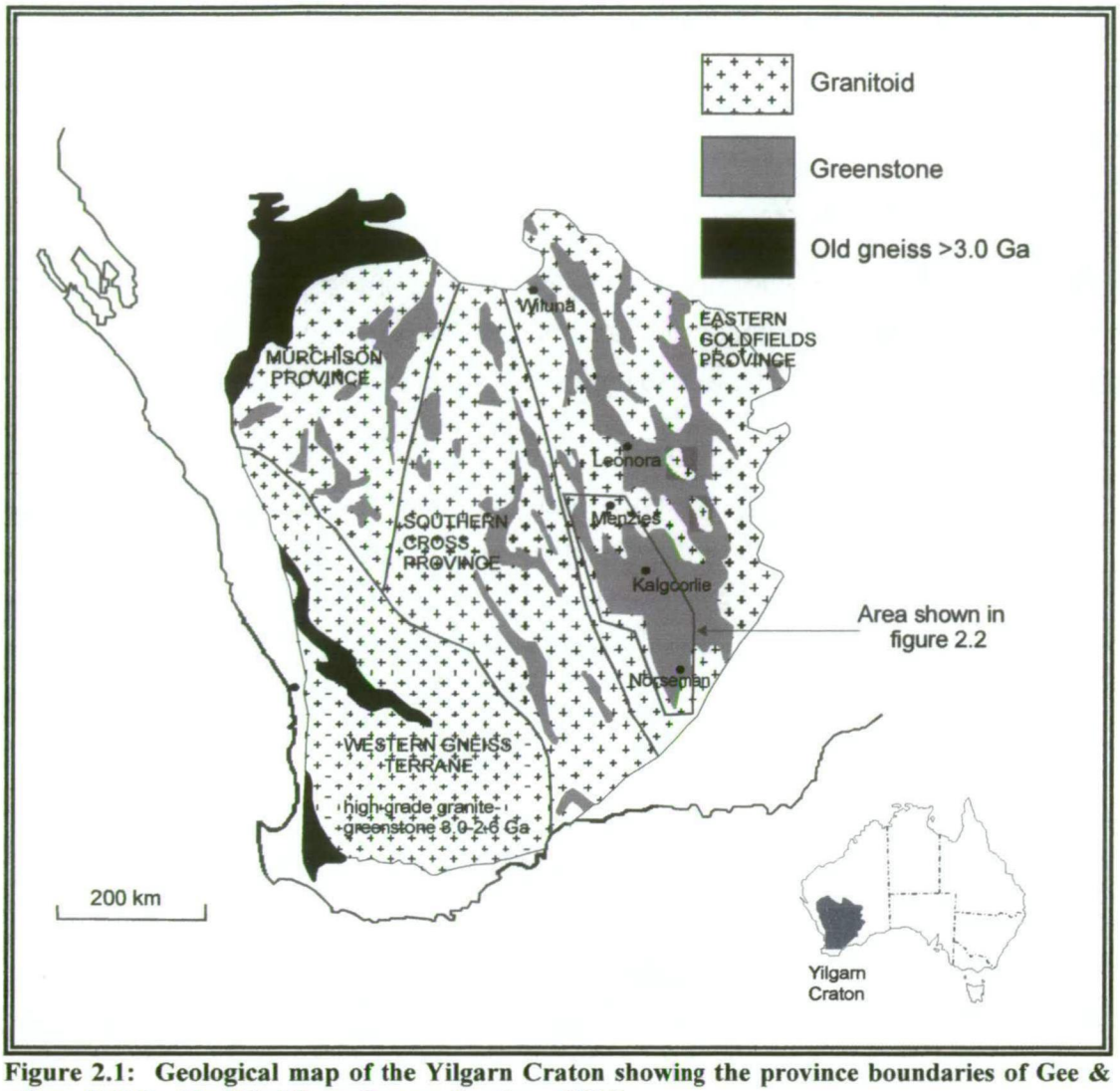

Figure 2.1: Geological map of the Yilgarn Craton showing the province boundaries of Gee & others (1981). Modified from Swager & others (1995).

- granitoid intrusions between 2.75 Ga and 2.55 Ga.

Gneiss complexes older than 3.0 Ga comprise two age groups dated at 3.68 Ga and 3.4 Ga, and are derived from monzogranite and syenogranite with inclusions of older gabbro-anorthosite and metasedimentary rocks. The oldest components are detrital zircons in quartzite and metaconglomerate, which have ages as great as 4.275 Ga, far older than the oldest known terrestrial rocks. All the rock types within the old gneiss complexes are metamorphosed to upper amphibolite or granulite facies and are strongly deformed.

Gneiss complexes younger than 3.0 Ga consist of granite and banded pegmatite gneiss that show a simpler geological history than the older gneiss. They have been deformed during and after the emplacement of younger 2.7-2.6 Ga granite.

Granitoid intrusions with ages of 2.75-2.55 Ga cut the gneiss complexes and form the largest component of the Western Gneiss Terrane. They can generally be divided into an older group of metamorphosed granulite or upper amphibolite facies rocks,

and a younger, less deformed group, metamorphosed at greenschist facies. The low metamorphic grade Saddleback Greenstone Belt is associated with the younger, low-grade granites.

2.2.2 Murchison Province

The Murchison Province occupies the north-western part of the granite-greenstone terrane of the Yilgarn Craton. The Murchison Province has a pattern typical of many Archaean granite-greenstone terranes, with linear, arcuate, synformal belts of greenstone lying between large domal masses of granitoid and gneiss. This pattern reflects three major phases of folding and subsequent shear zone and fault development. Gee & others (1981) distinguished the Murchison Province from the adjacent Southern Cross Province on the basis of slightly different tectonic trends and the apparent scarcity of komatiitic basalt in the Murchison Province compared to the Southern Cross Province. However, tectonic trends in much of the southern portion of the Murchison are parallel to those in the Southern Cross Province and komatiitic basalt appears to be as abundant as tholeiitic basalt, so there may be little basis for the subdivision into separate provinces.

The Murchison Province contains two greenstone sequences separated by an unconformity. The lower greenstone sequence has an age of about 3.0 Ga, but the basement upon which it was deposited is not seen. A pattern is recognisable in the stratigraphic development of the greenstones. Two episodes of basaltic lava plain-type volcanism formed laterally extensive, thick accumulations on an unknown basement. Each of these sequences was capped by extensive BIF. Subsequently, many distinct shield volcanoes and stratovolcanoes developed contemporaneously and were locally overlain by an epiclastic sedimentary basin in the southern part of the province.

Metamorphosed monzogranite that has been thoroughly recrystallised during regional metamorphism occupies the areas between the greenstone belts. Contacts between recrystallised monzogranite and greenstone belts are complex zones of high strain generally between 50 m and 1000 m wide in which greenstone belt rocks and monzogranite are interlayered. A number of geological features indicate that the monzogranite intruded the greenstone.

There appear to have been two phases of widespread metamorphism. The first phase was associated with the intrusion of the monzogranite sheets that caused metamorphism of adjacent greenstone to amphibolite facies. The second was a regional metamorphic event, mainly to greenschist facies.

2.2.3 Southern Cross Province

Poorly exposed granitoid and gneiss dominate the Southern Cross Province. Ages of these rock types are poorly constrained, however Pb-Pb dating on granitoid and gneiss suggests that the maximum age is 2800 Ma, similar to the greenstones. Contacts between granitoid or gneiss and greenstone generally are sheared or strongly foliated. In the southwest of the province, granitoid and gneiss, metamorphosed to granulite facies, grade into the Western Gneiss Terrane.

Greenstones within the Southern Cross Province broadly consist of an upper and lower sequence separated by a major unconformity. The lower sequence is dominated by mafic and ultramafic volcanic rocks, which overlie a basal quartzite unit. BIF is common throughout the lower sequence and clastic sedimentary rocks, accompanied by laterally restricted felsic volcanic rocks, are present near the top. The upper sequence is present only in the centre of the province and consists of clastic sedimentary rocks, conformably overlain by subaerially-deposited andesitic and rhyolitic volcanic rocks, and intrusive syenogranite of the Marda Complex.

The maximum thickness of the basal quartzite is 1 km and the unit extends discontinuously for 400 km through various greenstone belts. U-Pb dating of detrital zircons has returned ages of 3.6 Ga, 3.3 Ga and 2.9 Ga. The only known material of this age is in the Western Gneiss Terrane suggesting that the sediment was transported across the Murchison Province, or there is a basement of older crust on which the greenstones accumulated. The base of the quartzite is in contact with gneiss or granitoid but is generally covered or intensely sheared. In one greenstone belt, the contact has been described as an unconformity.

Most greenstone is metamorphosed to greenschist or lower amphibolite facies. Binns & others (1976) recognised two regional metamorphic domains, dynamic and static, in the Southern Cross and Eastern Goldfields Provinces. The dynamic domains are restricted to the margins of greenstone belts and have an extensive, penetrative deformation fabric. The static domains generally are lower grade and primary rock textures are well preserved. Binns & others (1976) argued that the two domains developed contemporaneously in previously deformed but unmetamorphosed greenstones.

2.2.4 Eastern Goldfields Province

The Eastern Goldfields Province is 900 km long and 400 km wide and occupies the eastern third of the Yilgarn Craton (figure 2.1). The province is richly mineralised with gold and nickel. Greenstones are more extensive than in the other provinces and form a belt up to 150 km wide with few granitoid intrusions (figure 1.1). The

greenstones are deformed and metamorphosed, mainly to greenschist facies. The southern and south-eastern boundary of the Eastern Goldfields Province is considered to be the area where deformation and metamorphism associated with the Albany-Fraser Orogen becomes dominant. The area with which this thesis is concerned lies close to Norseman at the southern end of the Eastern Goldfields Province.

2.2.4.1 Stratigraphy

A consistent lithostratigraphic scheme for the greenstones encompassing the entire province has not been established. However, a general pattern can be recognised with the older rock sequences dominated by mafic and ultramafic rocks, and younger sequences comprising clastic-sedimentary and felsic volcanic rocks.

The best documented greenstone stratigraphy occurs in a distinct tectono-stratigraphic entity known as the Kalgoorlie Terrane, in which consistent stratigraphy is recognised between Widgiemooltha and Menzies, a distance of approximately 200 km (figure 2.2). This stratigraphy is described in more detail in section 2.4. In brief, the lowest known unit is dominated by tholeiitic basalt successively overlain by komatiite; variolitic-textured komatiitic basalt; a thin unit of slate; a thick unit of high-Mg basalt intruded by mafic and ultramafic sills; and a felsic volcaniclastic and sedimentary unit. Isolated enclaves of mudstone, sandstone and conglomerate unconformably overlie this package.

At another area that has received detailed work, around Leonora and Laverton, a number of adjacent greenstone belts are separated by granitoid and major shear zones, which hinder the establishment of a generalised stratigraphy. The area contains extensive outcrops of dacite, andesite, and rhyolite volcanic rocks that are described in more detail in section 2.5. Polymict conglomerate and arkose, similar to the unconformable conglomerate in the Kalgoorlie Terrane, occurs in linear, fault-bounded belts.

Granitoid rocks within the Eastern Goldfields Province are more poorly exposed than greenstones and granite-greenstone contacts are generally obscured. Three types of granitoid are recognised: gneiss; large areas of foliated and unfoliated granitoid; and small discordant stocks, which intrude older granitoid, gneiss and greenstone.

The largest outcrops of gneiss are in linear zones adjacent to the greenstones in the west and northwest of the province (figure 1.1). Two types of gneiss are recognised. Type 1 gneiss is composed of lenses and pods of recrystallised BIF, talc schist, chlorite schist, calc-silicate schist and most abundantly, amphibolite. In all cases, type 1 gneiss is separated from the greenstone belts by major ductile shear zones. Type 2 gneiss is banded quartzo-feldspathic rock of tonalitic to granodioritic

composition. Banding within type 2 gneiss is typically discordant to contacts with greenstones and granitoids.

Isotopic dating has not identified gneiss older than the greenstones. Several type 2 gneiss occurrences have igneous protolith ages of *ca.* 2672 Ma (Nelson, 1997). These ages indicate that the gneiss does not represent basement to the greenstones. The gneissic fabric may have developed in granitoid and adjacent greenstones during tectonic emplacement of the granitoid to high level positions.

Foliated and unfoliated granitoid dominates the areas away from the greenstone belts and also intrudes gneiss and greenstone. Monzogranite and granodiorite are dominant but syenogranite, tonalite and quartz diorite are also found. All granitoid types plot on a calc-alkaline trend. Traditionally, granitoids have been divided into foliated "synkinematic" and unfoliated "post-kinematic" types (eg. Witt & Davy, 1993), but this may be invalid since the presence of a foliation is a function of the distribution of strain, which may be heterogenous (Champion, 1997). The large areas of granitoid between the greenstone belts could represent large sheeted intrusions or amalgamated multiple stocks intruding the base of the greenstones.

2.2.4.2 Deformation

Four compressional deformation events are recognised throughout the Eastern Goldfields (Wyche, 2000; Swager 1997), but there is disagreement between different studies about the earliest deformation events in the Eastern Goldfields (see Chapter 10). The earliest deformation event that most studies recognise is an early recumbent fold and regional scale thrust event that affected a wide area with a general north-south orientation. The second event comprised broadly east-west directed compression that formed open to tight folds with gently plunging N-S to NNW-trending fold axes, and thrust stacking, coincident with the peak of metamorphism. NNW-striking transcurrent faults were activated late under the same E-W directed compressional regime, but are typically classified as the third deformation event. The fourth deformation event comprised NNE faults with a dextral offset.

Other deformation events have been proposed, but remain controversial. Williams & Currie (1993) and Hammond & Nisbet (1993) suggested the juxtaposition of high-grade metamorphic gneisses against lower-grade greenstones along tectonised contacts could be explained by regional extensional deformation, related to uplift, causing the emplacement of the gneiss and granite domes as metamorphic core complexes. This event was suggested to be the first deformation and is commonly designated D_E. This extension model was later modified by Williams (1993) to reflect the fault architecture identified in a deep seismic line recorded north of

Kalgoorlie. The latter work recognised an earlier extension event related to asymmetrical rifting, which formed large-scale, half-grabens that were filled with voluminous mafic volcanic flows. The proposed core complex-forming event post-dated the rifting and hence was re-designated D_{E2}, and moved in time to postdate the north-south thrust faults.

In contrast, Archibald (1998a & 1998b) explained the compressed metamorphic gradients along the granite-greenstone contacts as the result of thrusts uplifting deep crust in a model involving multiple compressional events related to continental collision and obduction.

Other less well-recognised deformation events that have been described include early deformation responsible for a bedding parallel foliation in black shale and blastomylonitic fabrics in massive Fe-Ni sulphide ores (Archibald, 1998b), and cross-folding with broadly E-W trending axes (Spray, (1985). The latter event was described as a late event, which resulted in egg-carton interference patterns with earlier folds with NNW axial surfaces.

2.2.4.3 Seismic Imaging

The Australian Geodynamics Cooperative Research Centre (AGCRC) recorded deep seismic lines in 1991 and 1999 that have greatly aided understanding of the Archaean crust beneath the Eastern Goldfields Province. In the profiles, the greenstones are 4-7 km thick, overlying basement interpreted by gravity and seismics to be dominantly felsic to intermediate in composition (Goleby & Drummond, 2000). Granitoids within the greenstone are thin, tabular bodies with steep sides, dominantly hosted in dilational sites such as antiforms.

The contact with the basement at the base of the greenstone sequence is suggested to be a sub-horizontal detachment surface where folds and steeply dipping greenstone units are truncated against a strong reflector. A detachment surface implies substantial movement of tens or even hundreds of kilometres of the greenstone relative to the basement.

Drummond & Goleby (1998) have discussed the structures that are visible in the 1991 deep seismic line recorded north of Kalgoorlie (figure 2.2) and the following summary is derived from this source unless otherwise referenced.

Extensional shears (D_E) are not recognised. Similarly, D_1 N-S thrusts are poorly defined as the seismic line was badly located to record such structures. The seismic line crossed a major D_1 thrust duplex described by Swager and Griffin (1990) only where it is folded into the eastern limb of a D_2 fold dome. However, a D_1 thrust can

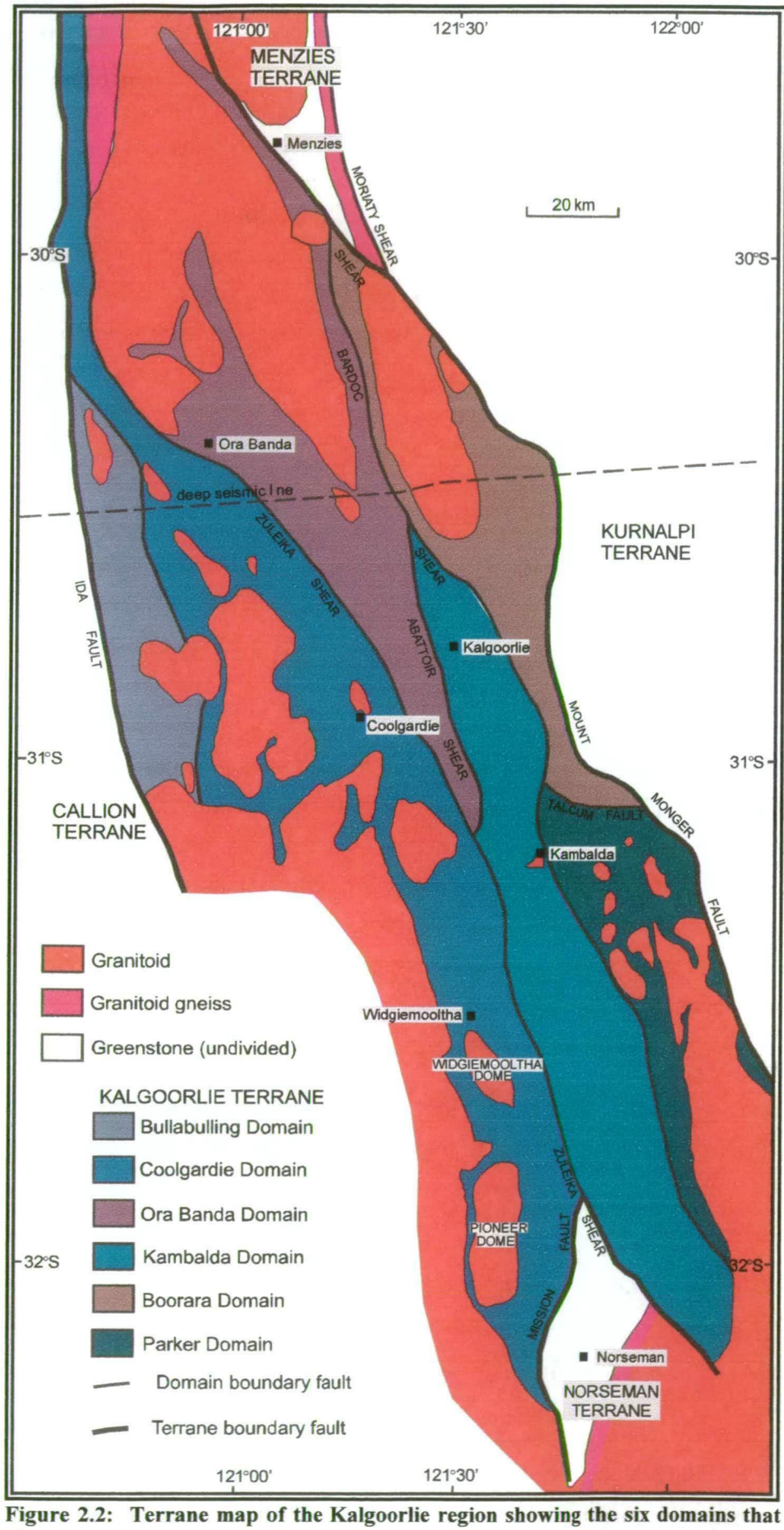

Figure 2.2: Terrane map of the Kalgoorlie region showing the six domains that constitute the Kalgoorlie Terrane. The Norseman Terrane lies at the southern end of the greenstone belt. Modified from Swager & others (1995). The location of this map is shown in figure 2.1.

be interpreted in the seismic image as a discontinuity separating units with opposing dips and soling into the basal greenstone detachment.

ENE-WSW shortening (D_2) involved crustal scale folding and thrust stacking above the detachment. Many D_2 antiformal structures are cored by granitoids. The Scotia-Kanowna Dome was imaged as consisting of west-directed thrust slices on the eastern limb of the dome and east-directed thrust slices on the western limb, all of which sole into the basal detachment. All these thrust slices were interpreted as being D_2. The dome therefore comprises a number of duplexes thrust from both east and west that repeat stratigraphy rather than a broad fold of coherent stratigraphy. As a similar effect is seen in the Mount Pleasant Dome, the D_2 domes are interpreted to be zones of stacked greenstone. East and west directed thrusts in the middle and lower crust that were imaged by the seismic profiles are also ascribed to D_2.

A number of regional scale, roughly N-S trending D_3 shear zones pass through the 1991 seismic line. In the field, the structures are several kilometres wide with an apparent sinistral movement but also a strong component of flattening (Wyche, 2000). In the seismic image, some of these structures, such as the Zuleika Shear, are non-reflective, but are traced by offsets in reflections and changes in the dip of the greenstone on either side of the fault, and appear to sole into the basal detachment. Other D_3 faults are reflective and penetrate through the detachment into the upper crust (e.g. Bardoc Shear) and into the middle to lower crust (Ida Fault). These structures may be reflective as a result of hydrothermal alteration along the structures.

The middle crust is typified by strongly reflective duplex structures. However, there is an anomalously non-reflective section of middle crust, measuring approximately 40 km wide by 15 km thick, adjacent to the intersection of the Ida fault and the Bardoc Shear at about 15 km depth. The greenstones between the Ida Fault and Bardoc Shear are rich with gold deposits. The lack of reflectors in this zone may be explained by: (i) a lack of structures; (ii) dehydration of the crust which would tend to homogenise the densities similar to the effects of metamorphism; or (iii) homogenisation by hydrothermal alteration. The second and third alternatives imply that this section of the crust could be the source for Au-bearing fluids responsible for the extensive gold mineralization in this area of the Eastern Goldfields.

2.3 TERRANES

Systematic regional mapping between Norseman and Menzies by the Geological Survey of WA allowed Swager & others (1995) to divide the southern part of the Eastern Goldfields Province into tectonostratigraphic terranes, distinguished from one another by distinct greenstone stratigraphy and deformation history. Terranes

may be further subdivided into tectonostratigraphic domains, units with similar geological histories, separated from each other by major faults.

The Kalgoorlie Terrane is the best known of the terranes in the Eastern Goldfields. It is subdivided into six domains (figure 2.2). The full stratigraphic succession comprising basalt, komatiite, shale, siliceous komatiitic basalt, felsic volcaniclastic and sedimentary rocks, and clast-bearing submarine fan or fluvial sequences above an unconformity, is present only in the Ora Banda and Kambalda Domains. In the Coolgardie & Boorara Domains, the upper siliceous komatiitic basalt is thin or absent such that komatiite is directly overlain by the felsic and sedimentary rocks (Swager & others, 1995).

As noted in Chapter 1, the Norseman Terrane was differentiated from the Kalgoorlie Terrane by the apparent minor volumes of komatiite and the presence of extensive "BIF" units and older pre-2700 Ma greenstone not seen in the Kalgoorlie Terrane.

2.4 KALGOORLIE TERRANE

2.4.1 Introduction

In the Kalgoorlie Terrane, the stratigraphy is well known and can be correlated between the Kambalda and Kalgoorlie areas. A formal stratigraphic nomenclature was proposed by Cowden and Archibald (1989) for the units in the sequence from which the following description is summarised unless otherwise referenced.

2.4.2 Kalgoorlie Terrane Stratigraphy

The Kalgoorlie Group, comprising five formations, is a well-defined association of mafic and ultramafic rocks which appear to be conformable. All rocks are metamorphosed to greenschist or lower amphibolite facies, but the meta-prefix is omitted for brevity.

The Lunnon Basalt is the lowest exposed unit in the sequence and is named after the prominent outcrops at the Lunnon nickel mine at Kambalda. It comprises a thick sequence of lava flows with minor gabbro-dolerite and thin, interflow sediments (figure 1.2). The base of the unit has not been found, but the minimum thickness is 2 km, the depth extent of drilling. Pillow basalts dominate and are typical Archaean low-K tholeiites. The rare interflow sediments are carbonaceous argillites.

The Kambalda Komatiite is a package of high-MgO lavas with a general decrease in MgO upwards from as much as 45% MgO at the base, to 16% MgO at the top. The unit is widespread in the Kambalda region, and is over 1 km thick in the east but thins markedly to the west where it pinches out. Most of the variation is attributed to primary thickness variations.

The Kambalda Komatiite is divided into lower and upper members, the Silver Lake and Tripod Hill Members respectively. Interflow sediments typically separate the Kambalda Komatiite from the underlying Lunnon Basalt except at the base of the komatiite lava channels, where sediments are typically thin or absent, possibly due to thermal erosion by the moving komatiite lava (*c.f* Lesher, 1989).

The Silver Lake Member directly overlies the Lunnon Basalt and typically consists of one or more thick (25-100 m), high MgO komatiite flows with thick, lower cumulate zones and thin, upper, spinifex-textured divisions. The member is characterised by ubiquitous, laminated, albitic and sulfidic, argillaceous interflow sedimentary rocks from 0.5 to 2 m thick. The upper boundary is taken to be the base of the flow immediately above the highest interflow sediment. The Silver Lake Member has a consistent thickness of approximately 100 m in the Kambalda area.

The Tripod Hill Member is a thick (up to 700 m) sequence of thin (1-10 m) komatiite flows ranging in composition from 16 to 35% MgO. Upper spinifex-textured divisions are well-developed. Interflow sediments are generally absent and the member is highly variable in thickness.

The Devons Consols Basalt (DCB) overlies the Kambalda Komatiite. It comprises high-MgO basalts, discontinuous massive dolerite units and rare interflow sediments. The basal contact of the formation with the underlying Kambalda Komatiite is sharp to gradational over 1 to 2 m and is often difficult to determine. The top of the formation is defined by the Kapai Slate. The basalt has a relatively constant thickness of 60 m to 100 m, but ranges up to 200 m in the Victory area. In common with the Kambalda Komatiite, it pinches out in the Foster area.

The lowermost member of the DCB in the Victory area is the Victory Dolerite, a stratiform unit up to 200 m thick, with internal chemical and mineralogical layering, and which is thought to be a thick flow. Where the dolerite members are absent, the bulk of the DCB consists of massive flows and pillowed, ocellar (variolitic) basalt. The ocelli (varioles) are pale spheroids composed of poikilitic zoisite and/or albite, which may preferentially develop in zones with high primary permeability (eg pillow basalt). Ocelli (variole)-rich zones of the basalts have high SiO_2 values and low FeO and MgO values. Unaltered basalt and dolerite were aluminous high-Mg rocks, enriched in light REE's, Al_2O_3, Zr and Ti compared with the Lunnon Basalt. In general, the MgO content decreases upwards from 12-14% at the base to as low as 4% at the top. The Devons Consols Basalt has a strong association with the underlying komatiites, having a transitional contact and a similar crystallisation sequence for lavas (clinopyroxene/plagioclase-orthopyroxene-quartz). This

association suggests that the basalt should be termed komatiitic basalt (Arndt & Brooks, 1980; Arndt & Nisbett, 1982).

The Kapai Slate is a prominent regional marker horizon that can be traced from north of Kalgoorlie to about 100 km to the south. It is tentatively correlated with the "Widgie Chert" around the Widgiemooltha Dome. It comprises well-laminated, carbonaceous and sulfidic argillite and lesser, massive, albite-quartz chert. Pyrrhotite and pyrite laminae and nodular pyrite are common in the argillite but less abundant in the chert units. Magnetite rather than sulphide minerals is common in some argillite and chert in the Victory area. At Kambalda, the unit is commonly intruded by layer-parallel, aphanitic and porphyritic felsic to intermediate sills up to 30 m thick. The Kapai Slate separates the underlying low SiO_2 lavas from the high Mg, high SiO_2 lavas of the overlying Paringa Basalt. It is interpreted to mark a major hiatus in volcanism.

The Paringa Basalt is over 1 km thick and consists of basalt, minor dolerite and rare, thin, interflow, sediment horizons. The Paringa Basalt is poorly exposed and has had little drilling coverage so that it is incompletely documented, particularly in its upper parts. Dolerite sills up to 300 m thick with internal zonation are known from the base of the unit but are not observed everywhere. The Paringa Basalt in the Kambalda area is predominantly massive, high-Mg lava with variable development of ocelli and rare pillow lava. Chemically, the Paringa Basalt is more siliceous and enriched in LREE, but depleted in Al_2O_3 and CaO than the Devons Consols Basalt. It does not seem to exhibit any systematic variation in chemical composition with stratigraphic position. The lavas crystallised in the sequence: orthopyroxene-clinopyroxene-plagioclase-ulvospinel-quartz.

The Black Flag Beds (BFB) were named in the early days of mining in the Kalgoorlie area and are generally poorly exposed throughout the south-eastern goldfields. They were raised to group status (Black Flag Group) by Swager & others (1995) and are defined as the felsic volcanic and/or sedimentary succession immediately above the mafic-ultramafic lavas of the Kalgoorlie Group. However, Hand (1998) prefers to retain the term Black Flag Beds as there is no regional correlation between members. The description below, intended as an introduction, is modified from Cowden and Archibald (1989) and describes the Black Flag Beds in the vicinity of Kambalda. The results of the more recent, detailed study by Hand (1998) are presented in section 2.5.4

The BFB are in excess of 1 km thick and at Kambalda appear to be conformable with the underlying ultramafic lavas. Two local members are known at Kambalda, a lower felsic unit called the Newtown Felsic Volcanics comprising massive

porphyritic rhyolite, lapilli tuff, thin shale and wacke, and an upper dominantly sedimentary unit named the Morgan's Island Sandstone containing felsic volcanic conglomerate, wacke and thin bedded arenites and argillites. The latter units show a range of sedimentary structures within Bouma sequences.

Thick, layered intrusive gabbro bodies are known from the base of the BFB, typically with a sill-like morphology. The best known is the Golden Mile Dolerite at Kalgoorlie, but the 500 m thick Condenser Dolerite in the Foster area south of Kambalda occupies a similar stratigraphic position and has a similar internal layering to the Golden Mile Dolerite

The top of the BFB is not seen in the Kambalda area. The contact against the overlying Merougil Beds has been traditionally described as a fault, but more recent work (AMIRA P437 study, Barley & others, 1998) has demonstrated that it is an angular unconformity.

The Merougil Beds is an informally named unit in the Kambalda area comprising conglomerate, pebbly arenite and arenite in fining upward units with well developed trough cross-bedding. Clasts comprise feldspar-quartz phyric felsic rocks, granodiorite, metasediment and rare mafic volcanic rocks deposited in a fluvial system. The granodiorite clasts, the angular unconformity, and the lack of strong cleavages contrast with the BFB and suggest a syn to post-tectonic timing for deposition of these rocks.

West of Kalgoorlie, another clastic group known as the Kurrawang Conglomerate overlies the BFB. It differs from the Merougil Beds by having less granite clasts and no trough cross-bedding. A similar conglomerate east of Kalgoorlie at Penny Dam is surrounded by turbidites. Barley & others (1998) consider the Kurrawang and Penny Dam conglomerate exposures to be the channel facies of a submarine fan that was once deposited in a laterally continuous basin, but has subsequently been segmented into isolated enclaves by uplift and erosion.

Barley & others (1998) suggest that the deposition of the turbidite system at the Kurrawang Syncline and Penny Dam, and the fluvial system of the Merougil Beds, marks craton-wide, compressive deformation, because the clasts in these units were derived from eroded older units.

A group of intermediate to felsic stocks, dykes and sills intrudes the Kalgoorlie Group and BFB. Three associations have been defined in a series of unpublished internal WMC reports on the basis of texture, composition and relative timing of emplacement. All felsic and intermediate intrusives show mineralogical and fabric evidence of peak metamorphism. The youngest intrusive, the Durkin Granodiorite,

which forms the core to the Kambalda Dome, is believed to be synchronous with the metamorphic peak and D_3 deformation.

2.4.3 Geochronology of the Kalgoorlie Terrane

The ages of units have been resolved by ion microprobe analyses of single zircon grains by various workers. The main episode of greenstone deposition commenced at *ca.* 2710 Ma with the eruption of felsic rocks from a number of centres found in the north-eastern goldfields. This was closely followed by the eruption of the mafic rocks and komatiites, the latter dated at 2705 Ma using zircons from interbedded felsic rocks in the Gindalbie, Boorara and Jubilee Domains (Nelson, 1995). The Kapai Slate overlying the Devons Consols Basalt at Kambalda has zircons aged between 2690 Ma to 2694 Ma, interpreted to be derived from airfall from a Plinian-style eruption (Claoue-Long, 1990) so the major phase of mafic greenstone deposition occurred between 2710 Ma and 2690 Ma. Ancient zircons that pre-date the greenstone deposition by hundreds of millions of years, found in the Victory Dolerite at Kambalda (a possible lava flow in the DCB) by Compston & others (1986), are interpreted as xenocrysts derived from sialic basement to the greenstone sequence.

The oldest *in situ* lava similar to those in the BFB, a dacite hyaloclastite at Golden Ridge 20 km southeast Kalgoorlie, is dated at 2698±6 Ma. A dacite clast in the BFB from Widgiemooltha has been dated at 2686±3 Ma. Taking into account the Kapai Slate age, deposition of the BFB is considered to commence around 2690 Ma and continued until after 2665 Ma based on the youngest zircons found in volcanic sandstones (Barley & others, 1998).

The youngest detrital zircons in the Kurrawang (2666±5 Ma) and Merougil conglomerates (2664±6 Ma), give a maximum age for these units of *ca.* 2665 Ma (Barley & others, 1998). The minimum age can be constrained by the 2662±5 Ma age of monzodiorite which intrudes conglomerate at Yilgangi Nelson (1997).

Deformation events can be roughly dated relative to the stratigraphy and emplacement of granitoids. Structural studies suggest the Buldania Granodiorite at Norseman was emplaced during D_E extension (Holcolme, 1997) and it is dated at 2686±6 Ma (Hill & others, 1992b), synchronous with commencement of BFB deposition. D_1 N-S directed thrusting is post-BFB, but faults considered to be part of a D_1 thrust duplex documented by Swager & Griffin (1990) are covered by Merougil Beds. Therefore D_1 occurred between 2665 Ma and 2657 Ma. Deformation relationships with granite suggest D_2 E-W orogenic compression and folding was underway at 2660±3 Ma and D_3 faulting occurred between 2663 Ma and 2645 Ma (Nelson, 1997). Regional metamorphism accompanied D_2 and was finished by

2632 Ma. Gold mineralization appears to have largely occurred between 2625 Ma and 2645 Ma (Yeats & McNaughton, 1997).

Therefore, the greenstone succession in the Kalgoorlie Terrane was emplaced on continental crust over about 40 million years, and cratonisation was completed with the cessation of deformation, plutonism and metamorphism after an additional 30 million years.

2.5 KEY FINDINGS OF AMIRA P437

AMIRA project P437 "Mineralised volcanic and sedimentary environments in the Eastern Goldfields" was undertaken between 1995 and 1997 to study the poorly known felsic and sedimentary successions with the aim of "reconstructing paleoenvironmental and tectonic settings of felsic volcanic and sedimentary rock associations in the Eastern Goldfields Province" (Barley & others, 1998). The felsic rocks within the Norseman Terrane were not included in the AMIRA project, but the findings of the project that impact on this study are summarised in this section.

Felsic to intermediate rocks in the Eastern Goldfields were divided into four associations in AMIRA P437 (figure 2.3). The subdivisions were primarily based on geochemistry and geochronology but they also considered the lithology. The information presented below about these associations was summarised from Barley & others (1998) and Hand (1998) unless otherwise referenced. The lithologies in the associations are described here; their geochemistry is described in Chapter 8.

2.5.1 Calc-alkaline andesite-dominated Association 1 (2720-2700 Ma)

Association 1 consists of volcanic complexes dominated by andesite lavas with minor rhyolite, abundant mass-flow deposits, shallow intrusives and voluminous aprons of andesite-derived volcaniclastic rocks interpreted to be deposited by submarine fans. Distal deposits interfinger with tholeiitic basalt. The andesite complexes form discreet centres that are interpreted to represent emergent stratovolcanoes with high relief, which were rapidly eroded to produce voluminous debris. The interfingering of basalt and andesitic epiclastic sediments indicates that andesitic and basaltic volcanism was coeval. An island arc tectonic setting is favoured for the Association 1 complexes.

These intermediate complexes are distinguished from other volcanic centres primarily by their relatively old age, slightly predating the komatiite volcanic event at *ca.* 2705 Ma in the Eastern Goldfields. These complexes are chiefly known in the Laverton area, but also extend north into the Duketon Greenstone Belt and south into the Edjudina, Mulgabbie and Pinjin Terranes of Swager (1995). The Bore Well, Welcome Well and Ida Hill complexes are included in Association 1 (figure 2.3).

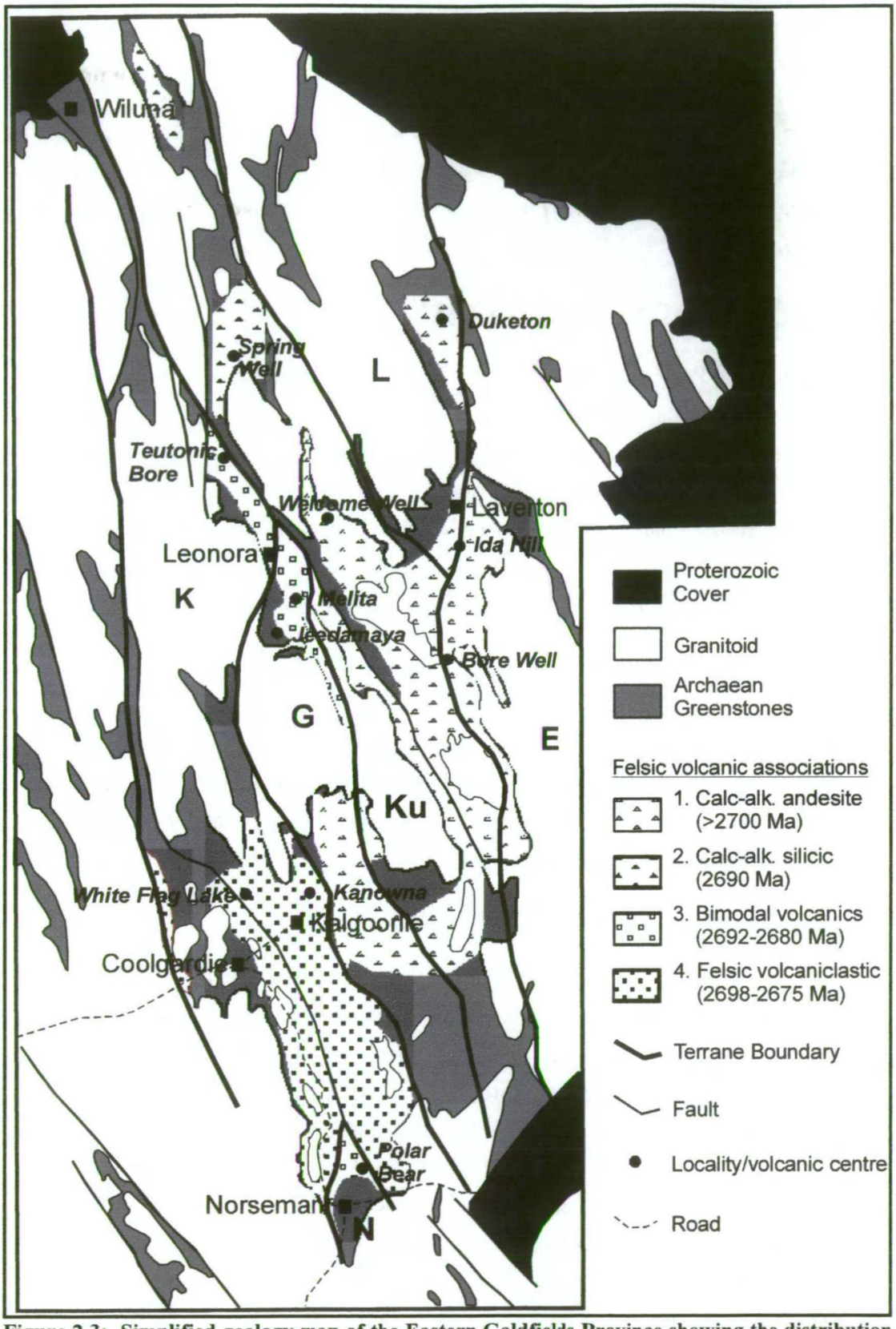

Figure 2.3: Simplified geology map of the Eastern Goldfields Province showing the distribution of felsic volcanic rock associations (modified from Barley & others, 1998; Hallberg & others, 1993). Terranes and terrane-bounding faults modified from Myers (1997). "K" indicates the Kalgoorlie Terrane, "N" the Norseman Terrane. Norseman pattern was added using data from this study.

2.5.2 Calc-alkaline intermediate-silicic Association 2 (2690 Ma)

Association 2 is dominated by calc-alkaline andesite lava, coarse volcaniclastic breccia and intrusive intermediate sills, but also includes significant volumes of rhyolite lava, felsic breccia and felsic conglomerate. This Association is interpreted to represent a submarine silicic volcanic complex formed in a continental marginal arc environment. It may have reached shallow subaqueous conditions.

The only representative of Association 2 is the Spring Well volcanic complex in the Yandal Greenstone Belt. Spring Well is younger than association 1 volcanic centres, having been dated at 2690±5 Ma. Lithologically, Spring Well differs from other calc-alkaline centres in the Eastern Goldfields by the large volumes of felsic lavas and silicic volcaniclastics present.

Spring Well was recently re-examined in an honours project (Crozier, 1999). In detail the stratigraphy has been found from bottom to top to consist of: lower black shale and siltstone representing ambient sedimentation; aphyric rhyolite and andesitic lava, intrusions and breccia; a second shale in distal localities; porphyritic and aphyric rhyolite and andesitic lava, intrusions and breccia and minor tuff beds; andesite and diorite intrusions; and late intrusions including dolerite, gabbro lamprophyre, dacite and trondhjemite. The entire succession covers 20-30 million years.

The initial shale comprises both turbidite and rocks derived from ambient sedimentation, and are considered to be deep water deposits. The majority of the clasts within the volcaniclastic are angular and possess characteristics suggesting they formed by quench fragmentation or gravitational collapse. Minor crystal-rich beds are interpreted as tuffaceous debris related to explosive volcanism. If the latter interpretation is correct, the explosive volcanism suggests that the volcanic edifice grew to shallow water depths.

2.5.3 Bimodal volcanic Association 3 (2692-2680 Ma)

Volcanic complexes in Association 3 are characterised by interfingered pillow basalts and rhyolite to dacite lavas, sills and epiclastic sedimentary rocks. They are intruded by thick mafic sills carrying felsic host rock xenoliths and high level granitoid intrusions of similar composition to the rhyolites. Epiclastic rocks range from coarse monomict breccias to crystal-rich sandstone that probably represents thick debris flow deposits and also chanellised breccia deposits. Fine-grained sediments display ripple cross-bedding and climbing ripple sets, suggesting a relatively shallow water, possibly tidal setting. The abundance of shard-rich volcaniclastic sandstones and breccias indicate that much of the volcanic debris was derived from subaerial

explosive volcanism. The bimodal association forms a linear chain of discreet volcanic centres separated by subaqueous tuffs and fine-grained sedimentary rocks representing more distal deposits. The favoured tectonic setting is back-arc rifting within arc crust.

The bimodal Association 3 has been traced from Teutonic Bore in the north to the Melita and Jeedamya volcanic centres south of Leonora (figure 2.3). SHRIMP dates range from 2692±5 Ma at Teutonic Bore to 2679±4 Ma at Melita and are coincident with the ages of felsic rocks (Black Flag Group) in the Kalgoorlie Basin. As well as the distinct bimodal lithologies, association 3 is distinguished by a distinctive incompatible element-enriched geochemistry (see Chapter 8).

2.5.4 Felsic volcaniclastic Association 4 (2698-2675 Ma)

Association 4 comprises volcaniclastic rocks within upper felsic and sedimentary successions of the Black Flag Beds (BFB) within the Kalgoorlie Terrane.

Hand (1998) noted abundant porphyritic felsic rocks present throughout the Kalgoorlie Terrane, but using contact relationships, found that the vast majority are intrusive in origin and post-date lithification of the BFB succession. Coherent lavas were found to be minor, (identified only at Golden Ridge 20 km SE of Kalgoorlie), but there are numerous proximal volcaniclastic deposits. The most voluminous products within the BFB's are felsic volcanic-derived sandstone and mudrock and all clastic facies within the BFB were deposited by turbidity currents or as slope apron deposits.

The submarine basin within which the BFB was deposited was named the "Kalgoorlie Basin" in Barley & others (1998). The Kalgoorlie Basin had a well established longitudinal depositional system with a northerly paleocurrent flow direction. Felsic volcanic activity along the basin margin or within the basin provided thick, proximal, volcaniclastic deposits in a more localised transverse depositional system. The total thickness of the BFB is difficult to estimate but may be 2 km to 3 km.

Coherent volcanic and coarse volcaniclastic rocks have yielded SHRIMP zircon age dates of 2698±6 Ma for dacite lava at Golden Ridge, 2676±5 Ma for dacite breccia at Gibson-Honman Rock and 2669±7 Ma for volcaniclastic breccia at Eight Mile Dam (Barley & others, 1998). These ages are consistent with dates of 2676±4 Ma at Kalgoorlie (Cloué-Long, 1990) and 2681±5 Ma in the Parker Domain (Nelson, 1995). The youngest detrital zircons from sandstones have an age of 2666±6 Ma, demonstrating that deposition continued at this time. Relatively old ages from some felsic to intermediate detritus such as the andesites at White Flag

Lake, dated as 2813±3 Ma, indicates there was input into the Kalgoorlie Basin from older volcanic terranes.

CHAPTER THREE

Upper Stratigraphy of the Norseman Terrane

3.1 INTRODUCTION

The upper stratigraphic units of the Norseman Terrane are poorly exposed, being largely covered by unconsolidated sediments infilling paleochannels over which Lake Cowan has developed. South and west of Lake Cowan, exposures of the felsic-sedimentary succession overlying the mafic Woolyeenyer Formation are limited to rubbly subcrop in a 500 metre wide band because the majority of the succession has been truncated by the Mission Fault (figure 1.3). However, an area with excellent exposures of the upper stratigraphic units occurs at the northern end of the Norseman Terrane. The outcrop lies in a north-south belt roughly 8 km long and 1.5 km wide at the eastern edge of the Polar Bear Peninsula (figure 3.1). Sporadic outcrop continues south and east of this area extending to the southeast of Killaloe Hill where the cover thickens.

The rock units exposed along the eastern shore of the Polar Bear Peninsula have been folded such that the entire upper stratigraphy from basalt through to felsic volcanic and sedimentary rocks is exposed in the narrow belt. Because this area has the best exposures, the primary task of investigating the upper stratigraphy of the Norseman Terrane was approached by detailed 1:2500-scale geological mapping of the Polar Bear Peninsula. These maps are included in Appendix 4 (maps 1 to 8) and a solid geology compilation at a scale of 1:10 000 is included in Appendix 4 as map 9. The poor exposures south of Lake Cowan were reconnoitred but not mapped.

There are certain localities ("key areas") at the Polar Bear Peninsula, which were crucial to this study in advancing the understanding of the stratigraphy. These key areas are described in Appendix 1, in order to present the evidence used for the stratigraphic interpretation to the interested reader.

Layout of the chapter

The geological and stratigraphic study of the Polar Bear Peninsula, based on geological mapping, occupies the bulk of this chapter. The work is used to determine the upper stratigraphy of the Norseman Terrane (above the basalt). Following the Polar Bear study, another locality, Microwave Tower that was reconnoitred is described, and geological characteristics of the felsic intrusions at Harlequin in Lake Cowan are described. Finally a stratigraphic synthesis and geological history of the Norseman Terrane is presented.

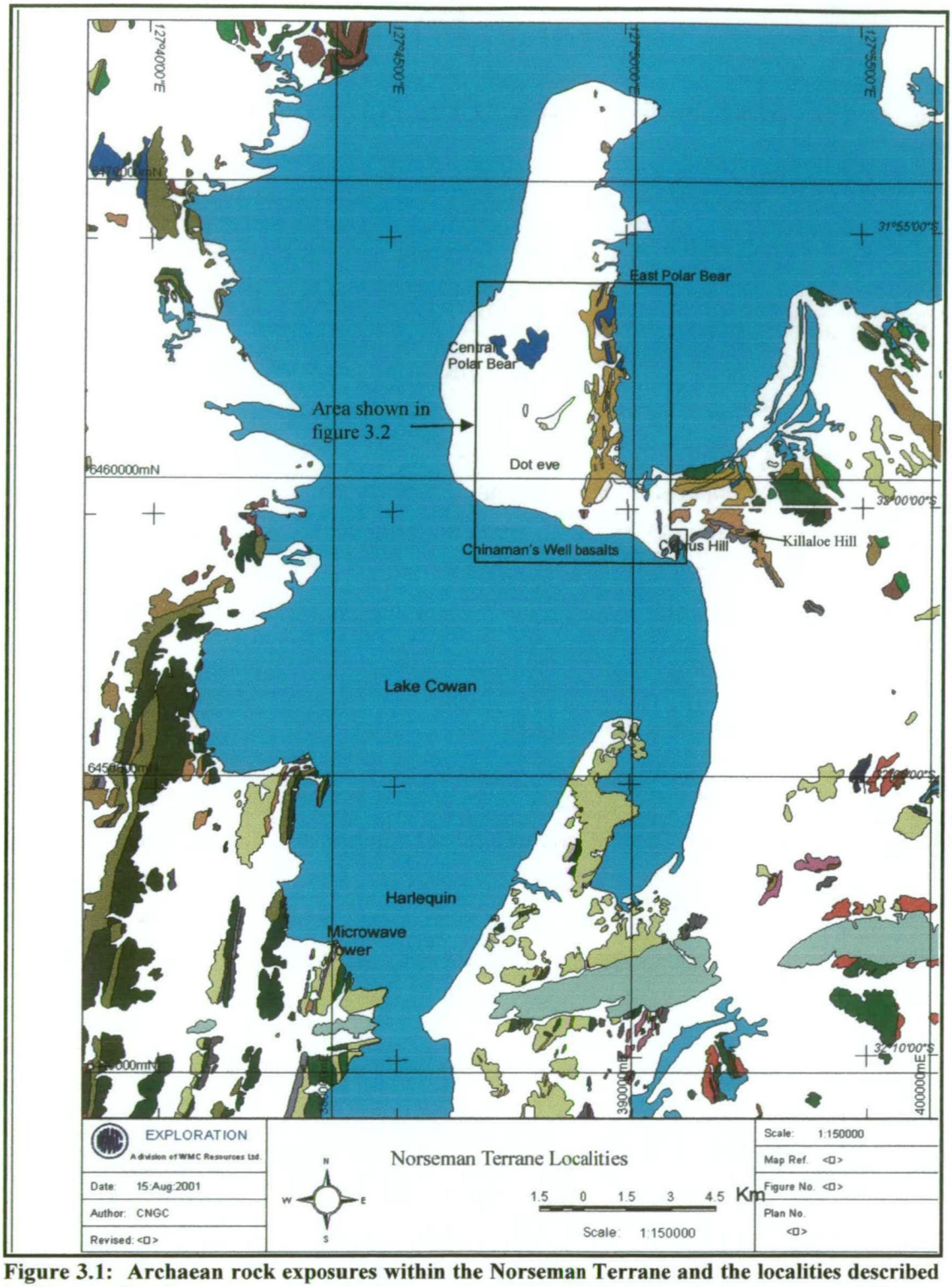

Figure 3.1: Archaean rock exposures within the Norseman Terrane and the localities described in Chapter 3. The outcrop mapping is from the GSWA 1:100 000-scale Norseman and Cowan Sheets. The Polar Bear Peninsula is the bear-shaped peninsula at the top–centre of the map. Green coloured outcrops are broadly mafic in composition, orange are felsic rocks, blue, mauve or grey are sedimentary rocks, brown are ultramafic rocks and red is granitoid.

3.2 POLAR BEAR STRATIGRAPHY

3.2.1 Introduction

The base of the Polar Bear Peninsula is located 23 km north of Norseman and it extends a further 15 km north, surrounded by Lake Cowan (figure 1.3). The

peninsula is dominantly a flat plateau, underpinned by a layer of ferricrete cementing transported sediment in the upper portion of the regolith. The ferricrete is, in turn, overlain by several metres of unconsolidated sediment dominated by aeolian sand. The western-most 1 km of the peninsula is elevated with thick sand dunes forming low hills. To the east, the plateau has been eroded and the bedrock is exposed along a belt of undulating topography. Exposures are typically rubbly subcrop interspersed with small areas of outcrop. However, In a few areas, soil cover has been entirely stripped off and exposure is close to 100 %.

All exposures have been affected to some degree by weathering. In some areas, this has altered outcrops to ferricrete, silcrete, saprolite or mottled saprolite. Strong silicification is also present in places.

3.2.2 Overview of the Geology

Prior to commencing the detailed rock unit descriptions, a brief overview of the geology is provided in this section, incorporating the stratigraphic interpretation of this chapter and the facies interpretations of Chapter 5.

The bedrock geology of the Polar Bear Peninsula (figure 3.2 and maps, Appendix 4) can be divided into five facies associations;

- Mafic volcanic rocks and dolerite intrusive.
- Ultramafic rocks.
- Mafic conglomerate and sandstone.
- Fine-grained sedimentary units, dominantly pyritic black shale and thin-bedded, siltstone-shale turbidite.
- Felsic volcanic rocks, including coherent rhyolite lava, *in situ* felsic breccia and resedimented breccia.

All these Archaean rocks have been metamorphosed to lower amphibolite facies in the Norseman area. In general, primary rock textures are readily identified so the rock names omit the prefix "meta" for clarity, although it is implied for all rocks.

The mafic and ultramafic associations are typical greenstone and are correlated with the Woolyeenyer Formation (figure 1.2). Mafic rocks occupy a far greater volume than ultramafic rocks in the Polar Bear Peninsula area, but are under-represented in the mapped area. Aircore drilling has demonstrated that large areas of the regolith-covered terrain both onshore and offshore of the Polar Bear Peninsula have basaltic or doleritic bedrock. Laminated shale is common in the basalt association as 1-2 m thick interflow sediment bands, representing ambient sedimentation during cessations in volcanic activity. An angular unconformity is interpreted to exist at the top of the

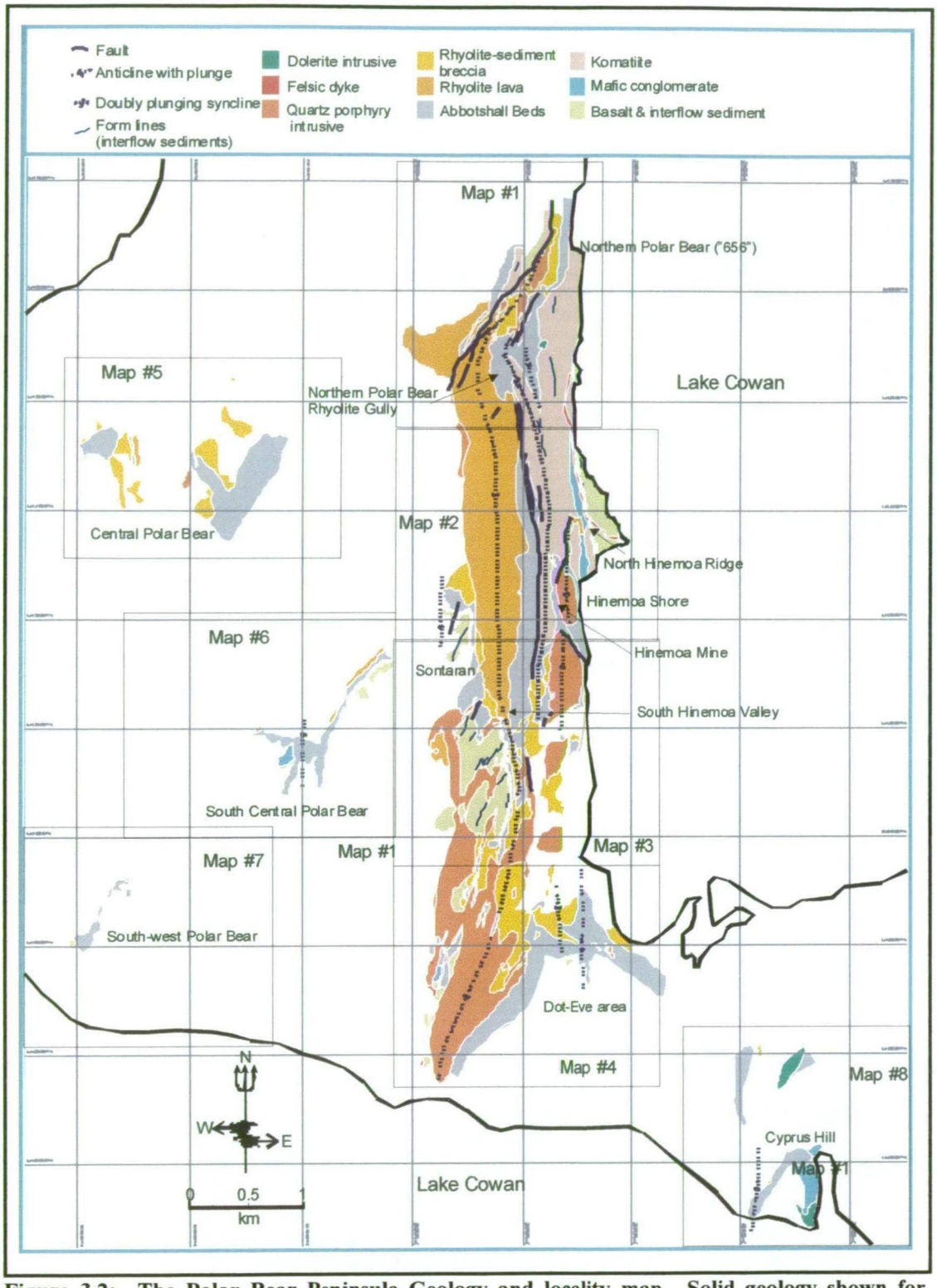

Figure 3.2: The Polar Bear Peninsula Geology and locality map. Solid geology shown for exposed areas. Note that the rhyolite lava represents a lava dome. Area of map shown in figure 3.1. A 1:10 000 scale version of this map is provided as map 9 in Appendix 4. The solid geology was developed by consolidating and interpreting 1:2500-scale geological maps 1 to 8 in Appendix 4. Map areas and the shoreline of the Polar Bear Peninsula are shown.

mafic succession based on the angular discordance between the orientation of interflow sediment bands in the mafic succession and the overlying sediments of the Abbotshall Beds.

The ultramafic rocks are komatiitic, with similar interflow sediment bands to the basalts. They overlie the basaltic succession but are present only in the east of the mapped area, constrained by a lateral stratigraphic pinchout. Spinifex textures are commonly preserved.

Mafic conglomerate is patchy in distribution and is not a widespread unit in the stratigraphy. Where found, it occupies a position between flows near the base of the komatiite, or directly beneath the fine-grained sedimentary rocks of the Abbotshall Beds where the komatiite is absent. Clasts in the conglomerate have been reworked in a subaerial or beach environment demonstrating exposure and erosion of the mafic greenstone prior to or coincident with the komatiite volcanic event. Based on the textures described in section 3.2.6, the conglomerate is interpreted as submarine fan channel facies.

The fine-grained sediment association variably overlies mafic rock, ultramafic rock or mafic conglomerate depending upon whether ultramafic and/or mafic conglomerate are present within the particular section of stratigraphy. The fine-grained sedimentary rocks are dominated by pyritic black shale and thin-bedded siltstone-shale turbidite with felsic volcanic-derived sandstone units as a minor interbedded constituent. The thickness of the fine-grained sedimentary package varies from 25 to 50 m, but the package is commonly thickened by contorted intrafolial folding. Hall & Bekker (1965) defined the Abbotshall Beds closer to Norseman as comprising similar shale and felsic rocks, but also included mafic rocks, which are suggested in this thesis to be structurally repeated Woolyeenyer Formation. Therefore, in this thesis, the name "Abbotshall Beds" will be used to refer only to the fine-grained sedimentary rocks and interbedded felsic-derived sedimentary rocks.

The felsic volcanic association overlies the Abbotshall Beds and is interpreted to comprise a proximal volcanic complex associated with a submarine rhyolite dome. It includes flow-banded rhyolite lava, proximal rhyolitic breccia and sandstone related to quenching and collapse, and interbedded shale bands representing ongoing ambient sedimentation. The felsic volcanic rocks form the uppermost stratigraphy in the Norseman Terrane as no overlying units are preserved.

Quartz porphyry intrusive is arbitrarily assigned to the felsic volcanic association, but the nature of the contacts suggests it is somewhat younger than the rhyolite.

Although evidence for the facing direction is scarce, ultramafic spinifex textures, sediment grading, and soft-sediment structures are preserved in enough sites to establish the stratigraphic succession.

3.2.3 Structural Overview

A full review of the structural development of the Norseman area is carried out in Chapter 10. The following notes about the structures at the Polar Bear Peninsula are provided to assist in the interpretation of the stratigraphy.

The outcrop pattern is complex, largely controlled by doubly-plunging, upright, tight to isoclinal folds (figure 3.2). The wavelength of the folds in an east-west direction is in the order of 500-600 metres and the plunge to the north and south is typically shallow. A broad section of stratigraphy is exposed as a result of the tight folding. Rhyolite is the uppermost stratigraphic unit exposed and typically occupies the cores of synclines. Basalt is the lowermost unit exposed in anticlinal cores.

A north-south cleavage related to the upright folding is strongly developed at the Polar Bear Peninsula. The cleavage is the result of shortening in an east-west direction with concurrent subhorizontal north-south, stretching (Holcolme, 1997). The stretching is prominently displayed as quartz fringes around the north and south sides of pyrite nodules in sulfidic shales, and in thin section as talc fringes around carbonate porphyroblasts in ultramafic rocks. The flattening and stretching distorts the shapes of clasts in rhyolitic breccias.

Reverse faults are the result of east-west compression with the Hinemoa Fault, which hosts gold mineralisation, being the best-known example. NNE-trending faults, some of which are mineralised, are also mapped, and a major fault with a NE orientation, splaying off the Mission Fault is apparent in aeromagnetic images, cutting the northern area of the mapped geology and causing offsets in the stratigraphy.

3.2.4 Mafic Rocks

Mafic rocks are exposed sporadically along the eastern shoreline of the Polar Bear Peninsula and along the western boundary of the well exposed area. Interflow sedimentary layers within the basalt act as form lines, indicating the strike of the basaltic succession on the maps in Appendix 4. The form lines in a number of areas are highly oblique to the sedimentary Abbotshall Beds which overlies the basalt (examples 6461500mN, 388800mE and the Sontaran Prospect at 6461500mN, 388800mE MGA, Appendix 1, section A1.2.3),. This evidence, combined with the presence of mafic conglomerates (section 3.2.6) suggests the upper boundary of the mafic succession is an angular unconformity.

3.2.4.1 Basalt & interflow sedimentary rocks

The description and interpretation of the basalt in this section is brief as a full description is provided with the Basalt studies in Chapter 4.

Description

The majority of the mafic rock exposures comprise distinctive fine-grained, aphyric, grey-green coloured basalt in which clear acicular minerals, less than 1 mm in length, can usually be distinguished. Pillow margins have been identified in outcrop and drill core from hole PEN1206 at the Sontaran prospect. In general, amygdales are rare

The majority of the mafic rock exposures at the Polar Bear Peninsula comprise distinctive fine-grained basalt. The basalt is grey-green in colour, aphyric and clear acicular minerals, less than 1 mm in length, can usually be distinguished. A well preserved pillow was identified in basalt by Offe (1994) and confirmed in the present study at location 388145mE, 6459300mN MGA in the south-western area. Pillow margins have also been identified in drill core from hole PEN1206 at the Sontaran prospect, which was drilled near the top of the sequence. In general, amygdales are rare, but they have been observed in PEN1206 drill core.

In areas where the bedrock is well exposed, interflow sedimentary horizons within the mafic sequence are common. These sedimentary rocks are commonly thin, with a width of one to two metres, but can in some cases be traced along strike for hundreds of metres. Near surface they typically have the appearance of laminated chert, but in holes drilled below the weathered zone, the sedimentary rocks can be either chert or black shale.

Individual basalt flows between the interflow sedimentary horizons range from 1 m thick to a maximum of 30 m thick at the Sontaran Prospect near the top of the mafic succession (Appendix 1, section A1.2.3).

Interpretation & discussion

The pillowed nature of the basalt indicates that it was erupted in water. The planar laminated and fine-grained nature of the interflow sediments is indicative of ambient sedimentation below wave base in an area starved of terrigenous sediment input.

The relatively thin basalt flows and extensive time periods represented by the interflow sedimentary rock horizons, at the top of the mafic succession indicates a waning magmatic flux at the end of the mafic volcanic event.

An unconformity at the top of the basalt succession would imply erosion, probably caused by uplift, which tilted the strata.

3.2.4.2 Dolerite

Description

Dolerite is typically intimately associated with basalt and is defined by a fine to medium grain size. The petrographic features of the dolerites are poorly known, as only one thin section of an equigranular dolerite was examined (CN851901 described in Chapter 4).

Interpretation & discussion

Rocks have been classified as dolerite on the basis of grain size alone and the classification does not necessarily imply an intrusive origin. It is likely that some or all of the dolerites may be fine to medium grained basalt flows. The basalt and dolerite are similar in appearance and the sporadic subcropping nature of the exposures combined with the strong cleavage renders it difficult to map basalt-dolerite boundaries.

3.2.5 Ultramafic Rocks

Several altered varieties of ultramafic komatiite occur in the north and east of the mapped area at the Polar Bear Peninsula, overlying the mafic succession. Spinifex textures have been used in some instances to infer the younging direction, assisting the investigation of the stratigraphic sequence. Thin interflow sediment units, similar to those within the basalt, are common within the komatiite succession and are inferred to have a similar origin, reflecting ambient sedimentation during volcanic hiatuses.

Komatiite is not present at the top of the mafic succession in all areas, including the western flank of the mapped area. Where it is not present, it is interpreted to have pinched out of the stratigraphy.

The contact between basalt and komatiite is observed at 6463750mN, 389650mE MGA, along the lake shore. At the contact, a band of shale approximately 1 m thick separates the top of the basalt from the base of the komatiite. The shale band is parallel to the interflow sedimentary units within the komatiite, but oblique to interflow sedimentary bands within the basalt, thus the basalt shale overlies the angular unconformity at the top of the mafic succession.

Talc-carbonate ultramafics with rounded shapes reminiscent of pillows are recognisable at a number of locations at both the top and the bottom of the ultramafic

sequence. Locations with "pillows" include 6463780mN, 389630mE MGA and 64464500mN, 389000mE MGA (Plate 3.8).

3.2.5.1 Talc-Carbonate Ultramafic

Description

Talc-carbonate is the most common composition for ultramafic rocks at the Polar Bear Peninsula. In outcrop, talc-carbonate ultramafic typically appears as rounded, massive boulders with a speckled brown surface (Plate 3.1). The speckles are cavities where carbonate has been weathered out, whereas the talc is preserved. On freshly broken surfaces, the talc is pale green and the carbonate stained orange by incipient weathering so that the overall colour of the surface appears slightly pink. Although the massive, rounded outcrops are conspicuous in some areas, more commonly, talc-carbonate ultramafic is recessive and a valley marks its location with subcrop exposed by erosion in gullies.

Plate spinifex textures are common and rounded textures were observed in some outcrops, which may represent volcanic pillow structures (Plate 3.2). The largest "pillow" observed has a diameter of approximately 1 m and the smallest about 5 cm. The typical size is 20-30 cm in diameter.

The carbonate within a sample of talc-carbonate drillcore from the Hinemoa Mine area was found to be magnesite by XRD. A small amount of chlorite was detected in the rock, but was probably intermixed with the abundant microcrystalline talc matrix and was not observed in thin section. Strain within the rock is exhibited by coarse talc fringes around carbonate porphyroblasts.

Interpretation & discussion

Both the spinifex textures and the interflow sedimentary units indicate that the ultramafic is extrusive and, therefore, komatiite.

Alteration of an ultramafic rock to a talc-carbonate mineralogy occurs in response to a significant flux of CO_2 (Winkler, 1979). The alteration is commonly texturally destructive with carbonate overgrowing any igneous mineralogical textures. However, spinifex textures are commonly preserved at the Polar Bear Peninsula, probably due to the low MgO abundances of spinifex-textured komatiites preventing substantial carbonate development.

Plate 3.1: Talc-carbonate ultramafic with the typical rounded outcrops.

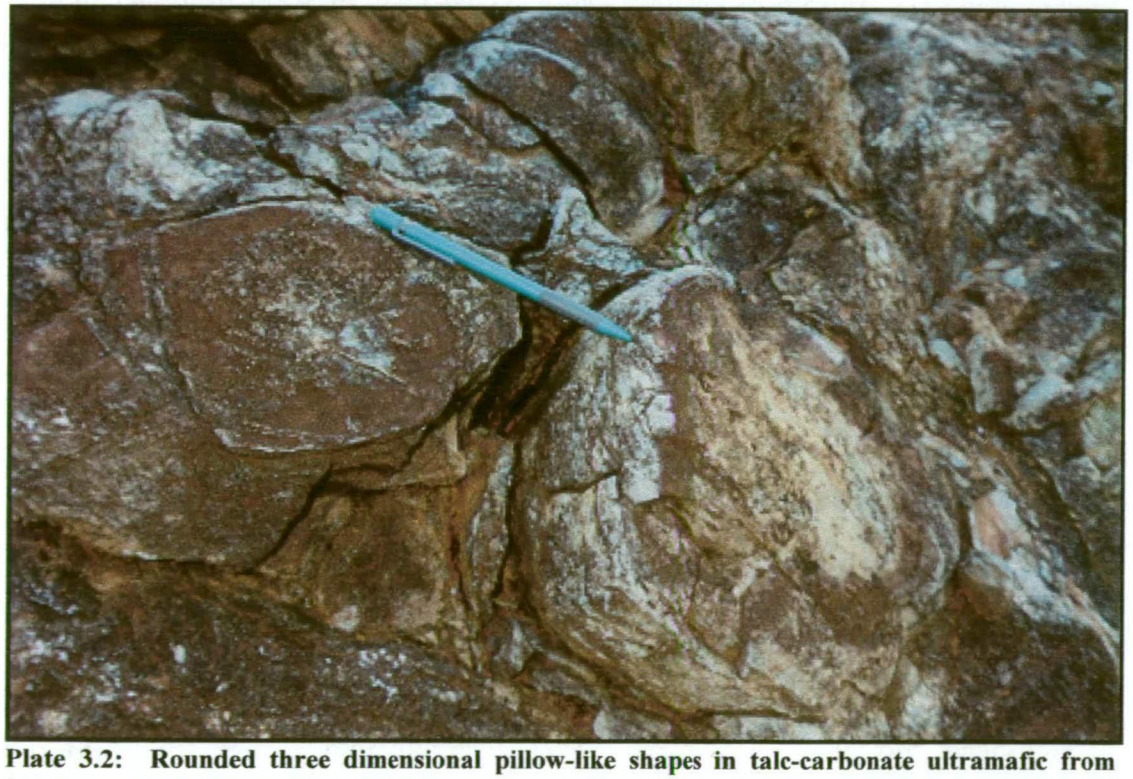

Plate 3.2: Rounded three dimensional pillow-like shapes in talc-carbonate ultramafic from locality 6463780mN, 389630mE MGA. The pencil is 6.5 cm in length and both ends rest against the sides of the pillow-like objects.

The interpretation of the rounded shapes as pillows has been questioned, and R. Cas (pers. comm., 2001) suggests they may actually represent some form of alteration rim. The pillow interpretation would certainly be unconventional as pillows in true komatiites (>18 wt%) MgO have not been previously described. The problem with the rounded shapes at the Polar Bear Peninsula being pillows is that most do not show the interlocking concave margins against other pillows and appear to sit in isolation.

The abundance of interflow sedimentary units within the komatiite at the Polar Bear Peninsula suggest that it is more closely related to the Silver Lake member of the Kambalda Komatiite than the Tripod Hill member. The latter member has thinner, less Mg-rich flows and sedimentary rocks are generally absent (Arndt & Jenner, 1986). This has important implications for the prospectivity of the komatiite for nickel sulfide mineralisation as the Silver Lake member hosts the nickel ore deposits at Kambalda.

3.2.5.2 Quartz-Carbonate Ultramafic

Description

Quartz-carbonate mineralogies are common within the ultramafic outcrops. This type of ultramafic can attain an almost fluted weathering pattern where carbonate abundances are high and quartz veinlets are few (Plate 3.3). If quartz veinlets are abundant, the outcrops have a very rough, hackly texture due to the protruding veinlets. The veinlets are typically only 2-3 mm wide.

The character of the quartz–carbonate ultramafic is best observed in diamond drill core. It is grey in colour with diffuse, white patches and may be present in small zones adjacent to talc-carbonate ultramafic, or in broad zones up to 80 metres thick downhole. Previous CNGC geologists working at the Polar Bear Peninsula submitted a number of samples from drill holes for XRD analysis. Typical analyses returned quartz, dolomite, minor chlorite and sometimes traces of albite.

A segment of quartz-carbonate alteration selected for this study from Hinemoa Mine drillcore consists almost entirely of carbonate, with very minor quartz veining (Plate 3.4). The carbonate grains have irregular, interlocking margins like a completed jigsaw puzzle and are particularly coarse-grained adjacent to a quartz veinlet. Traces of talc occur in veinlets and between carbonate grains in finer grained, less recrystallised areas. Opaque grains are rare. The geochemical analysis suggested the carbonate is approximately ankerite in composition with 28 wt% CaO, 14 wt% MgO and 10 wt% FeO(t). As would be expected, considering the carbonate abundance, the volatile contents are very high with 42 wt% loss on ignition.

Plate 3.3: silica-carbonate altered ultramafic. An almost fluted weathering pattern is visible un the surfaces, with small ridges where quartz veinlets protrude. Hammer is 31.5 cm in length.

Plate 3.4: Photomicrograph of sample CN851911. Carbonate with quartz vein cutting the bottom left quadrant. Field of view 5 mm. Plane polarised light.

It is likely that weathered samples of quartz-carbonate alteration are those rocks described in section 3.2.7.1 as type 1 silicification. It is also possible that some type 2 silicification may be quartz-carbonate rocks.

Interpretation & discussion

The segment of quartz-carbonate drillcore from the Hinemoa Mine selected for further study, lies one metre downhole from talc-magnesite ultramafic. Both these alteration types were studied using XRD, petrography and geochemical analysis. The objective was to determine whether chemical changes accompanied the alteration and in particular, whether the quartz in the alteration was introduced or was silica derived from the primary ultramafic minerals.

Marked chemical changes have occurred in the quartz-carbonate sample at least on the scale of tens of centimetres, so that the geochemistry bears little resemblance to an ultramafic composition. During recystallisation, all major elements not held by ankerite were depleted. The quartz-carbonate sample has a volatile-present composition strongly depleted in SiO_2 and MgO and with lesser reductions in Al_2O_2 and TiO_2 compared with the talc-carbonate sample. Abundances of CaO and volatiles have increased markedly and the CaO/Al_2O_3 ratio is 156 compared to the talc-carbonate sample one metre away, which has a ratio of 1 that Donaldson & others (1986) indicate is typical for ultramafic rocks. It is possible that a larger sample might have included more quartz veinlets and patches of exotic minerals and possessed a composition closer to that of a typical ultramafic. However, increasing quartz would further decrease the MgO by dilution, and the CaO abundance is so great that any sample that included significant ankerite would be enriched in CaO.

Drill core from the Hinemoa Mine area has talc-carbonate ultramafic intimately interfingered with the quartz-carbonate komatiite, therefore, the two varieties are likely to have originated from similar komatiitic rocks, but the quartz-carbonate rock has been more strongly metasomatised. Quartz-carbonate mineralogies produced during metamorphism of ultramafics are stable at lower temperatures or potentially a higher CO_2 flux than talc-carbonate compositions (Winkler, 1979). As it is not feasible that intimately interfingered rocks could have experienced different temperatures, the quartz-carbonate rocks at the Polar Bear Peninsula are thought to represent more permeable zones that received a higher flux of CO_2 than surrounding talc-carbonate-altered komatiites. This fluid flux added CaO as well as CO_2 and depleted MgO and a range of other elements. SiO_2 appears to have transferred into quartz veinlets and it is unclear whether there has been an overall depletion of silica from the rock.

Isobaric equilibrium curves for metamorphic reactions provided by Winkler (1979), indicate that between about 350°C and 450°C, the reaction of talc + CO_2 converting to quartz + carbonate is rather insensitive to the mole fraction of CO_2. However, between about 450°C and 520°C, the reaction becomes increasingly sensitive to the CO_2 abundance. Because the reaction at Polar Bear is believed to caused by a higher flux of CO_2, the equilibrium curves suggest that the alteration to quartz-carbonate mineralogies took place within this higher temperature range and potentially may indicate the temperature of metamorphism.

The intense quartz veining within silicified komatiite suggests that quartz formed during metamorphism to quartz-carbonate mineralogies and was directed into veinlets rather than spread homogenously through the rock. The majority of the veinlets strike east-west indicating that they formed during D_2 deformation as tension gashes, perpendicular to the extensional direction indicated by quartz fringes on pyrite nodules. This in turn gives a relative date for peak metamorphism as syn-D_2 (see Chapter 10).

3.2.5.3 Serpentinised Olivine Orthocumulate

Description

Ultramafic rock that appears to be serpentinised olivine orthocumulate and serpentinised porphyritic ultramafic overlies a unit with feathery random spinifex textures at location 6465255mN, 388915mE MGA. The rocks were not examined petrographically or with XRD.

Cleavage is poorly developed in the serpentinised ultramafic rock, hence it is massive, with a granular texture in weathered surfaces. It appears to be incipiently silicified, but does not have the quartz veining and siliceous appearance of the silicified ultramafic rock. The phenocrysts in the porphyritic ultramafic weather out on exposed surfaces, leaving cavities.

Interpretation & discussion

The presence of serpentine is a reliable indicator that the fluid phase present during rock alteration contained very little or no CO_2 otherwise it would be replaced by talc-carbonate minerals (Winkler, 1979). The reason serpentinites are preserved in this locality may be the poorly developed cleavage, preventing an easy conduit for CO_2 to access the rock.

3.2.6 Mafic Conglomerate and Mafic Sandstone

Mafic conglomerate and sandstone is a patchy unit that occurs overlies the mafic succession. At the best preserved localities (described in Appendix 1, sections A1.2.4 & A1.2.5), mafic conglomerate and sandstone overlie the mafic succession and underlie the Abbotshall Beds, and komatiite is not present in the stratigraphy, probably due to a lateral pinch out. However, along the eastern shore of the Polar Bear Peninsula, a poorly preserved occurrence (described in Appendix 1, section A1.2.6) indicates that the mafic conglomerate and sandstone may have been deposited between komatiite flows.

Mafic conglomerate and mafic sandstone are described together as they are intimately associated and together form one facies association. In some localities, there appears to be a fining up facies transition from conglomerate-sandstone to fine-grained sedimentary rocks. However, the fine-grained sedimentary rocks also are present where conglomerate is not present, so it is convenient to consider the conglomerate-sandstone and fine-grained sedimentary rock facies separately.

The mafic conglomerate and sandstone facies is probably genetically related to the angular unconformity at the top of the mafic succession.

Description

Mafic conglomerate and sandstone are exposed in a number of locations but have a patchy distribution and are not widespread. The thickness of the package is less than 50 metres. The mafic conglomerate and sandstone facies association is abruptly overlain by the fine-grained sedimentary rocks of the Abbotshall Beds, predominantly siltstone and shale

The conglomerate is clast-supported and poorly sorted, with a fine-grained, sandstone matrix. In general, the majority of the unit is massive, but conglomerate, grading into basaltic sandstone over a width of about 20 cm, is present in isolated exposures at Cyprus Hill (figures 3.1, 3.2). The outcrop preservation is insufficient to gain an overview of all the facies transitions through the unit.

Both sandstone and conglomerate are dominated by basalt clasts, which range in diameter from approximately 0.2 mm in fine sandstone to roughly one metre in boulder conglomerate. Basalt may comprise all of the clasts, but more commonly chert clasts are also a minor constituent. Basalt clasts larger than about 1 cm in diameter are well rounded and typically elliptical in shape but occasionally exhibit high sphericity. Basalt clasts smaller than one centimetre in diameter range from well rounded to subangular. The chert clasts larger than about 2 cm in length have

Plate 3.5: Mafic conglomerate with pebble-sized basalt and chert clasts from Cyprus Hill. Pencil is 13.5 cm in length.

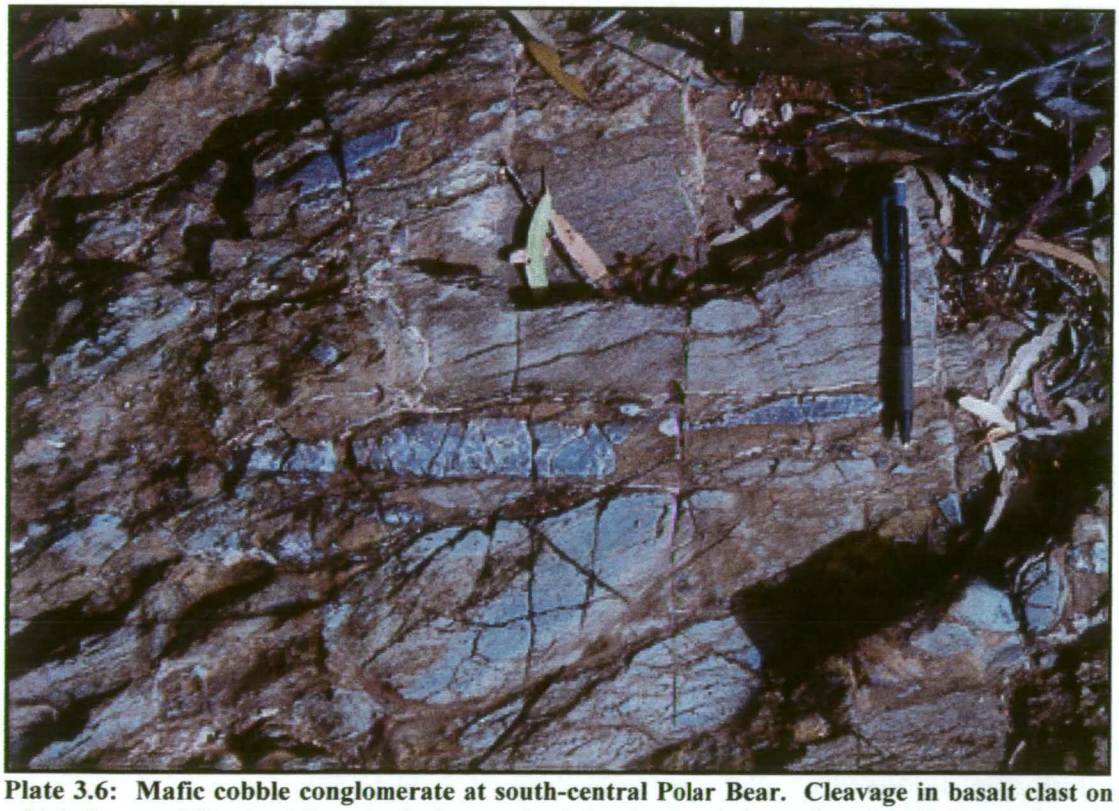

Plate 3.6: Mafic cobble conglomerate at south-central Polar Bear. Cleavage in basalt clast on which the pencil lies is oblique to the long axis of the elongated chert. Pencil is 13.5 cm in length.

well rounded edges whereas smaller clasts may be angular. Highly angular spinose grains occur in some sandstone. The shape of the chert clasts is typically elongate but spherical examples are present at Cyprus Hill (Plate 3.5).

The matrix between the pebbles is composed of sand-sized basalt and chert clasts, and quartz and skeletal leucoxene grains up to 0.3 mm, indicating erosion of slightly more coarsely-grained units (Plate 3.7). Sandstone units are typically well-sorted and comprise approximately 80% basalt and 20% chert lithics. Grading may be present.

Strong alteration is ubiquitous within the basalt clasts. The petrographic characteristics of the basalt clasts are discussed in Chapter 4. At Cyprus Hill, well-rounded clasts are typically elongate parallel to cleavage. It is likely that the clasts have been flattened, although a primary depositional origin for the fabric cannot be discounted. Elongate clasts exposed within a creek bed at south-central Polar Bear (figure 3.2) have a clast alignment slightly oblique to the cleavage which may indicate primary imbrication (Plate 3.6). No other depositional structures have been identified within the unit.

Interpretation & discussion

The clast assemblage within the conglomerate, basalt and chert, would be derived by erosion of the mafic succession, which includes thin, interflow sedimentary layers. The lack of other clast compositions suggests that only the mafic succession was eroded to form the conglomerate and sandstone. The well-rounded, and in some cases spherical clasts, are indicative of a high degree of abrasion requiring exposure to a shoreline or fluvial environment, both of which imply a shallow to emergent setting. Thus, irrespective of their final depositional site, the clasts within the conglomerate were eroded and reworked from exposed basalt flows in a fluvial or shoreline environment.

In section 3.2.4, it was noted that there is evidence for an angular unconformity at the top of the mafic succession. The presence of mafic conglomerate and sandstone, indicating erosion of the mafic succession, is further evidence for the angular unconformity. A more detailed facies interpretation of the mafic conglomerate and sandstone is provided in Chapter 5.

Doepel (1973), noted the conglomerate at Cyprus Hill and defined the top of the Woolyeenyer Formation at its base, placing it within the Mt Kirk Formation. This interpretation is now believed to be incorrect because the terrane-bounding Mission Fault separates the Polar Bear Peninsula from the Mt Kirk Formation type area, as described in Chapter 1. The conglomerates are currently not assigned to any formally defined stratigraphic element.

Hand (1998) described mafic conglomerate near the Junction, Kanowna Belle and Panglo Mines in the Kalgoorlie Terrane. 90% of the clasts in these conglomerates are mafic in composition, but the remaining 10% are felsic, ultramafic and fine-grained sedimentary clasts. These conglomerates differ from those found at the Polar Bear Peninsula due to inclusion of felsic and ultramafic clasts. The interpreted stratigraphic position of the conglomerates described by Hand as a part of the Black Flag Beds sequence, deposited within the Kalgoorlie Basin, is stratigraphically higher and younger than the mafic conglomerate at the Polar Bear Peninsula, which predates the Abbotshall Beds that cap the mafic and ultramafic volcanic sequence.

3.2.7 Silicified rocks

Pervasive silicification has altered many outcrops at the Polar Bear Peninsula. In some instances, primary textures are preserved despite the alteration, revealing the precursor rock-type. It is also commonly the case that silicified outcrops are spatially associated with one form of rock, allowing a reasonable inference of the precursor. Where the precursor rock-type can be deduced using these means, it has been found that different rock-types are generally affected by distinctive and characteristic forms of silicification. Three varieties of silicification have been recognised. Where textures are not preserved, the precursor rock-type may be tentatively inferred by the variety of silicification. However, it is not possible to be certain that all silicified outcrops of the same variety were derived from the same rock-type. This problem is mainly encountered where silicification has affected rocks of different composition which are interlayered, a situation that occurs along a ridge northeast of the Hinemoa Mine. In this locality, mafic conglomerate, sandstone and black shale are all interbedded with komatiite and silicification has locally affected all rock types.

3.2.7.1 Type 1 silicification

Description

Type 1 silicification is hard and crops out strongly, commonly forming ridges. The outcrops are dark brown to orange in colour and have a rough, hackly texture where weathering has caused silicified joints and quartz veins to protrude. A rough brecciated appearance is also common but not ubiquitous. Fresh rock shows quartz and minor carbonate but no primary igneous minerals.

Spinifex textures are well preserved in the some type 1 silicification outcrops. The most characteristic form are plate spinifex but random spinifex can be recognised in some instances. One outcrop with spinifex textures and a brecciated appearance could be recognised as hyaloclastite.

Interpretation & discussion

The preservation of spinifex textures identifies the precursor of rocks with type 1 silicification as komatiite. Silicified outcrops of this type are commonly found adjacent to talc-carbonate altered ultramafic. It is probable that this form of silicification is the weathered expression of the rock described above as quartz-carbonate ultramafic.

3.2.7.2 Type 2 silicification

Description

Type 2 silicification forms a hard, smooth, siliceous rock with a pale grey-green colour and lacks a stained weathering rind. Quartz veinlets within the rock are common, but in contrast to type 1 alteration, the veinlets do not protrude from the rock. A faint laminated texture may also be preserved. This form of alteration is less common than type 1 silicification, typically occurring as pods with limited strike extent.

Interpretation and discussion

The precursor rock-types that form this alteration are less well-defined than for type 1 alteration. Along north Hinemoa ridge (figure 3.2), northeast of the Hinemoa Mine, where a wide variety of rocks are interlayered, some type 2 alteration appears to be altered mafic sandstone. This is suggested by correlation along strike of a 1.5 m wide band of type 2 alteration with an outcrop of poorly altered sandstone with obvious graded units. The former grading in the silicified rocks is revealed by a faint laminated texture.

Rocks, with silicification similar to type 2, but with a slightly darker colour and a prominent laminated texture, crop out along the north Hinemoa ridge. The origin of this form is revealed by large rounded iron oxide casts after pyrite nodules, showing they were originally sulfidic black shale as discussed in section 3.2.8.3.

It is probable that type 2 silicification is altered sediment, largely mafic sandstone. However, some shales, when silicified, also obtain an appearance similar to type 2 silicification.

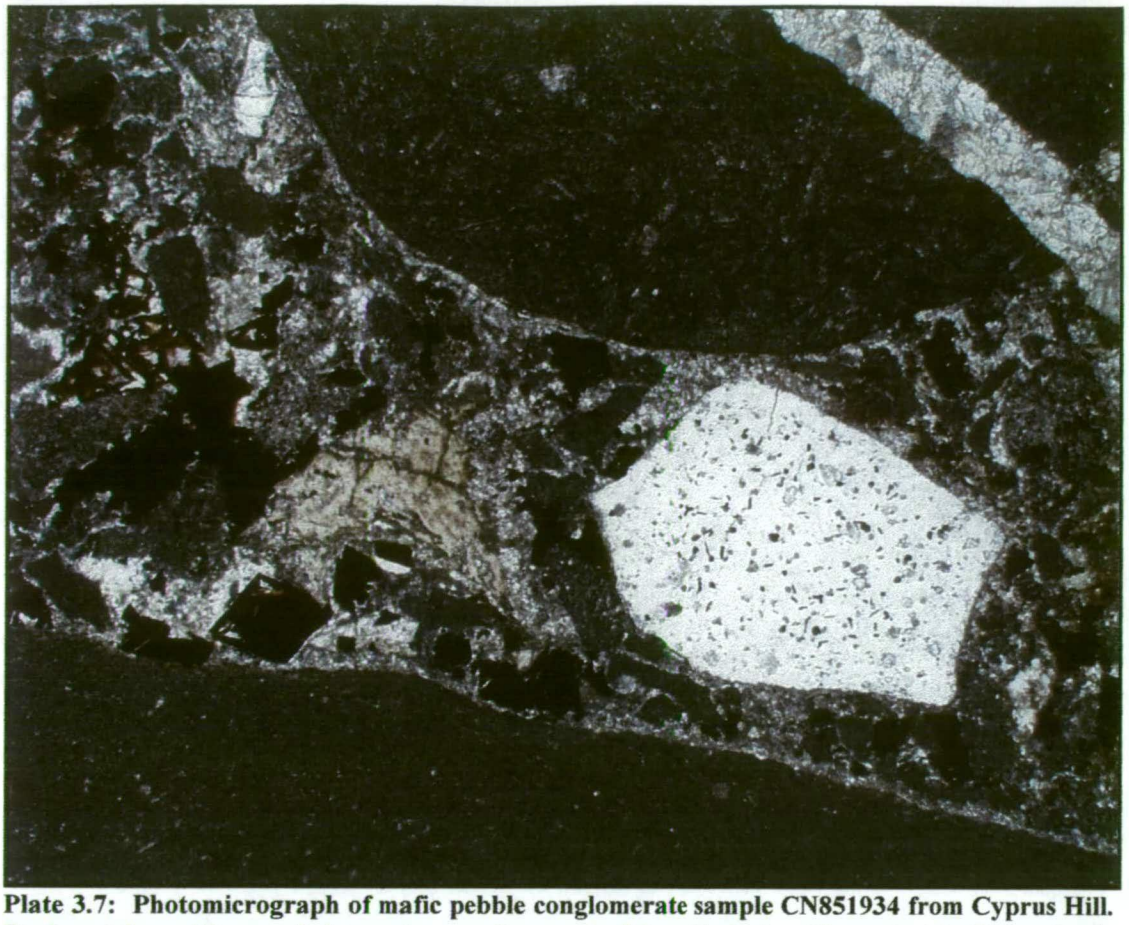

Plate 3.7: Photomicrograph of mafic pebble conglomerate sample CN851934 from Cyprus Hill. Dark patches with rounded margins are fine-grained basalt clasts. Clear clast in the centre is chert. The grains between these clasts are basalt clasts, quartz, and leucoxene. Field of view 5 mm. Plane polarised light.

Plate 3.8: Sandstone-shale turbidite from the North Hinemoa area. Felsic sandstone has scoured underlying shales and has small black shale rip-up clasts just above the shale contact. Upper grey shales display ripple cross-laminations. Pencil is 13.5 cm in length.

3.2.7.3 Type 3 silicification

Description

Type 3 silicification may be spatially associated with either of the other two forms. It is characteristically brecciated and has an appearance transitional between type 1 silicification and brecciated mafic rock. It is typically greyish in colour and the silicification tends to look patchy so that some fragments appear to be largely unaltered.

Discussion & interpretation

Type 3 silicification is the most enigmatic of the three varieties. In some areas it appears to be a weak form of type 1 silicification in a rock that is brecciated. In other localities, chiefly along north Hinemoa ridge, it is closely associated with type 2 silicification of mafic sandstone and appears to be moderately-silicified, heavily-deformed, mafic conglomerate. A single, common precursor has not been identified.

3.2.8 Fine-grained sedimentary rocks

The major occurrence of fine-grained sedimentary rocks at the Polar Bear Peninsula is in the package correlated with the Abbotshall Beds. The Abbotshall Beds typically range in thickness from 25 to 50 metres, but may be significantly thickened by intrafolial folding. In outcrop the Abbotshall Beds variably appear as broad zones of laminated chert, interbedded siltstone and shale, or sulfidic black shale. A range of other sedimentary rock types including slate, shale, volcanic sandstone and massive sulfide/gossan have been mapped locally.

Although fine-grained sedimentary rocks typically appear to be laminated chert at the surface, laminated black shale is the most prevalent rock type intersected in drillholes below the base of weathering, including beneath chert outcrops.

The fine-grained sedimentary rocks locally overlie komatiite, basalt or mafic conglomerate and sandstone. The range of rock types in the substrate is caused by the komatiite pinching out of the stratigraphy, and the mafic conglomerate and sandstone having a patchy, lenticular distribution. The contact between the underlying rocks and the fine-grained sedimentary rocks is abrupt.

3.2.8.1 Sandstone-Shale Turbidite

Description

Sandstone-shale turbidite is dominated by sandstone and occurs as graded units 1.5 to 8 cm thick. Shale occurs at the top of each normally graded unit and typically has a

Plate 3.9: Siltstone-shale turbidite from south Polar Bear. Siliceous siltstone band with bedding parallel to the pencil has been broken up by the cleavage.

Plate 3.10: Sulfidic shale with abundant hematite balls after pyrite nodules. The pencil points towards a small patch of white quartz on the northerly margin of a nodule, showing the subhorizontal, north-south stretching. Thin bands of quartz are also apparent on the margins of some other nodules. A pair of holes, which were previously occupied by pyrite, is visible above and to the left of the pencil tip.

thickness of only a few millimetres. Iron oxide layers, a few millimetres in width, are common between the sand-shale turbidite units and are considered to represent weathered sulfidic horizons. The basal unit is typically coarse-grained sandstone and gravel or fine-grained muddy sandstone. Isolated small chert pebbles have been found as rare oversized clasts (Plate 5.2). The sandstone may be plane laminated or massive and typically scours the underlying shale (Plate 3.8). The basal sandstone may be overlain by cross-laminated fine sands or may grade directly into grey-green shales.

Interpretation & discussion

Overall, the graded units display sequences typical of those derived from low-density turbidity currents. A more detailed facies analysis is presented in Chapter 5.

3.2.8.2 Siltstone-Shale Turbidite

Siltstone-shale turbidite is a common component of the Abbotshall Beds at the Polar Bear Peninsula.

Description

The rock type typically crops out as siliceous cherty units, interbedded with slaty rocks. The "chert" is dark in colour and is probably silicified, fine-grained sandstone or siltstone. The slaty rocks are deformed shale. Rounded cavities after pyrite nodules, typically 1 to 2 cm in diameter, are common within the slate, indicating an origin as sulfidic shale. The interface between the silicified siltstone and shale is generally sharp with no grading evident.

Drill core from the Hinemoa Mine shows the rock type in an unweathered state. The rock is dominated by sulfidic black shale with pyrite nodules, but has lesser interbedded centimetre-thick siltstone layers.

Siltstone–shale turbidite is strongly deformed by D_2 flattening which has led to disruption of the layers (Plate 3.9). The disruption is commonly so intense that the unit acquires a brecciated appearance in outcrop with blocks of dark "chert" hosted in a shale matrix. This has led to the unit being called "diamictite" in previous descriptions. Siltstone layers in brecciated outcrops can often be crudely traced through the unit as discontinuous blocks subparallel to the cleavage or as bands with lateral offsets.

Interpretation & discussion

Overall, this rock type tends to be dominated by sulfidic black shale indicating ambient sedimentation in a quiet, sub-wave base, anaerobic environment with biogenic sulphate reduction. However, the siltstone or fine sandstone interbeds are clastic sediments that would be transported by currents. The latter units represent the upper divisions of low-density turbidites, deposited below wave base and distal from a clastic sediment source.

The characteristic brecciation is due to a spaced cleavage. The discontinuous blocks of siliceous laminated siltstone are primarily a result of boudinage of the siltstone within the incompetent shale matrix. The bands with lateral strike-slip offsets are common where siltstone layers are oblique to the cleavage. The shales have responded to the compression in a ductile manner whereas the siltstones are shortened by faulting (Plate 3.9).

3.2.8.3 Sulfidic Black Shale

Sulfidic black shale is a major component of other units such as the siltstone-shale turbidites described above, but also occurs as a distinct unit on its own.

Description

Sulfidic black shale is characterised in outcrop by ubiquitous spherical iron oxide casts or cavities after pyrite nodules (Plate 3.10). The pyrite nodules are typically one to two centimetres in diameter, although specimens up to 7 cm have been observed. Fresh sulfidic black shale has been intersected by diamond drill holes at Hinemoa Mine and in reverse circulation percussion drilling at Sontaran and Killaloe Hill. These drill holes show that sulfide minerals also occur as pyritic laminae. The rock type differs from siltstone-shale turbidite, which also contains pyrite nodules, by the absence of siltstone interbeds.

Interpretation & discussion

The unit represents ambient pelagic sedimentation within an anoxic sub-wave base environment.

3.2.8.4 Massive sulfide and Gossan

A number of gossans were recognised by previous exploration companies outcropping at the southern end of the Polar Bear Peninsula. Two exploration prospects targeting the gossans were named Dot and Eve. Pyritic massive sulfide has

also been intersected in drill holes penetrating the Abbotshall Beds at the Sontaran prospect, 700 metres south west of the Hinemoa Mine.

Description

At the southern end of the Polar Bear Peninsula, the gossan forms a regular stratigraphic unit at the top of the sedimentary succession overlying either slate or laminated chert. It typically forms prominent outcrops up to 30 m wide. The regular position of the gossan in the stratigraphy distinguishes it from ferricrete that has a similar appearance. The ferricrete typically forms small irregular exposures amongst other rock types, or plateaus where the water table has formed a redox front.

The gossan comprises black, iron oxide, commonly with irregular cavities up to 1 cm across. Iron oxide bounding the cavities may have a nodular, crustiform or botryoidal texture indicating it has been mobilized and deposited after the cavity was formed. Orange, irregular limonitic patches generally 1 to 2 cm across are common. Internally, the oxide minerals form porous textures that may represent boxwork after sulfide minerals or another mineral that has been leached out.

At Dot, the ferruginous exposures that were tested by costeans and drilling, appear to represent ferruginised sediment and do not consist of massive iron oxide. At location 6459900mN, 389070mE MGA, the gossan interfingers with discontinuous bands of chert, while at 6460185mN, 389535mE MGA, a single hemisphere of an iron oxide cast after a pyrite nodule was found lying loose on the gossan exposure.

Pyritic massive sulfide was intersected in some RC holes drilling through the Abbotshall Beds at the Sontaran prospect, west of the Hinemoa Mine. The thickest interval of massive sulfide intersected was 24 m in two sections, separated by 3 m of intervening felsic rock, but the drill holes ended in sulfide so the true thickness is unknown. The massive sulfide is overlain by sulfidic black shale. As the base of the massive sulfide was not intersected, it is not known what the underlying unit is. Correlation between drillholes suggests that the massive sulfide zone grades into pyritic chert along strike.

Interpretation & discussion

A full discussion of the exploration history of the gossans and their petrography and geochemistry was carried out by Offe (1994), who reports the assessments of petrographic consultants to whom samples were submitted. The consultants found evidence for limonitic boxwork after iron sulfide in some of the samples, but it typically comprised less than 5% of the sample. The overall conclusion was that the samples represented ferruginised rock. Small inclusions of chromite were noted by

the consultants in several samples, which led them to suggest the original rock was ultramafic. Other samples contained granular quartz suggesting a siltstone origin.

The single pyrite nodule discovered at one of the gossans suggests that the irregular cavities and limonitic patches may be holes after pyrite nodules, implying the gossan was derived from unusually sulfidic black shale. Remobilization of iron oxide and its deposition as botryoidal masses within the cavities after pyrite nodules is suggested as the reason for irregular shape of the cavities in contrast to the rounded holes in sulfidic shale. This interpretation is consistent with the stratigraphic position of the gossan within the fine-grained sedimentary succession, interfingered with chert. Other gossan probably represents pyritic massive sulfide such as that intersected by drillholes in the Abbotshall Beds at the Sontaran prospect. The chromite inclusions noted by the petrographic consultants may have been derived from the underlying basalt or komatiite.

3.2.8.5 Shale

Shale that is not strongly sulfidic is present in some areas of the Polar Bear Peninsula. "Shale" has been used as a mapping term for these rocks.

Description

In outcrop, the shales may be black due to organic matter, or bleached. The feature that distinguishes shale from sulfidic black shale is the absence of pyrite nodules. In the best exposures, laminated shales consist of 1-1.5 cm units with basal 1-2 mm thick sandstone laminae, grading up into grey-green shale. Rare sandstone beds up to 4 cm thick are present. Thin millimetre-sized bands of sulfidic material weathered to iron oxide are concentrated along bedding laminae.

Interpretation & discussion

These units are dominated by mud deposited from suspension and differ from sulfidic sediments only by the lower quantity of sulfide, made conspicuous by the absence of the pyrite nodules that are ubiquitous throughout the sulfidic black shales. The laminated shales represent the fine fractions of low-density turbidites. They differ from sand-shale turbidites by the dominance of shale over sandstone and from siltstone-shale turbidites by the absence of the siliceous siltstone layers.

3.2.8.6 Slate

Prominent outcrops of slate up to 30 metres thick are found as interflow sedimentary rocks between the komatiite and mafic rocks. Outcrops of slate are also common in the southern end of the mapped area near Dot-Eve.

Description

Slate has been used as a map description for highly fissile mud rocks. They are typically pale in colour but commonly have iron oxide casts after pyrite nodules.

Interpretation & discussion

Slate is directly equivalent to the sulfidic black shale, laminated shale or siltstone-shale turbidites in which the silicified siltstone/sandstone beds are less prominent and the cleavage is better developed. The foliation may have allowed more effective penetration of weathering to bleach the slates.

3.2.8.7 Laminated Chert

Chert is prominent capping ridge tops across the Polar Bear Peninsula (Plate 3.11)

Description

The chert is pale grey to white in colour and is composed of fine-grained polygonal quartz with an even grain size of 0.03 mm. The chert possesses a planar lamination formed by thin layers with a finer grain size of 0.016 mm. In some areas ferruginous laminae are present within the chert and have been remobilized along fractures such that the rock has previously been termed "jaspilite" (banded iron formation) (Plate 3.12). The iron oxide minerals are haematite and goethite. Sulfidic chert has been intersected in drill holes.

Interpretation & discussion

The quartz grains are polygonal suggesting they have been recrystallised. The preservation of finer-grained laminae suggests a detrital origin, at least in part, rather than a chemical sediment. The laminated chert may be laminated siltstone and the iron oxide layers are probably weathered sulfides.

3.2.8.8 Felsic volcanic sandstone Interbeds

Felsic volcanic sandstone interbeds in turbidite successions occur in a number of areas including along the western shore of a small island in the north of the Polar Bear Peninsula at 6446500mN, 389380mE MGA, on the eastern side of a knoll, southeast of the Hinemoa Mine at 6463435mN, 389025mE MGA and at 6463880mN, 389435mE MGA.

Plate 3.11: Typical appearance of laminated chert at the surface.

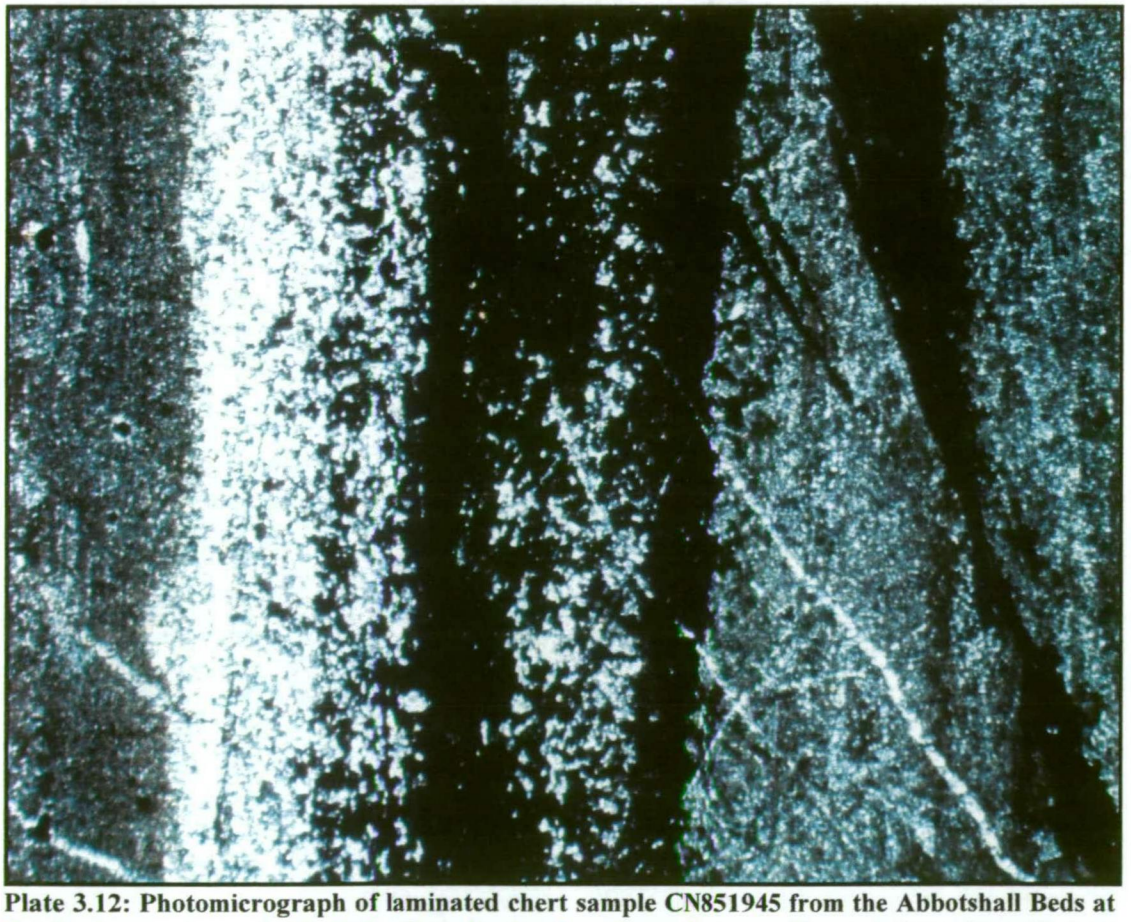

Plate 3.12: Photomicrograph of laminated chert sample CN851945 from the Abbotshall Beds at the Sontaran prospect, the Polar Bear Peninsula. Comprises very fine quartz grains with iron oxide laminae. Field of view 1 mm. Cross polarised light.

Description

Felsic volcanic sandstone typically occurs as non-graded but well sorted units, which range in thickness from a few centimetres to one metre, and are interbedded with sandstone-shale turbidite. The felsic units are generally ungraded but have scoured bases and laminations may be present in the top few centimetres. The sandstone is weathered, but euhedral feldspar shapes and quartz grains can be observed.

Interpretation & discussion

The euhedral shape of the feldspar precludes significant reworking in an abrasive environment. This suggests that the unit was likely deposited as a resedimented volcaniclastic following volcanic eruptions rather than erosion of an older felsic rock. This interpretation is consistent with the occurrence of the felsic units as episodic interbeds in a sand-shale turbidite-dominated succession.

The scouring common at the base of the felsic sandstone beds suggests they were resedimented as turbidites, so initial deposition of the pyroclasts into the water must have occurred in the source area for the fine-grained clastic sediments.

3.2.9 Rhyolite

A body of rhyolite lava is present in the Polar Bear Peninsula, overlying the Abbotshall Beds (figure 3.2; Appendix 4). The rhyolite body and associated breccias are the highest stratigraphic units preserved at the Polar Bear Peninsula. The majority of the lava is covered by alluvium in a north-south trending valley, but exposures occur along the margins and further south where the valley flattens out. Breccias are commonly associated with the rhyolite, but the rubbly nature of most outcrop, combined with strong weathering, a pervasive cleavage and muscovite/sericite alteration, typically renders identification of clast shapes and rock unit relationships difficult.

In certain localities, such as at the north-western edge of the area mapped at East Polar Bear (figure 3.2; map 1, Appendix 4), surficial silicification has strongly affected rhyolitic rubbly subcrop rendering it visually similar to chert. The rhyolitic origin can be discerned by close examination, which may show millimetre-scale euhedral pits where phenocrysts have weathered out and by the gradation between obvious rhyolite and siliceous rubble.

To map exposures of rhyolite with variable states of weathering, alteration and deformation, the rhyolite was, for convenience, divided into three major types, based on the appearances of the outcrops. Through detailed facies analysis of well-preserved exposures, more detailed categories of rhyolite with an implied genesis

were elucidated. The maps in Appendix 4 present a combination of major rhyolite types and detailed categories. Where the exposures are sufficiently preserved to determine the detailed categories of the rhyolite, those categories are presented on the maps, but where the exposures are poor, the maps present only the major rhyolite type. In some instances, the exposure of a detailed category is too small in area to be mapped at1:2500-scale, so the category of the rhyolite is indicated on the maps with annotation.

The major rhyolite units and detailed categories are:

- rhyolite, which includes subcategories of :
  - flow-banded rhyolite; and
  - quartz muscovite schist.
- rhyolite breccia, which may be subdivided into:
  - autobreccia;
  - *in situ* hyaloclastite;
  - resedimented rhyolite breccia; and
  - volcaniclastic sandstone.
- rhyolite-sediment breccia, which includes the categories of:
  - peperite;
  - xenolithic lava; and
  - resedimented rhyolite sediment breccia.

3.2.9.1 Rhyolite

"Rhyolite" is the label given to one of the three major rhyolite divisions, where the rock type is coherent rather than brecciated. The majority of exposures labelled as rhyolite comprise flow-banded rhyolite, although exposures of coherent rhyolite in which flow-banding is not apparent are also found, particularly where the rhyolite is silicified.

Rhyolite strongly affected by alteration and tectonic foliation, or weathering, such that the rhyolite is now quartz-muscovite schist or indurated saprolitic clays, is generally indicated to be quartz-muscovite schist. Typically the schist is intermixed with coherent rhyolite, such that the two together form a mappable unit.

Flow-banded rhyolite

Description

Flow banding within the rhyolite is prominent and distinctive, and forms parallel, centimetre-wide bands (Plate 3.13) or fine, swirling, sub-millimetre laminae, etched out by weathering. Flow-folds are common (Plate 3.14) and may become detached to form metre-scale clasts. Ductile flow-folding and blocky autobreccia commonly occur in the same outcrops (Plate 3.15).

Least altered rhyolite is black with small quartz and feldspar phenocrysts (Plate 3.16). Sparse euhedral plagioclase, 0.5-1 mm in length, comprises the most abundant phenocrysts and may be glomeroporphyritic. Euhedral quartz phenocrysts, typically square or triangular in section, are less abundant. The groundmass is extremely fine-grained and consists of cryptocrystalline material and fine-grained mosaics composed of quartz and feldspar, the latter typically comprising one third alkali feldspar according to XRD.

Within the groundmass, rounded shapes, approximately 0.3 mm in diameter, are visible in plane polarised light as clear areas that contrast with the surrounding grey-brown matrix. The clear shapes are patches of quartz-rich material, which consist of several irregular quartz grains rather than optically-continuous quartz. Many of the quartz grains are cloudy due to inclusions of extremely fine-grained crystals. The grey-brown matrix between the clear patches appears to be cryptocrystalline material in which minute crystals are visible. The best-defined quartz-rich patches were observed in the thin section for sample CN851924, where they comprise approximately 80% of the rock and in places coalesce to form dense mats (Plate 3.17). In other relatively fresh samples with a more prominent flow banding, the quartz-rich patches make up only 40 to 50% of the rock.

Relatively lighter and darker bands typically define flow banding (Plate 3.18). The colour of the bands represents the proportion of dark cryptocrystalline material versus paler quartz-rich patches and irregular coarse quartz and feldspar mosaics.

More altered rhyolite is generally pale green in hand specimen and is composed of sericite and quartz (Plate 3.19). Former euhedral plagioclase phenocrysts are transformed to irregular dense mats of sericite. Flow banding in these rocks is defined by variations in the proportion of sericite and quartz.

Plate 3.13: Typical appearance of flow-banded rhyolite. Pencil is 13.5 cm long.

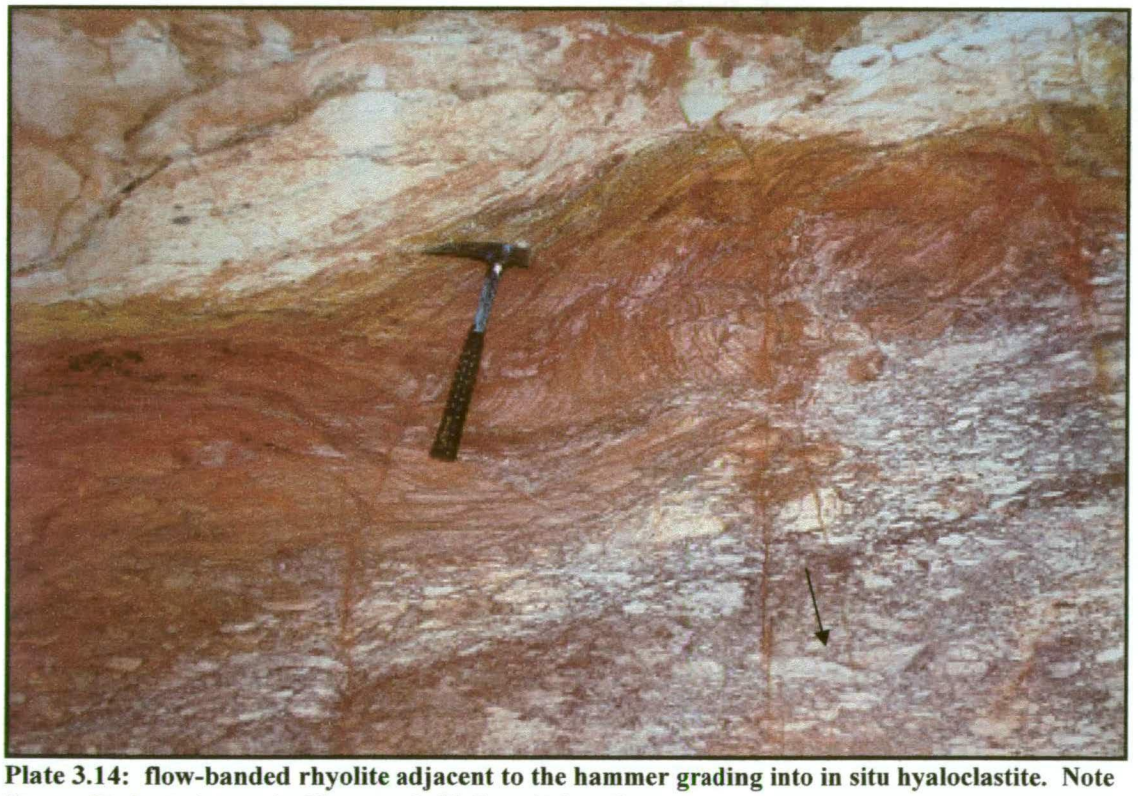

Plate 3.14: flow-banded rhyolite adjacent to the hammer grading into in situ hyaloclastite. Note jigsaw fit clasts (arrow). Hammer is 31.5 cm in length.

Spherulites visible in hand specimen are uncommon. Where found, they reach 6mm in diameter and are relatively sparse, comprising perhaps 5% of the rock volume. The only definitive spherulitic texture observed in thin section was bladed quartz and felspar forming a truncated fan spherulite 2 mm in width.

Isolated, tiny, millimetre-scale clasts are visible in thin sections of the flow-banded rhyolite where they comprise 1% or less of the rock. The most common clasts are rhyolitic and are defined by difference in the phenocryst textures. Locally, there are zones within the rhyolite with an unusually high abundance of fine-grained dark oxide material that appears to be black shale. In one thin section, a single angular clast of basalt was observed.

Discussion & interpretation

The rhyolite is mapped as a lens-shaped body, 3.3 km in length and reaching a maximum width of about 300 m (figure 3.2). Given the strong east-west shortening and concurrent north-south stretching that has affected the Polar Bear Peninsula (section 3.2.3), the original shape of the body would have been more equi-dimensional. The flow banding within the rhyolite, the dimensions of the body, and facies analysis of associated rhyolitic breccias suggest it formed as a submarine lava dome, erupted onto black shales. The folding has, in part, exposed a cross-section of the rhyolite, but the feeder to the dome is not observed at the current erosion level.

The quartz-rich patches most likely represent a micropoikilitic texture or pseudomorph spherulites. Both these textures are devitrification products of cooling glass and are common in rhyolite (McPhie & others, 1993). Micropoikilitic textures consist of optically continuous quartz enclosing smaller crystals of another mineral, whereas spherulites display radial crystal growth. Neither radial nor optically continuous textures are apparent, but this is considered to be due to recrystallisation caused by the metamorphism and deformation at the Polar Bear Peninsula. On balance, the slightly irregular to ragged rather than perfectly spherical shapes of the quartz-rich patches suggest that the micropoikilitic texture is a more likely origin, with the quartz strained and segmented by deformation.

The zones that are locally enriched with fine-grained dark oxide material, are interpreted to represent assimilation and disintegration of black shale fragments by the rhyolite. The black shale and the single basalt clast observed, were probably ripped from the vent wall prior to emplacement. The isolated rhyolite fragments have been formed in a similar manner to the autobreccia described below, and have been incorporated and dispersed from previously consolidated magma.

Plate 3.15: orange and dark grey flow-banded rhyolite with a mutual sharp contact (arrow). On the right side of the photo, the white rhyolite is autobrecciated. Hammer is 31.5 cm in length.

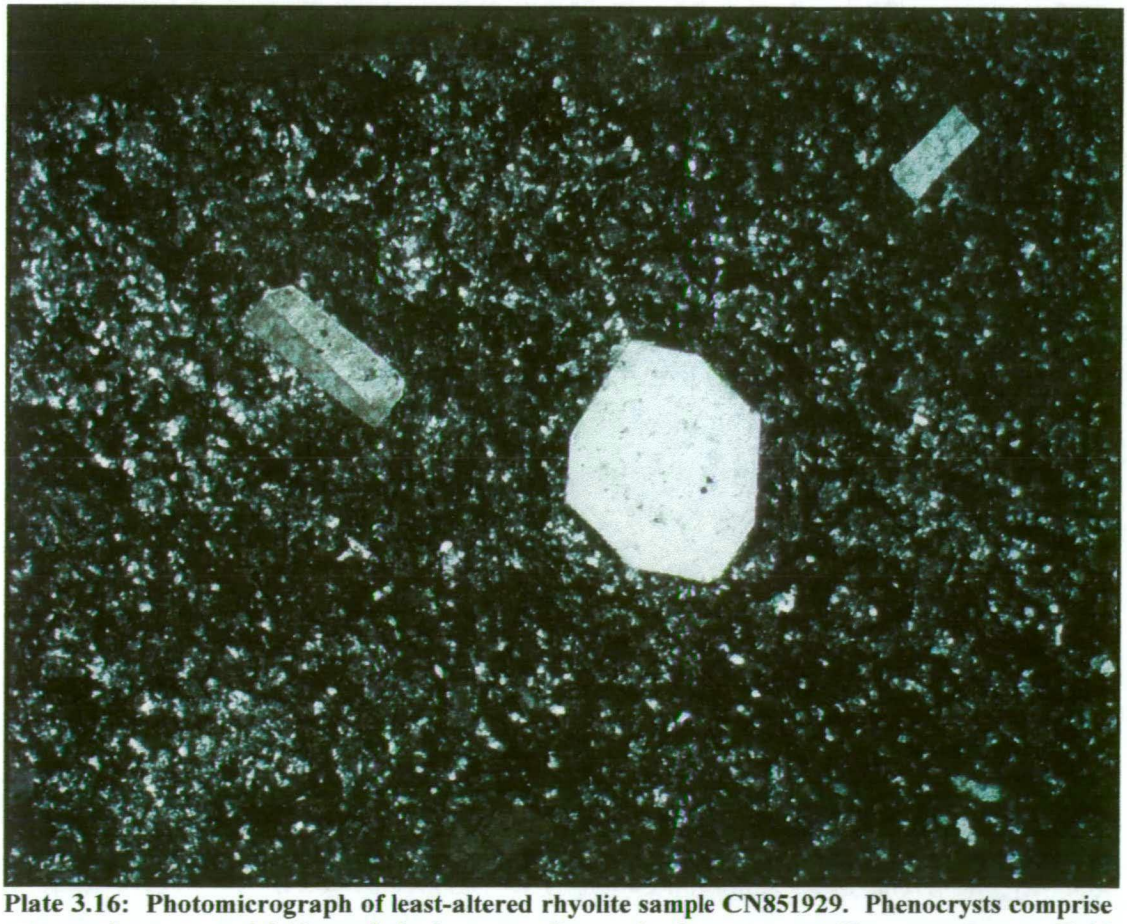

Plate 3.16: Photomicrograph of least-altered rhyolite sample CN851929. Phenocrysts comprise octagonal quartz and feldspar laths in a very fine-grained cryptocrystalline groundmass. Field of view 4 mm. Cross polarised light.

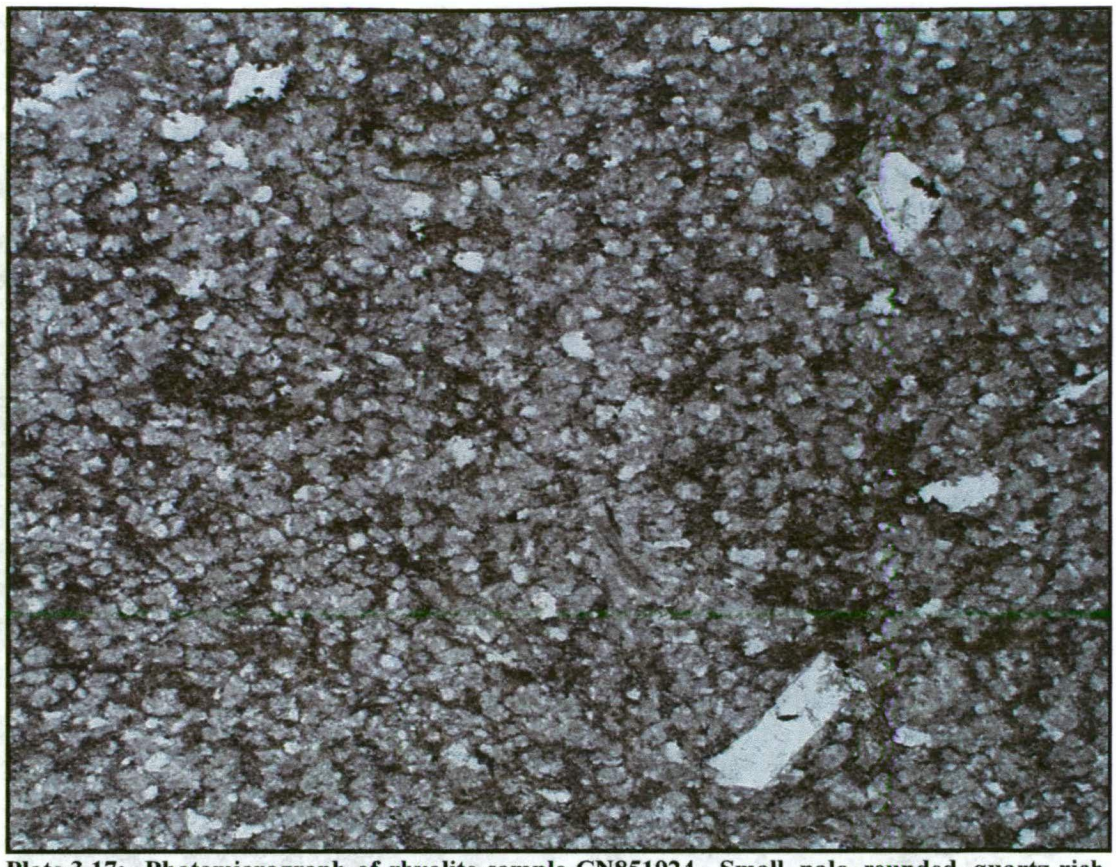

Plate 3.17: Photomicrograph of rhyolite sample CN851924. Small, pale, rounded, quartz-rich shapes in grey-brown cryptocrystalline groundmass. Pale shapes are interpreted as a micropoikilitic texture. Field of view 5mm. Plane polarised light.

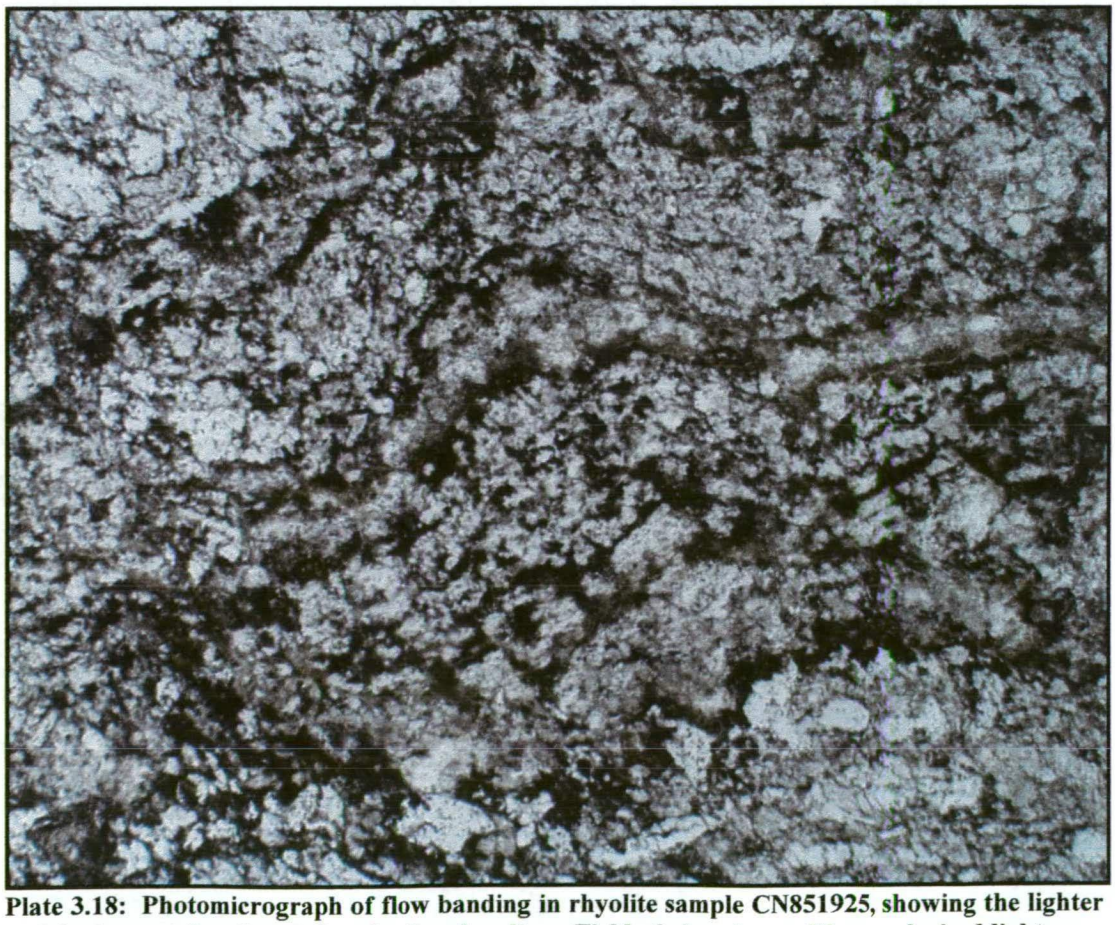

Plate 3.18: Photomicrograph of flow banding in rhyolite sample CN851925, showing the lighter and darker patches that define the flow banding. Field of view 4 mm. Plane polarised light.

Plate 3.19: Photomicrograph of intensely sericitised rhyolite. Sample CN851942. In the centre of the view, the homogenous shape is a sericitised feldspar phenocryst. Field of view 4 mm. Cross polarised light.

Plate 3.20: *In situ* rhyolitic hyaloclastite at northern Polar Bear. Closer view of the breccia shown in Plate 3.14. An example of jigsaw fit clasts is circled.

Quartz-muscovite schist

Quartz-muscovite schist is the name given to rhyolite that is strongly affected by alteration and tectonic foliation, or weathering, such that the rhyolite is now quartz-muscovite schist.

3.2.9.2 Rhyolite Breccia

Rhyolite breccia, one of the three major rhyolite divisions of this study, includes clastic rocks in which all the clasts are composed of rhyolite. Fragmentation processes that formed the clasts are interpreted to have been autobrecciation, quench fragmentation and gravitational collapse. The detailed rhyolite breccia categories related to these fragmentation processes are autobreccia; *in situ* hyaloclastite; resedimented rhyolite breccia; and volcaniclastic sandstone.

All rhyolite breccia occurrences, other than *in situ* hyaloclastite and autobreccia, are categorised as "resedimented rhyolite breccia". This category is volumetrically large and is interpreted to include clasts generated by quench fragmentation and gravitational collapse, which have been resedimented.

Exposures of *in situ* hyaloclastite, and autobreccia are commonly too small to be mapped, but are indicated on the maps in Appendix 4 with annotation.

Autobreccia

Description

Autobreccia is a subdivision of rhyolite breccia that occurs associated with flow-banded rhyolite. It is not restricted to the margins of the rhyolite body and may occur internally. The breccia is monomict, clast-supported and consists of angular rhyolite fragments, which range in size from millimetres to greater than a metre (Plate 3.15). Recognition of clasts is commonly assisted by the varying orientations of flow banding due to clast rotation.

Interpretation & discussion

The autobreccia is interpreted to have formed by movement of a flow or radial expansion in a dome, causing fragmentation of rhyolite that had partly consolidated due to cooling. Two methods for the formation of the autobreccia found internal to the dome can be envisaged. The rate of strain caused by shear stress driving the flow may exceed the rate at which a highly viscous magma can flow in a ductile manner, causing it to fragment, or flowing magma may surround and entrain marginal breccia during expansion of the lava.

In Situ Hyaloclastite

Description

In situ rhyolitic hyaloclastite has been recognised in a number of areas. The clasts possess curviplanar shapes with a "jigsaw puzzle-fit" texture and form units which are typically only a few metres thick (Plate 3.20)

Interpretation & Discussion

The curviplanar clast shapes are characteristic of quench fragmentation and the "jigsaw-fit" textures indicate that displacement of the clasts has been minor such that they remain where they formed (McPhie & others, 1993). From the presence of hyaloclastite, it can be inferred that the rhyolite was emplaced in a submarine setting as a lava dome rather than a cryptodome, as the latter would be characterised by peperite along all contacts.

Resedimented Rhyolite Breccia

Resedimented rhyolite breccia is closely related to the resedimented rhyolite-sediment breccia that is discussed below, and the two facies may have a similar origin. The fragmentation, transport and depositional mechanisms are discussed in Chapter 5.

Description

Resedimented rhyolite breccia is common and forms broad exposures of rubbly subcrop and outcrop. It is defined as breccia composed of rhyolite clasts, which are not autobreccia or *in situ* hyaloclastite. In part, designation as resedimented rhyolite breccia reflects a lack of evidence for the latter two facies. Positive evidence that the unit is resedimented rhyolite breccia is sporadic, thin beds of volcaniclastic sandstone that occur locally. These are typically 1-2 metres thick and discontinuous along strike. Typically, the rubbly nature of the outcrops combined with the strong cleavage obscures the origin of the breccia.

In better exposures, generally found along gullies where the bedrock has been stripped bare, resedimented rhyolite breccia comprises interbedded units of breccia, gravel and sandstone. The rhyolite clasts typically have a white or very pale grey colour caused by alteration to quartz and sericite. Many sandstone and breccia units have also been strongly flattened by D_2 deformation so that the original shape of the clasts is obscured. The following description is based on the best-preserved examples.

Breccia units are usually clast-supported but may have a finer-grained matrix. The typical clast size ranges from 1 to 20 cm, but clasts of rhyolite lava up to 1.5 m in length have been recognised locally. Subangular to angular clasts with curviplanar margins are common, as are clasts with highly irregular or even serrated margins. Clasts with subrounded to rounded margins are uncommon. Clasts of flow-banded rhyolite are less abundant than rhyolite clasts with a massive texture. Laminated volcaniclastic sandstones, 0.3 to 1 m thick are locally present within the breccia.

Interpretation & Discussion

Resedimented rhyolite breccia is interpreted to form through similar processes to resedimented rhyolite-sediment breccia, with which it is closely spatially associated. The genesis of these units is fully discussed in Chapter 5. The comments below are restricted to justifying the classification of the facies as "resedimented".

Many of the rhyolite clasts possess curviplanar margins and are hosted in a sandstone matrix. The curviplanar clast shapes are characteristic of quench fragmentation but the lack of "jigsaw-fit" textures and the sandstone matrix suggest they have been resedimented. The bedded nature of the units in better exposures is also a characteristic of resedimentation.

Volcaniclastic sandstone

Volcaniclastic sandstone is associated with areas of resedimented rhyolite breccia and resedimented rhyolite-sediment breccia. In Chapter 5, it is included as a component of the resedimented rhyolite breccia facies.

Description

Volcaniclastic sandstones are typically laminated, 0.3 to 1 m thick and generally show normal grading. Graded units passing from gravel to sandstone are also present. Fine-grained siltstone/shale units are typically less than 30 cm thick and may consist of multiple normally graded units.

3.2.9.3 Rhyolite-Sediment Breccia

Rhyolite-sediment breccia, the third major rhyolite division of this study, includes breccias with clasts composed of rhyolite and clasts composed of sedimentary rock. Fragmentation processes that formed the clasts are interpreted to have included quench fragmentation, gravitational collapse and rip up of unconsolidated sediment by currents. The detailed rhyolite-sediment breccia categories related to these fragmentation processes are peperite; xenolithic lava; and resedimented rhyolite-sediment breccia.

Plate 3.21: Rhyolitic peperite with black shale at Northern Polar Bear. Lobe of flow-banded coherent peperite shows spalled fragments (arrow). Excellent jigsaw fit clasts with curviplanar quench fragmented margins are circled. Width of view is 30 cm. Width of circled area is 7 cm.

Plate 3.22: Photomicrograph of rhyolitic peperite, sample CN851956. Pale shapes with curviplanar margins are sericite-altered rhyolite. Dark matrix is black shale. Note that white patches in top left quadrant are holes in the thin section. Field of view 5 mm. Plane polarised light.

All rhyolite-sediment breccia occurrences, other than peperite and xenolithic lava, are categorised as "resedimented rhyolite-sediment breccia". This category is volumetrically large and is interpreted to include clasts generated by quench fragmentation and gravitational collapse, which have been resedimented.

Exposures of peperite and xenolithic lava are commonly too small to be mapped at 1:2500-scale, but are indicated on the maps in Appendix 4 with annotation.

Peperite

Peperite is recognised in a number locations, the best exposed being in a gully bounding the alluvial channel at the northern end of the mapped area at 6465355mN, 388685mE MGA, and at 6462355mN, 388640mE MGA where it forms the eastern lower boundary to rhyolite lava. The western boundary of the rhyolite lava in this area is not well-exposed, but has breccias and a complex interfingering relationship with sediment that is also suggestive of peperite.

Description

Peperitic breccia is found at the contact between black shale and flow-banded rhyolite. The rhyolite clasts are typically white in colour due to intense sericitisation and contrast with the dark grey of the shale matrix. Rhyolite clasts range in size from millimetre scale to approximately one metre in diameter and the larger clasts are surrounded by jigsaw breccias showing progressive fragmentation (Plate 3.21). The rhyolite clasts are typically angular with curviplanar margins although some show more irregular margins (Plate 3.22).

The width of the zones of peperite varies, but in the best exposed areas is approximately 10 m. The contacts between the peperitic breccia and the rhyolite lava vary, but overall are generally gradational, with the rhyolite becoming increasingly sediment-rich towards the enclosing shale. Towards the rhyolite body, the quantity of intercalated sediment diminishes and the peperite becomes discontinuous, separated by increasing large lobes of coherent rhyolite lava.

Interpretation & discussion

Peperite is a rock generated by mixing coherent magma with unconsolidated wet sediment and is characterised by a clastic texture. The clastic texture may be generated by quench fragmentation ("peperitic hyaloclastite"), shattering by steam explosions, foundering or burrowing of parts of the magma into the sediment, or by fluidised vapour removing fine sediment, creating space that is filled by the magma ("globular peperite") (McPhie & others, 1993 and references therein). "Blocky peperite", the variety exhibited along the rhyolite contacts at the Polar Bear

Peninsula, has sharply angular, blocky clasts with common jigsaw puzzle-fit textures in contrast to the bulbous clasts of "globular peperite". The curviplanar margins of the rhyolite clasts at the Polar Bear Peninsula are characteristic of quench fragmentation processes, indicating the breccia is a variety of blocky peperite sometimes referred to as "peperitic hyaloclastite" (McPhie & others, 1993).

At 6465355mN, 388685mE MGA, in a gully at the northern end of the mapped area (described in section A1.2.7, Appendix 1), there are large lobes of coherent rhyolite with jigsaw-fit brecciated margins within the peperite exposures (Plate 3.21). These lobes have probably foundered or burrowed into the unconsolidated mud, so both foundering and quench fragmentation were involved in the generation of this peperite.

The presence of peperite along the contact between the rhyolite and the black shale indicates that the shale predated the rhyolite, and was unconsolidated and wet at the time the rhyolite was emplaced. Peperite contacts form along any rhyolite-sediment contacts and do not indicate whether the surface is the top, bottom or side of the magma body. However, at the northern end of the mapped area at the Polar Bear Peninsula, the presence of hyaloclastite indicates that at least the top of the rhyolite was exposed to the water, so the peperite, and the overall mapped shape of the rhyolite, indicates that the peperite is the base of the rhyolite which faces west at that locality.

Xenolithic Lava

Description

At a number of locations, flow-banded rhyolite lava has small fragments of sedimentary rock incorporated with it, forming about 1% of the volume. The best example is in the gully at north Polar Bear (6465355mN, 388685mE MGA), in which peperite is also exposed. At this location, which is approximately 25 m west of the peperitic base of the rhyolite, small fragments of sedimentary rock are evenly dispersed through flow-banded and flow folded rhyolite.

Interpretation & discussion

A number of methods by which these small fragments of sedimentary rock could have been incorporated can be envisaged. They may be xenoliths which were ripped from the margins of the lava conduit; burrowing magma may have remobilised and fragmented earlier formed peperite; or rhyolite may have intruded as a sill beneath a layer of unconsolidated sediment, which was lifted and subsequently incorporated into the rhyolite, breaking up due to shear stress within the flow.

Resedimented Rhyolite-Sediment Breccia

Resedimented rhyolite-sediment breccia is similar to and associated with resedimented rhyolite breccia. The origins of these two facies are interpreted to be similar but the presence of sediment clasts in resedimented rhyolite-sediment breccia adds the caveat that the proposed genesis must allow for their incorporation (Plate 3.23).

Description

Resedimented rhyolite-sediment breccia is widespread and forms broad exposures of rubbly subcrop and outcrop. It is defined as a breccia composed of rhyolite lava and abundant sediment clasts. Blocks of laminated chert up to 40 cm across are characteristic (Plate 3.23) and continuous bands of fine-grained sedimentary rock are present locally, generally sulfidic slate with holes after pyrite nodules, or bands of dark siltstone or chert, less than 0.5 m in thickness. Typically, the rubbly nature of the outcrops, combined with a strong spaced cleavage that disaggregates clasts, masks the original shape of the clasts and obscures the origin of the breccia. In places, tabular cherty clasts appear to be aligned over a few metres, suggesting remnants of bedding, but more often there is no internal organisation to the unit. Small zones of rhyolitic sandstone are present locally and are diagnostic of rhyolite-sediment breccia or its sediment-free relative, rhyolite breccia. The sandstone is typically laminated, less than a metre in thickness and cannot be traced for more than a few metres along strike.

Rhyolite-sediment breccia is clast-supported and rhyolite blocks observed in faces perpendicular to the flattening direction are typically angular with curviplanar margins, although subrounded clasts are also present. Chert blocks within the breccia are typically tabular. Some breccia contacts have scoured the tops of fine-grained sediment bands or sandstone that can be used to indicate facing.

Interpretation & discussion

The resedimented rhyolite-sediment breccia is marginal to a rhyolite dome. Where the rhyolite lava pinches out of the stratigraphy, resedimented rhyolite breccia or rhyolite-sediment breccia occupies the rhyolite's former stratigraphic position. The presence of these breccias away from the rhyolite margin indicates that the rhyolite body was not a cryptodome, as clasts of rhyolite were able to be transported laterally away from the dome.

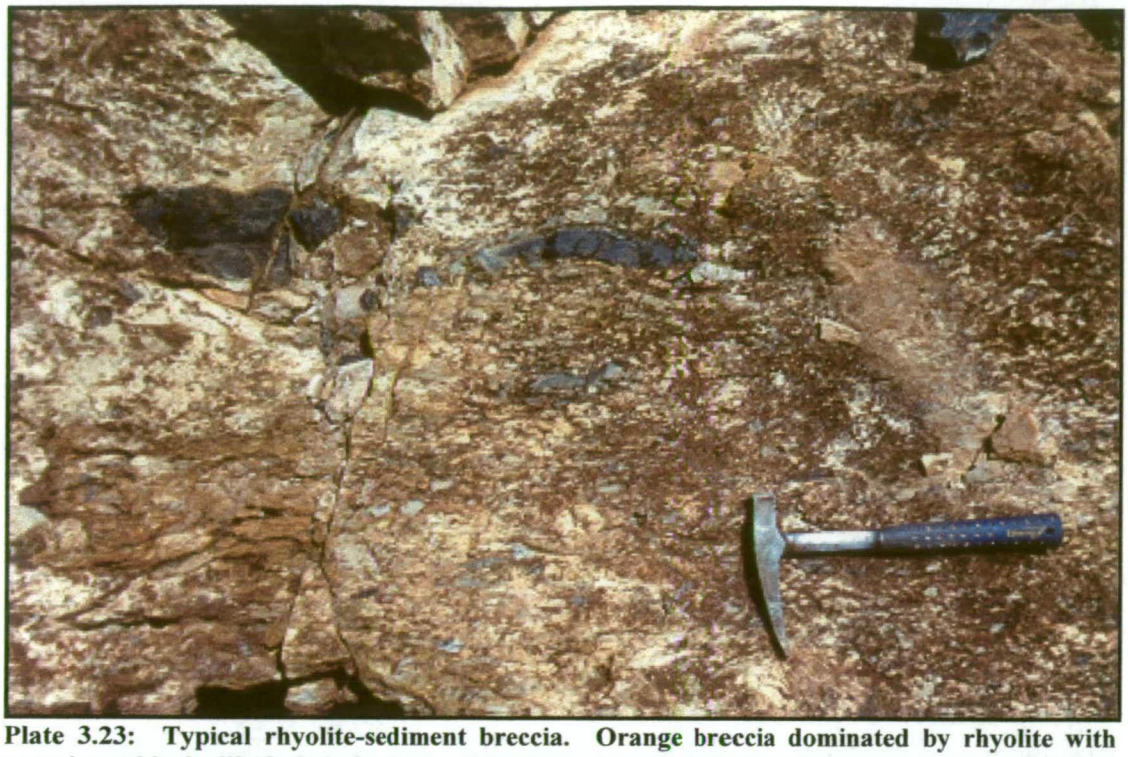

Plate 3.23: Typical rhyolite-sediment breccia. Orange breccia dominated by rhyolite with prominent black silicified shale clasts. Smaller sediment clasts are also present but are difficult to distinguish in this view. Hammer is 31.5 cm long.

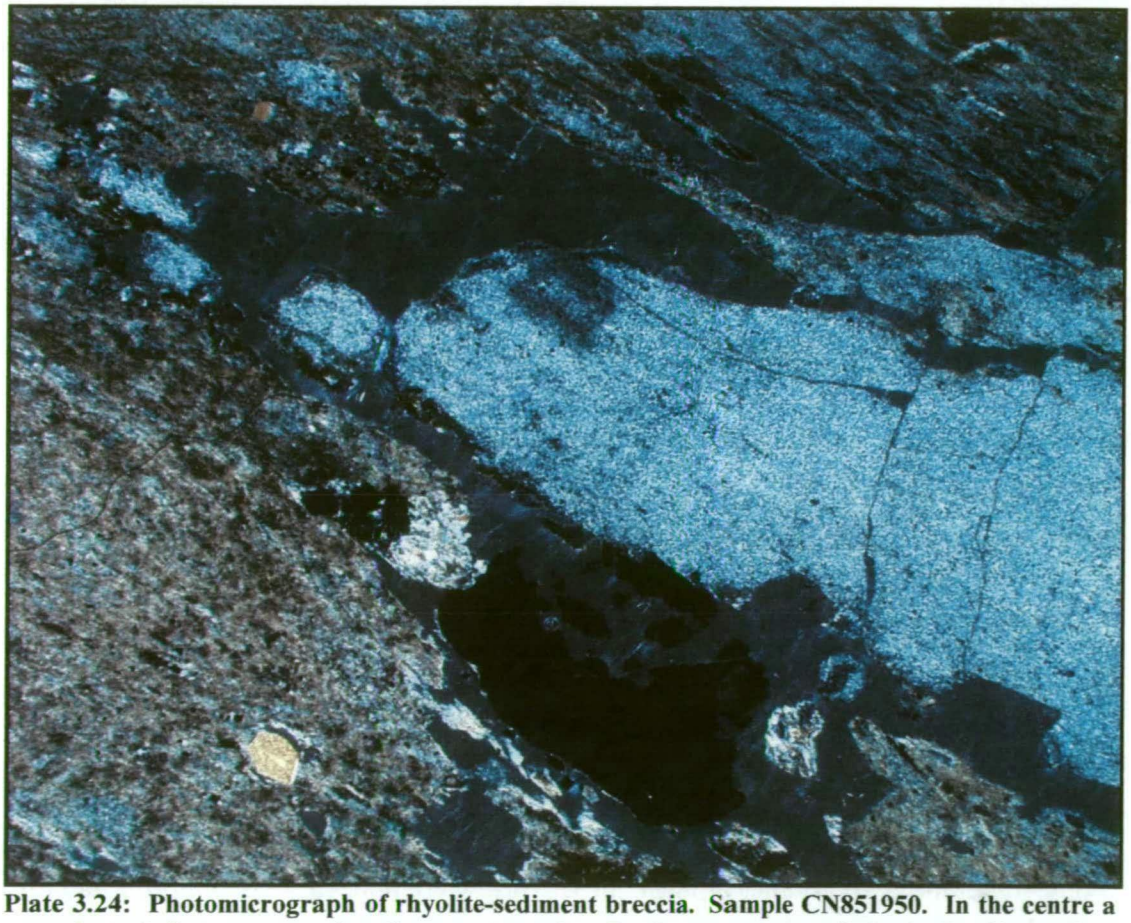

Plate 3.24: Photomicrograph of rhyolite-sediment breccia. Sample CN851950. In the centre a grey clast of siltstone comprises fine quartz grains. Dark grey areas are holes in the thin section. Black shapes are opaques, possibly pyrite. Grey-brown areas are intensely sericite-altered rhyolite. The yellow grain is a quartz phenocryst. Field of view 8 mm. Cross polarised light.

The stratigraphic change from rhyolite lava to rhyolitic breccia, where the lava pinches out, involves a dramatic change in the thickness of the unit occupying that stratigraphic position. At the centre of the rhyolite dome, it is 300 m wide, whereas south of the rhyolite dome, 10 m of rhyolitic breccia occupies the stratigraphic position. Thus, the stratigraphy is not a simple "layer cake" sequence with units of constant thickness. Instead, the stratigraphy has the complexity expected for a proximal volcanic sequence, with irregular changes in the thickness of strata and units pinching out.

A full discussion of the origin of the resedimented rhyolite-sediment breccia follows a detailed facies analysis of the unit in Chapter 5.

3.2.10 Felsic Intrusive Rocks

3.2.10.1 Quartz Porphyry

Quartz Porphyry forms prominent exposures east of the Hinemoa Mine where it appears to be concordant with stratigraphy, overlying the sediment in the position normally occupied by rhyolite. The porphyry also forms major exposures at the south end of the Polar Bear Peninsula where it is discordant with stratigraphy and appears to have replaced some stratigraphic units, suggesting an intrusive origin.

Description

Quartz porphyry is readily identified by prominent quartz phenocrysts up to 3 mm in diameter. The rock is evenly porphyritic, generally pale in colour and commonly displays polygonal jointing. Feldspar phenocrysts are occasionally visible, but more commonly cannot be discerned through the cleavage and sericite alteration that are prevalent within the unit. Laminations, a few centimetres thick, are widespread but typically difficult to detect due to being sub-parallel to the strong, upright, north-south cleavage (Plate 3.25). Although quartz porphyry contacts are rarely exposed, where they are seen, they are sharp and not brecciated (Plate 3.26).

The rock is almost invariably heavily sericitised, in many cases destroying all former feldspars so that it is composed entirely of quartz and sericite (Plate 3.27). In the least altered example, quartz phenocrysts range from 0.5 to 2 mm in diameter with less abundant, heavily sericitised, former plagioclase phenocrysts up to 4 mm in size. The groundmass comprises relict laths and tabular feldspars 0.1-0.2 mm in size with similar sized quartz. XRD indicates that the remnant plagioclase is sodic.

Plate 3.25: Quartz Porphyry. The prominent inclined jointing toward the top left corner is planar flow banding. The S_2 cleavage dips at a steeper angle (arrow). 31.5 cm long hammer is circled in yellow.

Plate 3.26: Quartz porphyry-sediment contact. The hammer lies on the quartz porphyry with a spotted appearance due to quartz phenocrysts. The pencil lies along the knife sharp contact with shale. There is no peperitic breccia at the contact.

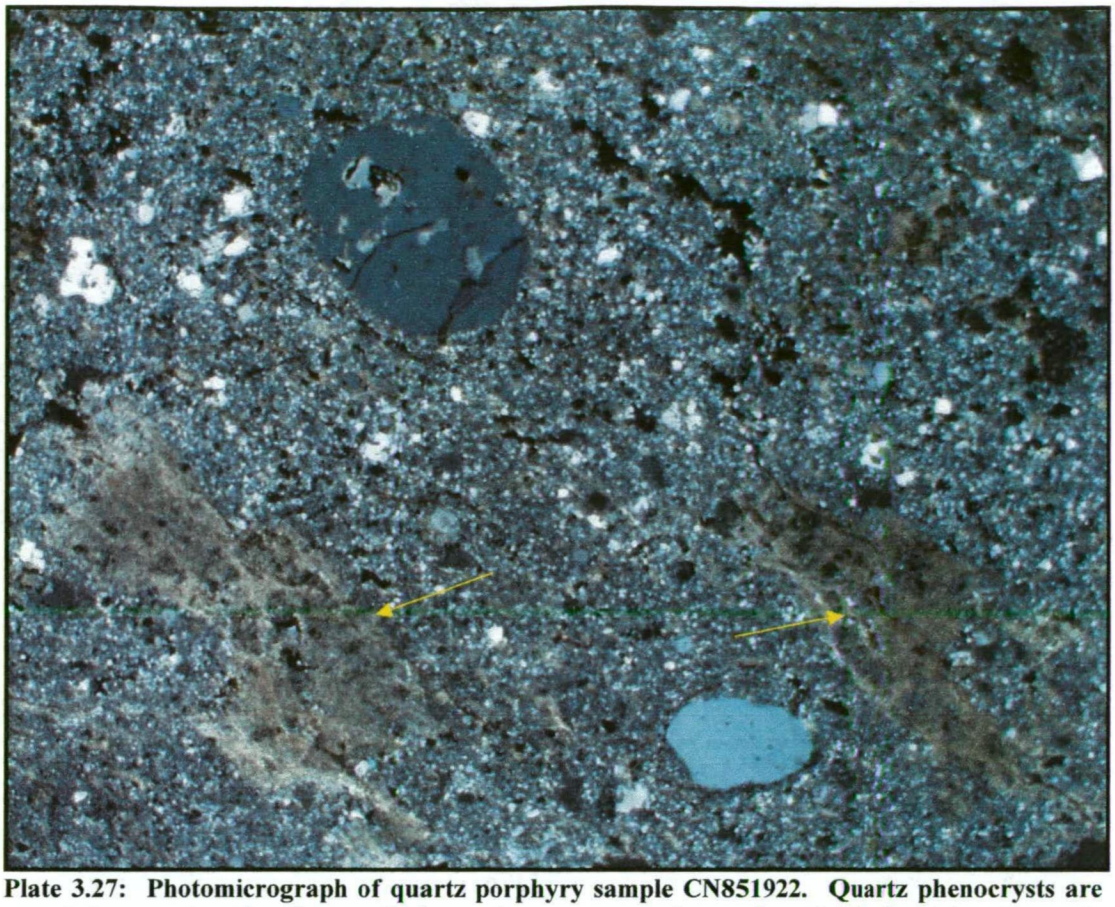

Plate 3.27: Photomicrograph of quartz porphyry sample CN851922. Quartz phenocrysts are rounded grey minerals. Former feldspar phenocrysts are intensely sericitised patches (arrows). Matrix is dominantly quartz and sericite. Field of view 8 mm. Cross polarised light.

Interpretation & discussion

The evenly porphyritic nature of the unit, with prominent quartz phenocrysts up to 3 mm in diameter, and the polygonal jointing constrain the porphyry to a magmatic origin. It is, therefore, considered that the laminations represent planar, continuous, flow banding.

The abundant porphyry intrusive at the south end of the Polar Bear Peninsula is commonly interfingered with both continuous and discontinuous chert bands and fragments of mafic and rhyolitic rocks. This interfingering suggests that the porphyry intruded as numerous dykes fingering their way through the stratigraphy and regularly spreading out to form small sills at numerous levels in the strata. Following east-west folding, which has made the units dip steeply, these sills are exposed with rafts of stratigraphy suspended between them.

Where sediment-porphyry contacts are observed, the absence of peperite suggests that sediment intruded by quartz porphyry was at least partly consolidated (Plate 3.26). When first deposited, muds contain up to 60% water by volume (Conybeare, 1980). In general, at a depth of 1 km, compaction has reduced the porosity of silty clay sediments to 20-25%, with most of this reduction in pore

volume having taken place during burial in the upper 500 metres. At depths greater than 1 km, it becomes progressively more difficult to squeeze water from the sediments (Conybeare, 1980). Thus, the absence of peperite suggests the sediment was buried at a depth of at least several hundred metres when the quartz porphyry intruded it. In part, the rhyolite dome would have buried the sediment, and where the dome pinched out, the sediment would have been buried by resedimented rhyolitic breccia. However, these units, particularly the resedimented breccia, do not appear to have the requisite thickness to explain the compaction. Greater thicknesses of rhyolitic breccia, or other units that have now been removed by erosion, must have been deposited prior to emplacement of the quartz porphyry. This requirement for thick sequences above the sediment, suggests a distinct age difference between the rhyolite and quartz porphyry.

The sodic composition of the remnant feldspars in the least altered quartz porphyry, suggest the rock could be trondhjemitic in composition. This is supported by the lack, in any of the four quartz porphyry samples examined petrographically, of calcic secondary minerals which might have formed had calcium been expelled from plagioclase. However, due to the strong sericitic alteration, any conclusions based on mobile elements remain inconclusive. XRD indicates the sericite is muscovite so the rock must become increasingly rich in potassium as sericitisation intensifies, indicating strong mobility of alkalies.

3.2.10.2 Feldspar Porphyry

Description

Feldspar porphyry has tabular feldspar phenocrysts 2-3 millimetres in length and slightly smaller quartz phenocrysts set in a black, siliceous groundmass. Feldspar is more prone to weathering than the remainder of the rock and the unit is often recognised in outcrop by the tabular to lath shaped cavities that remain after feldspar is weathered out.

One thin section was examined, from a sample of a thin dyke exposed in a gully south and west of the Hinemoa Mine that appeared very fresh in hand specimen. However, in thin section, twinning within the feldspar phenocrysts is obliterated by a dark amorphous alteration, possibly clay minerals. Minor patches of sericite are preserved within the amorphous mass. Quartz is present as 0.1 mm grains in the groundmass.

Feldspar porphyry differs from quartz porphyry in that tabular feldspar phenocrysts, a few millimetres in size are prominent, and quartz phenocrysts are typically smaller and less abundant or absent. At the southern end of the Polar Bear Peninsula,

feldspar porphyry grades into quartz porphyry with the disappearance of feldspar phenocrysts and the increase in size and abundance of quartz phenocrysts.

Discussion & interpretation

Feldspar Porphyry was mapped as a single unit but in retrospect, and with the assistance of geochemistry, it appears to comprise at least two distinctly different compositions. One type occurs as enclaves within quartz porphyry and has gradational contacts as described above at Dot-Eve. It appears to be a variant of the quartz porphyry in which feldspar becomes more prominent. The second type of feldspar porphyry occurs as thin dykes a couple of metres wide and this is the variety which was sampled for thin section and geochemistry. The dykes are volumetrically minor rocks, exposed in a few localities.

3.2.10.3 Granitoid

Description

A band of granitoid, subparallel to bedding and thus with a sill-like morphology, runs up the eastern shore of the Polar Bear Peninsula, north of the Hinemoa Mine (figure 3.2; map 1, 2 Appendix 4). It appears coarse-grained in hand specimen with quartz grains up to 6 mm in diameter. The granitoid is typically less than 10 metres in width, but extends for several kilometres, continuing beyond the northern boundary of the mapped area and outcrops have been noted around the Polar Bear "arms" to the north. The granitoid has a similar steep N-S cleavage to the other Archaean units and thus predates D_2.

One thin section of granitoid was studied and found to be seriate textured, with crystal sizes ranging from equant quartz, 6 mm in diameter to fine polygonal quartz in the groundmass, 0.03 mm in diameter. Abundant plagioclase forms euhedral phenocrysts 0.5 to 3 mm in length, but is also found as rare 0.2 mm grains in the groundmass. XRD indicates that the plagioclase is sodic. Biotite is a minor constituent scattered in irregular tufts. Alteration is confined to coarse-grained sericite flecking feldspar phenocrysts and within the groundmass.

Interpretation & discussion

The absence of calcium-bearing alteration minerals suggests that the sodic composition of the plagioclase is the primary igneous composition, thus, the granitoid has trondhjemitic affinities.

3.3 MICROWAVE TOWER

The microwave tower is situated 7 km northwest of Norseman, on the crest of a hill at location 6442955mN, 379985mE MGA (figure 3.1). The upper units of the Norseman Terrane are exposed in the surrounding area. The work for this study consisted of a reconnaissance to check the quality of the exposures. The units of interest in this study, chiefly the felsic rocks and their contacts with mafic rocks are poorly exposed, consisting largely of subcrop. No mapping was carried out in the area as the poor quality of the outcrop precluded any significant advance over the geology shown on the GSWA Norseman 1:100,000 geological sheet (McGoldrick. 1993).

The microwave tower area lies on the western limb of the regional scale Norseman anticline, so the stratigraphy faces west. Around the microwave tower, the Norseman 1:100,000 sheet shows two NNE-striking, parallel bands of sedimentary rock, 500 m apart, both underlain by basalt (figure 3.1). The eastern sedimentary band is overlain by felsic rock at the southern end close to the Coolgardie-Esperance highway.

Examination of the sedimentary rock indicates that it consist primarily of laminated chert, but also includes gossanous material exposed in shallow diggings interpreted as sulfidic shale. The felsic rocks are exposed only as sporadic subcrop with a blocky fracture pattern and quartz and feldspar phenocrysts. Minor monomict breccia is preserved although the rock is dominantly coherent. The felsic porphyry is either lava or intrusive, but no contacts or textures are preserved that might indicate one of these two options.

Due to the sporadic subcrop, the contact between felsic rocks and mafic rocks immediately west is not exposed. However, stretched felsic porphyry is found in the vicinity, which suggests the contact may be faulted.

Interpretation & discussion

The easternmost sedimentary band overlain by felsic rock is interpreted to be the Abbotshall Beds. The repetition of the mafic and sediment units is probably caused by a D_2 thrust fault (see Chapter 10). The stretched felsic porphyry found approaching the zone of basalt is consistent with this interpretation.

3.4 HARLEQUIN GRANODIORITE

A body of microgranitoid lies beneath Lake Cowan adjacent to the Harlequin Mine off the western shore of the Royal Peninsula, 9 km north of Norseman (figure 3.1, figure 9.15). Due to its location, it is known locally as the Harlequin granodiorite. The granodiorite intrudes the Desirable Pillow Lava member of the Lower

Woolyeenyer Formation close to the Harlequin mining operations. The Harlequin granodiorite is included in this study for comparison to the felsic rocks at the Polar Bear Peninsula. Other felsic intrusives known from the mining areas around Norseman were studied by Perring, (1989), but the Harlequin granodiorite was not known at the time of Perring's work, having first been intersected during exploration drilling in 1993.

The Harlequin granodiorite is of economic importance due to the gold mineralisation hosted within it and in adjacent greenstones (see Chapter 11). Although there is no outcrop of the Harlequin granodiorite, the geometry of the body is reasonably well understood due to the intensive drilling that has been undertaken around its central segment.

Description

The Harlequin granodiorite forms an elongate, tabular body, which has been traced by aircore drilling for approximately 3 km (figure 3.3). It has a NNE strike and dips about 80° west, steeper than the presumed moderate westerly dip of the surrounding greenstone, suggesting it is a dyke. The granodiorite reaches a maximum thickness of about 250 m, but pinches out to the north and thins to the south as far as it has been traced. The deepest drilling undertaken in the area has intersected the body at about 500 m below surface where no change in the characteristics has been noted. Easterly dipping shear zones offset the granodiorite at depth, most notably, the apparent reverse movement of up to 100 metres across the HV6 shear (figure 3.4).

The characteristics of the western margin of the granodiorite are poorly known as drilling is typically oriented subparallel to the contact and often intersects it in shear zones. Where it is unsheared, the western contact has alternating zones of thin felsic porphyry and granodiorite, with the porphyry possibly representing chilled zones. The eastern contact is better known and is marked by a tabular, felsic porphyry up to 50 m wide subparallel to the granodiorite. The width of the porphyry, its slight discordance to the granodiorite and mineralogical characteristics suggest the porphyry is a separate intrusion. This has been confirmed with trace element geochemistry, which indicates there is no petrogenetic relationship between the granodiorite and porphyry (see Chapter 8). The porphyry may postdate the granodiorite although the timing relationships are unclear. The porphyry has a greater strike extent than the granodiorite and continues north and south beyond the pinch-outs of the granodiorite to the extent of drill testing.

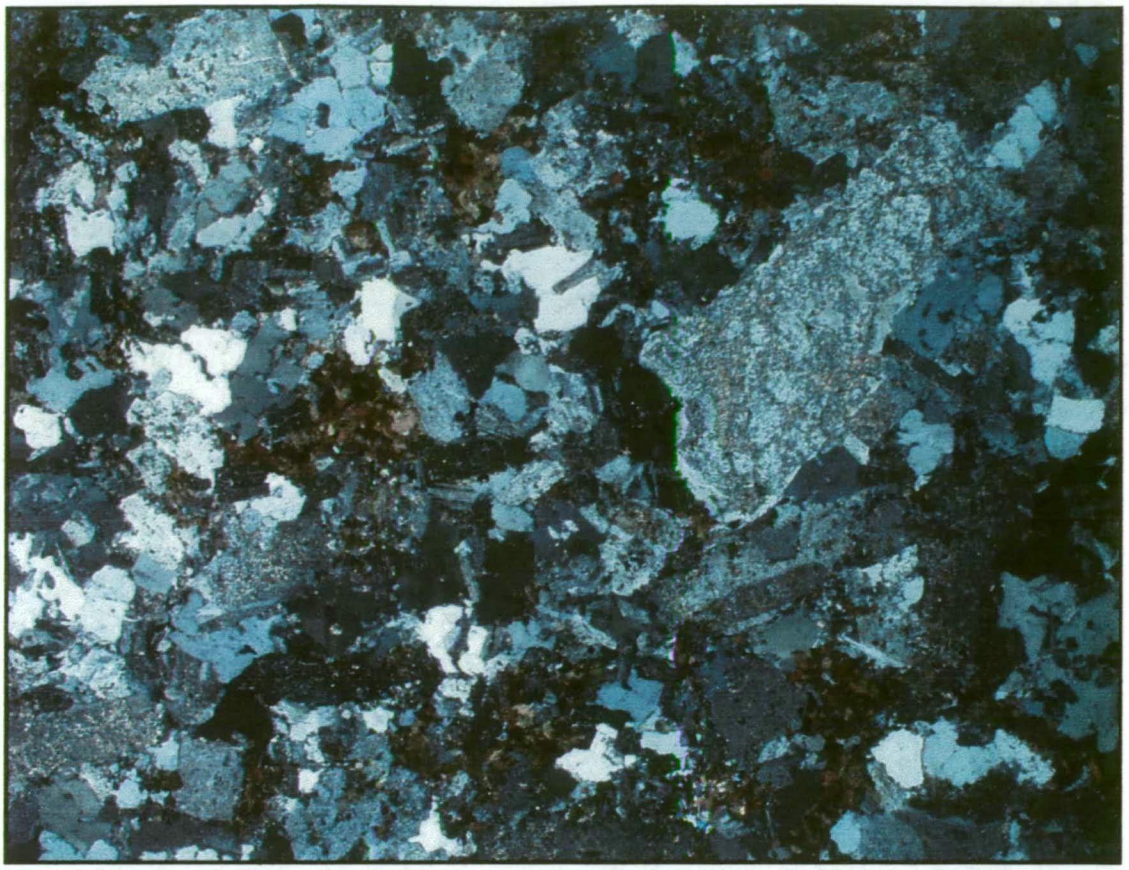

Plate 3.28: Photomicrograph of Harlequin granodiorite sample CN851940. Equigranular to seriate textured. sericite–dusted feldspar and quartz, both with irregular margins. Biotite in the interstices between feldspar and quartz. Field of view 6.4 mm. Cross polarised light.

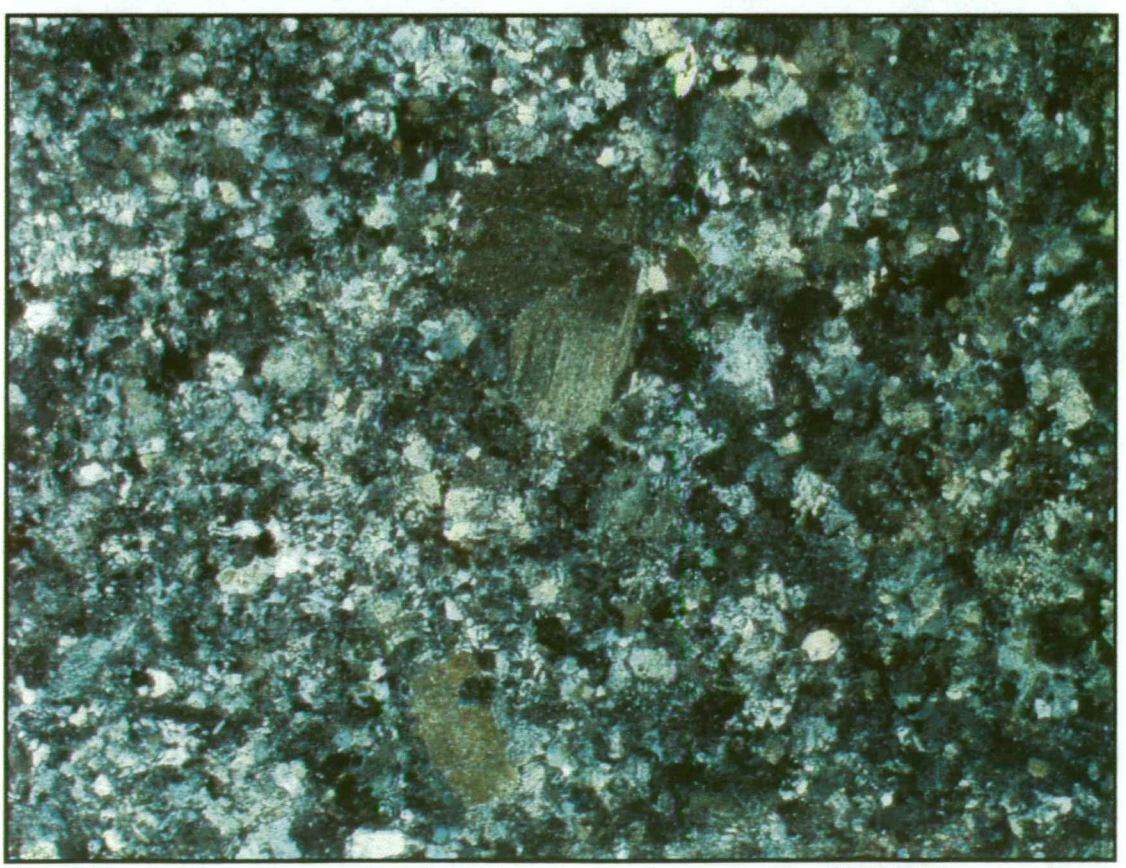

Plate 3.29: Photomicrograph of Harlequin porphyry sample CN851946. Sercitised. Glomeroporphyritic plagioclase phenocrysts in a plagioclase-alkali feldspar-quartz matrix. Field of view 4.0 mm. Cross polarised light.

The granodiorite is holocrystalline, consisting of equigranular grains of quartz and feldspar approximately 2 mm in diameter, and aggregates of biotite which constitutes about 5% of the rock (Plate 3.28). These characteristics are fairly uniform throughout the body. The proportion of granular felsic xenoliths tends to be the most variable characteristic of the granodiorite. Close to the eastern margin, there is a change in the character of the granodiorite as the biotite content diminishes to 1-2%, present as fine spots, and there is a gradational transition until the rock becomes porphyritic, still carrying a small proportion of biotite. The contact between porphyritic granodiorite and the separate felsic porphyry body is difficult to pinpoint.

Complete cross sections of the granodiorite margin as described above are uncommon. More commonly, there are sharp contacts between equigranular granodiorite and felsic porphyry, suggesting the felsic porphyry has stoped out the marginal zones of the granodiorite.

Within the granodiorite, quartz and feldspar are present in sub-equal quantities and both range in size from 0.5 to 2 mm in diameter. Feldspar is typically euhedral to subhedral with the interstices filled with quartz, which may become poikilitic. Twinning in the feldspars is generally poorly defined but may consist of Carlsbad, albite or Pericline varieties. XRD identified only sodic plagioclase and this is thought to be a primary characteristic because alteration is generally minor, largely comprising sericite flecking of the feldspars. Biotite typically has minor alteration to chlorite or sericite.

The porphyritic granodiorite has glomeroporphyritic plagioclase up to 2 mm across and lesser quartz phenocrysts 1 mm in diameter. The groundmass comprises tabular and anhedral grains of plagioclase and quartz typically 0.2 mm in size, with granophyric textures common in the feldspar. Like the granodiorite, alteration is largely restricted to sericitisation and the feldspar is sodic in composition.

The body of felsic porphyry has similar mineral textures to the porphyritic granodiorite, having glomeroporphyritic plagioclase, quartz phenocrysts and granophyric textures in the groundmass (Plate 3.29). However, mineralogically the felsic porphyry differs from the granodiorite in that plagioclase is more calcic and alkali feldspar is also present. The compositions of the groundmass feldspar could not be resolved in thin section, but XRD indicated just over two-thirds plagioclase and one-third alkali feldspar.

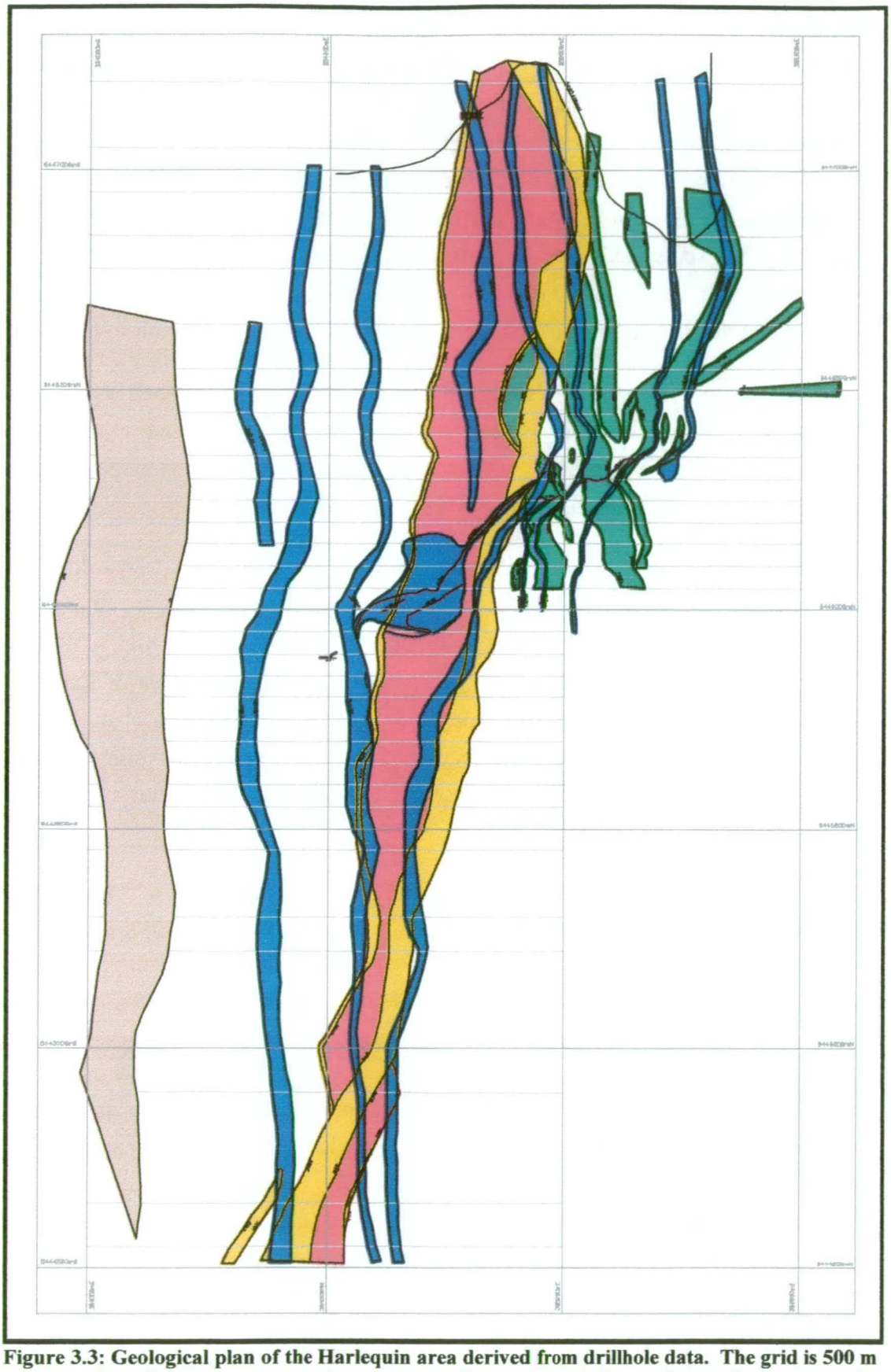

Figure 3.3: Geological plan of the Harlequin area derived from drillhole data. The grid is 500 m square. E-W lines are cross section traces used to interpret the geology. Red area is the Harlequin Granodiorite; orange the Harlequin rhyolite porphyry; green areas are dolerite dykes interpreted in closely spaced drilling in the vicinity of the Harlequin Mine on the HV1 reef; Blue zones are shear zones forming a shear network; pink lines are reefs within shears; Brown is the Norseman komatiite.

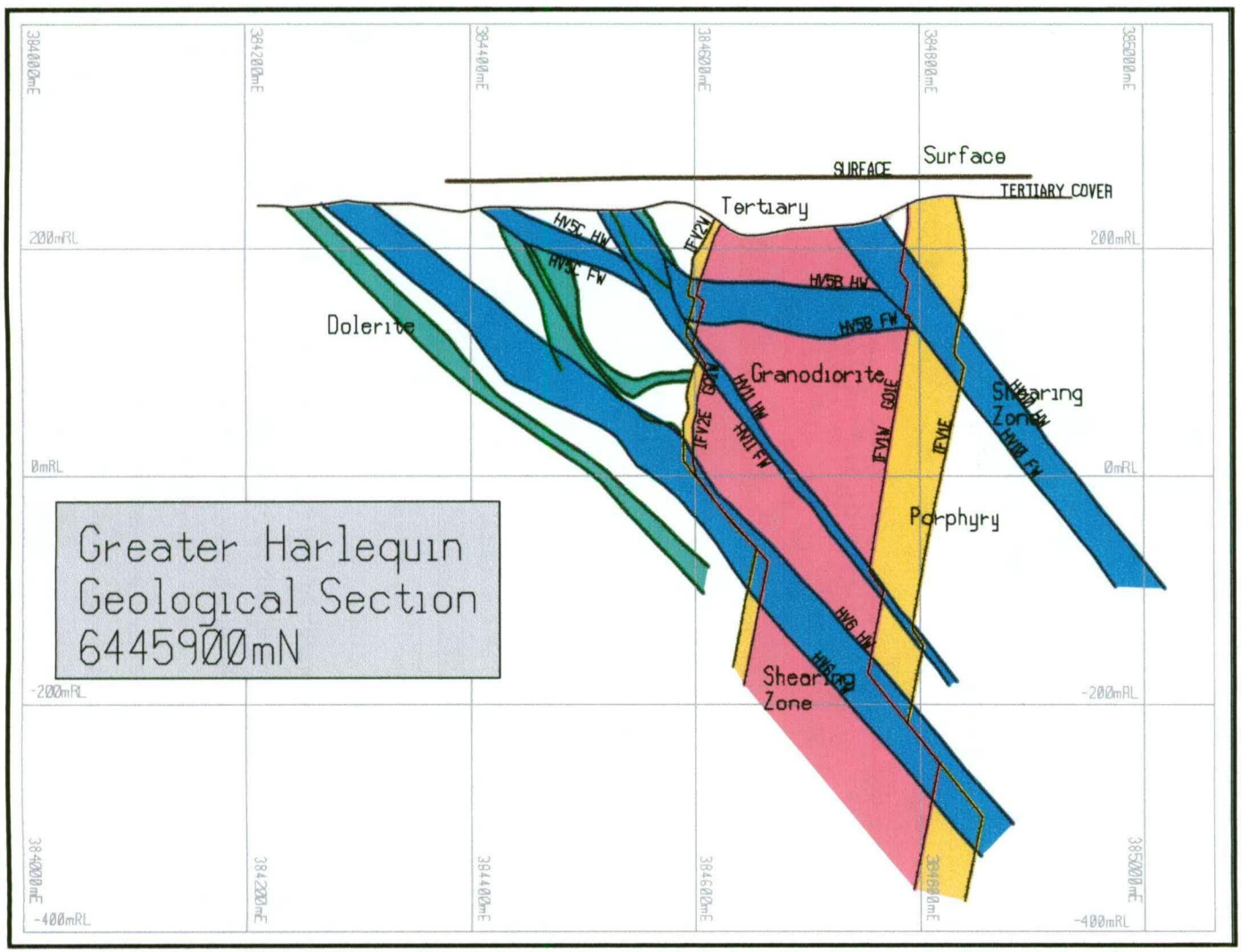

Figure 3.4: Cross section of the Harlequin area derived from drillhole data.. Looking north. Colour code is the same as used for figure 3.3.

Other geometrically more irregular porphyries are encountered in the greenstone east of the Harlequin granodiorite. One variety is distinguished mesoscopically by the abundance of quartz phenocrysts and is similar to porphyry that invades parts of the Harlequin Mine at HV1. The quartz phenocrysts, typically 1 mm in diameter, are recrystallised to polygonal mosaics and rare feldspar phenocrysts are heavily altered with biotite and microcline. The groundmass quartz and feldspar is generally about 0.2 mm in size and one 2 mm spherulite was noted. XRD again indicated two-thirds plagioclase and one-third alkali feldspar.

Discussion & interpretation

Proportions of plagioclase to alkali feldspar, indicated by XRD, suggest that both the felsic porphyry that transgresses the Harlequin granodiorite and the irregular quartz-rich porphyry in the Harlequin Mine have similar compositions, but differ from the granodiorite. The Harlequin granodiorite has only sodic plagioclase, suggesting a trondhjemitic rather than granodiorite composition. These interpretations are supported by geochemical studies (see Chapter 8). Due to "Harlequin granodiorite" being entrenched in the local Norseman vernacular, the latter name will be retained in this study.

3.5 UPPER NORSEMAN TERRANE STRATIGRAPHIC SYNTHESIS

The stratigraphy of the upper Norseman Terrane, as summarised in the geological overview (section 3.2.2), is largely understood from geological mapping and key area studies at the Polar Bear Peninsula. The Polar Bear Peninsula is particularly useful for the stratigraphic study as the tight to isoclinal folding, with a wavelength of a few hundred metres, exposes all the stratigraphy from basalt to the uppermost preserved units in the Norseman region. The Microwave Tower area was of little benefit and is not discussed further. In this section, the development of the upper stratigraphy of the Norseman Terrane is synthesised (figure 3.5) using the interpretations and conclusions derived from individual units as discussed in this chapter.

The lowest stratigraphic unit exposed at the Polar Bear Peninsula is basalt. The character of the uppermost basalts just below the Abbotshall Beds is exposed at the Sontaran prospect (Appendix 1, section A1.2.3). Interflow sedimentary bands are common and the basalt units between the sedimentary layers reach a maximum thickness of about 30 m. In contrast, the lower Woolyeenyer Formation closer to Norseman has a minimum basalt thickness between interflow sedimentary layers of about 100 m, being the width between the Gee Cee and Empress Slate members (Thomas & others, 1990). This difference suggests a lessening flux of basaltic magma with larger quiescent periods near the top of the Woolyeenyer Formation.

The basaltic magma is also highly amygdaloidal at the Sontaran prospect. Amygdaloidal basalt is present at other locations in the Woolyeenyer Formation, such as the causeway section (see section 4.2.2), but on the whole, they are rare. The water depth necessary to prevent vesiculation may be as little as 200 m for ocean floor basalts (Wilson, 1989) so the appearance of amygdales at the top of the sequence may indicate shoaling of a basaltic edifice to less than 200 metres depth or alternatively, a batch of magma with unusually high volatile contents (see section 4.4.3 for further discussion of water depths and vesiculation).

An angular unconformity is present at the top of the mafic succession. At the Sontaran prospect, the unconformity lies between basalt and the Abbotshall Beds, whereas at North Hinemoa Ridge (Appendix 1, section A1.2.6), the unconformity is interpreted to lie between the basalt and a shale band at the base of the overlying komatiite. The angular unconformity indicates that the basalt has been through a deformation and erosional event prior to the deposition of the overlying units. This erosional event is independently verified by the presence of the mafic conglomerate and sandstone. The rounding of the mafic pebbles and cobbles requires a fluvial or shoreline environment, necessitating a shallow marine or subaerial edifice. The presence of chert pebbles in the conglomerate shows that interflow sedimentary bands were also eroded, so the eroded source consisted of exposed submarine basalt, not an emergent volcanic vent. Exposure of submarine basalt could be the result of a sea level drop or tectonic uplift. The latter is more consistent with the deformation indicated by the angular unconformity.

No other examples of angular unconformities or mafic conglomerates at this level in the stratigraphy have been described in the Eastern Goldfields suggesting that the causative event is not widespread. The unconformity at the Polar Bear Peninsula may be the only example of such early basalt erosion in the Eastern Goldfields, in which case the inferred tectonic uplift would have to have been a local event.

At North Hinemoa Ridge (Appendix 1, section A1.2.6), deformed mafic conglomerate is apparently underlain and overlain by komatiite, although the underlying unit is only 10 to 60 m thick. This sequence suggests that deposition of the mafic conglomerate was approximately coeval with the eruption of the komatiite, occurring after the initial flows, but before the main komatiitic volcanic event. Unfortunately, the conglomerate is heavily deformed so that the stratigraphy remains a little ambiguous.

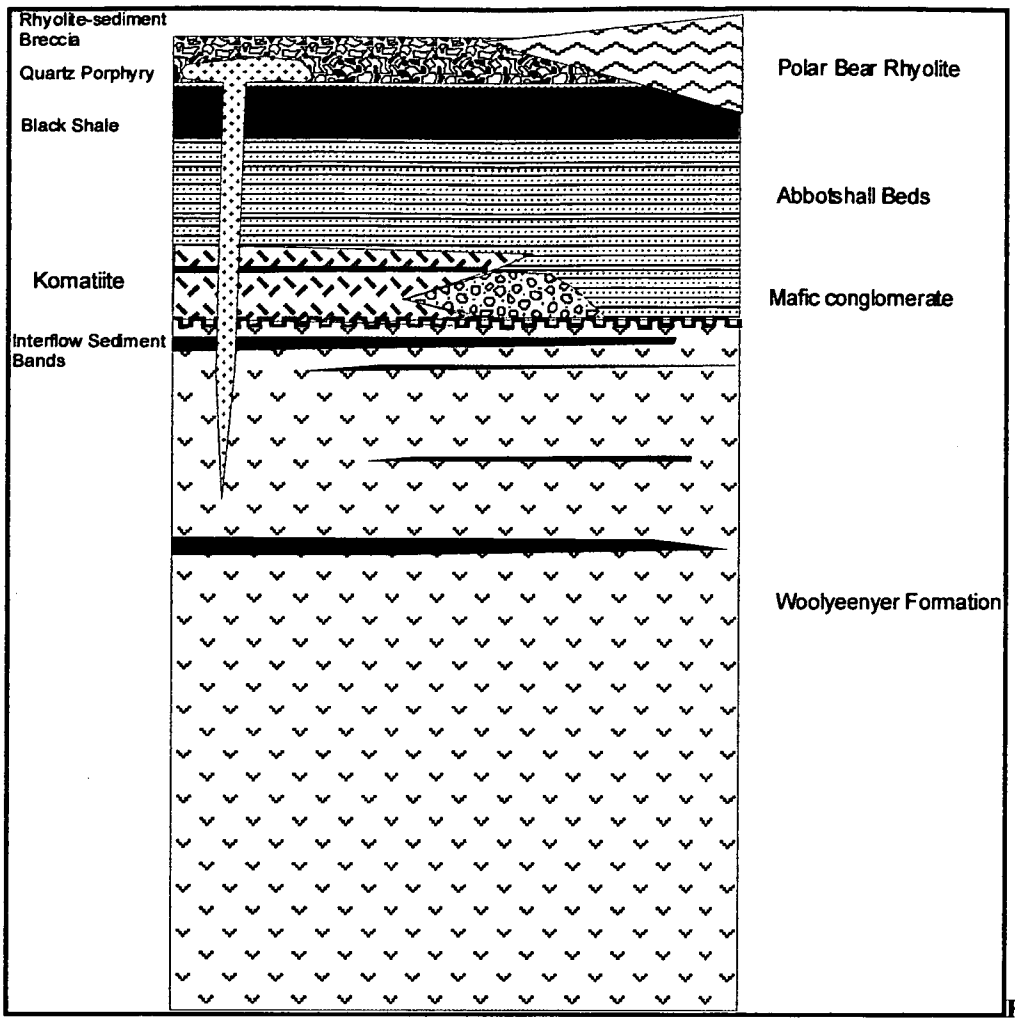

Figure 3.5: Simplified stratigraphic column for the upper stratigraphy of the Norseman Terrane as seen at the Polar Bear Peninsula after removing all structural repetitions.

Where komatiite has pinched out in the stratigraphy, the mafic conglomerate and sandstone is overlain by fine-grained sedimentary rocks of the Abbotshall Beds. At south central Polar Bear (Appendix 1, section A1.2.4), cobble conglomerate is overlain by sandstone-shale turbidite in which rare chert pebbles can be found as oversize clasts, indicating affinity with the sedimentary source of the conglomerate. The turbidite in turn is overlain by laminated chert. The sequence change from conglomerate to sandstone-shale turbidite could have been caused by local abandonment of the channel, but the overlying widespread laminated chert of the Abbotshall Beds suggests starvation and abandonment of the entire submarine fan.

The komatiite erupted over an extended period as evidenced by the common interflow sedimentary horizons. Spinifex textures are abundant which suggests a succession of dominantly thin flows. Together, the features of the komatiites at the Polar Bear Peninsula suggest thin, episodic flows with a low magma flux and long quiescent periods. If the komatiitic volcanism within the Eastern Goldfields formed as a cataclysmic eruption from a single vent as postulated by Hill & others (1993), the textures at the Polar Bear Peninsula imply a position distal from the vent near the

margins of the komatiite flood. This interpretation is consistent with the stratigraphic pinch-out of the komatiite evident at the Polar Bear Peninsula.

There is no upper basalt overlying the komatiite at the Polar Bear Peninsula, so the stratigraphy differs from that at Kambalda. Instead, the komatiite is overlain by the Abbotshall Beds, which consists of thin, low-density turbidites that may represent distal lobe fringes in a submarine fan system, grading into shales with drowning of the clastic sediment source. Sulfidic shales are abundant within the Abbotshall beds, both as part of the siltstone-shale low-density turbidites and as individual units. Sulfidic shale implies ambient sedimentation in an anoxic environment with biological sulfate reduction. Thus the 25 to 50 m true thickness of the Abbotshall beds represents a long period of time and the sulfidic shale intervals are condensed sections of stratigraphy. The water depth in which black shales can form is poorly known, particularly for the Archaean. It can only be said with certainty that they formed below wave base.

Rhyolite was erupted onto the Abbotshall Beds with a peperitic contact, which indicates the sediment was wet and unconsolidated when the lava was emplaced. The flow-banded and autobrecciated lava defines a rhyolite dome with a N-S length of 3.8 km and a maximum E-W width of about 500 m (figure 3.2). These dimensions have been affected by regional E-W shortening including folding, and concurrent N-S extension (see Chapter 10), so the original dimensions of the lava dome were probably more equant.

Being vent-proximal, there are rapid changes in the rhyolitic volcanic facies and thicknesses along strike and down dip. To the west, north and south, rhyolite breccia and rhyolite-sediment breccia replace the flow-banded rhyolite in the stratigraphy. This volcanic stratigraphy is not simple "layer cake"-style strata as the rhyolite dome typically has a much greater width than the breccias. This leads to complex map patterns where 1150 m southwest of the Hinemoa Mine, a 300 m width of rhyolite pinches down to a 30 m width of rhyolite-sediment breccia.

The stratigraphy at the Polar Bear Peninsula is intruded by voluminous quartz porphyry. The sharp contacts with adjacent shale indicate the shale was compacted and dewatered prior to the quartz porphyry intrusion, indicating a distinctly younger age than the rhyolite. Other minor intrusives in the area are felsic porphyry and granitoid with possible trondhjemitic affinities.

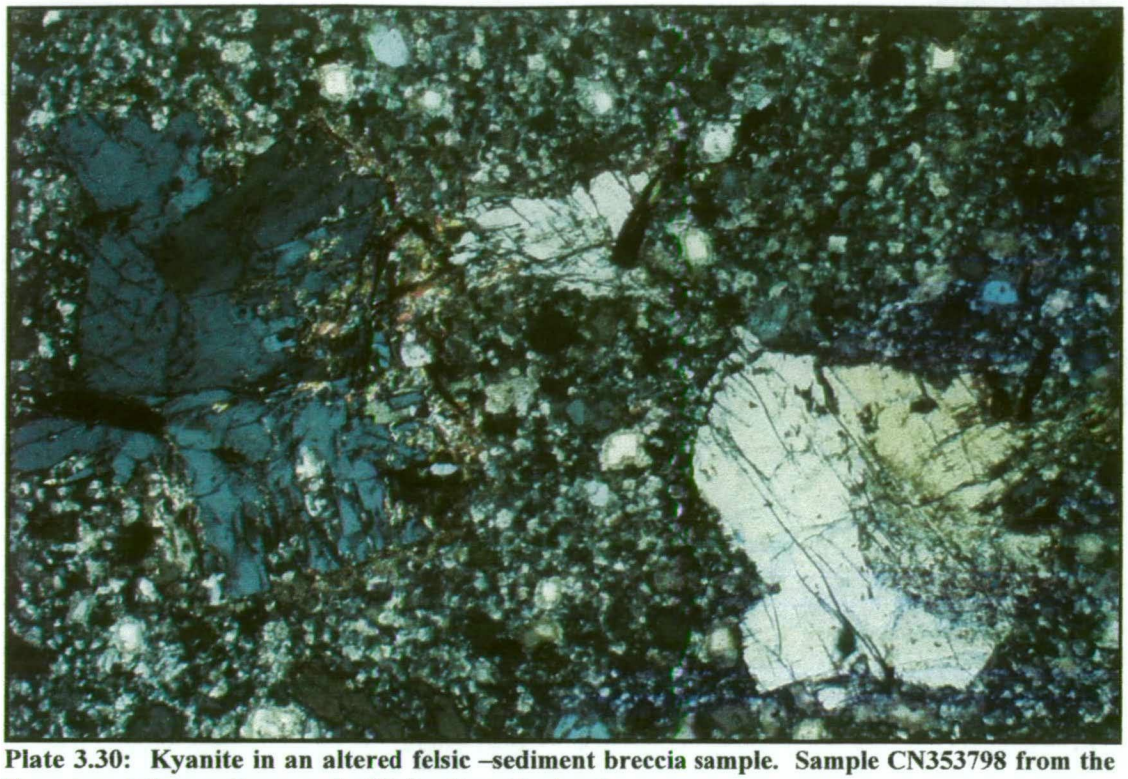

Plate 3.30: Kyanite in an altered felsic –sediment breccia sample. Sample CN353798 from the Eve area at the southern end of Polar Bear Peninsula.

All the Archaean units described above have been deformed and metamorphosed to lower amphibolite facies. The local changes in the mineralogy of the komatiite from talc-carbonate to quartz-carbonate compositions at the Hinemoa Mine, suggests a temperature between 450 °C and 520 °C (Winkler, 1979). Using this temperature range, the pressure can be estimated to have been between 3.5 to 4 Kb, based on the presence of kyanite porphyroblasts in felsic sediments at the south end of the Polar Bear Peninsula (Plate 3.30). The estimated pressure indicates the observed stratigraphy was buried to a depth of 10 to 12 km prior to the metamorphism. No evidence of the nature of the former overlying units remains in the Norseman Terrane.

The zircon dating throughout the Eastern Goldfields suggests that there is only one komatiitic unit, which forms a marker bed (Nelson, 1997). Therefore, the Norseman komatiite beneath Lake Cowan should correlate with the Polar Bear komatiite. As the Norseman komatiite and Polar Bear komatiite are spatially separated, there must be some form of structural repetition. However, there are significant differences between the stratigraphy at the Polar Bear Peninsula and Lake Cowan. The Norseman komatiite is overlain by Chinaman's Well basalts, which in turn, is overlain by the Abbotshall Beds. At the Polar Bear Peninsula, the Abbotshall Beds directly overlie the Polar Bear komatiite (where it has not pinched out).

These findings suggest that the Chinaman's Well basalts are a thrust repetition of the lower Woolyeenyer Formation. The basalt at the Polar Bear Peninsula is the on-land

continuation of the Chinaman's Well basalts. The Polar Bear komatiite overlying the basalt is, therefore, a thrust repetition of the Norseman komatiite. However, the lateral pinchout of the Polar Bear komatiite, evident at the Polar Bear Peninsula, continues to the south and west so that the Chinaman's Well basalts are directly overlain by the Abbotshall Beds. The rhyolite and associated breccias that overlie the Abbotshall Beds at the Polar Bear Peninsula are the highest units seen in the Norseman Terrane.

3.6 SUMMARY & CONCLUSION

The Polar Pear Peninsula provides a view through the top of the Norseman Terrane stratigraphy. The units include basalt equivalent to the lower Woolyeenyer Formation, komatiite equivalent to the Norseman komatiite, sandstone-shale turbidites, cherts and black shales of the Abbotshall Beds and a rhyolite dome with associated proximal breccias.

Like the other greenstone terranes between Norseman and Menzies, the greenstone at Norseman includes an extensive mafic succession, greater than 6 km thick. The mafic succession is followed by komatiite, except for the areas where the komatiite has pinched out of the stratigraphy. However, unlike the Kambalda and Ora Banda Domains of the Kalgoorlie Terrane, there is no "hangingwall basalt" above the komatiite. In this respect, the sequence is more like the Coolgardie Domain of the Kalgoorlie Terrane, which also lacks the "hanging wall" basalts. The Chinaman's Well basalt that overlies the Norseman komatiite is suggested in this study to be a tectonic repetition of the lower Woolyeenyer Formation, and the Polar Bear komatiite is the structural equivalent to the Norseman komatiite.

A feature which may be unique to the Polar Bear Peninsula, is an angular unconformity at the top of the basalt. The angular discordance between the interflow sedimentary rocks in the basalt succession and the overlying Abbotshall Beds was first noted during mapping and confirmed by drilling. Further evidence is provided by local occurrences of mafic conglomerate and sandstone with a similar composition to the basaltic sequence including occasional interflow sediment chert pebbles. The rounding of the clasts requires erosion of the submarine basalt sequence which has become subaerial. The angular unconformity is probably the result of local tectonic uplift, although lowering of the sea level cannot be ruled out. There is some evidence that the mafic conglomerate may be coeval with the initial komatiite eruption, but the majority of the komatiite is younger than the mafic conglomerate.

A 25 to 50 m thick sequence of thin-bedded sandstone-shale turbidites and sulfidic sedimentary rocks overlies the ultramafic and basalts. This is a regionally continuous unit known as the Abbotshall Beds. Initially, it shows deepening water and drowning

of mafic sediment sources with a fining upward sequence, but eventually passes into sulfidic shales representing ambient sedimentation and a condensed section of stratigraphy.

The felsic and sedimentary units of the Norseman Terrane are also distinctly different to the Black Flag Beds (BFB) of the Kalgoorlie Terrane (see Chapter 2). The voluminous felsic-derived sediments that form the 2 km thick BFB in the Kambalda Domain to the east and the Coolgardie Domain to the west are not seen in the Norseman Terrane. Instead, ambient sedimentation took place forming the Abbotshall Beds followed by rhyolitic volcanism. The rhyolite dome at the Polar Bear Peninsula was probably extruded at depth as it is not associated with any pumiceous volcanics. The rhyolite dome has peperitic contacts with the underlying sulfidic shales, and associated breccias related to collapse events indicate the rhyolite was erupted on the ocean floor and is not a cryptodome. No units higher than the rhyolite are exposed in the stratigraphy. No date exists for the rhyolite volcanism but it predates D_2 deformation as it has the S_2 fabric, suggesting an age of greater than *ca.* 2660 Ma (see section 2.4.3).

The stratigraphy at the Polar Bear Peninsula is intruded by voluminous quartz porphyry which disrupts the stratigraphy and also forms sills, occupying the position above the Abbotshall Beds. There is a suggestion of trondhjemitic affinities for the quartz porphyry. The Harlequin granodiorite in the lower Woolyeenyer Formation shows a similar trondhjemitic affinity and may correlate with the quartz porphyry. Interestingly, the Harlequin granodiorite forms an elongate body trending directly towards the outcrop of quartz porphyry at the Polar Bear Peninsula. The Harlequin granodiorite could be a deeper magma chamber. Felsic porphyry at Harlequin has different composition of feldspars than the granodiorite. Other intrusives at the Polar Bear Peninsula are minor and volumetrically unimportant.

Metamorphic mineralogies indicate the rhyolitic exposures at the Polar Bear Peninsula were buried to a depth of 10-12 km at the time of peak metamorphism, but no trace of the overlying sequences remains.

CHAPTER FOUR

Basalt Geology and Geochemistry

4.1 INTRODUCTION

The mafic Woolyeenyer Formation is one of the best known stratigraphic units at Norseman, as it hosts the majority of the gold deposits. Numerous previous studies have addressed various aspects of the mafic rocks of the Woolyeenyer Formation including Hallberg (1970), Redman (1982), Thomas (1991), McCuaig (1996) and Ghaderi (1998). However, all the previous studies have been directed at the Woolyeenyer Formation close to Norseman, primarily because that is where drill holes and mine exposures were available, and have not examined mafic rocks from beneath the sediment cover north of the Royal Peninsula. Specifically, for the basalt overlying the Norseman komatiite, which is of particular importance for this study, there is a paucity of data.

As noted in Chapter 3, basalt is also known at the Polar Bear Peninsula north of Norseman. The basalt occurs beneath unconsolidated cover off the eastern shore of the Polar Bear Peninsula, under lake cover to the south of the Peninsula, and in certain locations on the Peninsula. However, there is a 6.5 km gap with no basalt exposures between outcropping Woolyeenyer Formation at the Royal Peninsula and basalt at Polar Bear (figure 3.1). Doepel (1973) concluded that the basalt at the Polar Bear Peninsula was unrelated to the Woolyeenyer Formation and included the Polar Bear Peninsula basalts within the Mount Kirk Formation.

As outlined in Chapter 1, the work of Doepel (1973) is challenged by the regional synthesis of Swager & others (1995), which suggested that the Mount Kirk Formation was restricted to the western side of the Mission Fault (figure 1.3). If the work of Swager & others (1995) is correct, the basalt at Polar Bear occurs in a different terrane to the Mount Kirk Formation.

Chapter 3 presented the results of geological mapping undertaken for this study at the Polar Bear Peninsula. Through the mapping, the stratigraphy at the Polar Bear Peninsula was established, with basalt being the lowermost unit, underlying komatiite. By correlating the komatiite from the Polar Bear Peninsula with the Norseman komatiite overlying basalts of the Woolyeenyer Formation, it was suggested in Chapter 3, that all the stratigraphy at the Polar Bear Peninsula represents a repetition of the Norseman stratigraphy, which has been thrust over the Norseman komatiite. If this is the case, then the basalt at Polar Bear is equivalent to the Woolyeenyer Formation at Norseman, being a structural repetition.

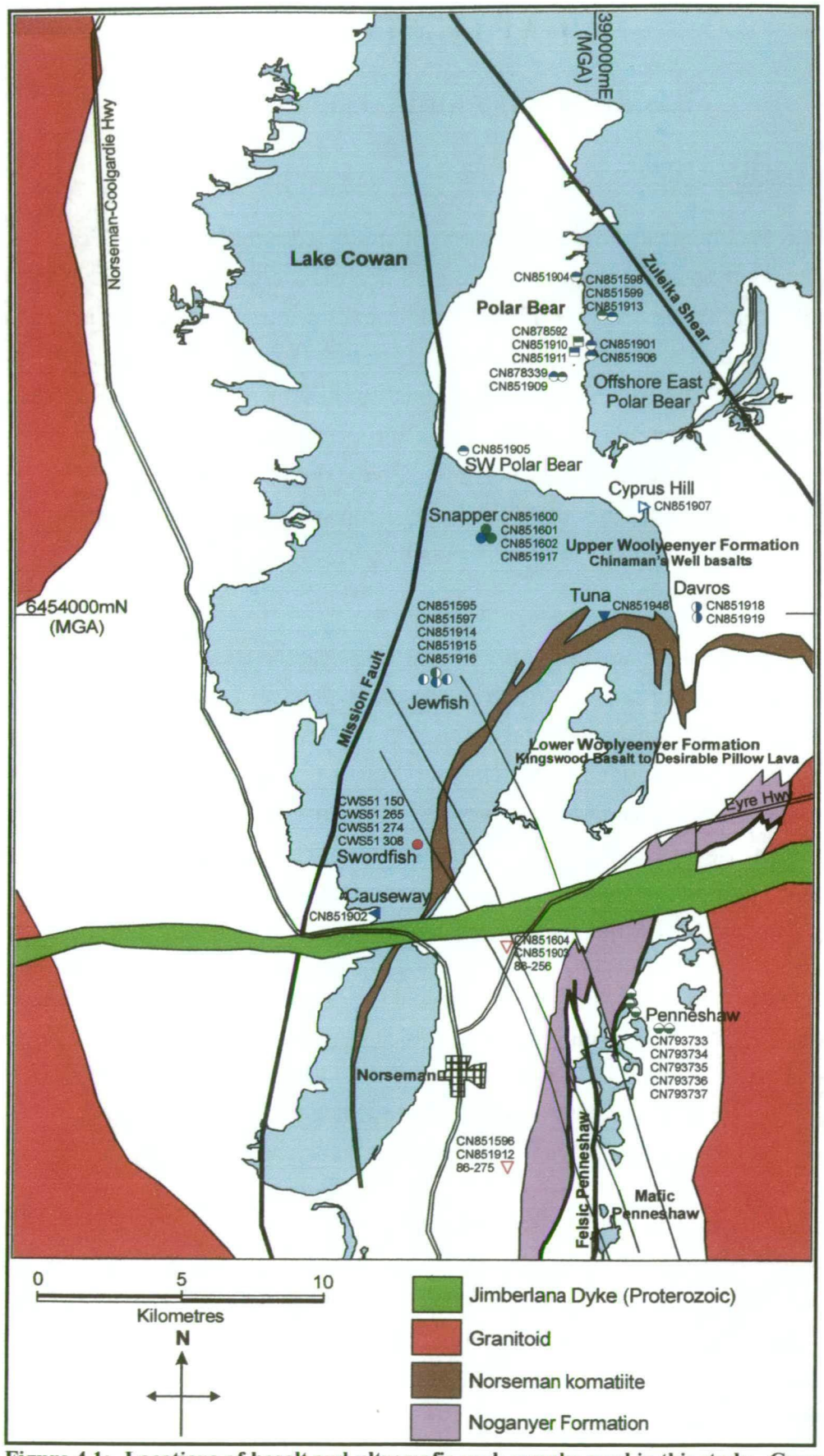

Figure 4.1: Locations of basalt and ultramafic rock samples used in this study. Green and blue circles and triangles are the new basalt samples. The red inverted triangles are the locations of the quality control samples. The two squares with three sample numbers at Polar Bear are the ultramafic samples discussed in Chapter 7. Noganyer Formation and Penneshaw faults after a compilation map by Connors (2000).

The thrust hypothesis outlined above represents a major departure from previous stratigraphic interpretations for Norseman. Previously, the Norseman stratigraphy was typically compared to that at Kambalda and the basalt overlying the komatiite at both locations was assumed to be similar (figure 1.2). If the thrust hypothesis is correct, then the basaltic rocks overlying the komatiite at Norseman and Kambalda would not be equivalent. The thrust hypothesis has important implications for understanding the stratigraphy of the Norseman Terrane and determining whether the Norseman Terrane is a distinct entity. These implications and ideas are explained in Chapter 12.

The thrust model can be tested using geochemistry and petrography. As described in Chapter 2, the Devons Consols Basalt and the Paringa Basalt overlying the Kambalda Komatiite have a distinctive geochemistry and mineralogy. These features can be used to determine whether the basalt overlying the Norseman komatiite from beneath Lake Cowan and from the Polar Bear Peninsula resembles the Woolyeenyer Formation from Norseman, which would support the basalt being a thrust repetition; or the Devons Consols Basalt or Paringa Basalt from Kambalda, which would suggest the previous stratigraphic correlation with Kambalda was correct.

The aim of this chapter is to testing the thrust model by examining the petrography and geochemistry of the basalt.

Layout of the chapter

The chapter commences with a description of the Woolyeenyer Formation at Norseman, then examines the petrographic features of basalt from above the Norseman komatiite, using drill core samples. Samples from the Polar Bear Peninsula, which are above the Norseman komatiite, but below the komatiite at the Polar Bear Peninsula are also examined (figure 4.1). The results of the petrographic studies are compared to the results of Redman (1982), which remains the most comprehensive petrographic study of mafic rocks from the Eastern Goldfields.

Following the petrographic examinations, the geochemistry of basalt samples is examined. Initially the geochemical results from previous studies are compiled to create a database for comparative purposes. The geochemistry of basalt samples from above the Norseman komatiite and the Polar Bear Peninsula are then compared to the database to test for similarities or differences. AFC geochemical modelling is undertaken for a number of samples.

Finally conclusions are drawn about the character of the basalts, and the validity of the thrust hypothesis.

4.2 CHINAMAN'S WELL BASALTS

4.2.1 Introduction

The mafic Woolyeenyer Formation in the vicinity of Norseman township has been intersected in numerous drill holes and mine openings. Detailed studies undertaken from these exposures have allowed a consistent stratigraphy to be recognised.

The Woolyeenyer Formation was first subdivided by Hall and Bekker (1965) and formally defined by Doepel (1973) as comprising nine members from the Kingswood Basalt at the base to the Desirable Pillow Lava at the top, all dipping steeply to the west at Norseman township. The members comprise:

- the Kingswood Basalt, pillow lavas 400 m thick;
- the Venture Slate, 10 m thick;
- the Mararoa Pillow Lava with a thickness of 1350 m;
- the Gee Cee Slate, 2 m thick;
- the Bluebird flows, a plagioclase megacrystic pillow lava with a thickness of 100 m;
- the Empress slate, 5 m thick;
- the Royal Amphibolite, an amygdaloidal basalt 150 m thick;
- the Crown Sills a mixture of pillow basalt slate and dolerite intrusives 100 m thick; and
- the Desirable Pillow lava with a thickness of 6 km..

The Woolyeenyer Formation is intruded by numerous mafic dykes and one ultramafic dyke.

Within each of the basalt members of the Woolyeenyer Formation, a more finely divided stratigraphy can be recognised by characteristic preserved volcanic textures and distinctive metamorphic mineralogies. Thomas (1991) described the basis of the methods used to recognise and correlate individual basalt units, and provided the results of a major project that involved relogging historic drill core to identify basalt stratigraphy within the Woolyeenyer Formation. Using the methods outlined by Thomas (1991), basalt strata were successfully correlated across a number of project areas and a detailed stratigraphy was established.

Under the formal definition of the Woolyeenyer Formation (Doepel, 1973), the Desirable Pillow Lava member, with a thickness of 6 km, has not been subdivided into thinner units due to insufficient exposures or drill intersections. The member is

largely covered by the unconsolidated sediments of Lake Cowan. However, subsequent additional data provided by regional aeromagnetics and drilling rigs capable of operating on Lake Cowan suggest that the Desirable Pillow Lava member should be divided into three separate units. Under the scheme in use at CNGC, the base of the original Desirable Pillow Lava member retains that name and the two new units are informally termed the Norseman komatiite and the Chinaman's Well basalts. In this study, the Woolyeenyer Formation from the Kingswood Basalt up to the base of the komatiite is termed the "lower Woolyeenyer Formation".

The Norseman komatiite outcrops on a small island adjacent to the eastern shore of Lake Cowan north of Norseman where it ranges from spinifex-textured ultramafic to serpentinised, olivine adcumulate. Cherry (2002) undertook a detailed study of the komatiite using diamond drill core. The komatiite is clearly defined in regional aeromagnetic images as a continuous magnetic unit extending east and west of the island and folding in sympathy with the regional Norseman anticline (figure 1.3).

The Chinaman's Well basalts overlie the Norseman komatiite and are a major focus of this section. They are exposed southwest of Norseman in the Lake Kirk area and at the northern end of the causeway, west of Norseman, on which the Coolgardie-Esperance Highway crosses Lake Cowan. Further to the north, the unit is largely covered by the unconsolidated sediments forming Lake Cowan except for some exposures on small islands within the lake.

The Chinaman's Well basalts occupies a similar structural position to the Devon's Consols Basalt (DCB) or Paringa Basalt at Kambalda, both of which overlie the Kambalda Komatiite (figure 1.2). The DCB and Paringa Basalt both have distinctive petrographic and geochemical features that allow testing of thrust theory. If the Chinaman's Well basalts stratigraphically overlies the Norseman komatiite, it should have a similar geochemistry to the DCB or Paringa Basalt. Conversely, if the Chinaman's Well basalts has represents lower Woolyeenyer that has been thrust over the Norseman komatiite, then the petrographic and textural features of the Chinaman's Well basalts should resemble the lower Woolyeenyer Formation.

Little previous work has been undertaken on the Chinaman's Well basalts. Morris & others (1991) provided a single analysis and Morris (1993b) an outcrop description of the basalts at the causeway area, and Ghaderi (1998) undertook major and trace element analysis of four drill core samples from the Swordfish prospect approximately 2 km north of the causeway.

Conventionally, the basalt at Polar Bear was considered to be part of the Mount Kirk Formation. However, the basalt near the base of the Peninsula seems to be part of the Chinaman's Well basalts. As outlined in Chapter 3, the basalt at the Polar Bear

Peninsula underlies komatiite, suggesting equivalence with the lower Woolyeenyer Formation.

Methods

This study utilises petrography and geochemistry from a suite of samples from holes drilled by CNGC on Lake Cowan since 1994 (figure 4.1). All samples are diamond drill core except for two from the Davros prospect, which are hand-picked fragments of unweathered basalt from aircore holes that achieved unusually deep penetration into the bedrock, and an outcrop sample from the causeway. The petrographic features of the rocks are discussed in this section and the geochemistry in sections 4.7-4.12.

Thin sections and XRD analyses were obtained for all batch #2 geochemical samples (see section 4.6.3). These comprise seven samples from the Chinaman's Well basalts south of the Polar Bear Peninsula, and six samples from the Polar Bear Peninsula. The Chinaman's Well samples comprise three from the Jewfish prospect, two from the Davros prospect, one from the Snapper prospect and one variolitic and amygdaloidal basalt from the causeway section (figure 4.1). One spinifex-textured sample from the Tuna prospect close to the Norseman komatiite was also included. The samples from the Polar Bear Peninsula were from offshore and onshore and comprise five basalts and a dolerite. All the basalts are typically aphyric and are metamorphosed but have minimal hydrothermal alteration.

4.2.2 Description

Morris (1993b) described the geology of the causeway area, where the Coolgardie–Esperance Highway crosses Lake Cowan west of Norseman, and correlated the basalt there with the Desirable Pillow Lava member using the formal stratigraphy of Doepel (1973). However, as noted above in section 4.2.1, correlation with a new informal unit, the Chinaman's Well basalts, is preferred due to the structural position, overlying the Norseman komatiite.

The causeway area is renowned for displaying excellent examples of pillow basalt. Individual pillows are fine-grained, usually aphanitic, may be amygdaloidal and are described as strongly variolitic in places. The apparent varioles range up to 1 cm in diameter (somewhat larger than described by Morris (1993b)) and are particularly well developed in comparison to Chinaman's Well basalts observed elsewhere.

Drill core of the Chinaman's Well basalts beneath Lake Cowan, reveals similar morphologies to those observed by Morris at the causeway. Basalts are typically very fine-grained, pillowed, may have faint varioles a few millimetres in diameter and amygdales are developed in places. Interflow sedimentary rocks have been

intersected in some diamond drill holes and dolerite is common and is interpreted to be intrusive on the basis of margins chilling against contacts with basalt.

The primary mineralogy of the basalt is strongly altered, most commonly by very fine-grained chlorite-quartz-carbonate mosaics, with small, clinozoisite grains and aggregates of fine-grained granular sphene common as accessory phases. In five of the seven basalt samples examined petrographically from the Chinaman's Well basalts, igneous plagioclase is visible, typically as small, heavily altered laths from 0.1 to 0.5 mm in length, in which remnant twinning can be detected. One sample has unusually large plagioclase phenocrysts up to 4 mm in length which are partially obliterated by chlorite alteration.

Of the samples that do not have visible plagioclase, one is from the Davros prospect and the other from the causeway area. The Davros sample (CN851918) has a moderate foliation induced by shearing and is completely altered to a very fine-grained chlorite-carbonate mosaic. However, XRD registered approximately 13% plagioclase, which may be present as tiny recrystallised grains within the alteration mosaic. A small percentage of plagioclase was also reported by XRD in the causeway sample but is not visible.

The causeway sample (CN851902) is variolitic and amygdaloidal and differs from the other samples by the absence of carbonate and presence of abundant amphibole with a strong pleochroism from green to blue-green. The apparent varioles do not possess spherulitic textures; they are finer-grained, quartz + amphibole nodules in which the amphiboles typically occur as needles, and rarely form patches with parallel needles approximately 0.1 mm in length that may pseudomorph dendritic pyroxenes (Plate 4.1). Outside the nodules there are no remnant igneous textures; the amphibole has a metamorphic texture forming tufts 0.5 mm in length.

Another sample with a moderate variolitic texture (CN851915 - from Jewfish) was found to have a mineralogy that differs from the other samples. It has higher MgO, 8.4 wt % (volatile free calculation), than most of the other samples, which typically have 3 – 5 wt % MgO (vol. free). Sample CN851915 is dominated by colourless chlorite and amphibole and also contains minor carbonate, quartz, clinozoisite and sphene. Plagioclase, as 0.5 mm laths, is a minor constituent. The variolitic texture was confirmed petrographically by one example of spherulitic pyroxene 1 mm in diameter, pseudomorphed by radial amphibole. Two other altered, igneous, ferromagnesian mineral forms are present. The first form (type 1) consists of acicular minerals, 0.3 mm in length, which possess amphibole rims and chlorite-altered cores giving them a hollow, skeletal appearance (Plate 4.2). The second form (type 2) consists of euhedral minerals, replaced by chlorite with minor quartz

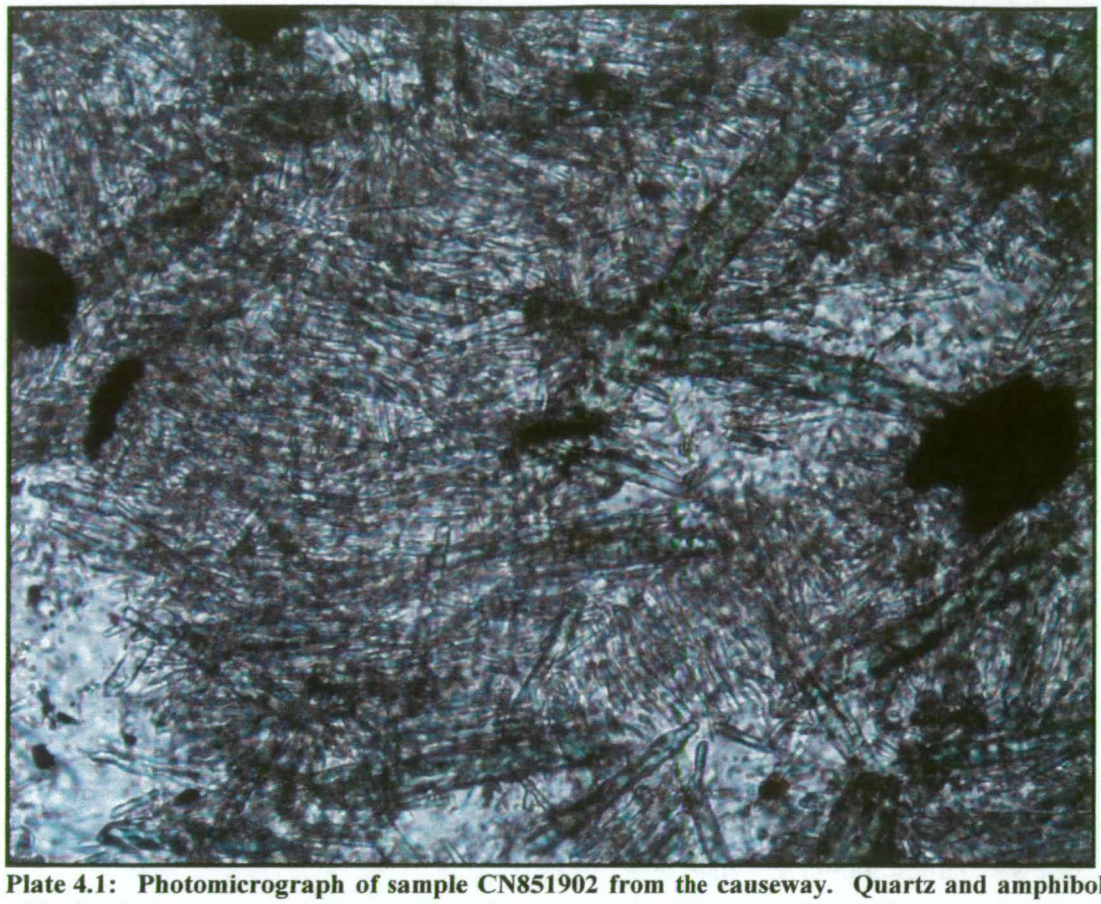

Plate 4.1: Photomicrograph of sample CN851902 from the causeway. Quartz and amphibole with dendritic texture within a nodule that appeared to be a variole. Field of view 0.25 mm. Cross polarised light.

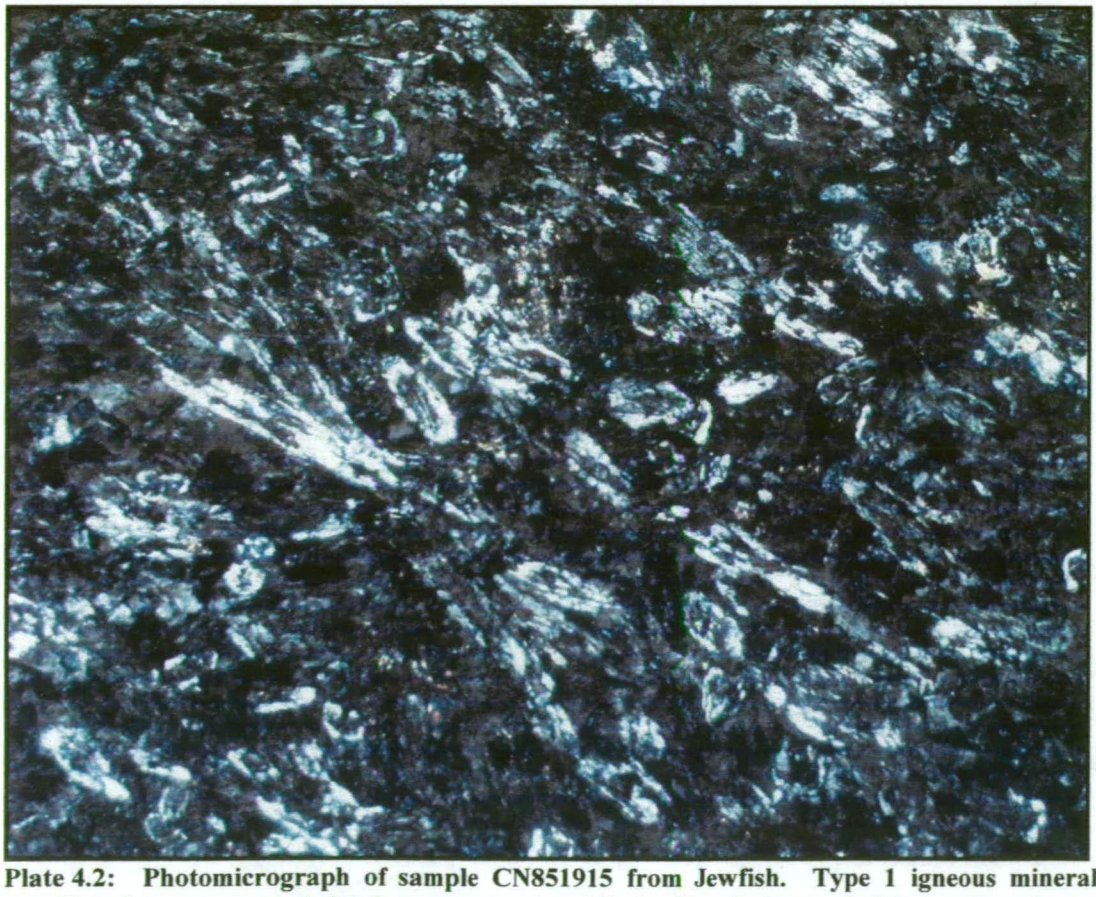

Plate 4.2: Photomicrograph of sample CN851915 from Jewfish. Type 1 igneous minerals, considered to represent skeletal pyroxenes. Amphibole-altered rims and chlorite-altered cores. Equant examples represent cross sections. Field of view 1 mm. Cross polarised light.

(Plate 4.3). With reference to the work of Redman (1982), discussed below, type 1 acicular minerals are thought to represent skeletal pyroxenes. Redman (1982-his Plate 3.13b) also illustrated a euhedral mineral with a form similar to type 2 that he suggested pseudomorphs a hopper olivine grain.

A spinifex-textured sample was collected from a diamond drill hole in the Tuna prospect (figure 4.1), collared just north of (stratigraphically above) the Norseman komatiite and angled to the south to drill into it. The drill core commenced with spinifex-textured rock and then entered rock that appears to be mafic. The sample examined (CN851948) came from the top of the hole and has a prominent spinifex texture in hand specimen consisting of groups of parallel acicular grains up to 1 cm in length intersecting other groups at high angles.

The spinifex texture is formed by acicular grains with a similar form to type 1 altered ferromagnesian minerals in sample CN851915 discussed above (Plate 4.4). The grains are altered and now consist of rims of amphibole surrounding cores of colourless chlorite giving a hollow, skeletal appearance. Square cross sections of the acicular grains are visible in places. These grains are similar to descriptions and illustrations by Redman (1982), of minerals he deduced were originally skeletal pyroxenes. Former dendritic pyroxenes and spherulitic fans, both replaced by amphibole, fill the majority of the spaces between the acicular grains.

4.3 POLAR BEAR BASALT

Mafic rocks underlie the unconsolidated sediments of the lake east of the Polar Bear Peninsula, and are exposed sporadically along the eastern shoreline. Mafic rocks are exposed in various other locations with the exposures at Polar Bear, most prominently along the western boundary of the exposures. The mafic rocks under the lake sediments south of the Polar Bear Peninsula, are the Chinaman's Well basalts. For brevity, basalt at the Polar Bear Peninsula is termed "Polar Bear basalt" in this thesis.

4.3.1 Description

The majority of the mafic rock exposures comprise a distinctive fine-grained, aphyric, grey-green coloured basalt, in which clear acicular minerals, less than 1 mm in length, can usually be distinguished. Pillow margins have been identified in outcrop and drill core from hole PEN1206 at the Sontaran prospect. In general, amygdales are rare but they have been observed in PEN1206 drill core.

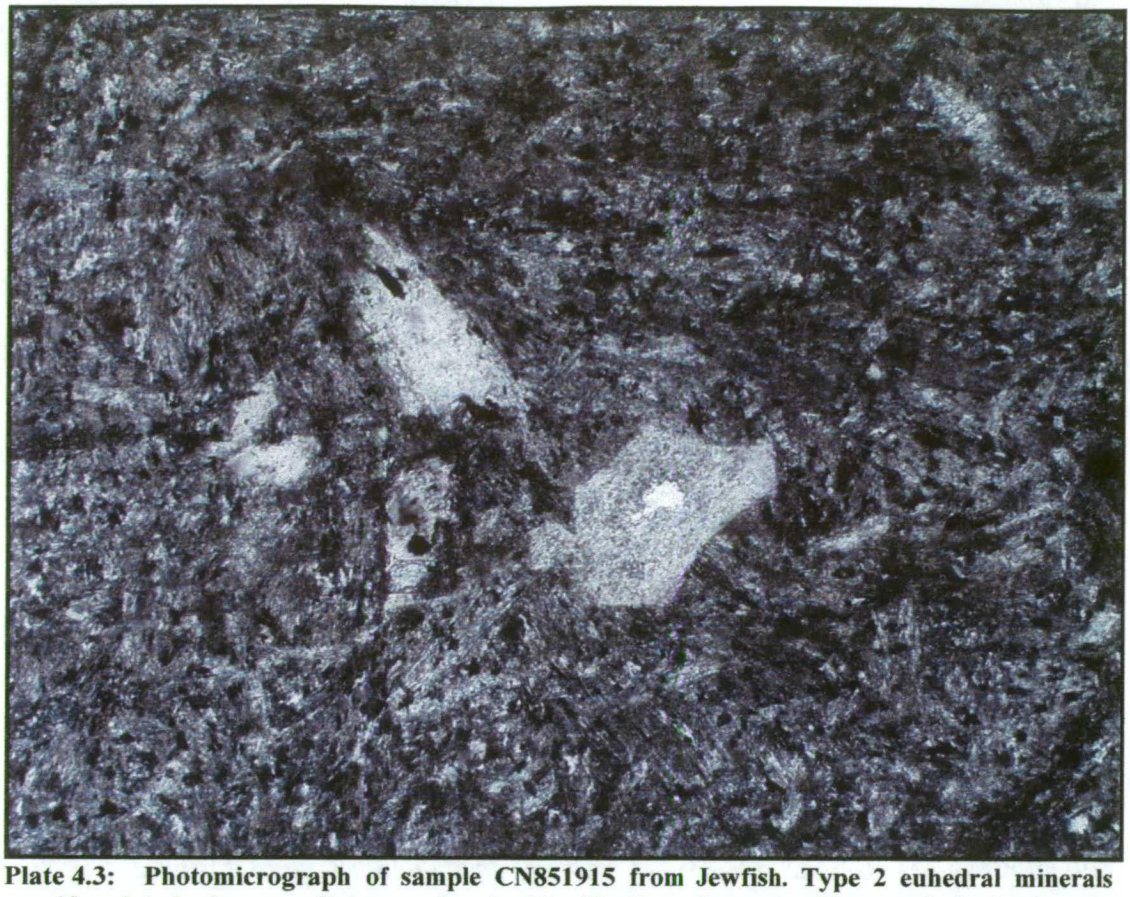

Plate 4.3: Photomicrograph of sample CN851915 from Jewfish. Type 2 euhedral minerals considered to be hopper olivines replaced with chlorite and quartz. The matrix is dominantly amphibole and chlorite. Field of view 1.6 mm. Plane polarised light.

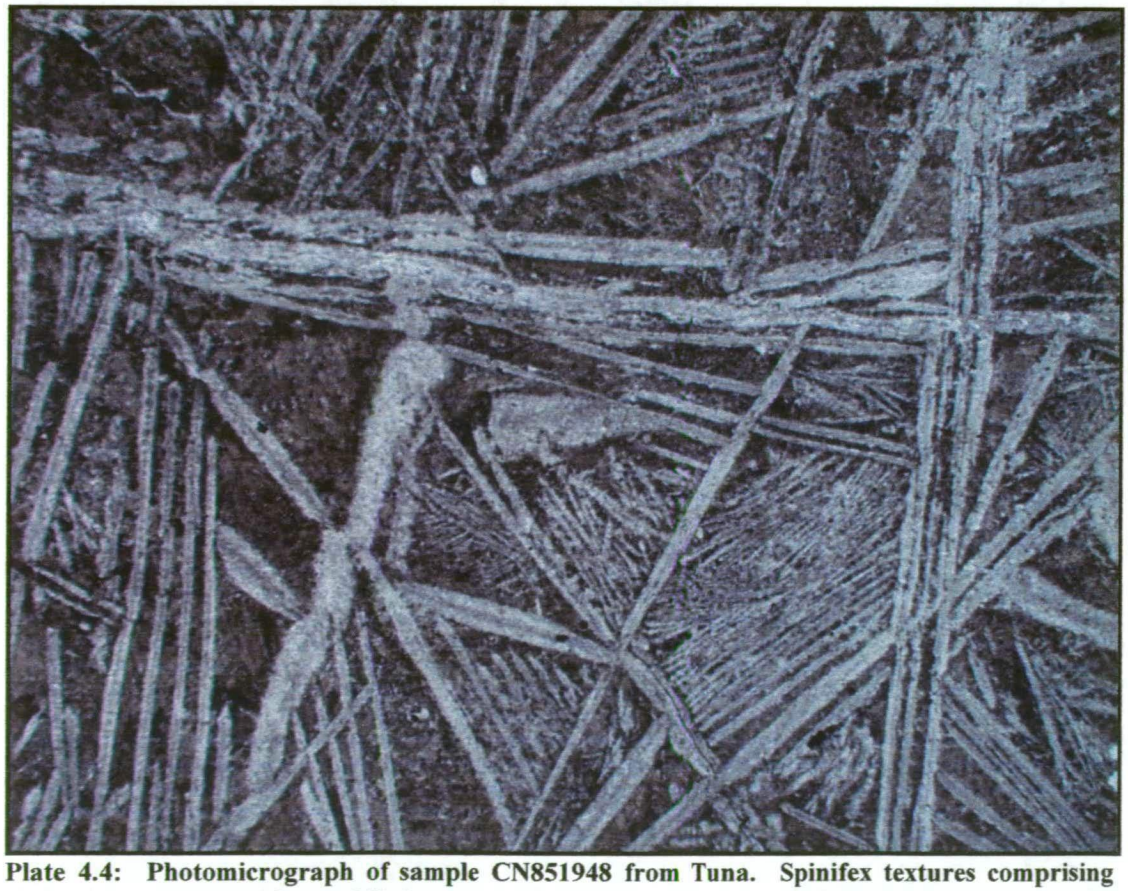

Plate 4.4: Photomicrograph of sample CN851948 from Tuna. Spinifex textures comprising skeletal pyroxenes with amphibole rims and chlorite cores. Parallel dendritic pyroxenes fill interstices between larger acicular forms. Field of view 8 mm. Plane polarised light.

The clear acicular minerals are plagioclase microlites typically 0.5 mm in length. Some microlites are entirely replaced by alternating segments of paragonite and quartz, or aggregates of quartz and calcite which have retained the crystallographic orientations of former plagioclase polysynthetic twins. Other feldspar microlites are partially preserved and remnant twinning can be discerned through a heavy alteration of minute quartz, carbonate, or chlorite. Plagioclase microlite textures are visible in all five basalt samples from the Polar Bear Peninsula examined petrographically.

Of the five petrographic samples, four have a groundmass altered to a fine-grained quartz-chlorite-calcite(±clinozoisite) mosaic and three of these samples have preserved no former igneous minerals other than the plagioclase microlites. One basalt sample (CN851904) has amphibole alteration with a preserved igneous textures comprising stubby, heavily altered plagioclase in a groundmass in which amphibole forms parallel needles pseudomorphing dendritic pyroxene, 0.1 mm in size (Plate 4.5).

One basalt sample (CN851905) with a groundmass alteration of fine-grained quartz-chlorite-calcite(±clinozoisite) has retained igneous mineral textures. In this sample, radial, spherulitic pyroxene textures, up to 2 mm in diameter, are abundant, now replaced by the chlorite and calcite (Plate 4.6). In addition, there are acicular altered minerals that may represent skeletal pyroxene and other small, irregular patches of quartz, carbonate and clinozoisite that are similar in composition and shape to textures Redman (1982) attributed to former hopper olivine grains. The spherulites in this basalt are visible in hand specimen as weakly defined pale circular shapes, textures that are common in basalts at Norseman.

Samples of mafic conglomerate were examined petrographically. Igneous textures are generally obliterated by very fine-grained chlorite-quartz mosaics, partly overprinted by patches of calcite and spatially associated goethite. However, remnant igneous textures consisting of carbonate altered feldspar laths 0.2 mm in length can typically be distinguished in basalt pebbles, suggesting they are dominantly LMSB (see section 4.4.1) and probably tholeiitic. Microscopic quartz and carbonate-filled amygdales are common within basaltic clasts. Chert clasts are recrystallised to evenly-sized, unstrained, polygonal quartz grains.

Interflow sedimentary rock horizons within the mafic sequence are common. These sedimentary units are commonly thin, with a width of one to two metres, but are laterally continuous.

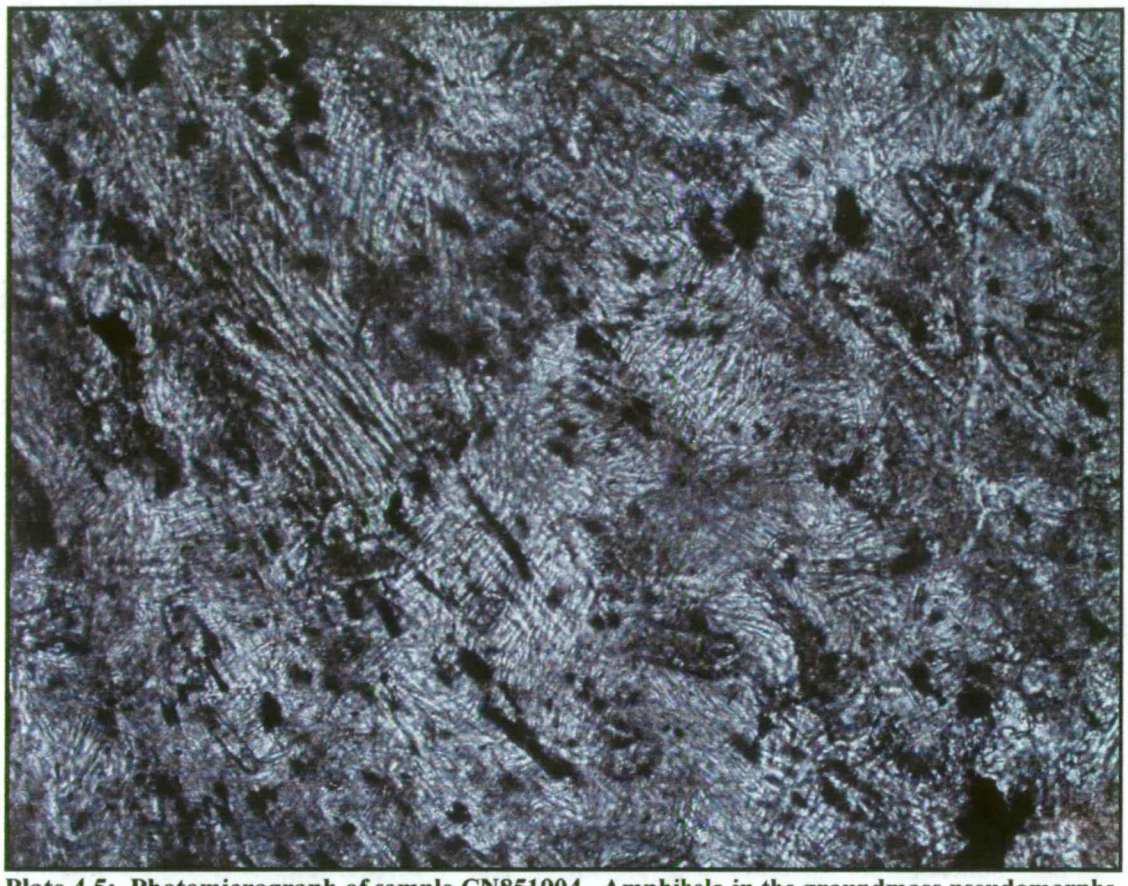

Plate 4.5: Photomicrograph of sample CN851904. Amphibole in the groundmass pseudomorphs dendritic pyroxenes. Field of view 0.5 mm. Plane polarised light.

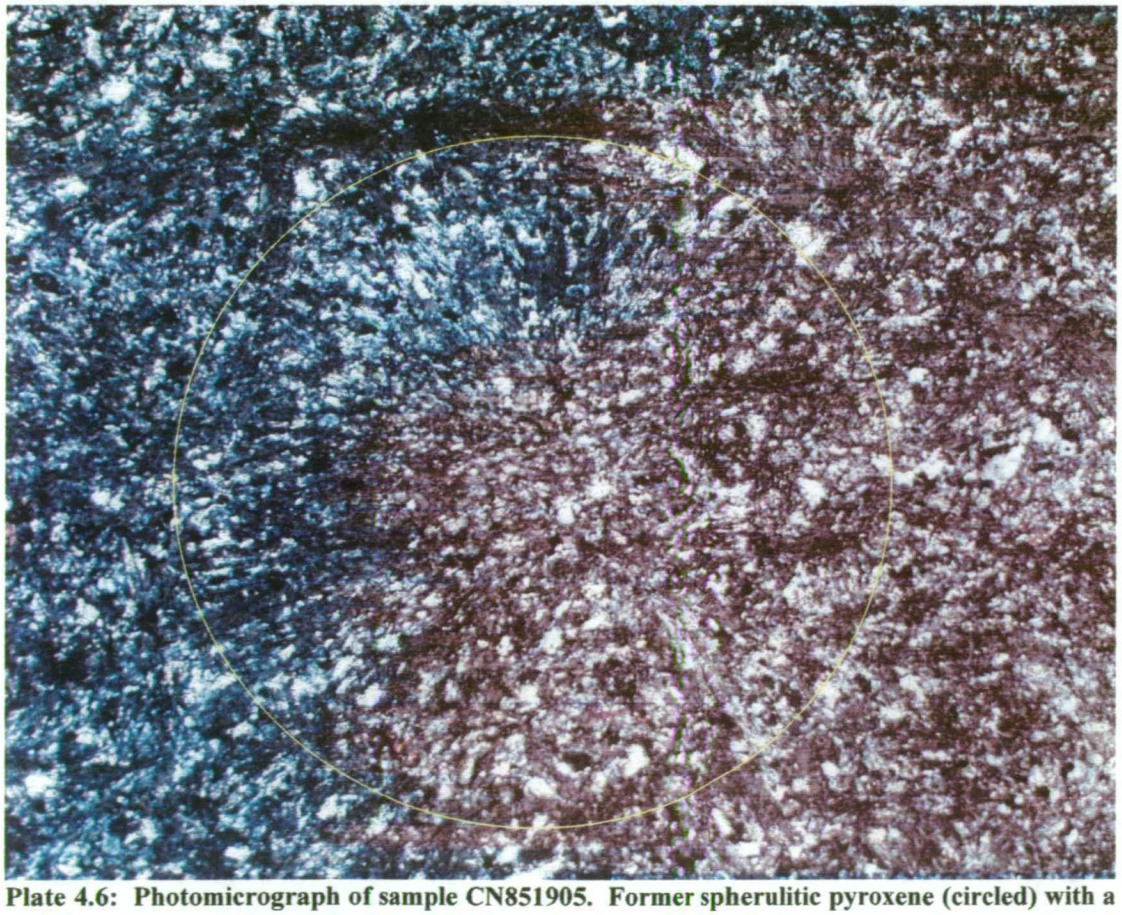

Plate 4.6: Photomicrograph of sample CN851905. Former spherulitic pyroxene (circled) with a radial texture, pseudomorphed by chlorite and calcite. Field of view 1.6 mm. Cross polarised light.

One thin section of an equigranular dolerite was examined (CN851901). Former plagioclase laths ranging in length from 1 to 4 mm are visible but are strongly altered by calcite and chlorite. Opaque grains range from 0.5 to 1 mm in diameter and possess a skeletal habit suggestive of ilmenite. A few grains of a former igneous phase now entirely replaced by calcite are identifiable by outlines formed by a brown mineral which may be iddingsite. One of the outlines has a shape typical for olivine and the iddingsite highlights former cracks through the mineral, a common characteristic of olivine. Like the basalts, the dolerite is heavily altered by fine-grained quartz-chlorite and carbonate mosaics, and no primary ferromagnesian phases are preserved.

4.4 INTERPRETATION OF THE BASALT PETROGRAPHY

4.4.1 Previous Studies

Petrographic studies of basaltic rocks around Norseman have been previously undertaken by Hallberg (1970) and Redman (1982). Hallberg (1970) found that partially-altered feldspar microlites and blades or needles of amphibole forming a feathery groundmass were ubiquitous and termed the rocks "uralitized basalts", concluding that there was no textural or mineralogical preservation of former igneous olivines or pyroxenes.

Redman (1982) undertook a comprehensive study of basalts between Kalgoorlie and Norseman using both petrography and geochemistry and his results differed substantially from those of Hallberg. Redman found that preserved igneous textures are common and concluded that the amphibole in Norseman rocks typically pseudomorphs acicular pyroxene. The work of Redman in subdividing the basaltic stratigraphy on the basis of geochemistry is discussed further in the mafic geochemistry section of this chapter (section 4.8). Redman's petrographic conclusions will be discussed below since they are relevant to the textures observed in the Chinaman's Well basalts.

From detailed work around Kalgoorlie and Kambalda, Redman (1982) recognised three basalt series:

- Siliceous High Magnesian Series Basalt (SHMSB);
- High Magnesian Series Basalt (HMSB); and
- Low Magnesian Series Basalt (LMSB).

The term "tholeiite" was avoided for reasons which are discussed in section 4.8.

The SHMSB and HMSB were largely distinguished using geochemistry and are difficult to separate on petrographic textures alone. SHMSB and HMSB can usually

be distinguished petrographically from the LMSB, because the former are characterised by variable quantities of altered skeletal olivines, hopper olivines, skeletal pyroxenes or dendritic pyroxenes. In contrast, LMSB basalts are typified by igneous plagioclase, which may be skeletal or lath shaped with interstitial dendritic, spherulitic or lath-shaped pyroxene forms. Variolitic textures formed by spherulitic pyroxene are generally better developed in the high magnesian rocks. It may, however, be difficult to distinguish the more MgO-rich LMSB from the lower MgO differentiates of the HMSB and SHMSB due to petrographic overlap. Redman found this to be more of a problem at Norseman than Kambalda.

The Paringa Basalt and Devons Consols Basalt sequences at Kambalda and Kalgoorlie were classified by Redman as SHMSB basalts. HMSB basalts were found to comprise the lower part of the Lunnon Basalt at Kambalda with a thickness of at least 1800 metres (the depth limit of the deepest drill holes) and were also found at Norseman within parts of the Mararoa Pillow Lava member of the Woolyeenyer Formation and the Penneshaw Formation. The sampling was not sufficiently methodical to delineate the limits of the HMSB at Norseman. The top 200 metres of the Lunnon Basalt was classified as LMSB as was the majority of the basalt that Redman sampled at Norseman from the lower Woolyeenyer and Penneshaw Formations.

4.4.2 Interpretation of the Chinaman's Well basalts

The samples of the Chinaman's Well basalts described in this study are generally more altered than those described by Redman (1982), with chlorite-quartz-carbonate mosaics commonly obliterating groundmass textures. This may be due to bias in the sample collection because available diamond drill holes all test gold prospects that may be broadly enveloped by carbonate alteration. Despite the alteration, plagioclase microlites can be recognised in the majority of the samples indicating they are LMSB in the classification of Redman (1982), which is compositionally equivalent to tholeiitic basalt.

The dearth of relict igneous textures in the causeway sample (CN851902) prevents the classification of this basalt on the basis of petrography. The apparent remnant dendritic pyroxenes in the sample may occur in all three basalt series (Redman, 1982). The basalt does, however, display some interesting alteration and metamorphic features. As the sample possesses little chlorite or plagioclase, the alumina analysed in the rock must be hosted by the amphibole with unusual blue-green pleochroism. Redman analysed amphibole with similar colours at Kambalda and found they were aluminous with hornblende compositions in contrast to the low alumina actinolite which have pale colours.

A second feature of interest in the causeway basalt is the prominent nodules, which appear similar in hand specimen to the varioles ubiquitous in the Devons Consols Basalt at Kambalda. Within the best preserved examples of the Devons Consols, Redman found the varioles are pyroxene-textured spherulites replaced by chlorite and plagioclase. More altered examples consist of sparse hornblende and chlorite grains in a quartz and plagioclase matrix with no preserved primary textures (Arndt & Jenner, 1986). The causeway nodules do not preserve spherulitic textures, but are finer-grained zones and may be heavily-altered varioles derived from pyroxene spherulites.

Sample CN851915 from Jewfish has a texture which suggests a more MgO-rich composition in the zone of petrographic overlap between the high and low MgO basalts. Plagioclase is sparse whereas skeletal pyroxene and spherulitic pyroxene textures more characteristic of high MgO basalts are preserved. There are also possible hopper olivine textures although this identification remains tenuous, being based on comparison with shapes illustrated by Redman (1982) that are also considered equivocal. However, the sample does not display the abundant skeletal and hopper olivines which, with skeletal pyroxene, characterise the SHMSB and HMSB.

The MgO content of the spinifex-textured rock from the Tuna Prospect (CN851948) is 10.4 wt % (volatile free), well below the required minimum of 18 wt % for the rock to be classified a komatiite. The pyroxene spinifex textures are consistent with the MgO contents. Komatiites typically have olivine spinifex textures rather than pyroxene and have MgO percentages ranging from 18 to 32 (Donaldson & others, 1986). The Tuna sample comes from a location close to the top of the Norseman komatiite. This would be consistent with the sample being a differentiated member of the komatiite succession and therefore a komatiitic basalt using the definition of Arndt & Brooks (1980).

4.4.3 Interpretation of the Polar Bear basalt

The pillowed nature of the basalt at the Polar Bear Peninsula indicates that it was erupted in water. The planar laminated and fine-grained nature of the interflow sediments is indicative of ambient sedimentation below wave base in an area starved of terrigenous sediment input.

Amygdale development is controlled by a combination of hydrostatic pressure and volatile content of the magma. The absence of amygdales can indicate either a low volatile content, a water depth sufficient to suppress vesiculation, or both. Conversely, the appearance of amygdales at the top of the sequence may indicate shoaling of the basaltic edifice, or a magma batch with unusually high volatile

contents. The water depth necessary to suppress vesiculation is imprecisely known. Wilson (1989) indicates that degassing of ocean floor basalts appears to be inhibited at depths greater than 200 m, and it is pointed out in section 4.11 that the basalts in this study are largely similar to N-type Mid-Ocean Ridge basalts. The maximum depth of possible vesiculation must certainly be less than 3000 m for sea water, which corresponds to the critical pressure above which the distinction between liquid and vapour phases does not exist and rates of expansion with pressure decrease are low (McBirney, 1963, cited in McPhie, 1998). Squire & others (1998) suggest a minimum emplacement depth of 700 m for poorly vesicular basalt at Kambalda, based on the presence of hyaloclastite and the absence of phreatic pyroclastic deposits. Hyaloclastite in pillow margins is also typical for the majority of the Woolyeenyer Formation.

Under the classification scheme of Redman (1982) discussed in section 4.4.1, the samples with abundant feldspar microlites are probably Low Magnesian Series Basalts (LMSB), a classification which is compositionally equivalent to tholeiitic basalts. The majority of the samples are more altered than basalts described by Redman (1982), however, one sample from north Polar Bear (CN851904) with amphibole and feldspar shows good preservation of igneous textures. In the latter sample, dendritic pyroxene textures are preserved in addition to plagioclase. Dendritic pyroxene is the characteristic mineralogy described by Redman for LMSB.

The basalt sample from southwest Polar Bear (CN851905) has plagioclase microlites but also possesses textures suggesting a higher MgO composition. Abundant spherulitic pyroxene, skeletal pyroxene and possible hopper olivine textures are preserved. The basalt is similar to sample CN851915 from the Chinaman's Well basalts, which was suggested to have a composition in the zone of petrographic overlap between the high and low MgO basalts. The MgO abundances at 7.2 wt% (volatile free), are higher than the other basalts, consistent with the petrographic features.

The basalt clasts within the mafic conglomerate have remnant feldspar lath textures, suggesting they are dominantly LMSB.

The dolerite has plagioclase laths, suggesting an LMSB composition. The ilmenite shapes of the opaques further suggests a high Ti content suggestive of a tholeiitic composition. The possible former olivines are consistent with this interpretation.

4.5 CONCLUSION

Of the seven samples from the Chinaman's Well basalts examined, petrographic techniques define five as LMSB using the classification of Redman (1982). The

LMSB are equivalent to tholeiite. Two samples were ambiguous, one having insufficient remnant igneous textures to characterise, the other having textures that place it in the zone of petrographic overlap between high and low MgO series. No basalt samples had definitive high MgO textures as possessed by the SHMS Devons Consols Basalt (DCB) and Paringa Basalt. This makes it doubtful that the Chinaman's Well basalts are stratigraphic equivalents to either the DCB or Paringa Basalt despite the apparently similar structural position in the hangingwall of the komatiite.

The Tuna sample has abundant pyroxene spinifex textures and may be a komatiitic basalt member of the Norseman komatiite.

Of the five basalt samples from the Polar Bear Peninsula, four have petrographic features indicative of the LMSB. One sample has textures that place it in the zone of petrographic overlap between high and low MgO series. No basalts were found with definitive high MgO textures. The Polar Bear basalt has similarities to the Chinamen's Well basalts.

4.6 INTRODUCTION TO GEOCHEMISTRY

During the 1990s, the volume of high precision major and trace element geochemistry available for rocks in the Eastern Goldfields has increased markedly. This work has led to geochemical signatures being recognised for a variety of stratigraphic units and intrusive rock types. Geochemistry can now be used to assist geological mapping and petrography to discriminate between volcanic successions and to identify the association of intrusive rocks, an advance that benefits this study. The major aim of geochemistry for this thesis is to identify the affinities of stratigraphic successions and thereby test the hypotheses raised in other chapters. The geochemistry also provides some insights into the petrogenesis of the rocks studied, which assists in elucidating the tectonic environment in which they were emplaced.

Layout of the geochemistry chapters

Major and trace element abundances were analysed for 60 samples. These comprised 28 mafic rocks, 29 felsic rocks, and 3 ultramafics. As discussed in Chapter 3, the mafic, ultramafic and felsic successions are all separated by sulfidic shale representing significant time intervals. There is no reason to suspect a geochemical linkage between the successions, hence, the geochemistry for the mafic, ultramafic and felsic rocks are considered separately. The geochemistry of mafic rocks is presented in this chapter, ultramafic rocks in Chapter 8 and felsic rocks in Chapter 9.

An introductory discussion about element mobility, trace element data and analytical techniques is presented below, which is applicable to all sample compositions.

4.6.1 Element Mobility

A problem for geochemical studies of ancient rocks is the mobility of some elements under conditions of metamorphism, hydrothermal alteration and weathering. Visible hydrothermal alteration and weathering were avoided when collecting samples, but all rocks collected for this study were deformed and metamorphosed to lower amphibolite facies.

Rollinson (1993) provides a summary of element mobilities. The most easily mobilised elements are generally the large ion lithophile elements (LILE) comprising Na, K, Ba, Rb, and Cs. Sr, Ca, Fe, Mg and Si may also be mobile. In contrast, the High Field Strength Elements (HFSE) are typically immobile during secondary processes and include Ti, P, Zr, Y, Hf, Nb, Ta, Th, U and the Rare Earth Elements (REE). Al is also generally regarded as immobile. Of the transition metals, Mn, Zn and Cu tend to be mobile, whereas Co, Ni and Cr are immobile.

Although REE are regarded as among the least soluble trace elements, they are not completely immobile. Humphries (1984) found no simple relationship between the degree of mobility of the REE and rock type or metamorphic grade and instead emphasised the importance of the mineralogy of the rock and composition of the fluid. REE are more susceptible to mobilisation from altered glassy volcanic rocks than crystalline rocks and are more easily mobilised by halogen or CO_2-rich fluids than aqueous compositions.

Published accounts of the mafic rock geochemistry at Kambalda and Norseman (Redman & Keays, 1985; Arndt and Jenner, 1986) are largely in accordance with the summary of Rollinson (1993) except that total Fe (Fe*) was found to be immobile, whereas the mobilities of Nb, Y and P were equivocal, with some inconsistent results that may be related to low-level analytical problems. McCuaig (1996) found that HFSE, REE, Al_2O_3, TiO_2 and MgO remained relatively unchanged by hydrothermal alteration and metamorphism at Norseman.

In this study, mobile elements are thought to include the LILE and Sr, based on erratic abundances in similar rock types. Ca and Si are also locally affected although this is not always easy to discern. In section 9.4, it is shown that the REE are extraordinarily immobile even during severe carbonation of rocks where all major element abundances are heavily altered.

4.6.2 Trace Element Geochemistry

Trace elements are often studied in groups and deviations from group behaviour or systematic behaviour within the group are used as an indicator of petrological processes (Rollinson, 1993). The rare earth elements (REE), metals with atomic numbers 57 to 71, are among the most useful of all trace elements due to their immobility and coherent group behaviour. Rollinson (1993) discusses the use of these elements. In this study, chondrite-normalised REE patterns are used and will be termed simply "REE patterns" for brevity.

Normalised multielement diagrams, commonly called spidergrams (Thompson & others, 1983), are an extension of the chondrite-normalised REE diagrams. A number of different element groups and ordering of the elements have been used for spidergrams.

There are a wide range of values used for normalising REE and spidergrams in the literature. Sun & McDonough (1989) compiled values for all the normalising agents in common use including C-chondritic meteorites and N-type Mid-Ocean Ridge Basalts (N-MORB). They also determined the order of incompatibility of trace elements in oceanic basalt to assist with ordering the elements in spidergrams by decreasing incompatibility. Their work is widely used, and is followed in this thesis. REE are normalised to C1-chondrites, and trace elements for spidergrams listed in the recommended order and normalised to N-MORB. Most of the LILE elements have been removed from the spidergrams as they are mobile and produce erratic patterns that obscure the overall picture.

Elements that deviate from a smooth trend in normalised REE patterns and spidergrams are known as anomalies. The size of the anomaly can be quantified by using a ratio that compares the actual value of the element with the value predicted from the trend of neighbouring elements with similar compatibility. Taylor & McLennan (1985) recommend using the geometric mean for these ratios and their suggested formula was used for Eu/Eu*. The formulas for Ti/Ti* and Nb/Nb* are those used by McCuaig (1996) and are listed in Table 4.2.

Trace elements are also useful for modelling petrogenetic processes in igneous rocks. In this study, Rayleigh fractionation, and assimilation-fractional crystallisation models are used to quantitatively assess the origin of some samples.

Theory

During the passage of magma towards the surface, continental crust may be assimilated. The heat required to melt the crust must come from the magma,

consequently cooling it and causing crystallisation (Wilson, 1989). The latent heat of crystallisation in turn produces thermal energy that may drive wall rock assimilation. Assimilation in magma chambers is, therefore, commonly concurrent with crystallisation. Where the crystallisation is fractional crystallisation, widely considered to be the usual case in mafic magma chambers, DePaolo (1981) termed the process Assimilation-Fractional Crystallisation (AFC). AFC processes give rise to magma suites with a positive correlation between indices measuring the degree of fractionation and incompatible trace elements indicating crustal contamination.

A second style of crustal contamination has been proposed for deep magma chambers at the base of the crust or upper mantle where fractional crystallisation proceeds without the involvement of assimilation due to the refractory nature of the wall rocks (Wilson, 1989). Magma that has undergone such fractionation, may rise to higher levels in the crust and become contaminated with more readily fusible wall rocks. However, only hotter, more primitive magmas are likely to show significant assimilation, resulting in a negative correlation between degree of fractionation and the degree of assimilation.

DePaolo (1981) and Powell (1984) developed equations for AFC processes (concurrent assimilation and fractional crystallisation), which describe the concentration of a trace element in a melt relative to the original magma composition and the crustal contaminant used. AFC equations of are used in this thesis.

4.6.3 Methods

Least-altered and weathered samples were collected for the geochemical studies. Diamond core was used as a sampling medium where available, particularly for basalt beneath Lake Cowan. Few diamond drill holes were available on the Polar Bear Peninsula so the majority of mafic and felsic samples from this area comprised rock chips from outcrops. Large samples without weathered joints were broken up and rock fragments free of weathering selected. These samples were supplemented with cuttings from reverse circulation holes drilled during the course of this study. Details of the samples and hole locations are tabulated in Appendix 2.

A major aim of the basalt geochemical study was to compare basalt from Chinaman's Well and the Polar Bear Peninsula with the lower Woolyeenyer Formation at Norseman, using detailed analyses provided by Ghaderi (1998). Ghaderi's work was undertaken using ANU research facilities and achieved detection limits as low as 1 ppb by using ICP-MS with the methods of Eggins & others (1997). For analytical quality control and to ensure comparability of the new analyses with those of Ghaderi, three basalt samples adjacent to intervals sampled by Ghaderi were selected for inclusion in the sample batches.

Samples were submitted to Analabs Pty Ltd in Perth for analysis in two batches five months apart. The first batch consisted of 24 samples which included three analytical quality control samples as described above. The second batch consisted of 43 samples including two quality control samples.

Samples were dried, jaw crushed to 6 mm and pulverised to a nominal 75 μm in a Cr-steel ring mill. Elements expected to be unreliable due to possible contamination from the mill are FeO*, Cr_2O_3 and MnO. Major elements were analysed by XRF on a fused glass disc and the volatile loss on ignition (LOI) at 1000°C was measured. For batch #1, a selection of 33 trace elements including the REE were analysed by ICP-MS using a 0.2 g split, digested in hydrofluoric, perchloric, hydrochloric and nitric acid. Elements with abundances greater than the upper detection limit of ICP-MS were analysed with ICP-OES using the same solution.

Several problems were identified in the initial analyses for batch #1. After further work with the laboratory, and re-analysis of the samples, adequate analyses were received, but analyses for Ta were excluded from the results for batch #1 basalt samples. In addition, Zr and Ti were re-analysed for the basalts from stored sample pulps using XRF on pressed powder pellets.

Following the problems encountered in batch #1, some changes in the analytical procedure were instituted for batch #2, which are described in Appendix 2. Changes included analysing Zr, Ba, Rb, Sr, Y, Zn, Cr and Ti using XRF on pressed powered pellets rather than ICP-MS. In batch #1, Bi did not register above detection so no further analyses of this element were undertaken. One remaining problem that could not be addressed was the anomalously low abundances of Hf measured by ICP-MS. Ghaderi (1998) investigated this problem and found Hf was not depleted when analysed by laser ablation on glass samples. Thus, it appears Hf is hosted by minerals that are resistant to acid dissolution. As Hf could not be analysed by XRF, anomalous depletions remain. To remove this effect, Hf has not been used in the spidergrams. Apart from Hf, all results for batch #2 are considered to be accurate as a result of the changes enacted.

Appendix 2 contains a full discussion of the analytical procedures.

4.7 INTRODUCTION TO MAFIC GEOCHEMISTRY

In detail, geochemical analysis was applied to mafic rocks for the following purposes:

- To test the hypothesis advanced from consideration of the stratigraphy at the Polar Bear Peninsula (Chapter 3), that the Norseman Terrane lacks the upper

basalt that overlies the komatiite in the Kambalda and Ora Banda Domains of the Kalgoorlie Terrane. If this is the case, the Chinaman's Well basalts north of the Norseman komatiite and the basalts at the Polar Bear Peninsula are lower Woolyeenyer Formation rocks that have been tectonically emplaced and should have similar chemistry to the lower Woolyeenyer Formation.

- To test a similar model suggested by CNGC geologists that the mafic part of the Penneshaw Formation is a structural repetition of the lower Woolyeenyer Formation.

- To compare analyses of Woolyeenyer Formation mafic rocks with the mafic units at Kambalda to assess the similarity and to match stratigraphy.

- To use the geochemical results and previous studies to assess possible models for the tectonic environment in which the basalts were erupted.

- To compare the composition of basaltic sand from a mafic conglomerate unit, with coherent basalts to determine whether they have comparable geochemistry, and therefore, whether the sand could be an eroded portion of the Chinaman's Well or Polar Bear basalt.

To achieve these aims, it was first necessary to determine the chemical characteristics of the lower Woolyeenyer Formation at Norseman, and the Kambalda mafic and ultramafic succession. The next section reviews previous geochemical studies that have been undertaken at Norseman and Kambalda.

Layout of the Mafic Geochemistry sections of this chapter

The geochemistry of the mafic rocks in the Norseman Terrane was not examined in isolation in this thesis, but was compared to other studies. Accordingly, I have reviewed previous work and produced a tabulation of geochemical groups that have been previously defined. Results from the new data collected for this thesis are then presented, similarly tabulated into groups with REE patterns, spidergrams. and a comment on the basis by which the results were grouped. Each of the groups is subsequently interpreted petrogenically and finally a conclusion is reached addressing the problems defined in section 4.7.

4.8 PREVIOUS STUDIES

4.8.1 Introduction

The results of previous basalt petrology studies at the Kambalda and Norseman areas are confusing. A number of significant geochemical studies have been previously carried out on the mafic stratigraphy at Kambalda and Norseman, but the authors

have each used their own terminology to name the groups they defined, and have treated their data differently. Data is generally not directly comparable between the studies. The mafic petrology requires a thorough review and clarification using modern concepts and standard terminology.

Such a clarification and review is outside the scope of this thesis. This thesis requires only an understanding of the previous results, and compilation of the available data in a standard format to determine what mafic geochemical groups have previously been defined at Kambalda and Norseman. This section documents the results of the previous studies. Data is then selected from some of these studies and compiled to create a list of all geochemical groups that have been previously defined.

4.8.2 Summary of conclusions of previous studies

In a major study of the geology in the Norseman area, Hallberg (1970) described the mafic rocks between Norseman and Coolgardie as tholeiitic with a remarkable lack of variation in major element chemistry. Hallberg also noted the presence of the komatiite series, which had been recently defined at that time.

During the 1970's, komatiite and magnesian basalt was redefined in the geological literature several times. Redman (1982) undertook a study of the mafic and ultramafic rocks between Norseman and Kalgoorlie with the objective of resolving the confusion in nomenclature and defining the mafic and ultramafic rocks rigorously. Redman noted that primary mineral textures could be recognised petrographically and combined this work with geochemistry to subdivide the mafic sequences into a number of different basalt series. Redman's petrographic studies are described in section 4.4; this section is restricted to the geochemistry.

Redman & Keays (1985) followed the work of Redman (1982) by proposing the subdivision of mafic and ultramafic rocks in the Eastern Goldfields into five series using a combination of trace element geochemistry and petrography:

- Low-Magnesium Series Basalts (LMSB) (MgO: 5-8.5%);
- High-Magnesium Series Basalts (HMSB) (MgO: 6-15%);
- komatiites (MgO >18%);
- Siliceous High-Magnesium Series Basalt (SHMSB) (MgO: 5-13%); and
- high iron tholeiites (MgO: 3-7%).

The latter series was not found by Redman (1982) but was based on published studies from other Archaean localities.

Redman & Keays did not provide characteristic SiO_2 abundances for the groups. However, perusal of their chemical data indicates that SHMSB typically has SiO_2 abundances of 52.7-54.7%, although abundances do become as low as 46.7% and as high as 57.3% in variolitic units. For comparison, LMSB and HMSB typically have SiO_2 abundances of 48.9-52.4%.

The HMSB and the SHMSB each comprise a high and a low MgO member with contrasting petrographic features, the two members being related by differentiation. The MgO abundances at the boundary between the high and low MgO members for each series are set at 9% MgO for the HMSB and 9.5% for the SHMSB.

Redman (1982) and Redman & Keays (1985) chose not to use the term "tholeiite" for any basalts at Kambalda or Norseman as both the LMSB and low MgO members of the HMSB have compositions that would be classified as tholeiite, but the distinction between these two series was considered important. Chemically, the basis of the subdivision is the lower PGE concentrations of the LMSB in comparison to the HMSB, SHMSB and komatiites. The low PGE abundance in the LMSB was attributed to S-saturation and consequent sulfide fractionation, which did not occur in the other series. A second difference is that textures of the low MgO member of the HMSB indicate higher eruption temperatures than the LMSB, although these two types cannot always be distinguished petrographically.

The LMSB, HMSB and komatiites are all slightly depleted in LREE relative to chondrites. In contrast the SHMSB are variably enriched in LREE, LILE and Zr and also have distinctly higher SiO_2. Redman & Keays (1985) suggested the former were all derived from a mantle source in which the prior removal of a small proportion of melt had lowered the concentrations of incompatible elements leaving a still relatively fertile mantle. Hydrous partial melting in a mantle source enriched in LILE and LREE was suggested to explain the siliceous yet magnesian-rich character of the SHMBS, and their elevated incompatible element abundances.

Redman & Keays (1985) found the upper 200 m of the Lunnon Basalt at Kambalda, most of the lower Woolyeenyer Formation and the mafic part of the Penneshaw Formation at Norseman, to comprise LMSB. The low MgO member of the HMSB was found to be minor at Norseman, occurring in parts of the Mararoa Pillow Lavas member of the Woolyeenyer Formation and in parts of the Penneshaw Formation. However, the low MgO member of the HMSB comprises all of the Lunnon Basalt below the top 200 m; a thickness of at least 1800 m, the depth limit of the deepest drill holes. The Devons Consols Basalt (DCB) and the Paringa Basalt at Kambalda were classified as SHMSB but were not found at Norseman (for further stratigraphic information, see section 1.2 for Norseman and section 2.4.2 for Kambalda).

An important paper was published in 1986 that changed the interpretation of the genesis of the basalts at Kambalda. The basalts were discovered to contain zircons with ages between approximately 2.7 Ga and 3.5 Ga (Compston & others, 1986). The zircons were interpreted as xenocrysts that were absorbed by a komatiitic magma parental to the basalt, as it assimilated older crustal basement on the way to the surface. The majority of zircon ages are around 3.1-3.2 Ga, taken to be the age of the crustal basement. The implications from this work were twofold: first, it confirmed that the greenstones were emplaced over sialic basement; and second, the upper basalts (DCB and Paringa Basalt), with their unusual incompatible element-enriched geochemistry, were formed by contamination of komatiite with crustal material.

Arndt & Jenner (1986) tested the implied crustal contamination with petrogenetic modelling. They first collected extensive geochemistry including REE for the komatiite and upper basalts at Kambalda, which allowed them to divide the upper basalts in greater detail than previously achieved. The Devons Consols Basalt and Paringa Basalt, which had been both classified as SHMSB by Redman & Keays (1985), were now seen to differ in that the former has only moderate LREE enrichment, whereas the latter has pronounced enrichment. In addition, the Devons Consols Basalt was further subdivided into two members, one having higher SiO_2 (up to 60 wt%) and lower MgO and FeO than the other. Arndt & Jenner (1986) suggested that the higher SiO_2 basalts have chemistry similar to ocelli-rich (variolitic) basalts, whereas the lower SiO_2 samples are more like the mafic matrix to the ocelli (varioles). Arndt & Jenner noted that the presence of spinifex textures and an association with the komatiite would normally qualify the Devons Consols Basalt to be classified as komatiitic basalt, but they did not do so, as they believed the chemical characteristics preclude a direct genetic relationship with the underlying komatiites.

Arndt & Jenner (1986) assessed the effect of fractional crystallisation and found it does not explain all the variations in the chemistry of the DCB and Paringa Basalt. The elevated abundances of Zr and Nd in the DCB and Paringa Basalt is best explained by crustal contamination, as these elements are enriched in continental crust, whereas V, Sc and Ti are not elevated, and these elements are relatively depleted in the crust. AFC models indicated that an average Paringa Basalt composition could be produced by adding 24% of a contaminant with the average modern upper crust composition of Taylor & McLennan (1981), to magma with the composition of a non-cumulate komatiite from Munro Township. This involves an assimilation to fractional crystallisation ratio of 0.4 accompanying 60% olivine, clinopyroxene and orthopyroxene fractional crystallisation. The other basalts in the sequence may have involved less contaminant, approximately 2% for the Lunnon Basalt and 5% for the Devons Consols Basalt. The composition of Kambalda

komatiite was not used for the initial magma composition because it has an anomalously high SiO_2 abundance in comparison with komatiite from other areas, perhaps due to later alteration, and it produces model basalts with SiO_2 contents slightly too high. If more mafic contaminants were used, such as average lower crust or Archaean crust estimations, then the concentrations and ratios of incompatible elements in the most extreme Paringa Basalts could not be generated.

The use of a highly evolved contaminant has been supported by the results of Nb/U studies. Hofmann & others (1986) found that the Nb/U values in OIB and MORB are nearly constant at 47±10 and quite different from the primitive mantle ratio of 30. In contrast the Nb/U of continental crust averages about 10 (Rudnick & Fountain, 1995). Sylvester & others, (1997) showed that the Nb/U decreased up the stratigraphy at Kambalda, supporting the accepted view that the upper basalts and dolerites have been contaminated with crust. The Paringa Basalt has Nb/U values lower than average crust, suggesting a highly evolved contaminant with Nb/U of approximately 3-4 if the degree of contamination was approximately 25%. Sylvester & others (1997) also argued that the high values for Nb/U in the Lunnon Basalt at Kambalda (30-47) indicate derivation from a mantle which may have been depleted by prior extraction of a large fraction of continental crust.

Subsequent studies have claimed success modelling the upper basalts at Kambalda using other AFC combinations. Sun & others (1989) modelled the Paringa Basalts using 14% assimilation of felsic crust by Al-undepleted komatiitic magma with 24 wt% MgO, and approximately 35% fractional crystallisation. Morris (1993b) found that assimilation of a 10-15% calc-alkaline granitoid (A/FC=0.5) by a komatiite accompanied by 20-30% fractional crystallisation produced a reasonable fit to the Wongi Basalt in the Ora Banda Domain.

Morris's choice of the Wongi Basalt as a representative of the upper basalts is odd considering that it lies below the ultramafic unit. The reasoning behind the choice is not explained but may be related to the reinterpretation of the stratigraphy by Morris (1993b) based on ratios of Ti, Zr and Al_2O_3. That methodology is not followed in this thesis as a wider range of elements, particularly the REE appear to be necessary to correctly classify the basalts.

A useful contribution by Morris (1993b) was an effort to standardise the nomenclature used to classify the basalts based on the Jensen cation plot, which is designed for mafic and ultramafic rocks. This plot uses the proportions of the cations Fe(total) + Ti, Al and Mg, which show variability in subalkaline rocks and tend to be stable under low grades of metamorphism (Rollinson, 1993). The Jensen cation plot is useful for classifying Archaean metavolcanics because it has individual fields for

komatiite, komatiitic basalt, High Mg tholeiitic basalts (HMTB), High Fe tholeiitic basalt (HFTB) and calc-alkaline basalt (CAB), as well as all the intermediate and felsic divisions.

Morris (1993b) found that the upper part of the Lunnon Basalt (LMSB) plots in the HFTB and CAB fields on the Jensen plot, whereas the lower parts (low MgO member of HMSB) plots in the HMTB field, a result consistent with the findings of Redman & Keays (1985). Morris (1993b) considered the Devons Consols Basalt to be the upper part of the komatiite unit due to its geological and geochemical affinities despite the objections raised by Arndt & Jenner (1986) who demonstrated the contaminated geochemistry. The Devons Consols Basalt plots in the Calc-Alkaline Basalt (CAB), HMTB and komatiitic basalt fields of the Jensen cation plot. The Paringa Basalt spans a similar range. The wide range is considered to be due to the variability in composition of these basalts. Overall, these units are crustally contaminated komatiite and have a siliceous high magnesium composition, consistent with the samples classified as HMTB and komatiitic basalt by the Jensen Plot. The CAB samples are undoubtedly highly variolitic, and therefore, siliceous.

Morris found that 69 analyses from the Woolyeenyer Formation at Norseman plot in a tight range spanning the HFTB and HMTB fields on the Jensen cation plot. Three intrusive dykes at Norseman have komatiitic basalt chemistry. The dykes have steep REE patterns that Morris (1993b) suggested maybe the first recorded occurrence of mafic rocks from an Ocean Island Basalt-type mantle source.

McCuaig (1996) examined the mafic rocks in the lower Woolyeenyer Formation using his own samples and some from Morris (1991) and divided them into six groups based on trace elements:

- tholeiitic basalt and gabbro, which constitutes the majority of the formation;
- High-MgO Tholeiitic intrusives (HMT) with similar spidergrams to the tholeiites at slightly lower abundances;
- Enriched High-MgO Tholeiite (EHMT), which are the samples of dykes from a single drill hole which Morris (1993b) likened to OIB;
- two groups of Enriched Tholeiites (ET1 & ET2) with high abundances of LREE; and
- one sample called a Transitional High-MgO Tholeiite (THMT) due to its characteristics transitional between HMT and EHMT.

The EHMT is strongly enriched in LREE, so McCuaig (1996) undertook AFC modelling to determine whether it could be produced by crustal contamination of magma. Several compositions were used for the starting magma, with a range of contaminants, but no combination could produce EHMT trace element abundances. McCuaig noted a number of important compositional differences between the EHMT and the Paringa Basalt at Kambalda, the latter considered to be crustally contaminated magma. For the EHMT, these include a greater LREE enrichment, a stronger fractionation in the HREE and the lack of an enrichment in SiO_2, which would be expected with crustal assimilation. McCuaig also concluded that the ET and THMT were unlikely to be produced by crustal contamination. Instead, he proposed that variable mixing of EHMT and HMT composition magmas at depth, followed by fractional crystallisation, produced ET and THMT. The abundant tholeiites were proposed to be end-members following clinopyroxene and plagioclase fractional crystallisation of HMT magma.

McCuaig (1996) noted that the incompatible element depletion in the tholeiites and HMT magmas is extremely common in Archaean terranes and is very similar to recent MORB, widely considered to be derived from melting of depleted upper mantle (Wilson 1989). McCuaig considered the EHMT magma to be similar to OIB and interpreted a genesis involving residual garnet in the source to account for the strong REE fractionation.

Ghaderi (1998) undertook extensive geochemical analysis of samples from Norseman and Kambalda to correlate the stratigraphy. The lower Woolyeenyer Formation is geochemically the same as the Lunnon Basalt having similar major element abundances, LREE depletion and Nd isotopic values. In addition, Ghaderi noted identical trace element compositions in the lower and upper parts of the Lunnon Basalt and suggested that the differences documented by Redman & Keays (1985) are not significant. The existence of the Norseman komatiite was well known by the time of Ghaderi's study and drill samples from the island outcrop were found to be LREE-depleted, similar to the non-contaminated samples of Kambalda Komatiite. They do not show Nb or Ta depletion, precluding significant crustal contamination.

Ghaderi (1998) was aware of the implication that the basalt overlying the Norseman komatiite should resemble the Paringa and Devons Consols Basalts overlying the Kambalda Komatiite, but, due to limited availability of drill core at that time, he was only able to test the Chinaman's Well basalts with five samples from the Swordfish Prospect. These samples are characterised by high MgO contents similar to those of the Paringa Basalt. However, the lower average SiO_2 contents, slight depletion in LREE and high Nb/U values clearly distinguish these samples from the basalts above

the Kambalda Komatiite. Ghaderi suggested that the Swordfish samples are geochemically similar to the Lunnon Basalt and suggested three possibilities to account for this result:

- a facies change between Norseman and Kambalda;
- a major, unrecognised fault above the Norseman komatiite repeating the lower Woolyeenyer Formation; or
- the possibility that the Swordfish samples are the equivalent of the upper basalts at Kambalda, but have not been crustally contaminated.

4.8.3 Discussion

The mafic stratigraphy at Kambalda is now typically defined as starting with Archaean tholeiites of the Lunnon Basalt and followed by komatiite series rocks with a general increase in crustal contamination with increasing stratigraphic height (Ghaderi, 1998). The Devons Consols Basalt is generally considered to be the upper, crustally contaminated, basaltic section of an extended Kambalda Komatiite package. The Paringa Basalt is separated from the extended komatiite by the Kapai Slate, so it is commonly called the "upper hangingwall basalt".

It is notable that the Paringa Basalt, which is the mafic rocks most strongly contaminated with crust at Kambalda, has prominent Nb, Ta and Ti depletion. Depletion of these elements is commonly considered to be the signature of convergent margin plate tectonic processes. It seems that the contaminant in the lower crust must have possessed this signature, a conclusion consistent with findings from granite studies which have found a similar signature for granites thought to be sourced from the lower crust (see section 8.5.2). The small range of trace element abundances for the Paringa Basalt led Ghaderi (1998) to suggest that the magma was homogenised after contamination, implying a long-lived magma chamber at deep crustal levels.

The suggestion by Ghaderi (1998), that the differences Redman & Keays (1985) documented for the upper and lower Lunnon Basalt are not significant, ignores the evidence of petrography and differing PGE abundances. The latter authors used this evidence to suggest lower temperatures and fractionation of sulfide for the upper Lunnon Basalt and the majority of the basalts at Norseman.

The majority of basalts in the lower Woolyeenyer Formation have been found to be N-MORB tholeiites. However, McCuaig (1996) also identified five other volumetrically minor compositions, particularly in dykes, none of which appear to be equivalent to basalts defined at Kambalda. McCuaig interpreted one of these

magmas, HMT, to be a primitive, high-MgO product of melting depleted upper mantle which, following fractional crystallisation of clinopyroxene and plagioclase, resulted in the tholeiites. Another magma, EHMT, was interpreted to have left residual garnet in the source implying a melt generated at depth within the mantle rising as a plume similar to those that generate OIB (McCuaig, 1996). Dykes with the EHMT composition are scarce, having been found only at Norseman and only in one drillhole. The other three magma compositions are interpreted to be the product of mixing HMT and EHMT.

Ti/Zr has been used to subdivide basalts of the Eastern Goldfields by Morris (1993). The ratio was originally used by Redman & Keays (1985) on the basis that the elements are cheap to analyse, reliable (being immobile under low grade metamorphism), and both elements are incompatible in common mantle minerals, so changes in the ratio should indicate different mantle compositions. However, the work of Compston & others (1986), which demonstrated that zircons and therefore, Zr, have been inherited by basalts from assimilated crust, makes interpretation of the ratio problematic. The Paringa Basalt invariably has lower Ti/Zr than other basalts at Kambalda, probably due to the effects of crustal assimilation; Zr increases while Ti does not, due to its low abundance in the contaminant, hence Ti is decreased by dilution.

REE are the most reliable method for separating the different basalts at Kambalda because the crustal contaminant was highly enriched in LREE and has imparted this characteristic to contaminated basalts. The advantage of REE over Ti/Zr is that a number of elements, commonly 12 to 15, which all behave in a similar manner are used, rather than just two.

4.9 COMPARISON OF DATA FROM PREVIOUS STUDIES

4.9.1 Introduction

Section 4.8 synthesised previous basalt studies to obtain a view of the basalt genesis and how the geochemistry should be considered. However, due to the differing classification schemes and nomenclature used, it remains unclear exactly how many groups have been defined by these studies. It is also unclear as to which parameters and values define the particular groups since the data has been treated slightly differently in each study. This section addresses these problems and generates a reference dataset to which the new basalt geochemistry collected for this study can be compared.

4.9.2 Results

High precision geochemical data from the lower Woolyeenyer Formation (McCuaig, 1996) and Kambalda (Ghaderi, 1998) is compiled in this section. To maintain consistency and comparability, the existing data and new data collected for this study have been treated in the same way. All the major element data were analysed by XRF. Iron oxide is calculated as FeO(t) and major element oxides are then recalculated to total 100%, the volatile-free basis. Trace elements were analysed using XRF and ICP-MS although Ghaderi (1998) obtained extremely high precision by using ICP-MS with the methods of Eggins & others (1997).

To avoid burdening the text with geochemical descriptions, the data is presented in Table 4.3 as ratios and values that together describe the geochemical characteristics of the various groups defined in the literature. The parameters in Table 4.3 are explained in Table 4.2. The groups used are the six defined by McCuaig (1996) for the lower Woolyeenyer Formation; plus the Devons Consols Basalt, the Paringa Basalt and the Lunnon Basalt from Kambalda, with the Lunnon basalt divided into two groups (LMSB and low MgO member of HMSB) based on the work of Redman & Keays (1985).

Some of the parameters in Table 4.2 are similar to those listed by McCuaig (1996 - his Table 3.3), but the values ascribed to the same groups differ, due to differing treatment of the same data. McCuaig listed major elements that were not recalculated to total 100% so his absolute values are lower than those presented in this study. Ratios using Ti also differ as the abundance of this element was calculated from the major element oxide percentage (TiO_2). Other changes are that Mg number (Mg_no) in this thesis is calculated as the molecular ratio rather than the weight%, and the values used to normalize the REE and trace elements in this thesis differ from those used by McCuaig. In this study, all normalizing values for trace elements are those published by Sun & McDonough (1989) and comprise C1-chondrite for REE ratios (including Eu/Eu*) and N-MORB for Sr/Sr*, Ti/Ti* and Nb/Nb*, to maintain consistency with the normalised REE plots and spidergrams respectively.

The data is also presented graphically as a series of plots: a Jensen cation plot for classification; bivariate plots which divide the samples up into groups; REE patterns; spidergrams; and a Winchester and Floyd (1976) discrimination diagram.

Alkalies versus silica bivariate plots are not used for classification due to the mobility of LILE as noted in section 4.6.1. Jensen cation plots are more reliable as Al, Mg, Fe and Ti, which are used by the diagram, are typically less mobile than the alkalies although Fe may be somewhat altered. The Jensen plot also removes one of the

effects of the "constant sum problem" of major elements being expressed as percentages in that additions or subtractions of mobile elements not used for the diagram, do not affect the plotted positions of samples. This is because the diagram is ternary and the ratios between the Al, Fe+Ti and Mg remain the same irrespective of the behaviour of other elements. However, statistical problems of induced correlations do occur with the diagram (Rollinson, 1993).

Fields are drawn on the bivariate plots enclosing sample groups (figures 4.3, 4.4 and 4.6). The same fields are used on similar bivariate plots later in the chapter to assist comparison between data collected in this study and the reference sample groups.

The bivariate plots are used in this section and section 4.10.3 to define fractionation trends for some basalt groups. The justification for this is based on the tight clustering of the samples in the groups for simple bivariate plots of immobile elements (figures 4.3, 4.4, 4.15a to 4.15f). Although all the samples in a group such as the tholeiites are unlikely to be sourced from a single fractionating magma batch, the marked similarity in trace element abundances for the samples suggest that all the tholeiites were derived from a similar primitive magma, which fractionated under similar conditions so that trace elements and major elements behave in a consistent manner. Batches of magma with a different source or magmas which fractionated differently have already been separated into different groups by McCuaig (1996) and Ghaderi (1998).

A legend is presented as Table 4.1, explaining the variety of symbols used in the plots.

Table 4.1: Symbol legend for diagrams in Chapter 4, mafic rocks.

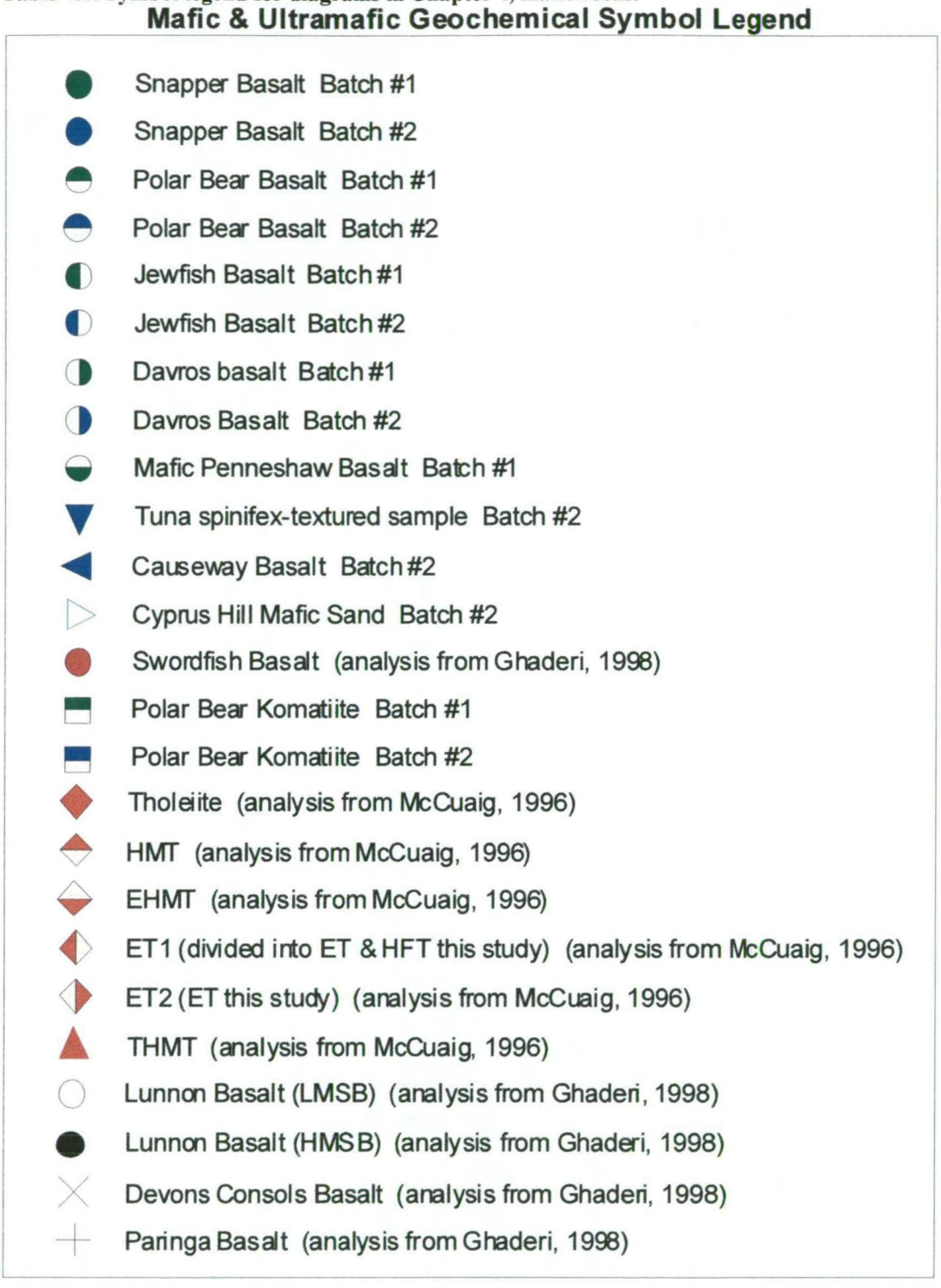

Table 4.3: Parameters which describe the geochemical characteristics of the groups defined by McCuaig (1996) and Ghaderi (1998).

GROUP	EHMT	ET1	ET2	THMT	HMT	Tholeiite	Lunnon LMSB	Lunnon HMSB	Devons Consols	Paringa
Area	Norseman	Norseman	Norseman	Norseman	Norseman	Norseman	Kambalda	Kambalda	Kambalda	Kambalda
Analyses by:	McCuaig	McCuaig	McCuaig	McCuaig	McCuaig	McCuaig	Ghaderi	Ghaderi	Ghaderi	Ghaderi
No. of samples	6	2	4	1	15	15	15	3	10	6
Jensen classification	komatiitic basalt	high-Fe tholeiite	high-Fe tholeiite	komatiitic basalt	komatiitic basalt	high-Mg T - high-Fe T	CA & Thol And. - Bas.	high-Mg tholeiite	CA-And - high-Mg T.	high-Mg T. - kom.bas.
SiO_2 wt%	47.1-51.0	52.0-54.8	50.3-51.2	53.2	49.1-51.6	50.0-55.0	49.1-56.44	47.3-51.8	50.3-60.7	51.3-54.7
TiO_2 wt%	1.3-2.0	1.1-1.8	1.6-1.9	0.7	0.4-0.8	0.7-1.2	0.88-1.36	0.68-0.74	0.64-0.85	0.60-0.65
Al_2O_3 wt%	6.2-8.8	14.7-14.8	13.6-14.4	4.7	10.2-15.3	14.2-15.6	14.9-23.89	14.0-15.2	13.8-17.9	12.1-13.8
MgO wt%	14.1-15.9	5.1-7.6	5.3-6.2	15.2	12.2-18.2	5.0-8.2	2.3-8.3	7.4-9.7	3.3-8.4	8.4-12.4
Cr ppm	936-1706	71-181	62-90	1180	1250-1950	112.322	286-522	302-356	482-696	429-917
Ni ppm	716-1384	124	61-65	-	333-379	65-132	53-163	100-124	175-331	119-248
U ppm	0.43-0.62	0.12-0.18	0.21	0.22	0.03-0.12	0.03-1.06	0.02-0.06	0.04-0.06	0.18-0.21	0.72-0.83
Al_2O_3/TiO_2	4.0-4.6	8.4-13.5	7.5-8.3	6.8	14.2-30.0	12.1-21.9	16.2-17.7	20.6-21.4	20.1-22.8	19.9-22.0
CaO/Al_2O_3	1.3-2.2	0.6-0.7	0.8	2.8	0.6-0.8	0.6-0.8	0.2-1.0	0.8-1.1	0.5-1.0	0.7-1.0
Ti/Zr	78-83	92-93	88-101	65	90-110	90-110	114-167	112-252	61-67	51-57
Zr/Y	7.7-8.0	3.8-4.0	4.1-4.9	5.4	2.1-3.2	2.1-3.2	1.8-5.2	1.0-2.4	2.7-3.7	3.9-4.4
Mg#	64-70	45-56	42-45	69	65-74	46-61	32-56	53-58	46.2-67.3	59-69
M/Si	0.63-0.73	0.31-0.39	0.37-0.41	0.62	0.57-0.72	0.29-0.46	0.23-0.45	0.40-0.54	0.16-0.40	0.39-0.53
(La)N	67-123	27-29	42-47	19	5-11	9-18	7-13	9-11	17-22	35-40
$(La/Yb)_N$	9.8-11.9	1.3-2.5	3.2-3.7	2.7	0.9-1.2	0.7-1.2	0.8-1.0	0.8-0.9	1.3-1.7	3.6-4.0
$(La/Sm)_N$	2.8-3.2	1.1-1.6	1.4-1.5	1.2	0.8-1.0	0.7-1.1	0.8-0.9	0.8-0.9	1.2-1.4	2.7-2.8
$(Gd/Yb)_N$	2.4-2.6	1.2-1.4	1.8-1.9	1.9	0.9-1.1	1.0-1.2	0.9-1.1	1.0-1.1	1.0-1.2	1.1-1.2
REE patterns	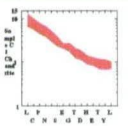	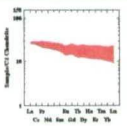	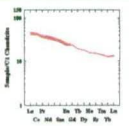	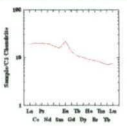	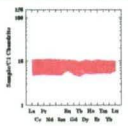	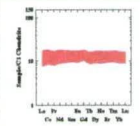	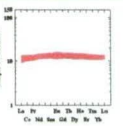	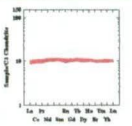	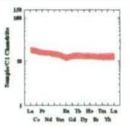	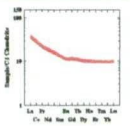
Eu/Eu*	0.8-1.0	0.9-1.0	0.9-1.0	1.6	0.8-1.6	0.8-1.0	0.6-1.1	0.9-1.1	0.7-0.9	0.9
Sr/Sr*	0-0.1	0.6	0.3-0.6	0.3	0.9-2.5	1.1-1.7	0.8-2.6	1.2-2.3	0.5-1.8	0.8-1.2
Ti/Ti*	0.9-1.0	0.9-1.0	0.9-1.0	0.7	0.7-1.3	0.8-1.0	1.0-2.3	0.9-1.0	0.7-0.8	0.7-0.8
Nb/Nb*	0.4-0.7	0.8	0.8-0.9	1.1	0.7-1.0	0.7-1.2	0.7-1.6	0.8-0.9	0.5-0.7	0.2-0.3

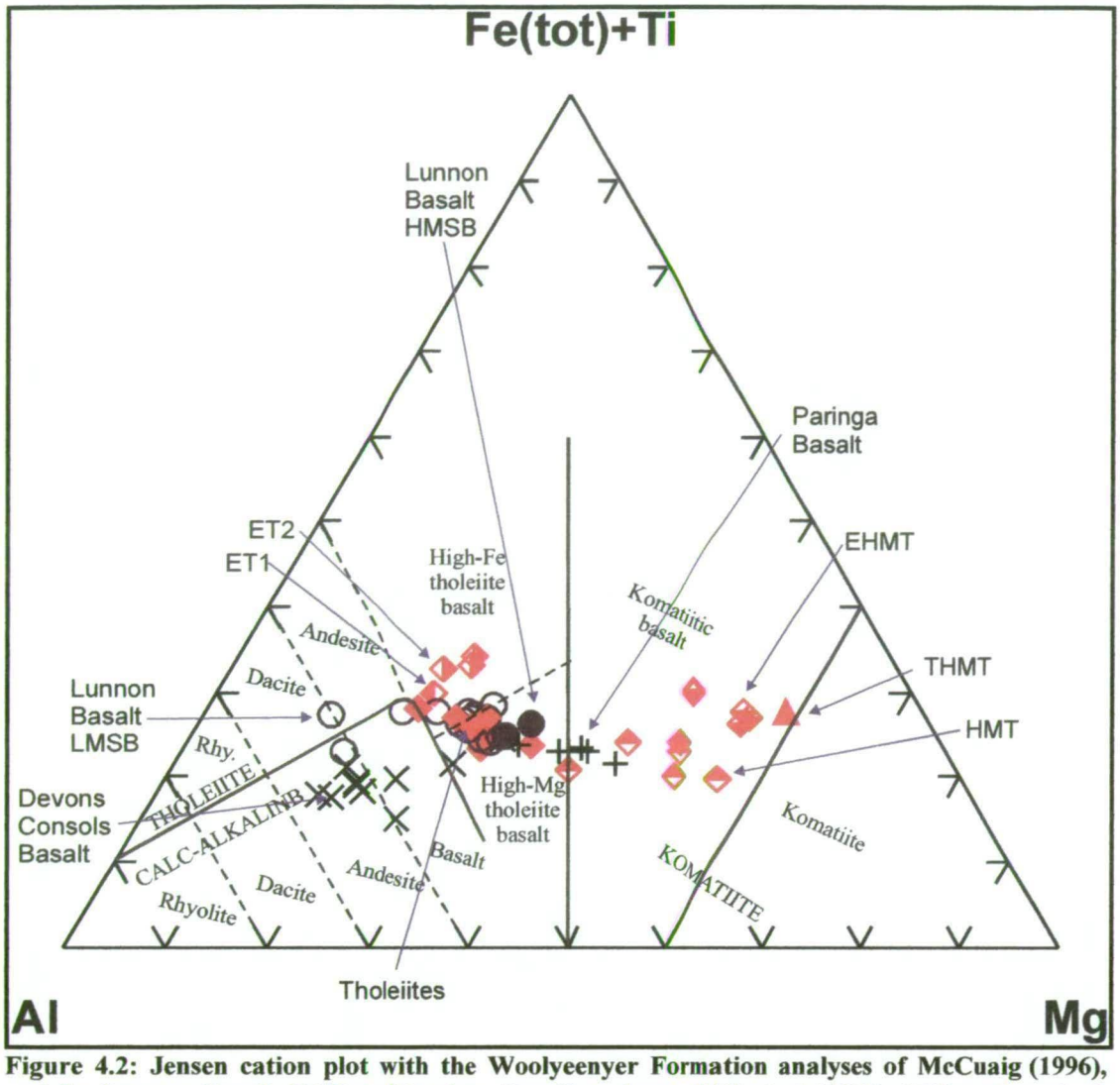

Figure 4.2: Jensen cation plot with the Woolyeenyer Formation analyses of McCuaig (1996), and the Lunnon Basalt, DCB and Paringa Basalt analyses of Ghaderi (1998). Different symbols represent the different groups tabulated in Table 4.2. The arrows point to a single representative of each group; all other symbols of that type are the same group.

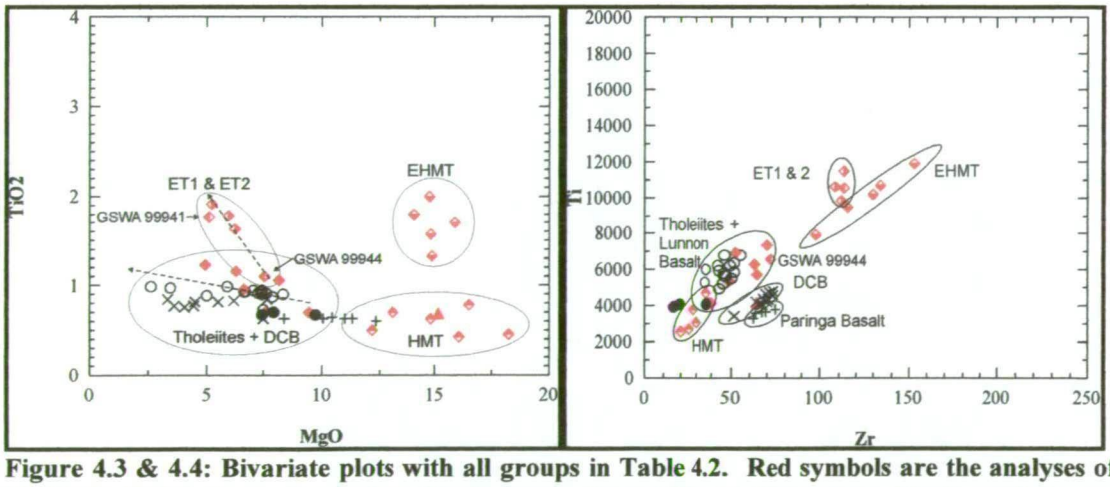

Figure 4.3 & 4.4: Bivariate plots with all groups in Table 4.2. Red symbols are the analyses of McCuaig (1996) from the lower Woolyeenyer Formation at Norseman; black symbols are analyses of Ghaderi (1998) from Kambalda. 4.3: TiO_2 vs MgO. Groups described by McCuaig form separate clusters. Dotted lines show general fractionation trend of tholeiites and run through ET1b and ET2 samples (see text). 4.4: Ti vs Zr (ppm). DCB and Paringa Basalt forms separate trend.

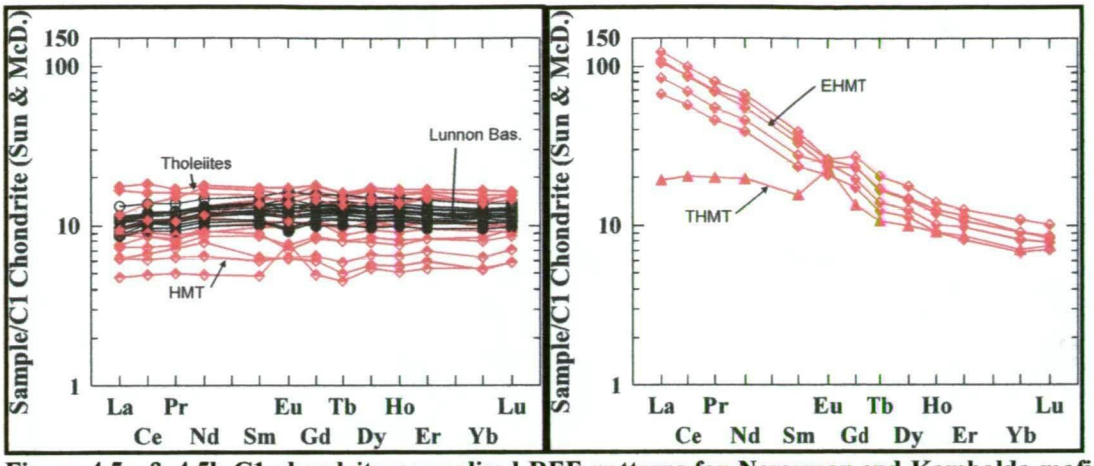

Figure 4.5a & 4.5b:C1-chondrite normalised REE patterns for Norseman and Kambalda mafic rocks using the normalisation factors of Sun & McDonough (1989). 4.5a has tholeiites and HMT from the lower Woolyeenyer Formation (analyses: McCuaig, 1996) (red diamonds); and Lunnon Basalt LMSB & HMSB from Kambalda (analyses: Ghaderi, 1998) (black circles). 4.5b has EHMT and the single THMT samples from the lower Woolyeenyer Formation (analyses: McCuaig, 1996).

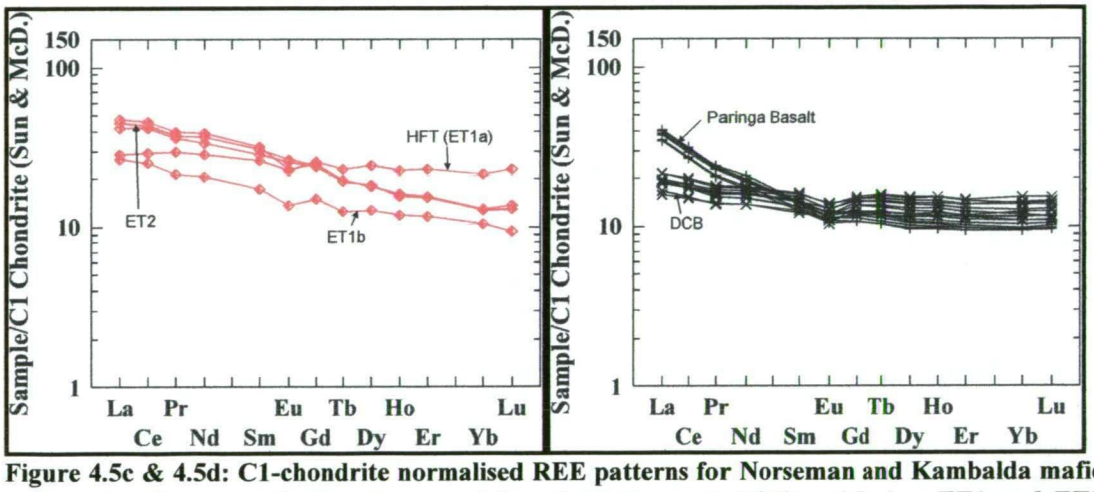

Figure 4.5c & 4.5d: C1-chondrite normalised REE patterns for Norseman and Kambalda mafic rocks using the normalisation factors of Sun & McDonough (1989). 4.5c has ET1 and ET2 samples from the lower Woolyeenyer Formation, the former divided into ET1a and ET1b (see text) (analyses: McCuaig, 1996). 4.5d has DCB and Paringa Basalt samples (analyses: Ghaderi, 1998).

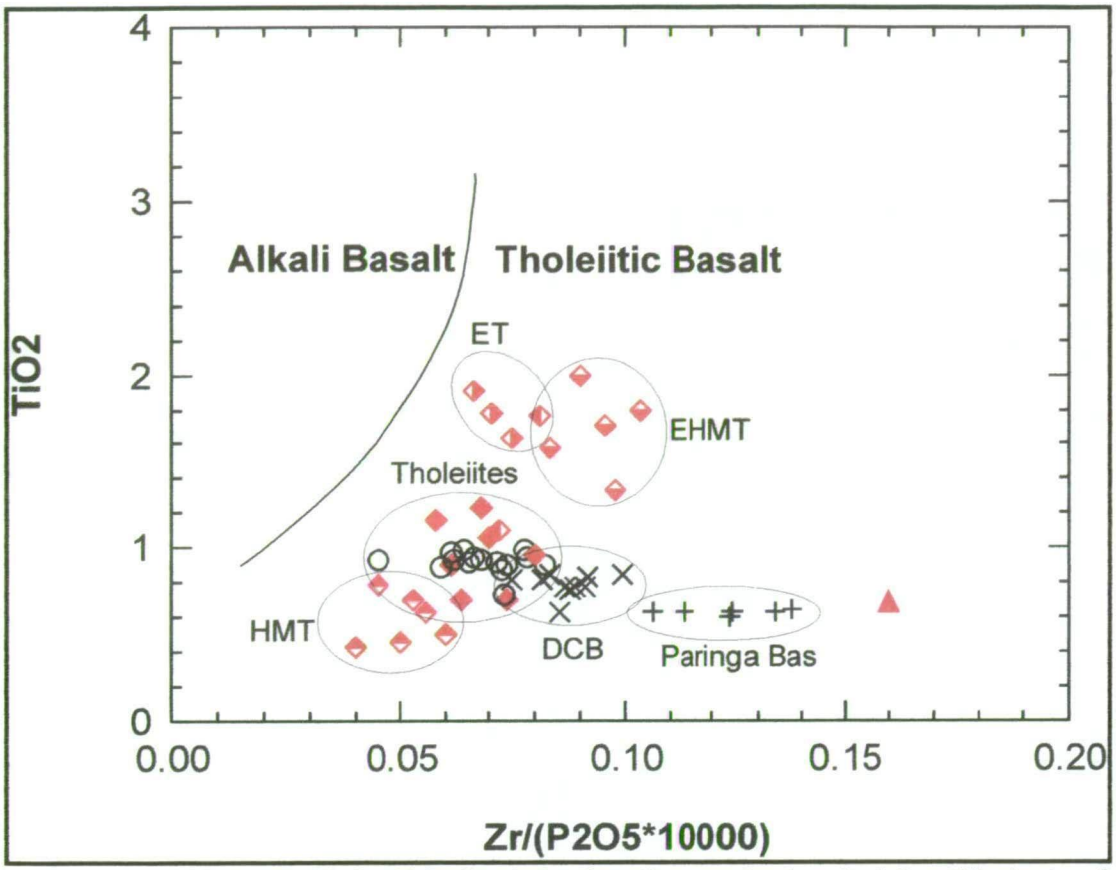

Figure 4.6: TiO_2 vs $Zr/(P_2O_5x104)$ discrimination diagram for basalts (after Winchester & Floyd, 1976). Red symbols are the analyses of McCuaig (1996) from the lower Woolyeenyer Formation at Norseman, black symbols are analyses of Ghaderi (1998) from Kambalda. Groups of McCuaig (1996) are modified as discussed in the text.

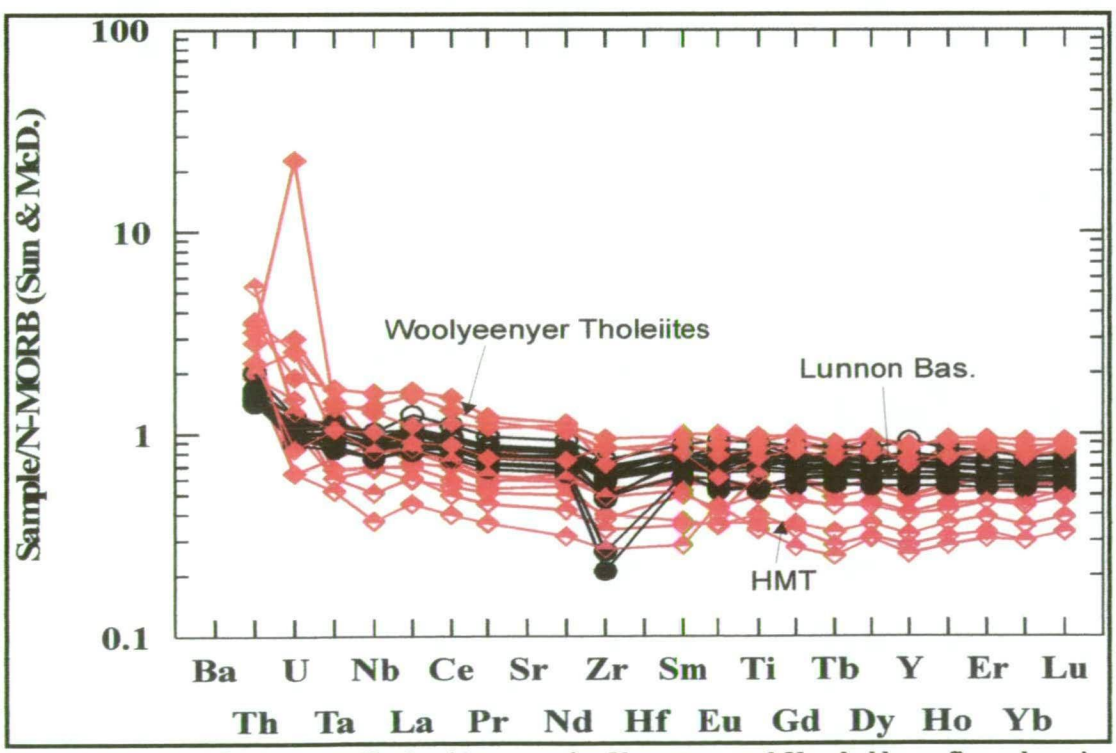

Figure 4.7a: N-MORB normalised spidergram for Norseman and Kambalda mafic rocks using the normalisation factors of Sun & McDonough (1989). Samples shown are tholeiites and HMT from the lower Woolyeenyer (analyses: McCuaig, 1996) (red diamonds); and Lunnon Basalt LMSB & HMSB from Kambalda (analyses: Ghaderi, 1998) (black circles).

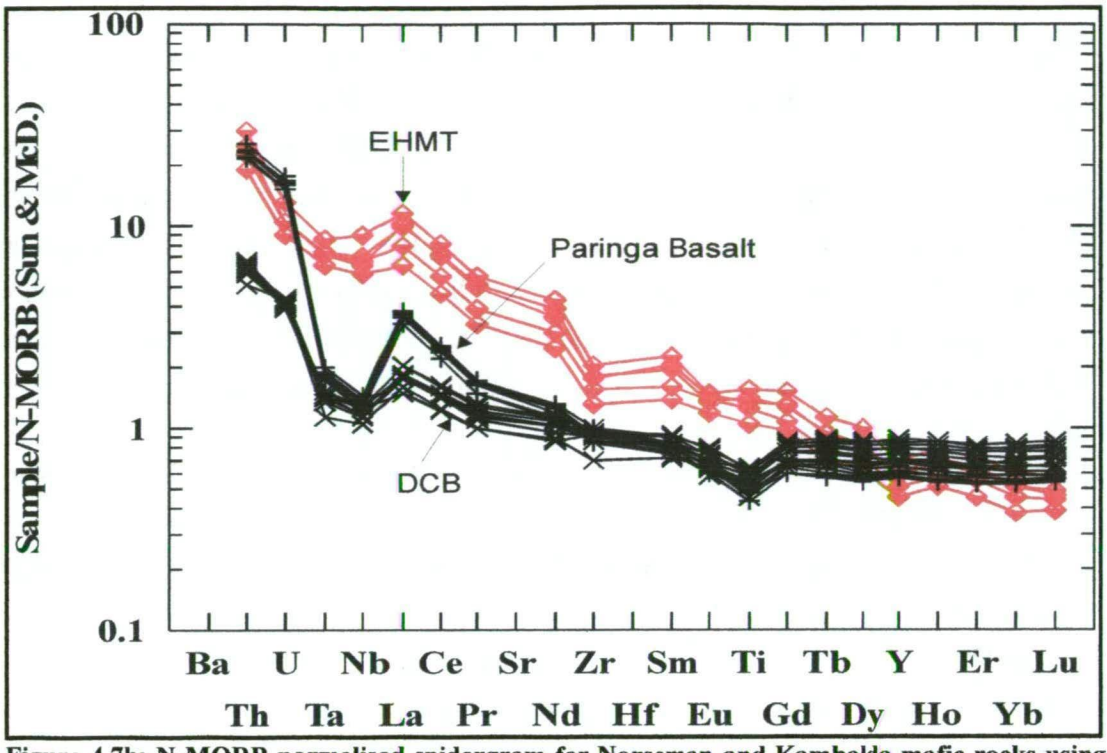

Figure 4.7b: N-MORB normalised spidergram for Norseman and Kambalda mafic rocks using the normalisation factors of Sun & McDonough (1989). Samples shown are EHMT from the lower Woolyeenyer (analyses: McCuaig, 1996) (red diamonds); and DCB (black X) and Paringa Basalt (black +) from Kambalda (analyses: Ghaderi, 1998).

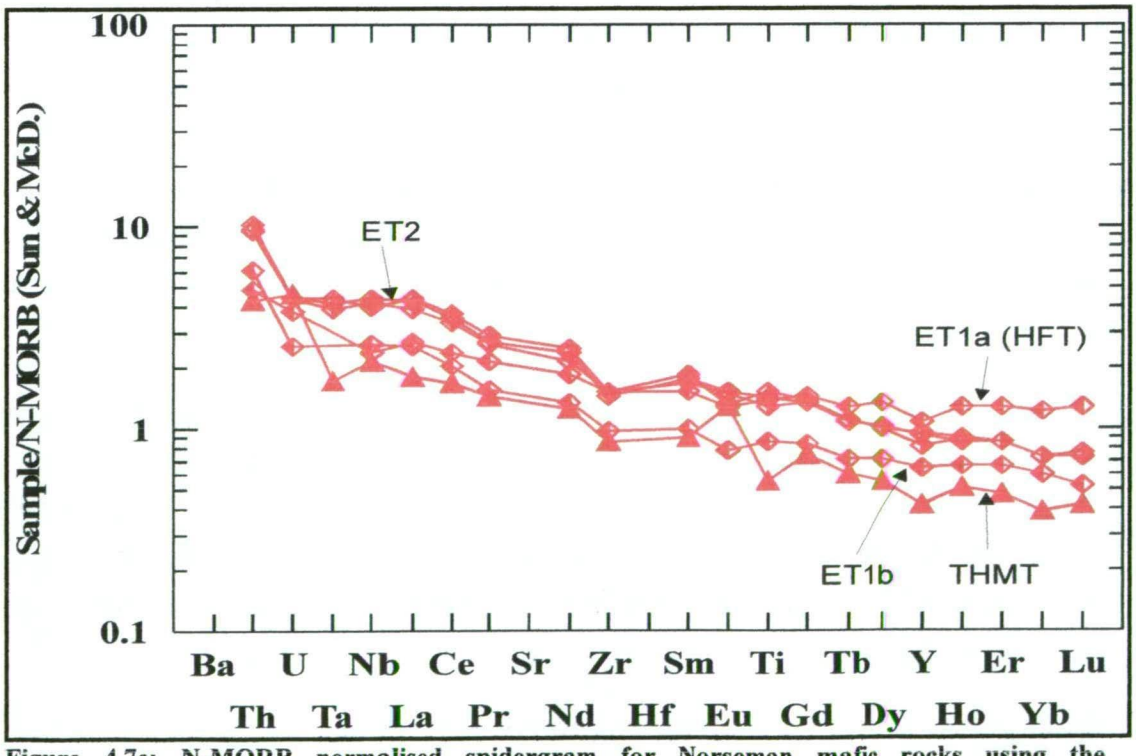

Figure 4.7c: N-MORB normalised spidergram for Norseman mafic rocks using the normalisation factors of Sun & McDonough (1989). Samples shown are EH1a&b, EH2 (red diamonds) and THMT (red triangle) from the lower Woolyeenyer (analyses: McCuaig, 1996).

4.9.3 Discussion about defined basalt groups

This section discusses the results of compiling the data of McCuaig (1996) and Ghaderi (1998) to create a reference dataset for lower Woolyeenyer Formation and Kambalda basalts. Eight groups of geochemically distinct basalts are found. The groups defined by McCuaig (1996) for the lower Woolyeenyer Formation are all distinct and accepted as individual groups except ET1. At Kambalda, all the groups are well-defined, but for this study, the two basalt varieties that comprise the Lunnon Basalt, the LMSB and low-MgO member of the HMSB, are combined with tholeiites. The reasons for combining some groups are discussed below.

The Jensen cation plot classifies most of the samples as basalt or komatiitic basalt, except for the majority of the DCB samples which are classified as andesite, and one Lunnon Basalt sample that approaches dacite in composition (figure 4.2). Classifying these samples on the more conventional basis of silica content, eight of the ten DCB samples are andesite or basaltic-andesite, and one of the Lunnon Basalt samples is basaltic-andesite. Although the latter samples are intermediate, rather than mafic in composition, all will be referred to as "basalts" for convenience.

The Woolyeenyer Formation tholeiites and Lunnon Basalt are geochemically similar, having coincident geochemical parameters. Within the Lunnon Basalt, the LMSB and the low MgO member of the HMSB, that Redman & Keays (1985) defined, are very similar, the only significant differences being the slightly lower Mg and higher Ti values for the LMSB, and differing ratios that involve these elements (figure 4.3). In the absence of PGE analyses, which Redman & Keays (1985) used to define the groups (see section 4.8), it is impractical to attempt a geochemical separation of these two varieties of Lunnon Basalt, therefore they are all grouped under the name "tholeiite" in this study.

Figure 4.7a shows the similarity of the tholeiite group to N-MORB, with flat patterns close to unity for the majority of the elements, but a slight enrichment in the more incompatible elements. There are strong enrichments or depletions in the mobile LILE, which is probably related to secondary alteration, so the LILE have been removed from the spidergrams. The high U in one tholeiite is also considered to be due to alteration.

HMT, defined in the lower Woolyeenyer Formation, are similar to the tholeiite samples in most parameters except for the low TiO_2 and the very high MgO (figure 4.3); which classify the group as komatiitic basalts on the Jensen cation plot (figure 4.2). The group has flat REE patterns (figure 4.5a) and spidergrams similar to the tholeiites but at lower overall abundances (figure 4.7a). The HMT and tholeiites were interpreted by McCuaig (1996) as having a similar mantle source, therefore, the

HMT can be regarded as the primitive magma to the tholeiite group. The HMT may be equivalent to the high MgO member of the HMSB of Redman & Keays (1985), but the latter group is not listed in Table 4.2 due to a lack of high precision data.

The EHMT is readily distinguished from other groups on the basis of very low Al_2O_3, steep REE patterns with elevated LREE (figure 4.5b), and high MgO and TiO_2 contents (figure 4.3). The THMT group consists of only one sample with characteristics distinct from all other groups. It will receive no further consideration.

ET1 & 2 cluster together in most bivariate plots. However, the ET2 samples have distinctive, straight, moderately sloping REE patterns with enriched LREE.

The establishment of the group called ET1 seems questionable. The two samples that comprise this group have diverse trace element characteristics with the only likeness being similar La abundances. The two ET1 samples probably do not belong to the same group, therefore, they are separated for this study and renamed ET1a and ET1b.

ET1a (sample GSWA 99941) has flat REE and spidergram patterns similar to the tholeiites, albeit at slightly higher overall abundances (figure 4.5c & 4.7c). The sample also has low MgO, indicating extended fractionation, but the TiO_2 abundances in the sample far exceed the enrichment expected by fractionation of tholeiites (figure 4.3). Although the REE and spidergrams are consistent with a more fractionated tholeiite having increased incompatible elements in the residual melt, the elevated TiO_2 abundances suggest a source with higher Ti than the tholeiites. The Jensen cation plot classifies ET1a as a high-Fe tholeiite (figure 4.2), a name that seems appropriate considering the similarity of the other characteristics to the tholeiite group.

ET1b (sample GSWA 99944) has a REE and spidergram pattern similar to the ET2 samples but with lower overall abundances and a slightly shallower trend. ET1b has both higher MgO and lower TiO_2 than the ET2 samples, but lies along the projection of their trend (figure 4.3). These characteristics suggest ET1b is a more primitive, less fractionated member of the ET2 group.

The Paringa Basalt is distinguished from all the other groups by the enriched LREE and flat HREE patterns (figure 4.5d), the low Ti/Zr (figure 4.4), and enriched U but Ta, Nb and Ti depleted spidergrams (figure 4.7b). All these geochemical features are consistent with crustal contamination. One of the simplest ways of geochemically discriminating Paringa Basalts is their position on the Winchester & Floyd (1976) diagram for basalts, which separates the Paringa Basalts from all other groups due to its low TiO_2 and P_2O_5 abundances and high Zr (figure 4.6).

The Devons Consols Basalt samples in this study are biased in favour of the felsic, ocelli-rich (variolitic) andesitic members rather than the komatiitic basalt members, because these are the analyses available from Ghaderi (1998). The samples possess similar distinctive characteristics to the Paringa Basalt, but with a lower intensity. The LREE enrichment is present but weak and not readily distinguished from the tholeiitic basalts (figure 4.5d). Similarly, the group is approximately coincident with the tholeiites on the TiO_2 versus MgO diagram (figure 4.3). The Winchester & Floyd (1976) discrimination diagram removes most of the overlap between tholeiites and DCB (figure 4.6), but the spidergrams are the most successful at fingerprinting the DCB, due to the depletion in Nb, Ta and Ti of a similar order to the Paringa Basalt (figure 4.7b).

4.9.4 Conclusion

If the LMSB and low MgO member of the HMSB within the Lunnon Basalt are both combined with the tholeiites, the samples can be geochemically divided into eight groups: Tholeiites, HMT, EHMT, THMT, DCB, Paringa Basalt, ET1a which will be called "high-Fe tholeiites" (HFT), and a group consisting of ET2 and ET1b, which will be known as "ET" in this study. These comprise all the geochemical groups for mafic rocks that have been defined by previous studies from Norseman and Kambalda.

4.10 CHINAMAN'S WELL, POLAR BEAR & PENNESHAW BASALTS

4.10.1 Introduction

The lower Woolyeenyer Formation is well characterised due to the previous basalt studies described in section 4.8, and stratigraphic studies based on the abundant drill holes and underground mine openings around the major gold deposits at Norseman. In contrast, the Chinaman's Well basalts above the Norseman komatiite, and the Polar Bear basalts are very poorly known, as they are largely covered by lake sediments. The development by CNGC of drilling rigs mounted on all-terrain vehicles has, since 1990, enabled drilling through the cover across Lake Cowan and extended the availability of diamond drill core into Chinaman's Well and Polar Bear basalts. This core has been utilised in the current study with the aim of testing a hypothesis that these basalts constitute a thrust repetition of the lower Woolyeenyer. This testing involves determining whether these basalts are geochemically similar to the upper basalts at Kambalda or the lower Woolyeenyer Formation.

CNGC geologists also have hypothesised that the mafic part of the Penneshaw Formation is a repetition of the lower Woolyeenyer Formation. The mafic rocks from the Penneshaw Formation are visibly similar to the Woolyeenyer Formation and

are thought to be structurally separated from the felsic rocks in the western Penneshaw (Chapter 6). The bedrock geology of the Penneshaw Formation is poorly exposed, being largely covered with lake sediments and gypsum dunes, so geological studies into this area have also benefited by the development of all-terrain drilling rigs. Five basalt samples, selected by CNGC Geologist Anthony Gray from diamond drill holes into the mafic part of the Penneshaw Formation, are included in this study, with the aim of determining their resemblance to the lower Woolyeenyer Formation.

Methods

For mafic rocks, aphyric, pillowed basalt was the preferred media for sampling as it is most likely to represent the magma composition, free from localised effects of crystal fractionation. In addition, these rocks offer sample homogeneity and are of known volcanic origin. Samples were collected from within pillows, away from the pillow rind and visible seafloor alteration, and from zones with minimal carbonate crackle veining.

The samples comprise nine from the Polar Bear Peninsula, seventeen from the Chinaman's Well basalts, five from the mafic Penneshaw Formation and one sample of basaltic sand from Cyprus Hill. The petrographic samples described in sections 4.2-4.5 are a subset of these geochemical samples. All the analyses were conducted for this study with the exception of the four basalt samples that Ghaderi (1998) analysed from the Swordfish prospect, which are included to round out the study with all the available geochemical data for mafic rocks above the Norseman komatiite. The locations of the samples and the prospect names used are shown in figure 4.1.

All Chinaman's Well samples were diamond core except for an outcrop sample of variolitic and amygdaloidal basalt from the causeway, and two samples of hand-picked, unweathered, basalt fragments from aircore holes that achieved unusually deep penetration into the bedrock at the Davros prospect. At the Polar Bear Peninsula, the poor availability of diamond drill core allowed collection of only three diamond core samples from offshore and two samples from one hole at the Sontaran prospect onshore. The four other samples from the Polar Bear area comprised rock chips from outcrops. Large samples without weathered joints were broken up and rock fragments free of weathering selected. The sample of basaltic sand from Cyprus Hill was also chipped from an outcrop. The five basalt samples from the Penneshaw Formation were selected by A. Gray from diamond drill core.

4.10.2 Results

The results are presented in the same style of tables and plots as the last section to avoid burdening the text with geochemical descriptions. The legend explaining the symbols used in the plots are presented as Table 4.3. The symbol shape given to each sample is based upon the location from which it was collected, noted as a prospect name, and the symbol colour, green or blue, indicates with which sample batch it was submitted to the laboratory; batch #1 samples are green, batch #2 samples are blue. Red circles are the Swordfish analyses of Ghaderi (1998). The oval fields in figures 4.9, 4.10 and 4.12 are for comparative purposes as they envelope the groups in figures 4.2, 4.3 and 4.5.

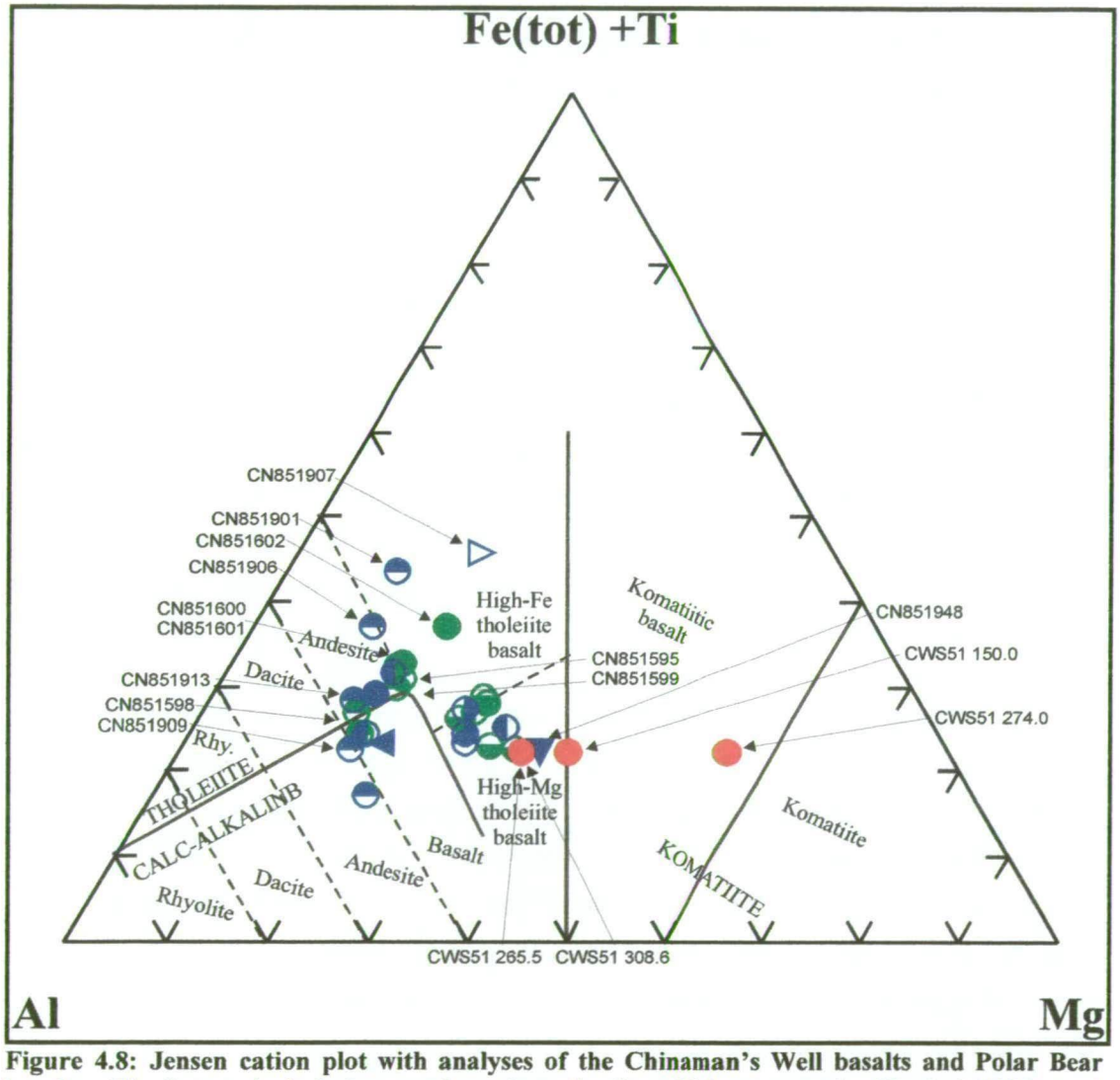

Figure 4.8: Jensen cation plot with analyses of the Chinaman's Well basalts and Polar Bear basalts. The former include four analyses from the Swordfish prospect by Ghaderi (1998), (red circles)

Table 4.4: Mafic samples from study listing parameters which describe the geochemical characteristics. Table 4.2 explains parameters.

GROUP	Tholeiite	Tholeiite	Tholeiite	Tholeiite	Tholeiite	Tholeiite	Tholeiite	Tholeiite	Tholeiite	Tholeiite	Tholeiite
Sample_no	CN793733	CN793734	CN793735	CN793736	CN793737	CN851339	CN851597	CN851902	CN851904	CN851905	CN851915
Analyses by:	This study	This study	This study	This study	This study	This study	This study	This study	This study	This study	This study
Prospect area	Penneshaw	Penneshaw	Penneshaw	Penneshaw	Penneshaw	Sontaran	Jewfish	Causeway	Polar Bear	Polar Bear	Jewfish
Jensen classification	High Mg Tholeiite	High Fe Tholeiite	High Fe Tholeiite	High Mg Tholeiite	High Fe Tholeiite	Calc-alkal. Basalt	High Fe Tholeiite	Calc-alkal. Basalt	Calc-alkal. Andesite	High Mg Tholeiite	High Mg Tholeiite
SiO_2 wt%	52.4	54.7	50.5	51.65	50.9	57.7	50.5	61.8	58.7	53.2	52.2
TiO_2 wt%	0.9	1.1	1.2	0.7	1.1	1.0	1.4	0.6	0.8	1.0	0.7
Al_2O_3 wt%	15.1	14.8	14.7	14.9	15.2	15.8	16.5	14.9	16.3	16.0	15.0
MgO wt%	8.2	6.3	7.3	8.8	7.8	3.8	7.5	4.1	4.6	7.2	8.4
Cr ppm	255	240	170	330	235	225	160	369	495	171	445
Ni ppm	134	117	143	152	121	129	98	200	147	134	148
U ppm	0.16	0.12	0.1	0.06	0.1	0.21	0.09	0.07	0.06	0.07	0
Al_2O_3/TiO_2	16.4	13.6	12.2	20.3	13.4	15.7	11.9	23.9	21.4	16.4	22.2
CaO/Al_2O_3	0.7	0.4	0.7	0.8	0.6	0.6	0.5	0.6	0.6	0.6	0.7
Ti/Zr	85.8	92.4	81.0	95.5	93.3	77.0	89.2	94.4	81.9	109.8	89.3
Zr/Y	1.6	1.4	1.5	0.8	1.0	1.7	1.5	2.3	2.5	2.5	2.5
Mg#	0.458.9	51.4	50.5	61.6	52.3	44.1	51.3	47.8	58.9	55.8	55.9
M/Si	0.40	0.34	0.43	0.41	0.44	0.23	0.44	0.21	0.20	0.37	0.43
$(La)_N$	20.7	13.3	19.4	12.4	17.9	19.2	17.5	11.8	12.4	16.7	12.4
$(La/Yb)_N$	2.9	2.6	2.6	2.3	2.4	2.7	2.9	1.3	1.3	1.3	1.2
$(La/Sm)_N$	1.3	0.8	1.0	1.0	1.0	1.2	1.0	1.1	1.1	1.1	1.1
$(Gd/Yb)_N$	1.2	1.2	1.2	1.2	1.3	1.3	1.2	1.2	1.3	1.2	1.2
Eu/Eu*	0.9	1.0	0.9	1.0	1.0	1.3	1.0	1.1	1.1	1.1	1.1
Sr/Sr*	0.7	0.8	0.7	0.9	0.9	0.4	1.5	1.4	1.9	1.0	1.1
Ti/Ti*	0.8	0.8	0.7	0.8	0.8	0.7	0.9	0.7	0.7	0.7	0.8
Nb/Nb*	0.8	1.1	0.8	1.2	0.9	0.7	0.9	0.5	0.5	0.5	0.5

GROUP	Tholeiite	Tholeiite	Tholeiite	Tholeiite	HMT	HMT	HMT	HMT	HMT	HFT	Tholeiite spoons
Sample_no	CN851916	CN851917	CN851918	CN851919	CN851948	CWS51-150.0	CWS51-274.0	CWS51-265.5	CWS51-308.6	CN851599	CN851595
Analyses by:	This study	This study	This study	This study	This study	Ghaderi	Ghaderi	Ghaderi	Ghaderi	This study	This study
Prospect area	Jewfish	Snapper	Davros	Davros	Tuna	Swordfish	Swordfish	Swordfish	Swordfish	Polar Bear	Jewfish
Jensen classification	Tholeiitic Andesite	Tholeiitic Andesite	High Fe Tholeiite	High Mg Tholeiite	High Mg Tholeiite	Komatiitic Basalt	Komatiitic Basalt	High Mg Tholeiite	High Mg Tholeiite	Tholeiitic Andesite	High Fe Tholeiite
SiO_2 wt%	52.0	50.5	55.40	57.6	51.6	49.1	52.9	46.4	54.2	51.0	50.3
TiO_2 wt%	1.3	1.4	0.7	0.7	0.5	0.6	0.6	0.4	0.6	1.8	1.3
Al_2O_3 wt%	15.7	17.2	16.4	16.8	15.3	14.5	15.0	10.2	14.8	17.7	15.9
MgO wt%	4.2	4.2	7.3	7.8	10.4	11.3	9.4	19.9	9.1	5.0	4.6
Cr ppm	202	213	413	464	1055	490	579	571	380	96	160
Ni ppm	113	108	136	128	157	377	161	695	138	81	93
U ppm	0.06	0.06	0.07	0.11	0.22	0.36	0.38	0.028	0.036	0.19	0.09
Al_2O_3/TiO_2	12.4	12.1	23.6	23.1	30.6	24.5	23.7	23.8	23.1	9.7	12.2
CaO/Al_2O_3	0.7	0.6	0.3	0.1	0.6	0.8	0.6	0.8	0.6	0.4	0.7
Ti/Zr	106.6	87.4	112.1	95.3	129.0	94.1	114.6	104.9	109.1	61.8	98.5
Zr/Y	2.5	2.8	1.8	3.3	1.5	2.4	2.0	2.3	2.5	2.6	2.9
Mg#	37.9	39.6	50.6	55.3	63.2	64.4	61.7	71.5	61.7	41.0	39.7
M/Si	0.32	0.32	0.39	0.37	0.48	0.5	0.4	0.9	0.4	0.36	0.35
$(La)_N$	21.9	22.6	12.2	11.0	7.0	7.1	5.6	4.9	6.8	30.0	19.2
$(La/Yb)_N$	1.5	1.4	1.2	1.3	0.9	0.9	0.6	0.8	0.9	3.4	3.5
$(La/Sm)_N$	1.2	1.1	1.0	1.1	1.1	0.8	0.8	0.8	0.8	1.0	1.1
$(Gd/Yb)_N$	1.4	1.4	1.2	1.3	1.0	1.1	0.8	1.0	1.1	1.3	1.3
Eu/Eu*	1.0	1.0	1.0	1.0	1.1	0.9	0.9	0.7	0.9	1.0	1.1
Sr/Sr*	1.3	0.4	0.8	0.6	2.7	0.4	1.6	0.3	1.1	0.5	1.4
Ti/Ti*	0.8	0.8	0.7	0.8	0.9	0.8	1.0	0.9	1.0	0.7	0.9
Nb/Nb*	0.4	0.5	0.5	0.6	0.2	0.8	1.0	0.9	0.9	0.6	1.2

GROUP	Tholeiite spoons	Tholeiite spoons	Tholeiite spoons	Tholeiite spoons	Contam. Tholeiite spoons	Contam. HFT spoons	Contam. HFT spoons	Contam. HFT spoons	Contam. Basalt (DC B-like)	EHMT (fraction.)
Sample no	CN851598	CN851600	CN851913	CN851914	CN851909	CN851602	CN851906	CN851901	CN851907	CN851601
Analyses by:	This study	This study	This study	This study	This study	This study	This study	This study	This study	This study
Prospect area	Polar Bear	Snapper	Polar Bear	Jewfish	Sontaran	Snapper	Polar Bear	Polar Bear	Cyprus Hill	Snapper
Jensen classification	Tholeiitic Andesite	High Fe Tholeiite	Tholeiitic Andesite	Calc-alkal. Basalt	Calc-alkal. Andesite	High Fe Tholeiite	Tholeiitic Andesite	High Fe Tholeiite	High Fe Tholeiite	Tholeiitic Andesite
SiO_2 wt%	53.1	48.2	49.7	57.5	58.5	51.9	61.8	53.2	52.7	53.9
TiO_2 wt%	1.1	1.4	1.2	0.7	1.0	1.6	1.9	2.0	1.0	3.1
Al_2O_3 wt%	17.2	17.0	18.3	16.9	16.6	13.8	15.1	14.8	10.6	14.7
MgO wt%	3.8	4.4	3.8	4.2	3.5	4.7	2.8	2.9	4.4	3.9
Cr ppm	205	160	301	418	212	52	124	123	271	24
Ni ppm	174	93	161	124	127	50	120	128	103	30
U ppm	0.08	0.07	0.06	0	0.25	0.17	0.29	0.18	0.11	0.45
Al_2O_3/TiO_2	15.9	12.4	15.7	23.7	17.1	8.6	8.0	7.4	11.1	4.8
CaO/Al_2O_3	0.6	0.6	0.7	0.4	0.6	0.7	0	0.4	1.1	0.6
Ti/Zr	95.9	90.0	112.2	124.8	78.3	79.9	81.7	85.3	132.4	64.9
Zr/Y	4.0	2.9	2.7	2.5	3.6	3.9	3.21	3.1	1.7	5.7
Mg#	39.5	36.5	36.5	44.0	44.8	35.8	26.8	21.7	29.3	38.9
M/Si	0.28	0.38	0.32	0.25	0.20	0.38	0.26	0.38	0.44	0.29
$(La)_N$	12.7	17.7	22.6	12.9	28.5	34.2	32.1	44.3	21.9	91.1
$(La/Yb)_N$	5.8	5.2	3.2	1.8	4.4	6.3	2.4	3.1	1.7	7.2
$(La/Sm)_N$	1.0	1.0	1.2	1.2	2.0	1.5	1.3	1.4	1.5	1.8
$(Gd/Yb)_N$	1.4	1.2	1.9	1.4	1.8	1.6	1.5	1.6	1.1	2.3
Eu/Eu*	1.1	1.0	1.0	1.1	1.1	1.0	0.9	1.0	1.1	0.9
Sr/Sr*	1.0	0.5	0.6	0.9	0.7	0.5	0.4	0.3	0.3	0.4
Ti/Ti*	1.2	1.1	1.1	1.0	1.0	1.0	1.2	1.0	0.8	0.8
Nb/Nb*	1.0	0.7	0.2	0.4	0.2	0.4	0.1	0.4	0.2	0.5

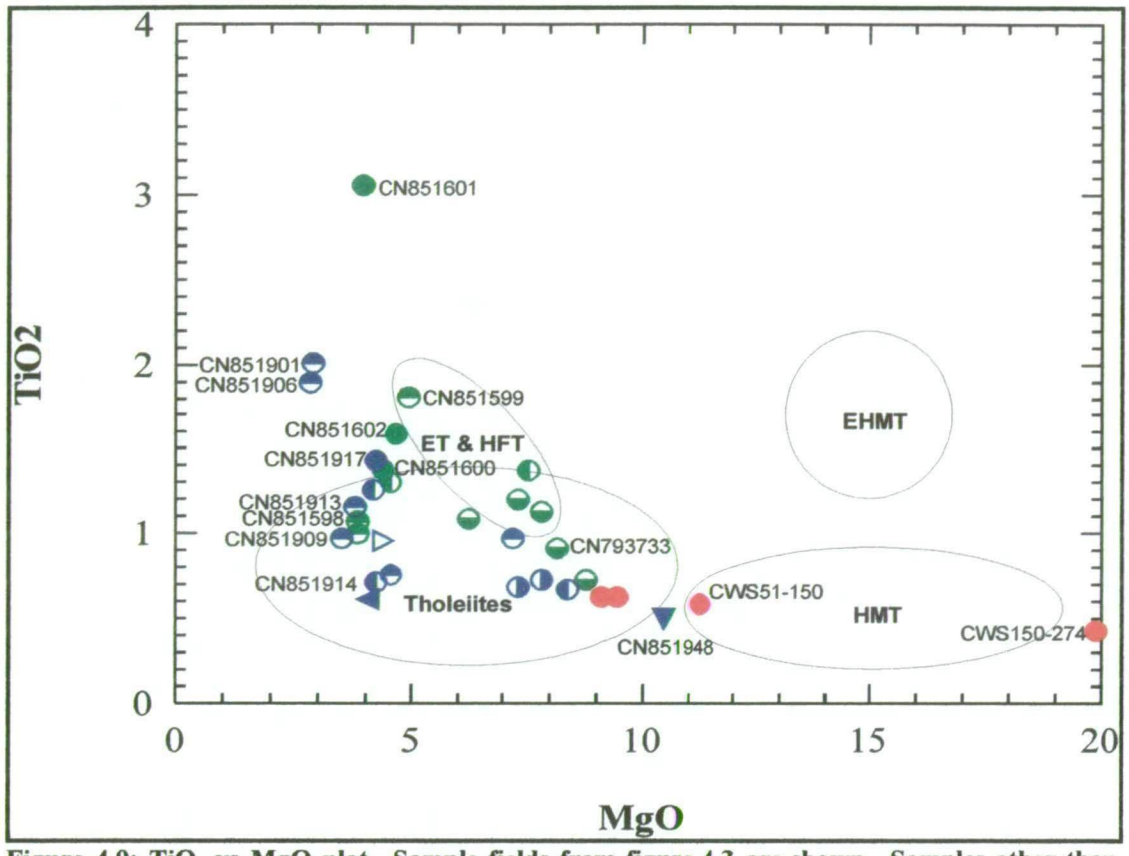

Figure 4.9: TiO_2 vs MgO plot. Sample fields from figure 4.3 are shown. Samples other than tholeiites (see Table 4.4) and samples lying outside the oval tholeiite field are labelled.

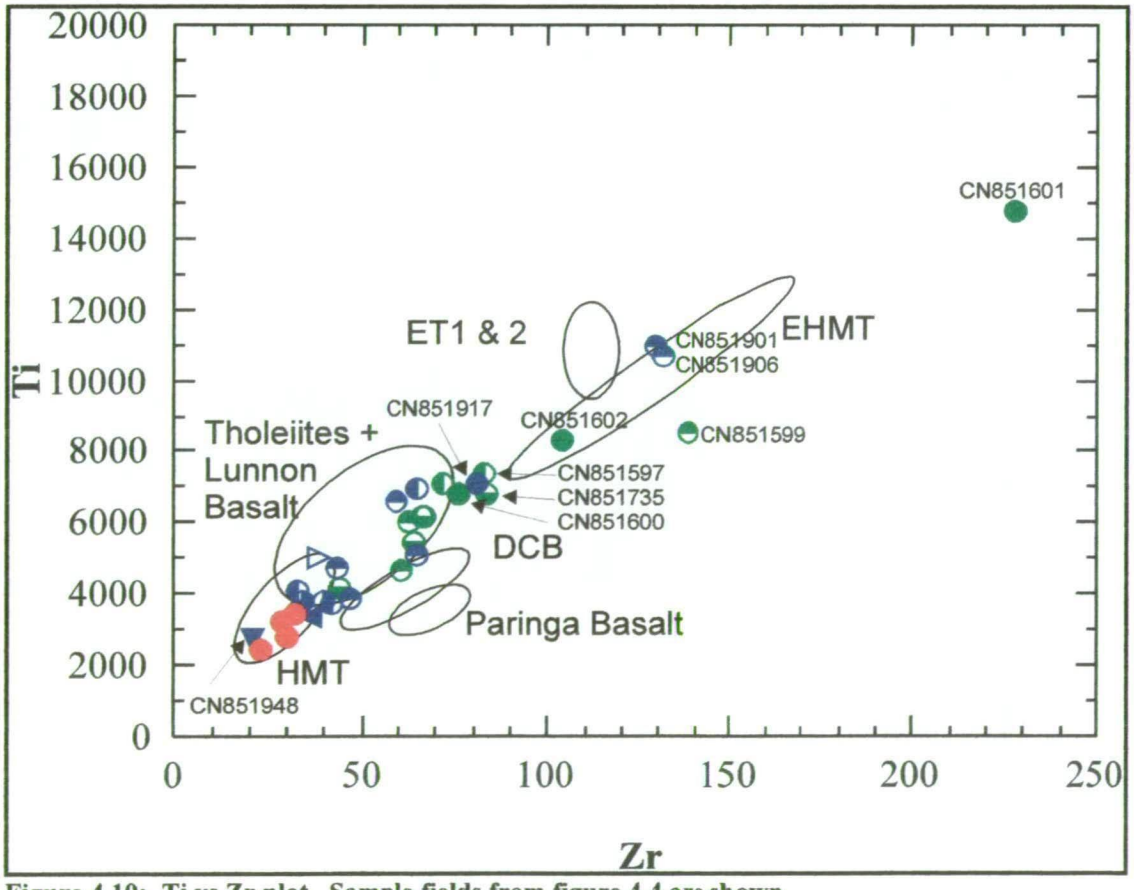

Figure 4.10: Ti vs Zr plot. Sample fields from figure 4.4 are shown.

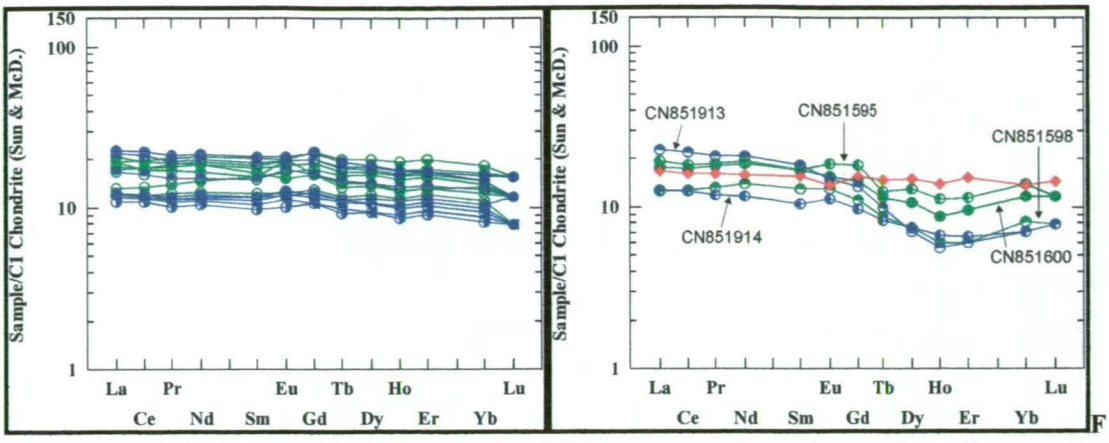

Figure 4.11a & 4.11b: C1-chondrite normalised REE patterns for Chinaman's Well and Polar Bear basalts using the normalisation factors of Sun & McDonough (1989). 4.11a has tholeiite samples1. 4.11b has spoon-shaped REE patterns thought to be tholeiites (see text) with a tholeiite analysis for comparison. (Comparison sample: SC1484-10; red diamond; McCuaig, 1996).

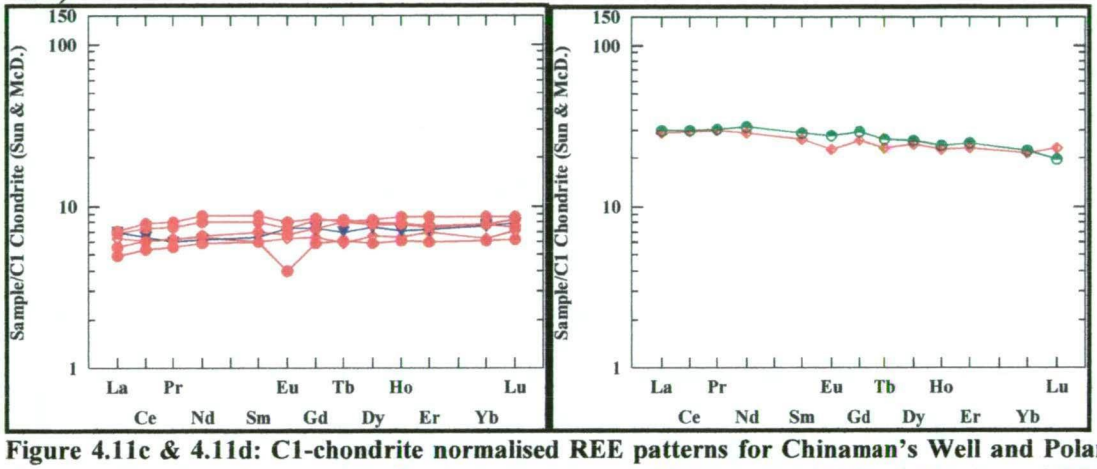

Figure 4.11c & 4.11d: C1-chondrite normalised REE patterns for Chinaman's Well and Polar Bear basalts using the normalisation factors of Sun & McDonough (1989). 4.11c shows HMT samples from Chinaman's Well with a single HMT analysis from the lower Woolyeenyer Fm for comparison. Four of the Chinaman's Well HMT samples are the analyses of Ghaderi (1998) from the Swordfish prospect ("CWS" prefix in Table 4.4, red circles); the other is a Spinifex-textured rock from the Tuna prospect (CN851948-inverted blue triangle). 4.11d has high-Fe tholeiite (HFT) REE patterns with HFT (ET1a) for comparison (Comparison samples: HMT-AB3727686; HFT-GSWA 99941; red diamonds; McCuaig, 1996).

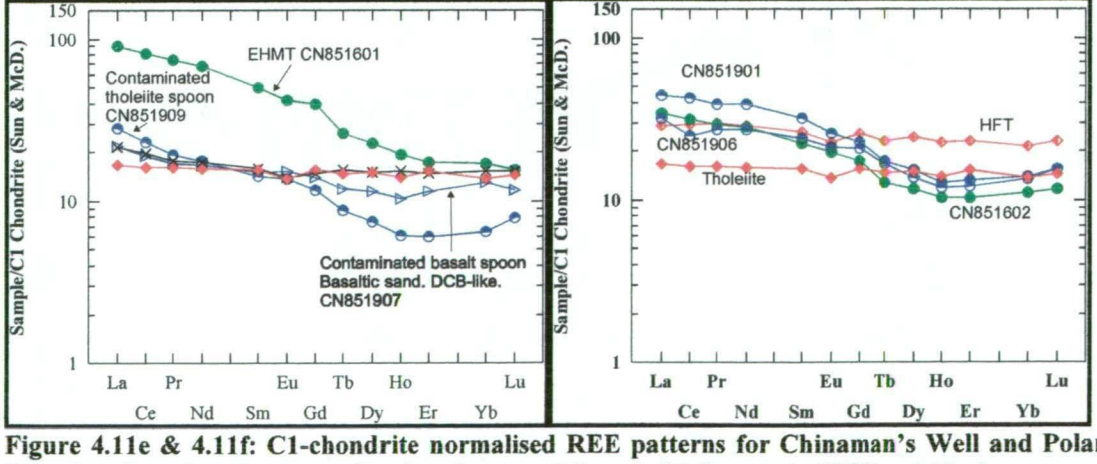

Figure 4.11e & 4.11f: C1-chondrite normalised REE patterns for Chinaman's Well and Polar Bear basalts using the normalisation factors of Sun & McDonough (1989). 4.11e has spoon-shaped, crustally contaminated basalts and a fractionated EHMT sample with a DCB sample and tholeiite for comparison. 4.11f has spoon-shaped REE patterns thought to contaminated HFT with HFT (ET1a) and tholeiite from the lower Woolyeenyer Fm for comparison. (Comparison samples: tholeiite-SC1484-10; DCB-KD1236 221.1; HFT-GSWA99941; Ghaderi, 1998; McCuaig, 1996).

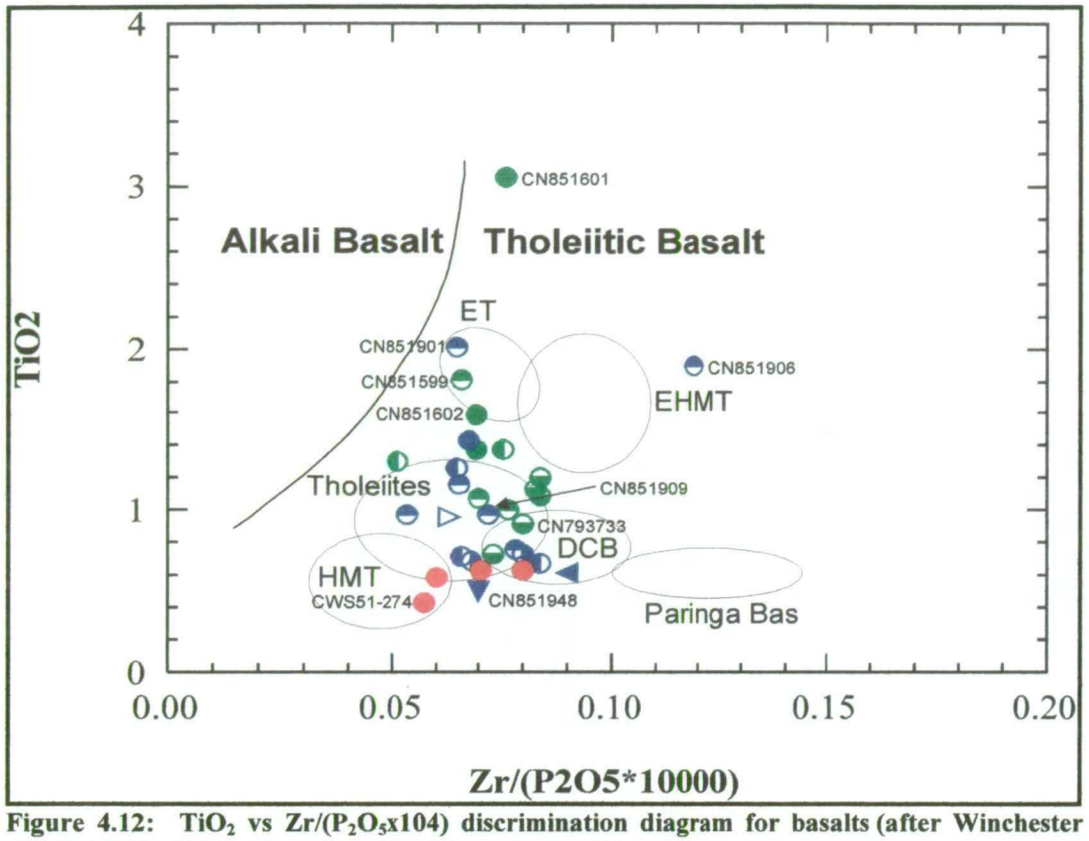

Figure 4.12: TiO_2 vs $Zr/(P_2O_5x104)$ discrimination diagram for basalts (after Winchester & Floyd, 1976). Fields shown are those from figure 4.6.

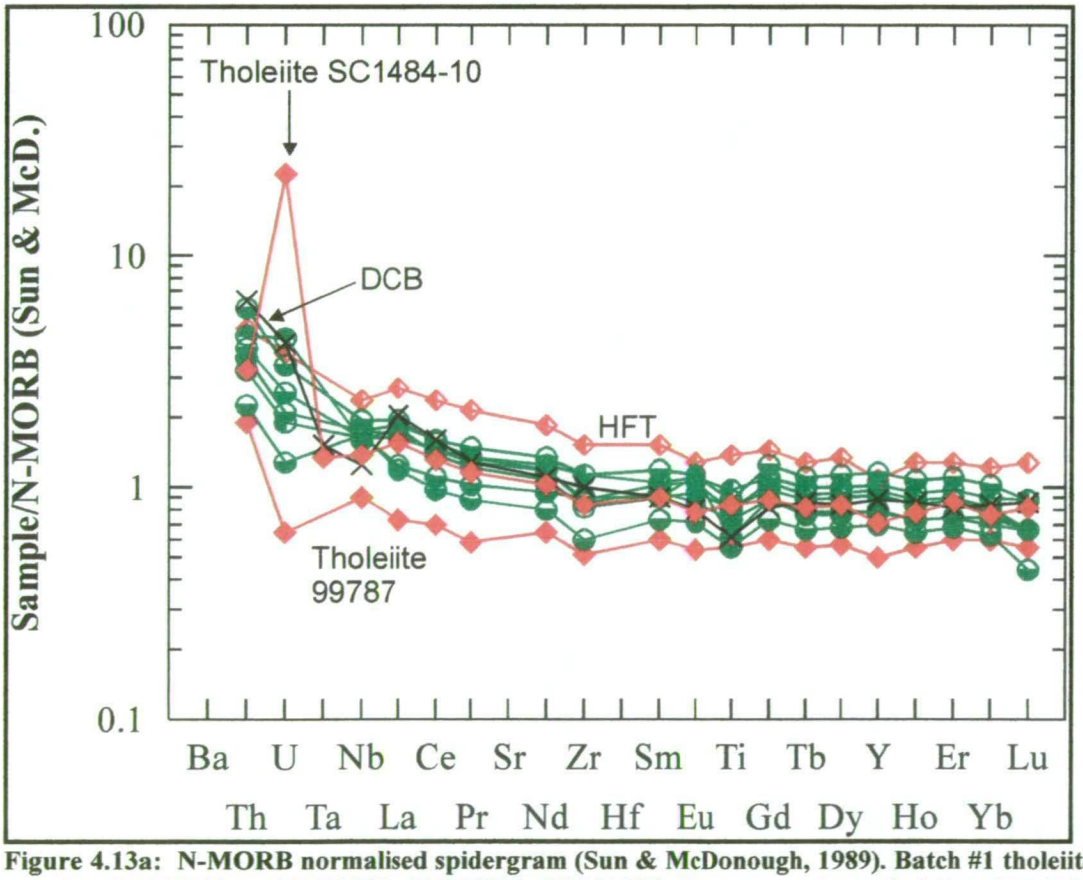

Figure 4.13a: N-MORB normalised spidergram (Sun & McDonough, 1989). Batch #1 tholeiites: samples CN793733 to CN793737, CN851339, CN851597. For comparison: tholeiites SC1484-10 & GSWA 99787; HFT (ET1a) GSWA 99941; DCB KD1236 221.1. Samples for comparison from Ghaderi (1998) & McCuaig (1996).

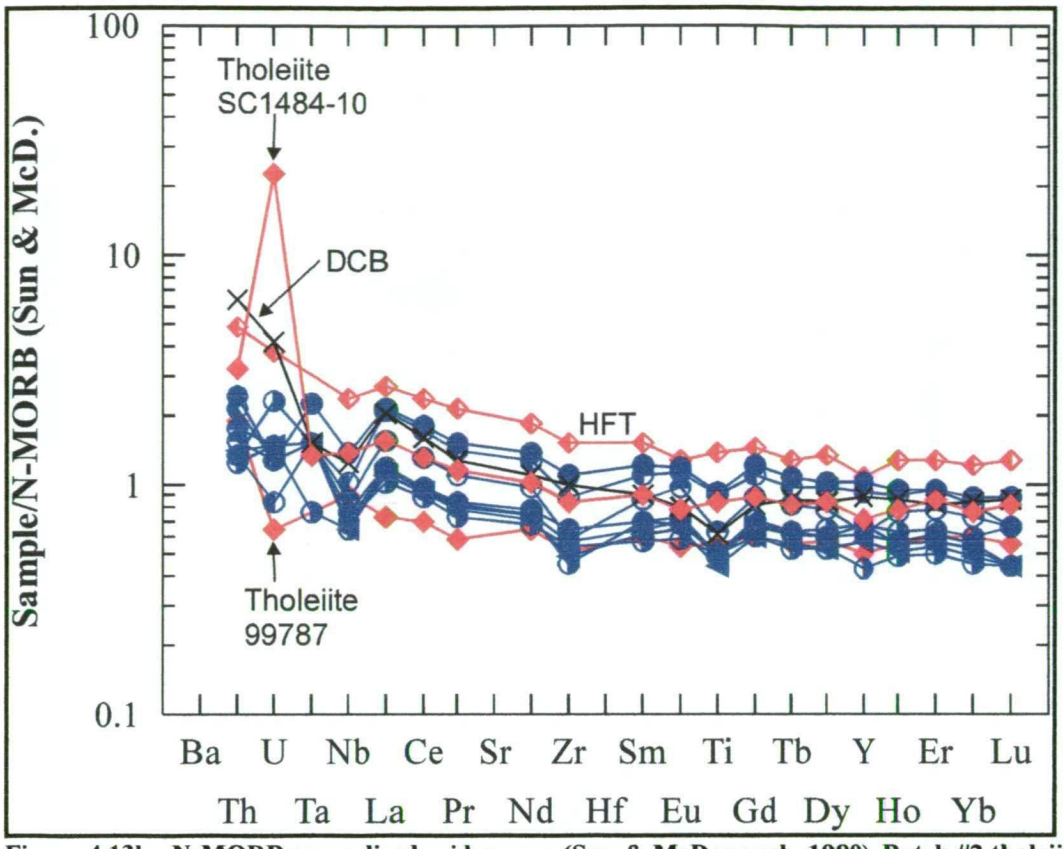

Figure 4.13b: N-MORB normalised spidergram (Sun & McDonough, 1989). Batch #2 tholeiites: samples CN851902, CN851904, CN851905, CN851915 to CN851919. For comparison: tholeiites SC1484-10 & GSWA 99787; HFT (ET1a) GSWA 99941; DCB KD1236 221.1. Samples for comparison from Ghaderi (1998) & McCuaig (1996).

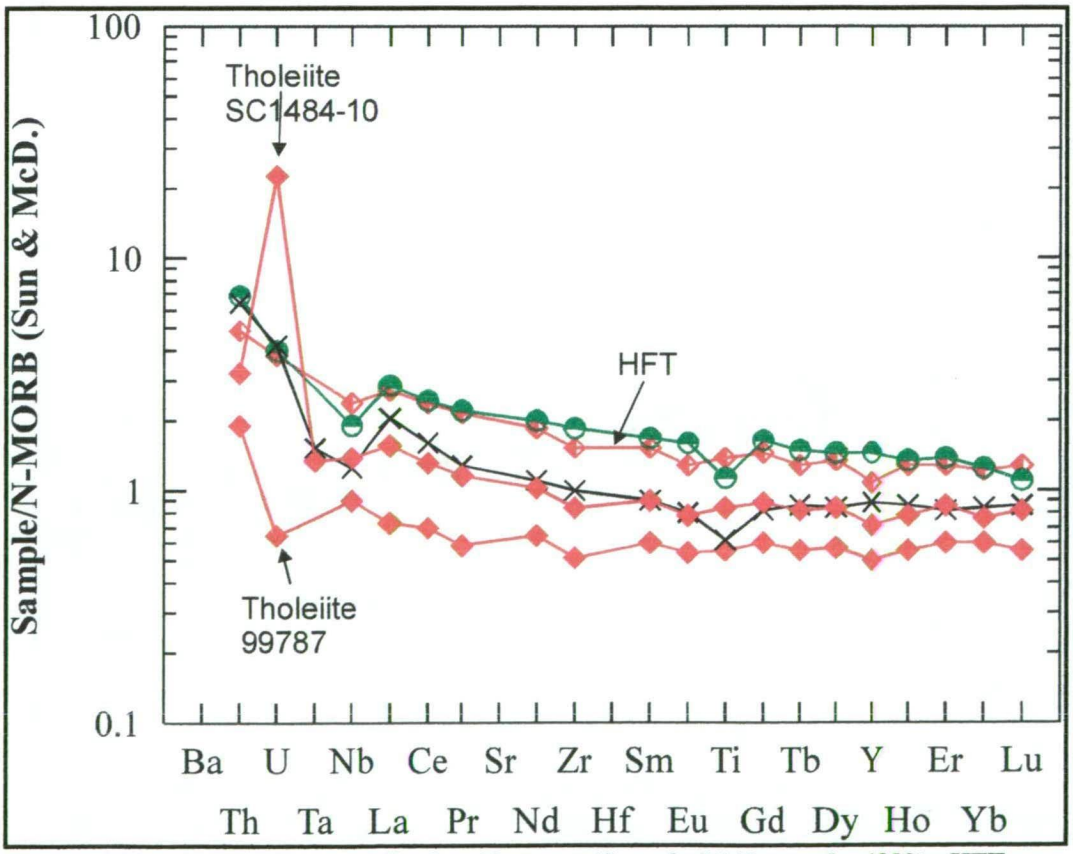

Figure 4.13c: N-MORB normalised spidergram (Sun & McDonough, 1989). HFT sample CN851599. For comparison: tholeiites SC1484-10 & GSWA 99787; HFT (ET1a) GSWA 99941; DCB KD1236 221.1. Samples for comparison from Ghaderi (1998) & McCuaig (1996).

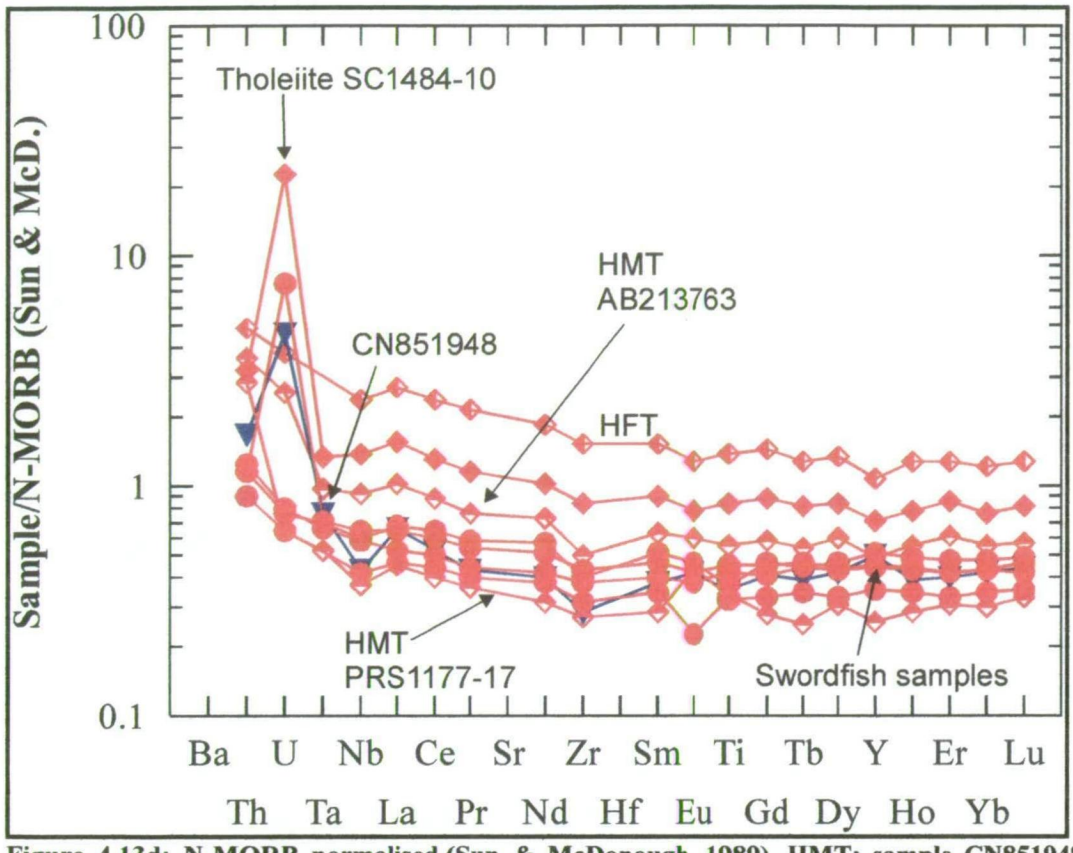

Figure 4.13d: N-MORB normalised (Sun & McDonough, 1989). HMT: sample CN851948 & Swordfish samples CWS51 150.0, CWS51 265.5, CWS51 274.0, CWS51 308.6. For comparison: HMT PRS1177-17 & AB213763; tholeiite SC1484-10; HFT (ET1a) GSWA 99941. Samples for comparison from Ghaderi (1998) & McCuaig (1996).

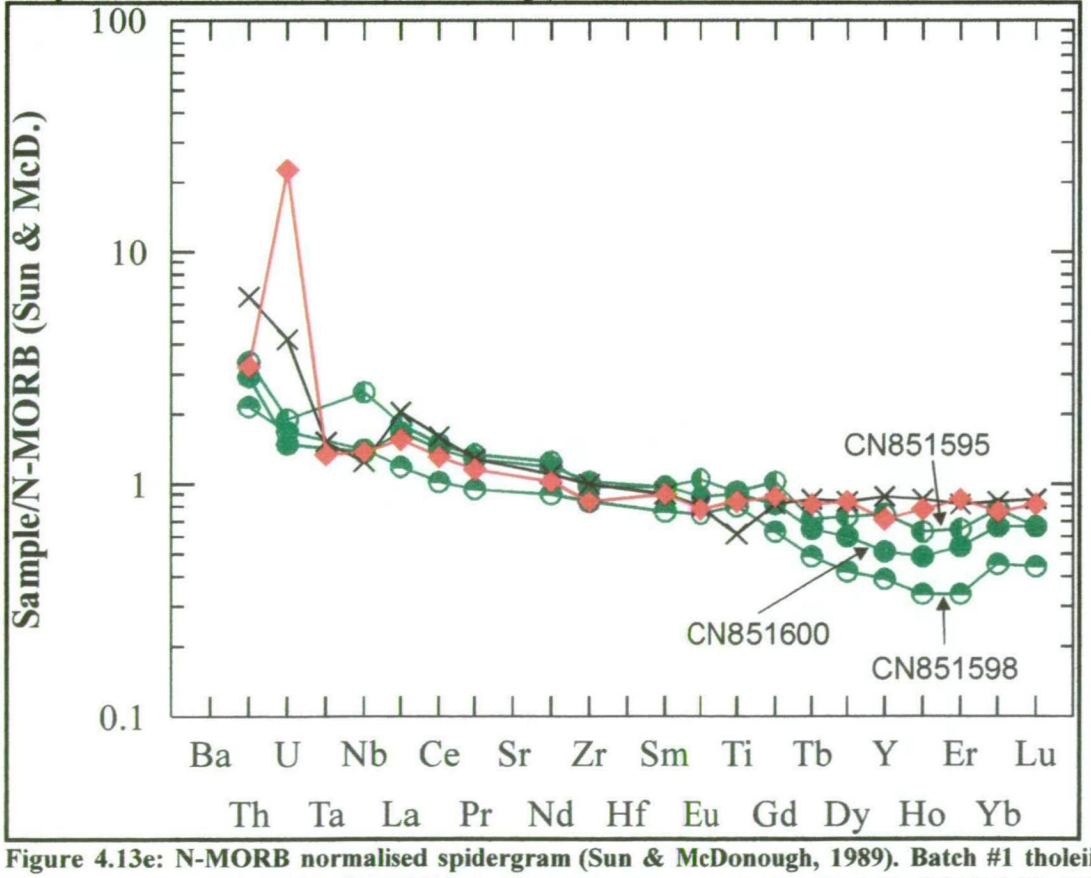

Figure 4.13e: N-MORB normalised spidergram (Sun & McDonough, 1989). Batch #1 tholeiite spoons: samples CN851595, CN851598 & CN851600. For comparison tholeiite SC1484-10; DCB KD1236 221.1. Samples for comparison from Ghaderi (1998) & McCuaig (1996).

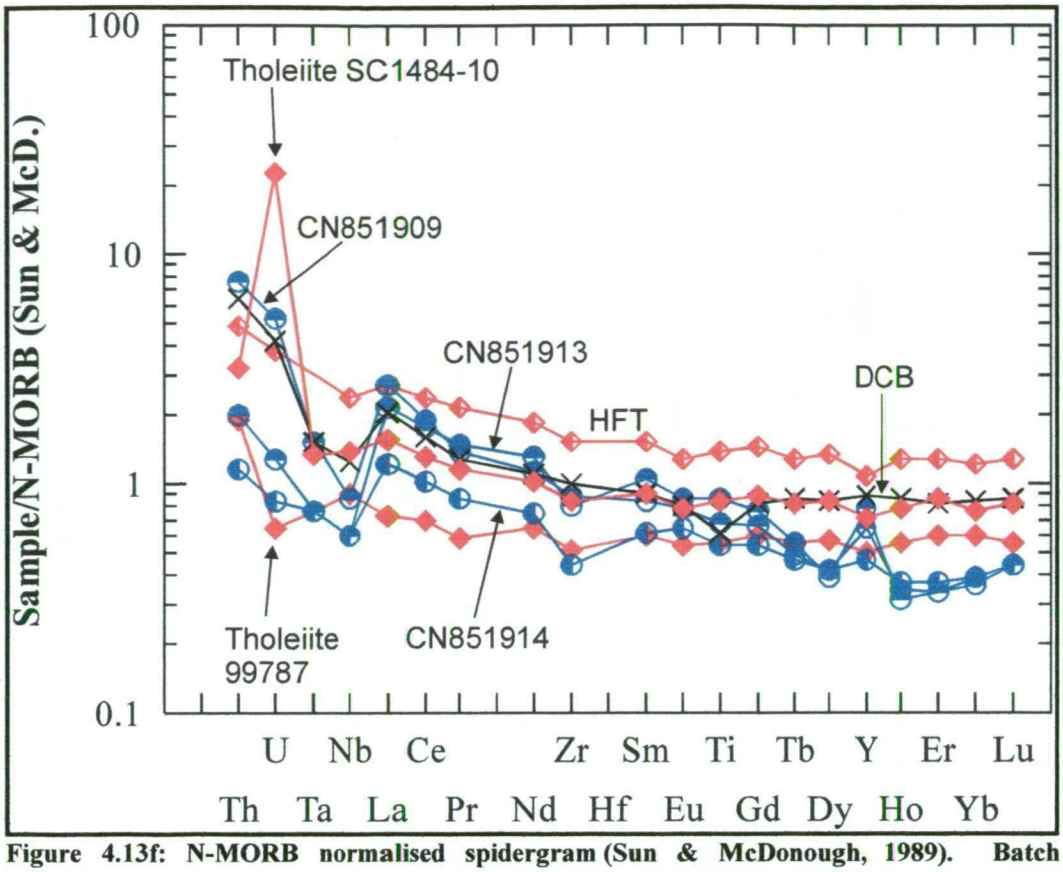

Figure 4.13f: N-MORB normalised spidergram (Sun & McDonough, 1989). Batch #2 contaminated tholeiite spoons: samples CN851909, CN851913 & CN851914. For comparison tholeiites GSWA 99787 & SC1484-10; HFT (ET1a) 99941; DCB KD1236 221.1. Samples for comparison from Ghaderi (1998) & McCuaig (1996).

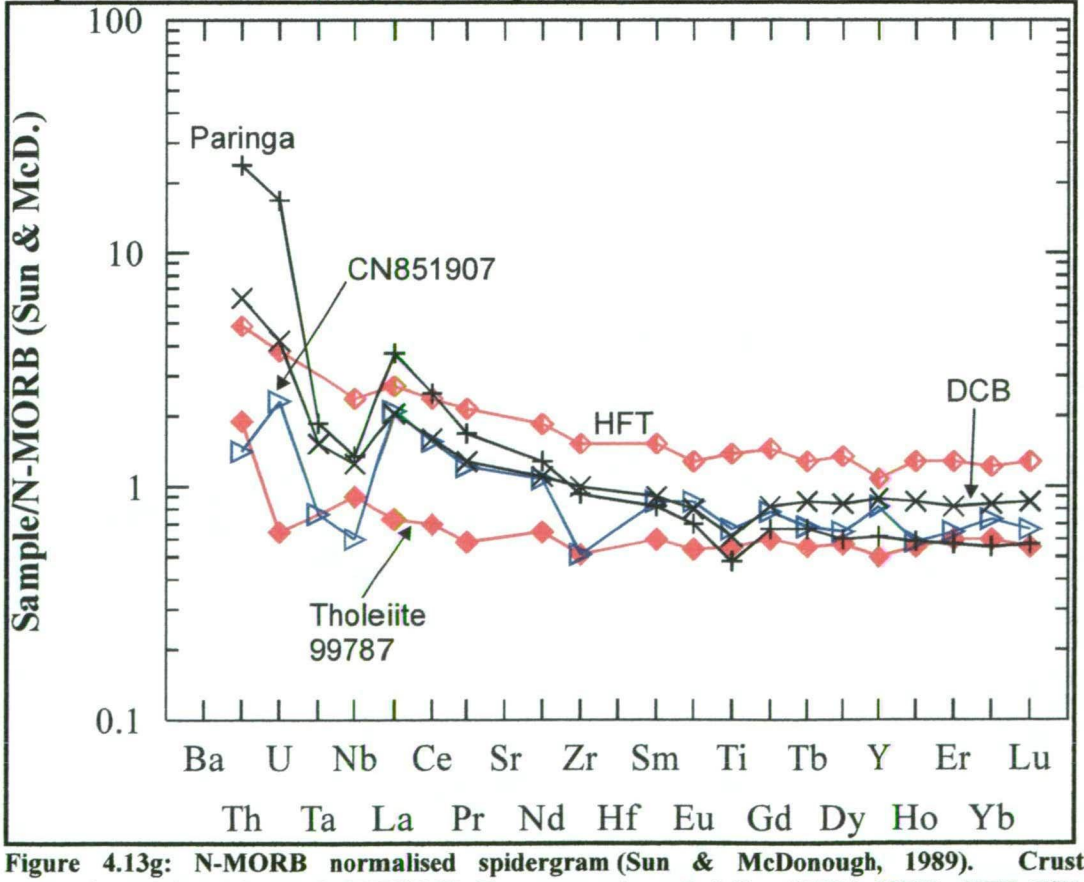

Figure 4.13g: N-MORB normalised spidergram (Sun & McDonough, 1989). Crustal contaminated basaltic sand CN851907. For comparison tholeiite GSWA 99787; HFT (ET1a) GSW 99941; DCB KD1236 221.1; Paringa Basalt KD122.5. Samples for comparison from Ghaderi (1998) & McCuaig (1996).

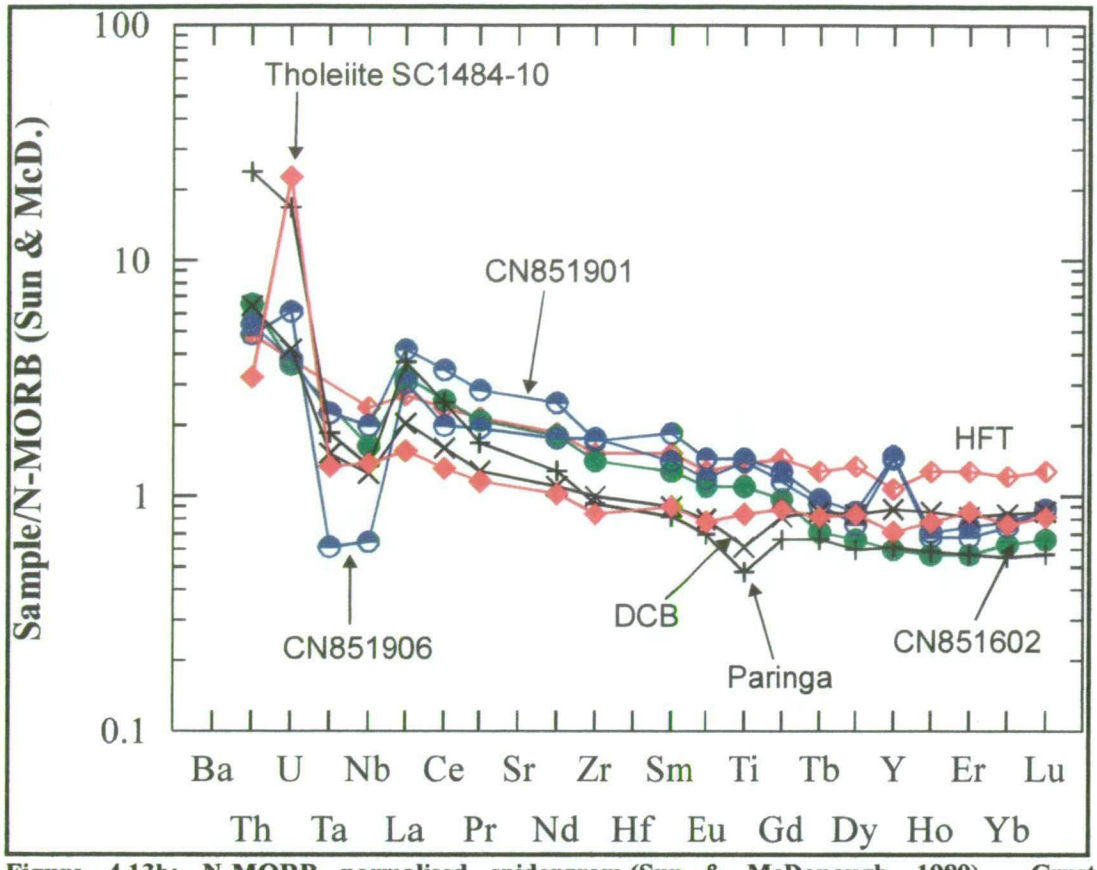

Figure 4.13h: N-MORB normalised spidergram (Sun & McDonough, 1989). Crustal contaminated HFT spoons: samples CN851901, CN851906 & CN851602. For comparison tholeiite SC1484-10; HFT (ET1a) GSW 99941; DCB KD1236 221.1; Paringa Basalt KD122.5. Samples for comparison from Ghaderi (1998) & McCuaig (1996).

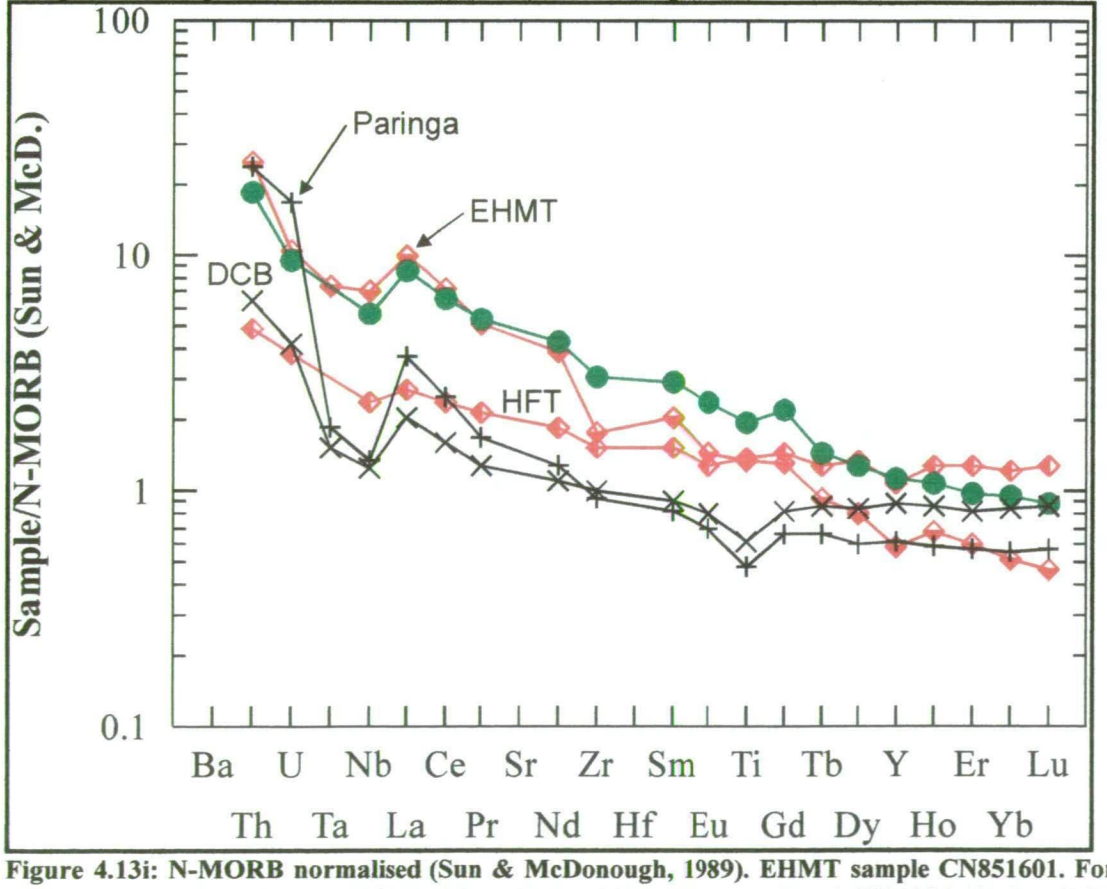

Figure 4.13i: N-MORB normalised (Sun & McDonough, 1989). EHMT sample CN851601. For comparison: EHMT GSWA 109064; HFT (ET1a) 99941; Paringa Basalt KD1236 122.5m; DCB KD1236 221.1. Samples for comparison from Ghaderi (1998) & McCuaig (1996).

4.10.3 Discussion & interpretation

The main object of this study was to determine whether the basalt that lies above the Norseman komatiite and in the mafic Penneshaw Formation are geochemically similar to the upper basalts at Kambalda, or the lower Woolyeenyer Formation or Lunnon Basalt. The results suggest that none of the samples collected are equivalent to the Paringa Basalt, which constitutes the majority of the upper basalt at Kambalda.

That none of the samples collected are equivalent to the Paringa Basalt is most clearly shown by the Winchester & Floyd diagram (figure 4.12). The Paringa Basalt spidergrams and REE patterns are also unlike any samples collected at Norseman. None of the Norseman samples possess the requisite combination of extreme LREE enrichment, flat HREE, enriched U and Th and strongly depleted Nb, Ta and Ti. As the Paringa Basalt at Kambalda has a thickness of around 1 km and comprises the majority of the upper basalt there, if any equivalent existed at Norseman, it would be expected that the expansive sample collection of this study would have found it.

The existence of a Norseman equivalent to the Devons Consols Basalt has not been comprehensively tested for in this study. At Kambalda, the unit has a maximum thickness of only 200 metres, grading up from the komatiite, so an equivalent unit at Norseman may have been missed in the sampling. CN851948 from Tuna, the sample collected closest to the top of the Norseman komatiite, is a high magnesian tholeiite (HMT), but does not possess the DCB crustal contamination signature of elevated LREE, Th and U and depleted Nb, Ta and Ti.

One sample collected in this study, CN851907, basaltic sandstone from Cyprus Hill, does possess trace element characteristics very similar to the DCB except that Zr is depleted and it lacks strong Th and U enrichment. Thin section examination revealed that approximately 20% of the sand clasts in this sample are chert. Hand (1998) found that fine-grained sedimentary rocks from the Black Flag Beds in the Kalgoorlie Terrane possess the geochemical characteristics of the felsic rocks from which they were derived. It is probable that the 20% chert clasts in CN851907 have an equivalent geochemical effect to assimilation of 20% bulk crust making the sample appear similar to the DCB. The lower abundances of Zr, Th and U can be explained as a lack of zircons within the chert, a heavy mineral which may not have been readily transported with the fine-grained sediments that formed the chert.

The remainder of the samples analysed in this study can be subdivided into groups previously defined from the lower Woolyeenyer Formation by McCuaig (1996). This subdivision is listed in Table 4.5. The majority of the samples are tholeiites but there are also representatives of the high-MgO tholeiites (HMT); the high-Fe tholeiites (HFT); both HFT and tholeiites with minor crustal contamination; and one possible

enriched high-MgO tholeiite (EHMT). Some of these groups have unusual REE patterns and have the suffix "spoons" added to the group name. This will be further discussed below.

Table 4.5: Mafic samples from the Chinaman's Well basalts, Polar Bear Peninsula and the Penneshaw Formation, divided into geochemical groups. Sample numbers and locality names are listed.

Tholeiites	HMT	HFT	Crustal contamin. tholeiite spoons	Contamin. HFT spoons	Contamin. mafic–sand (DCB-like)	EHMT
CN793733 Penneshaw	CN851948 Tuna	CN851599 Polar Bear	CN851595 Jewfish	CN851602 Snapper	CN851907 Cyprus Hill	CN851601 Snapper
CN793734 Penneshaw	CWS51 150.0 Swordfish		CN851598 Polar Bear	CN851906 Polar Bear		
CN793735 Penneshaw	CWS51 274.0 Swordfish		CN851600 Snapper	CN851901 Polar Bear		
CN793736 Penneshaw	CWS51 265.5 Swordfish *		CN851909 Polar Bear			
CN793737 Penneshaw	CWS51 308.6 Swordfish *		CN851913 Polar Bear			
CN851339 Polar Bear			CN851914 Jewfish			
CN851597 Jewfish						
CN851902 Causeway						
CN851904 Polar Bear						
CN851905 Polar Bear						
CN851915 Jewfish						
CN851916 Jewfish						
CN851917 Snapper						
CN851918 Davros						
CN851919 Davros						

*** indicates transitional between tholeiitic & HMT**

Tholeiites, HMT and HFT

Tholeiite is the most abundant basalt composition and was found at all prospects other than Swordfish and Tuna. All the samples from the mafic part of the Penneshaw Formation are tholeiitic.

The HMT samples were found at Swordfish and Tuna, in close proximity to the Norseman komatiite. Of the four Swordfish samples, one is komatiitic basalt, the others plot in the high-Mg tholeiite field of the Jensen diagram, but are divided between the HMT and tholeiite fields on the other diagrams. Two of the Swordfish

samples are transitional between tholeiite and HMT; Nevertheless, all these samples are classified as HMT as they have similar REE patterns and low TiO_2 values.

The classification of CN851599 from the Polar Bear Peninsula as HFT is based on its elevated Ti content and the similarity of the spidergram and REE patterns to GSWA 99941, which was designated HFT in section 4.9.3 of this study. The spidergram and REE patterns have a similar shape to tholeiite, but with higher abundances of all elements.

Crustal contamination

Ten samples display geochemical features indicative of crustal contamination. For reasons that are discussed below, it is considered that spoon-shaped REE patterns are the most definitive characteristic of basalts that have been contaminated by the crustal basement in the Norseman Terrane. More traditional geochemical evidence for crustal contamination, such as that shown by the Paringa Basalt and DCB (see section 4.9.3), centres on depleted Nb and Ta, observable at low degrees of contamination, and elevated LREE, U and Th, which become apparent in samples with higher degrees of contamination. Elevated U alone is not considered to be sufficient evidence, because in some samples it may be mobile, a situation apparently the case for SC1484-10, one of the tholeiites used for comparative purposes in the spidergrams. Ti may be depleted by crustal contamination, especially if the precursor magma was low Ti-bearing komatiite, but it is not always the case as some of the tholeiites, in particular the high Fe varieties, may be initially enriched in Ti.

Spidergrams for samples with characteristics suggestive of crustal contamination are shown in figures 4.13e, 4.13f, 4.13g and 4.13h. Contamination in the mafic-sand sample (figure 4.13g) by integration of chert clasts has been discussed above. The nine samples in the other three spidergrams are basalt, and crustal contamination must have occurred through assimilation of crust by the magma. Among the effects of crustal assimilation is that Zr will not be depleted, and if the crustal material contained significant quantities of zircons, U and Th may be elevated. This was apparently the case at Kambalda, as the DCB and Paringa Basalt, being contaminated komatiite, have elevated U and Th contents, and ancient zircons sourced from crust have been found (Compston & others, 1986).

Of the nine contaminated basalts, three are HFT, as indicated by elevated Ti and REE contents, and the other six are believed to be tholeiites. All nine contaminated basalt samples have relatively low MgO abundances (figure 4.9), an expected consequence of dilution of the magma with silicic material.

Five of the samples with crustal contamination came from the Polar Bear Peninsula, two came from Snapper and two from Jewfish. The samples from the Polar Bear Peninsula are from high in the stratigraphy. CN851909, the most strongly contaminated sample, was collected from a drillhole little more than 100 m from the overlying Abbotshall Beds, and CN851901 and CN851906 were located within 100 m of overlying komatiite. Similarly, the Jewfish and Snapper samples are all within 1.5 km of the overlying Abbotshall Beds and therefore are stratigraphically high in comparison to the total basalt thickness of about 6 km. The discovery of crustal contamination within basalt close to the top of the mafic succession, suggests that contamination may have been more prevalent in the latter stages of basalt eruption, when the magmas may have been the final, evolved products of magma chambers.

Spoon-shaped samples

As noted above, some samples have unusual spoon-shaped REE patterns (figures 4.11b, 4.11e and 4.11f). They have flat or gently sloping patterns for the LREE, are depleted in the heavier MREE, reaching a minimum at Ho and Er and then have a positive slope for the heaviest REE to return to levels close to those projected from the slope of the LREE. Spoon-shaped samples were returned from both sample batches (#1 & #2). Ghaderi (1998) noted similar REE patterns for the Silver Lake Peridotite at Kambalda, but provided no explanation.

To account for these unusual patterns, five possibilities are considered:

- Analytical error;
- Depletion due to hornblende or clinopyroxene fractionation;
- Mobilization of the REE as a response to alteration or metamorphism;
- Heavier REE hosted by minerals resistant to dissolution; and
- Contamination with crustal material.

The possibility of analytical error to account for the spoon-shaped samples is discounted as the spoon-shaped patterns were returned for only a few, non-sequential samples from both batches. There is no systematic error evident, and similar patterns were found by Ghaderi (1998).

Hornblende and clinopyroxene tend prefer MREE above other REE in their mineral structures (*cf.* partition coefficients of Arth (1976}, reproduced in Table 4.6). However, for basalts, the partition coefficients for all REE in these minerals are less

than one, indicating they are preferentially excluded. In this case, very high percentages of fractionation would be required to have any substantial effect on the REE patterns. In addition, the maximum partition coefficients for both hornblende and clinopyroxene are for Dy (partition coefficients of Arth (1976)), rather than Er and Ho. Nevertheless, this possibility is tested with fractional crystallisation modelling in section 4.10.4.2.

Secondary mobilization is a problematical explanation for the spoon-shaped patterns because REE are typically rather immobile. In addition, the heavy MREE have been selectively depleted rather than the larger, more incompatible LREE that would be expected to be more mobile (Rollinson, 1993).

The possible development of spoon-shapes as a result of alteration was further investigated with a bivariate diagram. Figure 4.14 shows a plot of Er_N/Yb_N versus volatile loss on ignition (LOI) measured as weight per cent. Samples with $Er_N/Yb_N<1$ have negative slopes for the HREE patterns which is typical for the spoons. All of the samples below the dashed line are spoon-shaped. The diagram indicates a very rough concurrence of spoon-shapes with higher volatiles, but it is not universal. The rocks with higher LOI are generally carbonate-rich and Humphries (1984) found CO_2-rich fluids to be more effective at mobilizing REE than aqueous fluids, which might support for the concept of mobile REE. However, this explanation is considered unlikely, based on evidence for the immobile nature of the REE discussed further in section 9.4. Ultramafic sample CN851911 is entirely altered to ankerite and minor vein quartz, probably by an intense flux of CO_2 through the rock, and yet has only a weak depletion of the LREE. MREE and HREE are unaffected and the rock retains a recognisable komatiite REE signature. It is considered highly unlikely that the spoon-shaped REE patterns were caused by alteration.

The possibility that minerals resistant to dissolution are responsible for the spoon-shaped patterns is based on Y analyses. Y is not a REE but has a similar ionic radius to Ho, the same +3 ionic charge and behaves in a very similar manner with equivalent partition coefficients to the HREE. A major difference between Y and the HREE is that its abundance is higher, sufficient to be measured using XRF for the basalt samples of this study.

For batch #1, all trace elements were initially conducted with ICP-MS, although Ti and Zr were later repeated with XRF. Spoon-shapes for these samples are smooth (e.g. CN851602, figure 4.13h, figure 4.13e). For batch #2, Y was measured using XRF. For the majority of the non-spoon-shaped, batch #2 samples, normalised-Y, analysed by XRF, is at a similar level to elements with similar

incompatibilities measured using ICP-MS. The result is a smooth spidergram pattern (e.g. figure 4.13b). However, batch #2 samples with spoon-shaped REE patterns, have a positive spike for Y in their spidergrams, breaking up the smooth curve of the HREE (figures 4.13f, 4.13g, & 4.13h). The evidence indicates that Y is similarly depleted to the HREE in spoon-shaped samples analysed by ICP-MS, but commonly returns a higher value when analysed using XRF. It is possible that the depleted REE and Y are hosted in a mineral resistant to acid dissolution so they do not register with ICP-MS, resulting in a spoon-shape.

The main problem with this possibility is that no common resistant minerals have a higher partition coefficient for Ho and Er over other REE (*cf.* mineral partition coefficients provided in Rollinson[1993]). The partition coefficients for zircon, for instance, increase steadily with REE atomic number so that Lu has the highest partition coefficient. Secondly, it must be questioned why the mineral is only in some samples, leaving other REE patterns normal. The analytical argument provided above may be reversed: perhaps the elevated Y in samples with spoon-shaped REE patterns are a result of analytical imprecision by XRF when measuring elements at low-levels, whereas the higher precision ICP-MS returned more accurate values.

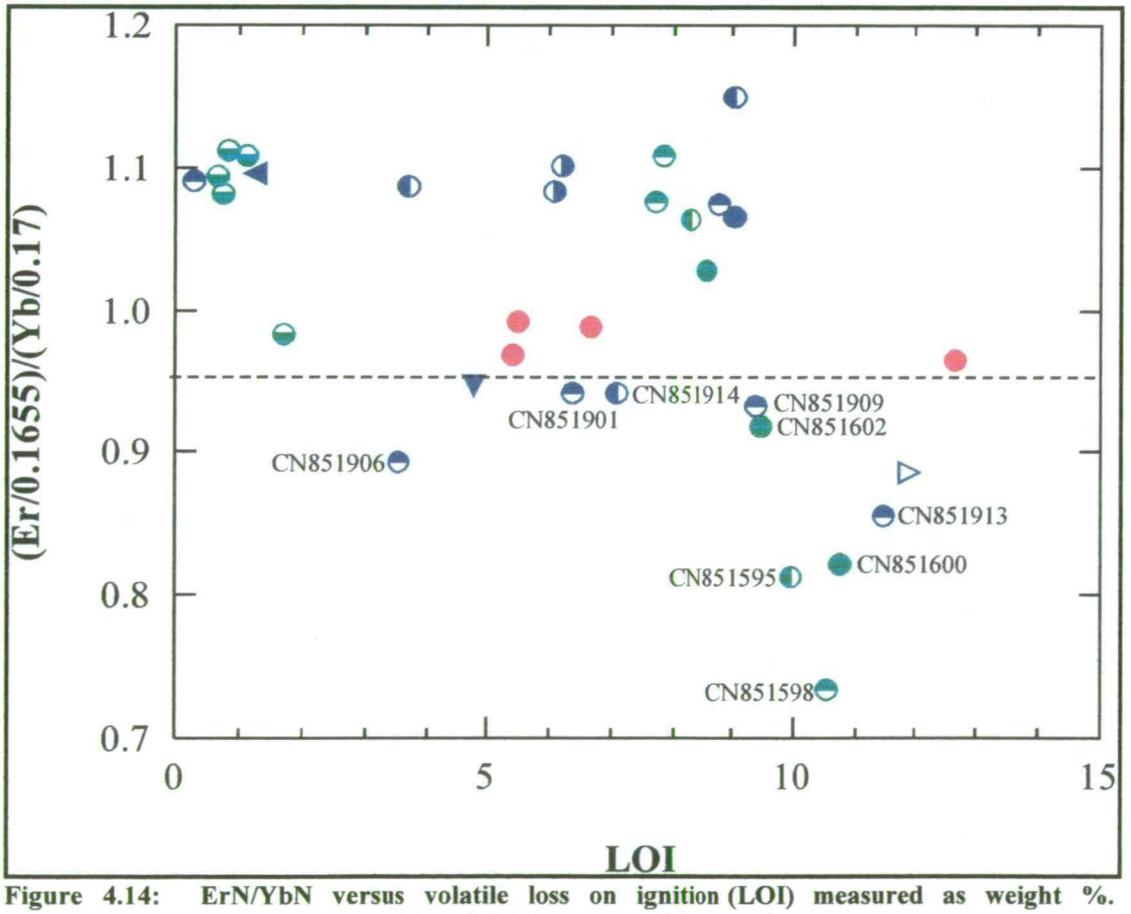

Figure 4.14: ErN/YbN versus volatile loss on ignition (LOI) measured as weight %. Normalisation factors are those of Sun & McDonough (1989) for C1 chondrite.

The fifth possibility to account for the spoon-shaped patterns is crustal contamination. This is considered to be the most likely explanation. No common estimates of bulk crustal composition possess Ho & Er depleted patterns (*cf.* data of; Taylor & McLennan (1985)). However, spoon-shaped chondrite-normalised REE patterns are characteristic of trondhjemites (Perring, 1989). Some felsic porphyries at Norseman (Dinky Buoys) and Kambalda have ladle-shaped REE patterns with intense depletion of the MREE to HREE (Perring, 1989). If a rock with such a REE signature occurred in the crustal basement, its assimilation by basalt may explain the spoon-shaped patterns. This possibility is tested with AFC modelling in section 4.10.4.

EHMT

Sample CN851601 from Snapper, is considered to be a highly fractionated member of the EHMT group. The sample's steep REE pattern resembles the EHMT group, but the low Mg number of CN851601 and the very low Ni and Cr, suggest significant fractional crystallisation of olivine and clinopyroxene respectively.

Bivariate plots of the incompatible elements TiO_2 and Zr against the Mg number as an index of fractionation (figures 4.15a & 4.15b), indicate that CN851601 is not a highly fractionated tholeiite, as it is enriched in these elements to a greater degree than expected from the fractionation trend of the tholeiites. The same bivariate plots show that EHMT magmas have steeper fractionation trends for TiO_2 and Zr that point roughly towards CN851601. The implication is that EHMT, or a primitive magma that gave rise to EHMT, may have generated CN851601 following extended fractionation. It is unlikely that contamination of magma with continental crust generated the steep REE pattern, because the sample does not have other trace element characteristics of known contaminated groups, such as strong Nb depletion in the Paringa Basalt (figure 4.13i).

The EHMT have extraordinarily low Al_2O_3 contents, which McCuaig (1996) attributed to residual aluminous garnet in the mantle source, whereas CN851601 has a tholeiitic alumina abundance (figure 4.15c). This can be explained through the fractionation trend for Al_2O_3 in the EHMT group, which is very steep and would reach tholeiitic levels at typical tholeiitic Mg numbers (figure 4.15c). Ni and Cr may increase over the small fractionation range of the EHMT (figures 4.15e & 4.15f), but more likely there is simply a wide range of values for these elements. McCuaig (1996) found evidence for clinopyroxene fractional crystallisation which should reduce both of these elements with decreasing Mg nunber. The interpreted origin of CN851601 as a fractionated member of the EHMT group is tested with FC modelling in the section 4.10.4.

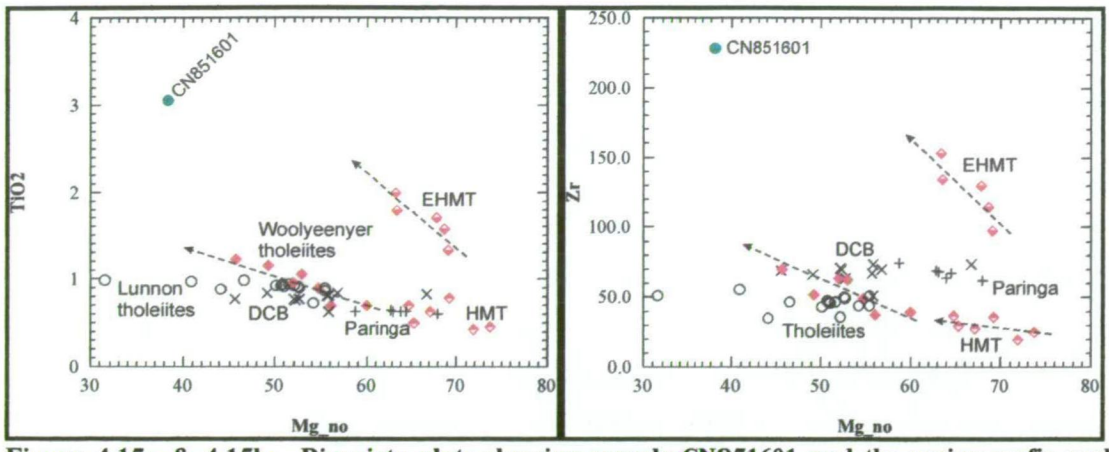

Figure 4.15a & 4.15b: Bivariate plots showing sample CN851601 and the major mafic rock groups from the data of McCuaig (1996) and Ghaderi (1998). Mg number (Mg_no) is the atomic fraction as shown in Table 4.2 and is used as an index of fractionation. Arrows show general trend with fractionation of Woolyeenyer Formation tholeiitic rocks and EHMT.

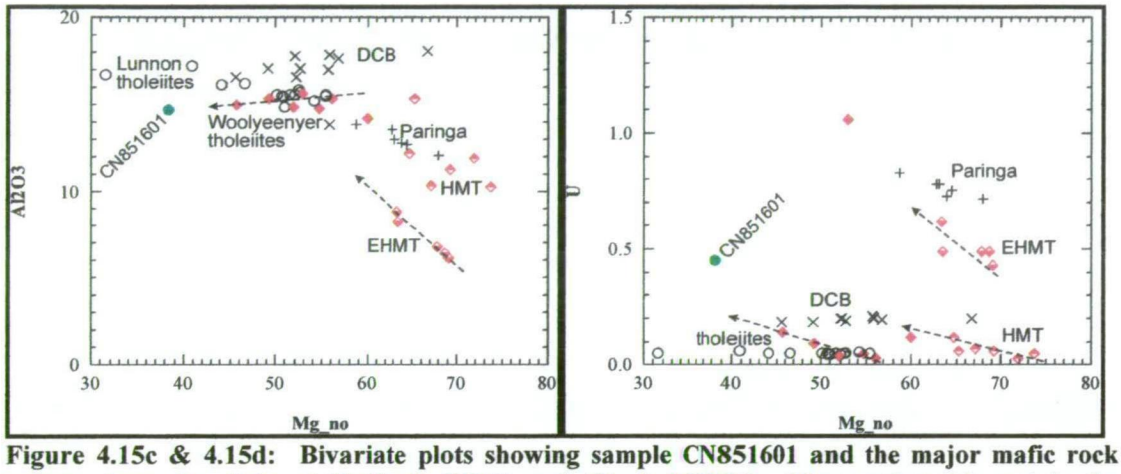

Figure 4.15c & 4.15d: Bivariate plots showing sample CN851601 and the major mafic rock groups from the data of McCuaig (1996) and Ghaderi (1998). Mg number (Mg_no) is the atomic fraction as shown in Table 4.2 and is used as an index of fractionation. Arrows show general trend with fractionation of Woolyeenyer Formation tholeiitic rocks and EHMT.

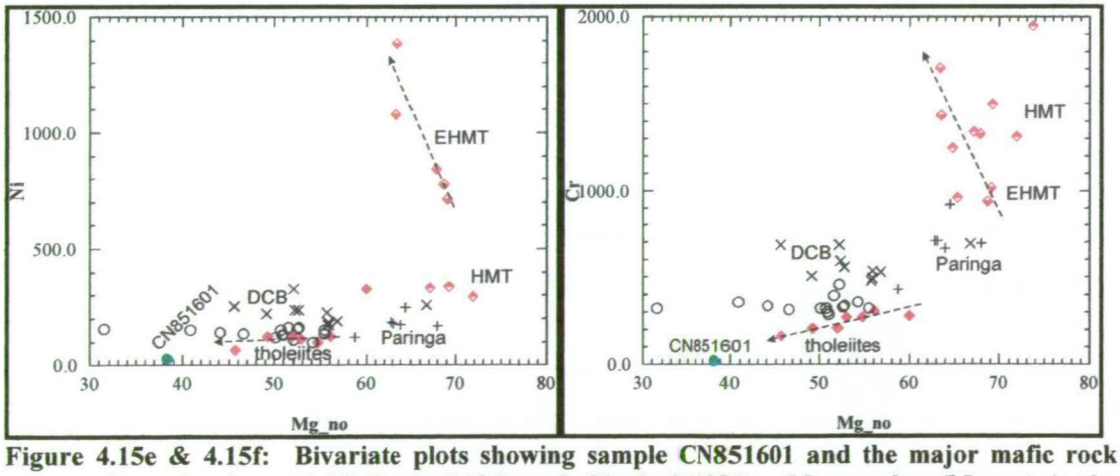

Figure 4.15e & 4.15f: Bivariate plots showing sample CN851601 and the major mafic rock groups from the data of McCuaig (1996) and Ghaderi (1998). Mg number (Mg_no) is the atomic fraction as shown in Table 4.2 and is used as an index of fractionation. Arrows show general trend with fractionation of Woolyeenyer Formation tholeiitic rocks and EHMT.

4.10.4 Petrogenetic Modelling

The results of petrogenetic modelling carried out for several of the basalt varieties are described in this section. The object of the work is to quantitatively test fractional crystallisation (FC) and assimilation, fractional crystallisation (AFC) models proposed for some samples in section 4.10.3. FC modelling is used to show that spoon-shaped REE patterns possessed by some basalt samples cannot be generated by amphibole or clinopyroxene fractionation. AFC modelling demonstrates that assimilation of crust with a ladle-shaped trondhjemitic REE pattern could be the origin of these patterns. Sample CN851601 was proposed in section 4.10.3 to be a fractionated member of the EHMT group and this argument is strengthened by the results of FC modelling.

To constrain the variables for this study, an assumption is made that the primitive mantle-derived magma source for the sample being examined was not unique and other basalts described in section 4.8 were also derived from a primitive melt of this composition. This assumption is considered reasonable because zircon dating in the Eastern Goldfields has shown that mafic volcanism occurred concurrently, at least across the southern part of the Province from Norseman to Menzies (figure 1.1), and possibly across the entire Eastern Goldfields (see Chapter 2). With such a large-scale magmatic event operating over a relatively short time period, it would not seem feasible that a small batch of magma with an unusual composition could be generated in some way and make its way from the mantle to the surface, past magma chambers without being homogenised by other magma batches. Under the assumption that the magma is not unique, the possibilities for the source magmas are reduced to komatiite, high MgO tholeiites (HMT) and EHMT, compositions identified by other authors as being precursors to all the other known basalt varieties (section 4.8).

4.10.4.1 Petrogenetic modelling of CN851601

AFC and FC modelling with a suite of eight trace elements was used to test whether CN851601 could be a highly fractionated member of the EHMT group. The elements were chosen based on their partition coefficients for minerals of interest, immobile behaviour and a sufficiently high abundance in the rock to reduce the influence of analytical precision at low levels as a controlling factor.

To measure fractionation of mafic minerals, Ni was chosen for olivine and Cr for clinopyroxene, while orthopyroxene preferentially includes both elements. Hornblende accommodates these elements but also has a high partition coefficient for Ti and Y, two other elements that were included. Plagioclase has low partition a coefficient for most elements except Sr, but this element is mobile so was not used in this study. Eu was used instead as it has a partition coefficient an order of magnitude

higher than other elements although it remains less than 1 for basalts (Table 4.6). To monitor the REE, Ce was used for the LREE, Gd the MREE and Y included as a proxy for the HREE. Zr is highly incompatible in most minerals in basalts but is enriched in the crust so can assist in detecting contamination. The partition coefficients for the elements used, and the references for the data are listed in Table 4.6.

Cr is an immobile element under metamorphic conditions, but Cr-steel mills used during sample preparation may contaminate the samples. However, there does not appear to have been any strong contamination because the samples are tightly constrained into groups in the bivariate plot in figure 4.15f. The sample of interest, CN851601, has low levels of Cr (24 ppm) so any Cr contamination has clearly been negligible and contamination of several ppm is unimportant as the original magma used has an abundance over 50 times greater (1324 ppm).

To plot the results (figure 4.16), the modelled elements were listed in order of decreasing incompatibility in oceanic basalts and normalised to N-MORB (after Sun & McDonough, 1989). The MORB values of Bevins & others (1984) were used for normalising Ni and Cr as values for these elements are not provided by Sun & McDonough (1989).

Table 4.6: Mineral /melt partition coefficients for basalts used in this study. References for data: (1) Arth (1976); (2) Arth (1976), Eu from Green & Pearson (1987).

Mineral: rock type (ref):	**Olivine** basalt (1)	**Orthopyroxene** basalt (1)	**Clinopyroxene** basalt (1)	**Hornblende** basalt (2)	**Plagioclase** basalt (1)
Y	0.010	0.18	0.900	1.00	0.030
Ti	0.020	0.10	0.400	1.50	0.040
Zr	0.012	0.18	0.100	0.50	0.048
Ce	0.0069	0.15	0.15	0.20	0.120
Nd	0.0066	0.31	0.31	0.33	0.081
Sm	0.0066	0.50	0.50	0.52	0.067
Eu	0.0068	0.51	0.51	0.40	0.340
Gd	0.0077	0.61	0.61	0.63	0.063
Dy	.00096	0.68	0.68	0.64	0.055
Er	0.0110	0.65	0.65	0.55	0.063
Yb	0.0140	0.62	0.62	0.49	0.067
Lu	0.0160	0.56	0.56	0.43	0.06
Ni	13	5	4	6.8	...
Cr	0.70	10	34	12.5	...

The hypothesis to be tested was that sample CN851601 was derived from EHMT magma. Accordingly, the starting magma chosen (C_O) was the most primitive MgO-rich EHMT magma (GSWA 99938).

Results

Rayleigh fractionation with 35% fractional crystallisation of an olivine and clinopyroxene mixture with a ratio of 0.65:0.35 gives a reasonable fit to CN851601 (Table 4.7, 4.8; figure 4.16). Importantly, the modelling indicates that fractionation of olivine and clinopyroxene sufficient to deplete the Cr and Ni to the appropriate low levels will cause both Ti and Zr to increase to around the same high levels as occur in CN851601. Eu, Gd and Y all increase although the levels are still below those in the target, and Ce continues to increases when the level in the EHMT starting composition is already higher than that in CN851601. There is, however, sufficient variability in range of these elements in the EHMT samples to account for these problems. Ce, for example, ranges from 34.6 to 60.8. In addition, the partition coefficients published in the literature vary rather widely, particularly for Ni in olivine and clinopyroxene, so these factors can account for all the error.

The effect of assimilating an average bulk crustal contaminant (Taylor & McLennan, 1985) while undergoing fractional crystallisation is to lower the concentration of all the elements. The percentage of crystallisation necessary to reduce Ni and Cr to appropriate values is reduced, but the concentration of the incompatible elements in the residual magma is also reduced (Table 4.8), producing model magmas with a less accurate fit than fractional crystallisation alone.

The conclusion is that CN851601 is a magma produced by fractional crystallisation of olivine and pyroxene from an EHMT parent with no crustal assimilation.

4.10.4.2 FC modelling for spoon-shaped REE patterns

Modelling was used to determine whether the spoon-shaped samples could be tholeiites or HFT in which fractional crystallisation has depleted the middle to heavy REE and produced the spoon-shaped patterns. Notwithstanding the thermal improbability in fractionating hornblende, basaltic hornblende and clinopyroxene were selected as the minerals to test, as they have a preference for MREE to HREE (Table 4.6) A suite of nine REE from Ce to Lu were modelled, and also Ni to monitor the degree of depletion of compatible elements.

McCuaig (1996) concluded that the tholeiites were produced by fractionation of magmas of HMT composition. The most MgO-rich sample of McCuaig (1996) for which a Ni analysis was provided (PRS1177-13), was used as the starting magma

composition for the modelling. CN851914, a tholeiite sample from Jewfish with a relatively subdued spoon-shape was selected as the target magma that the FC modelling would attempt to replicate.

Table 4.7: Results of Rayleigh fractional crystallisation modelling using a mixture of 65% olivine, 35% clinopyroxene.

	Ce	Zr	Eu	Ti	Gd	Y	Cr	Ni	Sample_no
C_O	54.0	130	1.5	9768	4.9	16.4	1325	844	GSWA109064
Target	49.6	228	2.5	14800	8.1	31.6	24	30	CN851601
									% Fractional Crystallisation
Model#1	75.5	182.9	2.0	13213	6.5	20.9	23.1	35.9	30%
Model#2	81	196.3	2.1	14069	6.8	22.0	10.0	18.6	35%

Table 4.8: Results of AFC modelling using 5% assimilation of bulk continental crust (A/FC = 0.2) to 25-30% fractional crystallisation of a mixture of 65% olivine, 35% clinopyroxene. C_O and target as in Table 4.6

AFC model: r = 0.2; A = bulk crust; FC = 65% olivine, 35% clinopyroxene									
Model #3	73.2	179.8	1.9	12764	6.3	19.7	23.9	34.8	**25%**
Model #4	78.6	193.9	2.1	13592	6.7	20.5	10.9	17.2	**30%**

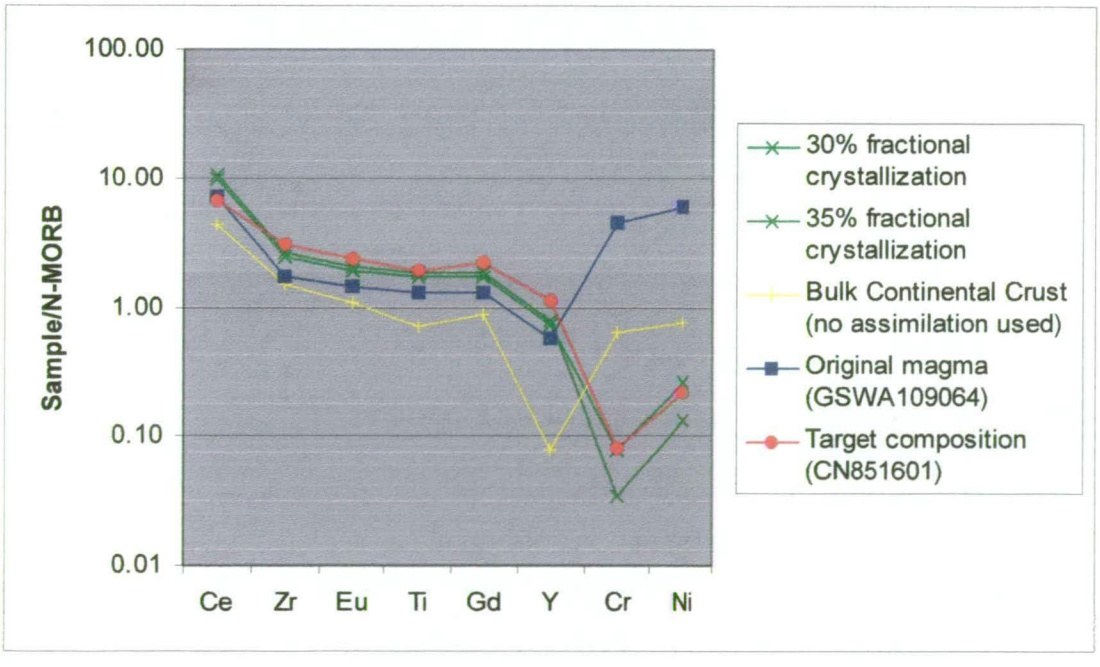

Figure 4.16: N-MORB normalised truncated spidergram (Sun & McDonough, 1989; Cr + Ni: Bevins & others, 1984) showing results of Rayleigh Fractional Crystallisation modelling from Table 4.7. Target composition is sample CN851601. Starting magma composition(C_O) is GSWA 109064 (McCuaig, 1996). 30% & 35% FC of 65% olivine, 35% clinopyroxene shown. Also shown: composition of bulk continental crust (Taylor & McLennan, 1985).

Results

Rayleigh fractionation of amphibole alone reduces Ni contents to the appropriate levels at about 15% crystallisation but the REE pattern continues to mimic the HMT shape with slightly higher overall abundances. Due to partition coefficients of less than one, amphibole fractionation does not produce a pronounced effect on the REE pattern of the residual magma until 70 to 80% crystallisation has taken place and then the minima is at Gd and Dy rather than Er.

Table 4.9: Results of modelled Rayleigh fractional crystallisation of clinopyroxene and amphibole

	Ce	Nd	Sm	Eu	Gd	Dy	Er	Yb	Lu	Ni	Sample_no
C_O	4.51	3.8	1.13	0.46	1.45	1.86	1.2	1.1	0.18	379	PR1177-13
Target	7.65	5.5	1.6	0.66	2.0	1.9	1.1	1.2	0.2	124	CN851914
											Cpx Fract. Crystallizat.
Model#1	6.1	4.9	1.4	0.5	1.7	2.1	1.4	1.3	0.2	130	30%
Model#2	17.7	11.5	2.5	1.0	2.7	3.1	2.1	2.0	0.4	3.0	80%
											Amph. Fract. Crystallizat.
Model#3	5.1	4.2	1.2	0.5	1.5	2.0	1.3	1.2	0.2	148	15%
Model#4	16.3	11.2	2.4	1.2	2.6	3.3	2.5	2.5	0.5	0.0	80%

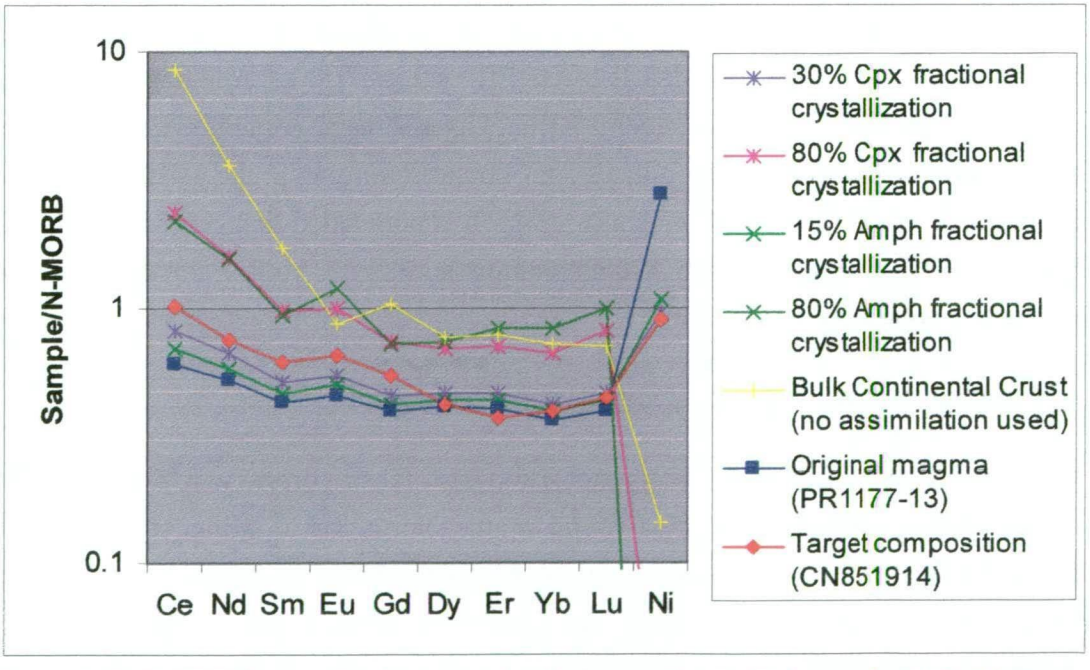

Figure 4.17: N-MORB normalised truncated spidergram (Sun & McDonough, 1989; Ni: Bevins & others, 1984) showing results of Rayleigh Fractional Crystallisation modelling from Table 4.8. Target composition is sample CN851914. Starting magma composition(C_O) is PR1177-13 (McCuaig, 1996). 30% & 80% FC of clinopyroxene and 15% & 80% FC of amphibole shown. Composition of bulk continental crust also shown (Taylor & McLennan, 1985).

Rayleigh fractionation of clinopyroxene alone reduces Ni contents to the appropriate levels at about 30% crystallisation at which point the REE pattern still mimics HMT but with slightly higher abundances. Due to partition coefficients of less than one, clinopyroxene fractionation does not produce a pronounced effect on the REE pattern of the residual magma until 70 to 80% crystallisation has taken place. At those levels of crystallisation, there is a broad, flat minima in the REE patterns between Dy and Yb rather than a low point at Er.

It is concluded that fractional crystallisation or assimilation with a typical crustal contaminant could not have produced the spoon-shaped REE patterns.

4.10.4.3 AFC modelling for spoon-shaped REE patterns

Assimilation fractional crystallisation modelling were used to test whether a spoon-shaped REE pattern could be produced by contamination of magma with crust. Contamination with bulk crust estimates are unsuccessful, as they have flat HREE to MREE. Assimilation with the Penneshaw granitoid, which may be a fragment of crustal basement, also does not produce spoon-shapes. However, a contaminant with a pronounced ladle-shape similar to the Dinky Buoys Porphyry can produce the appropriate shapes.

Results for AFC using bulk crustal estimates

Assimilation of Taylor & McLennan's (1985) estimate for the bulk continental crust would not produce spoon-shapes, as crust has no minima but has a steep LREE pattern and a gently sloping MREE to HREE pattern. Upper continental crust has flat MREE to HREE and very steep LREE. Upper crustal contamination combined with amphibole fractionation produces a pronounced minima in the MREE at Dy, not Er and only with 70% to 80% crystallisation. It is concluded that contamination of a HMT magma with crust with a composition similar to bulk estimates, will not produce spoon-shapes.

AFC modelling using a Dinky Buoys Porphyry composition

AFC models were run using the composition of a felsic porphyry at Norseman, the Dinky Buoys porphyry, which is found at the North Royal Mine (see Chapter 8, figure 8.15) as the contaminant. Perring (1989) presented average analyses for the Dinky Buoys suite and described the pattern as ladle-shaped. There is strong depletion of the HREE with a minimum at Er so it appears to be a contaminant that may provide a spoon shape. The Dinky Buoys Porphyry or its relations could not have been the contaminant as it is younger than the basalt. The assumption is that the

ancient crustal basement may contain substantial trondhjemitic granitoid with a similar REE pattern.

Table 4.10: Results of AFC modelling using 5% and 3% assimilation of crust with the composition of the Dinky Buoys Porphyry (A/FC = 0.2) concurrent with 25% & 15% fractional crystallisation of clinopyroxene or amphibole. Contaminant composition is the analysis of Perring (1989). C_O and target as in Table 4.9 & 4.10, HMT and spoon-shaped basalt respectively.

	Ce	Nd	Sm	Eu	Gd	Dy	Er	Yb	Lu	Ni	Sample_no
Co	4.5	3.8	1.1	0.5	1.5	1.9	1.2	1.1	0.2	379	PR1177-13
Target	7.65	5.5	1.6	0.66	2.0	1.9	1.1	1.2	0.2	124	CN851914
Contaminant	32.4	13.8	4.6	1.7	3.2	1.0	0.5	0.6	0.5	3	Dinky Buoys

Model	**Ce**	**Nd**	**Sm**	**Eu**	**Gd**	**Dy**	**Er**	**Yb**	**Lu**	**Ni**	**FC%**
AFC model: r = 0.2; A = Dinky Buoys porphyry; FC = amphibole; 3% assimilation											
Model#1	6.5	4.8	1.4	0.64	1.8	2.0	1.3	1.2	0.2	112	15%
AFC model: r = 0.2; A = Dinky Buoys porphry; FC = clinopyroxene; 5% assimilat.											
Model#2	8.3	5.6	1.6	0.6	1.8	2.0	1.3	1.2	0.2	120	25%

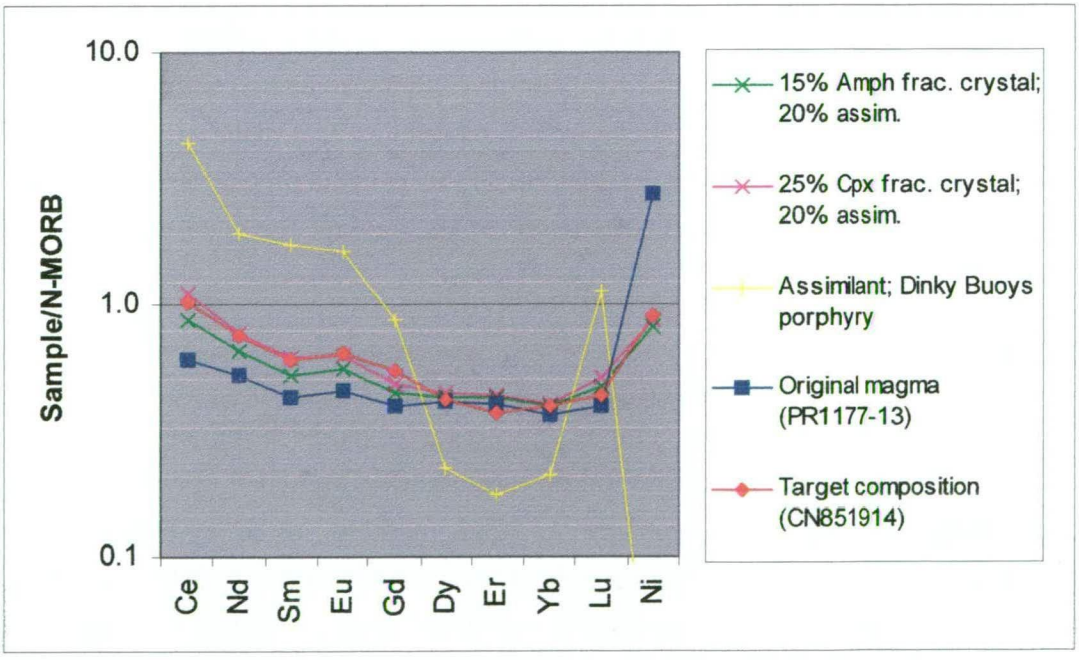

Figure 4.18: : N-MORB normalised truncated spidergram (Sun & McDonough, 1989; Ni: Bevins & others, 1984) showing results of AFC modelling from Table 4.10. Target composition is spoon-shaped sample CN851914. Starting magma composition (C_O) is PR1177-13 (McCuaig, 1996). Contaminant is Dinky Buoys Porphyry (Perring, 1989). Results plotted are 25% FC of clinopyroxene at an A/FC ratio of 0.2, and 15% FC of amphibole at an A/FC ratio of 0.2. Percentages of FC were chosen by their similar abundances of Ni to the target composition.

Results

The results of the AFC modelling are shown in Table 4.10 and plotted in figure 4.18. The ladle-shaped normalised trace element pattern of the Dinky Buoys porphyry is

conducive to developing a spoon-shaped pattern for the contaminated magma. Close results can be achieved using assimilation to fractional crystallisation ratios of either 0.1 or 0.2, with the latter being slightly better, and 15% to 25% clinopyroxene or amphibole fractional crystallisation. At an A/FC of 0.3, the LREE and increase to Lu becomes too steep. Clinopyroxene tends to give a slightly more accurate shape than amphibole because the highest partition coefficients are at the appropriate HREE. Fractionation of clinopyroxene is also more likely than amphibole in a basalt.

With sample PR1177-13 as the composition of the original magma, Er cannot achieve the minima of the spoon shaped sample. A more primitive magma with lower REE is necessary. Apart from Er, it is concluded that a reasonable fit can be achieved using assimilation of 5% crust with the composition of the Dinky Buoys Porphyry and 25% concurrent fractional crystallisation of clinopyroxene.

AFC modelling using a Penneshaw Granitoid composition

The granitoid in the felsic domain of the Penneshaw Formation has been dated at *ca.* 2930 Ma, suggesting it may be a fragment of the crustal basement beneath the greenstone (see Chapter 7). If this is the case, it is possible that magmas have assimilated basement with a similar composition so AFC models were run to determine whether spoon-shaped REE patterns could be generated using the granitoid as the contaminant. Only one trace element analysis of this material was available, sample 86-222, analysed by Ghaderi (1998), so this is the composition used. Models were run with amphibole and clinopyroxene as the mineral fractionating from HMT magma PR1177-13.

Results

The closest result to the target composition was achieved by using an A/FC ratio of 0.1 with 15% fractional crystallisation of amphibole. The LREE abundances in the contaminant are very high causing a rapid increase in these elements with contamination of the magma. If higher A/FC ratios are used, the LREE exceed target levels well before a sufficient percentage of fractional crystallisation has taken place to suppress Ni to the appropriate level. Using clinopyroxene as the fractionating mineral has a similar effect to increasing the A/FC ratio. The partition coefficient for Ni in clinopyroxene is lower than that for amphibole, requiring a greater amount of fractional crystallisation to lower the Ni abundances while concurrent assimilation is raising LREE abundances. Lowering the ratio of A/FC to 0.05 and using clinopyroxene gives a similar result to amphibole.

Table 4.11: Results of AFC modelling using ratios of 10% and 20% assimilation/fractional crystallisation and 15%, 20% and 25% concurrent fractional crystallisation of 100% amphibole and 100% clinopyroxene. Contaminant has the composition of Penneshaw granitoid sample 86-222 (Ghaderi, 1998). C_O and target as in Table 4.9 & 4.10, HMT and spoon-shaped basalt respectively.

	Ce	Nd	Sm	Eu	Gd	Dy	Er	Yb	Lu	Ni	Sample_no
Co	4.5	3.8	1.1	0.46	1.5	1.9	1.2	1.1	0.2	379	PR1177-13
Target	7.7	5.5	1.6	0.66	2.0	1.9	1.1	1.2	0.2	124	CN851914
Contamin.	*108*	*35.1*	*5.1*	*0.80*	*3.2*	*2.2*	*1.1*	*1.2*	*0.2*	*2*	*86-222*

Model	**Ce**	**Nd**	**Sm**	**Eu**	**Gd**	**Dy**	**Er**	**Yb**	**Lu**	**Ni**	**FC%**
AFC model: r = 0.1; A = Penneshaw granitoid 86-222; FC = amphibole; 1.5% assim.											
Model#1	7.2	4.9	1.3	0.5	1.6	2.0	1.3	1.2	0.2	131	**15%**
AFC model: r = 0.2; A = Penneshaw granitoid 86-222; FC = amphibole; 3% assim.											
Model#2	9.7	5.7	1.4	0.5	1.6	2.0	1.3	1.2	0.2	112	**15%**
AFC model: r = 0.1; A = Penneshaw granitoid 86-222; FC = clinopyrox.; 1.5% assim											
Model#3	9.6	5.8	1.5	0.5	1.7	2.1	1.3	1.2	0.2	141	**25%**
AFC model: r = 0.2; A = Penneshaw granitoid 86-222; FC = clinopyrox.; 3% assim.											
Model#4	12.0	6.5	1.5	0.5	1.7	2.0	1.3	1.2	0.2	155	20%

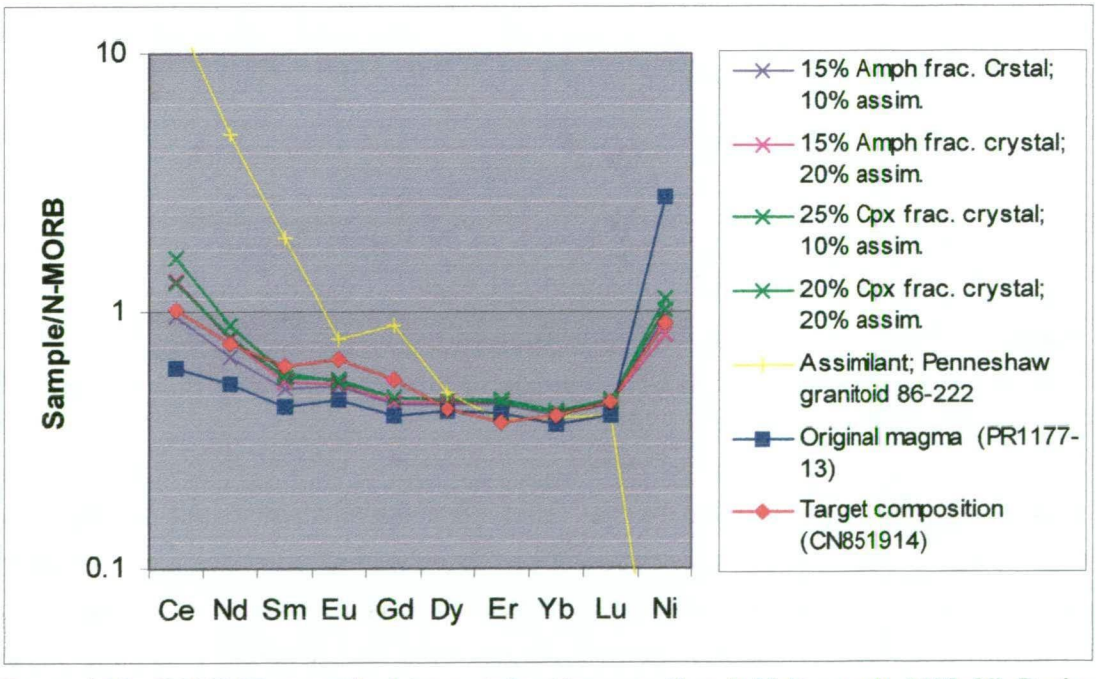

Figure 4.19: N-MORB normalised truncated spidergram (Sun & McDonough, 1989; Ni: Bevins & others, 1984) showing results of AFC modelling from Table 4.11. Target composition is sample CN851914. Starting magma composition (C_O) is PR1177-13 (McCuaig, 1996). Contaminant is Penneshaw granitoid sample 86-222 (Ghaderi, 1998). Results plotted are 15% FC of amphibole at A/FC ratios of 0.1 & 0.2, and 25% & 20% FC of clinopyroxene at A/FC ratios of 0.1 & 0.2. Percentages of were FC chosen by their similar abundances of Ni to the target composition.

None of the results give a particularly close fit to the target composition (figure 4.19, Table 4.11). The elevated LREE can be achieved, however the modelled results for the MREE are too low and the HREE are too high, continuing to mimic the HMT and not achieving a spoon shape. It is concluded that spoon-shapes cannot be achieved using the Penneshaw granitoid as a contaminant.

Conclusion

AFC modelling suggests that spoon-shaped REE patterns can be achieved by assimilating a contaminant with a ladle-shaped REE pattern. Ladle-shapes are characteristic of some trondhjemites (Perring, 1989), which must have undergone substantial subtraction of amphibole from a felsic melt composition to achieve these REE patterns. Approximately 5% contamination of a high magnesian tholeiite slightly more primitive than PR1177-13 with crust having the composition of the Dinky Buoys Porphyry, combined with 25% concurrent clinopyroxene fractional crystallisation, achieves the spoon-shaped pattern of CN851914. More intense spoon-shapes such as CN851909 would require somewhat greater degrees of assimilation.

Four other suggestions for the production of spoon-shaped REE patterns were examined in section 4.10.3, but all were concluded to be unlikely. Therefore spoon-shaped REE patterns in basalt are considered to be the result of crustal assimilation by a contaminant with a trondhjemitic-style, ladle–shaped REE pattern.

4.11 DISCUSSION

The main purpose of this geochemical study of the Polar Bear and Chinaman's Well basalts was to test a hypothesis, advanced in Chapter 3, that the basalts overlying the Norseman komatiite is a structural repetition of the lower Woolyeenyer Formation. This test was achieved through a comparison of the geochemistry of the basalts with Kambalda.

Previous studies have divided basalts from the Kambalda area into several types based on geochemistry and stratigraphy using the komatiite as a regional chronostratigraphic marker unit. The basic theme is that footwall basalts to the komatiite (Lunnon Basalt) may be classified as tholeiitic, whereas overlying basalts are all derived from a komatiitic parent magma by AFC processes. The komatiite magma becomes increasingly contaminated by crust with increasing stratigraphic height giving the upper basalts a distinctive chemistry that has been termed siliceous high magnesian basalt (SHMSB). The characteristic trace elements for these basalts are enriched LREE, flat HREE and depleted Nb, Ta and Ti. The Paringa Basalt, a

unit with a thickness of greater than 1 km, has this chemistry at Kambalda and Kalgoorlie.

GSWA 1:100 000 scale geological mapping of the area between Norseman and Menzies in the Eastern Goldfields, indicates that tholeiitic basalt is not found above the komatiite. Tholeiitic volcanism ceased and was replaced by komatiitic volcanism. If the basalts overlying the Norseman komatiite are *in situ*, they would be expected to share the distinctive SHMSB chemistry of the hangingwall basalts at Kambalda. Conversely, if the Chinaman's Well and Polar Bear basalt units are a structural repetition of the lower Woolyeenyer Formation, then the basalts should have similar geochemical characteristics to this unit.

Within the lower Woolyeenyer Formation, the majority of rocks are tholeiitic, with N-MORB style trace element patterns, equivalent in composition and stratigraphic position to the Lunnon Basalt at Kambalda. However, McCuaig (1996) also found five other groups, largely occurring as mafic intrusives. HMT rocks are similar to the tholeiites, but have higher MgO. The tholeiitic basalt may have been derived from HMT magmas by fractional crystallisation. EHMT rocks are rare, but have a very different chemistry to the main group of N-MORB tholeiites. EHMT rocks have distinctive low-alumina and steep REE patterns. They may be sourced from deep within the mantle, leaving aluminous garnet in the residuum. Two other groups, ET and THMT, are rare and may represent mixing of HMT and EHMT magmas. The final group identified has similar trace element characteristics to the tholeiitic basalt but with overall higher abundances of incompatible elements including Ti. It has been classified as high Fe tholeiites (HFT) in this study.

This study compared the compositions of 26 basalts from the Chinaman's Well and Polar Bear areas; and 5 basalts from the mafic Penneshaw Formation, with basalt in the lower Woolyeenyer Formation and at Kambalda. No samples were found to have the distinctive trace element signature of Paringa Basalt; instead, they are largely equivalent to the units from the lower Woolyeenyer Formation, with tholeiitic basalt being the dominant group rather than the uniform SHMSB that comprises the Paringa Basalt. This supports the hypothesis that the basalt units overlying the komatiite and within the mafic part of the Penneshaw Formation are thrust repetitions of the lower Woolyeenyer Formation.

An alternative suggestion, that repetition of the basalt above the komatiite may be magmatic, based on complex dynamics of a plume in the model of Campbell and Hill (1988), is not supported because it would fail to explain the repetition of the Norseman komatiite beneath Lake Cowan at the Polar Bear Peninsula. An even more complex plume model involving repetition of komatiitic magmas would be

inconsistent with the geochronological testing across the Eastern Goldfields that suggests there is only one komatiitic event (Nelson, 1997).

Basalt types found in this study that can be directly equated with the groups in the lower Woolyeenyer Formation are fifteen tholeiites, which includes all five of the Penneshaw Formation samples, five HMT, one HFT and one basalt which is suggested to be a fractionated EHMT. Another nine basalts have unusual spoon-shaped chondrite-normalised REE patterns that have previously been detected in komatiites at Kambalda. The petrogenetic modelling in this study indicates that spoon-shaped REE patterns cannot be generated by fractional crystallisation of clinopyroxene or amphibole, but are probably the result of HMT assimilating trondhjemitic crust with a ladle-shaped chondrite-normalised REE pattern, similar to the composition of the Dinky Buoys Porphyry.

Six of the samples with spoon-shaped REE patterns can be geochemically modelled as HMT magmas, contaminated with Dinky Buoys Porphyry with concurrent fractional crystallisation, whereas three may be contaminated HFT. In addition to the spoon-shaped REE patterns, evidence for contamination is the depleted Nb and Ta and, with higher degrees of contamination, enriched LREE, U and Th, as occurs for the Paringa Basalts and DCB. Ti depletion is not apparent, possibly because it is already enriched in these tholeiitic samples in comparison to the low Ti abundances of the komatiitic magmas that gave rise to the DCB and Paringa Basalt.

The discovery of, and interpretation placed on the basalts with spoon-shaped REE patterns raises two questions: If the basalts overlying the Norseman komatiite are a thrust repetition of the lower Woolyeenyer Formation, why have basalts with spoon-shaped REE patterns not been reported from the lower Woolyeenyer Formation? Second, high degrees of crustal contamination have occurred at Kambalda, 15 to 24% for the Paringa Basalt, yet these basalts have flat HREE patterns. Why do contaminated basalts at Norseman have spoon-shaped REE patterns whereas the contaminated basalts at Kambalda do not?

The most reasonable explanation for the first question is sampling bias. The majority of the samples with REE analyses from the lower Woolyeenyer Formation come from diamond drill core in the vicinity of the gold mines at Norseman. They have been collected largely from the Mararoa Pillow Lava, the Royal Amphibolite and Crown Basalt members of the Woolyeenyer Formation that occur near the base of the 6 km-thick unit. In contrast, most of the samples for this study were collected from close to the top of the basaltic formation, typically, between 1500 m and 100 m from the contact with the overlying Abbotshall Beds or komatiite, as these were the localities where samples were available. Therefore, directly equivalent stratigraphic

units have not been analysed as appropriate samples and pre-existing analyses were not available. Contaminated basalts with spoon-shaped REE patterns may occur in the Desirable Pillow Lava member of the lower Woolyeenyer Formation, which has not been sampled.

The lack of spoon-shaped REE patterns in the Paringa Basalt at Kambalda may indicate a different basement composition hosting the mafic magma chambers that were undergoing fractionation and assimilation. At Norseman, AFC modelling suggests the basement has trondhjemitic affinities, formed by a large proportion of amphibole being extracted from felsic magma, leaving a ladle-shaped REE pattern. In contrast, AFC modelling by Arndt & Jenner (1986) and Sun & others (1989) suggests that below Kambalda, the basement may have a composition similar to estimates for either bulk continental crust or felsic (but not trondhjemitic) upper crust. The difference between Norseman and Kambalda may indicate that batholithic-sized trondhjemitic intrusions are present in the basement beneath Norseman.

Although this study has shown that the Polar Bear and the Chinaman's Well basalts are dominantly tholeiites, and not contaminated komatiite like the Paringa Basalt, the possibility remains that DCB-equivalent lavas may occur immediately above the Norseman komatiite. The DCB has a thickness of only 200 m at Kambalda, far too narrow for the sample spacing of this study to define. High MgO basalts have been located at the Tuna and Swordfish prospects, close to the upper contact of the Norseman komatiite. These are considered to be highly differentiated members of the komatiite package, but there is no evidence for crustal contamination of these units. These high MgO basalts are similar in chemistry to the HMT dykes that McCuaig (1996) suggested are rather primitive magmas from which the tholeiites were derived by fractional crystallisation.

The composition of the dominant basalts, tholeiites with N-MORB trace element patterns, places constraints on the models by which they have formed. Tholeiitic magmas typically involve fractionation of the anhydrous mineral assemblage plagioclase, olivine, clinopyroxene and oxides, at low pressure and low $f(O_2)$. The depletion of incompatible elements in N-MORB may be generated by partial melting of upper mantle previously depleted of incompatible elements in previous melting events. As the temperature of the upper mantle is below the solidus under normal conditions, the melting is thought to occur due to adiabatic decompression caused by upwelling of the mantle beneath crust that is undergoing extension (Wilson, 1989).

A basaltic sand sample had a strong geochemical similarity to DCB. This is caused by mechanical contamination by crustal material in the form of chert clasts rather

than assimilation. Without the chert, the basaltic clasts probably had a tholeiitic signature, so it is geochemically feasible that this sample was derived by erosion of Polar Bear basalt equivalent to the lower Woolyeenyer Formation.

4.12 CONCLUSION

The aims listed for the mafic geochemical study listed at the start of this chapter can now be addressed. It is concluded that:

- The Chinaman's Well and Polar Bear basalts are dominantly tholeiitic sequences that are geochemically equivalent to the lower Woolyeenyer Formation. They are not similar to the Paringa Basalt at Kambalda. Therefore, the hypothesis that the basalt overlying the Norseman komatiite is a thrust repetition of the lower Woolyeenyer Formation is supported.

- Similarly, five basalts from the Penneshaw Formation have a tholeiitic composition, consistent with the mafic part of the Penneshaw Formation being a structural repetition of the lower Woolyeenyer Formation.

- As the komatiite within the Eastern Goldfields is considered to be regional marker bed, the Lunnon Basalt beneath the Kambalda Komatiite is considered to be the stratigraphic and time equivalent of the lower Woolyeenyer Formation below the Norseman komatiite. The crustally contaminated komatiite above the Kambalda Komatiite (DCB and Paringa Basalt), is not recognised at Norseman. The Paringa Basalt has a distinctive geochemical signature, is homogenous and has a thickness of more than 1 km. The sampling program in this study is sufficient to show that a similar thick unit does not occur at Norseman. The DCB, which directly overlies the Kambalda Komatiite, has a thickness of only about 200 m. There is insufficient sampling of the equivalent stratigraphic position in the Norseman Terrane, immediately above the Norseman komatiite, to preclude the possibility of sliver of DCB equivalent overlying the komatiite at Norseman. High MgO basalt samples occur at Tuna and Swordfish close to the top of the komatiite, but these samples display no evidence for crustal contamination. They are considered to sample a differentiated part of the Norseman komatiite.

- The tholeiitic basalt that dominates the mafic sequences at Norseman and the Lunnon Basalt at Kambalda has a geochemical signature very similar to N-MORB. Rocks in the tholeiite series differentiate an anhydrous assemblage of minerals typically under low pressure, low $f(H_2O)$ and a reduced oxidation state. Depletion of incompatible elements in N-MORB is widely considered to be evidence for its formation as a partial melt of the upper mantle from which the

incompatible elements were removed by previous magmatic events. The temperature of the upper mantle is below the solidus under normal conditions, so melting to form N-MORB-style basalts is considered to form by pressure-release melting of upwelling mantle in an extensional plate tectonic setting (Wilson, 1989). A similar mechanism must have led to the development of the Archaean N-MORB basalts. Tectonic models are considered further in Chapter 12.

- A significant number of basalt samples from Chinaman's Well and the Polar Bear Peninsula were found to have spoon-shaped REE patterns. AFC modelling suggests these patterns could be the result of about 5% crustal contamination of a high MgO basalt (HMT) with concurrent clinopyroxene fractionation. The contaminant would need to have a ladle-shaped REE pattern similar to the Dinky Buoys Porphyry. These REE patterns are possessed by some trondhjemites. The absence of spoon-shaped patterns from contaminated magmas (Paringa Basalt) at Kambalda and their presence at Norseman may be explained by a difference in composition of the basement between Norseman and Kambalda.

- The basaltic sand sample from Cyprus Hill has a crustal contamination signature, probably derived from the approximately 20% chert clasts in its composition. Without the crustal signature, the basalt would probably be similar to a tholeiite, consistent with its suggested derivation by erosion of the basalt at the Polar Bear Peninsula.

CHAPTER FIVE

Sedimentary Facies Analysis for the Norseman Terrane

5.1 INTRODUCTION

Chapter 3 presented the results of mapping at the Polar Bear Peninsula, to establish the stratigraphy of the upper Norseman Terrane. That work reported the presence of mafic conglomerates and resedimented rhyolite-sediment breccias, which required detailed study to determine their origins. This chapter presents the detailed studies of these sediment facies which leads to conclusions about the paleo-environment

Layout of the chapter

The chapter first discusses the genetic processes involved in the deposition of the mafic conglomerate and sandstone units, and what the facies indicates about the paleo-environment. The chapter then examines the genesis of the resedimented rhyolite breccia and resedimented rhyolite-sediment breccia, by examining three key exposures and then considering the character of the exposures against likely processes of formation.

5.2 FACIES ANALYSIS OF THE MAFIC CONGLOMERATE AND SANDSTONE; SANDSTONE-SHALE TURBIDITE AND LAMINATED CHERT.

In section 3.2.7, mafic conglomerate and mafic sandstone overlying the mafic succession were described. The two best exposures of the facies are at localities known as Cyprus Hill and south central Polar Bear (figure 5.1), which are described in sections A1.2.5 and A1.2.4 of Appendix 1 respectively.

The conglomerate and sandstone units are intimately associated and together form one facies. The facies is patchy in distribution and only found in certain localities. At Cyprus Hill, the conglomerate and sandstone is overlain by chert of the Abbotshall Beds. At south central Polar Bear, there is a rapid fining up transition, from conglomerate and sandstone, to sand-shale turbidites and then chert of the Abbotshall Beds.

In section 3.2.7, it was noted that the clast assemblage within the conglomerate, basalt and chert, indicates erosion of the mafic succession with the chert clasts derived from the interflow sedimentary layers (Plate 5.1). The absence of other clast compositions suggests that only the mafic stratigraphy was eroded. It was also noted that the well-rounded, and in some cases spherical clasts, indicate exposure to a shoreline or fluvial environment, both of which imply a shallow to emergent setting.

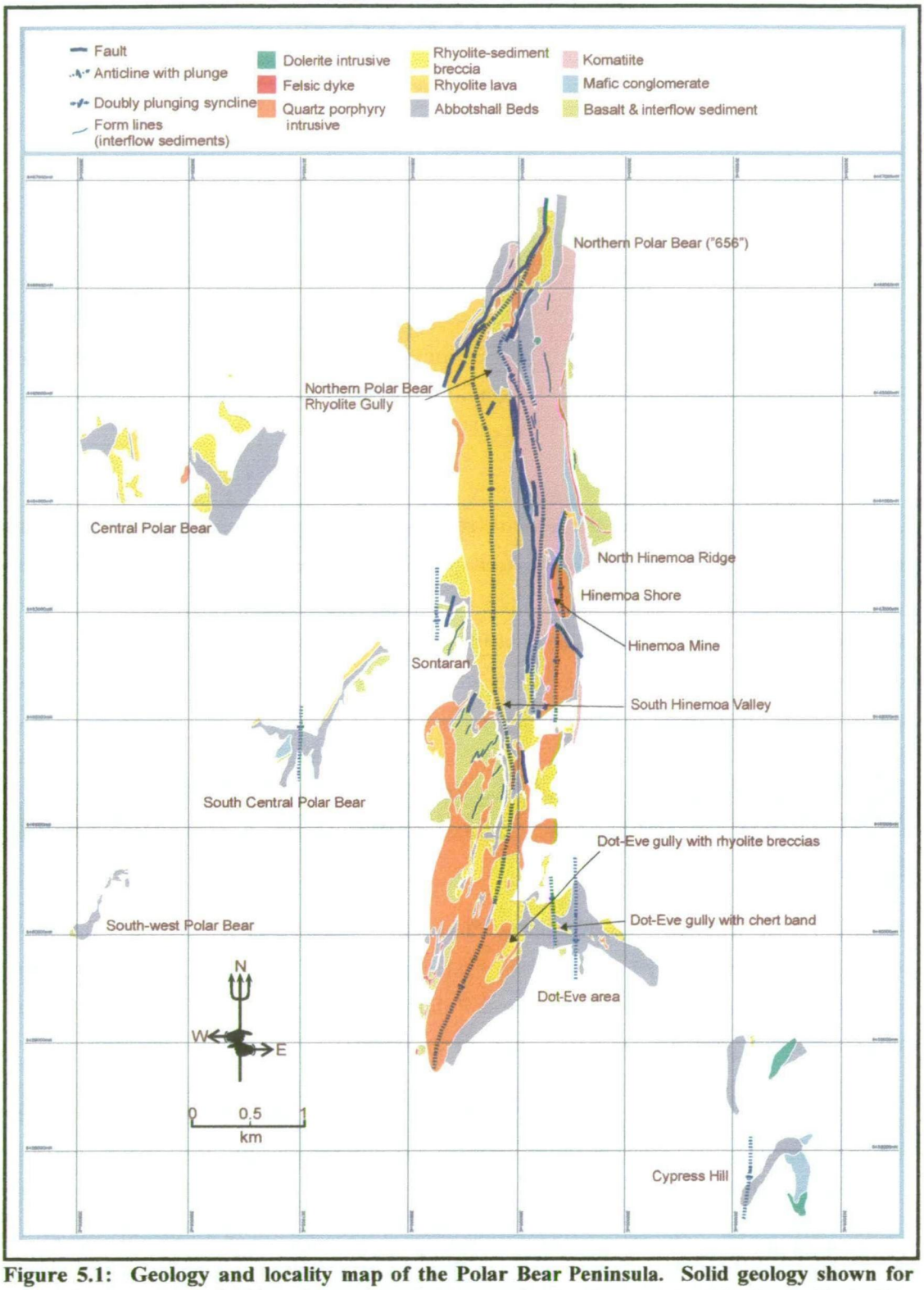

Figure 5.1: Geology and locality map of the Polar Bear Peninsula. Solid geology shown for exposed areas. A 1:10 000-scale version of this map is provided as map 9 in Appendix 4. The solid geology was developed by consolidating and interpreting 1:2500-scale geological maps 1 to 8 in Appendix 4. The rhyolite lava represents a lava dome.

Thus, irrespective of their final depositional site, the clasts within the conglomerate were eroded and reworked from exposed basalt flows in a fluvial or shoreline environment.

The internally massive, poorly sorted and clast-supported nature of the conglomerate, and instances of conglomerate grading into sandstone, are consistent with deposition from high-density turbidites. Another possibility, fluvial channel facies, can be discounted by observation of the surrounding units. The conglomerate has limited width and passes laterally and vertically into fine-grained sediments, which in some cases display partial Bouma sequences, indicative of low-density turbidite. Such sequences would not be found in a fluvial environment.

Low and high-density turbidity currents involve similar processes, but the latter have a greater concentration of particles, which influences support mechanisms, and they operate at greater velocities and deposit coarser and thicker deposits (McPhie & others, 1993). Such turbidite sequences are believed to form the channel facies of submarine fans. In the model for submarine fan facies presented by Walker (1984), the channels are characterised by conglomerate and commonly become finer-grained and increasingly well-graded downstream. In contrast, classical low-density turbidite is typically widespread rather than channelised, and is thought to comprise the suprafan lobes or levee banks on upper lobes of submarine fans. Thinning upward sequences, in which facies become progressively thinner bedded, passing from high-density to low-density turbidites, are interpreted to represent gradual channel filling and abandonment.

The mafic conglomerate and sandstone at the Polar Bear Peninsula show several features consistent with the submarine fan model of Walker (1984). The conglomerate units are localised within the stratigraphy rather than widespread, indicating a lenticular geometry. Coarse conglomerate, such as that at south central Polar Bear, lacks associated sandstone facies and represents a higher energy, more proximal location than the pebbly conglomerate with graded sandstone at Cyprus Hill.

The mafic source for the clasts in the conglomerate and sandstone was probably local. In section 3.2.4, it was noted that an angular unconformity overlies the mafic succession at the Polar Bear Peninsula, implying that the top of the mafic succession has been eroded. Evidence for the unconformity is documented for the Sontaran prospect at the Polar Bear Peninsula (figure 5.1) in A1.2.3 of Appendix 1.

Plate 5.1: Mafic conglomerate at south central Polar Bear comprising rounded chert clasts and basalt clasts.

Plate 5.2: Sandstone shale turbidite from south central Polar Bear. Pencil lies along a shale layer between turbidites. Rounded chert pebbles, similar (but smaller) than those found in the underlying mafic conglomerate occur at the base of the sandstone layer as oversize clasts (arrows).

The combination of relatively thin channel facies, with a thickness of no greater than 50 metres, and the possibility of a local source for the clasts suggests that the submarine fan was small in size, rather than the vast systems discussed by Walker (1984). It is possible that the channels were only a few kilometres in length, but the gradient must have been high in order to transport the large clasts present at south central Polar Bear. An environment that would fulfil these requirements is a small basin adjacent to an exposed block of the mafic succession.

The presence of chert clasts from eroded interflow sedimentary bands, demonstrates that the source of the clasts was a submarine sequence that became exposed, and not an emergent volcanic centre. The submarine mafic sequence may have been shoaling, and have become exposed by eustatic changes, or exposure could have resulted from uplift due to compressional tectonics.

Sandstone-shale facies

Sandstone-shale is one of the units that make up the fine-grained sedimentary facies association of the Abbotshall Beds and is described in section 3.2.8.1. Sandstone-shale overlies the mafic conglomerate at south central Polar Bear (figure 5.1). It is also present higher within the Abbotshall Beds where the sandstone is composed of felsic volcanic material.

Overall, the graded units of the sandstone-shale display sequences typical of those derived from low-density turbidity currents, but individual units differ as to which divisions of a classical Bouma sequence are present.

Massive sandstone that grades into shale and has sulfidic laminae at the top represents the A, D and E divisions of a Bouma sequence. The turbidity currents depositing these sequences were probably travelling sufficiently rapidly that only the A division was initially deposited while the finer sediments continued on down-slope. The passage of the turbidity current left a cloud of suspended mud in its wake, the gradual deposition of which, generated the thin shale horizons. The sulfidic laminae, now weathered to iron oxide minerals, indicate significant quiescent periods with biogenic sulphate reduction in the pelagic mudstone between turbidity currents.

Sandstone-shale turbidites where plane laminated sandstone is overlain by ripple cross-laminated sand, display the B and C divisions of a classical Bouma sequence. These turbidites were probably deposited by a waning turbidity current that had previously deposited the coarser A division. The B and C divisions, being finer-grained, continued to be transported by the turbidity current until the velocity dropped sufficiently that they could no longer be suspended.

The rare chert pebbles present as oversized clasts in the sandstone-shale that overlies the mafic conglomerate and sandstone at south central Polar Bear (Plate 5.2), indicates a link between the sediment sources of the conglomerate and the sandstone-shale turbidite. The transition from conglomerate-sandstone to sandstone-shale marks a change from high-energy, high-density turbidity currents to low-energy, low-density turbidity currents.

At south central Polar Bear, the sandstone-shale turbidite is overlain by laminated chert, which is actually very fine-grained siltstone with sulfidic shale. This facies may be either the fine fraction of turbidity currents and ambient sedimentation, deposited at the distal lobe front of a submarine fan system, or be unrelated to a submarine fan and be deposited through settling of pyroclastic ash into the ocean. As support for the latter contention, it is noted that the geochemistry of black shale from the Abbotshall Beds at the Polar Bear Peninsula resembles the Black Flag Beds (see Chapter 8), which suggests that Black Flag Beds volcanic material is present within the black shale. It is likely that volcanism was underway in the Kalgoorlie Terrane and fine-grained pyroclastic ash was deposited across a wide expanse.

Under the model of Walker (1984) discussed in section 5.2, the transition from conglomerate-sandstone channel facies to sandstone-shale turbidite to very fine-grained siltstone represents a thinning upwards sequence, indicating the filling and abandonment of submarine fan channels. The thickness of the sandstone-shale turbidite facies is not great at the Polar Bear Peninsula, suggesting starvation and abandonment of the entire submarine fan rather than the filling of a single channel and switching of channel axes with ongoing deposition in a submarine fan system. Starvation and abandonment of the submarine fan was probably caused by rapid subsidence and drowning of the shallow-subaerial source.

5.3 FACIES ANALYSIS OF RESEDIMENTED RHYOLITE BRECCIA AND RHYOLITE-SEDIMENT BRECCIA

5.3.1 Introduction

In section 3.2.9.2 and 3.2.9.3, resedimented rhyolite breccia, and resedimented rhyolite sediment breccia were described. It was noted that these rock units are similar, with the difference being that rhyolite breccia is composed of clasts of rhyolite only, whereas rhyolite sediment also has sedimentary rock clasts. Both units form extensive outcrops in the areas marginal to the rhyolite lava at the Polar Bear Peninsula. There is typically no apparent internal organisation to the units, but weathering, alteration and deformation commonly obscure the clast shapes.

A number of areas, typically gullies or hillsides where the soil cover has been stripped, have excellent exposures of the rhyolitic breccia and sandstone. Graphic

logs have been drawn for three of these areas in order to collect detailed data to assist in interpreting the origin of the units. The three areas are described with interpretations of local features and then a final comprehensive discussion and interpretation of the breccia and sandstone is presented.

5.3.2 Dot-Eve gully with chert band

Description

A gully north of the Eve prospect at 6460155mN, 389310mE MGA exposes a band of chert approximately 20 cm thick, bounded on both sides by rhyolitic breccias and sandstone (Plate 5.3). A graphic log was prepared for the exposure (figure 5.2). Although the bedding within the exposure is parallel to a strong cleavage so that textures are flattened, important observations can be made. A westward facing is defined by a small soft sediment slump in a thin band of sandstone overlain by shale.

Typical rubbly subcrop of resedimented rhyolite-sediment breccia on the hillside gives way to almost 100% exposure within the gully. A continuous band of vertically dipping, laminated chert about 20 cm wide trends roughly north-south through the centre of the gully. The chert consists of well-sorted, unstrained, polygonal quartz grains typically 0.03 mm in size. Finer-grained laminae occur associated with iron oxide minerals. Grading between the laminae is poor and the grain size changes tend to be sharp.

Plate 5.3: Dot-Eve gully with chert band. Yellow notebook lies on chert band bounded by rhyolite breccia on the RHS and sandstone on the LHS. The graphic log starts in the outcrop on the left side of the photo and runs along the line shown.

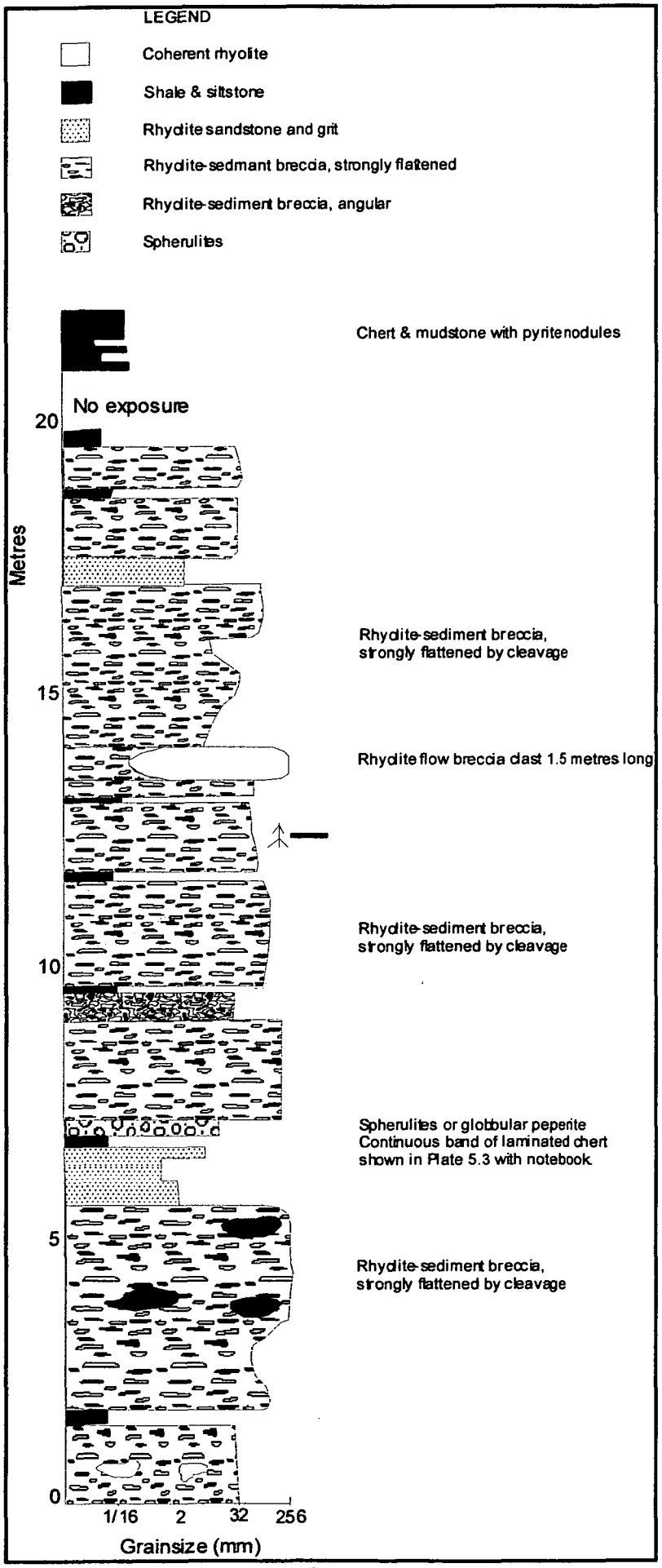

Figure 5.2: Graphic log across Dot-Eve rhyolite-sediment gully

East of the chert band, a 1 m wide band of volcanic sandstone with tractional laminae lies between the chert and rhyolite-sediment breccia. Both medium and coarse-grained volcanic sandstone are present with sharp mutual contacts. West of the chert band, beds of rhyolite breccia typically 1-2 m thick separated by thin lenses of shale form a broad zone with obscure textures due to strong flattening (figure 5.2).

The rhyolite-sediment breccia is clast-supported. Although the shapes of rhyolite clasts are difficult to determine due to flattening, in faces perpendicular to the flattening direction, some clasts have curviplanar margins whereas others show subrounded shapes indicating some abrasion during transport. Quartzite blocks within the breccia are typically tabular with laminae parallel to the quartzite band. The rhyolite-sediment breccia has a complex interfingering relationship with coarse-grained volcanic sandstone, but the contacts between sandstone and breccia are sharp.

Rhyolite clasts within the breccia are intensely sericitised. The sandstone and gravel comprises very fine-grained sericite and quartz with larger anhedral quartz grains 0.3 mm in diameter and dense patches of sericite that may represent altered feldspars up to 2 mm across.

Interpretation & discussion

The band of chert bounded by rhyolite-sediment breccia indicates a sedimentary origin for the breccia and sandstone. In addition, the chert band shows that deposition of breccia was infrequent as a 20 cm layer of fine sediment was deposited between breccia units. Other shale units in the sequence are discontinuous lenses, due both to boudinage and scouring by overlying breccia units. The strong cleavage obscures clast textures in the breccia, preventing detailed facies analysis.

Quartz grains within the chert are unstrained and polygonal indicating that they are recrystallised. Nevertheless, variations in grain size that define each lamination appear to be a preserved primary texture that suggests a detrital origin for the quartz. Thus, the chert is probably a recrystallised siltstone rather than a chemical sediment. Bands of oxide minerals associated with the finer-grained laminae may be weathered sulfide minerals.

5.3.3 Dot-Eve creek with rhyolitic breccias

Description

A well-exposed example of rhyolite-sediment breccia is present in a gully at 6449955mN, 388960mE MGA. The exposure commences with rhyolite-sediment breccia on the east embankment and finishes in quartz porphyry on the west bank. Between these rock-types, interbedded felsic sandstone and rhyolitic breccia units are

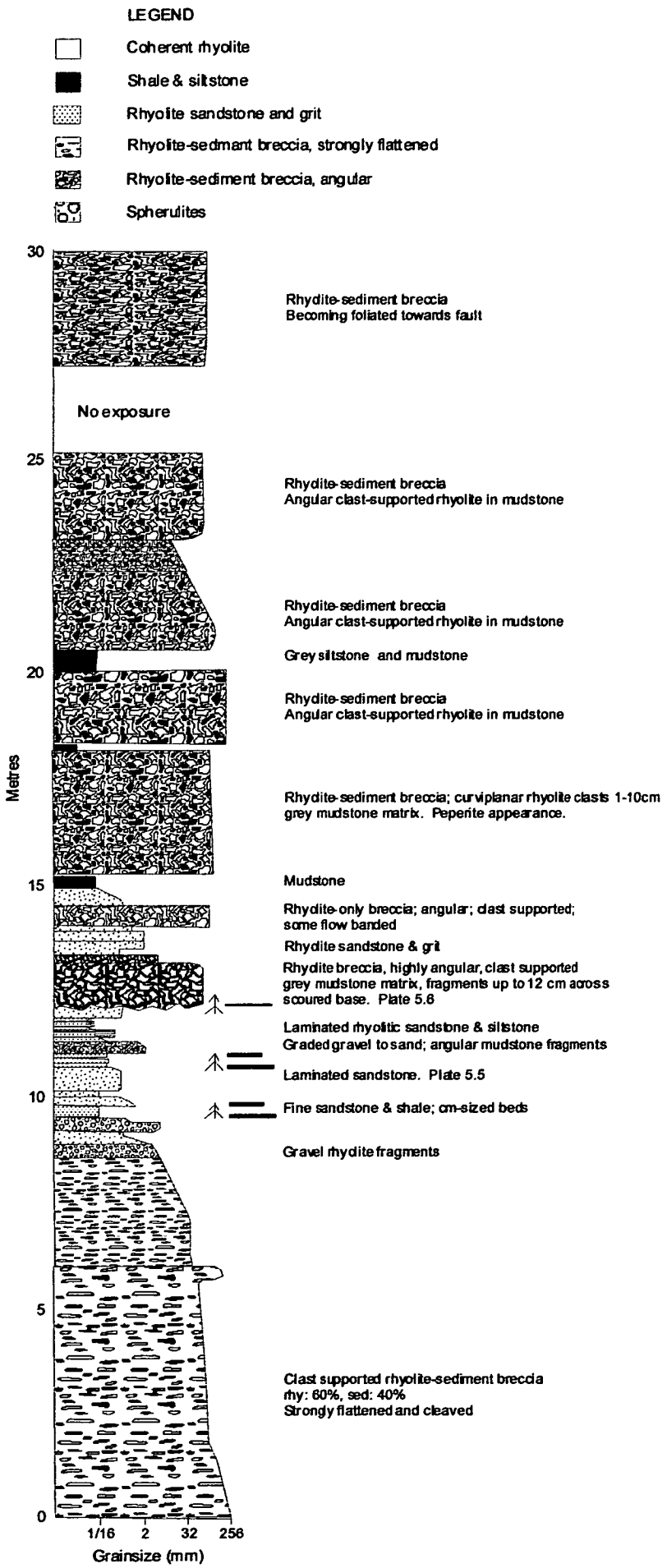

Figure 5.3: graphic log across Dot-Eve rhyolite breccia creek

exposed within the gully (Plate 5.4). A graphic log was prepared for the exposure (figure 5.3)

Younging indicators, including scouring of underlying units, cross bedding in sandstone and soft sediment deformation, such as slumps and flame structures, are abundant. Grading of sandstone and gravel units is also common, but was not used as a facing indicator. At the southern end of the gully where the graphic log (figure 5.3) was constructed, flame structures and scouring indicate the sequence faces east and that gravel-sandstone units are normally graded. However, approximately 100 m to the north, younging indicators face both east and west; the cleavage intensifies and folds with a wavelength of approximately 5-10 m can be traced by following sandstone units.

The graphic log (figure 5.3) commences with clast-supported rhyolite-sediment breccia on the east bank that is rubbly and poorly exposed. The thickness of the breccia unit cannot be determined, but exceeds 6 m. The composition of the breccia is 40 to 60% rhyolite with the remainder comprising sediment. Rhyolite clasts are both black and cream-coloured and appear to be angular, although the shapes are difficult to distinguish due to the cleavage. Sediment clasts are orange to tan-coloured mudstone that are elongated due to flattening. The breccia fines upwards overall.

The breccia is overlain by 6 m of normally graded gravel, sandstone (Plate 5.5) and siltstone units (figure 5.3). Towards the top of this bedded zone, two tabular units, 0.5 and 1 m thick, composed of closely packed, clast-supported, highly angular rhyolitic breccia with a grey, mudstone matrix, are interbedded with the sandstone and gravel (Plate 5.6). Similar, but thicker, clast-supported, angular rhyolite and mudstone breccia units overlie the gravel and sandstone units.

Shale and siltstone beds separate breccia units, but disappear along strike with abrupt ragged terminations. Within breccia units, large clasts consisting of segments of shale and siltstone beds are present (Plate 5.7).

At the far western embankment of the gully there is a zone of sericitic schist possibly representing sheared felsic rock. Quartz porphyry intrusive, which is unrelated to breccia, crops out 10 m from the edge of the gully. The latter units are not shown at the top of the graphic log (figure 5.3).

Interpretation & discussion

The rhyolite-sediment breccia at the base of the sequence is not well-preserved, due to strong flattening, but it is apparent that the breccia can form thick units.

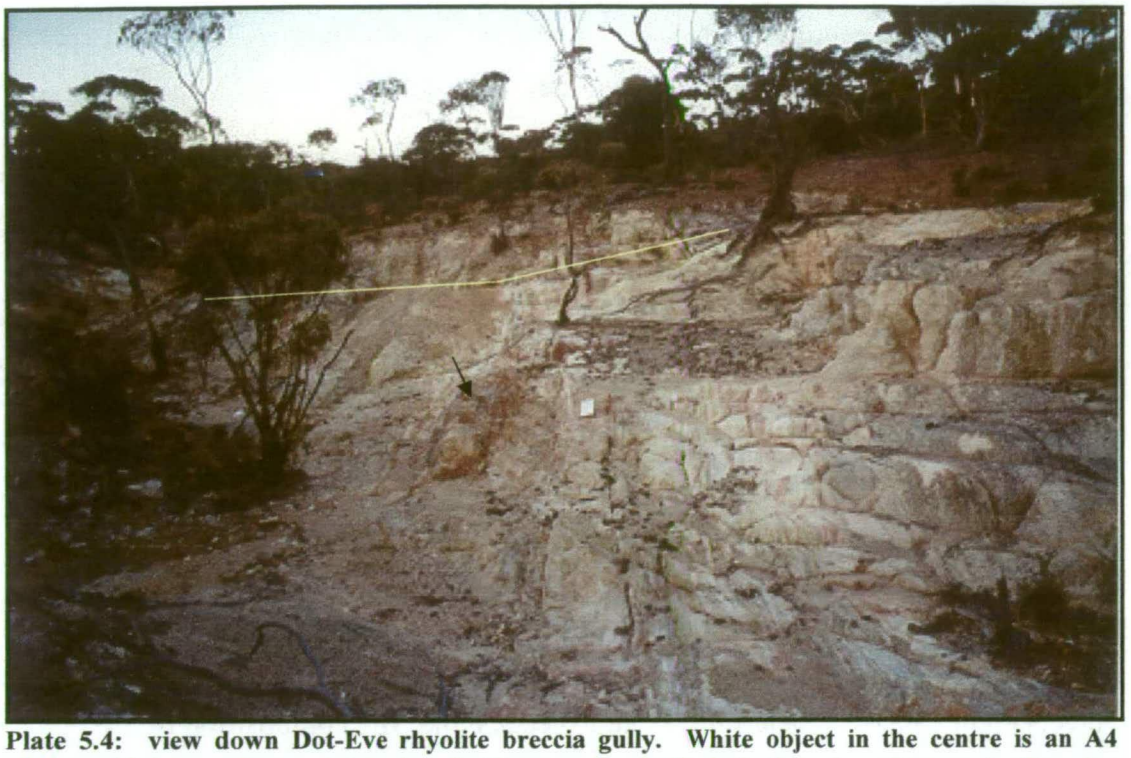

Plate 5.4: view down Dot-Eve rhyolite breccia gully. White object in the centre is an A4 clipboard lying on the sandstone band. Hammer lies to the left of the board (arrow). Breccias on the far right and far left of the photo, sandstones in the centre. Graphic log in figure 5.3 commences on the RHS of the photo and runs along yellow line.

Plate 5.5: Graded rhyolitic gravel and weakly plane-laminated sandstone at 10 metres in figure 5.3. Interpreted as R3 suspension sedimentation of the gravel passing into S1 traction sedimentation sandstone sections of a high density turbidite. From Dot-Eve rhyolite Gully

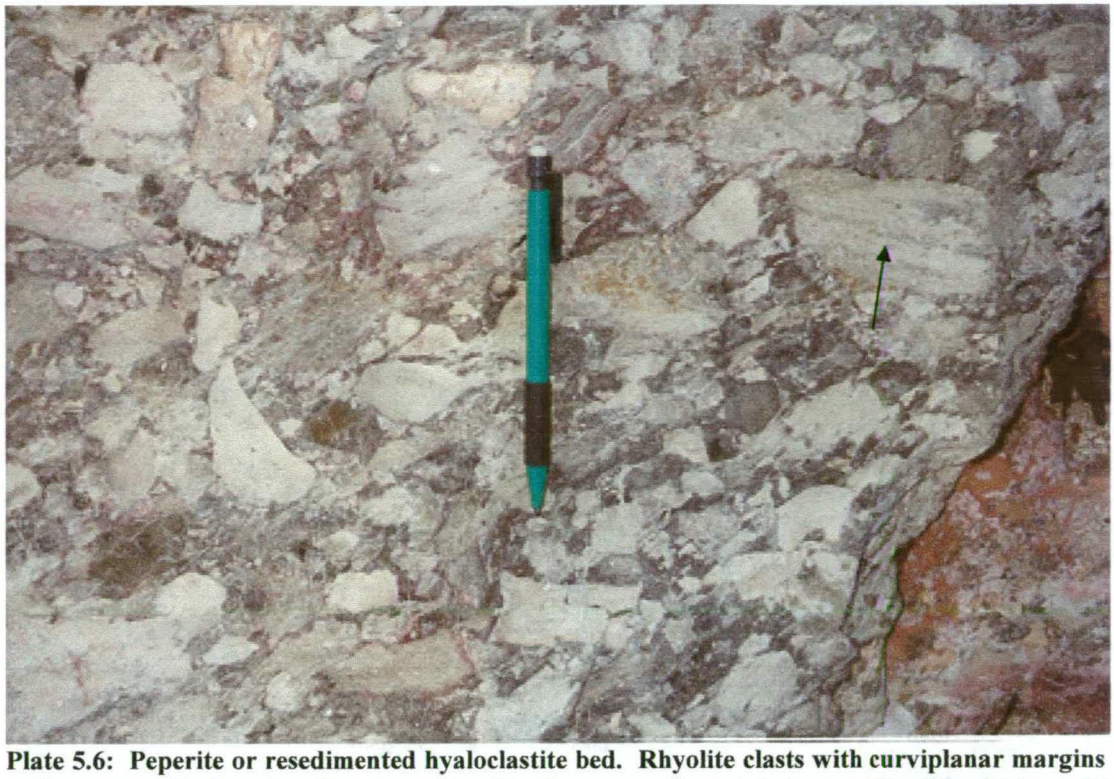

Plate 5.6: Peperite or resedimented hyaloclastite bed. Rhyolite clasts with curviplanar margins and some with flow banding (arrow). Dark grey sediment between rhyolite clasts. At 12.5 metres in figure 5.3.

Plate 5.7: Large laminated shale clast in rhyolite sediment breccia (arrow). The fold within the shale is interpreted as a soft sediment feature. The shale clasts form as rip-up clasts of interbreccia shales.

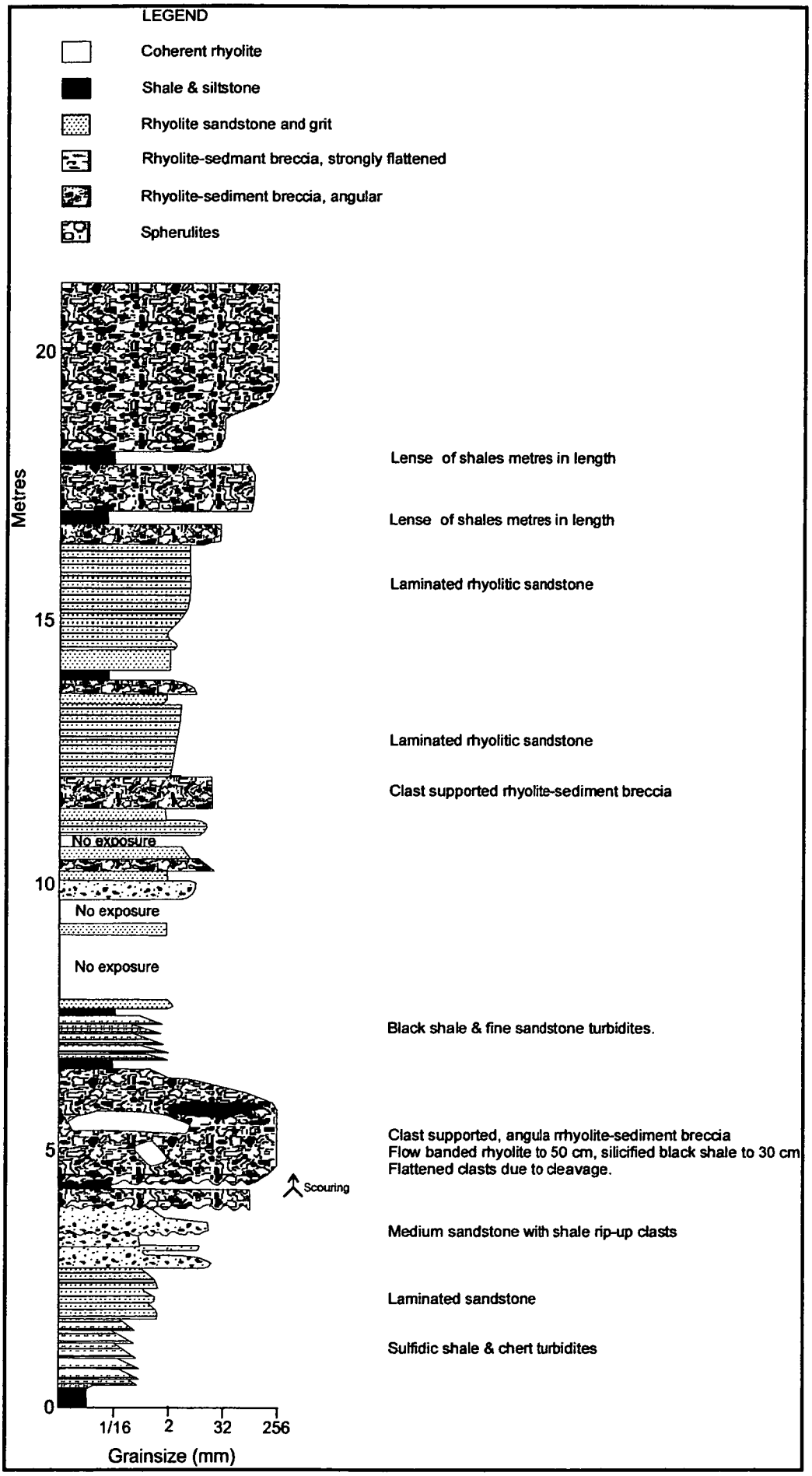

Figure 5.4: Graphic log across "656" rhyolite-sediment breccia.

Angular clasts in the breccia near the top of the sequence have curviplanar margins indicative of quench fragmentation (Plate 5.6). Jigsaw-fit clasts although rare, are also present. Internally, the breccia has similar characteristics to peperite, albeit with a lesser proportion of mud matrix than other peperitic exposures. A difficulty with a peperite interpretation is that no coherent rhyolite body is exposed and two of these breccia units are interbedded with sandstone (figure 5.3). Breccia-sandstone sequences are not typical of peperite.

It is possible that the units could be peperite, formed as shallow sills that intruded along wet sandstone-mudstone sequences, became wholly quench fragmented, and gained both sandstone and mud as matrix, while remaining relatively intact as tabular units. However, a preferred interpretation is that the breccia units are resedimented hyaloclastite, spalled from a rhyolite lava, transported and deposited with a mud matrix gained by scouring underlying units during transport. McPhie & Gemmell (1998) suggest two processes that may be responsible for jigsaw-fit clasts in resedimented hyaloclastite at Newton Dam Spillway in the Mount Read Volcanics of western Tasmania; quench fragmentation after deposition, or progressive opening of prepared fractures during transport.

5.3.4 Northern Polar Bear ("656" area) - stratigraphy

At the northern end of the mapped area at the Polar Bear Peninsula (known as the "656" prospect in old exploration reports), there is a good exposure of rhyolite-sediment breccia and rhyolitic sandstone on the side of a hill at 6465955mN, 388920mN MGA. A graphic log was prepared for this exposure (figure 5.4)

Description

Poorly defined rhyolite-breccia is exposed at the top of the hill and is overlain to the west by shale and siltstone, which is in turn overlain by sandstone and breccia. The graphic log (figure 5.4) commences near the top of the slope in the shales and siltstones, 1.7 m from the western rhyolite breccia contact. It extends through the sandstone and breccias to the track at the base of the slope. The facing is elucidated by weakly defined scours at the base of the coarse sandstone and is supported by shale rip-up clasts at the base of sandstone beds.

Sandstone units are typically medium to coarse-grained, and consist of rhyolitic material and sand-sized, dark, shale fragments. The sandstone beds typically are 10-15 cm thick with sharp to diffuse contacts, and may amalgamate to form units 1-2 m thick. Dark siltstone bands cap some sandstone sequences but are rarely continuous along strike due to scouring by overlying flows. Some sandstone units

have siltstone rip-up clasts near the base. Poorly defined laminae caused by traction are ubiquitous in the sandstone beds.

Breccia units are typically 0.5-3 m thick and are clast-supported. They are dominated by rhyolite clasts, but also contain minor sedimentary clasts. The most common rhyolite lithology is pale green, textureless, and intensely sericitised. The clasts are flattened, consistent with the strong upright, north-south-trending cleavage. Notwithstanding the flattening, the angular shape and typical curvilinear margins of the rhyolite clasts remain apparent. The typical clast size is 3-10 cm. A second common clast type is flow-banded rhyolite, which tends to be more blocky and less flattened and often larger in size than the textureless rhyolite. The largest block observed was approximately 0.5 m along its axis. Dark coloured, laminated, siliceous siltstone or silicified shale are the least abundant clasts. These range in size from a couple of centimetres to 0.3 m. The larger clasts tend to be lens shaped in outline, in part due to flattening. At 6 m along the traverse, a 2 m thick breccia unit grades into sandstone about 20 cm thick which is overlain by shale. All other breccia units are overlain by sandstone with sharp rather than gradational contacts.

Dark coloured, siltstone and shale units lie between many sandstone and breccia units. The siltstone and shale units may be discontinuous due to scouring at the base of the overlying breccia or laminated sandstone unit. Near the base of the slope, at 17 to 18 m along the traverse, two discontinuous siltstone-shale bands approximately 30 cm thick and several metres in length lie approximately 1 m apart, enclosed by rhyolite-sediment breccia.

Interpretation & discussion

This exposure shows ubiquitous scouring of fine-grained sediments and the incorporation of the rip-up clasts into the overlying breccia and sand units. Rip-up is probably the origin of all sedimentary clasts in the rhyolite-sediment breccia. Residual bands of fine-grained sedimentary rock that remain unscoured form beds several metres in length in this outcrop.

5.3.5 Discussion: Origin of resedimented rhyolite-sediment breccia and rhyolitic sandstone

Interpreting the transport and deposition mechanisms for the breccia and sandstone deposits that constitute resedimented rhyolite and resedimented rhyolite-sediment breccia involves consideration of the possible processes versus the evidence provided by the deposits.

Deposits of breccia and sandstone are commonly 0.5 to 3 m thick (although units greater than 6 m thick are present) and are typically divided by siltstone or shale

bands 10-30 cm thick, suggesting that all the units have a sedimentary origin. The deposits indicate that intermittent high-energy mass flows of probable short duration were separated by longer quiescent periods in which fine-grained material, representing ambient sedimentation, settled from suspension.

McPhie & others (1993) describe the characteristics of the most important types of mass flows in volcanic environments. Volcanic slides, debris avalanches and grain flows are supported by grain interactions and involve gravity acting on unstable deposits, whereas density-modified grain flows, debris flows and turbidity currents all involve water-support for the grains.

Volcanic slides consist of coherent masses of an edifice sliding down-slope along a shear plane and are difficult to identify in ancient environments. Slides are commonly associated with debris avalanches that are rapid, gravity-driven flows of unsorted mixtures of rock and sediment. Deposition occurs en masse by frictional freezing and deposits are non-graded and very poorly sorted with clasts ranging from centimetres to tens of metres in size. Debris avalanches have small-scale variations from clast to matrix-supported but are unstratified. They may be gigantic in size, are highly mobile and can travel kilometres from the initiation point. The key areas described at the Polar Bear Peninsula are well-bedded, precluding their deposition from avalanches or volcanic slides.

Grain flow affects cohesion-less grains on steep slopes which roll and slide down-slope under the action of gravity until they reach a more stable angle of repose. Multiple grain flows contribute to restoring a stable angle of repose so grain-flow deposits are characterised by thin, centimetres thick, lenticular beds which are reversely graded and clast-supported. Density-modified grain flows involve sediment mixtures in which larger and denser clasts become buoyant in a silt-sand suspension. These deposits may transport cobble-sized clasts, are typically reverse-graded and have a matrix of poorly-supported sand to clay-sized particles. Density-modified grain flows are expected to be common around subaqueous lava domes such as the rhyolite at the Polar Bear Peninsula, as steep slopes are common in the talus breccias that typically surround such bodies. Nevertheless, no multiple, thin, reversely graded sandstone beds consistent with grain flows have been observed at the Polar Bear Peninsula.

Cohesive debris flows have clay-sized particles forming a slurry with sufficient strength to support large clasts whereas clay-poor volcaniclastic deposits may involve both grain collisions and cohesion between fine ash-sized particles to support clasts. In either case, debris deposits are generally very poorly supported, non-graded and

have sharp but rarely erosive contacts. Rhyolite-sediment breccias with the characteristics of cohesive grain flows have not been observed at the Polar Bear.

High-density turbidity currents have a greater concentration of particles and travel faster than the low-density currents that deposit the fine-grained, graded deposits often called Bouma sequences. Grain support and depositional processes are also more complex, involving grain interaction and hindered settling in addition to water turbulence. Sandy and gravelly turbidites have been described by Lowe (1982). Gravelly turbidites consist of a basal, reversely-graded traction carpet layer (R2) that is deposited when the flow velocity declines sufficiently, overlain by normally graded suspension sedimentation layer (R3). Deposition of these coarse divisions generally leaves a sandy high-density turbidity current that may continue down-slope or deposit sand over the gravel.

An ideal sandy turbidite consists of a lower sequence of sand and gravel with plane laminations and cross-stratification (S1), generated by interaction between deposited sediment and the current (traction sedimentation); an intermediate division of reverse graded, thin beds of sand to gravel, representing traction carpet deposits (S2); and an upper division of massive or normally graded sand, commonly with water-escape structures, deposited directly and rapidly from dense suspension (S3). The latter sands are envisaged as having become a "fluidized flow" slurry immediately preceding deposition, which would destroy any possible sedimentary structures except graded bedding (Walker, 1984). The residual fine material may form a low-density turbidite overlying the S1 to S3 sand units, or continue down-slope.

Typically, turbidite units are deposited progressively as the current wanes so that rather than the complete gravel to mud sequence described above, only a few of the divisions are deposited in any single location. The resedimented rhyolite-sediment breccias described in the key areas have characteristics consistent with deposition from high-density turbidity currents.

The breccia and sandstone beds from the logged sections comprise divisions of sandy and gravelly high-density turbidites. Breccia units are interpreted to be gravelly turbidites, whereas the sandstone dominated units are sandy turbidites. The majority of the sandstone units are planar or cross-laminated indicating traction processes, and in the absence of reverse grading, they are interpreted as S1. Units that exhibit some reverse grading are interpreted as R2 or S2 traction carpet divisions. The normally graded sections of gravel and breccia are interpreted as R3 divisions, and S3 has not been identified. Normally graded units passing from gravel to laminated sand (Plate 5.6) indicate deposition from suspension for the gravel (R3) passing into planar laminated S1 traction sedimentation sands.

The fine-grained units between the sandstone and breccia beds are typically dark siltstone, laminated "chert" (which may be recrystallised siltstone), or grey-green mudstone. The fine-grained units may be the upper divisions (Td and Te) of low-density turbidites, or represent ambient suspension sedimentation unrelated to turbidites. In either case, successive high-density turbidity currents, particularly those that deposited breccia beds, have scoured fine-grained units such that fine grained sedimentary units are now found as discontinuous remnants of beds or rip-up clasts in the breccia (Plate 5.7).

Further consideration needs to be given to processes that may have generated the volcaniclastic turbidites at the Polar Bear Peninsula The paleo-environment at the time of deposition was proximal to a rhyolite lava dome. The volcanic clasts within the breccia beds are all sourced locally from the rhyolite dome, indicating the high-density turbidite is not the vast, far-travelled varieties feeding submarine fans that were described by Walker (1984).

The majority of rhyolite clasts are massive (textureless) and angular with curviplanar margins characteristic of quench fragmentation, although flow-banded blocks are also present (Plate 5.6). These clast textures would be expected in talus breccia aprons around the margins of a submarine rhyolite dome. Spalling of quench-fragmented rhyolite would generate significant thicknesses of resedimented hyaloclastite. With continued inflation of the rhyolite dome, the carapace would be further fragmented, and segments may fall to the talus apron, adding flow-banded lava blocks from the interior of the dome. Mega-clasts might be expected from significant collapses, but would be difficult to recognise with the available patchy exposures. Sand-sized particles would be formed directly from quench fragmentation and by attrition within the talus.

Significant thicknesses of fine-grained sediment would not be expected within talus breccia deposits. Spalling, collapse and cascading of breccias down the talus apron would be continuous, disrupting the blankets of fine sediments deposited by ongoing ambient sedimentation. Suspension sediments that were deposited across the talus would fill the cavities between coarse blocks and be overlain by further breccias. In this way, clast-supported breccias intermixed with muds and volcanic sand could be generated.

Talus breccias would be identified by characteristics such as clast support, paucity of matrix, and massive or weak stratification (McPhie & others, 1993). Within the talus apron, resedimentation would be dominated by density modified grain flows yielding lenticular, reverse graded beds. Although aprons of talus are most likely to have surrounded the rhyolite lava dome at the Polar Bear Peninsula, no breccia with the

appropriate characteristics have been identified. Instead, the clasts expected in the talus aprons are found in high-density turbidites, suggesting resedimentation.

Density modified grain flows cascading down the talus slope would be unlikely to transform into turbidity currents capable of transporting coarse breccias. Instead, it seems likely that major events such as large slumps of the talus or collapse of segments of the lava dome involving the mass movement of sediment at considerable velocity would be necessary to initiate these flows. The necessity for such major events is supported by their infrequent occurrence as indicated by the sequences of shale or chert that have been deposited between turbidites in the localities described.

As the rhyolite-sediment breccias remain proximal to the rhyolite dome, it is also apparent that once the turbidity currents were initiated, they did not travel far before the sequences that are now found at the Polar Bear Peninsula were deposited. This can be explained by the coarse nature of the deposits. R2, R3 and S1 are the most commonly preserved sequences. S2 is uncommon and S3 has not been identified. Thus, it appears that only the coarse basal sections of high-density turbidites are preserved close to the lava dome. The majority of the sandy turbidites that would require less energy to transport are not found, suggesting they continued down-slope.

Thus, resedimented rhyolite breccia and sandstone layers are interpreted to be basal sections of high-density turbidites that resedimented rhyolitic debris from talus slopes. Commonly, significant layers of fine sediment were deposited from suspension between turbidite events and these were, in part, ripped up by successive gravelly turbidites. Clasts of fine-grained sediment were not destroyed in the flow because they travelled only a short distance before being redeposited. Rip-up sediment clasts, incorporated into gravelly turbidites are now seen as the widespread resedimented rhyolite-sediment breccias (Plate 5.7).

5.4 SUMMARY & CONCLUSION

A feature which may be unique to the Polar Bear Peninsula is an angular unconformity at the top of the mafic succession. The local occurrences of mafic conglomerate and sandstone with a similar composition to the mafic succession are probably related to the angular unconformity. The mafic succession was exposed and eroded, generating clasts. The clasts were rounded in a fluvial or shoreline environment prior to being deposited as high-density turbidites in channels, representing a small submarine fan system.

The thin-bedded sandstone-shale turbidite and laminated chert of the Abbotshall Beds, which overlies the mafic conglomerate, indicates abandonment of the

submarine fan channels. Abandonment was probably caused by starvation of the submarine fan due to subsidence leading to drowning of the sediment source.

The angular unconformity is probably the result of local tectonic uplift, although lowering of the sea level cannot be ruled out.

At the Polar Bear Peninsula, a submarine rhyolite dome was extruded onto black shale of the Abbotshall Beds. The rhyolite lava has peperitic contacts with the underlying sulfidic shales and *in situ* hyaloclastite adjacent to other contacts.

The rhyolite-sediment breccias that are lateral equivalents of the rhyolite dome, where it pinches out of the stratigraphy, are the submarine equivalent of ring plain breccias. They were formed by collapse of portions of the dome, and resedimentation of large masses of hyaloclastite spalled from the dome, which were transported as high density turbidite flows. The breccias represent the coarsest fractions of high-density turbidites that have travelled only a short distance before being redeposited; hence, they remain proximal to the rhyolite dome. mud and silt beds, deposited between collapse events, were scoured by the high-density turbidites. Ripped-up mud and silt fragments were intermixed with rhyolite clasts to form rhyolite-sediment breccias. The sediments were not completely disaggregated in the turbidity currents because they travelled only a short distance before being redeposited.

CHAPTER SIX

Upper Stratigraphy of the southern Coolgardie Domain

6.1 INTRODUCTION

The Coolgardie Domain is a fault-bounded block of the Kalgoorlie Terrane separated from the Ora Banda and Kambalda Domains by the Zuleika Shear and from the Norseman Terrane by the Mission Fault (figure 2.2). The Coolgardie Domain occupies the western side of the study area beneath the sediment cover of Lake Cowan and onshore to the west (figure 1.3). Outcrop west of Lake Cowan is dominated by two large, differentiated, mafic sills. The upper felsic and sedimentary units are not well exposed (figure 6.1).

The stratigraphy within the Coolgardie Domain is better defined than the Norseman Terrane, but most of the previous studies have been undertaken in the Widgiemooltha area, approximately 80 km north of Norseman, where nickel deposits are found. The regional stratigraphy within Coolgardie Domain is similar to the Kambalda Domain except that the upper basalt (Paringa Basalt equivalent) is absent (Swager & others, 1995). The contact between the komatiite and the overlying felsic-sedimentary succession is marked by a regionally continuous thin shale or chert bed ("Widgie chert" at Widgiemooltha) that is correlated with the Kapai Slate at Kambalda.

The Coolgardie Domain contains the type section of the Mount Kirk Formation (Doepel, 1973) (figure 1.2, 1.3). The stratigraphy of the Norseman area, as compiled by Doepel (1973), has the Mount Kirk Formation as the uppermost unit, so it is important to compare the upper stratigraphy at the Polar Bear Peninsula with the Mount Kirk Formation. If the terrane map of Swager & others (1995) is correct, then the Mount Kirk Formation should be part of the Coolgardie Domain rather than the Norseman Terrane and the Mount Thirsty Beds member of the Mount Kirk Formation (figure 1.2), may be the equivalent to the Black Flag Beds.

The felsic and sedimentary succession within the Coolgardie Domain is of interest in this study for comparison with the upper units in the Norseman Terrane. However, in the Norseman area, exposure of the felsic and sedimentary succession within the Coolgardie Domain is very poor, and a good representation cannot be observed in any single locality. Instead, the characteristics of the succession have to be pieced together by studying isolated exposures. For this study, field work consisted of:

- reconnaissance of felsic and sedimentary rocks adjacent to the Coolgardie-Esperance Highway near Mt Thirsty and below the Mission Sill (figure 6.1, 6.2);

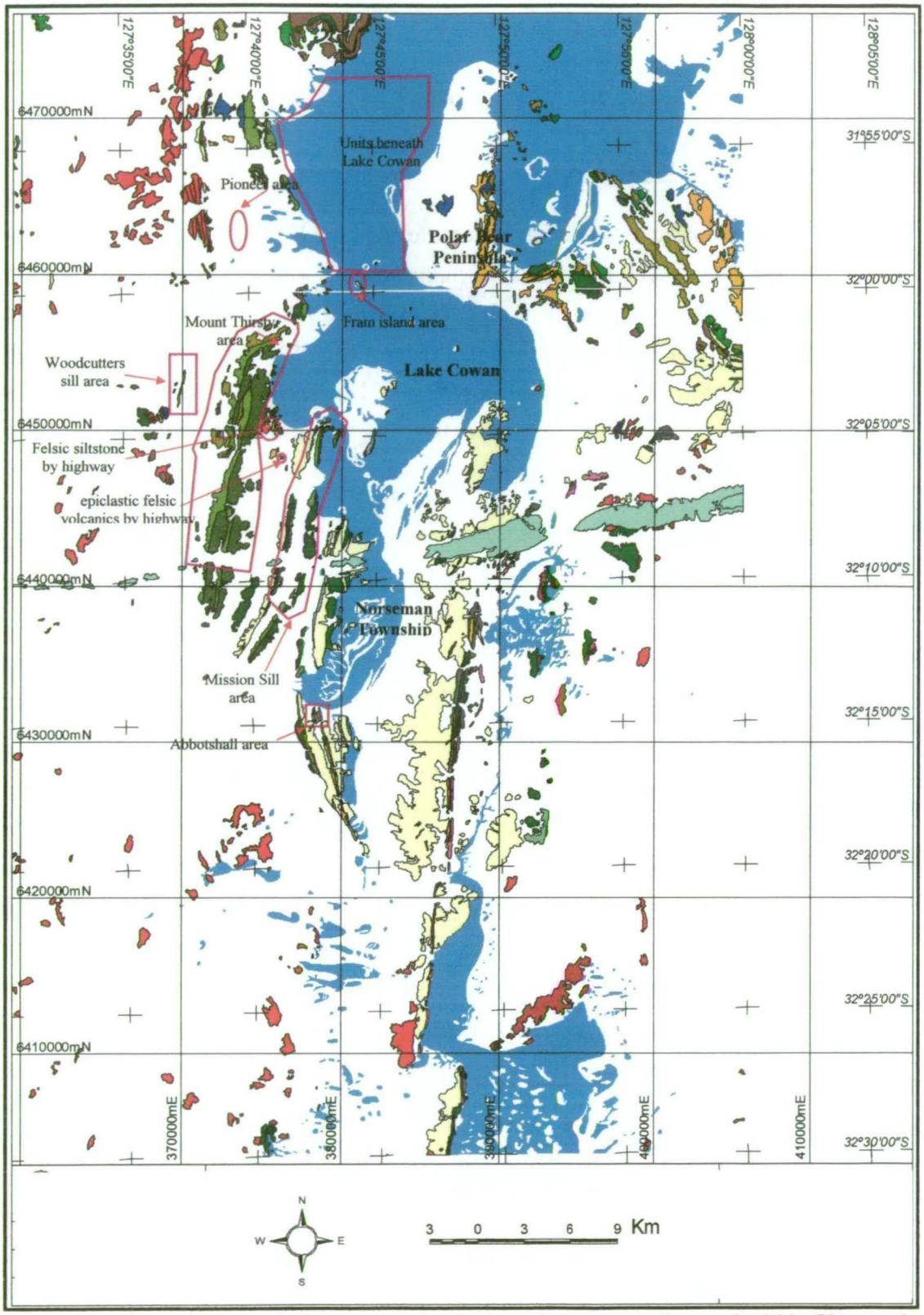

Figure 6.1: Regional geological outcrop map, showing the locations discussed within Chapter 6. Geology is from the GSWA 1:100,000-scale Norseman Sheet (McGoldrick, 1993) and Cowan Sheet (Griffin, 1988).

- preparation of detailed graphic logs across the best exposed sections of felsic outcrop;
- check mapping and minor modification of a 1:12,000 scale geological map of the Mt Thirsty area, compiled by Anaconda Inc. in 1968 (Gemuts, 1968);
- 1:2500 scale mapping of a small area below the Mt Thirsty sill where the Anaconda map showed mafic rock (figure 6.1, 6.3); and
- 1:2500 scale mapping of the Woodcutters north area to the west of the Mt Thirsty, where komatiite is overlain by a small differentiated mafic sill (figure 6.1, 6.3, 6.4).

Other work completed for the Coolgardie Domain comprised relogging of some stored end-of-hole rock samples from aircore holes drilled by CNGC across Lake Cowan and the covered area between Mt Thirsty and the Woodcutters North exposures to obtain an indication of what rock types are beneath the cover.

Layout of the chapter

The geological study begins with a summary of recent work describing the Coolgardie Domain in the vicinity of Widgiemooltha. The focus then shifts 80 km to the south to the area bounding the Norseman Terrane with a review of regional mapping for AMIRA Project 437 (Barley & others, 1998). The new work in this thesis for the southern part of the Coolgardie Domain commences with an overview of the geology to provide a framework for the more detailed descriptions and interpretations that follow. Important areas that were reconnoitred in the Coolgardie Domain to assist the study will be described under their area headings. Finally there will be an overall synthesis and the geological history of the Coolgardie Domain will be described.

6.2 PREVIOUS STUDIES

Hand (1998) studied one location in the Coolgardie Domain at Mount Edwards, 5 km north of Widgiemooltha, and about 85 km north of Norseman. Unless otherwise referenced, the following description of the upper stratigraphy at Mount Edwards is a summary of his work for comparison with the findings in this study.

At Mount Edwards, basal mafic and ultramafic rocks outcrop and are overlain by the felsic-sedimentary succession known as the Black Flag Beds (BFB).

The first BFB unit is massive volcaniclastic sandstone, which overlies a black shale unit immediately above the ultramafic rocks. The black shale is assigned to the

ultramafic succession because it represents ambient background sedimentation after eruption of the komatiite. The contact between the volcaniclastic sandstone and black shale is scoured and Hand considered it to be a disconformity. The sandstone consists of abundant feldspar grains and ubiquitous intraformational black shale clasts 1-10 cm in length. Up section, the volcaniclastic sandstone becomes coarser grained and shale clasts are rare. A 1-2 m wide shale band within the massive sandstone indicates a deep-water depositional environment.

Volcaniclastic conglomerate overlies the sandstone. The conglomerate is poorly sorted and supported by a medium-grained feldspar-rich sandstone matrix. Clasts are subrounded and dominantly 5-10 cm long, although 1 x 0.5 m specimens have been found. The clasts are dominantly feldspar-phyric dacite and flow banding is common. The conglomerate is not confined to channels and is interbedded with clast-poor massive sandstone. The juvenile and monomict nature of the dacitic conglomerate may reflect synchronous dacitic volcanism proximal to the source. Due to the apparent sheet-like, rather than channelised, nature of the conglomerate, Hand interpreted it to have been deposited in a slope apron environment that may have flanked the dacite source.

The dacite-derived conglomerate is overlain by a 20-30 cm thick band of black shale. A thick layer of interbedded massive sandstone, horizontally stratified sandstone and laminated mudstone overlies the shale bed. Individual beds are tabular and laterally continuous and rare polymict conglomerate intervals up to 30 cm thick are present. Hand considered that these units represent deposition by high to low-density turbidites in a lobe or lobe-fringe environment at the distal end of a submarine fan.

SHRIMP U-Pb dating on dacitic conglomerate and sandstone yielded three main zircon age populations: 2686±3 Ma, which is interpreted as the age of dacitic volcanism and synchronous sedimentary deposition; 2661±4 Ma, which may reflect Pb loss during amphibolite facies metamorphism; and 2629±4 Ma, which may be younger, low temperature alteration and Pb loss.

B. Krapez undertook regional geological mapping in the Norseman region for AMIRA Project 437 project (Barley & others, 1998). Within the southern Coolgardie Domain, Krapez found two sedimentary sequences. The lower sequence is at least 150 meters thick but the base is not exposed. One fining-upwards unit is preserved, passing from clast-supported gravelly turbidite with cobble-sized clasts of quartz-feldspar porphyry, to massive sandy turbidite, to low-density Bouma turbidite to black shale. The upper sequence varies along strike from a single laminated chert unit representing silicified shale to interbedded quartzo-feldspathic massive sandy turbidite; pelitic schist (or metamorphosed thinly bedded turbidite) and black shale.

Mafic amphibolite units within the shale bed sequences were interpreted as sills rather than basalt flows. Krapez suggested that these sedimentary sequences predate the BFB and preferred correlation with the Kambalda Group, placing the sedimentary rocks above the lower basalt sequence (Lunnon Basalt) but below the komatiite (Barley & others, 1998). His correlation is not supported by this study.

6.3 SOUTHERN COOLGARDIE DOMAIN

6.3.1 Introduction

The stratigraphy of the southern part of the Coolgardie Domain (hereafter called the "southern Coolgardie Domain") is disrupted by major faults and sills and the felsic and sedimentary sections are poorly exposed. The package was classified as the "Mount Kirk Formation" by Doepel (1973), with the type area defined as the location where the Esperance-Coolgardie Highway skirts the shoreline of Lake Cowan ENE of Mount Thirsty (figure 1.3, 6.2). "Mount Kirk Formation" is not used in this study because it was defined as including the entire greenstone stratigraphy of ultramafic, mafic, felsic and sedimentary rocks, and therefore is not considered to be a useful definition.

6.3.2 Overview of the Geology

The lowest unit exposed within the southern Coolgardie Domain is basalt, exposed sporadically along the western shore of Lake Cowan and along the western margin of the Mission Sill. In these areas, the basalt is overlain by fine-grained sedimentary rocks such as chert and shale or by the Mission Sill (figure 6.1, 6.2).

Komatiite is widespread within the southern Coolgardie Domain. Given the known stratigraphy of the Coolgardie Domain at Widgiemooltha, the komatiite probably overlay the basalt originally, but this transition was not observed in the field due to disruption of the stratigraphy by thrust faults. Where the basalt is overlain by fine-grained sedimentary rocks, the komatiite is interpreted as having pinched out of the stratigraphy.

The komatiite sequence is capped by chert approximately 2 m thick. Extensive mafic sills commonly intrude the sequence at this level. The sills are overlain by felsic-derived sedimentary rocks, typically epiclastic siltstone, sandstone and conglomerate, but also with rare, resedimented volcanic breccias. The sedimentary rocks are correlated with the Black Flag Beds (BFB).

The internal stratigraphy within the felsic and sedimentary succession is poorly defined. The lower-most BFB unit may be tuffaceous siltstone facies deposited as low-density turbidite, followed by the epiclastic felsic volcanic rocks deposited as

high-density turbidite. It is noted that Hand (1998) found coarse clastics at the base of the sequence at Mount Edwards. However, the evidence presented in Chapter 8 indicates that the felsic epiclastic rocks sampled by Hand at Mount Edwards, have a different provenance that the rocks sampled in this study, and therefore are probably separate depositional systems.

Three large, differentiated, mafic sills are present within the Coolgardie Domain in the Norseman region. From east to west, these sills are the Mission Sill, the Mount Thirsty sill and the smaller Woodcutters sill (figure 6.1). The former two sills have been previously described (Hudson, 1966; Hallberg, 1970; McCall, 1970; McCall, 1973; Williams & Hallberg, 1973; Witt, 1995). The sills tend to be emplaced close to or at the base of the BFB sedimentary rock sequence.

The stratigraphic facing within the Coolgardie Domain in the Norseman region can be determined by compositional layering attributed to differentiation within these sills. The Mission Sill is tightly folded into a syncline so that the eastern limb faces west but is truncated by the Mission Fault (figure 6.2). The western limb of the Mission Sill faces east as do the Mount Thirsty and Woodcutters sills.

6.3.3 Structural overview

The stratigraphy within the southern Coolgardie Domain is heavily dissected by D_2 thrust faults with a northerly strike and steep dip. These typically occur at the base of komatiite sequences and throw the komatiite over BFB. The ubiquitous co-occurrence of the thrusts with the ultramafic is presumed to be due to ultramafic minerals altering under the influence of metamorphism to form minerals such as talc and serpentine with low internal strength and with low friction coefficients on propagating shear planes.

D_2 folding within the southern Coolgardie Domain has tilted all units so they have a moderate to steep dip to the east. West dipping fold limbs are rarely found onshore, however, aeromagnetic images suggest they are found beneath Lake Cowan.

6.3.4 Mission Sill Area

Description

Differentiation within the Mission Sill has been described in previous studies. Hudson (1966) described the southern part of the sill as comprising bronzite (orthopyroxenite) cumulate overlain by norite and gabbro. Hallberg (1970) found the northern portion of the sill to be more complex, consisting of a basal layer of orthopyroxenite, overlain by ultramafic harzburgite cumulate passing into felspathic bronzite cumulate and norite. The Mission Sill is tightly folded and the eastern limb

is partially exposed on a hook-shaped promontory where two pyroxenite layers are separated by a band of norite (figure 6.2). The complete fold closure is not exposed at the surface, but is visible in aeromagnetics due to a highly magnetic band, probably serpentinised harzburgite.

Fresh orthopyroxene and intercumulus feldspar is found in some orthopyroxenite layers of the larger differentiated sills including the Mission Sill. This preservation of igneous minerals is unusual since the sills have been exposed to peak metamorphism. Hallberg (1970) suggested the preservation may be related to the lack of olivine to initiate breakdown and insufficient Ca to form amphibole due to a deficit of plagioclase.

Reconnaissance field work at the Mission Sill for this study broadly agrees with previous work in the area. Along the limbs of the Mission Sill, fresh orthopyroxenite and sedimentary rock both form prominent ridges to the east of west respectively of a 150 metre-wide alluvial plain. Near the fold closure at the northern end of the sill, black and green, serpentinised harzburgite with a medium to coarse grain size was found at the localities shown on the Norseman 1:100 000 geological sheet (McGoldrick, 1993) as "peridotite in the Mission Sill" (figure 6.2). At 6450150mN, 378435mE MGA, altered pyroxenite with elongate, bladed amphiboles up to 2 cm in length occurs immediately west of harzburgite outcrop near the crest of a hill. The main pyroxenite ridge occurs about 200 m further to the east. The altered pyroxenite is only about 30 m in width at this location and is underlain by felsic intrusive and sediment. These outcrops suggest that the harzburgite is underlain by a thin belt of altered pyroxenite and overlain by a thick body of fresh pyroxenite, as suggested by Hallberg (1970).

Sedimentary rocks approximately 100 m wide lie between the base of the Mission Sill and basalt. The sedimentary rocks dip at 50° towards the east suggesting a true thickness of about 60 m. The basal part of the sedimentary package consists of plane-laminated, sandstone-siltstone rocks with layers less than 1 cm in thickness. These rocks are overlain by thinly-bedded volcanic sandstone consisting of 3-15 mm wide sandstone beds, separated by siltstone 1-3 mm thick.

Quartz-veining and a fine-grained felsic intrusive with green amphiboles separate the uppermost sedimentary rock outcrops from the basal altered pyroxenite at the north end of the sill. Further south in the alluvial plain, along the contact between pyroxenite and sedimentary rock, there are sporadic exposures of quartz veining and silicification of weathered serpentinite.

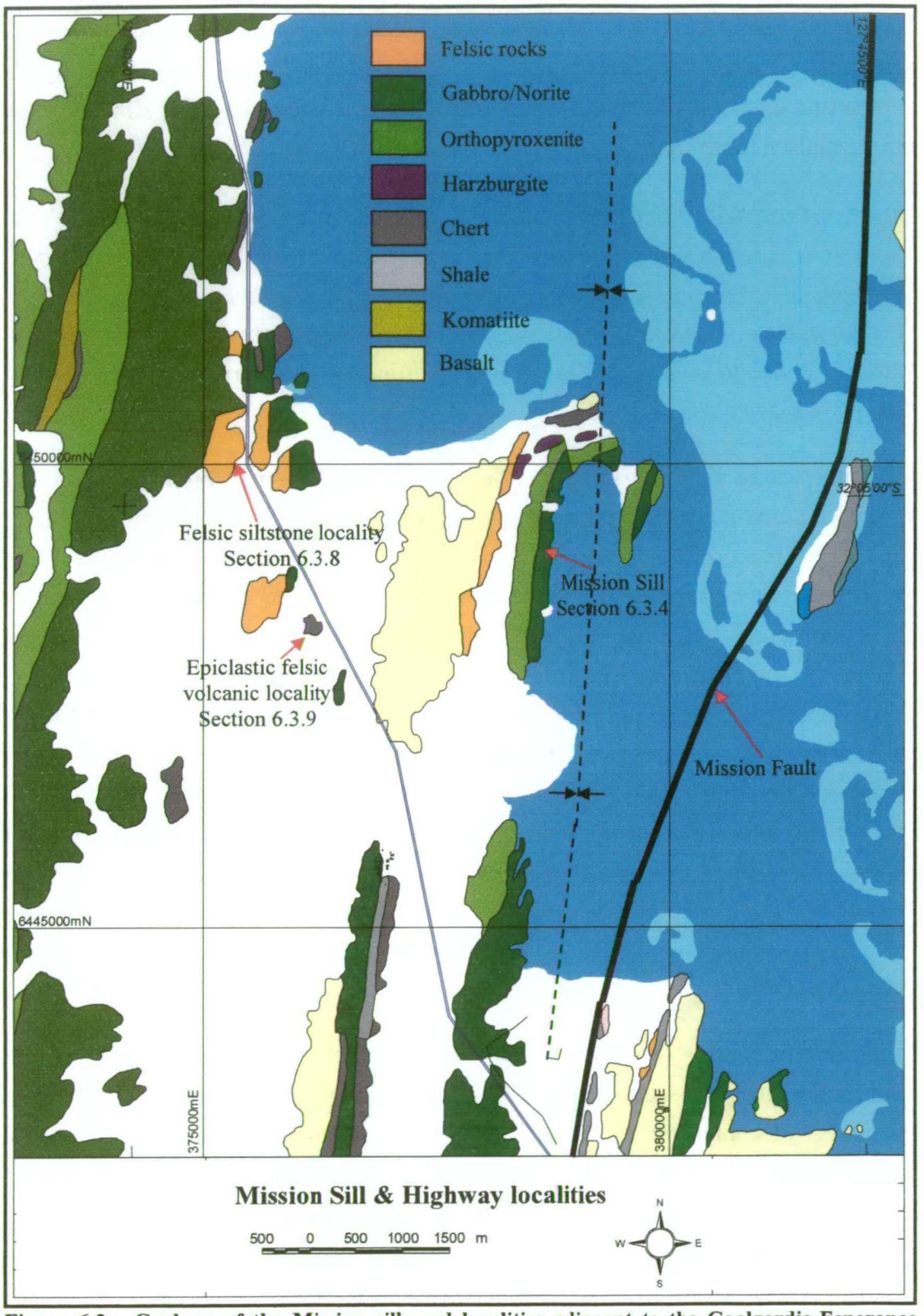

Figure 6.2: Geology of the Mission sill, and localities adjacent to the Coolgardie-Esperance Highway. Outcrop geology is from the GSWA Norseman 1:100 000-scale Sheet (McGoldrick, 1993). Section numbers refer to sections within the chapter where the localities are discussed.

Interpretation & discussion

The sedimentary package at the Mission Sill area directly overlies basalt. There is no indication of structural dislocation, so the contact is regarded as conformable. As noted in section 6.3.2, 80 km to the north at Widgiemooltha, and 15km to the northwest adjacent to the Pioneer Dome, the basalt is overlain by komatiite. The reason komatiite does not overlie the basalt in the Mission Sill area is considered to be its termination within the stratigraphy caused by a stratigraphic pinchout.

The thinly-bedded sandstone and siltstone is low-density turbidites and is correlated with the BFB. The turbidite become slightly coarser upwards and also show a more pronounced felsic volcanic provenance. The BFB are estimated to be 2-3 km thick by Barley & others (1998) whereas the true thickness of the sedimentary rocks below the Mission Sill is about 60 m, suggesting the Mission Sill has intruded the lowermost portion of the BFB. It is also possible that the contact between the sedimentary rocks and the sill is tectonic. Evidence to support the latter contention is the massive vein quartz below the sill, which may mark the location of a fault, and the apparent absence (in hand specimen) of contact metamorphism in the sedimentary rocks below the sill.

South of the fold closure defined by the Mission Sill (figure 6.2), aircore drilling has not located any rocks types other than intrusive units belonging to the sill. The absence of the rock sequences that originally overlay the sill from the core of the syncline is probably due to erosion having removed most of the upper units near the fold closure. As D_2 fold axes in the Norseman Terrane have a shallow plunge, these upper units would make their first appearance in the stratigraphy several kilometres to the south.

6.3.5 Mount Thirsty area

The Mount Thirsty sill was mapped at 1:12,000-scale by Anaconda Australia Inc. (Gemuts, 1968). Check mapping confirmed the accuracy of this map and it has been only slightly modified and the lithologies renamed following petrographic examinations (figure 6.3). The rock units of the Coolgardie Domain beneath the sill were investigated by check mapping and logging of aircore holes (figure 6.3).

Description

The basal unit of the Mount Thirsty sill comprises serpentinised harzburgite, which forms a prominent magnetic band about 200 m wide in aeromagnetic images. The harzburgite is successively overlain by altered orthopyroxenite, pristine orthopyroxenite, norite, gabbro and a granophyric unit, which includes bladed

amphiboles up to 12 mm in length with subhedral granophyric felspar and quartz. The units overlying the harzburgite are not magnetic and are not visible in aeromagnetic images.

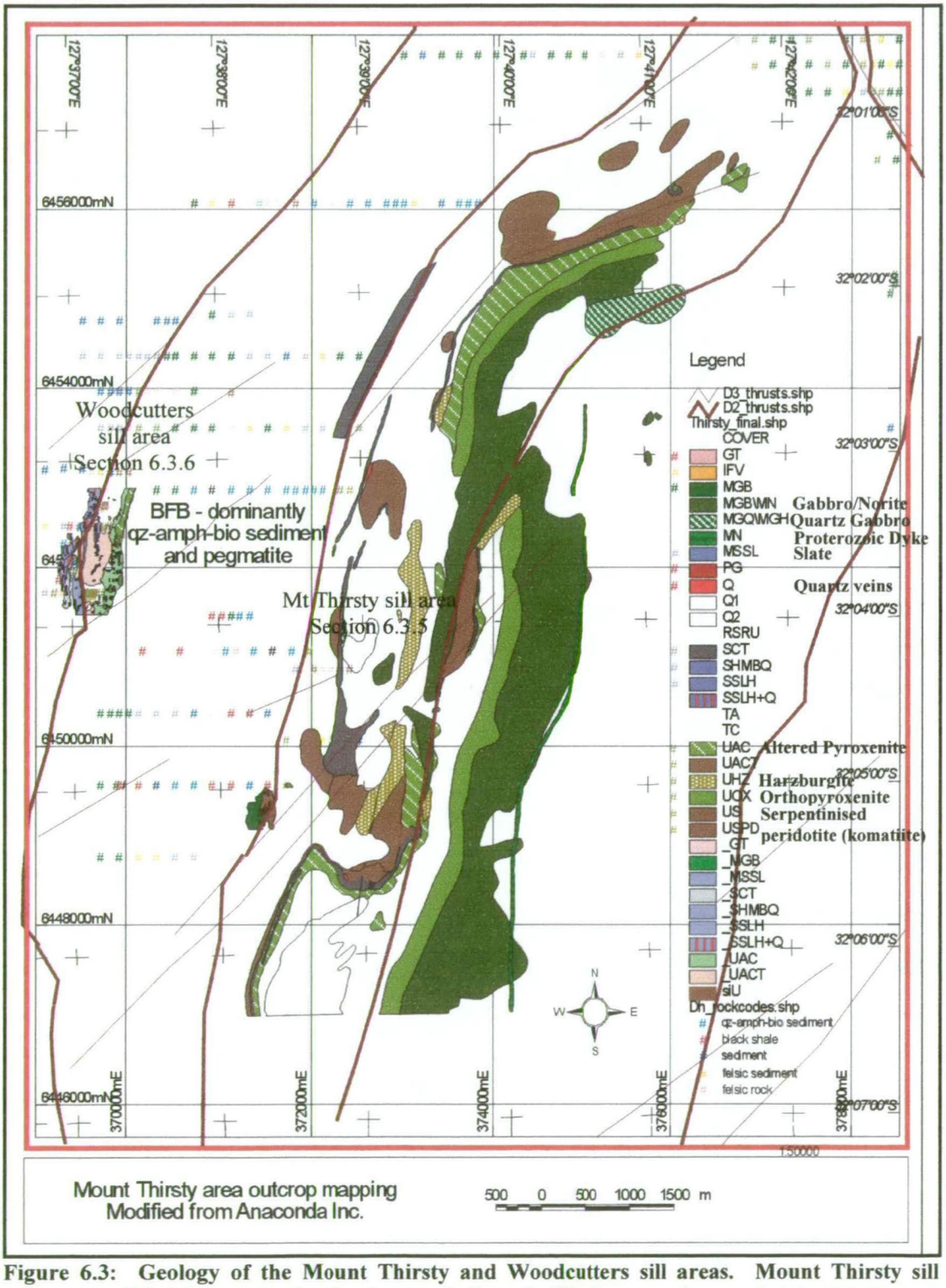

Figure 6.3: Geology of the Mount Thirsty and Woodcutters sill areas. Mount Thirsty sill geology modified from mapping by Anaconda Inc. Drillholes are colour coded by lithology at end of hole. The black lines are D_2 thrust faults. Rock types are noted next to the relevant codes on the legend.

A band of chert about 2 m thick, separates the base of the Mount Thirsty sill from underlying komatiite. Plate spinifex textures in the komatiite adjacent to the chert indicate the same easterly facing as the sill. The komatiite is visible in aeromagnetic images as a magnetically high belt adjacent to the harzburgite band. The komatiite has a width of about 600 m, although aeromagnetic images show it being broader in some areas due to folding. The base of the komatiite is covered with alluvial sediment.

A small patch a mafic rock shown on the Anaconda map (Gemuts, 1968), near the base of the komatiite, was mapped at 1:2500 scale to determine whether or not, it represents a basal basalt-komatiite contact. The mapping suggested the mafic rock is dolerite intruding the komatiite due to the fine to medium-grain size, the irregular and patchy distribution of the mafic and the presence of a thin metamorphic aureole in komatiite adjacent to the mafic.

Aircore drilling of the 2 km wide area covered with unconsolidated transported sediment, between the komatiite below the Mount Thirsty sill and the top of the Woodcutters sill, has provided data about the rock sequence in this area. It is dominated by quartz-feldspar-amphibole-biotite rocks and lesser felsic rocks, all intruded by abundant pegmatite dykes.

The unconsolidated cover comprises Tertiary-aged marine sediments, including sponge spicule-bearing clay, overlain by Recent alluvial gravels, which include maghemite fragments. The magnetic fragments cause a stippled pattern in magnetic images of the covered area.

The komatiite, away from spinifex zones, is dominated by serpentinised, fine-grained, olivine orthocumulate. Former olivine grains are typically 0.25-0.5 mm in diameter replaced in the core with serpentine and rimmed by acicular amphibole. Chlorite typically forms the intercumulus mineral and magnetite typically comprises around 3% of the rock. Texturally destructive forms of alteration, consisting of amphibole overgrown by flaky masses of serpentine are also common.

In hand specimen, the harzburgite has a similar appearance to the altered orthopyroxenite, except that the fresh surfaces are darker in colour and crystals are poorly defined. The darker colour is due to the presence of fine-grained magnetite and chlorite. Harzburgite is most readily distinguished by its magnetic character, caused by serpentinisation of former olivine grains, which has generated up to 5% magnetite. The olivines are now equant patches of serpentine 0.25-0.5 mm in diameter, which retain curving fracture patterns typical of olivine. The serpentine is commonly enclosed by tremolite-talc±chlorite replacing former poikilitic

orthopyroxene up to 2 mm in diameter. The magnetite is in tremolite-talc patches adjacent to serpentine.

The fresh orthopyroxenite layer is uniformly about 120 m wide and forms prominent ridges with little soil and strong, rubbly subcrop. These ridges have only low, sparse shrubs rather than the eucalypt woodland more common in the Norseman area, thereby forming vegetation anomalies. The orthopyroxenite consists of mesocumulate textured, fresh orthopyroxene grains, 1-2 mm in size, which are a glassy green colour. XRD suggests that the pyroxene is enstatite, but the pyroxenes display a faint pleochroism from yellow to grey in thin section, suggesting that they are the less magnesium-rich bronzite, consistent with the findings of Hudson (1966) for the Mission Sill. Plagioclase may comprise as much as 10% of the rock, forming anhedral, intercumulus grains. Minor tremolite and talc has formed within the pyroxenes as alteration along fractures. Opaque oxides are rare.

The strongly-altered orthopyroxenite forms a rind, 150-300 m wide along the lower contact of the pyroxenite. Former orthopyroxene sites are now a mixture of talc and amphibole (tremolite+anthophyllite). Intercumulus sites between former orthopyroxenes are occupied by chlorite. Opaque oxides are rare.

Norite typically comprises around 40% subhedral tabular and lath-shaped plagioclase, partly enclosed by talc and tremolite after subophitic orthopyroxenes up to 3 mm in diameter. Traces of granular sphene are associated with plagioclase but opaque oxides are rare.

Interpretation & discussion

The quartz-feldspar-amphibole-biotite rocks beneath the covered area are probably metamorphosed, mafic-derived sediments. Felsic rocks are also abundant but the aircore samples are insufficient to determine whether they are coherent, fragmental or epiclastic. This felsic and mafic-derived sedimentary rock package is considered to correlate with the BFB and therefore belongs at the top of the stratigraphic package. The komatiite and the Mt Thirsty sill have been thrust over the BFB sedimentary rocks. A similar relationship is present at the Woodcutters area described in section 6.3.6

The Mt Thirsty sill overlies a thin chert band at the top of the komatiite that may equate with the Widgie chert at Widgiemooltha and Mount Edwards. If this is the case, the sill intrudes the very base of the BFB.

6.3.6 Woodcutters sill area

The Woodcutters sill was mapped at 1:2500 scale (figure 6.4). It is a previously undocumented layered mafic sill at the Woodcutters North prospect west of Mount Thirsty.

Description

The Woodcutters sill is much smaller, and contains fewer differentiated phases, than the Mission and Mount Thirsty sills. From it west to east it consists of an amphibole-altered orthopyroxenite layer overlain by gabbro, which is poorly exposed. No fresh orthopyroxenite is preserved and there is no basal serpentinised harzburgite. In a simple differentiation model, gabbro would overlie pyroxenite, hence Woodcutters Sill is considered to face east.

The Woodcutters sill is underlain by amphibole-chlorite-talc ultramafic interpreted to be komatiite. It outcrops poorly and is mainly exposed in costean spoil and drill holes. Chert and mica schist interflow sedimentary rock bands can be traced through the komatiite defining the strike. Unlike Mount Thirsty, there is no sedimentary rock band at the contact between the komatiite and the base of the sill.

The base of the komatiite is truncated by a fault (figure 6.4), which is shown to be discordant to the strike of the interflow sedimentary units by the komatiite flows being successively cut out to the north. Thinly-bedded, sandstone-shale rocks on the west side of the fault are now in contact with the base of the komatiite. The contact between komatiite and the juxtaposed sandstone-shale is marked by abundant quartz-vein float, which costean spoil shows is the surficial expression of micaceous schist cut by stockwork quartz-veins. This schist is considered to be the expression of the fault in sandstone-shales. A WNW-trending fault visible in aeromagnetic data also cuts the komatiite at its southern end, causing it to thin. The pyroxenite is not offset across the fault, but the width of the sedimentary rock expands.

Interpretation & discussion

The amphibole-chlorite-talc composition of the komatiite suggests moderate MgO abundances and a non-cumulate protolith. Talc-carbonate compositions, likely to be more MgO-rich, were encountered at depth in a diamond drillhole.

As the Woodcutters sill overlies komatiite, but underlies the quartz–feldspar-amphibole-biotite rocks beneath the Mount Thirsty sill that are interpreted as BFB, it appears that the sill intrudes the contact at the base of the BFB.

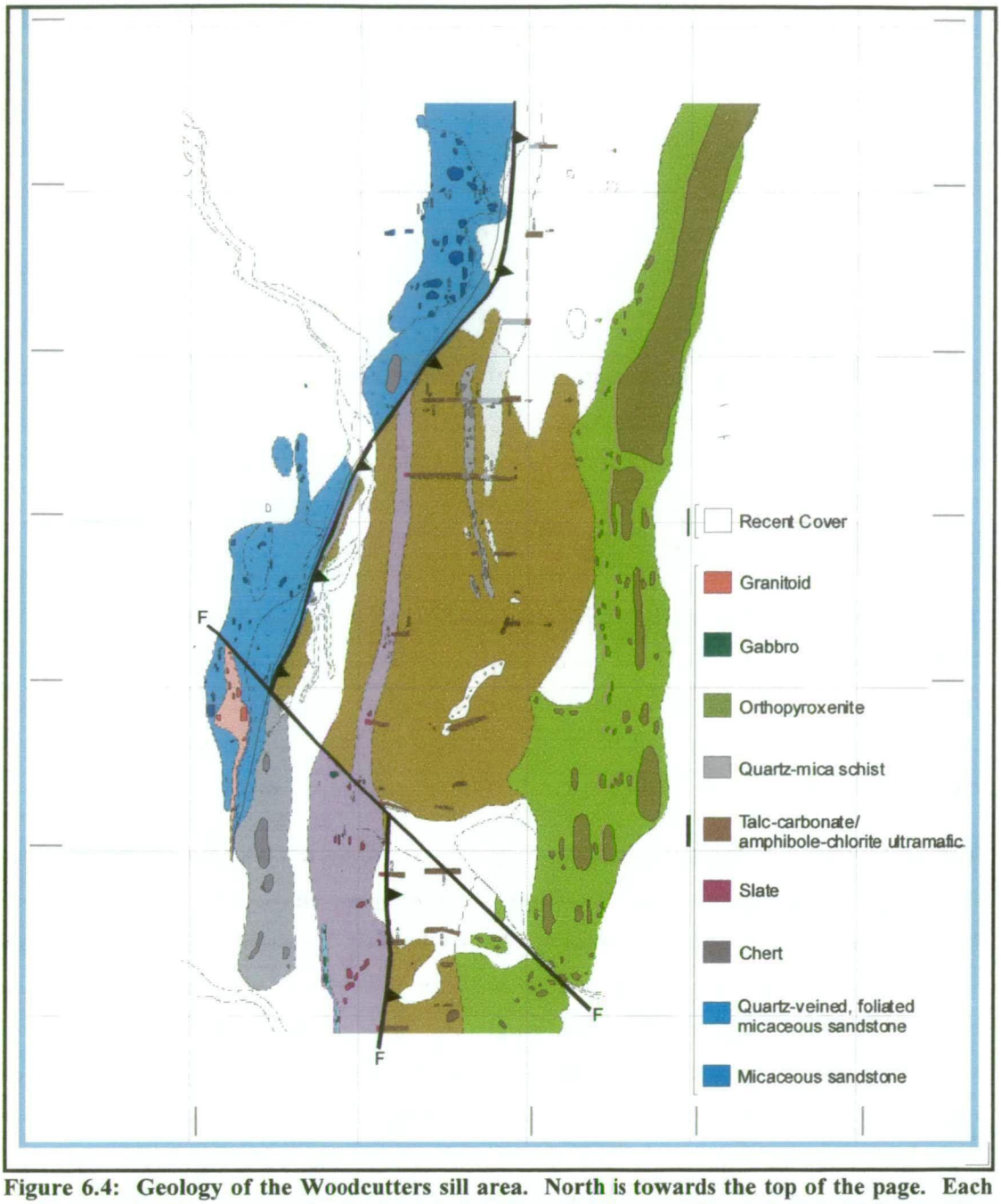

Figure 6.4: Geology of the Woodcutters sill area. North is towards the top of the page. Each grid square is 250 m across. See figure 6.3 and figure 6.1 for a smaller scale view of the location. The north-south trending interflow sedimentary rock bands within the ultramafic demarcate separate komatiite flows. The progressive wedging out of the komatiite flows and interflow sedimentary rocks against micaceous sandstone indicates a fault. The micaceous sandstone, chert and slate are considered to be Black Flag Beds, which the komatiite has been thrust over. A later NW trending fault has offset the thrust.

The thinly-bedded sandstone-shale, faulted against the base of the komatiite at the Woodcutters area is interpreted to be low-density turbidite, which is correlated with the BFB. As the strata are steeply east-dipping and face eastwards, the komatiite overlies the BFB, separated by the fault. The sequence of lower stratigraphy over higher is consistent with the fault being a thrust. This structure is discussed further in section 10.4.7.2.

The WNW fault expands the width of the BFB, thins the komatiite and does not affect the pyroxenite. These offsets would be consistent with a block fault if the pyroxenite has a vertical dip while the other units have a lesser dip. NNW-trending faults, initiated as block faults within the Norseman Terrane are discussed in section 10.4.8. This is the only example identified of a possible block fault within the Coolgardie Domain.

6.3.7 Pioneer area

The Pioneer prospect lies approximately 9 km north of Mt Thirsty and NNE of the Woodcutters sill (figure 6.1).

Description

The komatiite beneath the Woodcutters sill strikes to the north in aeromagnetic images, and bends around the southeast corner of the Pioneer Dome until 10 km to the NNE of Woodcutters, the sill again strikes north-south at the Pioneer prospect. The komatiite is demagnetised as it bends around the corner of the Pioneer Dome, probably by intense shearing and alteration, but the magnetic intensity increases again as it deflects back to a north-south orientation.

The Pioneer prospect is entirely covered by unconsolidated, transported sediment, but aircore and RC drilling at this location has revealed the bedrock geology. Amphibole-chlorite-talc-dolomite ultramafic with a sheared base at its western margin, overlies micaceous metasediments, consistent with Woodcutters North prospect stratigraphy. One difference between Woodcutters area and the Pioneer prospect is that quartz–phyric felsic rock, rather than a mafic sill, overlies the komatiite at Pioneer.

Interpretation & discussion

The Woodcutters thrust (figure 6.4) is continuous and remains at the base of the komatiite between Woodcutters and Pioneer. It juxtaposes similar rock types at Pioneer as at Woodcutters, being ultramafic and micaceous metasediments interpreted as BFB.

Plate 6.1: Laminated felsic siltstone from the location adjacent to the Coolgardie-Esperance highway described in section 6.3.8.

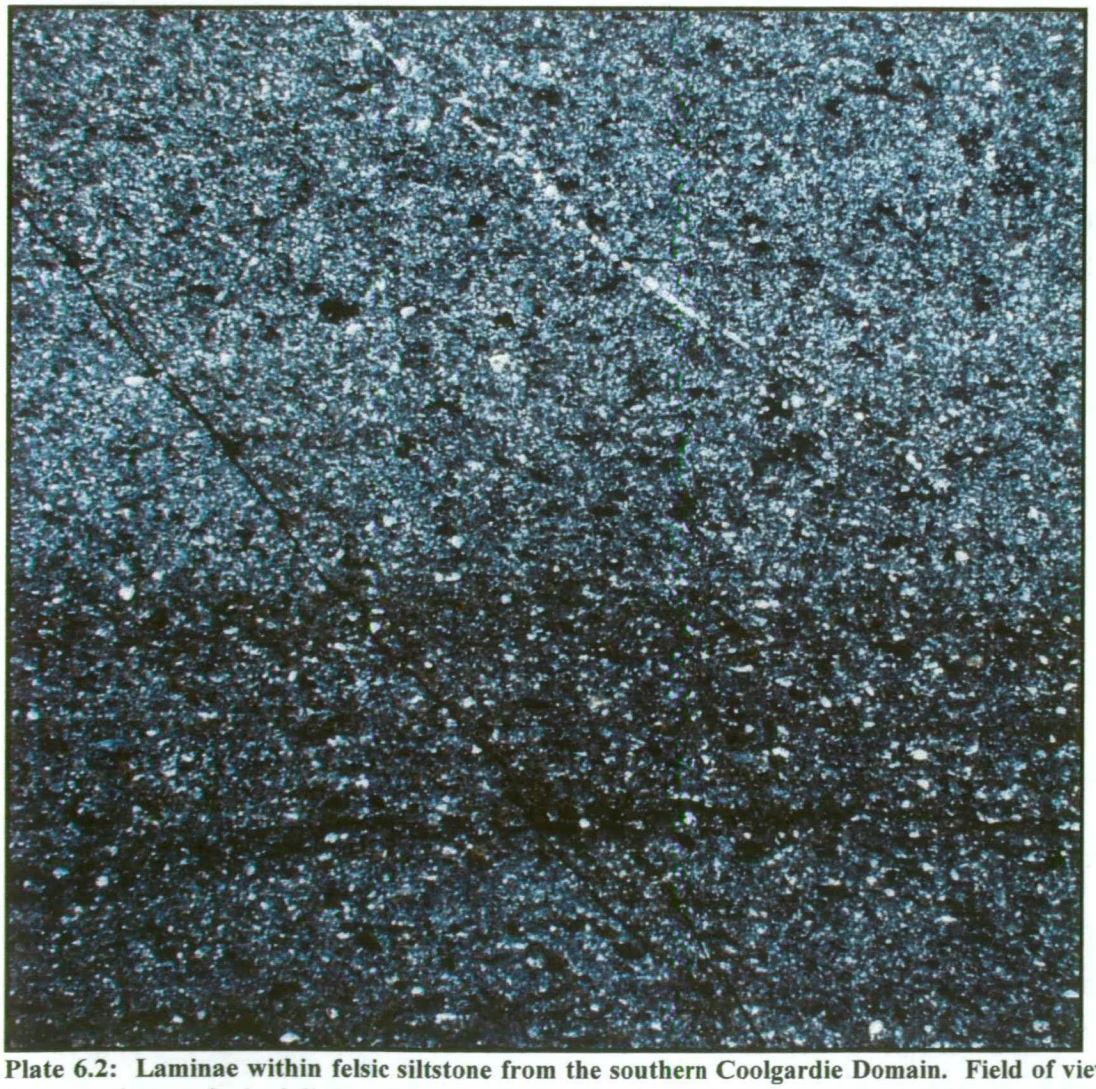

Plate 6.2: Laminae within felsic siltstone from the southern Coolgardie Domain. Field of view 8 mm. plane polarised light. Sample CN851921. See Plate 6.3 for magnified view of the minerals.

The ultramafic rocks at Pioneer were analysed for MgO content and returned levels in the mid-20's wt% (volatile-free). These levels indicate that the komatiite was not an olivine cumulate prior to alteration. Any cumulate komatiites that may originally have occurred has been cut out by the fault at the base of the ultramafic.

A likely intrusive felsic unit overlying the ultramafic appears gneissic in texture and has quartz phenocrysts up to 7 mm in diameter.

6.3.8 Felsic siltstone adjacent to the highway

This area lies at 6450150mN, 375450mE MGA, along the west side of the Coolgardie-Esperance Highway (figure 6.1 & 6.2). The exposure is cut by a creek, which, for convenience, can be used to divide this locality into northern and southern portions.

The geology in detail is rather complex. Rubbly subcrop to outcrop is extensive but contacts between units are poorly exposed. Evidence for the younging direction is not present in the local geology, but the area lies close to the upper differentiated layer of the Mount Thirsty sill, so the facing is assumed to be to the east, like the sill.

Description

North of the creek cutting the area, a band of laminated chert a few metres wide, probably representing silicified shale, dips about 50° towards the southwest (130°). The chert is successively overlain by a few metres of dark-coloured felsic siltstone; several metres of felsic breccia that is interbedded with black shale; and another few metres of dark-coloured felsic siltstone and silicified shale immediately adjacent to the highway (Plate 6.1 & 6.2).

Immediately below the chert to the west, hornblende-bearing, coarse-grained gabbro outcrops. The gabbro-chert contact is, in part, sulfidic and has been the focus of a number of prospecting trenches. Approximately 70 m west of the chert band and beneath the gabbro, there is a second outcrop of chert, suggesting that intrusion of the gabbro split the sedimentary rock unit.

South of the creek cutting the area, there is a broad, low hill about 250 m wide, dominated by subcropping, dark-coloured, felsic siltstone with a smaller area of plane-laminated, coarse-grained, felsic volcanic sandstone at the north end of the hill closest to the creek. At least one unit of felsic breccia approximately 2 m wide, is interbedded with the felsic siltstone. Down-section, about 40 m west of the hill and across a southwest-trending fork in the creek, a band of laminated chert is exposed underlying the felsic siltstone. The chert is approximately 10 m in width and divided into two bands, separated by approximately 3 m of recessive shale. Further west of

the chert, there is about 100 m of soil cover below a large hill, on which sporadic outcrops of hornblende gabbro are exposed.

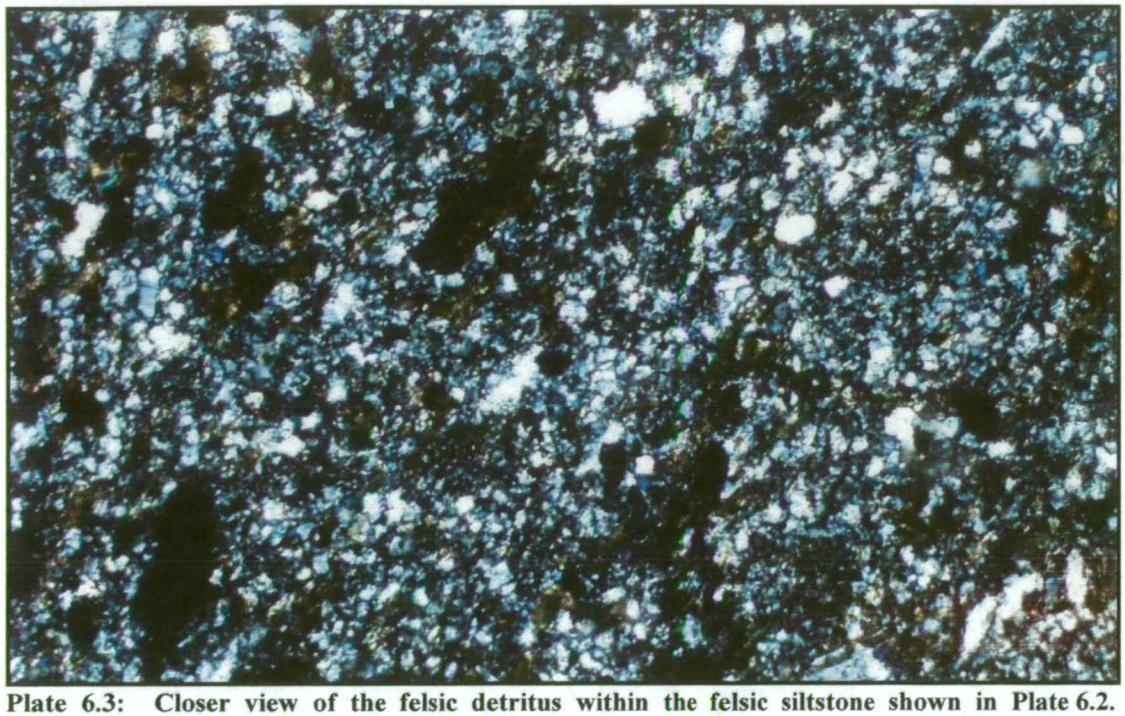

Plate 6.3: Closer view of the felsic detritus within the felsic siltstone shown in Plate 6.2. Irregular, corroded-shaped feldpars and quartz with opaque minerals and patches of biotite. Field of view 1 mm. Cross polarised light. Sample CN851921.

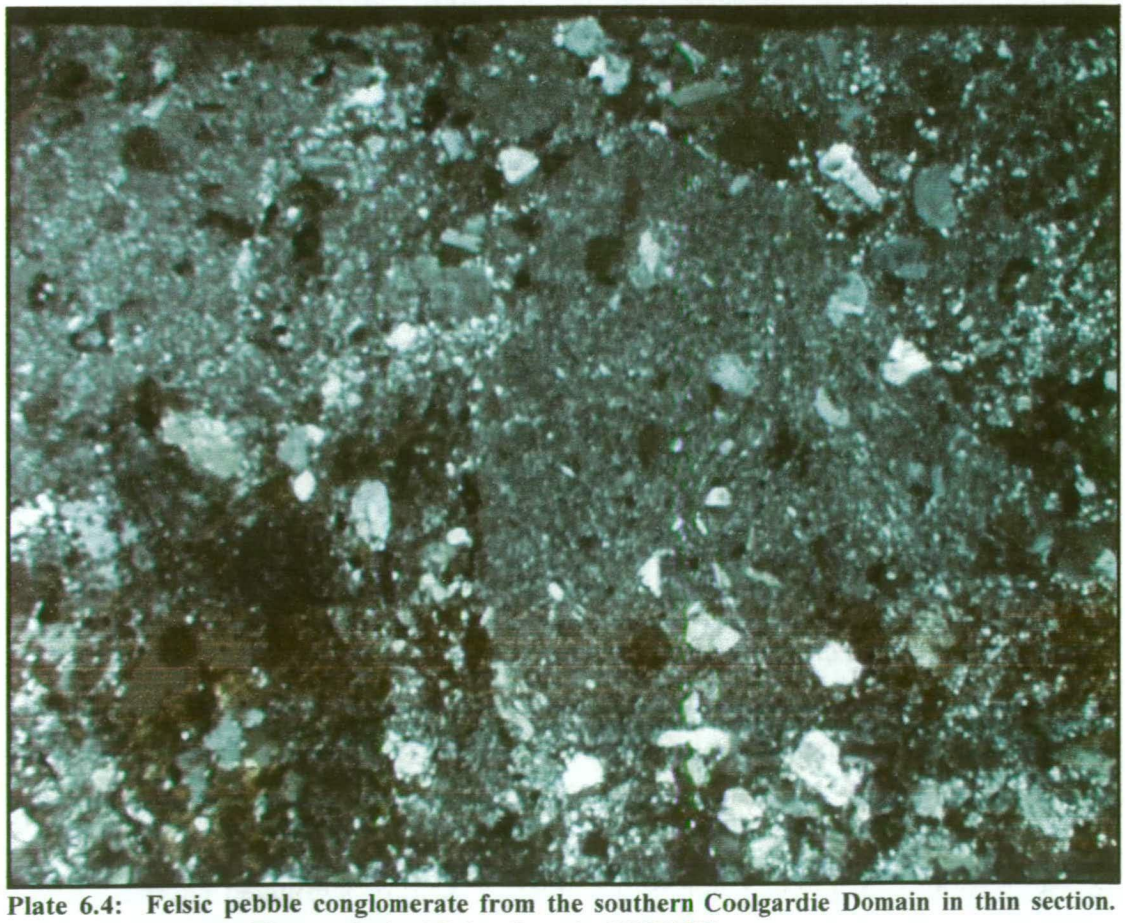

Plate 6.4: Felsic pebble conglomerate from the southern Coolgardie Domain in thin section. Field of view 8 mm. Plane polarised light. Sample CN851928.

Linking the chert bands north and south of the creek, the stratigraphy in the area can be roughly assembled. Chert, which may be silicified shale, appears to be stratigraphically the lowest sedimentary rock unit overlying the hornblende-bearing, coarse-grained gabbro at the top of the Mount Thirsty sill. The chert is overlain by a considerable thickness (perhaps 200 m) of dark-coloured, felsic siltstone with rare interbeds of felsic breccia, black shale and felsic sandstone. The felsic breccia has angular, gravel-sized, clasts of felsic volcanic, felsic siltstone and black shale in a matrix of dark-coloured felsic siltstone. The clasts are matrix supported and some volcanic clasts have curviplanar margins. The units appear to be several metres in width, but contacts are not exposed.

The dark coloured felsic siltstone is widespread in this area and is typically weakly cross-laminated. Most of the rock consists of recrystallised, quartzo-feldspathic grains 1/20 mm in size. However, larger, angular fragments of phenocrysts, up to 1/6 mm are also present, distributed evenly throughout. The largest grains have not been recrystallised and consist of microcline, plagioclase, and lesser quartz (Plate 6.3).

Interpretation & discussion

The sedimentary rocks are considered to be part of the BFB. The felsic siltstone probably represents deposition from low-density turbidite. The angular phenocryst fragments may have originated as pyroclasts, shattered by an explosive eruption. The crystals have not been subsequently reworked in an abrasive environment, so the textures are consistent with resedimentation of pyroclasts that fell into the ocean.

The extreme angularity of the clasts within the felsic breccia units interbedded with the siltstone also precludes significant transport or storage in an abrasive environment. A pyroclastic origin for the felsic fragments is possible, but not favoured, due to the relatively coarse grain-size. The curviplanar shapes that many of the felsic volcanic clasts possess, suggests quench fragmentation. Conclusions about the deposition of the breccia are tentative due to the poor exposure of the units. Considering the submarine origin of surrounding units, the gravel-sized, grain-size would be consistent with transport and deposition from high-density turbidity currents. The sedimentary rock fragments are best explained as rip-up clasts scoured from the black shale and felsic siltstone substrate. Thus, the units are considered most likely to represent high-density turbidite flows that have transported hyaloclastite spalled from a submarine felsic volcanic centre, down the flanks of the edifice and out into the basin plane.

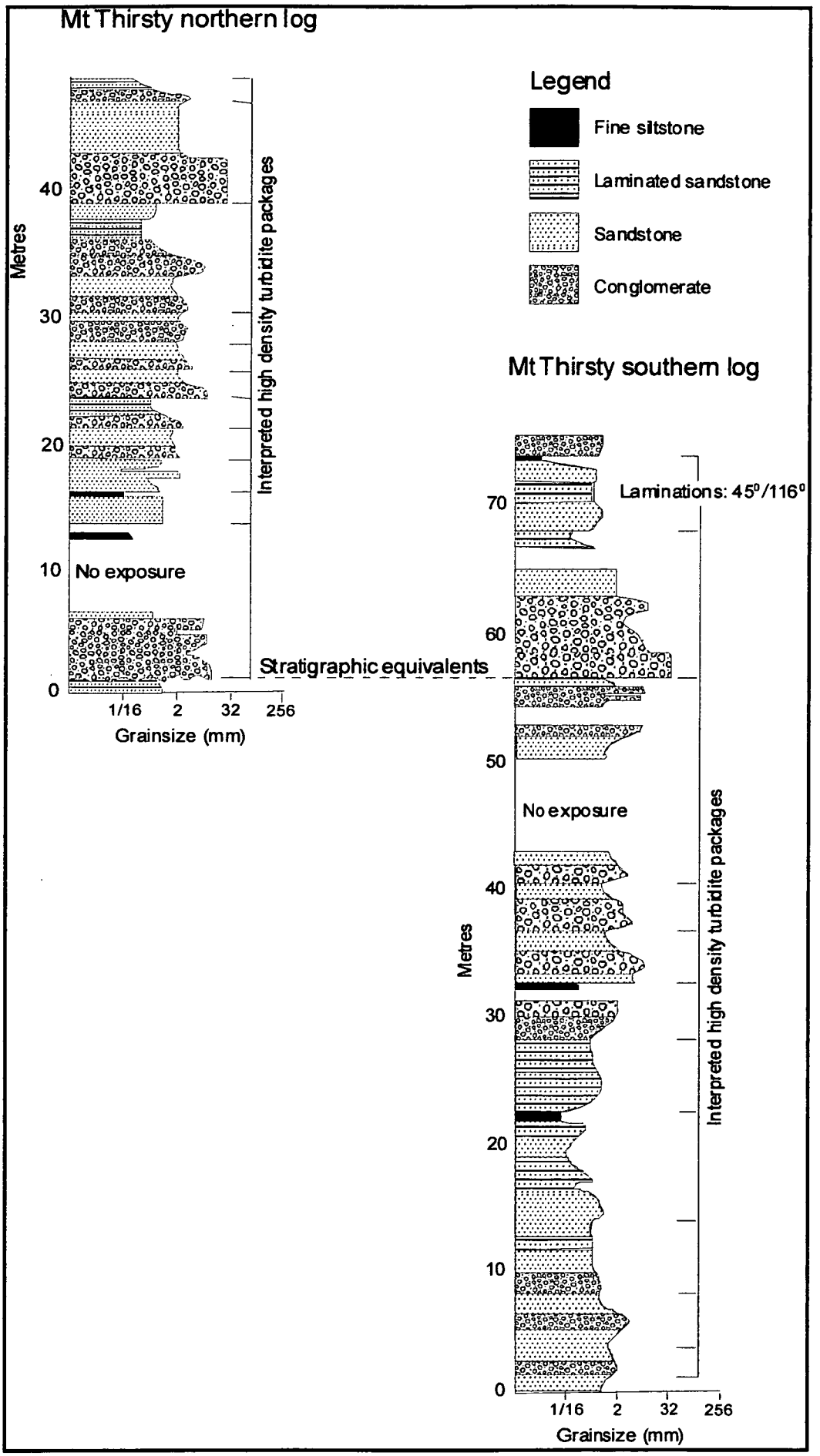

Figure 6.3: Graphic log across epiclastic felsic volcanic rocks of the Black Flag Beds adjacent to the Norseman-Coolgardie Highway.

6.3.9 Epiclastic felsic volcanic rocks adjacent to the highway

Epiclastic felsic volcanic rocks within the Coolgardie Domain are exposed at 6448350mN, 376450mE MGA, an area about 150 m across, immediately adjacent to the Coolgardie-Esperance Highway, 2.6 km northwest of the Tjirntu Parapara Aboriginal Mission (figure 6.1 & 6.2). The exposure is about 150 m across and consists of rubbly subcrop, in which contacts cannot be observed. Nevertheless, these felsic epiclastic rocks are the best exposures located, so two graphic logs were constructed in this area (figure 6.3). The first log commences in the felsic subcrop and extends to the upper limits of the exposure in that area. The second log commences about 50m along strike to the northeast of the first log. There is an overlap between the logged stratigraphy such that the second log commences in the conglomerate unit at 56 m in the first log.

Description

The strike of felsic sedimentary rock units is defined by low hummocks of subcrop trending at about 20°. Between the hummocks, subcrop is generally poor and largely consists of float. The entire subcrop consists of epiclastic felsic volcanic rocks with lithofacies varying between pebble conglomerate; gravel; both massive and planar laminated sandstone; and fine-grained, laminated sandstone to siltstone (Plates 6.6-6.8). These lithologies form repetitive sequences with pebble conglomerate or coarse-grained sandstone at the base of a sequence, passing through finer sandstones and with siltstone at the top of the sequence.

Contacts are generally not exposed and direct evidence for the younging direction is not present, but the facing is assumed to be east, as defined by differentiation in the Mt Thirsty and Mission Sills, so the sequences appear to be normally graded.

The thickest sequence logged is about 11 m wide at surface, which corresponds to a true thickness of about 8 m when the measured dip of 52° towards 116° is taken into account.

The pebble conglomerate is monomict and clast-supported with sub-rounded to well-rounded pebbles of low to moderate sphericity reaching a maximum size of about 4 cm in diameter. The pebbles consist of porphyritic dacite with euhedral and subhedral, tabular sodic plagioclase[1] phenocrysts up to 1.5 mm length and fine-grained, recrystallised, polygonal quartz matrix. Rare quartz phenocrysts are present in some clasts and approximately 5% biotite is present, considered to be a metamorphic product because it is typically associated with recrystallised areas and

[1] Mineral composition determined by XRD.

Plate 6.5: Texture within a felsic pebble in thin section. Large plagioclase laths within a quartzo-felspathic groundmass. Field of view 2 mm. Cross polarised light. Sample CN851928.

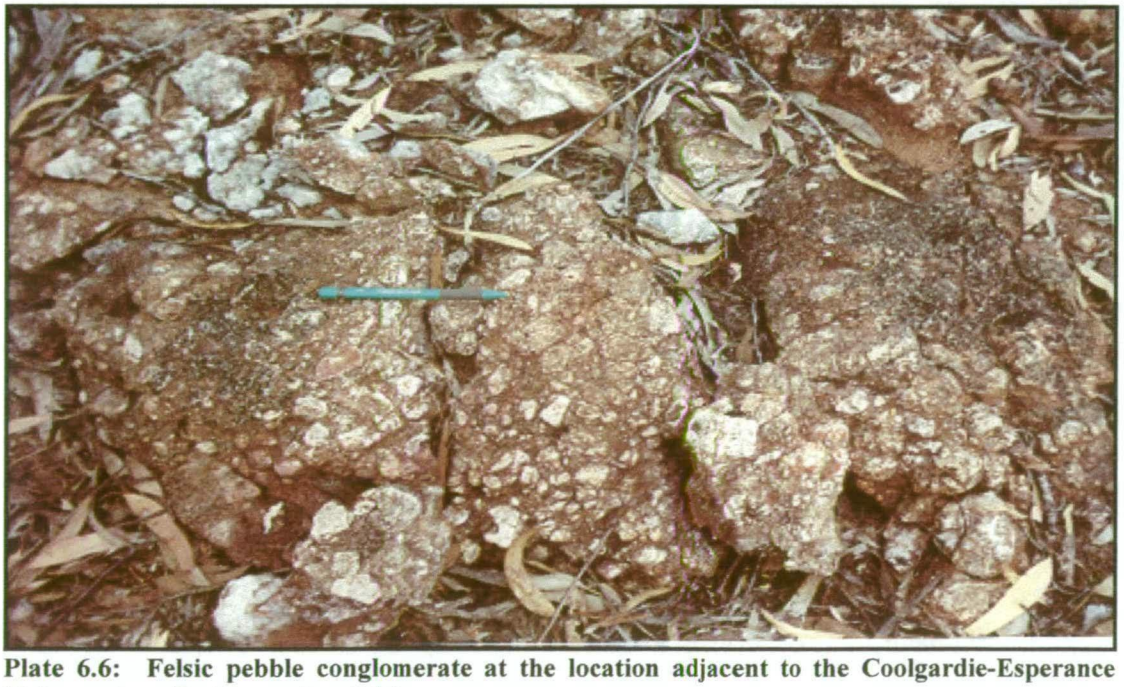

Plate 6.6: Felsic pebble conglomerate at the location adjacent to the Coolgardie-Esperance highway described in section 6.3.9.

occurs around clast margins. Rare chert fragments with a maximum size of around 1 cm can be found within the conglomerate.

The felsic gravel has a similar composition to the pebble conglomerate but differs in grain size. The sandstone is arkosic in bulk composition and planar laminated. The majority of the sandstone units are well sorted, although some coarse-grained sandstone contains matrix-supported gravel fragments. The clasts are poorly defined in thin section but appear to consist of rounded, calcic plagioclase phenocrysts and clasts of fine-grained, recrystallised, quartzo-feldspathic groundmass (Plates 6.4 & 6.5). Some plagioclase phenocrysts have granophyric quartz intergrowths and they are all partly replaced with unstrained, polygonal quartz. Trace muscovite is commonly associated with feldspars and biotite is distributed evenly throughout the sand. The medium and fine-grained sandstone appear to show wavy, possibly ripple cross-laminations. No climbing ripples were observed.

Interpretation & discussion

The sequences are interpreted to be high-density turbidites. The upper units grade from fine sandstone to shale and probably represent residual, low-density turbidites, but are not always present due to non-deposition or scouring by overlying flows. The conglomerate and gravel units show zones with reverse grading from gravel back into conglomerate suggesting a pulsing long-lived turbidity current. However, this interpretation is tentative due to the rubbly nature of the subcrop, which may conceal sharp or scoured contacts. The area of exposure is insufficient to determine whether the high-density turbidites represent channels.

The rounding of the felsic volcanic clasts indicates abrasion within a fluvial or shoreline environment, suggesting that the epiclasts were eroded from a subaerial environment. The monomict clast composition requires a single rock type at the source. An emergent volcanic cone is considered the most probable source. The small, rare, chert fragments within conglomerate and gravel units may be rip-up clasts from underlying fine-grained units.

The dacite pebbles in the conglomerate appear texturally and compositionally similar to the porphyritic dacite at Fram Island (section 6.3.10), apart from the recrystallisation of the groundmass and smaller size of the phenocrysts. It differs from the rhyolite at the Polar Bear Peninsula by having abundant tabular feldspar phenocrysts rather than the sparse quartz phenocrysts typical of the rhyolite. The two sandstone samples examined differ from the conglomerate in that the composition of plagioclase in the former is calcic rather than sodic.

6.3.10 Fram Island area

"Fram Island" is the informal name for a small island approximately 1 km off the western Shore of Lake Cowan (figure 6.1). Fram Island itself, exposes serpentinised

and talc-altered, olivine orthocumulate, which may be komatiite beneath the north plunging extension of the Mission Sill. A few hundred metres to the south, a small

Plate 6.7: Laminated felsic volcanic sandstone. From location adjacent to Coolgardie-Esperance Highway described in section 6.3.9.

Plate 6.8: Closer view of laminated felsic sandstone. From location adjacent to Coolgardie-Esperance Highway described in section 6.3.9.

island consists of porphyritic felsic rock.

Description

A diamond hole drilled at Fram Island intersected the felsic rock and a sample was submitted for analysis as described in Chapter 8. The felsic rock consists of plagioclase phenocrysts from 0.25 to 4 mm in size in a fine-grained quartzo-feldspathic groundmass. The feldspars are sodic in composition[2]. Traces of biotite are present, largely hosted by veinlets.

Interpretation & discussion

The quartzo-feldspathic nature of the rock with sodic feldspar phenocrysts but few ferromagnesian silicates suggests that the rock is a dacite with trondhjemitic affinities. Petrographically, the porphyry is similar to the clasts within the felsic conglomerate described in section 6.3.9.

6.3.11 Abbotshall area

The Abbotshall area gains its name from the Abbotshall Mine that lies 8 km SW of Norseman township, at the southern tip of Lake Cowan (figure 6.1, 6.4). The Abbotshall Mine is an historic underground mine that exploited gold in the Abbotshall Beds. It was reworked in 1997-1998 by an open cut operated by Australasian Gold Mines. The importance of the area for this study is that U-Pb zircon ages have been published for felsic units in this area.

The dated felsic units were reported to be "felsic volcanic and associated sedimentary rocks" of the Mount Kirk Formation with an age of 2688±8 Ma by Hill & others (1992b). With further dating and pooling of all zircon ages, the date was refined to 2687±3 Ma (Campbell, 1989). The local stratigraphy includes the Abbotshall Beds and felsic rocks, and the terrane-bounding Mission Fault is interpreted to pass through this area.

Description

The GSWA 1:100 000-scale Norseman Sheet (McGoldrick, 1993), shows that the geology of the Abbotshall Mine area from east to west comprises west-facing pillow basalts and dolerites of the Woolyeenyer Formation; cherts and other fine-grained sedimentary rocks with associated felsic rocks in the immediate vicinity of the mine; another package of west facing dolerites and pillow basalts about 700 m thick; and the NNW-trending, eastern limb of the Mission Sill, being amphibole-altered pyroxenite and gabbro (figure 6.4). The Mission Sill is part of the Coolgardie

[2] Mineral composition determined by XRD.

Domain, whereas at least some of the sedimentary rocks correlate with the Abbotshall Beds of the Norseman Terrane. Therefore, the terrane bounding Mission Fault is interpreted to pass through the Abbotshall Mine area, to the east of the 700 m thick succession of dolerite and basalt that forms the footwall to the Mission Sill.

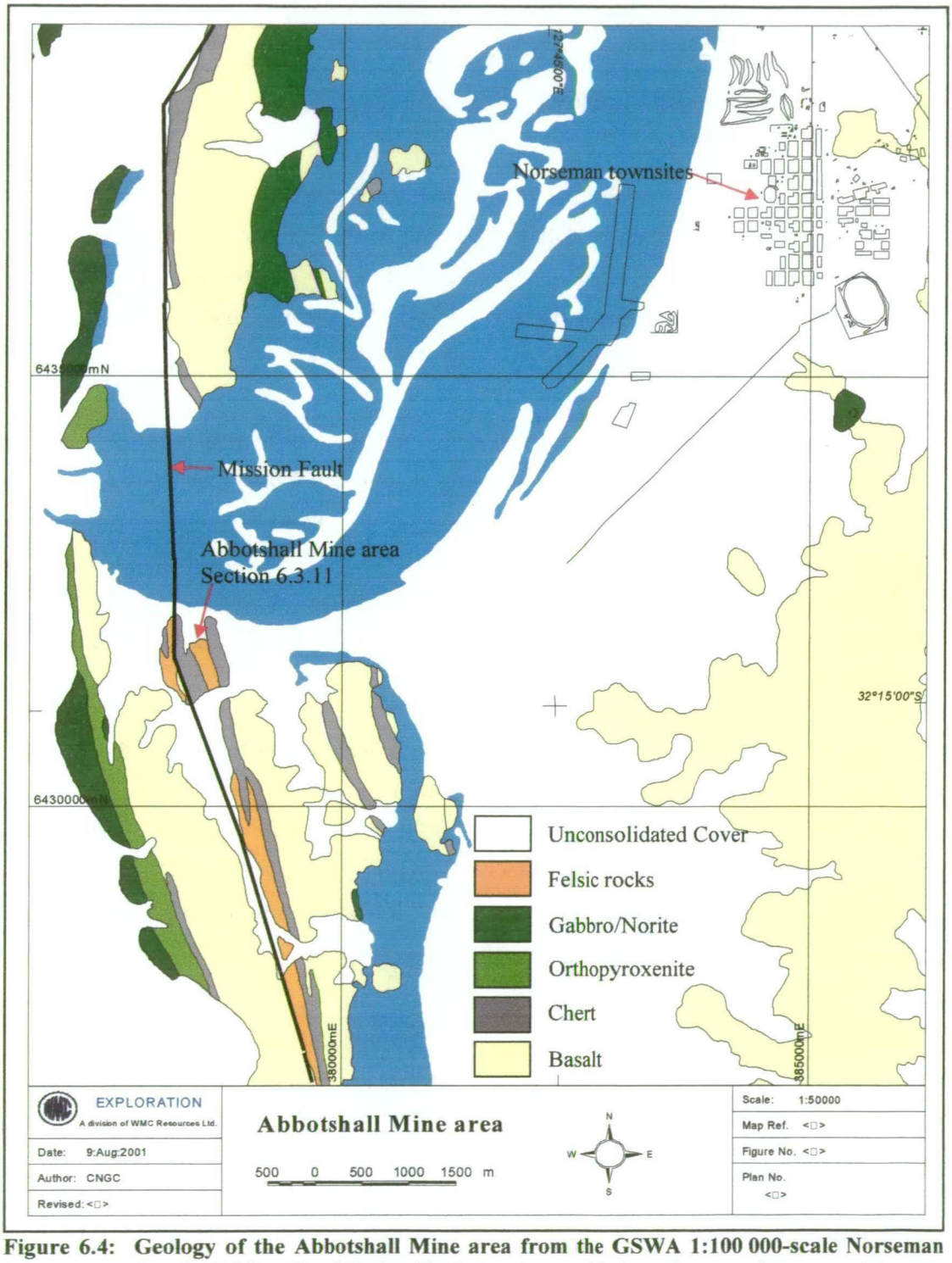

Figure 6.4: Geology of the Abbotshall Mine area from the GSWA 1:100 000-scale Norseman Sheet (McGoldrick, 1993). The Mission Fault has been added to the map, interpreted to pass through the Abbotshall Mine sequence, separating the Coolgardie Domain to the west from the Norseman Terrane to the east. The blue areas represent Lake Cowan and the white strands are sand dunes.

The felsic and sedimentary rocks in the immediate vicinity of the Abbotshall Mine are now covered and obliterated due to earth works associated with the open pit. However, they are, described in annual reports by BHP-Utah, which explored the area between 1986 and 1988. The local geology of the mine sequence is described as follows:

"Abbotshall is situated within a north-trending zone of metasediments, felsic volcanic rocks and metabasalts known as the Abbotshall Beds....The felsic volcanic rocks can be subdivided on the basis of texture, into an upper porphyritic, generally non-mineralised unit and a lower tuffaceous, mineralised unit....The youngest unit exposed in the mine area is a tremolite-chlorite schist which overlies the felsic volcanic rocks. Stratigraphically below the...(mineralisation)...are siliceous, biotite-amphibole-pyrrhotite rich sedimentary rocks, graphitic shales, cherts and greywackes." (Murphy, 1988).

It is the upper, porphyritic felsic unit that was dated (Hill & others, 1992; Campbell, 1989) using samples from BHP diamond hole DAH-3. This porphyritic felsic rock was described as "fragmental...consist(ing) of clasts of porphyritic dacitic lava comprising large plagioclase phenocrysts...in a groundmass of fine quartz, plagioclase microcline and biotite. The matrix around the clasts appears to be a similar mineralogy". The unit is 15 to 55 m in width (Murphy, 1988).

In detail, the sedimentary rocks below the porphyritic unit are: (i) mine chert (1-4 m in width); (ii) biotite and amphibole-rich, mafic sedimentary rocks and garnetiferous amphibolite all with abundant patches and layers of calc-silicate minerals (60-70 m in width); (iii) black shale, chert, "shale conglomerate" and greywacke (>100 m in width). Many of the fine-grained lithologies are sheared and foliated (Murphy, 1988).

The biotite and amphibole unit was described by BHP petrography as comprising a variety of rock types, many being fine-grained, banded and foliated. The fine-grained rocks are composed of a fine matrix of quartz and a little plagioclase with oriented amphibole laths and biotite. It was interpreted as mafic-derived sediment.

Interpretation & discussion

The calc-silicate minerals in the sedimentary rocks are interpreted to be alteration as a result of mineralisation. Garnet and diopside are present, in addition to ubiquitous biotite alteration, indicating mineralisation at upper amphibolite facies metamorphic grade, similar to the Scotia Mine, and higher grade than the lower amphibolite facies rocks in the mines at Norseman.

The description of the quartz-biotite-amphibole-rich mafic sedimentary rocks is remarkably similar to rocks located within aircore drillholes beneath the komatiite west of the Mount Thirsty sill (see section 6.3.5). At Mount Thirsty, the mafic sedimentary rocks were interpreted as BFB, with a thrust contact against the komatiite. A similar interpretation can be made at the Abbotshall Mine. The mafic-derived sedimentary rocks are interpreted as BFB, and the overlying tremolite-chlorite rocks to the west are interpreted as low-MgO komatiite thrust over the sedimentary rocks.

Interpreting the mafic sedimentary rocks as BFB implies that the Abbotshall Mine sequence is in the Coolgardie Domain. The black shales, cherts and greywackes immediately to the east could also be BFB, but the preferred interpretation is that they constitute the Abbotshall Beds as the lithologies are appropriate and the unit can be traced to this locality. With this interpretation, the Mission Fault, which separates the Norseman Terrane and the Coolgardie Domain follows the top of the Abbotshall Beds for some distance.

The Mission Fault is a major terrane-bounding structure and considerable width is expected. The shearing, foliation and stretching recorded in the finer-grained lithologies at the Abbotshall Mine sequence is probably related to the fault. The tremolite-chlorite schist has not been noted to the north or south outside the mine area so it may be an ultramafic enclave within the fault. The upper amphibolite grade of the metamorphism at the mine sequence is anomalously high and therefore the sequence is interpreted as a fragment of greenstone from depth, exposed within the fault zone.

The porphyritic dacite is not reported by BHP as being sheared. This lack of shearing could be interpreted as emplacement following the major movement on the Mission Fault or that strain was partitioned around the unit. It is noted that the dacitic composition and feldspathic porphyry texture are similar to other BFB felsic rocks (section 6.3.9; 6.3.10). The age of the felsic unit is also consistent with other ages for the BFB, but geological relationships, the description of the rock and its width all suggest that the porphyritic felsic is intrusive. Therefore, the date reported by Campbell (1989) is interpreted as the date of the intrusion of a porphyritic felsic rock. It is not regarded as providing an age for the Mission Fault as the amount of strain within the rock cannot be assessed and any lower degree of strain could be the result of partitioning into surrounding finer-grained lithologies.

6.3.12 Units beneath Lake Cowan

Aircore drilling of the northern end of Lake Cowan off the western shore of the Polar Bear Peninsula intersected abundant felsic rocks. Aeromagnetic images and the

geological constraints such as the position of the Abbotshall Beds suggests that the Mission Fault trends north along the western shoreline of Polar Bear, so the units offshore are interpreted to be within the southern Coolgardie Domain. Stored end-of-hole samples for 118 of the 417 aircore holes drilled were relogged for this study to obtain additional information about the felsic units. The samples logged comprised basalt, dolerite, ultramafic, black shale and felsic rock. It is the latter group that is of particular interest for this study.

Description

Seven different types of felsic rocks were recognised among the end-of-hole aircore samples. The two most abundant are felsic rocks that appear to be coherent, at least in the small rock fragments that constitute the stored samples (maximum length: 5 cm and diameter: 2.5 cm). Of the two coherent felsic rocks, one type appears to be rhyolite or dacite with feldspar and quartz phenocrysts in a felsic groundmass with trace biotite. The other type is similar, but is distinguished by a greater abundance of biotite. These samples may be lavas or intrusives based on their coherent textures, or samples of lava clasts in a coarse-grained breccia. A third felsic rock type is a probable intrusive, having an equigranular, holocrystalline, microgranitoid texture similar to the Harlequin Granodiorite (section 3.4).

The other four felsic rock types are clastic. They include felsic volcanic sandstone and siltstone with minor feldspar and spotted with biotite, similar to the felsic siltstones described in section 6.3.8, and felsic sandstone, differing from the siltstone by the coarser grainsize and visible layering. Another, less abundant felsic rock type has volcaniclastic textures. The clasts comprise variable rock-types such as dacites with siltstone or shale fragments. The final clastic felsic rock type is dark-coloured rock with abundant biotite and sometimes amphibole, with variable quartz and feldspar. This is considered to be mafic-derived sediment, similar to the units at Abbotshall and beneath the Mount Thirsty sill.

Interpretation & discussion

A wide variety of felsic rock types were encountered in lake drilling with many similar to varieties that have been encountered in the BFB on the land. However, given the limitations in dealing with small aircore samples, any interpretations must be treated cautiously.

A possible interpretation of the data is that the rock compositions indicate proximity to a volcanic centre. The features that indicate this are the abundance of apparently coherent, fine-grained felsic rocks. The very-fine-grain size suggests they are either lavas or high-level, subvolcanic intrusives, both of which are characteristic of vent

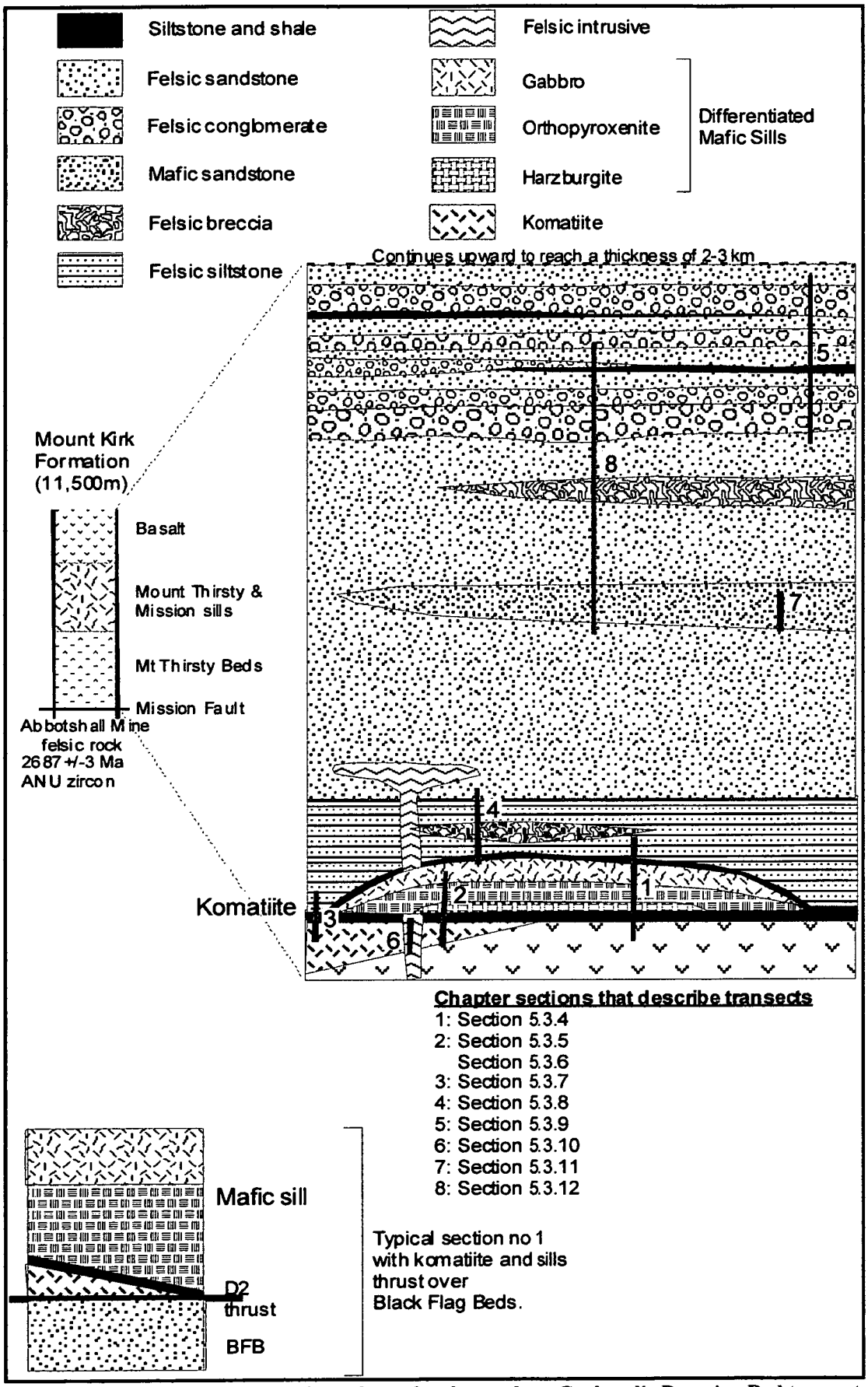

Figure 6.5: Schematic stratigraphic column for the southern Coolgardie Domain. Red transects show where the areas described in the sections of this chapter lie. The "Mt Kirk Formation" part of the stratigraphic column of Doepel (1973) (see figure 1.2) is shown for comparison.

proximal locations (McPhie & others, 1993). An alternative interpretation is that the coherent rock samples are segments of lava clasts from conglomerates deposited in sites distal to a volcanic centre.

6.4 SYNTHESIS

The localities in the southern Coolgardie Domain described in this chapter confirm that the greenstone stratigraphy passes from komatiite into felsic volcanic-derived sedimentary rocks of the BFB with no upper basalt such as the Paringa Basalt, which is present at Kambalda and Kalgoorlie. The units below the komatiite are not exposed in the areas examined due to the occurrence of thrust faults at the base of the komatiite that have thrown the ultramafic over the BFB. However, komatiite is presumed to have been originally emplaced over a thick mafic sequence as seen further north in the Coolgardie Domain.

The base of the BFB is observed at two locations, at the Mission Sill area (section 6.3.4) where it directly overlies basalt; and adjacent to the highway as described in section 6.3.8, where it overlies the top of the Mount Thirsty sill that intruded the contact. These basal sections are somewhat similar, dominated by felsic siltstone which coarsens upwards. The Mission Sill exposure has a thinly-bedded sandstone-siltstone package suggested to be low-density turbidites, which become coarser and shows a more pronounced felsic volcanic provenance, upwards. The highway exposure has basal chert overlain by up to 200 m of tuffaceous felsic siltstone, which then passes into coarser felsic sandstone. The basal chert band at the latter locality may correlate with a chert band a couple of metres wide overlying the komatiite at the base of the sill (see section 6.3.5) suggesting the Mount Thirsty sill may have split the chert. A schematic stratigraphic column is presented in figure 6.5.

Exposures of the BFB are patchy and discontinuous throughout the southern Coolgardie Domain so the stratigraphy has to be spliced together from various exposures. The two BFB highway localities described in sections 6.3.8 and 6.3.9 have a similar dip and strike even though they are 2 km apart. If this northeast strike and a 50°SE dip is assumed to be continuous between the two areas, then the locality with the epiclastic felsic volcanic rocks would lie approximately 1300 m above the basal contact of the chert and felsic siltstone. There is at least one gabbro intrusive between the two areas that may have split the sedimentary rocks, thickening the succession by about 200 m, so the epiclastic rocks may actually overlie the basal chert by a true distance of about 1 km.

It is unknown whether a cosistent and recognizable stratigraphy for the BFB exists on a regional scale at the southern Coolgardie Domain, as the internal divisions are poorly exposed. The sedimentary rocks at most localities were interpreted in this

study to have an origin as high-density or low-density turbidite, and show evidence of an emergent felsic volcano because they display rounded epiclasts or angular, fragmental pyroclasts. Offshore, beneath Lake Cowan, abundant samples of rhyolite or dacite that appears to be coherent have been returned by aircore drilling. These coherent felsic rocks may be lavas or subvolcanic intrusives, suggesting proximity to a vent. Alternatively, the coherent felsic rocks may be samples of felsic lava clasts in a conglomerate deposited distal from the vent.

At the Mount Thirsty and Abbotshall localities, and beneath Lake Cowan, quartz-amphibole-biotite-feldspar rocks are present, which appear to be metamorphosed quartzose sediments, derived from a mafic source. It is not known where in the BFB sequence, these sedimentary rocks belong. They are not unique as Hand (1998), has previously described mafic sedimentary rocks within the BFB.

Both tholeiitic and high-Mg compositions for the large, late-stage, mafic sills were described by Witt (1995). He noted that they are particularly common in the various domains of the Kalgoorlie Terrane in comparison to all other terranes. This is true for the study area as the Norseman Terrane has only minor examples of the sills, whereas three differentiated mafic sills are recognised in the southern Coolgardie Domain; the Mission Sill, Mount Thirsty sill and smaller Woodcutters sill. The larger pair have serpentinised harzburgite at the base and pass through altered and pristine bronzitite orthopyroxenite to norite to gabbro to granophyric hornblende-bearing gabbro. The Mount Thirsty sill is the best defined as the Mission Sill is less well-exposed, has a complex repetitive zonation and is bent into a fold closure defining a syncline. North of the Mission Sill closure on Lake Cowan near Fram island, a magnetic unit is visible in aeromagnetic images defining a fold closure and fresh pyroxenes are present in thin sections from aircore holes intersecting units near these magnetic highs. The magnetic units and surrounding rocks may be the north-plunging continuation of the synclinal Mission Sill, where it re-enters the preserved stratigraphy due to a plunge reversal.

It is possible that the Mission Sill, Mount Thirsty Sill and Woodcutters Sill may be the same unit, sliced up by D_2 thrusts. The sills all occur at the same stratigraphic level, immediately above the komatiite, where the latter has not pinched out, or above the basalt where has pinched out. The composition of the units within the sills are similar and they are side by side in an east west direction. The Woodcutters Sill is the smallest of the three sills and lacks harzburgite and differentiated gabbro, which may indicate it is close to the margin of the interpreted original single sill.

The Mount Thirsty and Mission Sills are high-Mg in composition, whereas other examples such as the Condensor Dolerite and Junction Dolerite at Kambalda, and the

Golden Mile Dolerite at Kalgoorlie, are tholeiitic (Witt, 1995),. The tholeiitic sills typically include magnetite-bearing, granophyric zones, which can be important hosts for epigenetic lode gold mineralisation. In contrast the granophyric zones in high-Mg composition sills do not contain magnetite.

The mafic sills are typically emplaced at the base of the BFB. The stratigraphic level of these sills, indicates they are younger than the majority of the BFB (2690-2665 Ma), but older than D_1 thrusts (2665-2657 Ma) (see Chapter 2). Although the mafic sills postdate commencement of BFB deposition, they may have been intruded late in the depositional history of the unit, when it was several kilometres thick. They form a second, mafic igneous event in the greenstone successions, albeit more limited in extent than the initial basaltic volcanism. All mafic intrusives that cut the komatiite, but do not have the composition of crustally contaminated komatiite (eg. Paringa Basalt-see Chapter 4), are inferred to belong to this generation of mafic intrusives.

The abundance of young mafic magmas in the Kalgoorlie Terrane, relative to all other terranes, indicates that the former terrane must have certain characteristics favourable for magma emplacement. A factor favouring the emplacement of magmas at high levels is an extensional tectonic regime (Lentz, 1998; Smith & others, 1997). Extension was occurring within the Kalgoorlie Terrane during BFB deposition as it created a deep basin (the "Kalgoorlie Basin") into which the 2-3 km thick sequence was deposited (Barley & other, 1998).

It is unlikely that the mafic sills were generated through the same magma generating processes that produced the dacite in the BFB because the trace element characteristics are different (section 8.6). Instead, the data indicates that the mafic magmas were the result of the crustal extension unloading the mantle sufficiently to cause adiabatic melting (Chapter 12).

6.5 CONCLUSION

In this study, it was determined that the felsic and sedimentary succession in the southern Coolgardie Domain is distinctly different from the rhyolites and Abbotshall Beds at the Polar Bear Peninsula in the Norseman Terrane. The southern Coolgardie Domain felsic and sedimentary succession is very similar to descriptions of the BFB provided by Hand (1998), consisting largely of dacitic conglomerates and sandstones. As the felsic and sedimentary sequence along the western shore of Lake Cowan in the southern Coolgardie Domain, was defined by Doepel (1973) as the Mount Thirsty Beds member of the Mount Kirk Formation, the Mount Thirsty Beds are equivalent to the BFB. The Mount Kirk Formation is regarded in this study as a composite unit,

consisting of basalt, komatiite, BFB equivalents and mafic sills and thus is of little use as a defined stratigraphic unit. It will not be referred to any further.

The lower greenstone sequence of the southern Coolgardie Domain is similar to the Norseman Terrane in that there is no upper basalt sequence overlying the komatiite, but the felsic and sedimentary sequences differ substantially. The southern Coolgardie Domain exhibits a thick sequence of felsic sedimentary rocks that were deposited predominantly by low-density and high-density turbidity currents. These felsic sequences commence with siltstone that contains fragmented clasts, suggesting explosive volcanism and, therefore, a possible origin as resedimented tuffs. The grainsize coarsens upwards to sandstones and ultimately to felsic conglomerate that was derived by erosion of an emergent volcanic cone. The coarsening up sequence may indicate growth of a volcanic cone, generating coarser products by erosion as the cone became emergent, and sedimentary sequences that prograded outwards from the growing edifice.

Some komatiite units in the southern Coolgardie Domain are overlain by chert, which may correlate with the Abbotshall Beds. However, the chert is not present at Woodcutters North or the Mission Sill for reasons that are unclear. Similarly, other units within the BFB appear to display little regional continuity. For instance, mafic-derived, quartz-amphibole-biotite sedimentary rocks rather than felsic siltstones and sandstones dominates the BFB above the Woodcutters sill, west of the Mount Thirsty sill.

The BFB at the southern Coolgardie Domain has some differences to those described by Hand (1998) at Widgiemooltha 80 km to the north. The southern Coolgardie BFB coarsens upwards from the base, whereas Hand (1998), described sequences fining upwards. This is interpreted to indicate separate depositional systems and probably different sediment provenances. Sedimentary sequences in the two areas are interpreted to be unrelated.

The abundance of thick, differentiated, high MgO and tholeiitic sills intruding the base of the BFB in the various domains of the Kalgoorlie Terrane suggest that extension within the terrane enabled ready ascent of the mafic magmas to a position where they achieved neutral buoyancy above the komatiite, but below the BFB. This extension was probably the same event responsible for the "Kalgoorlie Basin" in which the BFB was deposited.

7.2 BASE OF THE WOOLYEENYER FORMATION

7.2.1 Introduction

Keele (1984) refers to work by P. MacGeehan who logged a line of diamond drill holes across the Noganyer and Woolyeenyer Formations and encountered "Spinifex-textured ultramafics in the top of DDH S219..." which "forms the base to the Kingswood Basalt Member...". Given that spinifex-textures are commonly considered to be evidence of komatiitic lavas, and there is only one known komatiitic volcanic event in the Eastern Goldfields (Nelson, 1997), the report of this unit at the base of the Woolyeenyer Formation required examination.

Description & interpretation

Two holes shown on the section of P. MacGeehan as containing the ultramafic (S219 & S175) were examined. The rock was found to be medium-grained dolerite, with rare plumose amphibole alteration.

There is no spinifex-textured ultramafic at the base of the Woolyeenyer Formation.

7.3 NOGANYER FORMATION

7.3.1 Introduction

The Noganyer Formation is predominantly a sedimentary sequence that overlies the Penneshaw Formation with an obscured contact. At its broadest extent, the Noganyer Formation consists of five defined jaspilite members (Doepel, 1973) variously separated by conglomerate, schist, ultramafic and gabbro. The jaspilite members have traditionally been considered to be banded iron formation (BIF) as they consist of alternating seams of magnetite and siliceous rock. More recently, it has been recognized that the jaspilites are in fact clastic rather than chemical sediments comprising thin-bedded turbidite (Holcolme, 1996; Barley & others, 1998). The siliceous layers are siltstone in which graded bedding can be detected in thin section, whereas the iron oxide layers are a later, poorly understood, alteration event (Plate 7.1). The members will continue to be referred to as "jaspilite" in this study to maintain clarity of nomenclature.

The number of jaspilite bands multiplies from south to north such that there is one band near the Scotia Mine 30 km south of Norseman and five bands east of Norseman. Isoclinal folding has been proposed as responsible for some of the duplication (Keele, 1984; Holcolme, 1997) and thrust surfaces also identified (Holcolme, 1997).

Plate 7.1: Drill core from the Bon Accord Jaspilite – weak iron oxide alteration in this section allows the grading and clastic origin to be clearly observed. The jaspilite is interpreted as turbidite. The facing direction is the same as the arrow, demonstrated by grading and by soft sediment slumps at the base of a siltstone layer (arrow).

The issue to be addressed for this study is the original stratigraphic position of the Noganyer Formation prior to regional deformation. While it has traditionally been regarded as conformably underlying the Woolyeenyer Formation, reported similarities with Abbotshall Beds at the top of the Woolyeenyer require investigation. Holcolme (1996) noted the similarity of the rhythmically laminated siltstone packages (jaspilite) in the Noganyer Formation and the Abbotshall Beds and first raised the possibility that they may be equivalent, although this was not followed in Holcolme (1997). Further, pebbly conglomerate is well known in the Raggedy and Iron King Members of the Noganyer Formation and mafic conglomerate underlying segments of the Abbotshall Beds has been described in this study (Chapter 3 & Chapter 5). If the ultramafic present within the Noganyer Formation is komatiite, then it should be correlated with the other komatiites in the region as they are regarded as chronostratigraphic marker units (Nelson, 1997). This in turn would indicate major structural discontinuities bounding the Noganyer Formation rather than a conformable contact.

To address the problem, a segment of a diamond hole which passes through all the lithologies discussed above, was logged in detail (figure 7.1). In addition zircon U-Pb age dating undertaken in the formation was reassessed given the change in interpretation of the origin of the jaspilite.

7.3.2 Noganyer Lithologies

Description of S4172

Diamond hole S4172, collared in the Hopetoun Jaspilite Member adjacent to the Wheel Fault, was drilled east at 60° declination. The final 65 m of this hole (from 270 to 334.5 m) passed through jaspilite, conglomerate, dolerite and the hole ended in talc-carbonate ultramafic rock (figure 4.1). Although the sedimentary lithologies are strongly-altered with biotite and pyrrhotite, primary textures remain well preserved. Younging indicators include grading and load casts and indicate that the jaspilite faces west (up hole).

The ultramafic has a down hole width of 26 m. Although the majority of the unit is talc-carbonate in composition, with carbonate stockwork veining and a weak foliation, the hole terminates in amphibole-chlorite rock. The top metre of the ultramafic also has an amphibole-chlorite mineralogy, but the upper contact is tectonic with a quartz-carbonate veining and a shear fabric less than 1 m wide.

A fine-grained mafic unit with glomeroporphyritic feldspars overlies the ultramafic and remains uniform in texture for 9 m before rapidly coarsening in grainsize to a fine to medium grained dolerite. The dolerite body becomes finer-grained towards a margin interpreted as a chilled contact against clastic sediments of the Raggedy Member.

Pebble conglomerate and sandstone units with diffuse contacts overlie the dolerite and have a down-hole width of 9 m. The conglomerate is monomict, composed of well-rounded and dominantly clast-supported, sparsely-porphyritic, rhyolite pebbles with rare quartz phenocrysts. Zones with pebbles supported by a matrix of coarse sandstone also occur. The sedimentary rock then switches abruptly from conglomerate and coarse-sandstone, to fine-sandstone and siltstone turbidite across a 5 mm thick transition layer of coarse-sandstone. The fine-grained turbidite becomes the Hopetoun Jaspilite Member with the introduction of siliceous quartz-siltstone layers with magnetite laminae.

Interpretation & discussion

The evidence from this hole allows three possible origins for the ultramafic; a komatiite flow, an ultramafic intrusive, or the lower differentiated part of a gabbroic intrusion. The lack of a lower contact, the shearing at the upper contact and overall poor textural preservation does not provide unequivocal evidence for any of the possibilities, but the origins considered most likely are suggested below.

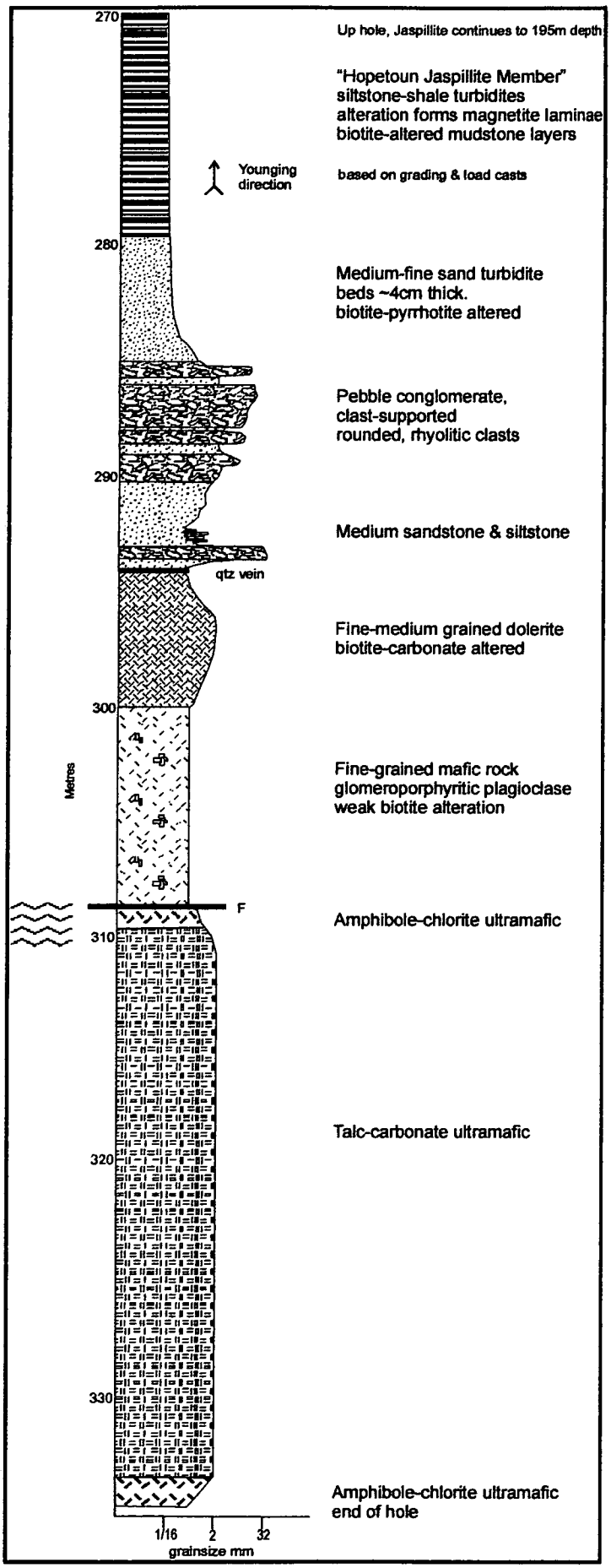

Figure 7.1: Graphic log of part of drill hole S4172

Amphibole-chlorite mineralogies are characteristic of a lower MgO content than talc-carbonate. The upper contact of the ultramafic has an amphibole-chlorite mineralogy, suggesting a potential chill composed of lower MgO ultramafic than the talc-carbonate ultramafic, which may represent former olivine cumulate within the centre of the unit. Likewise, the amphibole-chlorite at the end of the hole may indicate proximity to the lower contact. If this morphology is correct, it would suggest the ultramafic is an intrusion, with chilled upper and lower contacts and a central cumulate zone.

The shear between the ultramafic and mafic rock units is unfortunate as it does not allow the relationship between the two units to be observed. However, it appears that no significant movement has occurred along the structure as it is less than one metre in width and the foliation is not strong.

The rapid grading of the fine-grained dolerite into fine-medium grained dolerite after remaining uniform for 9 m suggests a differentiated dolerite. This in turn raises the possibility that further differentiation may occur down hole and that the ultramafic unit may be an olivine cumulate base to the dolerite. While the data allows this possibility, it is considered unlikely as such differentiation is more common in sills hundreds of metres to kilometres thick. However, if the dolerite and ultramafic are part of the same intrusion, the relative widths of the units (26 m for the ultramafic and 15 m for the dolerite) would indicate that the intrusion must be ultramafic in bulk composition with an upper mafic differentiate.

The felsic pebble conglomerate indicates erosion of a subaerial source as rounding occurs only in beach or fluvial environments. The monomict nature of the clasts indicates an emergent volcanic centre, perhaps a rhyolite dome. Uplift of a felsic terrane is considered unlikely as it would probably comprise a number of rock types, which would produce a polymictic conglomerate.

The conglomerate was probably deposited as high-density turbidite, although textures are not sufficient to precisely determine the boundaries of individual depositional units. The absence of scouring and the diffuse contacts between conglomerates and sandstones may indicate surging turbidity currents depositing coarser and finer units. The thick jaspilite sequence was deposited by low-density turbidites.

The transition from coarse-clastic deposits to thin-bedded turbidites (jaspilite) indicates a fining-up sequence. The relative thinness of the coarse clastic deposits may indicate that the source of the pebbles was not large and was rapidly eroded, or that the structure was rapidly drowned after becoming emergent during sea level rise or basin formation. Rhyolite in the Penneshaw Formation will be described in the

next section, which could be the source of the felsic detritus in the Noganyer Formation, although there are problems with this interpretation.

7.3.3 Age dating of the Noganyer Formation

Campbell & Hill (1988) undertook age dating of jaspilite from the Noganyer Formation and interpreted the age to be 2706±5 Ma, based on the analysis of a single high-U grain and supported by results from rims around a number of clastic zircons. The interpretation of the dates was based on the understanding of the Noganyer as comprising BIF. The zircon rims and the high-U zircon were proposed to be the product of new growth produced by the hydrothermal activity which led to deposition of the BIF, in which case the zircons would record the depositional age of the Noganyer Formation. Campbell & Hill (1988) also reported clastic zircons from the BIF with ages of *ca.* 3650-3670 Ma, appreciably older than known xenocrystic zircons in the Eastern Goldfields. A number of other zircon analyses lie on a U/Pb concordia diagram close to a cord between the ages 2706 Ma and 3652 Ma, suggesting they are 3652 Ma age grains which have been partially reset by the 2706 Ma event.

The more recent understanding of the Noganyer Formation as a clastic sequence is problematical for the isotopic age interpretation of Campbell & Hill (1988), which was based on the premise that the jaspilite represents an exhalative chemical sediment (BIF). The zircons should now be interpreted as detrital. This is supported by the original description of the 50 zircons recovered from dated sample 86-215 as "well-rounded (and thus almost certainly detrital)" (Hill, 1987). The younger zircons (*ca.* 2706 Ma) therefore provide a maximum age for deposition of the Noganyer and were probably derived originally from felsic volcanics of that age, which are well known from the north-eastern goldfields (eg. Bore Well; Barley & others, 1988). It is also possible that the *ca.* 2706 Ma rims are recrystallisation resulting from the hydrothermal alteration that introduced the magnetite. If the young zircons are clastic, they provide the maximum age for the Noganyer Formation, whereas, if the rims are hydrothermal, they provide the minimum age of the jaspilite. A third explanation, for the *ca.* 2706 Ma age, that it is a result of Pb-loss due to radiation damage caused by the higher U contents of the younger grains, is considered unlikely as some of the ages approach concordia.

A second attempt has been made to age date the Noganyer Formation. Barley & others (1998) reported zircon ages from a sample of fuchsitic quartzite at the base of the Noganyer Formation near south Scotia. U contents for the zircons were high (up to 900 ppm) and the zircons were mostly small, dark metamict grains with angular, broken morphologies. Consistent with the appearance of the grains, most analyses had a high degree of discordance indicating significant recent and possibly ancient

Pb-loss. The youngest near concordant group gives an age of 2864±5 Ma with two older groups of 2901±7 Ma and 2983±3 Ma. Two grains gave much older ages of 3132 Ma and 3402 Ma. The latter ages are approaching those found in the jaspilite sample suggesting that, at least in part, the turbidite of the jaspilite and the sandstone sampled the same source. The *ca.* 2864 Ma zircons are discordant so they provide only a minimum age whereas the true zircon age may be greater.

Table 7.1 provides a summary of the dating of zircons that has been undertaken for the Noganyer Formation, with the previous interpretation, and the new interpretation provided in this study.

Table 7.1: Summary of SHRIMP U-Pb dating of zircons in Noganyer Formation.

unit	age	comment	Previous interpretation	New interpretation
Jaspilite	2706±5 Ma	One zircon + rims of others. Campbell & Hill, 1988	Age of zircon rims formed during hydrothermal activity that deposited the BIF.	Maximum age – detrital zircons as jaspilite is clastic not chemical sediment.
Jaspilite	3650-3670 Ma	Campbell & Hill, 1988	Clastic zircons	Clastic zircons
Jaspilite	3652-2706 Ma discordant zircons	Lie on a chord. Campbell & Hill, 1988	Clastic zircons reset by BIF hydrothermal event.	Clastic zircons rest by mafic volcanic event?
Fuchsitic Quartzite	2864±5 Ma 2901±7 Ma 2983±3 Ma 3132 Ma 3402 Ma	Most analyses discordant, high-U dark, metamict zircons. Barley & others, 1998.	No reliable age provided by the grains.	

7.3.4 Facing of the Jaspilite bands

Green (1997) examined the part of the Noganyer Formation from directly east of town to south of the Iron King and Lady Miller mines. This area contains the maximum number of jaspilite bands (five) which decrease to the north and south as the bands wedge out. The primary purpose of Green's study was to obtain facings for the jaspilite members to aid the understanding of structural deformation in the area. Green attempted to obtain younging directions using oriented thin sections, but the evidence was tentative and commonly contradictory. Younging directions obtained from grading and soft sediment slumps and flame structures in old drill core from the area were found to be more reliable.

It was concluded that the Hopetoun Jaspilite, Lady Miller Jaspilite and Attlee Jaspilite face west, whereas the Holstein Jaspilite and Bon Accord Jaspilite face east. The Bon Accord Jaspilite has long been known to face east, the facing having been noted by Keele (1984), Holcolme (1997) and reconfirmed in this study based on grading in jaspilite intersected in diamond drill core drilled in 2000 (Plate 7.1). However, an east facing for the Holstein Jaspilite is a surprising outcome as the

jaspilite directly underlies the mafic Woolyeenyer Formation. The Woolyeenyer Formation faces west, as shown by many younging directions obtained from pillow basalts noted on the GSWA Norseman 1:100,000 scale geological sheet (McGoldrick, 1993).

Interpretation & discussion

If the Holstein Jaspilite, which lies directly beneath the Woolyeenyer Formation, faces east, as suggested by Green (1997), then there must be a major structural discontinuity between the Noganyer and Woolyeenyer Formations.

The Bon Accord Jaspilite at the base of the Noganyer Formation also faces east and a major shear is now recognised between the Noganyer and the Penneshaw Formations based on the work of Holcolme (1997) (section 10.4.4.5).

Green's findings that the Holstein Jaspilite appears to be overturned with respect to the Woolyeenyer Formation cannot be readily dismissed because it is supported by the paucity of dolerite dykes, as argued below.

The abundance of dolerite dykes in the base of the Woolyeenyer Formation and the profuse pillow basalts indicate eruption of the basalts from multiple centres, each with a low volcanic flux. The dolerite dykes are considered to form feeders to the pillow basalts. The volcanic textures within the Woolyeenyer Formation do not support eruption from a flood basalt-style fissure as that would lead to a high volcanic flux forming thick flows in lava tubes.

The basalt that forms the 6 km thick Woolyeenyer Formation must have passed through whichever rocks formed the substrate to the unit. The felsic part of the Penneshaw Formation (see section 7.4) illustrates what such a footwall to the Woolyeenyer Formation would be expected to look like, being cut by swarms of dolerite dykes, similar to the lower part of the Woolyeenyer Formation itself. However, the units in the Noganyer Formation show relatively few mafic intrusives other than an extensive gabbro sill (Lady Mary Member), which is considered to belong to the group of late-stage differentiated mafic sills (see section 7.5) and some other young dykes that fill NNW trending extensional fractures. Extensive sections of outcropping jaspilite can be traversed that are cut by no dolerite dykes. The absence of swarms of mafic dykes of the Woolyeenyer age in the jaspilite suggests the basalts of the Woolyeenyer Formation did not pass through and erupt onto the Noganyer Formation. The implication is that the Noganyer Formation was structurally emplaced over the felsic part of the Penneshaw Formation and under the Woolyeenyer Formation after the mafic volcanic event.

The age dating that has been undertaken is not sufficiently precise to confirm the hypothesis of an allocthonous Noganyer Formation. Hill R.I. & others (1990) dated a zircon from the felsic part of a differentiated dyke within the Woolyeenyer Formation (Crown Main Dyke) and obtained an age of 2714±5 Ma. This zircon could be interpreted as a xenocryst (section 2.4.2), but the age is consistent with the widely accepted age of the greenstone deposition in the Eastern Goldfields (*ca.* 2710 Ma) and the accepted age of the komatiitic volcanic event capping the mafic volcanics (such as the Norseman komatiite) at *ca.* 2705 Ma.

As pointed out in section 7.3.8, zircons of 2706±5 Ma age are found in the jaspilite members of the Noganyer. While this age is considered to be a maximum age, given that the Noganyer is a clastic sequence, it may also be close to the depositional age as the zircon is likely to have been derived from an emergent volcanic centre and deposited within the turbidites of the Noganyer Formation within a geologically short period of time. The Noganyer Formation and Woolyeenyer Formation ages are within error of each other, such that either could be the younger unit.

7.3.5 Conclusion

Drill hole S4172 provides a view of the coarser clastic material in the Noganyer Formation. While the jaspilite is similar to the Abbotshall Beds, the felsic clasts within the conglomerate and sandstone underlying the jaspilite differ in composition from the mafic clasts in the conglomerate that underlies parts of the Abbotshall Beds, thus these stratigraphic units are not regarded as directly equivalent.

The jaspilite appears to have been deposited predominantly as low-density turbidite and suspension sedimentation while the conglomerate and sandstone are more likely to be high-density turbidite. The clastic sedimentary rocks overall, define a fining up sequence.

The contacts and primary textures of the ultramafic rocks examined in drill core from the Noganyer Formation are insufficiently well-preserved to determine whether it is volcanic or intrusive. The change in composition to amphibole-chlorite at the top and bottom of the drill core may favour an intrusive origin, but the hole ended in ultramafic so it cannot be determined whether the lower amphibole-chlorite is actually the bottom of the ultramafic unit.

The mafic unit is probably part of the Lady Mary Member, which is described as being located beneath the Hopetoun Jaspilite.

S4172 also revealed that the coarse clastic rocks and ultramafic are more widespread in the Noganyer Formation than previously thought. The Hopetoun Jaspilite, into which S4172 was collared, is known to be underlain by the Lady Mary Member, but

there is no previous record of the coarse clastics and ultramafics. Therefore, the existing stratigraphic columns for the Noganyer Formation that imply variations in local stratigraphy, with some jaspilites underlain by clastics and others by ultramafic or gabbro, may be incorrect.

Based on the presence of coarse clastic rocks, additional to those previously known, it is inferred that all the jaspilites were originally underlain by coarse clastics in a fining up sequence. Similarities between the jaspilite sequences, and the presence of a single jaspilite band 30 km to the south at Scotia, is compatible with only one depositional sequence, if the single horizon has been structurally duplicated in the vicinity of Norseman. As three consecutive jaspilite bands in the Noganyer Formation are all west facing, the duplication of these was probably caused by thrusts rather than folding. However, the overturned, east-facing units at the top and bottom of the Noganyer Formation may be folds in which the upper limb has been thrust out.

Overturned jaspilite at the top and bottom of the Noganyer Formation could imply that the entire sequence is structurally emplaced beneath the Woolyeenyer Formation. This theory is consistent with the absence of mafic dyke swarms cutting the jaspilites, such as those seen in the Penneshaw Formation, which would be expected as feeders for the 6 km thick mafic succession if the Woolyeenyer Formation was erupted onto the Noganyer Formation.

The zircon age dating suggests that both the sandstone in the coarse clastic base to the formation and the siltstone and shale of the jaspilite have sampled the same source, providing ancient >3400 Ma zircons. However, there are differences in the ages of the younger age zircons. The sandstone contains zircons with a population that has a poorly defined age of around 2865 Ma, whereas the jaspilite has ages of *ca.* 2706 Ma. Considering the clastic rather than chemical sedimentary origin now recognised for the jaspilite, these zircons are probably detrital and therefore provide a maximum age for the Noganyer Formation. It is considered that the *ca.* 2706 Ma zircons may have been derived from an early felsic volcanic event similar to those found in the north-eastern goldfields (see section 2.5.1).

In summary, the Noganyer Formation is not the stratigraphic equivalent of the Abbotshall Beds because there are significant differences in the underlying conglomerate. There is evidence suggesting an allochthonous origin for the Noganyer Formation.

7.4 PENNESHAW FORMATION

7.4.1 Introduction

The Penneshaw Formation is conventionally considered to be the oldest sequence in the Norseman area as it lies in the core of the Norseman Anticline. Doepel (1973) described the composition of the Penneshaw as metamorphosed fine to coarse-grained basic volcanic rocks with minor fine-grained metasediments in the vicinity of the Penneshaw Mine and an occurrence of foliated quartzite. The easternmost part of the formation was considered to be intruded and truncated by granite.

Spray (1985) changed the interpretation of the relationship between the granite and the Penneshaw Formation by identifying early mylonite fabrics between the Buldania granitoid and the amphibolite. The mylonite was interpreted as having formed as sub-horizontal structures at a low angle to stratigraphy and to have been subsequently rotated to a steep orientation and retrogressed to greenschist facies. The mylonite was considered to represent a thrust surface along which the greenstone was tectonically juxtaposed against granitoid gneiss.

Seven stratigraphic drill cores, each 500 to 700 m in length, which had been drilled across the western part of the Penneshaw Formation in 1965, were re-examined in 1986 in order to select suitable samples for an Australian Mineral Industry Research Association (AMIRA) isotopic dating project using the (then) newly developed (SHRIMP) ion microprobe. MacGeehan (1986) noted that these holes intersected a thick rhyolitic volcanic complex invaded by dolerite dykes and sills that comprised 60-80 of the drill intersections. Zircons from felsic samples in one of these holes, (PE1) were analysed and the (U-Pb) ages returned were the numerically dominant set of 2921±20 Ma; a variety of older ages up to *ca.* 3100 Ma; and a few zircons at *ca.* 2700-2730 Ma. The 2921 Ma age was interpreted as the date of crystallisation of the felsic. The older ages were interpreted as zircon grains inherited from the magmatic source rock and the younger ages were considered to be hydrothermal disturbance related to the mafic volcanic event (Campbell & Hill, 1988).

With further analyses, the interpreted crystallisation age for the felsic in PE1 was refined to 2938±10 Ma (Hill & others, 1990). The GSWA tested the old age for the felsic part of the Penneshaw Formation by dating a felsic unit interpreted as a "metamorphosed rhyolitic glassy lapilli tuff" in another of the stratigraphic holes (PE6). A number of old dates were returned, which included the presumed crystallisation age of 2930±4 Ma (Nelson, 1995).

A summary of the zircon dating that has been undertaken for the Penneshaw Formation is provided in Table 7.2.

Table 7.2: Summary of SHRIMP U-Pb dating of zircons in Penneshaw Formation.

unit	age	comment	Previous interpretation	New interpretation
Felsic Penneshaw	2938±10 Ma	Drillhole: PE1. Hill & others, 1990	Crystallisation of rock: Fine-grained banded rhyolite	Rock: Sheared granitoid with coarse grainsize.
Felsic Penneshaw	2700-2730 Ma	Campbell & Hill, 1988	Hydrothermal disturbance related to mafic volcanic event.	As previous.
Felsic Penneshaw	Up to *ca.* 3100 Ma	Campbell & Hill, 1988	Inherited from magmatic source rock	As previous.
Felsic Penneshaw	2930±4 Ma	Drillhole: PE6. Nelson, 1995	Metamorphosed rhyolitic glassy lapilli tuff	Felsic porphyry and equigranular microgranitoid with pseudo-breccia texture due to bleached patches.

These isotopic ages have been widely accepted such that the Penneshaw Formation is typically considered to be a fragment of crust predating the post-2710 Ma mafic to felsic greenstone stratigraphy by some 200 million years. The tectonic relationship between the old crust represented by the felsic in the Penneshaw Formation, and the mafic to felsic greenstone stratigraphy is unclear.

Subsequently, further drilling has enabled a reinterpretation of the stratigraphy and structural relationships of the Penneshaw Formation by CNGC geologists. A. Gray, M. Briggs and I. Pegg recognised that the formation could be divided into three domains (pers comm. 1999; Connors, 2000). The central domain consists of basalts and dolerites very similar to the Woolyeenyer Formation. Textural preservation is excellent such that pillow margins in basalt and chilled margins of dolerites can be recognised. The eastern domain consists of a complex tectonic intercalation of basalt, granite, porphyry and mylonite zones, all with an upper amphibolite metamorphic grade. The western domain includes the rhyolitic units with the 2930±4 Ma isotopic age date.

The western rhyolitic domain of the Penneshaw Formation was suggested by CNGC geologists to be upper amphibolite facies based largely on the observations of almandine garnets. In contrast, the central mafic domain of the Penneshaw has no garnets and appears very similar to the "main field" segment of the Woolyeenyer Formation that McCuaig (1996) has shown is lowermost amphibolite facies. The perceived higher metamorphic grade, the rhyolitic to sedimentary rocks and the old isotopic age were considered by CNGC geologists to indicate the western domain of the Penneshaw is an up-thrust fragment of deeper, older crust.

Consideration of the results of regional studies indicates a modification to the above theory is required. If the western Penneshaw domain has a higher metamorphic

grade, it would not indicate a deeper position during the metamorphism. Rather, it would imply that this domain was exposed to a metamorphic event prior to deposition of the greenstone sequence, because the later widespread greenstone metamorphic event occurred after the structural assembly of the greenstone stratigraphy into its current state.

The central domain of the Penneshaw was suggested by CNGC geologists to be a thrust repetition of the mafic Woolyeenyer Formation while the eastern domain was regarded as an extensional tectonic zone following the work of Holcolme (1997). These interpretations were compiled into a structural geology map by Connors (2000).

If the above interpretation is correct, then the felsic Penneshaw Formation may be unique in the Eastern Goldfields: an upthrust slice of the felsic lower crust that seismic reflection, zircon dating and geochemical studies suggest lies beneath the greenstone. For this reason, and the implications for the structural architecture of the Norseman Terrane, a reconnaissance study of the felsic Penneshaw Formation was undertaken.

For this study, PE1, the hole that was dated by Hill R.I. & others (1990), was once again resurrected and was relogged to examine the textures and rock types.

7.4.2 Penneshaw Lithologies

7.4.2.1 Description of PE1 from the felsic Penneshaw domain

Diamond drill hole PE1 comprises mafic rock, rhyolite and granitoid, none of which have a pervasive tectonic fabric throughout the hole. The locality of the hole collar is shown in Chapter 8, figure 8.15 and a graphic log is presented in figure 7.2.

The rhyolite occurs between the start of the hole and 200 m (652 feet). It is homogenous throughout this depth, having a very fine grainsize and a siliceous appearance. Tabular to irregular feldspars 1-2 mm in size form sparse phenocrysts. Biotite occurs dominantly along fractures suggesting an alteration origin although isolated clusters are also present. Alteration minerals comprise sericite and chlorite, the latter altering biotite, disseminated pyrite and sparse, acicular to bladed pale-yellow amphiboles typically less than 1 mm in length.

Texturally the rhyolite varies from coherent with minor crackle brecciation fractures to monomict, poorly sorted, rubble breccia comprising clasts which range from angular to subrounded (Plate 7.2). Clasts vary from a few millimetres in diameter to approximately 200 mm. Banding resembling flow banding was observed in one clast. The breccia appears to grade in and out of coherent rhyolite.

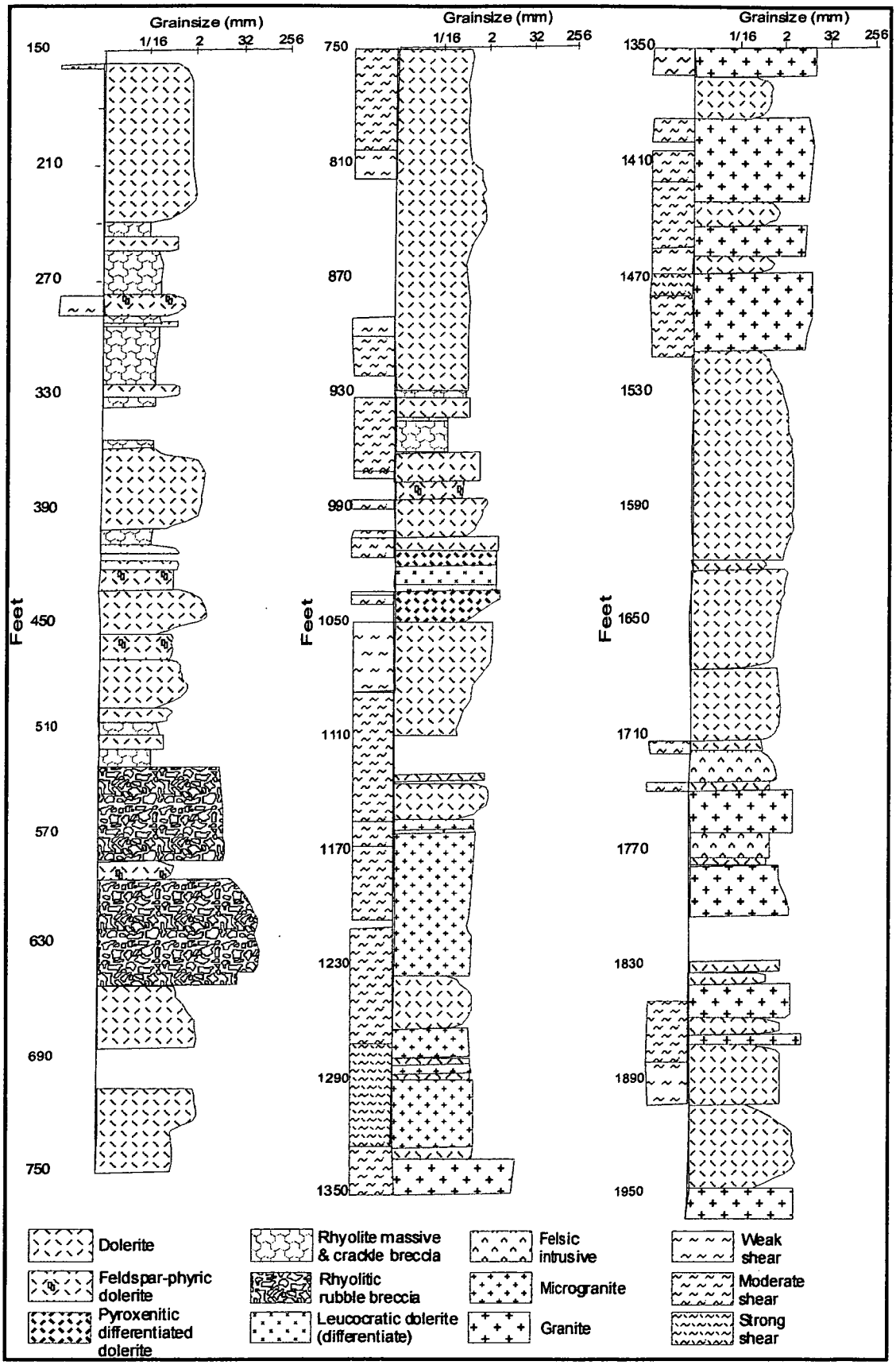

Figure 7.2: Graphic log of drill core from PE1 in the felsic part of the Penneshaw Formation, showing lithology and shearing,. The log extends from 150 feet to 1962 feet depth. The locality of the hole collar is shown in Chapter 8, figure 8.15. The core comprises rhyolite and granite intruded by dolerite. Blank sections indicate no core due to lack of drill recovery or missing core trays. The U-Pb age of 2938±10 Ma (Hill & others, 1990) was derived by pooling zircon ages from sheared granite collected at 1355', 1356'6", 1470', 1471'4" and 1489'7". Ghaderi (1998) conducted a geochemical analysis of granite at 2262', which is below the segment logged.

Plate 7.2: Rhyolite breccia in drill core from PE1 at a depth of 565 feet. The tip of the pencil points to "jigsaw puzzle" breccia composed of clasts with curviplanar margins, characteristic of *in situ* quench fragmentation. However, rubble breccia, in particular the clast to the left of the top of the pencil with apparent rounding in a fine matrix, implies a greater degree of abrasion and transport.

The first occurrence of granitoid in the drill core occurs at approximately 350 m (1154 feet), where it is a fine-medium grained microgranitoid. The granitoid continues with a gradually coarsening grainsize to the end of the hole at 801.7 m (2630 feet). At around 350 m, best preserved segments are holocrystalline, equigranular and have a grainsize of about 1 mm. Primary minerals are feldspar, quartz and probably biotite, although there is some uncertainty in the latter as it often appears to be unstrained in sheared rocks suggesting a later alteration origin.

From approximately 400 m (1330 feet) the granitoid becomes coarse-grained with quartz grains up to 10 mm in diameter. Feldspar is commonly sheared out and forms a cream-coloured amorphous, sericitic mass, but where it is preserved, it is typically white in colour, tabular and 4-5 mm in size. Biotite remains prevalent. At approximately 710 m (2380 feet), the granitoid is very coarse-grained with feldspars reaching 30-40 mm in diameter.

Segments of felsic rock within the drill core are separated by mafic rock, which is volumetrically dominant. The mafic rock typically has a doleritic fine-medium grainsize, with former pyroxenes replaced by chlorite and amphibole, subhedral feldspar and oxides which commonly include leucoxene. Biotite is a common alteration mineral, pervasive through the rock with pyrrhotite and carbonate in sheared sections and as a selvage to fractures in un-sheared mafic.

Contacts between dolerite and rhyolite are not well preserved in the core, and are commonly altered with chlorite and biotite. Where observed, contacts are irregular and diffuse over two to three centimetres composed of cream-coloured felsic material with abundant chlorite. The cream-colour persists into rhyolite for another few centimetres and then grades away into typical grey-colour of the rhyolite. Apart from the colour change and an increase in crackle fractures, the rhyolite appears to have no other textural change approaching the contacts. In contrast, the grain-size of the dolerites typically diminishes near the contacts. No change in grain-size is apparent for the granitoid, but preserved contacts are rare as granitoid is most abundant in a tectonic zone of the core where primary textures have been destroyed by shearing.

Shearing is prominent in some sections of the core, most noticeably in the section that was sampled for age dating. This shear zone ranges from weak to intense and extends from 268 m (880 feet) to 460 m depth (1510 feet), a down-hole width of 192 m. The angle of the shear to core axis ranges from about 60° in the outer zones to 80° in the most highly sheared sections. The most intense sections of the sheared zone are almost perpendicular to the drill hole, which was vertical, and therefore, the shear zone is suggested to be almost horizontal in its current orientation and to have a true thickness of 190 m.

The shearing is strongest along the rock contacts and then diminishes in intensity in the centre of the dolerite units. The fine-medium grained granitoid locally becomes intensely strained, forming a strongly sheared greenish white rock composed almost entirely of sericite and minor quartz, or a fine-grained banded rock, the banding caused by variations in the biotite abundance.

7.4.2.2 Description of age dated zone from PE6 from the felsic Penneshaw

PE6 is another of the deep stratigraphic holes drilled in 1965 into the western Penneshaw domain. Nelson (1995) used a SHRIMP to date zircons from a section of "metamorphosed rhyolitic glassy lapilli tuff", which provided an interpreted age of 2930±4 Ma. For this study, the hole was not logged, but the dated section was examined. Nelson's samples for dating consisted of half-core grab samples from the interval 759-765 m (2489-2510 feet).

The rock in this interval largely comprises feldspar porphyry and also a fine-medium grain-size equigranular felsic rock. Feldspar phenocrysts in the felspar porphyry are obscured in bleached patches, giving a brecciated appearance to the rock. In better preserved areas, the bleached patches are evenly porphyritic with tabular feldspars identical to the non-bleached patches; therefore, it is considered that the rock is a pseudo-breccia. However, there are some exceptionally biotite-rich zones, which may represent heavily-altered xenoliths.

The textures of these felsic rocks are similar to the textures observed in PE1 for the less sheared sections of the fine-medium grained granitoid between 350 m (1154 feet) and 360 m (1181 feet) depth. The equigranular rock in PE6 is nearly identical to microgranitoid samples in PE1. The felspar porphyry in PE6 can also be observed in better preserved patches of PE1, although shearing in the latter has converted most feldspars to shapeless masses of sericite.

7.4.2.3 Interpretation & discussion of the geology in the PE1 and PE6 drill core

Contact relationships suggest that dolerite has intruded felsic units rather than vice versa. The grain-size of the dolerite fines down towards the contacts but chilled zones are not found. The few-centimetre-sized, cream-coloured felsic and chloritic rock, located at the best preserved felsic-dolerite contacts, is interpreted as a zone of hybridised felsic, melted by the mafic intrusion. There are few contacts preserved between the mafic rock and the granitoid (due to missing core and shearing), but the fining of the dolerite towards the contacts again suggests the dolerite has intruded the granitoid.

The voluminous dolerite intrusives are interpreted as feeders involved in the eruption of mafic greenstone equivalent to the Woolyeenyer Formation. The basis for this suggestion is that only two mafic magmatic events are recognised. The first, the eruption of lavas and emplacement of synvolcanic dykes was the largest event and generated dykes in the Woolyeenyer Formation, which are very similar to those observed in PE1. In particular, alteration of former skeletal ilmenite to leucoxene is extremely common in the Woolyeenyer Formation as are glomerporphyritic plagioclase phenocrysts, two features common in the PE1 dolerites. In contrast the second mafic event is recognised as the emplacement of differentiated sills which typically have granophyric zones with magnetite as the oxide phase. These intrusives are recognised within the Norseman komatiite but do not resemble the dolerites observed in PE1.

The textures of the rhyolite are consistent with an extrusive dome or high level intrusive. The fine grain-size implies emplacement close to the surface where surrounding rocks or water are cold and heat loss is rapid. The crackle and rubble brecciation are consistent with autobrecciation, caused by movement in a partially solidified and highly viscous magma. Alternatively, some sections comprise "jigsaw puzzle" textured breccia composed of clasts with curviplanar margins (Plate 7.2). These textures are characteristic of quench fragmentation (McPhie & others, 1993). The Penneshaw rhyolite, in fact, looks remarkably similar to the rhyolite dome at the Polar Bear Peninsula. However, the actual emplacement environment cannot be interpreted as outer contacts of the rhyolite are not exposed in PE1.

There is extensive dolerite between the last obvious rhyolite at 199 m (652 feet) and the first unequivocal microgranitoid at 351 m (1153 feet), so the relationship between the two is not exposed. Both rhyolite and microgranitoid appear to predate the dolerite intrusions and therefore, by inference, the Woolyeenyer Formation. The holocrystalline nature of the granitoid suggests it is intrusive and the increase in grainsize down hole from fine-medium grain-size to very coarse grained, suggests the drillhole passed through the contact towards the interior of a major granitoid body rather than a minor felsic intrusive. The rhyolite is unlikely to be a fine-grained marginal phase of the granite because the breccia resembles autobreccia and thus implying cold wallrocks, air or water, indicating a very high level of emplacement, unlikely for a major granitoid. Trace element geochemistry would be required to test the relationship.

A shear zone commences in the zone between the rhyolite and granitoid and extends well into the granitoid. With a width of 190 m, it is a major structure. The horizontal orientation is unusual as most large structures were originally subhorizontal at a low angle to stratigraphy and became steep following the regional folding event. The shear postdates mafic intrusions so it does not represent an early pre-greenstone structure.

7.4.2.5 Metamorphism in the felsic Penneshaw

The metamorphic grade of core in the seven stratigraphic diamond drillholes across the western felsic domain of the Penneshaw Formation (PE1 to PE7) was determined by Keele (1984) to be low pressure amphibolite facies. This is consistent with the work of Nelson (1995) whose sample from PE6 indicated a metamorphic grade between upper greenschist facies to lower amphibolite facies.

1.7 km to the WSW, petrography for diamond hole PE260 at the Perkins prospect identified cummingtonite amphibole in felsic or sedimentary rocks indicating lower amphibolite facies metamorphism (Chapman, 1989).

Therefore, the available evidence suggests the grade of metamorphism in the western felsic domain of the Penneshaw Formation is lower amphibolite facies, similar to the Noganyer Formation and the main field segment of the Woolyeenyer Formation. This is consistent with the location of the felsic domain of the Penneshaw Formation during peak regional metamorphism, adjacent to the Noganyer Formation and close to the Woolyeenyer Formation. It does not support the ideas from previous work ,presented in the introduction, that the western felsic domain of the Penneshaw Formation is upper amphibolite facies, having been through an earlier metamorphic event.

7.4.2.6 Reinterpretation of the dating and geology of PE1 and PE6

It is unfortunate that the zones sampled for dating in PE1 contain the most sheared and ambiguous rocks in the hole. In this study, all of the samples are re-interpreted as granitoid. Two of the dating samples are from strongly sheared zones at 448 m (1470' & 1471'4"). The samples were described in the geochronology report as "fine-grained, banded rhyolite", but it is suggested here that the samples are granitoid and the banded textures are caused by shearing. The other three geochronology samples (from depths 413 m [1355' & 1356'6"] and 454 m [1489'7"]) were described as "coarse-grained porphyry". Again the rocks are granitoid but the shearing has altered the feldspars to sericitic shear bands while leaving quartz so the rock attains a porphyritic appearance. Ages from all these samples were pooled to give the final ages of 2938±10 Ma.

The samples from PE6 dated by Nelson (1995) as having an age of 2930±4 Ma, appear to have been derived from a microgranitoid that is not sheared. The microgranitoid appears to be a fine-medium grained variety of the granitoid samples dated from PE1. Therefore, the published origin of these rocks as felsic extrusive is not supported by this study. The rock that is interpreted as a possible extrusive in this study, the fine-grained rhyolite in PE1 between the start of the core and 200 m (652 feet), was not dated.

7.4.2.7 Implications of the re-interpretation for the felsic Penneshaw and Noganyer Formation

In this section, the findings for the individual rock types in drill holes PE1 and PE6 through the felsic domain of the Penneshaw Formation are considered in relation to the other rocks in the Penneshaw, Noganyer and Woolyeenyer Formations.

If the mafic dolerites that intruded the granitoid and rhyolite in the western domain of the Penneshaw Formation are indeed equivalent to the Woolyeenyer Formation then the rhyolite in PE1 must pre-date the mafic rocks. However, it is uncertain what the age of the rhyolite is because it was not dated. Its relationship with the granitoid is uncertain due to shearing and dolerite intrusions removing the contact.

It is possible that the rhyolite represents an early, pre-basalt felsic volcanic centre such as those recognised in the north-eastern goldfields (eg. Welcome Well, Bore Well) with an age of *ca.* 2710 Ma. Alternatively, it may be ancient like the granitoid that was dated at *ca.* 2930 Ma. If the latter is the case, there is a question as to what happened to the rhyolite in the 200 Ma gap between its crystallisation and emplacement below the Noganyer Formation. As no pre-2700 Ma structural fabrics

or metamorphic grade are imposed, how did a supracrustal rock-type survive and become emplaced, apparently without undergoing any significant tectonic event?

Another consideration is the structural relationship between the Noganyer Formation and the felsic Penneshaw Domain. As described in section 10.4.4.5, Holcolme (1997) identified a major ductile D_1 fault at the base of the Noganyer Formation north of the Jimberlana Dyke, and the Bon Accord Jaspilite Member has been recognised as being overturned.

A further question is whether the conglomerates in the Noganyer Formation, with clasts of an apparent rhyolite composition were derived from the Penneshaw rhyolite? The available age dates (section 6.3.3) of zircons derived from quartzite in the base of the Noganyer Formation are consistent with the ages of zircons derived from the granitoid in PE1.

For the last question, there are four possible models are considered below:

i. *The Penneshaw rhyolite is aged ca. 2930 Ma (like the granitoid) and the Noganyer conglomerate is derived from it, but deposited ca. 2706 Ma.* This model implies that the first event in the development of the *ca.* 2700 Ma greenstones is the uplift and erosion of rhyolite that had been previously buried for >200 Ma. As the conglomerate is monomict, this model implies that no other rock types including supracrustal sedimentary rock was exposed. It is also noted that no tectonic fabric was imposed during the uplift event. The model is not supported as the necessary conditions pointed out seem unlikely.

ii. *The Penneshaw rhyolite is aged ca. 2930 Ma (like the granitoid) and the Noganyer conglomerate is coeval and derived from it at the same time:* In this model there is an erosional unconformity over the Penneshaw rhyolite. The conglomerate is monomict as it was derived from the Penneshaw rhyolite as it became emergent. In this model, the interpreted original single BIF layer that existed prior to deformation, which has a maximum age of *ca.* 2706 Ma, represents greater than 200 Ma of turbidite deposition. This is unreasonable considering it is only about 60 m thick. It is also unreasonable to argue that a basin remained open for more than 200 Ma, longer than any current ocean. It is difficult to argue that some undefined structure may have removed a thick package of overlying sedimentary rock from between the BIF and the conglomerate because drill hole S4172 contains no such structure.

iii. *The Penneshaw rhyolite is aged ca. 2720 Ma (younger than granitoid) and the Noganyer conglomerate is coeval and derived from it at the same time:* Similar to the above model in that the conglomerate is directly derived from an emergent volcanic centre with a timing similar to that found in volcanic centres in the

north-eastern goldfields (eg. Bore Well). This argument suggests that the Noganyer Formation represents a fining up sequence possibly due to extension immediately prior to the onset of mafic volcanism. The model places the 200 Ma time gap indicated by geochronology in the sheared zone between the granitoid and rhyolite of drill core PE1.

iv. *The Penneshaw rhyolite is aged ca. 2930 Ma (related to granitoid) but the Noganyer conglomerate is younger and unrelated to it:* In this model, the Noganyer conglomerate and the Penneshaw rhyolite are actually unrelated, consistent with a fault with a large displacement (10's of km's) at the base of the Noganyer Formation. The emergent felsic volcanic centre that gave rise to the Noganyer conglomerates is not represented in the Penneshaw Formation. Some other ancient eroding source provided the oldest zircons incorporated into the Noganyer Formation.

With the dearth of evidence available, none of these alternative models can be uniquely selected. However, models (i) and (ii) appear to be the most problematical. In addition, the age dating in the Noganyer suggesting the quartzite and BIF have received ancient zircons from a similar source does not support model (ii). Models (iii) or (iv) seem the most likely.

7.4.3 Conclusion

The updated geological interpretation developed by CNGC (Connors, 2000), which divides the Penneshaw Formation into three domains is accepted in this study. Based on this interpretation, the Penneshaw Formation should be subdivided into two separate formations consisting of the central and eastern domains, which are dominated by mafic rocks and the structural margin to the Buldania Granodiorite, and the western felsic domain.

Within the western felsic domain, drill hole PE1 intersected rhyolite with a fine grain-size and brecciated textures that would be consistent with an extrusive or a high level intrusive. The margins of the rhyolite are not exposed, so there is insufficient data to distinguish between these two emplacement options. Almost 200 m of mafic intrusions and sheared rock separate the rhyolite from the next recognisable felsic phase of granitoid. The relationship (if any) between the rhyolite and the granitoid is unclear. Both these lithologies are intruded by abundant dolerite dykes that probably represent feeders to the Woolyeenyer Formation. Shearing postdates the mafic dykes. The metamorphic grade of the rhyolite is lower amphibolite, consistent with the Noganyer Formation and main field of the Woolyeenyer Formation. No structural fabrics are found in the rhyolite that are not also present in the mafic dykes.

The rhyolitic conglomerate at the base of the Noganyer Formation has visual similarities to the rhyolite in the Penneshaw Formation. However, the granitoid in the Penneshaw Formation has been dated at *ca.* 2930 Ma whereas zircon ages in the Noganyer indicate a maximum age of *ca.* 2706 Ma. As it is not considered geologically feasible for the Noganyer to represent in excess of 200 Ma years of sediment deposition, the two most probable explanations are either that the Penneshaw rhyolite is much younger than the granitoid and there is an erosional or structural unconformity between the two, or that the Penneshaw rhyolite is also aged *ca.* 2930 Ma and the clastic units of the Noganyer Formation are unrelated to it, consistent with the evidence of a major fault.

This study has shown that further work is required on the Penneshaw Formation. In particular, useful work would be careful relogging of core holes through the western Penneshaw Domain to determine volcanic facies and detect any structural fabrics that may be in the rhyolite but not the dolerite dykes; trace element geochemistry of the Penneshaw rhyolite, Penneshaw granitoid and Noganyer conglomerate for comparative purposes; and further SHRIMP dating with the models presented above in mind.

7.5 DIFFERENTIATED GABBROS AND DOLERITES.

Differentiated gabbro and dolerite need to be considered separately in the stratigraphy as they are younger than the mafic greenstone and are the dominant hosts for gold mineralisation in the Kalgoorlie Terrane. Differentiated mafic intrusives are described in this study in the Coolgardie Domain (Chapter 6). Prominent examples are the Mount Thirsty Sill, the Mission Sill and the Woodcutters Sill, the former reaching a maximum of 2 km thick. This section describes differentiated dolerites found in the Norseman Terrane that may be equivalent to the large differentiated mafic sills in the Coolgardie Domain. In the Norseman Terrane, the differentiated mafic units are thinner than in the Coolgardie Domain, ranging from less than one metre to hundreds of metres in thickness.

Description

As a group, these mafic intrusives are typically differentiated and emplaced as sills just above the stratigraphic level of the komatiite and in the base of the Black Flag Beds (BFB). Major sills with a high MgO composition in the southern Coolgardie Domain are described in Chapter 6. Differentiated tholeiitic sills are common in the Kambalda and Kalgoorlie areas and commonly have magnetite and quartz-bearing, granophyric layers (Witt, 1995; Travis & others, 1991). Examples in the Norseman Terrane include dolerite dykes intruding the Norseman komatiite and possibly the gabbroic Lady Mary Member of the Noganyer Formation.

Diamond drill hole ETS18, intersected a fine to medium grain-sized magnetite-bearing dolerite at 251.6-280.5 m, within the Norseman komatiite. The Norseman komatiite in this area is sheared talc-carbonate with the shear orientation consistent with a D_1 structure called the Hill Island thrust (see Chapter 10). The dolerite intrudes this sheared komatiite and is itself sheared along its margins, although the fabric disappears within the interior of the intrusion.

The Lady Mary Member (LMM) is a medium to coarse-grained gabbro sill which attains a maximum thickness of 120 m (Doepel, 1973). It is composed of pyroxene replaced by chlorite and actinolite, with minor feldspar and traces of quartz. The LMM is not entirely concordant with bedding and in places truncates the Noganyer Formation jaspilite units (Briggs, 1997). An additional suite of gabbroic dykes which may be related to the LMM are associated with 340° trending faults cross-cutting the Noganyer Formation. These dykes are dark in colour and comprise relict clinopyroxène, hornblende, feldspar and locally biotite alteration (Briggs, 1997).

Interpretation & discussion

Differentiated dolerite and gabbro sills in the Norseman Terrane are considered to be equivalent to other well-known, late-stage, tholeiitic sills including the Golden Mile Dolerite at Kalgoorlie, and the Condenser Dolerite and Junction Dolerite south of Kambalda. Similarities include sill morphology, and their differentiation sequences. The layered sills in the Kalgoorlie Terrane are commonly emplaced at the base of the BFB, overlying the contaminated komatiites of the Paringa Basalt. In the Norseman Terrane, one example is hosted in the Norseman komatiite and another possible example, the Lady Mary Member, is located within the Noganyer Formation

The age of the differentiated dolerites and gabbros is constrained by the stratigraphic levels of the examples and the evident metamorphic replacement of igneous minerals. In the Norseman Terrane, an example is provided, which intrudes the Norseman komatiite. In the Kalgoorlie Terrane the sills intrude the base of the BFB. Therefore the differentiated dolerites and gabbro are younger than the komatiite (*ca.* 2705 Ma) and BFB (2690-2665 Ma), but older than the peak metamorphism events, which were synchronous with D_2 and were underway by at least 2650 Ma (Nelson, 1997).

Evidence from the drill hole into the Norseman komatiite (ETS18) further indicates that the dolerite was pre or syn D1 (2665-2657Ma), as it is sheared by the Hill Island thrust (see section 10.4.4). The BFB were deposited coeval with D_E so the sills were probably intruded between D_E and D_1. The differentiated dolerites and gabbros form a second, mafic igneous event, albeit of more limited in extent than the first major mafic greenstone forming event. All mafic intrusives which cut the komatiite and do

not have siliceous high magnesian compositions, equivalent to the Paringa Basalt at Kambalda (see section 2.4.2 and Chapter 4), are inferred to have been generated in the second mafic igneous event.

7.6 CONCLUSION

This chapter has raised several issues concerning previous geological interpretations of the Penneshaw and Noganyer Formations. Although a lack of time and data precluded firm conclusions to be drawn about the geological evolution of these formations, the evolution of the Noganyer Formation and Penneshaw Formation are important constraints on the structural and tectonic interpretation of the Norseman Terrane (Chapters 10 & 12). The majority of the concepts presented in this chapter are tentative and are raised largely to clarify issues requiring further study.

The Woolyeenyer Formation is underlain by the Noganyer Formation. The Noganyer Formation is interpreted to have originally comprised one fining up sequence composed of monomict felsic conglomerate, sandstone and low density turbidite. The siltstone and mudstone of the turbidite has been altered with magnetite to resemble BIF. The fining up sequence has been structurally duplicated in the Norseman region by isoclinal folding and thrust faulting.

The Bon Accord Jaspilite at the base of the Noganyer is overturned to face east and is separated from the underlying Penneshaw Formation by a major thrust (see Chapter 10). Green (1997) reported that the facing direction of the Holstein Jaspilite at the top of the Noganyer Formation is also east as indicated by grading within a thin section. If correct, this facing indicates the Holstein Jaspilite is overturned with respect to the Woolyeenyer Formation, indicating a major structural discontinuity at the top of the Noganyer Formation.

Both the lower section of the Woolyeenyer Formation and the felsic part of the Penneshaw Formation are extensively intruded by dolerite dykes considered to be feeders to the basalts of the Woolyeenyer Formation. However, the Noganyer Formation has few dolerite dykes other than late stage gabbro sills and dykes filling NNW extensional structures.

It is tentatively proposed in this study that the entire Noganyer Formation may be allochthonous, thrust into position beneath the Woolyeenyer Formation.

The Penneshaw Formation is divided into three domains. The eastern and central domains are dominated by mafic rocks, intercalated with granitoid and mylonite zones in the east towards the contact with the Buldania Granodiorite. The mafic rocks of the eastern and central domains are considered to be a structural repetition of

the Woolyeenyer Formation (Connors, 2000). The western felsic domain was the subject of this chapter. An age of *ca.* 2930 Ma has been reported from granitoid in the western felsic domain of the Penneshaw Formation, approximately 220 Ma greater than the greenstones.

A review of petrography from the felsic Penneshaw Formation indicates that the metamorphic grade is lower amphibolite, the same as the Woolyeenyer Formation in the vicinity of Norseman.

PE1, a drill hole into the felsic Penneshaw includes an upper rhyolite and a lower granitoid, both intruded by swarms of dolerite dykes. The rhyolite has textures consistent with autobrecciation or quench fragmentation. However, the origin of the unit cannot be proposed due to the lack of preservation of the rhyolite margins. The microgranite and granite beneath the rhyolite is the dominant felsic unit within the drill hole and was dated at *ca.* 2930 Ma by Hill R.I. & others (1990). It is unclear whether the rhyolite and granite are related, as the contact between the units is obliterated by extensive dolerite intrusions and shearing. As a consequence, the age of the rhyolite is uncertain. It may be *ca.* 2930 Ma like the granite, or *ca.* 2710 Ma like some early greenstone felsic to intermediate volcanic complexes known from the north-eastern goldfields. It is also unclear whether there is any relationship between the rhyolite and felsic conglomerate in the Noganyer Formation.

A stratigraphic column for the lower Woolyeenyer, Noganyer and felsic Penneshaw Formations, which incorporates the concepts discussed in this chapter, is presented as figure 7.3.

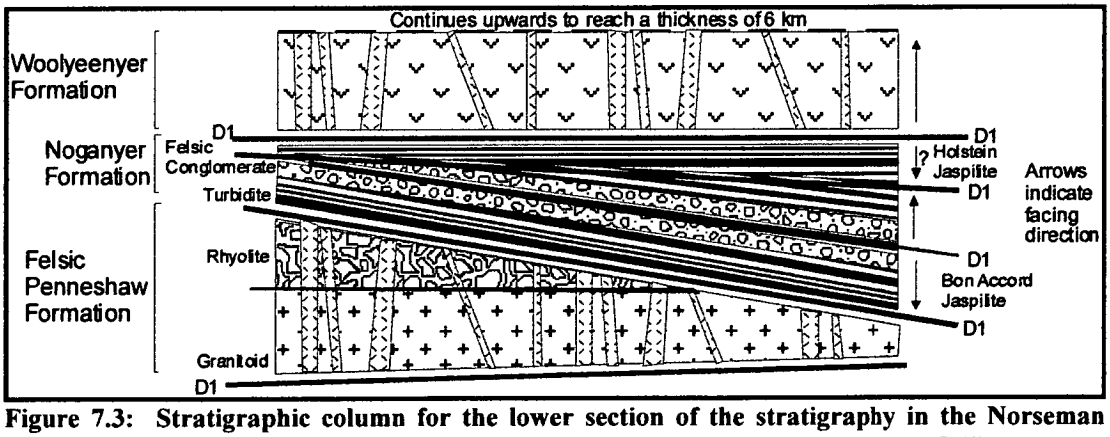

Figure 7.3: Stratigraphic column for the lower section of the stratigraphy in the Norseman region, presenting the concepts discussed in this chapter. The lines marked "D1" represent proposed thrusts.

CHAPTER EIGHT

Geochemistry of the felsic rocks

8.1 INTRODUCTION

The felsic rocks examined in this study include felsic volcanic and subvolcanic intrusive rocks from the upper felsic and sedimentary part of the succession, felsic porphyries and microgranitoids emplaced at a deep level in the mafic strata, and granitoids. Granitoids are conventionally studied separately from felsic volcanic rocks in Archaean greenstone terranes because relationships between the two are unclear. For clarity, this study first examines the high-level felsic rocks and then extends the study to porphyries and granites deeper in the stratigraphy.

This is the first study in which high precision geochemistry has been collected for felsic volcanic rocks in the Norseman Terrane. The geochemistry is used for comparison with data that has become available from Barley & others (1998) and Hand (1998) for the Black Flag Beds (BFB) around Kalgoorlie and for felsic volcanic centres in the northeastern goldfields. If the greenstone succession west of the Mission Fault in the Norseman region is part of the Coolgardie Domain, as proposed by Swager & others (1995), then the felsic epiclastic rocks should be equivalent to the BFB and have the same distinctive geochemical signature. Conversely, felsic volcanic rocks in the Norseman Terrane at The Polar Bear Peninsula appear lithologically different to the typical volcanic-derived rocks within the BFB, and geochemistry is used to show that this is indeed the case.

Felsic volcanic rocks and high-level porphyries erupted and emplaced at the Polar Bear Peninsula passed through the deeper mafic stratigraphy during their passage to the palaeo-surface. As the Norseman Anticline has tilted the mafic stratigraphy such that a cross section of the entire thickness of mafic stratigraphy (approximately 6 km) is near surface in the Norseman Terrane, some evidence of the passage of the felsic magmas might be expected. The geochemistry of some of the felsic microgranites and porphyries in the Woolyeenyer Formation are compared with volcanic rocks to test for any relationships between them.

In detail, geochemistry is being applied to felsic volcanic rocks and high-level porphyries for the following purposes:

- To test whether felsic epiclastic rocks near Mount Thirsty in the Coolgardie Domain have comparable geochemistry with the dacites in the Kalgoorlie Terrane and are thus part of the Black Flag Beds of the "Kalgoorlie Basin" of Barley & others (1998).

- To compare the felsic rocks at the Polar Bear Peninsula in the Norseman Terrane with felsic epiclastic rocks near Mount Thirsty in the Coolgardie Domain and determine whether there are any geochemical differences.

- To determine the affinities of the felsic rocks described in this study with other felsic centres in the Eastern Goldfields by comparing all the felsic rock analyses with the database collected in the AMIRA P437 study (Barley & others, 1989).

- To use the geochemistry to obtain petrogenetic information about samples to assist in establishing the palaeo-tectonic environment.

- To compare all the felsic rocks with published data for the granitoid plutons in the Eastern Goldfields to determine whether there are any geochemical relationships.

Layout of the chapter

To achieve these aims, it was first necessary to review previous geochemical studies that have been undertaken for felsic centres in the Eastern Goldfields to define the geochemical associations to which the Norseman samples will be compared. The findings of Perring (1989) about the felsic porphyries intruding the mafic stratigraphy of Norseman and Kambalda are also summarised.

The analytical results of this study are then presented as tables and diagrams to avoid geochemical descriptions in the text. The results are used to classify the felsic rocks, compare them with established associations and assign them to petrogenetic groups. Volcanic rocks and subvolcanic porphyries from the Polar Bear Peninsula and Mt Thirsty are discussed first, followed by felsic porphyries from the Woolyeenyer Formation.

Models for the genesis of felsic magmas are then discussed as an introduction to the petrogenetic section. The petrogenesis of established suites are reviewed and the origins of the groups delineated in this study postulated.

Granite studies are introduced and reviewed. As the geochemical data for the granitoids of interest were only published as normalised trace element patterns rather than raw data, the published REE patterns were compared with those created in this study and the results noted.

Implications of the work are discussed and it is found that the felsic rocks in the Norseman Terrane differ from those in the southern Coolgardie Domain. The nature of that difference and its implications for tectonic models and the terrane-bounding structures are pointed out.

Finally, the results are synthesised and conclusions are given for the aims introduced in section 8.1.

8.1.1 Methods

Samples with minimal alteration were collected from the Polar Bear Peninsula and near the Harlequin Mine in the Norseman Terrane, and adjacent to the highway near Mount Thirsty and "Fram island" in the Coolgardie Domain. Outcropping rocks were broken up and the freshest pieces collected to comprise the samples. The Harlequin and Fram Island samples were diamond drill core.

Sericitisation was impossible to avoid at the Polar Bear Peninsula, particularly for the quartz porphyry, but the freshest samples possible were obtained. Rhyolite was better preserved and some black, fairly unaltered samples were obtained from drill holes. The samples from near Mount Thirsty in the Coolgardie Domain were two volcanic sandstones and a volcanic conglomerate which appeared particularly fresh. The exposure that these samples were collected from were collected from was described in section 6.3.9.

The analytical procedure is described in section 4.6.3.

8.1.2 Element Mobility

This section evaluates the mobility of elements for the felsic rocks. An introductory description of the element mobility concept is presented in section 4.6.1.

The variable major element results for some rocks which appear similar in hand specimen suggests that there has been considerable mobility of the LILE and possibly SiO_2 in the rocks from the Polar Bear Peninsula. The mobility may be due to the combined influences of strong cleavage development, strong carbonation and incipient weathering of outcrop samples. The most affected samples are the quartz porphyries, for which it proved impossible to find non-sericitised samples. In contrast, samples from the other localities have less variable results and appear to have undergone much lower degrees of LILE mobility, particularly the drill core samples from Harlequin. Nevertheless, for all samples, results need to be treated with caution for SiO_2, K_2O, Na_2O, CaO, FeO*, Sr, Rb, and Ba. These latter trace elements have been removed from the spidergrams in this chapter.

8.2 PREVIOUS STUDIES

8.2.1 Felsic Volcanic Sequences

Felsic successions have not been as intensively studied as mafic and ultramafic successions in the Eastern Goldfields, as traditionally felsic successions have been

considered to host little mineralisation of significance other than the massive sulfide deposit at Teutonic Bore. This lack of study has only recently begun to be rectified.

One of the earliest comprehensive studies of the substantial felsic and intermediate centres in northeastern goldfields was a PhD study by Giles. This work led to a number of publications including Hallberg & Giles (1986), which documented a number of the felsic volcanic centres. Geochemical and lithological similarities over a wide extent of the Eastern Goldfields were perceived, allowing Hallberg & others (1993) to divide felsic successions into three associations. Barley & others (1998) for the AMIRA P437 study, used geochronology to add a further subdivision, resulting in four felsic volcanic associations defined using lithology, geochemistry and age. These are:

- the calc-alkaline andesite-dominated association 1 (2720-2700 Ma);
- the calc-alkaline intermediate-silicic association 2 (2690 Ma);
- the bimodal volcanic association 3 (2680-2692 Ma); and
- association 4, the volcaniclastic Black Flag Beds (BFB) of the Kalgoorlie Basin (2698-2675 Ma).

The lithologies of these four associations are described in section 2.5. This section describes the geochemistry of the associations based on the work of Barley & others (1998). Two examples from each of the four associations are plotted in figures 8.1-8.7. These use the most silicic analyses available for each group to ensure comparability with the Norseman felsic rocks.

8.2.1.1 Association 1

The calc-alkaline andesite-dominated association 1 (>2700 Ma) is widespread in the north-eastern goldfields around Laverton, but also extends south to the Gindalbie terrane. It includes volcanic centres such as Welcome Well, Bore Well and Ida Hill (figure 2.3).

The association is dominated by andesite, with subordinate basalt, basaltic-andesite, dacite and rhyolite lavas. The andesites are medium-K and compared to N-MORB, they are enriched in LILE, somewhat enriched in the more incompatible HFSE but approximately equivalent to N-MORB for the HREE. There is a small negative anomaly for Ta-Nb, and a strong negative Ti anomaly. Rhyolites and dacites are typically more enriched in all REE than andesites and have moderate Eu anomalies when normalised to chondrite (figures 8.1-8.7). The similarity in multielement patterns between andesite and rhyolite suggests they are comagmatic.

8.2.1.2 Association 2

The calc-alkaline intermediate-silicic association 2 (2690 Ma) has only one known example being the Spring Well complex (figure 2.3). The major differences between association 1 and association 2 are the younger age and the abundance of felsic volcanic rocks in the latter. Geochemically, they are indistinguishable (figures 8.1-8.7). The younger age is similar to association 3 (bimodal volcanic rocks) and the beginning of BFB deposition in the Kalgoorlie Basin.

8.2.1.3 Association 3

Association 3, the bimodal volcanic rocks (2692-2680 Ma), is best known from the Melita complex south of Leonora but extends further north to Teutonic Bore (figure 2.3). It hosts the only known example of VHMS mineralisation in the Eastern Goldfields.

The rhyolites and the inter-fingering basalts at Melita together define a tholeiitic iron enrichment trend on AFM diagrams. Rhyolites are high in silica (>74%) and highly enriched in all incompatible elements relative to other Eastern Goldfields felsic associations (figures 8.1-8.4). N-MORB normalised spidergrams show slight to moderate negative Ta-Nb anomalies and strong Ti depletions, similar in form to the calc-alkaline rocks (figure 8.7). Chondrite-normalised REE patterns are LREE enriched, but relatively flat in comparison to the calc-alkaline rocks due to high levels of HREE (figure 8.5). The rhyolites have moderate negative Eu anomalies indicating the removal of plagioclase. In detail, there are two rhyolite types, with one being more enriched and the other closer to calc-alkaline abundances.

Felsic rocks from association 3 differ from the other associations by plotting in the "within-plate granite" field of the Nb-Y discrimination diagram for granites of Pearce & others (1984), indicating an affinity with A-type, within plate, anorogenic granites (figure 8.6). A-type granitoid plutons with a similar geochemistry and age to the felsic rocks occur in the same geographic belt.

8.2.1.4 Association 4

The volcaniclastic rocks of the BFB (2698-2665 Ma) in the "Kalgoorlie Basin" of Barley & others (1998) are divided into three lithological and geochemical groups; basalt, andesite and dacite. All three types together define a calc-alkaline trend with respect to alkali oxides versus silica. Dacites, however, have strikingly different major and trace element characteristics to other felsic associations in the Eastern Goldfields. They have higher Al_2O_3, Na_2O and Sr than rhyolites from the other associations and are highly enriched in LILE, less enriched in HFSE and strongly

depleted in HREE. There is also strong depletion in Nb and Ta, a moderate negative Ti anomaly and importantly, no Eu anomaly. Andesites are somewhat similar to the dacites, indicating a likely petrogenetic relationship, but show less enrichment in LILE and less depletion in HREE. Basalts and dolerites are distinct from both andesites and dacites in the BFB, with flat HREE similar to N-MORB, slightly-enriched HFSE including LREE, enriched LILE and a slight negative Nb anomaly but no Ta anomaly.

The dacite characteristics of strongly fractionated REE patterns with no Eu anomaly and high Al and Na ratios are characteristic of trondhjemite-tonalite-dacite (TTD) suites that form a significant proportion of Archaean volcanic and plutonic rocks world-wide. The TTD suite is described in more detail in section 8.2.3.

Table 8.1: Symbol legend for Chapter 8.

Felsic Geochemical Symbol Legend	
▲	Flow banded rhyolite Batch #1 (Polar Bear)
▲	Flow banded rhyolite Batch #2 (Polar Bear)
▼	Quartz Porphyry Batch #1 (Polar Bear)
▼	Quartz Porphyry Batch #2 (Polar Bear)
▶	Feldspar Porphyry Batch #2 (Polar Bear)
◀	Granitoid dyke Batch #2 (Polar Bear)
▲	Felsic Grit Batch #2 (Polar Bear)
▶	Felsic rock Batch #2 (Polar Bear)
■	Black Shale Batch #2 (Polar Bear)
◆	Felsic sandstone & conglomerate Batch #2 (Mt Thirsty area)
◇	Feldspar Porphyry Batch #2 (Fram Island - Lake Cowan))
▽	Harlequin trondjhemite Batch #2
▷	Harlequin porpphyry Batch #2
◁	Swordfish Rhyolite (analysis from Ghaderi, 1998)
▲	Felsic Penneshaw (analysis from Ghaderi, 1998)
◭	Ajax Suite Porphyry (analysis from Perring, 1989)
▽	Ajax Suite Microgranitoid (analysis from Perring, 1989)
◑	Dinky Buoys Quartz Keratophyre (analysis from Perring, 1996)
◧	Big Porphyry Microgranodiorite (analysis from Perring, 1989)
◆	(Black Flag Beds) Dacite volcaniclastics (analyses from Barley & others, 1998)
◆	(>2700 Ma group) Bore Well rhyolites (analyses from Barley & others, 1998)
◭	Spring Well rhyolite & dacite (analyses from Barley & others, 1998)
◭	(Bimodal group) Melita rhyolites (analyses from Barley & others, 1998)

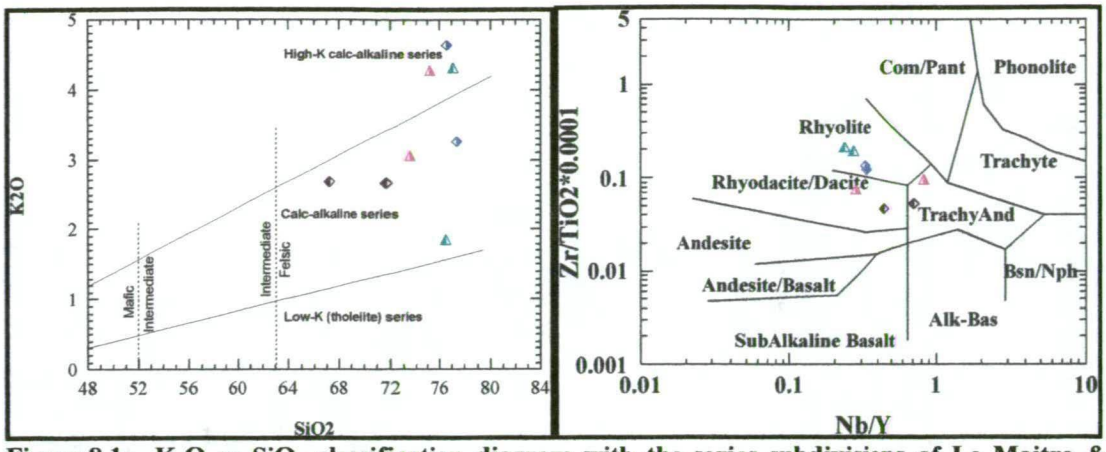

Figure 8.1: K_2O vs SiO_2 classification diagram with the series subdivisions of Le Maitre & others (1989). Figure 8.2: Zr x 10,000/TiO_2 vs Nb/Y (immobile element) classification diagram of Winchester & Floyd (1976). Two samples from each of the four associations defined by Barley & others (1989) are plotted.

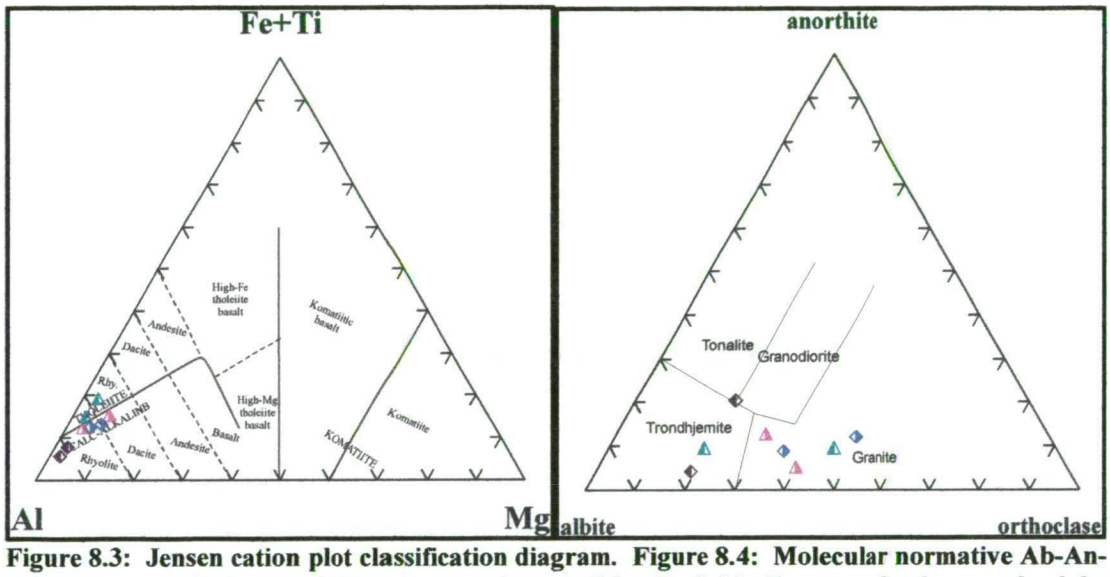

Figure 8.3: Jensen cation plot classification diagram. Figure 8.4: Molecular normative Ab-An-Or diagram after Barker (1979), showing the trondhjemite field. Two samples from each of the four associations defined by Barley & others (1989) are plotted.

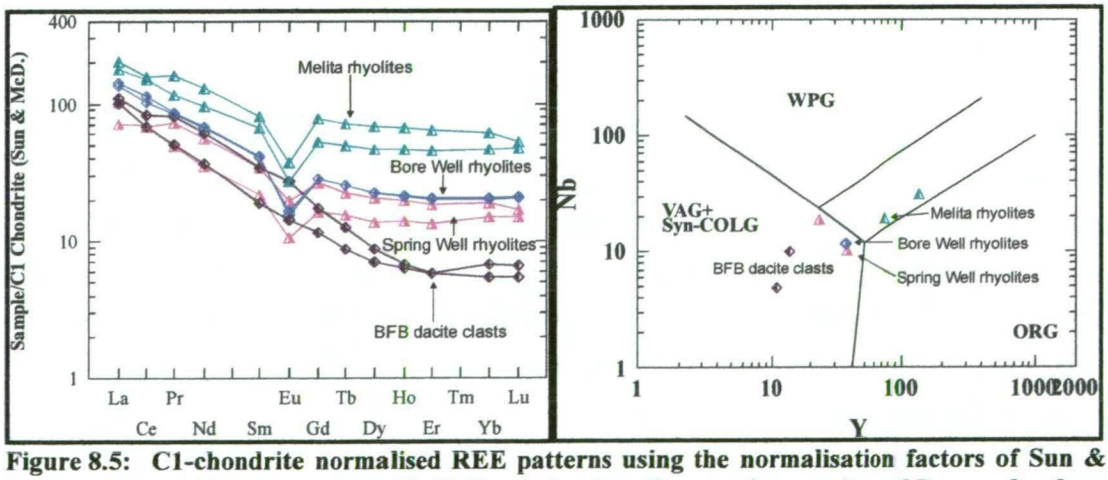

Figure 8.5: C1-chondrite normalised REE patterns using the normalisation factors of Sun & McDonough (1989). Figure 8.6: Nb-Y discrimination diagram for granites of Pearce & others (1984). VAG & syn-COLG = volcanic arc granites and syn-collisional granites; ORG = ocean ridge granites; WPG = within-plate granites; the area between the parallel lines is the overlapping field of within-plate granites and ocean ridge granites from anomalous ridges. Two samples from each of the four associations defined by Barley & others (1989) are plotted.

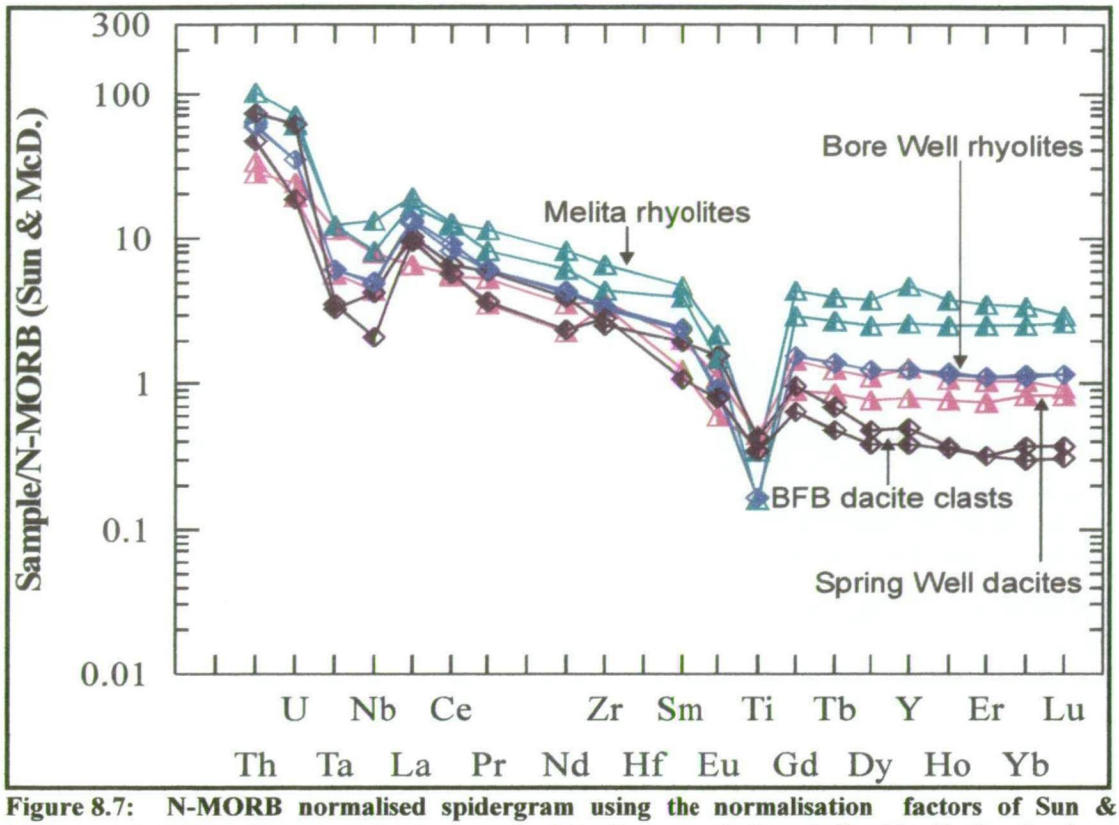

Figure 8.7: N-MORB normalised spidergram using the normalisation factors of Sun & McDonough (1989). Two samples from each of the four associations defined by Barley & others (1989) are plotted.

8.2.2 Small Felsic Intrusives ("Porphyries") within mafic successions

This section is based on the work of Perring (1989), who undertook a study of the small felsic to intermediate intrusions commonly known as "porphyries" within the mafic successions at Norseman and Kambalda. At Norseman, Perring divided the "porphyries" into three compositional groups. The Kambalda porphyries appear to form a geochemical continuum.

8.2.2.1 Ajax suite (Norseman)

The most abundant group of porphyries throughout the Woolyeenyer Formation around Norseman are known collectively as the Ajax suite, which includes the Ajax dyke swarm of quartz-alkali feldspar-phyric rhyolites and the Ajax Porphyry microgranite near the Ajax Mine (figure 8.15). The rhyolite dykes vary in width from a few centimetres to 40 m but are commonly 1 to 10 m thick. The microgranite has a thickness of 100 m and was included within the group, as the chilled margins bear similarities to the rhyolite dykes.

The rhyolites are sparsely porphyritic with 1 to 7% albite and/or quartz phenocrysts. The texture of the groundmass varies from granular to spherulitic. The Ajax porphyry has an almost flat REE pattern and a moderate negative Eu anomaly. The chemistry is distinctive, being siliceous (approximately 77 wt% SiO_2), with rather

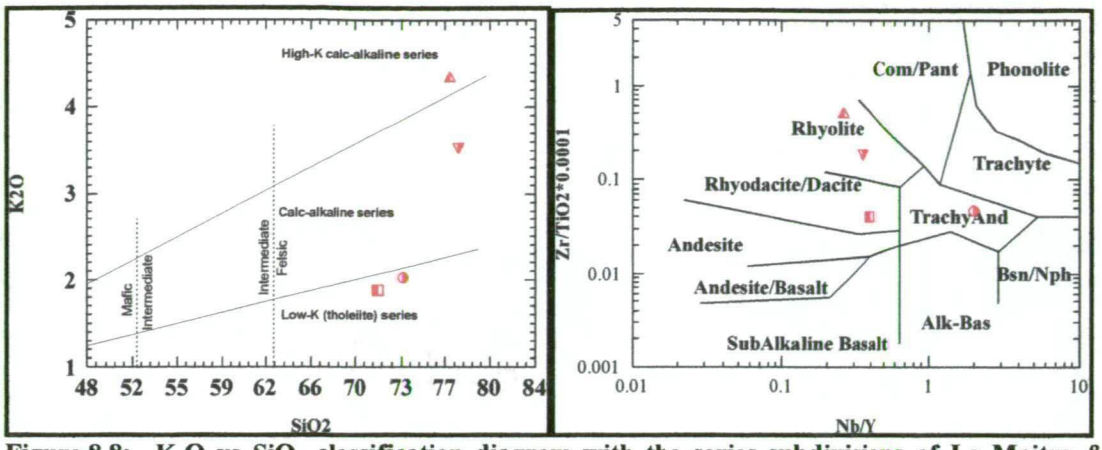

Figure 8.8: K_2O vs SiO_2 classification diagram with the series subdivisions of Le Maitre & others (1989). Figure 8.9: Zr x 10 000/TiO_2 vs Nb/Y (immobile element) classification diagram of Winchester & Floyd (1976). Norseman porphyries are plotted using analyses of Perring (1989).

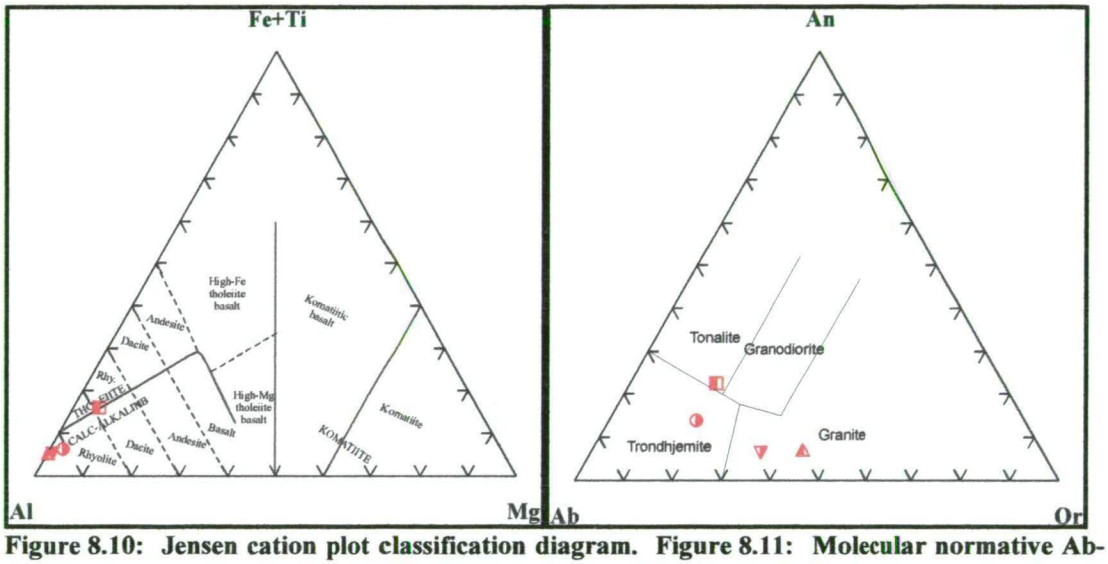

Figure 8.10: Jensen cation plot classification diagram. Figure 8.11: Molecular normative Ab-An-Or diagram after Barker (1979), showing the trondhjemite field. Norseman porphyries are plotted using analyses of Perring (1989).

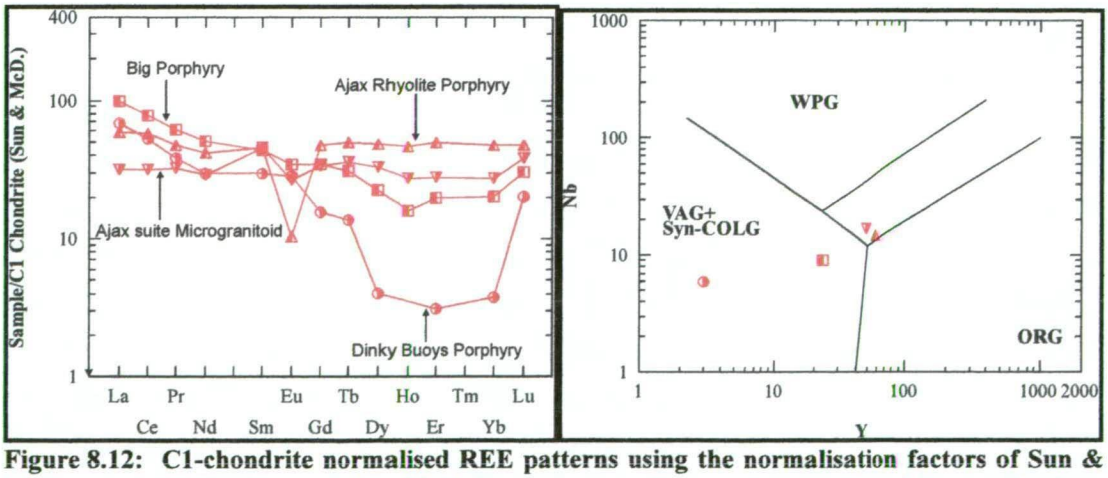

Figure 8.12: C1-chondrite normalised REE patterns using the normalisation factors of Sun & McDonough (1989). Figure 8.13: Nb-Y discrimination diagram for granites of Pearce & others (1984). VAG & syn-COLG = volcanic arc granites and syn-collisional granites; ORG = ocean ridge granites; WPG = within-plate granites; the area between the parallel lines is the overlapping field of within-plate granites and ocean ridge granites from anomalous ridges. Norseman porphyries are plotted using analyses of Perring (1989).

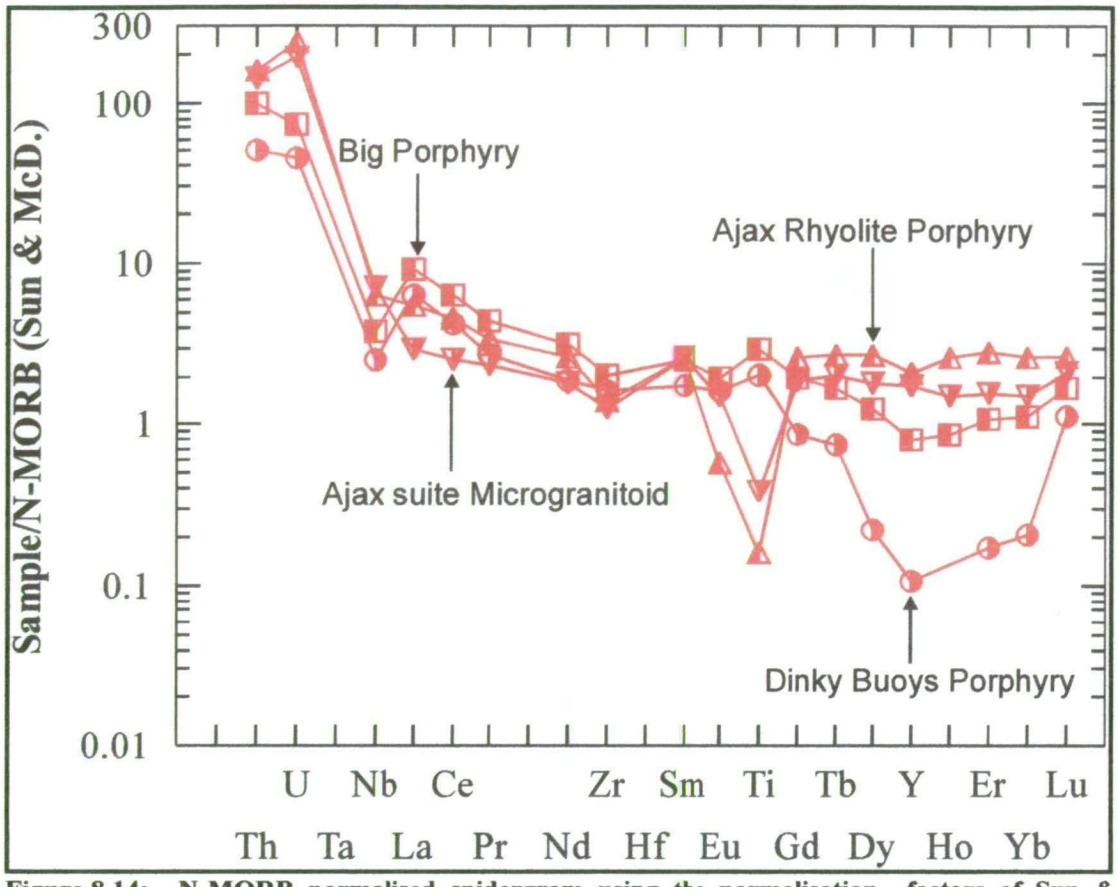

Figure 8.14: N-MORB normalised spidergram using the normalisation factors of Sun & McDonough (1989). Norseman porphyries are plotted using analyses of Perring (1989).

low K_2O (approximately 4.5 wt%), and high Y, Nb & U. Similarities to Sn-U granites were pointed out by Perring (1989).

Perring (1989) suggested the Ajax suite is oldest group of felsic intrusives, based on the work of Keele (1984), who noted the Ajax porphyries in the North Royal Mine pre-date the quartz reef and are rotated into shear fabrics.

8.2.2.2 Dinky Buoys suite (Norseman)

The Dinky Buoys suite (DBS) is spatially restricted, being mainly found in the vicinity of the North Royal Mine from where it gained its name from a well-known porphyry (figure 8.15). Hodgkison (1995) found a second example of this suite at the Swordfish prospect beneath Lake Cowan approximately 4 km west of the North Royal. Keele (1984) suggested the Dinky Buoys Porphyry in the North Royal pit cuts the quartz reef but was deformed by the NNW Princess Royal Shear. However, McCuaig (1991) noted that the quartz reef cuts the Dinky Buoys Porphyry in the area of the Surface Winze at the North Royal Mine and suggested that the porphyry actually pre-dates reef formation and gold mineralisation.

The DBS comprises quartz+plagioclase-phyric sodic rhyodacites. These are distinctive due to the characteristic plagioclase phenocrysts up to 3 mm, which

constitute 10-25 modal % in an aphanitic groundmass (McCuaig, 1991). The DBS was described by Perring (1989) as being calc-alkaline with trondhjemitic affinities and chemistry almost identical to a group of felsic rocks at Kambalda which includes the "Kambalda Granodiorite" in the core of the Kambalda Dome. It has a moderately fractionated REE pattern with flat HREE but relatively elevated Lu giving rise to an unusual "ladle-like profile".

8.2.2.3 Big Porphyry Complex

The third group is a 200 m-thick sill known as the Big Porphyry complex located west of the OK Mine and south of Norseman township (figure 8.15). This body largely comprises a xenolithic granodiorite but also includes enclaves of various compositions, with narrow dykes of quartz-alkali feldspar-phyric rhyolite similar to the Ajax suite being the latest phase. The texture is very heterogenous but at least in part, the Big Porphyry consists of sparsely porphyritic microgranite with plagioclase, quartz and clots of biotite and hornblende. It has a rather flat REE pattern with HREE levels marginally lower than LREE, no Eu anomaly and is thought to have tholeiitic affinities.

The porphyry was suggested by Perring (1989) to be relatively young based on an alteration assemblage of sericite-chlorite, proposed to be a retrograde metamorphic event, in contrast to the biotite-stable assemblages in the other suites. However, McCuaig (1991) found the Big Porphyry to be pre-mineralisation and therefore pre-peak metamorphism. Zircons within the Big Porphyry have returned two population ages of 2685±3 Ma and 2665±3 Ma which are interpreted as inheritance from the source and the age of emplacement respectively (Campbell, 1989).

8.2.2.4 Kambalda porphyries

At Kambalda, Perring (1989) found that field relationships, petrography and geochemistry indicate genetic relationships between most of the groups. Petrography and geochemistry indicate that the mafic end-members are lamprophyres whereas the felsic members have trondhjemitic chemistry. It is unclear whether the sodic character of the latter is entirely primary, as Na metasomatism may have taken place; nevertheless, the spoon-shaped REE patterns are characteristic of trondhjemites (TTD suite). All the REE patterns lack negative Eu anomalies and are steep, but flatten in the HREE. Some increase at Lu (possibly due to analytical error) giving them spoon shape or in extreme cases, a ladle-shape similar to the Dinky Buoys Porphyry.

The alumina content of all the samples is greater than 15 wt% at 70 wt% silica; thus they can be described as members of the high-Al TTD suite (see section 8.2.3). The

analyses presented by Perring (1989) with steep REE patterns but without the upward tick at Lu are very similar to the association 4 BFB patterns of Barley & others (1998) and are regarded as equivalent.

8.2.3 Trondhjemite-tonalite-dacite (TTD) suite

Rocks with trondhjemitic affinities are very important in this study and have been referred to in previous sections. They include the BFB, many of the porphyries at Kambalda and a number of samples in this study. Given the importance of these rocks to this study, their abundance in Archaean terranes and relative rarity in Phanerozoic sequences, trondhjemites will be defined in this section to aid classification of the samples from this study. The origin of the trondhjemitic rocks is discussed in section 8.4.2.3.

Trondhjemites are felsic plutonic rocks with sodic plagioclase and quartz but little or no K-feldspar. Plagiogranite is another name for rocks of this composition and is most commonly used for the varieties that occur in oceanic environments, ophiolites and island arcs (McBirney, 1984). Trondhjemite is the usual term for the varieties that are common in Archaean cratons and continental margins.

Trondhjemites are a member of a subalkaline series, the trondhjemite-tonalite-granodiorite (TTG) suite that have a distinctly different differentiation trend than the calc-alkaline series when plotted on a K-Na-Ca ternary diagram. Whereas the calc-alkaline series trends towards the K apex of the ternary diagram with differentiation, normative feldspars in the TTG suite become more albitic and the felsic members trend towards the Na apex. The TTG suite lacks the potassium feldspar so conspicuous in the felsic members of the calc-alkaline series and has lower contents of K and other LILE (McBirney, 1984). The series occurs not only as granitoids, but also as volcanic rocks; thus it may be labelled the trondhjemite–tonalite-dacite (TTD) suite. As this thesis is largely concerned with volcanic and subvolcanic porphyries, TTD will be used in preference to TTG.

A division of the TTD suite into two types can be made, using the alumina contents at 70 wt% SiO_2: the low-Al type have less than 15 wt% Al_2O_3 and the high-Al type have greater than or equal to 15 wt% Al_2O_3 (Barker, 1979). These two types have distinctive geochemical differences and appear to be found in different tectonic settings. Plagiogranites from ophiolite complexes and island arcs are typically low-Al types (McBirney, 1984) and have low Sr contents (<200 ppm), slightly enriched LREE, a negative Eu anomaly and flat HREE (Barker & Arth, 1976). Trondhjemites from continental margins and Archaean cratons are typically the high-Al types and have low Nb (<10-11 ppm), high Sr (>200-2000 ppm), enriched LREE and depleted

HREE with either no or only a small positive or negative Eu anomaly (Drummond & Defant, 1990).

8.3 FELSIC ROCKS OF THE NORSEMAN REGION

8.3.1 Introduction

The map of Barley & others (1998) showing the distribution of the four felsic associations through the Eastern Goldfields has Norseman as part of the BFB volcaniclastic suite, whereas the Polar Bear Peninsula is left blank. The mapping undertaken at the Polar Bear Peninsula for this study found a rhyolite volcanic complex consisting of a lava dome with flanking breccias stratigraphically above basalt and komatiite. In comparing the Polar Bear rhyolite to the four felsic associations described above, it appears most like association 2 at Spring Well. However, more detailed petrogenetic considerations and some bivariate plots (eg figure 8.39) indicate a closer relationship to the rhyolites in association 3 (Melita). Accordingly, in figure 2.3, the Norseman area has been given an association 3 pattern.

In contrast, felsic rocks adjacent to the Norseman-Coolgardie Highway near Mt Thirsty in the southern Coolgardie Domain are felsic volcanic-derived pebble conglomerate, sandstone and shale turbidite packages consistent with the BFB.

Thirty samples were analysed for this study. These comprise 19 volcanic rocks and intrusives from the Polar Bear Peninsula, 7 intrusives from the Harlequin prospect and 4 samples from the southern Coolgardie Domain. These samples were supplemented by two analyses of intrusives from the Sailfish prospect and the Penneshaw Formation listed in Ghaderi (1998). The samples have been compared to the four associations defined by Barley & others (1998) and the felsic porphyry suites defined by Perring (1989). The locations of all the samples are shown on figure 8.15.

8.3.2 Geochemical Results for Felsic Volcanic & subvolcanic Sequences

The samples have been divided into groups using the field classification, which involved consideration of visible mineralogy, textures, lithofacies and location. The general coherence of the geochemical results for each group indicates that the groupings are valid. The only problematical group is the quartz porphyries at the Polar Bear Peninsula for which two samples, collected as examples of this group, were subsequently reclassified on the basis of their geochemical characteristics. CN851923 has been reclassified into a group of its own representing a hybrid rock and CN878584 has identical trace element patterns to the Harlequin porphyries and is included with that group in section 8.3.5.1.

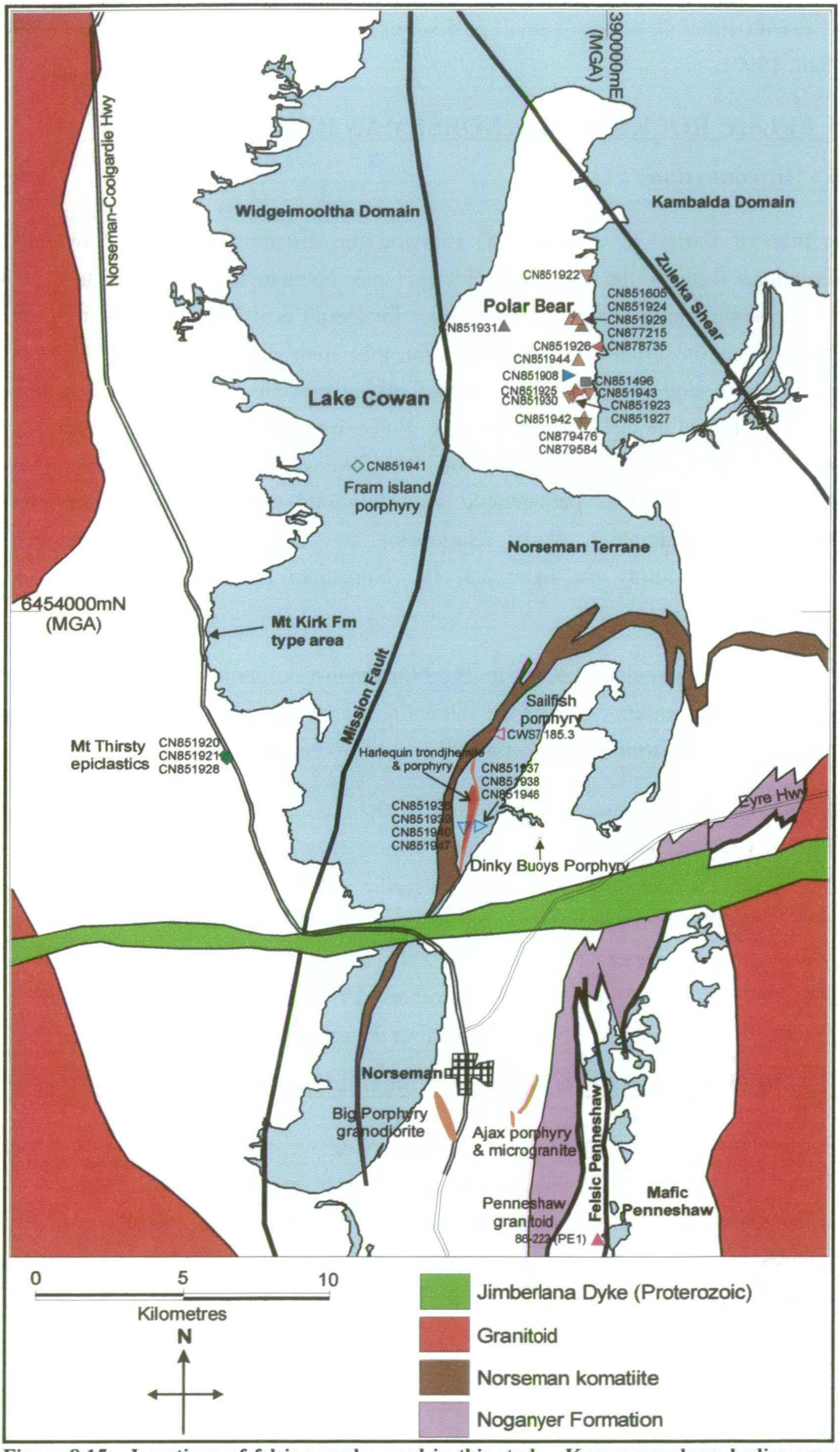

Figure 8.15: Locations of felsic samples used in this study. Known porphyry bodies are also shown. Noganyer & Penneshaw Faults after a compilation map by Connors (2000).

The felsic volcanic and small felsic intrusions sampled in this study are tabulated in Table 8.2 with geochemical values and ratios that together, describe the geochemical characteristics of the groups. The Ajax microgranite of Perring (1989), is included, as it is considered important for comparative purposes. The felsic rocks are assembled into petrogenetic groups in Table 8.3.

Another table in Appendix 3 contains typical geochemical characteristics of felsic reference groups, taken from Lentz (1998). It also lists the geochemical characteristics of the most felsic pair of samples for each of the four felsic associations defined in the Eastern Goldfields by Barley & others (1998). The characteristics of the Dinky Buoys Porphyry are included in the table using the data of Perring (1989).

Seven types of diagrams are used to present the data. Four of these are used to classify the individual samples. A K_2O vs silica diagram with the subdivisions of Le Maitre & others (1989) and a Jensen cation plot divide the felsic rocks into series. The alkalies and silica are highly mobile so little importance is placed in the positions of samples in the first, although general group trends may have some relevance. The Jensen cation plot is better for subdivision as it uses elements that are less mobile, although iron may be somewhat altered.

Petrologically, some samples appeared to have trondhjemitic affinities and this was tested geochemically using the An-Ab-Or classification for granitic rocks calculated as molecular norms and using the fields defined by Barker (1979). This classification scheme uses major elements and therefore is prone to error from direct element mobility and the constant sum problem. It was found to be of little use for most of the Polar Bear Peninsula samples, but has some utility for the Harlequin samples where major element mobility appears to have been lower.

The most reliable rock classification diagram for the ancient rocks of this study is the Zr x 10 000/TiO_2 vs Nb/Y diagram of Winchester and Floyd (1976), as it uses elements that are typically immobile. It does not, however, classify the rocks into series.

REE and other immobile trace elements are presented as chondrite-normalised REE patterns and N-MORB-normalised spidergrams, with reference samples to compare the shapes of patterns.

Finally the Nb-Y discrimination diagram for granites (after Pearce & others, 1984) is presented because Barley & others (1998) found that it discriminated between the felsic rocks from association 3 (Melita-Teutonic Bore) and the other associations.

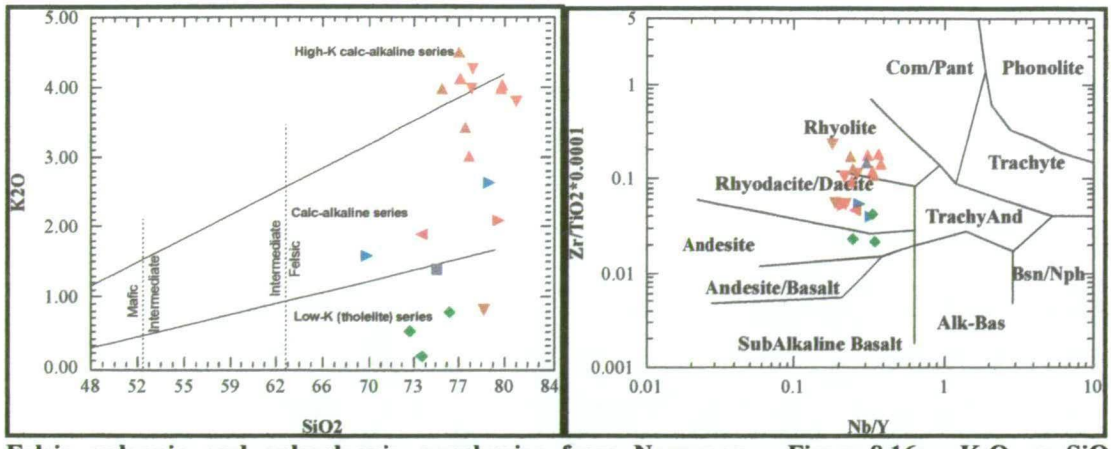

Felsic volcanic and subvolcanic porphyries from Norseman. Figure 8.16: K_2O vs SiO_2 classification diagram with the series subdivisions of Le Maitre & others (1989). Figure 8.17: Zr x 10 000/TiO_2 vs Nb/Y (immobile element) classification diagram of Winchester & Floyd (1976).

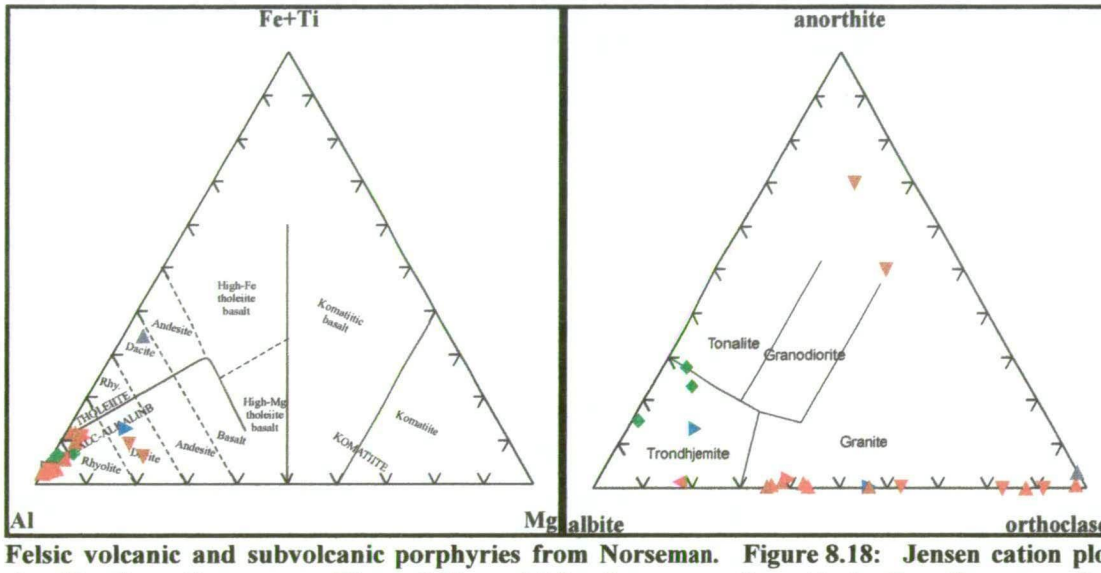

Felsic volcanic and subvolcanic porphyries from Norseman. Figure 8.18: Jensen cation plot classification diagram. Figure 8.19: Molecular normative Ab-An-Or diagram after Barker (1979) showing the trondhjemite field.

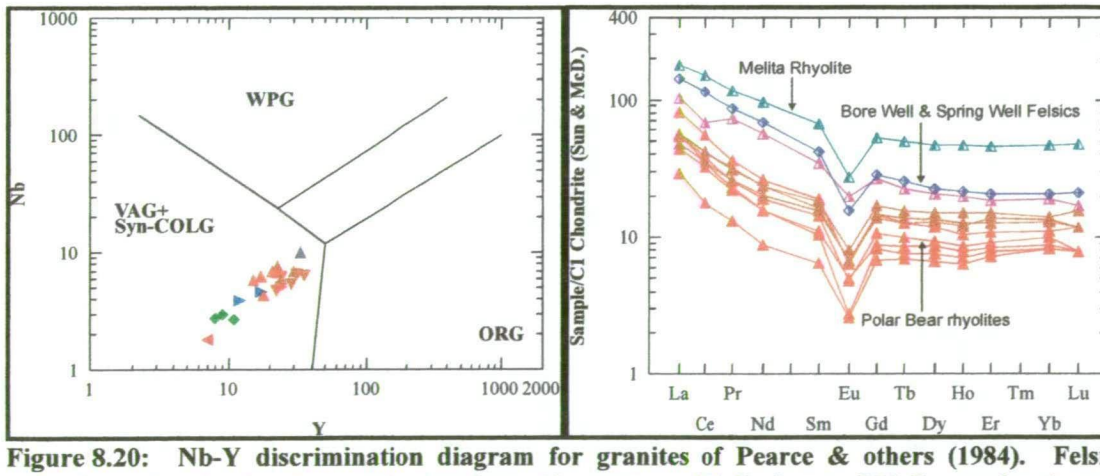

Figure 8.20: Nb-Y discrimination diagram for granites of Pearce & others (1984). Felsic volcanic and subvolcanic porphyries from Norseman. VAG & syn-COLG = volcanic arc granites and syn-collisional granites. Figure 8.21: C1-chondrite normalised REE patterns using the normalisation factors of Sun & McDonough (1989). Polar Bear rhyolites with reference Bore Well, Spring Well & Melita felsic rocks using analyses of Barley & others (1998).

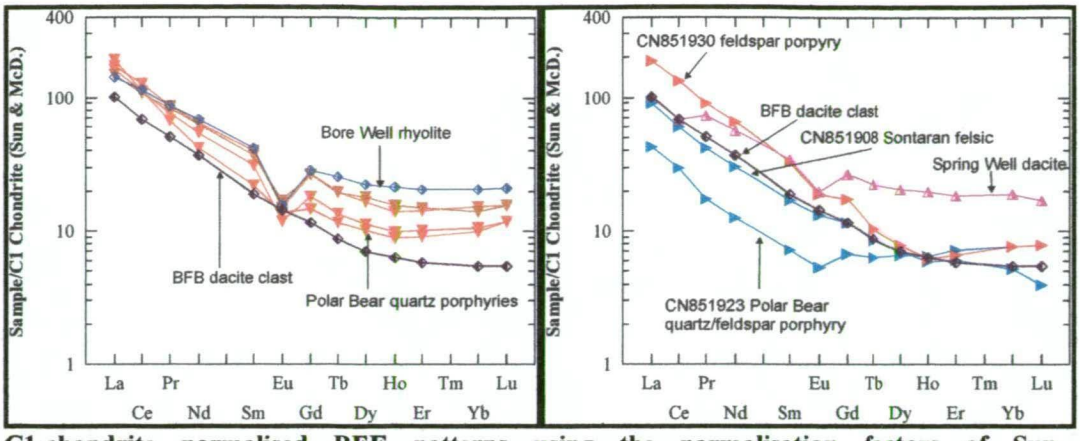

C1-chondrite normalised REE patterns using the normalisation factors of Sun & McDonough (1989). Figure 8.22: Polar Bear quartz porphyries with reference Bore Well, Spring Well and BFB samples using analyses of Barley & others (1998). Figure 8.23: Polar Bear feldspar porphyry, Sontaran felsic and quartz/feldspar porphyry with reference Spring Well and BFB samples using analyses of Barley & others (1998).

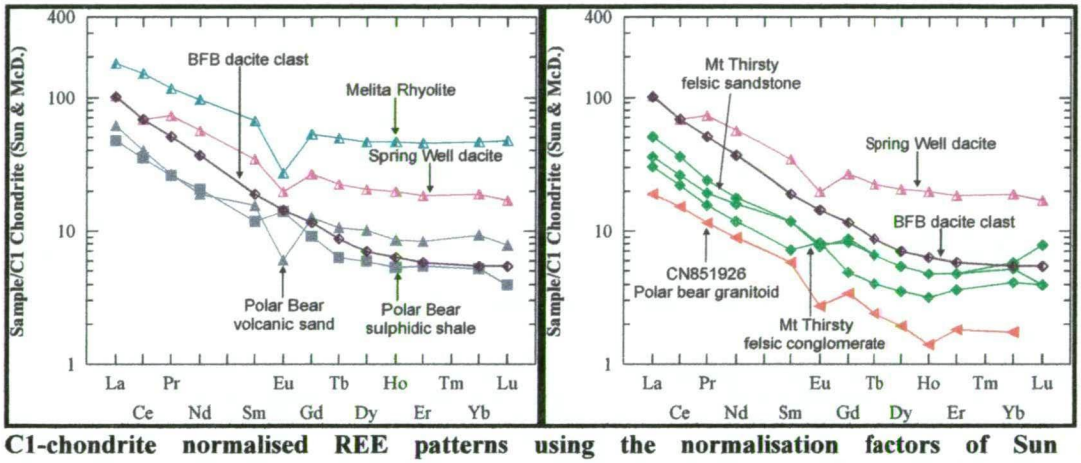

C1-chondrite normalised REE patterns using the normalisation factors of Sun & McDonough (1989). Figure 8.24: Polar Bear sediments with reference Spring Well, Melita and BFB samples using analyses of Barley & others (1998). Figure 8.25: Mt Thirsty epiclastic rocks, and Polar Bear granitoid with reference Spring Well and BFB samples using analyses of Barley & others (1998).

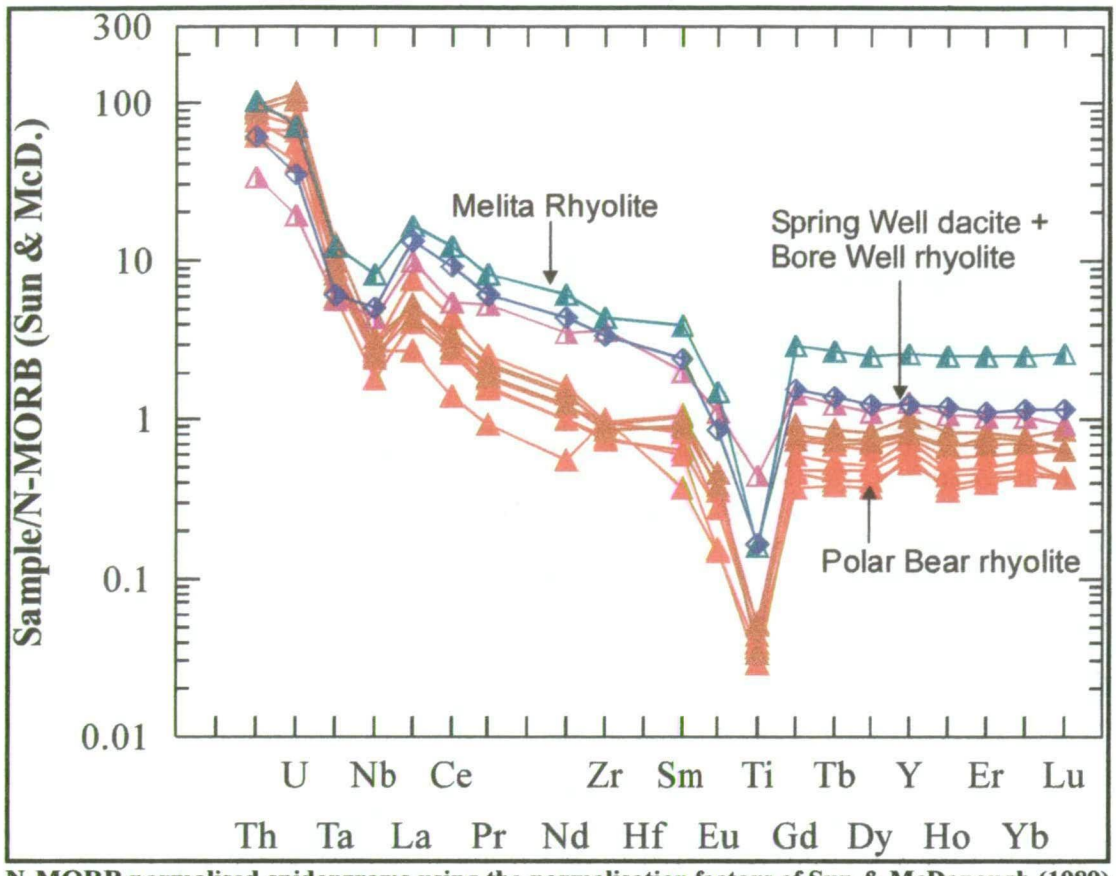

N-MORB normalised spidergrams using the normalisation factors of Sun & McDonough (1989).
Figure 8.26: Polar Bear rhyolites with reference Bore Well and Spring Well felsic rocks using analyses of Barley & others (1998).

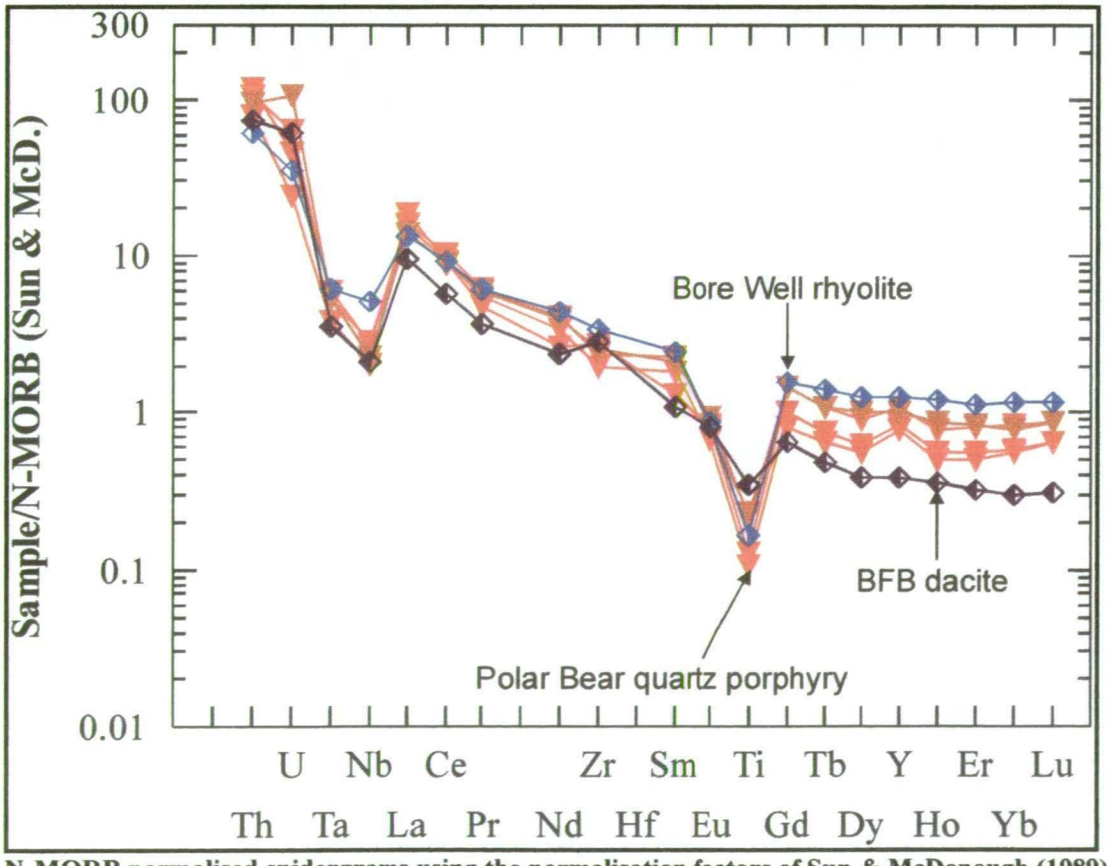

N-MORB normalised spidergrams using the normalisation factors of Sun & McDonough (1989).
Figure 8.27: Polar Bear quartz porphyries with reference Bore Well, Spring Well and BFB samples using analyses of Barley & others (1998).

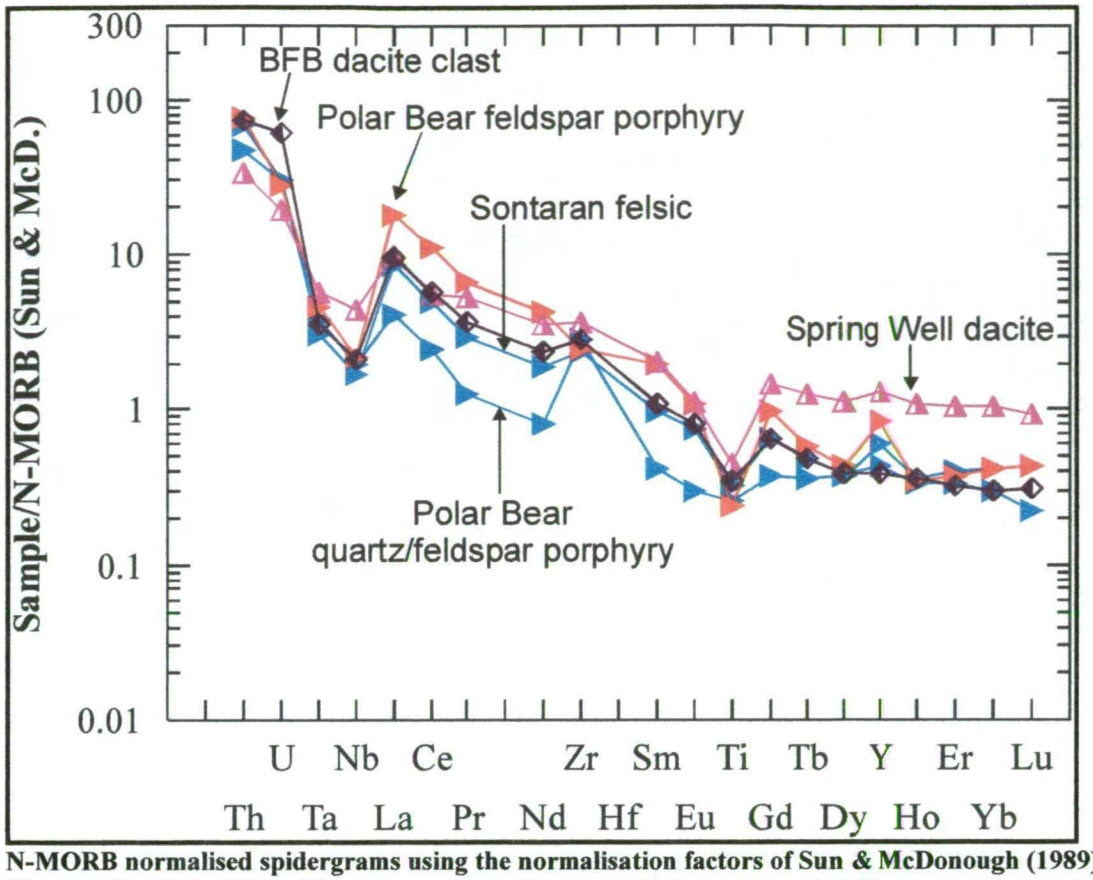

N-MORB normalised spidergrams using the normalisation factors of Sun & McDonough (1989).
Figure 8.28: Polar Bear feldspar porphyry, Sontaran felsic and quartz/feldspar porphyry with reference Spring Well and BFB samples using analyses of Barley & others (1998).

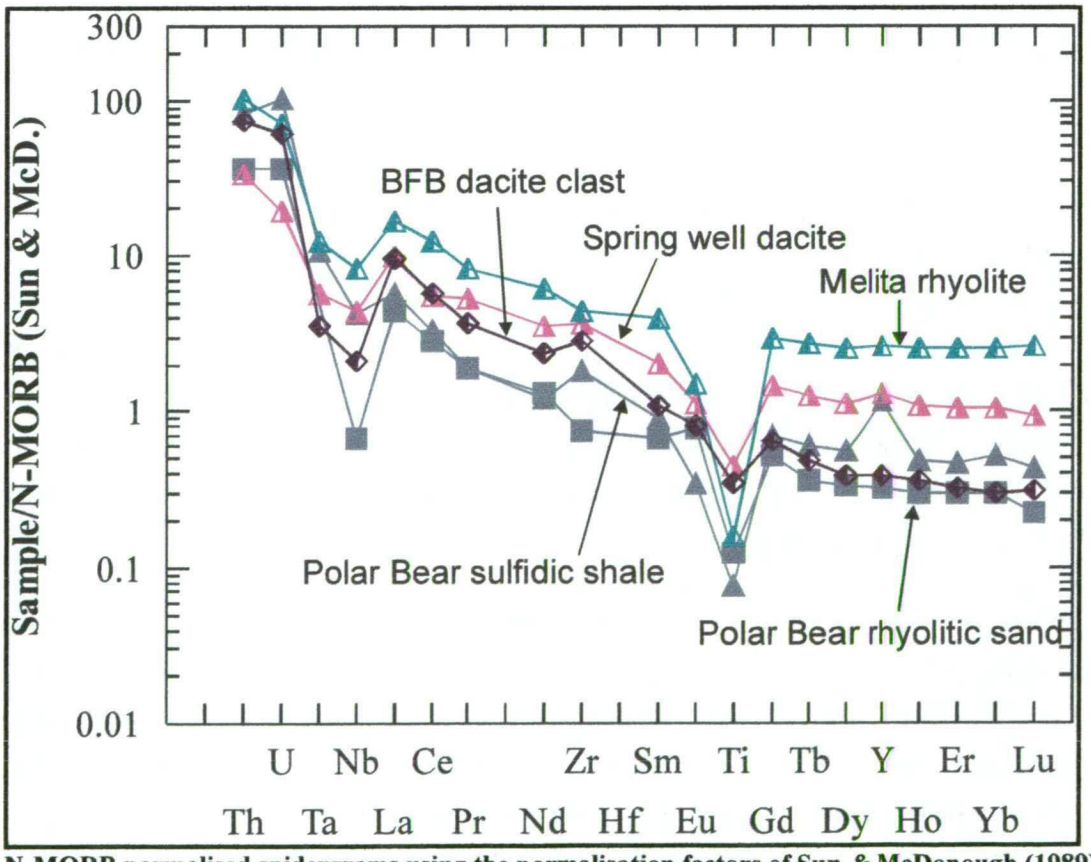

N-MORB normalised spidergrams using the normalisation factors of Sun & McDonough (1989).
Figure 8.29: Polar Bear sediments with reference Spring Well, Melita and BFB samples using analyses of Barley & others (1998).

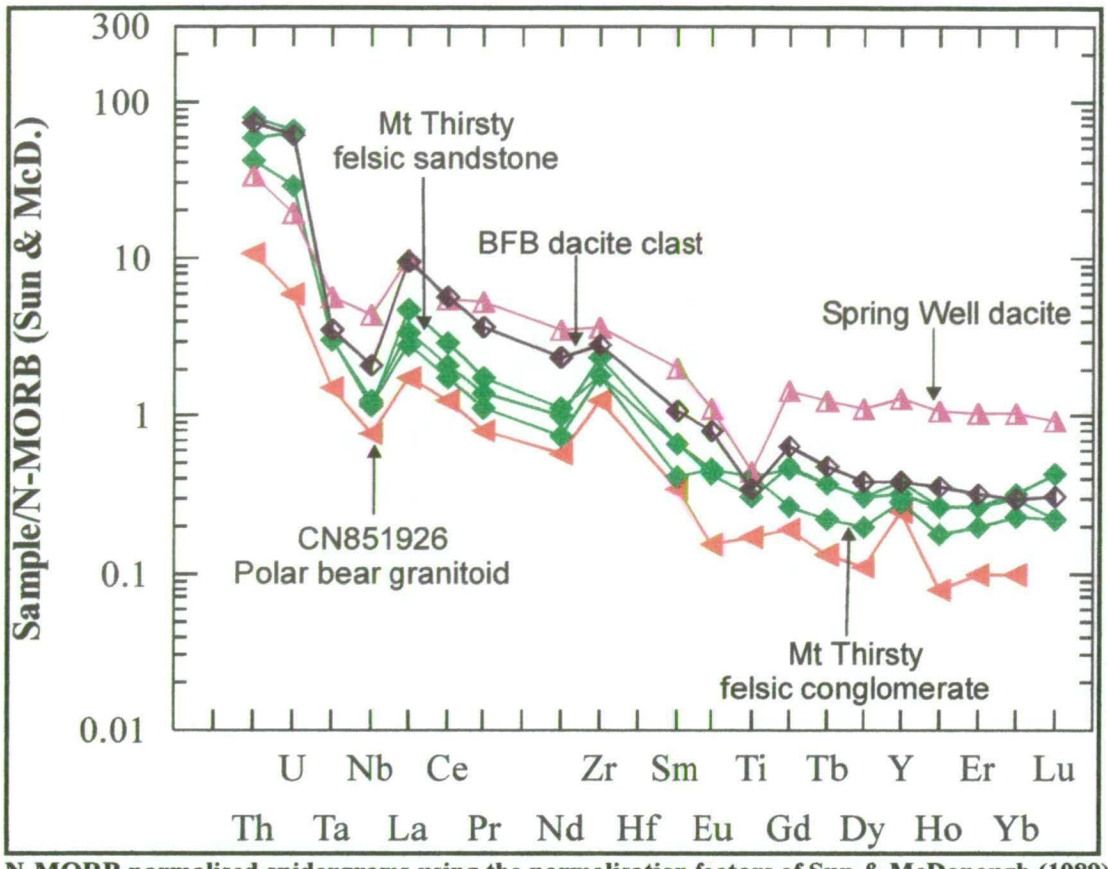

N-MORB normalised spidergrams using the normalisation factors of Sun & McDonough (1989). Figure 8.30: Mt Thirsty epiclastic rocks, and Polar Bear granitoid with reference Spring Well and BFB samples using analyses of Barley & others (1998).

8.3.3 Classification & petrogenetic groupings: volcanics & subvolcanics

8.3.3.1 Rhyolites

The rhyolites have high silica, generally 75-80 wt% and plot as calc-alkaline and high-K calc-alkaline in figure 8.16. They are also classified as calc-alkaline rhyolite and rhyolite in figures 8.17 & 8.18, which use immobile elements. There is almost no calcium in the rocks, probably due to calcium mobility, and as a consequence the rhyolites plot along the base of the An-Ab-Or plot (figure 8.19). Overall, it appears they may be classified as high silica, Calc-Alkaline (CA) rhyolites although it will be argued in section 8.4.4.1 that they have transitional characteristics between calc-alkaline and tholeiitic rhyolites.

The rhyolites have rather similar REE patterns to felsic volcanic rocks from associations 1 & 2 (>2700 Ma CA andesites & 2690 Ma CA silicic) albeit at lower levels (see figure 8.21) and the shapes of the REE patterns are almost identical to association 3 rhyolites from Melita, but at much lower abundances. HREE are flat, there is a strong, negative Eu anomaly and the LREE steepen, with a slight concave upwards shape. The spidergrams (figure 8.26 have a small negative Nb anomaly and highly depleted Ti. There is no negative Ta anomaly

Rhyolite is assigned to a petrogenetic group called "group-A" that will be discussed further in section 8.4.4.

8.3.3.2 Quartz Porphyry

Based on major elements, quartz porphyries cam be assigned to two groups, probably due to mobility of alkali and alkali earth elements. The two batch #1 samples were taken from adjacent RC drill holes and were unweathered and apparently unaltered, whereas the batch #2 samples from surface outcrops were heavily sericitised. Using K_2O vs SiO_2, the quartz porphyries extend from the tholeiitic field to high-K calc-alkaline (figure 8.16). They have even higher silica than the rhyolites (77 wt% to 82 wt%) and alumina is variable (12.3 to 16.7 wt%). The batch #1 samples have high Ca and very low K so plot very high on the An-Ab-Or diagram (figure 8.19)whereas batch #2 samples have no Ca and plot along the base. In the Jensen cation diagram (figure 8.18), batch #1 are classified as calc-alkaline dacites whereas batch #2 are calc-alkaline rhyolites. In figure 8.17 using immobile elements, the samples plot largely in the rhyodacite/dacite fields, with two samples lying in the rhyolite field and with no separation between batches.

It is difficult to classify the quartz porphyries due to the mobility of the alkalies. It was suggested in Chapter 3 that the sodic plagioclase may indicate a trondhjemitic affinity, but it could also be explained by alteration or metamorphism-related albitisation. The chemical analyses are highly variable but are most consistent with rhyodacite, possibly of the calc-alkaline series.

In terms of trace elements, one of the batch #1 "quartz porphyries" was found to have identical characteristics to the Harlequin Porphyry and is added to that group. The remainder of the quartz porphyries have higher overall abundances of REE than the Polar Bear rhyolites and a steeper pattern. They also differ by having concave-upwards rather than flat HREE-MREE patterns. The abundances are similar to the associations 1 & 2, but the LREE are slightly steeper. The LREE shape is parallel to association 4 (BFB) but the HREE are flatter and there is a prominent negative Eu anomaly (figure 8.22). The spidergrams also resemble associations 1 & 2 with strong negative anomalies for Ta, Nb and Ti (figure 8.27).

Quartz porphyry is assigned to a petrogenetic group called "group-B" which will be further discussed in section 8.4.4.

8.3.3.3 Feldspar Porphyry

The feldspar porphyry (CN851930) from the Polar Bear Peninsula is a high-silica, calc-alkaline, rhyodacite or dacite (figures 8.16-8.18) with moderate alumina

(12.9 wt%). It plots at the base of the An-Ab-Or diagram as there is almost no Ca in the rock, probably due to alkali and alkali earth mobilization (figure 8.19). The REE pattern is very steep, resembling association 4 (BFB) except for a very slight negative Eu anomaly (figure 8.23). The MREE-HREE are concave upwards. The spidergram also resembles association 4 with strong negative Ta, Nb and Ti anomalies (figure 8.28).

Feldspar porphyry is assigned to a petrogenetic group called "group-G" which will be further discussed in section 8.4.4.

8.3.3.4 Granitoid

One sample (CN851926) of the granitoid dyke that extends along the shoreline at north Polar Bear was analysed. It has low Ca abundances similar to the rhyolite and quartz porphyry but has higher Na so that it plots in the trondhjemite field of figure 8.19. Alumina is 16.24 wt% indicating the high-Al TTD suite. Immobile trace elements indicate a dacite or rhyodacite bulk composition (figure 8.17).

The granitoid has a steep REE pattern similar in shape to the BFB dacites but at much lower levels (figure 8.25). There is a small negative Eu anomaly and an unusual negative Ho anomaly. It has an irregular spidergram without a negative Ti anomaly and with positive Zr and Y anomalies (figure 8.30).

The cause of some irregularities of the spidergram and REE pattern can be explained as analytical error caused by the extreme depletion of the heavier incompatible elements, particularly the MREE & HREE. Ho, for instance, which has a small negative anomaly, was analysed at 0.08 ppm, whereas the anomaly would be eliminated if it were 0.10 ppm. The optimistically quoted detection limit of ICP-MS is 0.05 ppm for Ho, so the element abundance is at the near-detection-limit-level where ICP-MS is imprecise (see Appendix 2 for further discussion about analytical issues). Lu abundances were so low that none was detected.

A similar problem is thought to cause the positive Y spike in the spidergrams. The Y analysis is 7 ppm, a level far below that of the basalts and matched only by the ultramafic rocks. An abundance of 3 ppm would be required to remove the anomaly, but that is the quoted detection limit of Y (analysed with XRF), so again the problem appears to be imprecision of the analytical technique caused by background "noise" as the element abundance approaches the optimal detection limits. The Ti and Zr abundances are well above detection limits and are similar to patterns for Mount Thirsty rocks, hence they are regarded as accurate.

Ignoring the erratic results for Ho, the overall REE pattern is steep with extreme depletion of the heavier REE. It mimics the BFB trend but at a much lower total abundances, commencing at basalt levels then sinking far below. Similarly, if erratic spikes in the spidergrams are ignored, then the pattern again is steep, with a small negative anomaly at Nb and Ta.

The granitoid is assigned to a petrogenetic group called "group-D" which will be discussed further in section 8.4.4.

8.3.3.5 Other felsic rocks

There are two individual felsic rocks that were not recognized as belonging to any identified field groupings. One of these was a felsic rock from diamond drill core at Sontaran, originally interpreted as a mafic rock. The second is a rock similar to quartz porphyry but with unusually sparse quartz phenocrysts and high abundances of feldspar phenocrysts.

The Sontaran sample (CN851908) is considered to be dacite of the high-Al TTD suite, consistent with its plotted position in all the classification diagrams (figure 8.16-8.19) and the alumina content of 15.72 wt% at 69.4 wt% SiO2. It has a REE pattern and spidergram almost identical in shape and element abundance to dacite clast from the BFB (figure 8.23 & 8.28). Sample CN851908 is assigned to petrogenetic "group-C" which will be further discussed in section 8.4.4.

The quartz-feldspar porphyry sample (CN851923) has high silica and very low calcium levels like many of the quartz porphyry samples at the Polar Bear Peninsula, possibly caused by element mobilization. It plots inconsistently on the classification diagrams (figure 8.16-8.19) but appears to be calc-alkaline and has either a dacite or rhyodacite composition based on immobile trace elements (figure 8.17). The REE pattern of this rock is similar in shape to the Spring Well dacites but at lower levels. It also resembles the REE patterns of the rhyolites from the Polar Bear Peninsula with the exception of the negative Eu anomaly which is much less pronounced (figure 8.23). The negative Ti anomaly in the spidergram is also weak in comparison to the rhyolites and Zr is anomalously high (figure 8.28).

Quartz-feldspar porphyry is assigned to a petrogenetic group called "group-E" which will be further discussed in section 8.4.4.

8.3.3.6 Volcanogenic Sediments

Two sedimentary rocks from the Polar Bear Peninsula were analysed. One was a volcanic sandstone from central Polar Bear. The other was a partially weathered sulfidic black shale. Neither of the samples can be classified geochemically on the

basis of major elements as the abundances fall outside the bounds of most igneous rocks. However, immobile trace elements may be used to determine the geochemistry of the source, consistent with the work of Hand (1998), who found that sandstone and mudrock facies of the BFB have very similar immobile trace element compositions to andesite-dacite clasts.

In terms of trace elements, the volcanic sand (CN851931) plots as a rhyolite on figure 8.17 and has a REE pattern identical to the Polar Bear rhyolites (figure 8.24). It is considered to be resedimented rhyolitic sand.

The black shale sample (CN851496) has a REE pattern and spidergram rather similar to the dacitic BFB (figure 8.25 & 8.29), suggesting it may be derived from the BFB volcanic source. As these samples are not magmas, they are not assigned to any petrogenetic groups and will not be discussed in the next section. However, they are considered in the conclusion, section 8.7.

8.3.3.7 Felsic epiclastic rocks (from east of Mt Thirsty)

The felsic epiclastic samples from the southern Coolgardie Domain (see section 6.3.9) are from adjacent to the highway, east of Mt Thirsty. They are called the "Mt Thirsty samples" in this study. The samples are low-K series based on the K_2O-SiO_2 diagram (figure 8.16), but lie within the calc-alkaline field on the Jensen cation plot (figure 8.18). The dominant alkali is Na and alumina is elevated (14-17 wt%). The samples plot within or at the boundaries of the trondhjemite field in the An-Ab-Or diagram (figure 8.19). The evidence is consistent with the epiclastic rocks being members of the high-Al TTD suite. The immobile trace elements classify the rocks as andesite and dacite (figure 8.17) but the high silica (73-76 wt%) indicate that these rocks are dacites, not andesites. Quartz does not appear to have been concentrated during the sedimentation process as the conglomerate has similar abundances as the sands (73.9 wt%).

REE show a similar steep pattern with no Eu anomaly to the BFB dacite clasts but with lower overall abundances (figure 8.25). Spidergrams are likewise similar to the BFB except there is no negative Ti anomaly and the positive Zr anomaly is of greater magnitude than that in the BFB (figure 8.30).

The felsic epiclastic rocks from the Mt Thirsty area are assigned to petrogenetic group "group-D" which will be further discussed in section 8.4.4.

8.3.4 Geochemical Results for Small Felsic Intrusions ("Porphyries")

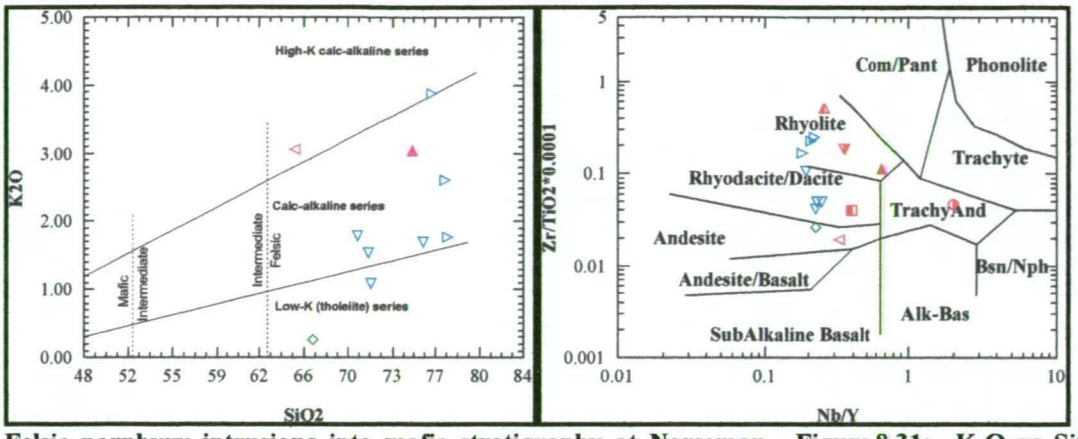

Felsic porphyry intrusions into mafic stratigraphy at Norseman. Figure 8.31: K_2O vs SiO_2 classification diagram with the series subdivisions of Le Maitre & others (1989). Figure 8.32: Zr x 10 000/TiO_2 vs Nb/Y (immobile element) classification diagram of Winchester & Floyd (1976).

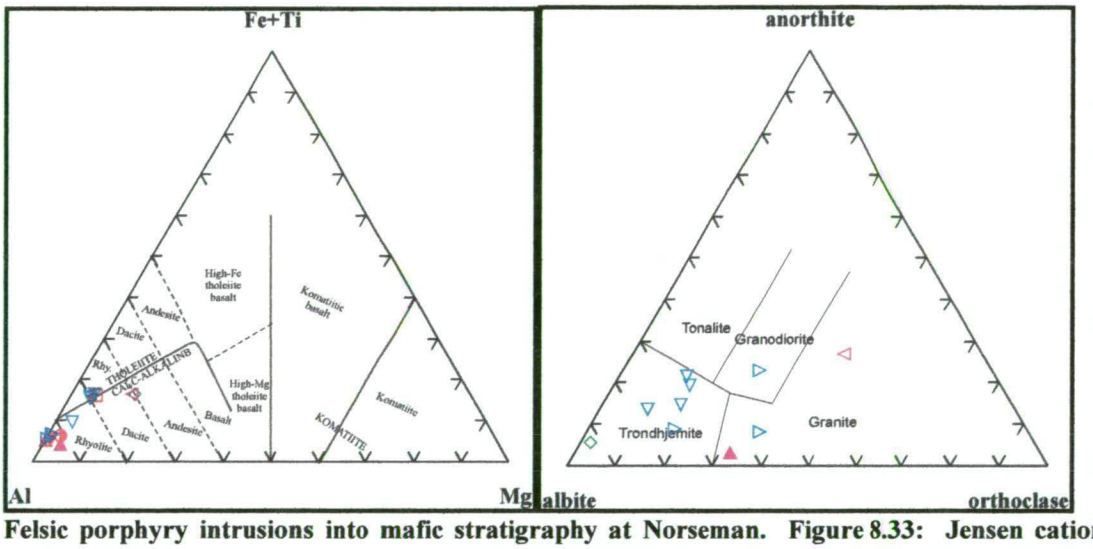

Felsic porphyry intrusions into mafic stratigraphy at Norseman. Figure 8.33: Jensen cation plot classification diagram. Figure 8.34: Molecular normative Ab-An-Or diagram after Barker (1979), showing the trondhjemite field.

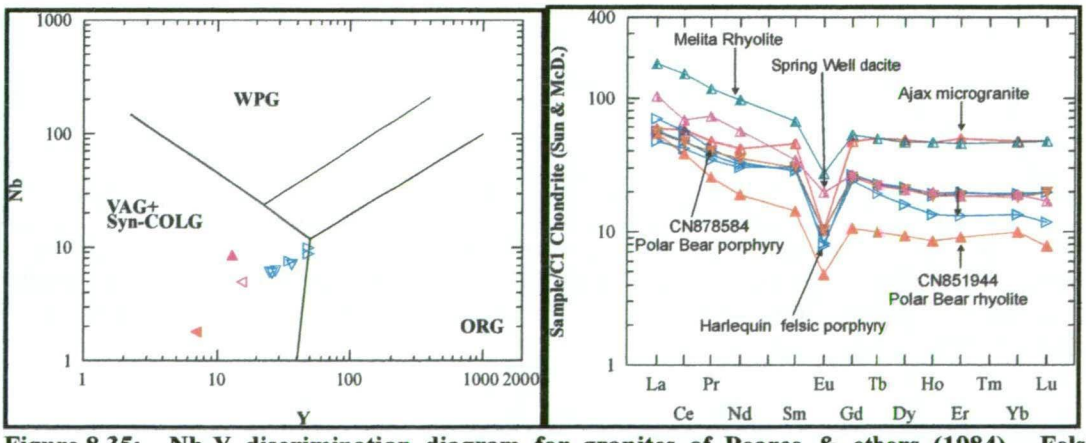

Figure 8.35: Nb-Y discrimination diagram for granites of Pearce & others (1984). Felsic porphyry intrusions into mafic stratigraphy at Norseman. VAG & syn-COLG = volcanic arc granites and syn-collisional granites. Figure 8.36: C1-chondrite normalised REE patterns using the normalisation factors of Sun & McDonough (1989). Harlequin porphyry with reference Polar Bear rhyolite, Ajax microgranite & porphyry using the data of Perring (1989) and BFB dacite using analyses of Barley & others (1998).

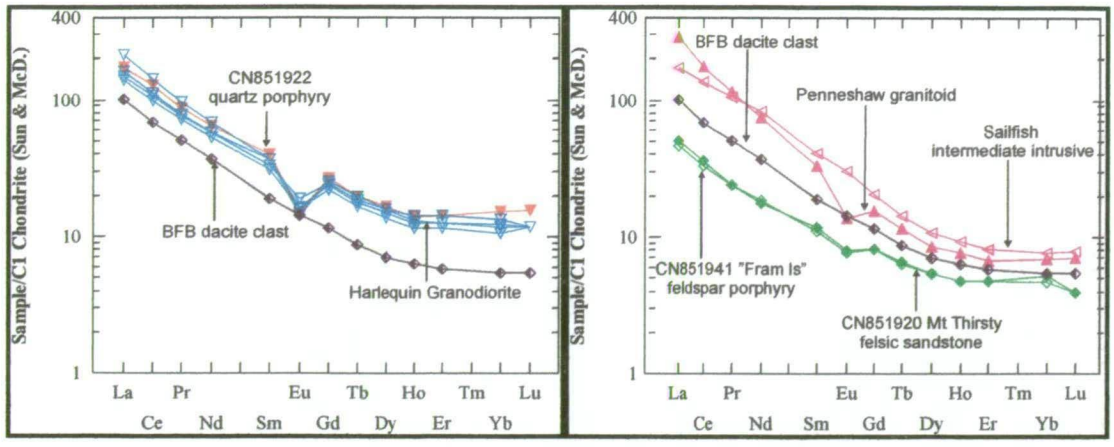

C1-chondrite normalised REE patterns using the normalisation factors of Sun & McDonough (1989). Figure 8.37: Harlequin "Granodiorite" with reference Polar Bear quartz porphyry & BFB dacite using analysis of Barley & others (1998). Figure 8.38: Fram island and Sailfish Porphyries with reference Mt Thirsty epiclastic & BFB dacite using analysis of Barley & others (1998). Sailfish and Penneshaw samples from Ghaderi (1998).

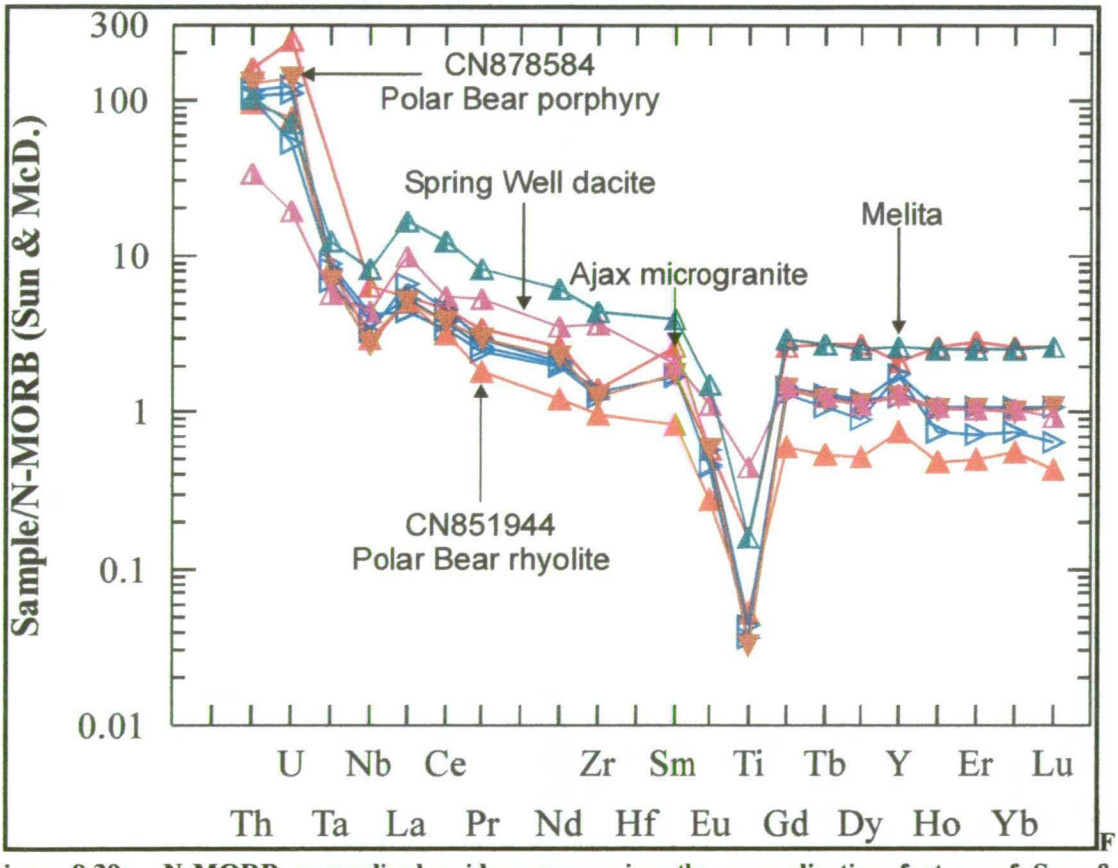

Figure 8.39: N-MORB normalised spidergrams using the normalisation factors of Sun & McDonough (1989). Harlequin porphyry with reference Polar Bear rhyolite, Ajax microgranite & porphyry using the data of Perring (1989) and BFB dacite using analyses of Barley & others (1998).

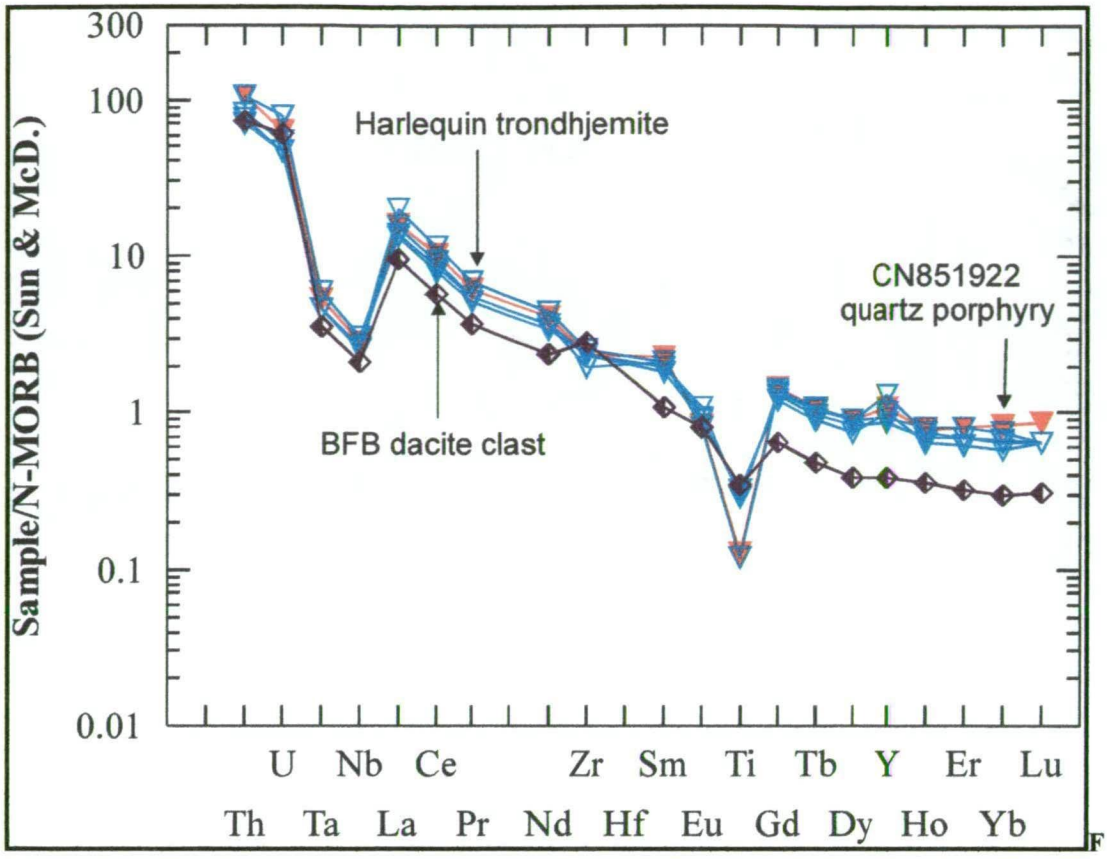

Figure 8.40: N-MORB normalised spidergrams using the normalisation factors of Sun & McDonough (1989). Harlequin "Granodiorite" with reference Polar Bear quartz porphyry & BFB dacite using analysis of Barley & others (1998).

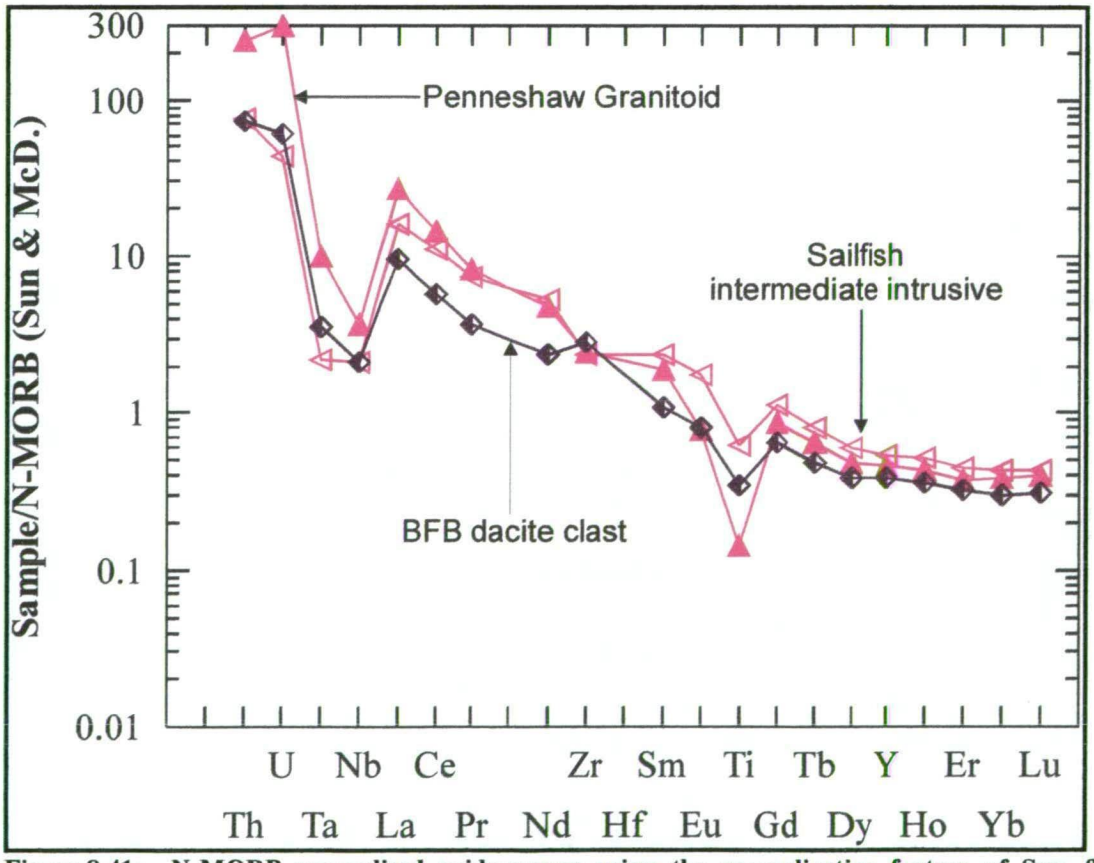

Figure 8.41: N-MORB normalised spidergrams using the normalisation factors of Sun & McDonough (1989). Sailfish porphyry and Penneshaw granitoid from Ghaderi (1998) with reference BFB dacite using analysis of Barley & others (1998).

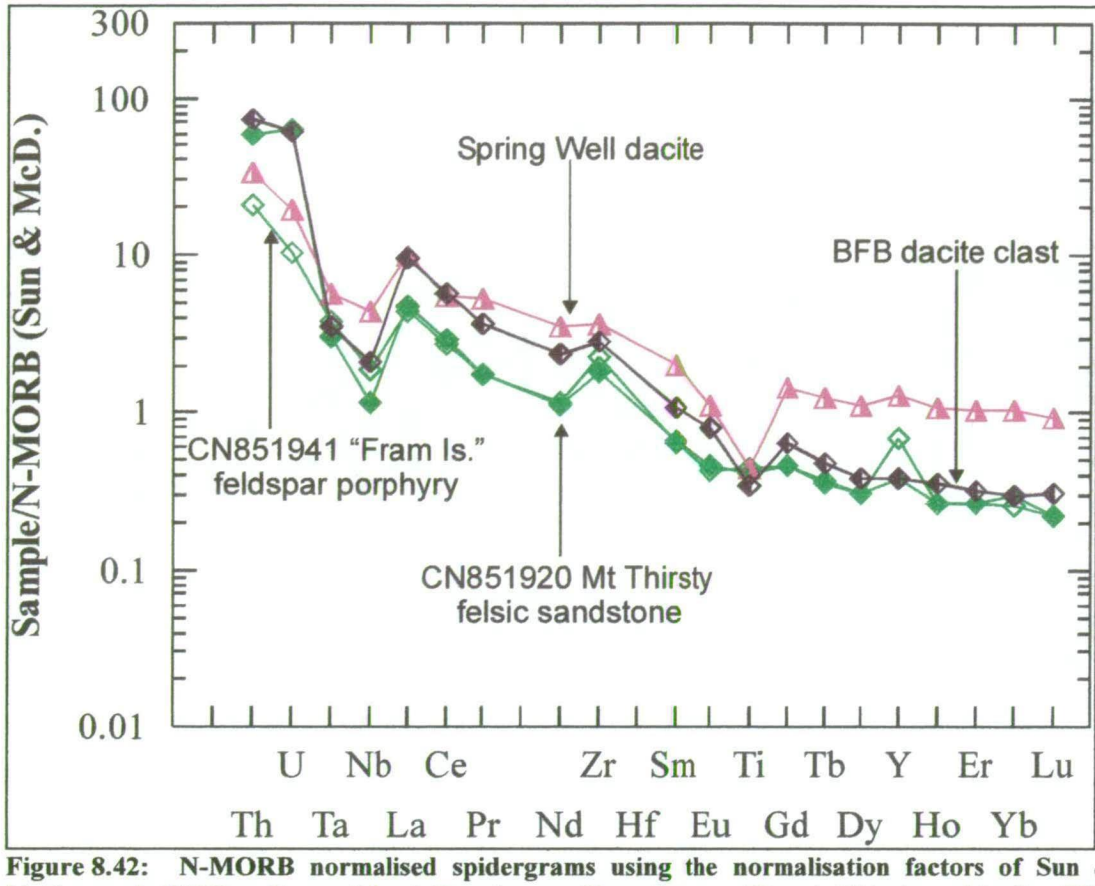

Figure 8.42: N-MORB normalised spidergrams using the normalisation factors of Sun & McDonough (1989). Fram Island Porphyry with reference Mount Thirsty epiclastic; BFB dacite & Spring well dacite using analyses of Barley & others (1998).

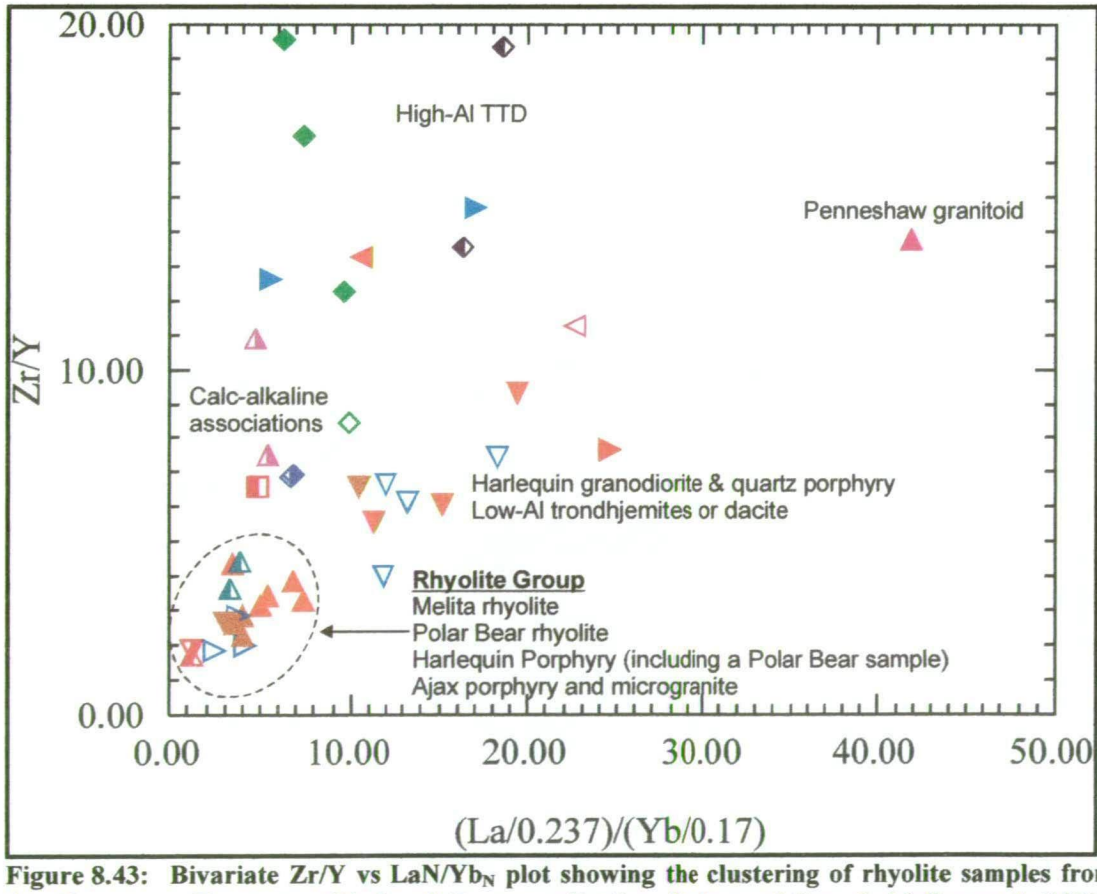

Figure 8.43: Bivariate Zr/Y vs LaN/Yb_N plot showing the clustering of rhyolite samples from the Norseman Terrane. C1-chondrite normalisation factors of Sun & McDonough (1989). Samples from this study, Barley& others (1998), Perring (1989) and Ghaderi (1998).

8.3.5 Classification & petrogenetic groupings, porphyry intrusions

8.3.5.1 Harlequin porphyry

The Harlequin porphyry borders the eastern margin of the Harlequin "granodiorite". It is sparsely porphyritic and was described in Chapter 3. A sample consisting of reverse circulation percussion drill chips from the Polar Bear Peninsula (CN878454), thought to be quartz porphyry is added to the group due to its identical REE pattern and spidergram.

The Harlequin porphyry has a rather uniform SiO_2 of 76-77 wt% but K_2O values vary significantly (figure 8.31). It has a highly restricted composition at the upper end of calc-alkali rhyolite field on the Jensen cation plot (figure 8.33) and immobile elements also indicate a rhyolite composition (figure 8.32). K, Ca & Na abundances are variable, probably due to mobilization so the porphyry plots at diverse compositions on the An-Ab-Or diagram (figure 8.34). It is classified as calc-alkaline rhyolite.

Hodgkison (1995) pointed out that the Harlequin porphyries are compositionally and texturally similar to the Ajax suite of rhyolite porphyries documented by Perring (1989), the most abundant felsic porphyries in the Norseman field. There are also geochemical and textural similarities between the Harlequin Porphyry and the rhyolite lava at the Polar Bear Peninsula. These three rock types (Harlequin Porphyry, Ajax suite and Polar Bear rhyolite) are similar in that they are all high-silica rhyolites with sub-equal abundances of K_2O & Na_2O, they have flat HREE with flat to sloping LREE and very strong negative Eu anomalies. The spidergrams have intense Ti depletion, a small negative anomaly for Nb but not Ta, and high U and Th abundances (figure 8.39). The differences between the groups are the abundances of REE and somewhat different (but flat) patterns.

It was pointed out in section 8.3.3.1 that the Polar Bear rhyolites have similarities to the Melita samples but with lower REE abundances. The Harlequin Porphyry and Ajax suite have higher REE, closer to those of the Melita samples but with flatter REE patterns (figure 8.36).

The similarity of these groups, Ajax rhyolite suite, Harlequin porphyry, Polar Bear rhyolite and association 3 rhyolites (Melita) is shown in figure 8.43. All these samples cluster closely in a bivariate plot of the ratios Zr/Y against La_N/Yb_N and are clearly separate from the other sample groups. The basis for using this diagram is that these ratios have been used to delineate Archaean felsic rocks prospective for VHMS deposits by Lesher & others (1986). The La_N/Yb_N ratio reflects the slope of the chondrite-normalised REE profiles. Because La and Zr have similar

incompatible element behaviour and Yb and Y even more so, the Zr/Y ratio closely corresponds with the LaN/YbN ratio in most intermediate to felsic sequences (Lentz, 1998). Low LaN/YbN values are characteristic of tholeiitic sequences and high ratios are indicative of calc-alkaline affinity caused by the higher partition coefficients of HREE in amphiboles and garnets for intermediate to felsic magmas (see section 8.4.2.4). Therefore, the tight clustering of the rhyolites close to the origin of the diagram indicates their flat REE patterns and affinity towards tholeiitic rather than calc-alkaline rocks. The contrary interpretations of the affinity of the Harlequin Porphyry as calc-alkaline using K_2O vs SiO_2 and the Jensen cation plot, and tholeiitic using the shape of normalized trace element diagrams, is discussed with the petrogenesis in section 8.4.4.1.

Due to the similarities between the groups, the Harlequin Porphyry is assigned to the same petrogenetic group as the Polar Bear rhyolite, "group-A".

8.3.5.2 Harlequin granodiorite

The Harlequin granodiorite analyses cluster rather tightly on the K_2O-SiO_2 plot in comparison to the volcanic rocks from the Polar Bear Peninsula (figure 8.31), indicating lower mobilities of LILE. They plot largely within the calc-alkali field. On the Jensen cation plot they lie in the tholeiitic rhyolite field very close to the calc-alkali boundary (figure 8.33) and in the trondhjemite field of the An-Ab-Or plot.(figure 8.34). Immobile elements suggest a rhyodacite or dacite composition (figure 8.32). The trondhjemitic affinity accords with the sodic character of the feldspars noted in Chapter 3, however, the Al_2O_3 abundances are all below 15 wt%, hence it appears to be a dacitic member of the low-Al TTD suite, or with regard to its grain size, a low-Al trondhjemite.

The Harlequin trondhjemite ("granodiorite") has a steep REE pattern similar to the BFB dacites, apart from a strong Eu anomaly (figure 8.37). The steep character is more akin to the high-Al TTD suite than low-Al. The pattern is almost identical to that of the quartz porphyry from the Polar Bear Peninsula in both levels and shape. The spidergrams are also similar to the quartz porphyry and BFB dacites, and have strong depletions in Ta, Nb and Ti (figure 8.40).

Based on the similarity of the trace element patterns to quartz porphyry, the Harlequin trondhjemite is assigned to petrogenetic "group-B".

8.3.5.3 Sailfish Porphyry

The Sailfish porphyry was analysed by Ghaderi (1998) and the analysis is included here to enable a thorough representation of all the "porphyries" at Norseman. At

65 wt% SiO_2, it is the least silicic sample included, but the Al_2O_3 levels are very high at 18.4 wt%. It falls in the high-K calc-alkali field of the SiO_2 vs K_2O diagram (figure 8.31) and in the calc-alkali andesite–dacite boundary on the Jensen cation plot (figure 8.33). Using immobile elements it is classified as andesite (figure 8.32) or granite using the An-Ab-Or diagram (figure 8.34). The diverse classifications suggest the alkalies have been mobile. The sample is dacite based on the silica abundance which is considered to be consistent with the immobile element classification of an andesite as the silica contents are close to the andesite-dacite division of 63 wt%. The Jensen cation plot accurately reflects the transitional nature of the sample.

The Sailfish porphyry has a very steep REE pattern parallel to a dacite clast from the BFB but at higher overall abundances (figure 8.38). The spidergram is also similar to the BFB with Ta, Nb and Ti depletions (figure 8.41). The steep REE pattern, and the high alumina abundance suggests the sample is a member of the high-Al TTD suite. The elevated K in the rock is considered to be a result of K-metasomatism.

Based on its similarity to the BFB sample and in particular the feldspar porphyry from the Polar Bear Peninsula, the porphyry is assigned to petrogenetic "group-C".

8.3.5.4 Fram island feldspar porphyry

The Fram island porphyry is a feldspar-phyric sample collected from diamond core drilled at a small island off the western shore of Lake Cowan known informally as "Fram island". The porphyry has silica contents of 67 wt% SiO_2, elevated alumina at 16.4 wt% and plots in the low-K field (figure 8.31). It lies on the calc-alkali andesite–dacite boundary of the Jensen cation plot (figure 8.33), is classified as andesite by immobile elements (figure 8.32) and trondhjemite by the An-Ab-Or diagram (figure 8.34). The silica abundances are too high for an andesite so it is considered to be dacite, although at the mafic end of that range which may explain the immobile element classification. The characteristics are all consistent with the sample being a dacite member of the high-Al TTD suite.

The REE pattern of the Fram Island sample is steep but with lower overall abundances than the reference BFB dacite clast and with a very subtle negative Eu anomaly (figure 8.38). The trace element characteristics of the spidergram are almost identical to the Mt Thirsty epiclastic samples with a positive Zr and no Ti anomaly (figure 8.42), hence the sample is assigned to petrogenetic group F.

8.3.5.5 Penneshaw Granitoid

An analysis of Penneshaw granitoid by Ghaderi (1998) is the only trace element data that exists for the felsic rocks dated at *ca.* 2930 Ma in the western Penneshaw Domain. The sample was from granitoid towards the bottom of diamond hole PE1 for which the log was presented in Chapter 7. It was included in this geochemical compilation for completeness.

It has about 76 wt% silica, 16 wt% alumina and the K_2O contents of the calc-alkaline suite (figure 8.31). On the Jensen cation plot it lies in the calc-alkaline rhyolite field (figure 8.33) and is a rhyolite based on its immobile trace element characteristics (figure 8.32). It plots in the granite field of the An-Ab-Or diagram (figure 8.34). Based on these characteristics, it is classified as a high-silica, calc-alkaline granite. Some of the characteristics such as alumina and the steep REE patterns are similar to the high-Al TTD suite (see section 8.4.2.2). The K_2O abundances in the sample and the silicic nature of the sample are inconsistent with the high-Al TTD suite sample although these may be altered by element mobility.

The REE pattern is steep, similar to the reference BFB dacite clast but with higher overall abundances and a small negative Eu anomaly (figure 8.38). The spidergram has a strong negative Nb and Ti anomalies, but a weak Ta negative anomaly and is highly enriched U and Th (figure 8.42).

Based on the very high radiogenic elements, the Penneshaw granitoid is considered to be unique and is assigned to a new petrogenetic group E, which will be discussed further in section 8.4.4.

8.4 PETROGENETIC INTERPRETATIONS

8.4.1 Introduction

This section examines the various felsic suites and groups that have been defined and discusses their petrogenesis. The origins of felsic magmas and models for TTD and calc-alkaline silicic melts are examined first to provide framework within which the petrogenesis of the samples can be considered.

8.4.2 Origin of felsic magmas

Silica over-saturated felsic magmas cannot be produced directly from the mantle. Low fraction partial melting of the mantle can yield magmas only as felsic as basaltic-andesite, alkali basalt or boninite (Drummond & Defant, 1990 and references therein). There remain two major categories of petrogenetic models to explain the origin of these magmas: (1) derivation from basaltic parents by fractional

crystallisation or AFC processes; (2) partial melting of crustal rocks. These models are discussed below

8.4.2.1 Derivation from basalt by FC or AFC

This model allows the production of relatively small volumes of magma only, as the production of batholith-size magma batches would require the crystallisation of an unreasonably large volume of basalt (Borg & Clynne, 1998). 90% crystallisation of a tholeiitic basalt is necessary to produce a felsic rock with a trondhjemitic composition, thus the felsic derivative should be volumetrically unimportant in comparison to the accompanying mafic and intermediate products of fractional crystallisation (Drummond & Defant, 1990 and references therein). The dearth of intermediate crystallisation products such as diorite or andesite in comparison to the abundance of felsic rocks in Archaean sequences suggests the role of fractional crystallisation as an origin for these felsic magmas is minor.

8.4.2.2 Derivation by partial melting of crust

This model allows great volumes of felsic magma to be produced but requires a thermal anomaly beneath the crust to provide heat for melting. This thermal anomaly is commonly attributed to basaltic underplating that may be coupled with crustal thinning.

Crustal melting can be divided into two types: fusion of mid-continental crust with a bulk composition thought to be intermediate to felsic and fusion of lower continental crust or oceanic crust with a broadly mafic composition.

Partial melting of mid-continental crust

A large number of granite studies have examined the melting of continental crust. "S"-type granites are attributed to melting of rocks which have been exposed to weathering processes whereas "I"-type granites are believed to be derived by melting intermediate composition igneous rocks that have not been exposed to weathering processes (Chappell & White, 1974). More recently, "A"-type, within-plate, anorogenic granites (Whalen, & others, 1987) have been defined, typified by a strong enrichment in HFSE. These magmas are essentially tholeiitic felsic rocks (Lentz, 1998) and have been variously interpreted as being sourced from the mantle, the lower crust, or remelting of melt-depleted, granulite or mafic crustal underplate (Craske, 1997). They characteristically occur in anorogenic intracratonic rift settings. At their least evolved end member, they overlap the compositions of I-type and S-type granites. Perring (1989) suggested the Ajax Porphyry has affinities to A or

S-type granites and suggested it was produced by crustal melting (see section 8.4.3.4).

Partial melting of basaltic crust

Fusion of lower continental crust and possibly oceanic crust is believed to be important in magma generation at convergent margins. Borg & Clynne (1998) argued that rhyolites in the southern Cascades volcanic arc in North America are the result of melting underplated arc-derived basalts. Drummond & Defant (1990) postulated that high-Al TTD suite are related to fusion of subducted oceanic crust.

As all the samples analysed for this study have the characteristic Ta, Nb & Ti-depleted signature of subduction-style processes and some of the samples belong to the TTD suite, partial melting of basaltic crust will be examined in some detail. TTD magma models are described first, followed by a discussion of high-silica calc-alkali models.

8.4.2.3 Origin of TTD magmas

It was noted in section 8.2.3 that the TTD suite can be divided into low-Al and high-Al types with different geochemical characteristics. These disparities are believed to be caused by differing processes involved in the genesis of the magmas.

The geochemical signature of the low-Al type TTD suggests that they were generated either by low-pressure (<5 kb) fractionation or partial melting where plagioclase + pyroxene differentiation was important and garnet and hornblende were not involved (Drummond & Defant, 1990).

The high-Al type TTD is attributed to either fractionation of a wet basalt or partial melting of a former basalt altered to amphibolite or quartz eclogite. This conclusion is based largely upon the steep REE patterns that require subtraction of a mineral with an affinity for the heavier REE. Drummond & Defant (1990) suggested the high Al_2O_3 levels may result from the presence of subaluminous hornblende in the petrogenesis; the removal of the hornblende from the magma due to fractional crystallisation or as a refractory product in the source would elevate the Al_2O_3 abundances of the resultant magma.

The results of investigations on the liquids produced by partial melting experiments of various types of basalt are also consistent with amphibolite being the source of trondhjemites (McBirney, 1984). Partial melting of amphibolite can produce siliceous magmas, because amphibole has a low silica content; hence any melt in equilibrium with it will be more silica-rich than one formed by partial melting of an equivalent anhydrous assemblage. Regardless of the initial composition of the

amphibole-bearing basalt, with progressive melting, magma compositions become poorer in normative orthoclase as the majority of that component enters the first melt, leaving little in the solid phased so that further melting dilutes the initial concentration. Thereafter silica declines as more amphibole enters the melt. In this way, partial melting of amphibole-rich mafic rocks can yield liquids rich in silica and with large ratios of sodium to potassium.

Drummond & Defant (1990) pointed out that the age and heat content of the downgoing slab in subduction zones appears to have a role in producing high-Al TTD suites at convergent margins. For Cenozoic high-Al TTD production, there is a positive correlation with the subduction of young (<20 Ma) hot, oceanic crustal material and conversely an antithetic relationship with arcs where old oceanic crust is being subducted. Similarly, Archaean terranes have a tremendous volume of high-Al TTD and are thought to have had a higher heat flow driving smaller oceanic plates at faster spreading rates, resulting in subduction of hot plates.

The steep, negatively-sloping, chondrite-normalized REE patterns of high-Al TTD suites indicate high-pressure garnet and/or hornblende extraction. Garnet removal causes a very steep, straight HREE-depleted slope, whereas amphibole involvement causes the slope to be steep but concave upwards (Drummond & Defant, 1990). Anatexis of subducted MORB with sea-floor alteration, leaving quartz eclogite or garnet amphibolite residue, could produce magma with this geochemistry. Under the present tectonic and heat flow regime, the conditions where a subducted slab could produce a TTD melt are highly specific, between 75 and 85 km depth at temperatures of 700° to 775°C. Under Archaean conditions of higher heat flow and possibly smaller oceanic plates with faster spreading rates, the resulting subduction of hotter plates would enlarge the P-T regime under which TTD could form (Drummond & Defant, 1990).

An alternative to slab melting for the origin of high-Al TTD may be partial melting of arc basalts that underplate continental crust in active arcs. Drummond & Defant (1990) suggested that this process could only produce low-Al TTD, as calcic plagioclase would inevitably be left in the restite, producing flat REE patterns with negative Eu anomalies. However, this assertion is not supported by studies of the origin of felsic magmas in the Cascades, (see section 8.4.4.4). These magmas are calc-alkaline, but have concave-upwards REE patterns, which are considered to be the result of partial melting under hydrous conditions leaving amphibole in the residue (Borg & Clynne, 1998).

As pointed out above, the origin of the TTD suite has been suggested to involve amphibole subtraction with or without the involvement of garnet. Similarly, many

authors have invoked amphibole fractionation from hydrous basaltic magmas at depth as a fundamental control in producing the calc-alkaline series (Wilson, 1989 and references therein). Clearly, some other mechanism must be involved in causing one series to have high Na and the other high K. This may, perhaps, be the scale of involvement of LILE-enriched subduction-zone fluids or subducted sediment in the magma genesis. The correlation between the high-Al TTD magmas and the subduction of young oceanic lithosphere pointed out by Drummond & Defant (1990), may indicate that little sediment is subducted with the young plates, so the trend of partial melting follows that described above where melts become increasingly poorer in normative orthoclase with increased melting. Calc-alkaline magmas, on the other hand, are believed to be enriched with LILE by fluids or hydrous melts, which may involve a greater degree of subducted sediment and devolatilisation of the slab.

Whatever the ultimate cause may be, it appears that TTD magmas are emplaced over subduction zones and were particularly voluminous in the Archaean.

8.4.2.4 Origin of felsic calc-alkaline magmas

Most petrogenetic studies of calc-alkaline rock suites have focussed on basaltic magmas, as these are the most primitive lavas within a given suite and are the most informative about the magmas sources (Borg & Clynne, 1998). Felsic magmas have received less petrogenetic attention as they may be highly crystalline and potentially extensively modified by fractional crystallisation and AFC processes.

Felsic calc-alkaline magmas are common at active continental margins. Their presence is a conspicuous difference between island arcs and continental margin calc-alkaline series (Wilson, 1989). Most of the silicic rocks are apparently associated with thickened continental crust and may be derived by partial melting of the crust. These magmas were discussed in section 8.4.2.2. However, felsic magmas in the Cascades arc have been modelled as resulting from partial melting of basaltic crust and are the subject of this section.

Borg & Clynne (1998) and Tepper & others (1993) modelled the production of calc-alkaline rhyolites and granitoids in the Cascade arc by partial melting of underplated basaltic arc magmas. These workers demonstrated that dehydration melting at 850-1000°C produces high-SiO_2 melts, leaving a residuum of plagioclase, pyroxene, and Fe-Ti oxides. Under higher fugacities of H_2O, similar amounts of melt are produced at slightly lower temperature that have higher Si and Al and leave a residuum of amphibole, plagioclase, clinopyroxene and Fe-Ti oxides. Thus the $f(H_2O)$ controls the appearance of the REE patterns with steep, concave upwards patterns developed by amphibole-bearing sources and flat REE trends from anhydrous assemblages.

The variable $f(H_2O)$ is produced by the variable quantities of water exsolved from crystallizing underplated basalts, which are also the heat source for the partial melting. Borg & Clynne (1998) argued that rhyolites produced under higher $f(H_2O)$ are more siliceous, have hydrous ferromagnesian phases (biotite or amphibole) and have concave upwards REE patterns showing the depletion of MREE due to the removal of amphibole. These patterns also have some negative Eu anomalies but this was considered to be caused by fractionation of plagioclase in the upper crust. In contrast, the rhyolites produced under anhydrous conditions have lower silica contents, anhydrous ferromagnesian phases (pyroxene) straight REE patterns, and negative Eu anomalies. Therefore high-silica, calc-alkaline magma can be produced by partial melting of basalts in arcs and need not involve remelting of felsic crust or extensive differentiation. Both concave-upwards and straight REE patterns can be produced for calc-alkaline magmas in subduction zones controlled by $f(H_2O)$, which in turn determines the abundance of amphibole. The involvement of amphibole is characteristic of calc-alkaline magmas.

8.4.3 Origin of felsic associations and suites previously defined.

Perring (1989) investigated the origin of the felsic porphyritic intrusive suites at Norseman and Kambalda and Barley & others (1998) suggested an origin for the four felsic volcanic associations defined in the Eastern Goldfields. The following summaries are derived from these studies. A table listing the geochemical characteristics of the groups is provided as Appendix 3.

8.4.3.1 Kambalda porphyries

Porphyries at Kambalda are related, probably by hybridisation of mantle-derived lamprophyre and felsic trondhjemite. The trondhjemite may have originated by partial melting of a garnet-bearing amphibolite. Pb-isotopic compositions are not very radiogenic suggesting a primitive source.

8.4.3.2 Dinky Buoys Suite (Norseman)

The sodic rhyodacites of the Dinky Buoys Suite bear a strong resemblance to the Kambalda trondhjemite. It was concluded that they formed in a similar manner, by partial melting of a garnet-bearing amphibolite.

8.4.3.3 Big Porphyry Suite (Norseman)

The Big Porphyry has tholeiitic affinities. It was concluded that it was derived by partial melting of tholeiitic mafic rocks, modified by late stage fractionation of biotite and plagioclase at low pressures (~1 Kb).

8.4.3.4 Ajax Porphyry (Norseman)

The Ajax Suite is the most voluminous suite of felsic porphyries at Norseman. Perring (1989) concluded that it to be the result of partial melting of relatively fractionated crustal material modified by feldspar fractionation. This model was based on the following reasoning.

The unusually flat REE patterns with the negative Eu anomalies and the extremely low Sr suggest significant removal of plagioclase. Involvement of K-feldspar is also indicated by behaviour of the LILE. Moderate Rb levels and high Y, Nb and HREE preclude substantial fractionation of biotite and hornblende respectively. Use of a normative Ab-Or-Qz diagram with a grid based on experimental data, shows that fractionation occurred at low pressure (<3 Kb for anhydrous conditions, <1 Kb for water saturated). The exceptionally radiogenic Pb-isotopic composition of the Ajax Porphyry precludes its derivation from mantle material. The signature is more radiogenic than many batholithic granitoids in the southern portion of the Eastern Goldfields and probably reflects an old Th and U-enriched crustal source. The presence of rare almandine/spessartine garnet xenocrysts suggests the source material may have comprised felsic to intermediate igneous material.

8.4.3.5 Association 1-Calc-alkaline andesites (northeastern goldfields)

The calc-alkaline andesites have compositions similar to those from volcanic arcs at convergent margins. They are considered to be derived by melting of LILE enriched mantle at a convergent plate boundary. The volcaniclastic facies are similar to those from island arcs.

8.4.3.6 Association 2-Calc-alkaline intermediate-silicic (Spring Well)

The calc-alkaline intermediate-silicic association has a similar geochemistry to association 1 suggesting a volcanic arc. The silicic character would appear to require the presence of continental crust to host a long lived magma chamber in which fractionation could take place or for partial melting of mafic or intermediate crust. The association was suggested as being similar to continental marginal settings.

8.4.3.7 Association 3-Bimodal (Melita-Teutonic Bore)

The highly evolved and enriched rhyolites at Melita have been likened to anorogenic (A-type) granites that occur in extensional settings. Crustal melting in rift environments are a potential source for these granites. The less enriched type of rhyolite at Melita was suggested as resulting from the least ev77olved magma, closest in composition to the crustal source. The most evolved magma formed the more

Table 8.2: Geochemical characteristics of felsic volcanic and small felsic intrusions in the Norseman area

GROUP	Ajax microgran.	Polar Bear Rhyolite	Harlequin porphyry	Penneshaw Granodiorite	Polar Bear quartz porph	Harlequin granodiorite	Mt Thirsty epiclastics	Fram island porphyry	Feldspar Porphyry	Sailfish/ Sontaran
Prospect area	Norseman	Polar Bear	Harlequin	Fel. Penneshaw	Polar Bear	Harlequin	Mt Thirsty	Fram island	Polar Bear	Sail/PBear
Classification	rhyolite	rhyolite	rhyolite	Granite	Dacite	Trondhjemite	Epicl. dacite	Dacite	Dacite	Dacite
Series	Tholeiite	CA-thol	CA-thol	CA/TTD	Low-Al TTD?	Low-Al TTD	High-Al TTD	High-Al TTD	Calc-Alk.	hi-Al TTD
SiO_2 wt%	77.3	75.5 – 80.2	76.5 – 77.7	75.1	77.2 – 81.3	70.5 – 75.8	72.9 – 76.1	66.7	79.9	65.3 – 69.4
Al_2O_3 wt%	13.1	11.8 – 14.7	12.9 – 13.4	15.8	13.2 – 16.7	13.2 – 14.8	14.0 – 17.0	16.4	12.9	15.7 – 18.4
Na_2O+K_2O	7.6	4.4 – 10.3	5.5 – 7.9	7.04	1.8 – 5.9	6.2 – 6.7	5.1 – 6.2	7.8	4.2	4.4 – 7.1
FeO_t/MgO	51.3	2.7 – 20.1	11.7 – 21.6	1.7	1.0 – 5.8	4.3 – 5.9	2.5 – 6.2	2.0	4.1	1.8 – 2.0
Zr (ppm)	104	57 – 75	93 – 101	181	147 – 205	148 – 173	134 – 176	169	184	173 – 176
Y (ppm)	59	15 – 29.6	35 – 49	13	22 – 31	25 - 37	8 – 11	20	24	12 – 15.4
Zr/Y	1.8	2.3 – 4.4	1.9 – 2.9	13.8	5.6 – 9.3	4.0 – 7.5	12.3 – 19.6	8.5	7.7	11.2 – 14.7
Nb (ppm)	15	4.3 – 7.7	7.7 – 10.1	8.7	4.8 – 6.6	6.1 – 7.1	2.7 – 3.0	4.5	5.1	3.9 – 5.0
Nb/Y	0.3	0.2 – 0.4	0.2	0.7	0.2 – 0.3	0.2	0.2 – 0.4	0.2	0.2	0.3
La (ppm)	13.9	6.9 – 19.5	11.2 – 16.5	68.9	35.1 – 46.1	33.3 – 50.8	7.2 – 12.0	11.1	44.6	21.4 – 41.2
Yb (ppm)	8	1.4 – 2.4	2.3 – 3.3	1.2	1.7 – 3.1	1.8 – 2.3	0.7 – 1.0	0.8	1.3	0.9 – 1.3
Th (ppm)	19.0	7.5 – 11.6	12.2 – 13.7	28.7	9.6 – 14.1	8.5 – 12.6	5.1 – 9.4	2.6	9.1	5.7 – 9.0
Th/Yb	2.4	4.7 – 6.8	3.9 – 5.3	24.4	4.8 – 7.8	4.2 – 6.0	7.2 – 9.4	3.2	7.0	6.3 – 6.9
Th/Y	0.3	0.4 – 0.6	0.2 – 0.4	2.2	0.4 – 0.6	0.3 – 0.4	0.6 – 1.0	0.1	0.4	0.5 – 0.6
Zn (ppm)	56	0 – 42	29 – 35	57	0 – 173	42 – 57	0 – 14	42	11	35 – 59
Cu (ppm)		0 – 23	0 – 4	6	0 – 25	3 – 6	6 – 183	0	76	13 – 19
Pb (ppm)	28	9 – 32	15 - 23	4	10 – 36	9 – 21	9 – 17	4	37	6 - 7
$(La/Yb)_N$	1.2	3.7 – 7.4	2.4 – 4.1	41.2	10.5 – 19.5	11.9 – 18.2	6.2 – 9.6	10.0	24.6	17.1 – 22.6
$(La/Sm)_N$	1.3	3.0 – 5.3	1.5 – 2.4	8.8	4.0 – 8.8	4.0 – 5.8	3.1 – 4.3	4.2	5.6	4.3 – 5.3
$(Gd/Yb)_N$	1.0	0.8 – 1.3	1.4 – 1.8	2.3	1.5 – 1.9	1.8 – 2.1	1.2 – 1.6	1.8	2.3	2.2 – 2.7
Eu/Eu*	0.2	0.3 – 0.5	0.3 – 0.4	0.6	0.5 – 0.8	0.5 – 0.7	0.8 – 1.4	0.8	0.8	0.9 – 1.0
Ti/Ti*	0.01	0 .04 – 0.10	0.02 – 0.03	0.1	0.08 – 0.3	0.08 – 0.2	0.6 – 1.4	0.9	0.2	0.4 – 0.5
Nb/Nb*	1.0	0.2 – 0.5	0.4 – 0.7	0.1	0.1	0.1	0.1 – 0.3	0.3	0.1	0.1

enriched types of rhyolite. Association 3 volcanics were suggested as having formed in a rifted volcanic arc, similar to the Taupo Volcanic Zone in New Zealand.

The basalts show similar trace element characteristics to the calc-alkaline andesites of association 1 but without the negative Ti anomaly. The basalts are suggested to have either been extracted from a subduction modified source or are MORB-like basalts that have undergone significant crustal contamination.

8.4.3.8 Association 4-BFB (Kalgoorlie Terrane)

The andesites and dacites of association 4 are derived from high-Al TTD magmas. There is a general consensus that this must involve garnet or amphibole subtraction to account for the depleted HREE. The model of Drummond and Defant (1990) of subduction of young, hot and buoyant oceanic crust was accepted by Barley & others (1998)

8.4.4 Origin of the felsic groups defined in this study

Felsic rocks in the Norseman region in this study can be divided into nine groups on the basis of geochemistry. (Note the rocks are divided into "groups" rather than "associations" to prevent any confusion between the results of this study and Barley & others (1998)).

Three of the groups were defined by Perring (1989) and were discussed above. An additional five groups are defined using geochemical samples collected in this study, and one group using an analysis of Ghaderi (1989). Two of the groups defined by Perring (1989), the Big Porphyry suite and Dinky Buoys suite were not encountered in this study and will not be considered any further. The remaining seven groups are listed in Table 8.3.

The objective of this section is to evaluate the genesis of the groups.

Table 8.3: List of all the defined petrogenetic groups in the Norseman region.

CA rhyolite	Fractionated high-Al TTD	high-Al TTD	High-Al TTD (no Ti anomaly)	high-Al TTD (enriched radiogenic)	Hybrid CA rhyolite/TTD	CA rhyodacite/ dacite
Group A	**Group B**	**Group C**	**Group D**	**Group E**	**Group F**	**Group G**
Ajax suite	Harlequin Granodiorite	Sontaran felsic	Mt Thirsty epiclastics	Penneshaw trondhjemite	Polar Bear qz-fspr porphyry	Polar Bear Feldspar Porphyry
Harlequin Porphyry	Polar Bear quartz porphyry	Sailfish felsic	Fram Is. Feldspar Porphyry			
Polar Bear rhyolite			Polar Bear granitoid			

8.4.4.1 Petrogenesis of Group A

Group A comprises sparsely porphyritic rhyolites, both the Ajax suite dykes, which are the ubiquitous "porphyries", that are intersected by drilling in the lower Woolyeenyer Formation including at Harlequin, and the lave dome at the Polar Bear Peninsula.

Group A rocks have intense negative Eu anomalies in REE patterns and low Sr abundances, both of which are characteristic of plagioclase subtraction. The group has a muted subduction signature with only weak negative anomalies for Nb, no disturbance of Ta but intense depletion of Ti.

The REE patterns are relatively flat, lacking the concave upwards, MREE-depleted, steep pattern characteristic of amphibole subtraction. Therefore, if these magmas were generated as partial melts of basaltic lower crust, the melting must have occurred under anhydrous conditions because amphibole remains in the residuum during partial melting under high pressure, relatively high $f(H_2O)$ conditions. Under less hydrous conditions, plagioclase dominates the restite assemblage (Tepper & others, 1993). A less hydrous plagioclase-dominated restite would be consistent with the negative Eu anomaly in the REE patterns.

Perring (1989) concluded that the magmas that produced Ajax suite dykes, which are included in group A, were not derived from basalt, but rather by partial melting of relatively evolved crustal material, followed by feldspar fractionation, as discussed in section 8.4.3.4. Certainly, the muted subduction signature of the rhyolite suggests it is not primary subduction zone magma, but that it has inherited a weak geochemical reflection by partial fusion of a source rock that was emplaced in a convergent margin.

If group A rhyolites, were derived from a magma generated by partial melting of crustal material, then the source rock must have had similar silica contents to the rhyolites, which have a mode of about 77 wt%. This deduction is derived from the work of Borg & Clynne (1998, and references within) evaluating the origin of similar calc-alkaline, silicic (68-75 wt%) rhyolites from the Cascades. Using liquidus temperatures of between 890°C and 950°C, calculated using geothermometry, they suggested nearly complete melting of a granitic country rock would take place if it was the source, thus the magma would have equivalent silica to the source. At lower temperatures of 700-800°C, smaller more silicic melt fractions are generated, but experimental melts with silica compositions equivalent to the Cascade rhyolites have only been generated at these temperatures and mid-crustal pressures (2 Kb) with variable $f(H_2O)$ by starting with highly siliceous source compositions (76.8-79.4 wt% SiO_2). As the Group A rhyolites evaluated in this study are even

more silicic than those of Borg & Clynne, it is considered that this result is applicable.

The Penneshaw granitoid sample (86-222 of Ghaderi, 1998), which is 240 Ma older than the rhyolites and may represent a fragment of the sialic basement (Chapter 7), appears to have appropriate source characteristics if the single available geochemical analysis is considered representative. It has higher Th and U abundances than any other rock sampled and so is presumably a repository of significant radiogenic Pb, one of the features noted by Perring (1989); it has a Th/U value of 2.1 similar to the Ajax suite; a similar (but stronger) subduction signature with Nb and strong Ti negative anomalies, but weak Ta depletion; and SiO_2 contents of almost 76 wt%.

The Penneshaw granitoid as a source for group A rocks cannot be evaluated using the equations for partial melting models (Wood & Fraser, 1976) because sufficient data is not available. There is currently only a single sample of the Penneshaw granitoid from a drill hole with significant biotite alteration, so it is unclear whether it is representative. In addition, the phases entering the liquidus cannot be modelled as temperature and $f(H_2O)$ are not constrained.

The group A samples have geochemical similarities to association 3 felsic rocks from Melita, which have been likened to A-type granitoids. Barley & others (1998) suggested that the magmas responsible for association 3 rocks at Melita formed by melting a calc-alkaline tonalitic source, and that Nd model ages suggest an old source (2.9-3.2 Ga). This suggested origin, through melting crustal material, is similar to the suggested origin for the Ajax rhyolite suite of Perring (1989. The range of ages possible for the source of the magmas at Melita, encompasses the age of the granitoid (*ca.* 2930 Ma) in the western felsic domain of the Penneshaw Formation at Norseman. A-type magmas are typically considered to be the product of extensional tectonic settings and association 3 is considered by Barley & others (1998) to be the product of a rifted arc. Field evidence at the Polar Bear Peninsula suggests deepening of the ocean, and therefore some extension prior to the onset of volcanism, but rifting is not supported (see Chapter 12).

The key differences between group A rhyolites and association 1 & 2 calc-alkaline magmas are the lower degree of Ta and Nb depletion, the extreme depletion of Ti and Eu, and the flat REE patterns of the former, that show little evidence of amphibole subtraction. Also there are high levels of Th and U, suggestive of a crustal origin.

Although the Polar Bear rhyolite, Harlequin Porphyry and Ajax suite are all regarded as the same petrogenetic group, the differences in REE patterns indicates that they are not from the same magma batch. The lower absolute REE abundance and steeper LREE of the Polar Bear rhyolite suggests that it is the least evolved and closest in

composition to the source, whereas the Ajax microgranite is the most evolved. The Polar Bear rhyolite is considered to be transitional between calc-alkaline magmas and felsic tholeiites. The magma that formed the Polar Bear rhyolite, was generated by partial melting of calc-alkaline or TTD crust and has inherited parts of that signature, modified by partial melting and fractional crystallisation. The REE pattern is flatter than the calc-alkaline felsic associations in the north-eastern goldfields due to the effects of plagioclase subtraction. Harlequin porphyries have even flatter REE patterns the Polar Bear rhyolite and they are further evolved from the calc-alkaline source. The Ajax microgranite essentially has an inverse plagioclase REE pattern (*c.f.* Rollinson, 1993), attesting to the dominant role of plagioclase subtraction in the petrogenesis of the Ajax suite.

The feldspar fractionation, which has flattened the REE patterns from that of the source, has brought about the intense, negative Eu anomalies evident in group A. Feldspar fractionation is one of the characteristics of magmas evolving along the tholeiitic liquid line of descent, so the chemistry of the group A magmas are transitional between the probable calc-alkaline or TTD source rocks and tholeiites. With increasing fractionation, they become more tholeiitic in composition

Ti depletion is intense in group A, whereas Ta and Nb negative anomalies are very slight. The reason for the decoupling of Ta-Nb and Ti, is not clear. A double depletion mechanism is one explanation for the strong Ti depletion - Ti was originally at low levels in the source rock due to its evolved composition and probable subduction signature and during the crustal melting event, Ti behaved as a compatible element, remaining with the restite. Ti behaving as a compatible element would suggest somewhat oxidised magmatic conditions during partial melting, to stabilise Fe-Ti oxides. However, the very weak Ta and Nb negative anomalies indicate that these elements were incompatible during the crustal fusion and it is unclear why these HFSE should behave differently to Ti. Another explanation for the decoupling of Ta-Nb and Ti is substantial Fe-Ti oxide fractionation (A. Crawford, pers. comm.).

Overall, the conclusion of this study is that the Group A rhyolites are most like the Melita samples (association 3), having been generated by crustal melting.

8.4.4.2 Petrogenesis of Group B

Group B members, the Polar Bear quartz porphyries and Harlequin granodiorite, were grouped together based on their similar trace element patterns. The Harlequin granodiorite (actually trondhjemite) has the major element characteristics of low-Al TTD. The quartz porphyry has diverse major element characteristics due to strongly

affected mobile elements, but petrography and XRD of the least-altered sample are consistent with an originally sodic composition.

The REE patterns of both members are similar. The steep and concave upward shape suggests amphibole was removed from the melt. The REE patterns are similar to those for high-Al TTD except that group B has a strong negative Eu anomaly and a low abundance of Sr, suggesting plagioclase subtraction.

Based on the trace element characteristics, it is suggested that group B originated as high-Al TTD magma, but subsequently fractionated significant plagioclase, depleting Eu, Sr and Al. As a result the samples now have steep REE patterns with negative Eu anomalies and typically Al_2O_3 abundances of <15 wt%.

Table 8.4: Results of Rayleigh fractional crystallisation modelling using plagioclase.

	Ce	Nd	Sm	Eu	Gd	Dy	Er	Yb	Lu	Ti	
C_O	50.9	289	5.3	1.6	3.6	2.2	1.0	1.2	0.2	3274	E179 (BFB)
Target	69.4	26.8	5.1	1.1	5	4.1	2.4	2.3	0.3	2220	CN851947
											% Fractional Crystallisation
Model#1	62.7	36.2	7.0	1.1	4.7	2.9	1.3	1.5	0.2	4242	25%
Model#2	66.0	38.2	7.5	1.1	5.0	3.1	1.4	1.6	0.2	4513	30%
Model#3	69.6	40.5	8.1	1.0	5.3	3.3	1.5	1.7	0.3	4825	35%

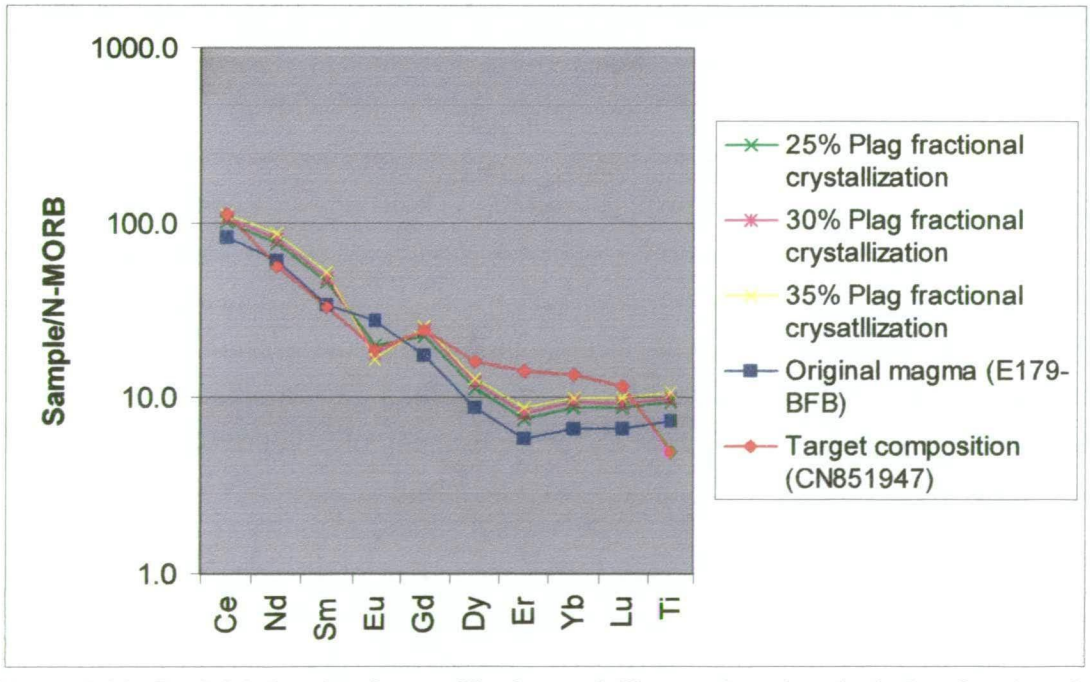

Figure 8.44: Rayleigh fractional crystallisation modelling results using plagioclase fractionation from a magma with the composition of BFB dacite E179 (Barley & others, 1998). The target magma is Group B Harlequin granodiorite(CN851947).

Table 8.5: Partition coefficients for plagioclase used in figure 8.44 and Table 8.4. (Arth, 1976).

Ce	Nd	Sm	Eu	Gd	Dy	Er	Yb	Lu	Ti
0.27	0.21	0.013	2.15	0.097	0.06	0.055	0.049	0.046	0.1

Plagioclase fractionation from a high-Al TTD was modelled using the equations for Rayleigh fractional crystallisation (see section 4.6.2) and partition coefficients suitable for plagioclase in a rhyolite (Table 8.5). Generating a Eu anomaly of sufficient magnitude was readily achieved with about 30% plagioclase fractionation (Table 8.4). The main concern in the modelling was choosing an appropriate composition for the initial magma to achieve the correct levels of the remaining REE, so the process in fact became reverse modelling to determine the composition of the original magma. Compared to the BFB sample (E179 from Barley & other, 1998) used in the model, the original magma composition requires lower Ti, lower LREE and flatter MREE.

The results for fractional crystallisation of 25, 30 and 35% plagioclase are tabulated with the compositions of the original liquid and the target magma in Table 8.4. The results are also shown in a N-MORB-normalised spidergram in figure 8.44.

8.4.4.3 Petrogenesis of Group C

Group C are members of the high-Al TTD suite and comprise two members, the felsic rocks from the Sailfish and Sontaran prospects. These rocks were classified as andesite and dacite or rhyodacite in section 8.3.3 and 8.3.5. They have steep REE patterns and negative anomalies for Ta, Nb and Ti, consistent with magmas derived from a subduction setting that left amphibole or garnet in the residuum. Sr is low also and Na is not high for the Sailfish sample, but these are mobile elements that may not be significant.

8.4.4.4 Petrogenesis of Group D

Group D comprises the felsic rocks from the southern Coolgardie Domain, namely the epiclastic rocks from Mt Thirsty and the feldspar porphyry from Fram Island. The granitoid dyke from the Polar Bear Peninsula is included in the group on the basis of the similar shape of the trace element pattern.

The southern Coolgardie Domain felsic rocks are members of the high-Al TTD suite and are considered to have an origin similar to group C and as discussed in section 8.4.2.3. The curvature in the steep REE patterns suggests amphibole was left in the residuum with or without garnet.

The high-Al TTD suite commonly is found at convergent margins and typically has the characteristic subduction zone signature of depleted Ta-Nb-Ti. A feature that is not understood for the southern Coolgardie samples is the lack of a negative Ti anomaly and the presence of a positive Zr anomaly. The anomalies are not related to the Mt Thirsty samples being sedimentary rocks because the same pattern occurs in

the feldspar porphyry intrusive sample from Fram island. The reference BFB rocks display a slight Zr enrichment which may have been stronger had XRF been used for the analysis, but the lack of Ti depletion is peculiar to the Norseman area.

The granitoid from the Polar Bear Peninsula marginally fails the high-Al TTD threshold test of 15 wt% alumina at 70 wt% silica. Nevertheless, it is included in group D as the spidergram is very similar to the Mount Thirsty epiclastic rocks, possessing the flat Ti and positive Zr anomaly. The REE pattern is also similar to the epiclastic rocks, except that there is a prominent Eu anomaly. The Eu anomaly suggests plagioclase has been fractionated and may be reason the sample is now low-Al, similar to the reasoning used for group B.

One of the most interesting outcomes of the analysis of samples for this group is the coincidence of the trace element patterns of the Fram island porphyry and Mount Thirsty samples. Although the Fram Island is considerably less siliceous than the epiclastic rocks, only in abundance of U and Th do the immobile trace elements significantly differ. The other elements are nearly identical suggesting that the epiclastic rocks are not significantly contaminated with non-volcanic products, and that the Mount Thirsty epiclastic rocks were eroded from a proximal emergent source. The reference BFB sample (E7a of Barley & others, 1998) from Widgiemooltha, to the north, differs by having a negative Ti anomaly.

8.4.4.5 Petrogenesis of Group E

Group E has only one member, represented by the granitoid sample 86-222 of Ghaderi (1998) from the felsic Penneshaw Formation drilled with PE1. The sample is classified as a calc-alkaline granite, but it has a steep and concave upward REE pattern similar to the trondhjemites. Like the high-Al TTD, the genesis of group E may have involved partial melting of an amphibole-bearing source. A small negative Eu anomaly is also present suggesting fractionation of plagioclase.

The sample is important because of the age of the granitoid (*ca.* 2930 Ma) and its possible origin as a slice of the sialic basement (see section 7.4). The sample has very high levels of Th and U and a low Th/U value of 2.1. As noted in section 8.4.4.1, these characteristics are compatible with the precursor that Perring (1989) suggested was involved in the genesis of the Ajax Porphyry.

8.4.4.6 Petrogenesis of Group F

Group F has only one member, represented by the quartz-feldspar porphyry from the Polar Bear Peninsula. This porphyry has characteristics between group A and group D. Like group D, it has a Zr anomaly and no Ti depletion. However, the REE

pattern is similar to group A rhyolites, (flat across the HREE and increasing for the LREE), except that the negative Eu anomaly is small.

These analyses lead to the conclusion that the sample may be a hybrid between group A and group D, possibly caused by magma mixing.

8.4.4.7 Petrogenesis of Group G

Group G has only one member, represented by the feldspar porphyry from the Polar Bear Peninsula, which was classified in section 8.3.3.3 as a high-silica, calc-alkaline rhyodacite, with mobile alkalies. The REE are identical to the high-Al TTD, but the alumina levels are much lower, being approximately13 wt% at a silica level of close to 80 wt%. It differs from the group B samples by the lower HREE abundances and the lack of a strong negative Eu anomaly. The latter indicates that feldspar fractionation cannot be invoked to explain the lower alumina contents.

The very high silica contents may indicate secondary enrichment, supported by the amorphous alteration observed in thin section (section 3.2.10.2). The low alumina contents for a high-Al TTD may actually be a consequence of the constant sum problem for major elements measured as percentages. With silica at 80%, only 20 wt% remains for all other elements. Group D may in fact be a high-Al TTD with silica enrichment or possibly has a similar genesis to the group 2 rhyolites of Borg & Clynne (1998), which are interpreted as partial melts of arc-derived amphibolite under hydrous conditions.

8.5 GRANITOIDS

8.5.1 Introduction

U-Pb dating of zircons at Norseman has found that the felsic porphyries exposed at the Abbotshall Mine (see section 6.3.11) have an age of 2687±3 Ma (Campbell, 1989), which is not resolvable from the age of the Buldania Granodiorite (2686±6 Ma) (Hill & others, 1992b). Structural studies (Holcolme 1997) support this conclusion, suggesting that the Pioneer Dome and Buldania Granodiorite are syn-deformation granitoids that intruded during extensional tectonics thought to have created the basin that hosts the BFB felsic rocks and sediment (see Chapter 10). These findings raise the question as to whether the granitoids are geochemically related to the felsic volcanic rocks and porphyries. No new data was collected from the granitoids for this study. Instead, existing information by Hill & others (1992b) has been compared with the data collected for the felsic volcanic rocks and small felsic intrusives.

8.5.2 Previous Studies

Schemes to classify granitoids in the Eastern Goldfields Province into suites have not been standardised and differ between authors. Nevertheless, there are some common themes. A widely used first order of subdivision, introduced by Soufoulis (1963), is based on whether the granitoid is a pluton within the greenstone belt (internal) or part of the "granite" terrains that form extensive areas of batholithic size between the greenstone belts (external). A further subdivision, used before geochronological data became widely available, classified granitoids based on the relationship to structural fabrics to define the ages of the granitoids relative to the deformation events. In this scheme, granitoids were classified as pre-folding (or pre- or syn-kinematic), post-folding (or post-kinematic) or gneiss. However, more recently Champion (1997) noted that there is not a simple relationship between structural history, age and composition of granitoids. Some gneissic granitoids have relatively young ages (2.65-2.64 Ga) whereas some older granitoids (2.68-2.65 Ga) are non-foliated, probably due to diachronous deformation or strain partitioning. Conversely granitoids with similar compositions exhibit a range of ages and structural states.

Due to the unreliability of deformation-based schemes, Champion and Sheraton (1997) subdivided granitoids in the north of the Eastern Goldfields Province into five groups based only upon geochemistry and petrography. The bulk of the granitoids are mineralogically similar, being biotite-bearing granodiorite or trondhjemite, and all of the groups exhibited a range of deformation or metamorphic fabrics. The volumetrically dominant groups were classified as high-Ca and low-Ca and comprise 60% and 20% of all granitoids respectively. The three minor groups are high-HFSE granitoids, syenite and mafic granitoids.

The high-Ca granitoids, particularly those with lower Y contents, share common features with typical Archaean TTG suites including strongly fractionated REE patterns with LREE enrichment. However, the high-Ca granitoids are more felsic, have higher LILE contents and lack more mafic end-members. The depleted Y and lack of Sr depletion in TTG suites is typically attributed to derivation from a mafic source at high pressure such that garnet remains in the source residue while plagioclase is melted. High pressure melting of a thickened crust or a subducting slab are commonly invoked models for TTG petrogenesis. Problems for these models for the high-Ca granitoids are; the presence of inherited zircons and high LILE contents implies either subducted sediment or assimilated crustal component; the variation of Y and Sr depletions within the group implies melting at a range of pressures; and seismic evidence suggests that the present day crust is too thin and felsic to derive TTG from thickened crust unless the 'eclogite' residue was subsequently delaminated. Possible scenarios for the generation of the high-Ca

group are hydrous melting at more typical crustal pressures (presumably leaving amphibole restite), remagmatization of more typical TTG rocks or fractionation from more mafic Y-undepleted magmas such as the mafic group. Sm-Nd isotope analyses constrain the granitoids to have formed from an isotopically uniform source.

The low-Ca granitoids are strongly enriched in LREE and HFSE, and Rb, Sr and K ratios suggest that crystal fractionation was significantly more important than in the high-Ca granitoids. Nd-Sm isotope trends suggest that the source rocks for these granitoids, or an assimilated component, becomes progressively younger to the east, spanning several hundred million years. The Nd-Sm data provide evidence for the existence of old continental crust, particularly in the western half of the northeastern Goldfields. The low-Ca granitoids clearly represent reworked crust. An appropriate source would be less siliceous Archaean TTG suite rocks.

High-HFSE granitoids have A-type affinities and were derived from an intermediate to silicic crustal source with low LILE. The LILE contents suggest that high-HFSE granitoids have sampled a different source than the low-Ca group. The syenitic group are clearly A-type in character and may have been formed by high temperature crustal partial melting along localised zones. The mafic group comprises a variety of suites with lower SiO_2 contents than the other groups. One possible model for their petrogenesis is partial melting of a mafic source generating a high-Ca type melt combined with varying amounts of a more mafic LILE-enriched component.

Hill & others, (1992a; 1992b) undertook geochemical analysis and SHRIMP geochronology of granitoids in the vicinity of Norseman. In a regional view, vast areas of the external "granite" terrain west and east of Norseman are dominated by biotite monzogranite, with biotite-hornblende-titanite granodiorite also making up a considerable proportion of the area. Internal granitoids are compositionally much more diverse. Considering both internal and external granitoids, Hill & others (1992b) identified a range of different compositions and ages and found that granitoids of a particular composition could form at different times. Two magmatic episodes of granitoid emplacement were identified: approximately 2685-2690 Ma and approximately 2660-2665 Ma. The majority of granitoids contain older xenocrystic zircons giving ages in the 2700-2800 Ma range, showing the involvement of continental crust in their petrogenesis. There is little correlation of geochemistry with age, and therefore, granites were divided into broad compositional groups, which included granitoids of differing ages and in some cases, differing trace element characteristics.

Hill & others (1992b) divided the granites into eight groups using different structural settings, textural differences, and minor groups. Three main groups were identified:

granodiorites, granites and tonalites. Hill & others (1992b) concluded that the variation in the major and trace elements compositions of these groups required significant differences in their petrogenesis. They tentatively suggested that the observed variations were more likely to be related to source rather than to magma chamber processes: K-rich phases were far less important in sources that yielded tonalites than in those that gave rise to granodiorites and granites. The granodiorites and granites both have steep REE patterns that were attributed to the source rocks retaining garnet as a residual phase. However, the granite source was suggested as also retaining residual plagioclase, to account for negative Sr and Eu anomalies. REE and Sr abundances for the tonalites vary considerably. All three major granite suites are relatively depleted in Nb and Ti, a feature thought to have been inherited from the source and which is found in magma related to subduction processes.

Two minor groups, the incompatible element-enriched late fractionated granites and syenites, range in age from 2600±12 Ma to 2646±6 Ma. Hill & others (1992b) noted that these had been compared with A-type granitoids by other authors and required a different origin to the more voluminous older rocks.

The classification schemes of Hill & others (1992a; 1992b) and Champion & Sheraton (1997) were both based on composition. Intrusions belonging to the granodiorite suite of Hill & others would be largely included within the high-Ca group of Champion & Sheraton, while the granite suite is similar to the low-Ca group. The tonalite (mafic), syenite and high HFSE groupings appear to be the same in both classifications.

8.5.3 Comparison of the granitoid data with volcanic rocks and porphyries

Hill & others (1992b) published their data as chondrite–normalized REE patterns and primordial mantle-normalized spidergrams. The actual values were not published so the data could not be manipulated for this study. The chondrite-normalized REE patterns are comparable to the data used in this study, so selected samples are reproduced below.

Comparing the REE patterns, some of the samples can be correlated with volcanic rocks and porphyries. The granodiorites (equivalent to high-Ca group) include the Buldania Granodiorite, the Pioneer Dome and the Widgiemooltha Dome, bodies that are all considered to be syn-deformation and syn-volcanism (see Chapter 10). The granodiorites have steep REE patterns with very weak negative Eu anomalies and appear to be high-Al TTD suite (figure 8.45 & 8.46). The Pioneer and Widgiemooltha Dome granodiorites have the steepest patterns and most HREE-depleted REE patterns seen in this study, with no concave-upwards shape

(figure 8.46), and are likely to have involved garnet subtraction. The Buldania Granodiorite and Stennet Rocks granodiorites (figure 8.45), that form parts of the eastern and western batholiths, have less steep and depleted patterns and are similar to the association 4 BFB, and high-Al TTD samples found in this study, including the Mt Thirsty samples from the southern Coolgardie Domain.

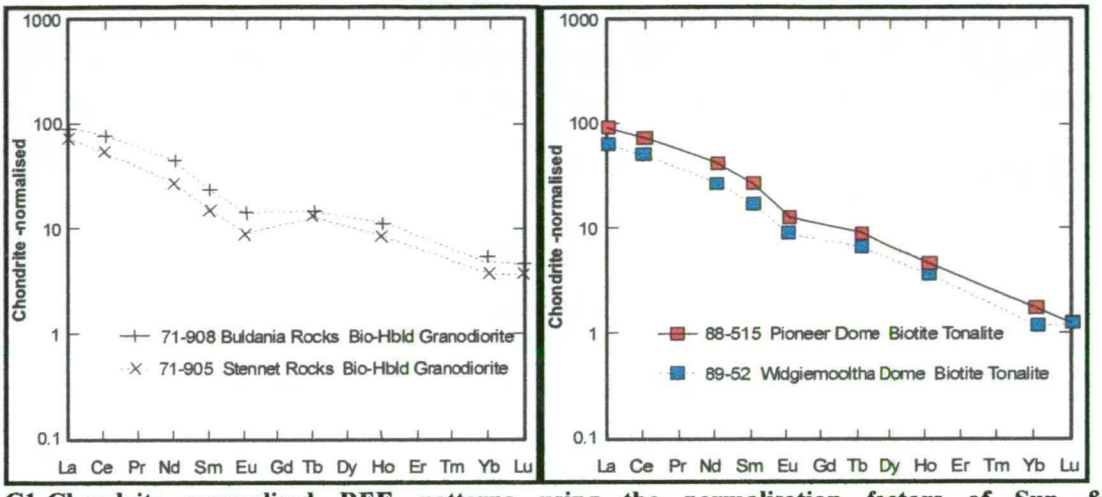

C1-Chondrite normalised REE patterns using the normalisation factors of Sun & McDonough (1989). Reproduced from Hill & others (1992b). Figure 8.45: Biotite-hornblende granodiorites from eastern and western batholiths. Similar REE patterns to association 4 BFB & petrogenetic groups C & D. Figure 8.46: Biotite tonalite associated with internal domes in the Coolgardie Domain. REE patterns steeper than association 4 BFB & petrogenetic groups C & D.

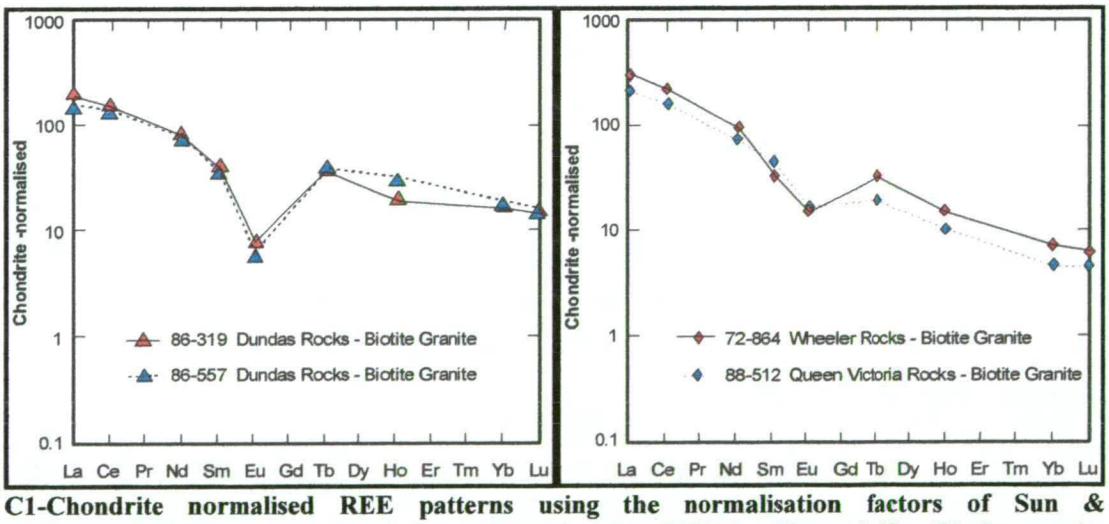

C1-Chondrite normalised REE patterns using the normalisation factors of Sun & McDonough (1989). Reproduced from Hill & others (1992b). Figure 8.47: Biotite granite associated with domes, Dundas Rocks samples from within the Norseman Terrane. Similar REE pattern to petrogenetic group A rhyolites. Figure 8.48: Coarse-grained biotite granite from the western batholith. Similar REE pattern to petrogenetic group B quartz-porphyry & Harlequin Granodiorite.

Of the granites (equivalent to low-Ca group), two Dundas Rocks analyses from within the Norseman Terrane have strong Eu anomalies and relatively flat patterns that resemble the petrogenetic group A rhyolites (figure 8.47). Champion & Sheraton (1997) suggested that low-Ca granites in the northern goldfields represent

reworked crust, which accords with the origin postulated by Perring (1989) for the Ajax suite.

The other granite samples are from the western batholith and have steep REE patterns with moderate Eu anomalies (figure 8.48). The patterns resemble the quartz porphyry and Harlequin Granodiorite of petrogenetic group B. This group includes external batholith samples dated at *ca.* 2660-2665 Ma and is attributed to a source retaining garnet and plagioclase by Hill & Campbell (1992b).

8.6 DISCUSSION

The most significant findings from the geochemical analysis of the felsic rocks is the matching of volcanic rocks with corresponding intrusives as summarised below.

- Ajax rhyolite suite = Harlequin porphyry = Polar Bear rhyolite = Dundas granite

The above rocks are derived from crustal basement by partial melting.

- Mount Thirsty epiclastic rocks = Fram island porphyry = BFB
- Kambalda high-Al trondhjemite suite = BFB high-Al TTD = high Ca granitoids

The implication that can be drawn by equating these rocks is that there is a major change in the composition of the felsic rocks between the Norseman Terrane and the Coolgardie Domain. This change in composition probably results from a change in tectonic conditions under which the felsic magmas were generated and emplaced. Therefore, the change in composition of the felsic rocks between the Norseman Terrane and the Coolgardie Domain suggests that the Mission Fault, dividing the Coolgardie Domain from the Norseman Terrane, is a major structure dividing areas that developed under differing tectonic conditions. The ideas leading to this conclusion are discussed below.

It is clear that the southern Coolgardie Domain felsic rocks examined near Mt Thirsty belong to the BFB based on the characteristic epiclastic textures and the dacitic high-Al TTD composition. This identification of the Mt Thirsty epiclastic rocks as BFB is important because it is the major difference between the Coolgardie Domain and the Norseman Terrane. The Norseman Terrane does not possess BFB; it has rhyolite lava and associated breccias of about the same age and in the same stratigraphic position.

The recognition that the Ajax suite of rhyolite dykes belong to the same petrogenetic group as the Polar Bear rhyolite makes the entire group (group A) more significant. The Ajax suite is the most voluminous group of porphyry dykes in the Norseman

Terrane and with the Polar Bear rhyolite lava, it shows that group A rhyolite was the major type of felsic magmatism in the Norseman Terrane. It cannot be argued that the Polar Bear rhyolite was simply a local magmatic event with little significance and that a major package of BFB, which has been subsequently eroded away, was actually the main magmatic event.

As discussed in section 8.4.4.1, group A rhyolites are believed to have been produced from melts of highly silicic, radiogenic crust with a subduction signature. In contrast, the high-Al TTD magmas of the BFB are considered to have formed by melting of a subducted slab or lower crustal amphibolite.

High-Al TTD magmas are found within the Norseman Terrane but they are a relatively minor product in comparison to the group A rhyolites. Only two high-Al TTD dacitic porphyry intrusives were identified in the Norseman Terrane in this study. Another type of felsic magma found in the Norseman Terrane appears to have some relationship to the high-Al TTD suite. These are the voluminous group B intrusives found at Harlequin and the Polar Bear Peninsula in the form of granodiorite and quartz porphyry respectively. These magmas are considered to be high-Al TTD magmas that have undergone extensive feldspar fractionation in magma chambers.

Thus, it is evident that the Norseman Terrane was exposed to high-Al TTD felsic magmas but the result was not the intrusion of abundant TTD dykes and eruption of volcanic rocks forming the BFB as seen in the southern Coolgardie Domain, at Kambalda and in the Kalgoorlie Terrane in general.

In the Kalgoorlie Terrane, the BFB contains felsic magmas derived from deep within the mantle or from the base of the crust, that have reached the surface with little fractionation. REE patterns do not show evidence of any mineral subtraction other than garnet or amphibole. The typical high-Al TTD signature is not modified. Based on this evidence, it is proposed that the Kalgoorlie Terrane was undergoing strong extension coincident with the felsic magmatism, allowing ready passage of magma to the surface. It is also suggested that extension within the Norseman Terrane was far more limited than the Kalgoorlie Terrane, such that TTD magmas had difficulty penetrating the crust and ponded in magma chambers, undergoing feldspar fractionation to form the group B magmas. Processes such as fractional crystallisation are typical of neutral, compressional or transient tensional stress regimes, rather than extensional environments where residence times of partial melts en route through the crust will be considerably less (Lentz, 1998).

Young, differentiated mafic sills are further evidence for this extension hypothesis. It was pointed out in Chapters 6 and 7 that young mafic sills are present in both the

Norseman Terrane and the southern Coolgardie Domain. Only minor mafic sills are found in the Norseman Terrane as described in Chapter 7. However, major mafic sills are especially common in the Kalgoorlie Terrane (Witt, 1995), where they are typically emplaced at the base of the BFB. These sills include the Mount Thirsty and Mission Sills in the southern Coolgardie Domain (described in Chapter 6), the Condensor Dolerite and Junction Dolerite at Kambalda, the Golden Mile Dolerite at Kalgoorlie, and numerous sills in the Ora Banda Domain where they form up to 30% of the greenstone (Witt, 1995). These magmas clearly postdate commencement of BFB deposition but may have been intruded late in the history of the unit, when it was several kilometres thick. The abundance of young mafic sills in the Kalgoorlie Terrane, relative to all other terranes, suggests that their emplacement was favoured in the former, possibly due to greater development of tectonic extension.

Witt (1995) described the composition of some of the mafic sills as tholeiitic and high-MgO. Ghaderi (1997) presents trace element analyses for the Junction Dolerite, Condensor Dolerite and Golden Mile Dolerite, which have flat REE patterns at abundances similar to the Lunnon Basalt. These results suggest an N-MORB trace element signature, generally attributed to decompression melting of upwelling, depleted, upper mantle, typically in extensional regimes (Wilson, 1989). The extension that allowed the high-Al TTD magmas to reach the surface, may eventually have unloaded the mantle sufficiently to cause adiabatic melting, forming the late stage mafic sills.

In section 8.4.4.4, it was noted that the high-Al TTD rocks found in the Kalgoorlie Terrane have a subduction signature. The character of the epiclastic volcanic rocks derived from emergent volcanic cones (see Chapter 6) suggests that the Kalgoorlie Terrane formed the core of a volcanic arc over a subduction zone. As noted above, the Norseman Terrane also was exposed to high-Al TTD magmas, but these ponded within the crust, probably due to a lack of substantial extension to assist the rise of the magmas. Similarly, the Norseman Terrane was also exposed to the late stage mafic magmas, but these rarely reached greenstone depths, also due to the lack of extension to provide pathways. The magmas probably remained deeper within the crust, or underplated the crust where they may have provided the heat source that caused crustal melting and generated the group A rhyolite suite.

Details of the model developed above, which explains the major differences in felsic magmatism between the Norseman Terrane and the Kalgoorlie Terrane, are examined below.

Although the Mt Thirsty felsic epiclastic rocks in the southern Coolgardie Domain are clearly BFB, there are some trace element differences between these rocks and

the other BFB occurrences such as the dacites at Widgiemooltha, 80 km to the north (see section 8.2.1.4 & 8.3.3.7), suggesting these felsic components of the BFB have different provenances. These differences are supported by the trace element composition of the Fram Island porphyry that is remarkably similar to the Mt Thirsty epiclastic rocks (section 8.3.5.4). The presence of an intrusive within a few kilometres of the Mt Thirsty epiclastic rocks, having the same geochemical fingerprint, suggests the epiclastic rocks have not been transported long distances - they were sourced from an eroding volcano within the district.

As the Fram Island porphyry is high-Al TTD suite and apparently related to the Mt Thirsty epiclastic rocks, the change from the TTD rocks to the rhyolites of group A must occur within the 2 km distance that separates Fram Island from the western side of the Polar Bear Peninsula, where aircore drilling has intersected rhyolite. This zone is where Swager & others (1995) proposed that the Mission Fault is located, confirming that the change in felsic rock types is related to the boundary between tectonostratigraphic terranes.

8.7 CONCLUSION

The aims stated at the start of this chapter can now be addressed:

BFB

The felsic epiclastic rocks near Mt Thirsty do indeed have comparable geochemistry with other dacites in the Kalgoorlie Terrane and can thus be termed "BFB".

The felsic epiclastic rocks have high-Al TTD compositions similar to the BFB dacites. However, there are some geochemical differences between the Mt Thirsty felsic epiclastic rocks and the dacites at Widgiemooltha. In particular, the Ti depletion is absent in the former and there are positive anomalies for Zr. The differences between the Widgiemooltha and Mt Thirsty epiclastic rocks suggest they have different provenances. A sample of feldspar porphyry from Fram Island in Lake Cowan has a nearly identical trace element pattern to the Mt Thirsty samples, suggesting that the porphyry and epiclastic rocks are co-magmatic and were derived from an emergent source within the district.

Comparison of felsic rocks at Mt Thirsty and the Polar Bear Peninsula

Rhyolite lava at the Polar Bear Peninsula in the Norseman Terrane is very different from the Mt Thirsty samples in the Southern Coolgardie Domain with respect to both trace elements and major elements.

Most intrusive rocks at the Polar Bear Peninsula are also different in composition from the Mount Thirsty rocks. A sample of porphyry from the Sontaran prospect has a high-Al TTD composition like felsic rocks from the Mt Thirsty area, but trace elements display some differences.

Affinities to other felsic centres in the Eastern Goldfields

The only volcanic rocks that can be directly compared with the associations defined by Barley & others (1998) are the Mt Thirsty epiclastic rocks that are high-Al TTD suite, similar to association 4 of the BFB. Two intrusive porphyry samples from the Norseman Terrane also have high-Al TTD compositions equivalent to association 4.

Rhyolite at the Polar Bear Peninsula has no exact correlation with any of the four felsic associations defined by Barley & others (1998), but detailed consideration of its geochemical attributes suggests it is most similar to association 3 (eg. Melita), although the absolute REE abundances are much lower. Ajax rhyolite suite porphyries are equivalent to the Polar Bear rhyolite, but have compositions even more closely related to the association 3 Melita samples.

Other felsic intrusive porphyries do not have compositions readily comparable with any of the four associations.

Petrogenetic information

The high-Al TTD felsic magmas of the BFB are considered to be related to a subduction setting because they have the signature of Ta, Nb, Ti depletions. High Al TTD compositions have undergone either garnet or amphibole subtraction, which causes depletion of HREE compared to LREE. These magmas are particularly common in the Archaean and Drummond & Defant (1990) suggested that they may have formed as partial melts of subducted, young, hot, oceanic crust. Subduction of such hot slabs may have been a common occurrence in the Archaean where heat flow was higher and tectonic plates are likely to have moved more rapidly. Although the model for their origin remains controversial, they are considered to indicate a subduction setting, similar to modern calc-alkaline arc magmas.

The young mafic sills that intrude the base of the BFB, including the Mount Thirsty and Mission Sill are broadly tholeiitic to high-Mg in composition. The limited trace element data available indicates they have N-MORB signatures. They may have been generated by extension in the Kalgoorlie Terrane causing unloading of the upper mantle.

Ajax rhyolite suite intrusives in the Woolyeenyer Formation have similarities to the rhyolite at the Polar Bear Peninsula, both texturally and chemically and are probably

related. The Ajax suite comprises the largest volume of felsic porphyry in the Norseman Terrane and includes the porphyry at the eastern margin of the Harlequin Granodiorite. Perring (1998) presented evidence that this suite was derived from a crustal source with highly radiogenic Pb.

The Ajax intrusives and other group A suite rhyolites have high silica, typically about 77 wt%. If group A were derived from a crustal source, the source must have similarly high silica abundances because such siliceous magmas could not be derived by either bulk crustal or small fraction melts of more mafic compositions. This evidence for a highly evolved crustal composition agrees with the radiogenic Pb evidence of Perring (1989).

Eu and Ti negative anomalies for all the rhyolite samples are particularly strong. The Eu indicates the importance of feldspar subtraction in the genesis of the rocks, most likely as restite in the source.

The intense Ti depletion suggests the Ti has behaved compatibly and remained with the source whereas, other HFSE, such as Nb and Ta, appear to have behaved relatively incompatibly and partitioned into the melt or there has been strong Fe-Ti oxide fractionation. The Nb, Ta and Ti anomalies suggest the crustal source had a subduction signature.

The heat source causing the crustal melting may be the mafic magma that forms young sills in the Kalgoorlie Terrane, and/or subduction melts intruding or underplating the crustal basement. These melts rarely reached the greenstone level in the Norseman Terrane due to poor development of tectonic extension.

The granitoid within the felsic Penneshaw Formation, considered to be a fragment of basement due to its age, is highly siliceous, has a high-Al TTD signature and abundant U and Th and therefore presumably, radiogenic Pb. It may be similar in composition to the crust from which the rhyolites were derived.

Quartz porphyry intrusive at the Polar Bear Peninsula is identical in trace element composition to the Harlequin granodiorite. These rocks have steep chondrite-normalised REE patterns with similarities to high-Al TTD suite rocks of the BFB but have prominent negative Eu anomalies and lower alumina contents. These samples were most likely derived by feldspar fractionation in a crustal magma chamber of a high-Al TTD magma. This fractional crystallisation directly resulted from the lack of extension within the Norseman Terrane, which increased residence time of the magma at depth in the crust.

The Harlequin granodiorite and Harlequin Porphyry are geochemically different and were derived by different petrogenetic processes. They bear no other relationship to each other apart from the spatial association.

A pair of samples with unmodified high-Al TTD compositions occurs within the Norseman Terrane, at the Sontaran prospect at the Polar Bear Peninsula and at Sailfish in Lake Cowan. These compositions are comparatively rare in the Norseman Terrane, whereas at Kambalda where they constitute the majority of the felsic rocks.

Other samples had singular unusual compositions, possibly related to mixing or other processes and no inferences of tectonic importance are drawn from them.

REE patterns indicate that a sample of somewhat weathered shale from the Abbotshall Beds at the Polar Bear Peninsula also has high-Al TTD affinities. This suggests that the sediment in the shale was derived from a source similar to the BFB, i.e. mud, transported from an eroding volcano or water-deposited pyroclastic material.

Limited data suggests that the granites have similar trace element geochemistry to the dominant felsic rocks of the Terrane in which they occur. Thus, the Pioneer and Widgiemooltha Domes, which occur in the Coolgardie Domain, are high-Ca granodiorites with high-Al TTD style signatures. In contrast, the Dundas Rocks Granite in the Norseman Terrane is a low-Ca granite with a REE pattern similar to the group A rhyolites. These low-Ca granites have been suggested as having been derived from crust, consistent with the rhyolite suite. The Buldania Granodiorite, forming the eastern margin to the Norseman Terrane, is a high-Ca granodiorite.

From the origins of the felsic rock groups proposed in this study, it can be concluded that the Mission Fault separates terranes with very different tectonic conditions. The various domains of the Kalgoorlie Terrane seem to have been subject to far greater extension than the Norseman Terrane.

CHAPTER NINE

Geochemistry of the Ultramafic Rocks

9.1 INTRODUCTION

Regional geological studies suggest that there is one komatiite unit throughout the Eastern Goldfields (Swager, 1997; Nelson, 1997). If this is the case, then the komatiite at the Polar Bear Peninsula is the same as the Norseman komatiite and Kambalda Komatiite. The geochemistry of the komatiites is of no special interest to this study. However, two talc-carbonate altered komatiites were analysed to determine whether high-MgO cumulates are present, which may represent lava channel facies and be of interest for Ni-sulphide prospecting. A silica-dolomite sample was also analysed to assess the geochemical changes that take place during alteration.

9.2 PREVIOUS STUDIES

Komatiites in the Eastern Goldfields have been comprehensively studied and the results widely published since the discovery of komatiite-hosted nickel sulfide deposits at Kambalda in 1965. Despite the comprehensive body of knowledge about the units, there remains disagreement about the source, emplacement, eruption characteristics and temperatures of komatiites.

Komatiites are defined as rocks which have crystallized from ultramafic magmas having MgO contents in excess of 18 wt% (Arndt & Nisbett, 1982). Conventionally, their parental magmas are thought to have had an initial MgO content of approximately 30 wt% MgO, requiring very high temperatures (1500-1650°C) (Lesher, 1989). The characteristic spinifex textures are interpreted to indicate eruption at the surface, on the basis that strong supercooling is necessary to form this texture.

Campbell & Hill (1988) used the high temperatures conventionally interpreted for Archaean komatiites to suggest that they formed by adiabatic melting of the tails to plumes, rising from the Earth's core-mantle boundary. The thick basaltic sequence typically predating the komatiites in Archaean greenstone belts was suggested to have formed by melting of the plume head, which modelling suggested would mix with surrounding cooler mantle during ascent of the plume.

However, Grove & others (1996, 1999), challenged the conventional views about komatiites by suggesting that at least some of the spinifex-textured komatiites in the Komati Formation type section are hypabyssal intrusions, and that petrological

evidence favours lower emplacement temperatures (1300-1350°C) and high magmatic H_2O contents (3-4 wt%). Their evidence included olivine microphenocrysts in chilled margins, difficult to explain using the supercooling explanation for spinifex textures, and the spatial association of amphibole-bearing wehrlite and gabbro. If komatiite magmas were hydrous, the liquidus temperature would not be far above the predicted Archaean upper mantle temperatures. The H_2O in the mantle may result from the latter stages of progressive degassing of the Earth's mantle of volatiles, or may provide evidence of subduction-related magmatic activity that recycled significant volumes of H_2O through the Archaean mantle.

Within the Norseman Terrane, the komatiites are not well studied, as the Norseman komatiite is exposed at only one location, and the Polar Bear komatiite has been generally ignored due to the lack of comprehensive work at the peninsula. The outcrop of Norseman komatiite occurs on a small island in Lake Cowan and was first recognised by GSWA mapping (McGoldrick, 1993), who also noted disseminated nickel sulfides (millerite). A number of diamond holes were subsequently drilled at this locality and have been analysed for trace elements. Hodgkison (1995) analysed fourteen samples and Ghaderi (1998) five. A detailed study of komatiites in the Norseman Terrane has been completed (Cherry, 2002).

9.3 RESULTS

Three samples of ultramafic from the Polar Bear Peninsula (figure 4.1; Table 4.1) were analysed for this study. The geochemical data are presented in a similar manner to chapter six. Selected ratios and values are presented in Table 9.1. The ratios are explained in Table 4.2. Figures 9.1 to 9.3 present data graphically.

Table 9.1: parameters which describe geochemical characteristics of the komatiite samples.

GROUP	Talc-carbonate komatiite	Talc-carbonate komatiite	Quartz-carbonate komatiite
Sample no.	CN878592	CN851910	CN851911
Analyses by:	This study	This study	This study
Prospect area	Polar Bear (North Leeders)	Polar Bear (Hinemoa Mine)	Polar Bear (Hinemoa Mine)
Jensen classification	Komatiite	Komatiite	Komatiite
SiO_2 wt%	43.27	44.59	3.55
TiO_2 wt%	0.33	0.21	0.04
Al_2O_3 wt%	1.96	1.58	0.04
MgO wt%	43.66	40.46	26.69
Cr ppm	415	1055	89
Ni ppm	>2000	1500	186
U ppm	<0.05	0	0
Cu ppm	85	15	0
Al_2O_3/TiO_2	5.9	7.5	9.0
CaO/Al_2O_3	0.2	1.0	156.8
Ti/Zr	15.2	131.4	-
Zr/Y	5.1	1.4	0
Mg#	88.6	86.4	72.8
M/Si	1.70	1.57	15.59
(La)N	5.0	4.6	3.4
(La/Yb)N	5.1	3.9	-
(La/Sm)N	1.3	1.4	1.0
(Gd/Yb)N	1.7	2.5	-
Eu/Eu*	0.9	0.8	1.8
Sr/Sr*	0.1	0.4	9.1
Ti/Ti*	0.2	0.7	0.2
Nb/Nb*	0.3	0.3	0

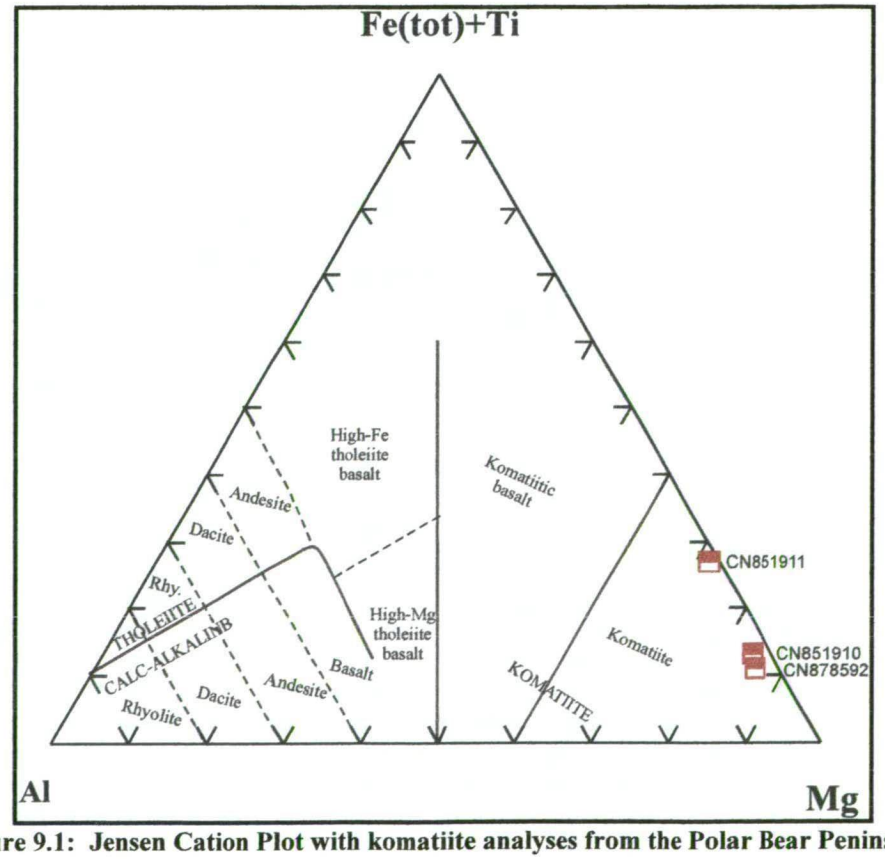

Figure 9.1: Jensen Cation Plot with komatiite analyses from the Polar Bear Peninsula.

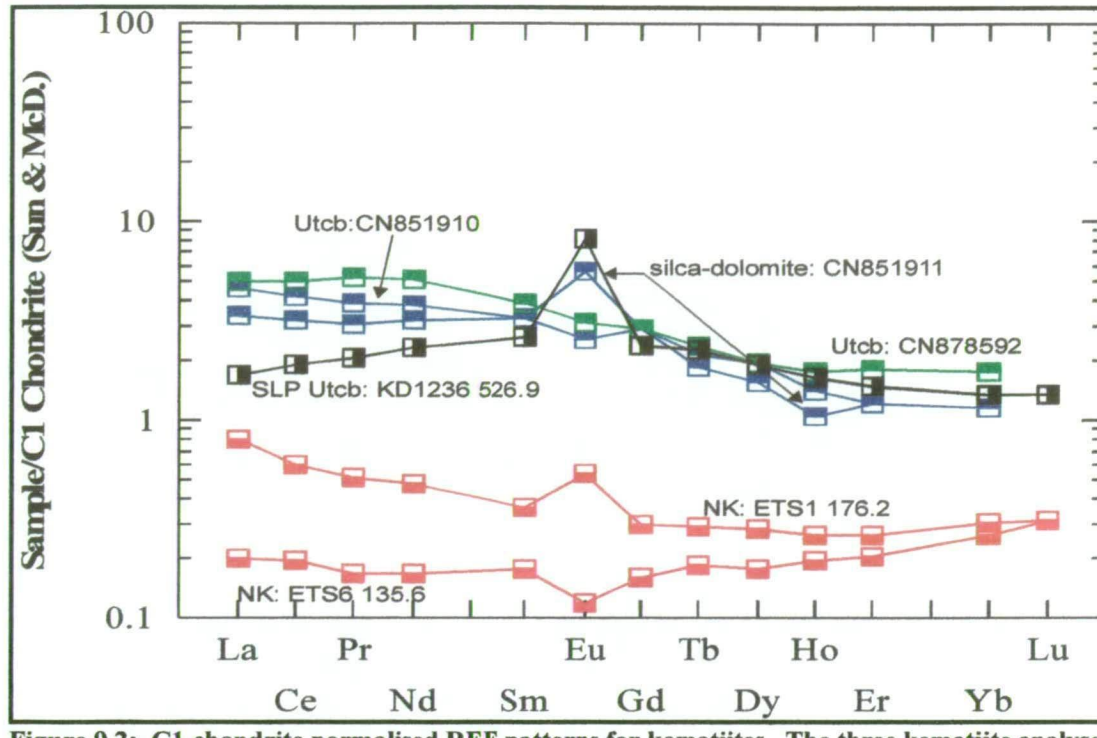

Figure 9.2: C1-chondrite normalised REE patterns for komatiites. The three komatiite analyses from the Polar Bear Peninsula with two serpentinised dunite samples from the Norseman komatiite (NK) and a talc-carbonate (Utcb) altered sample of the Silver Lake Peridotite member (SLP) of the Kambalda Komatiite for comparison (Comparison samples from Ghaderi, 1998). The Polar Bear samples and the SLP are spoon-shaped, see text.

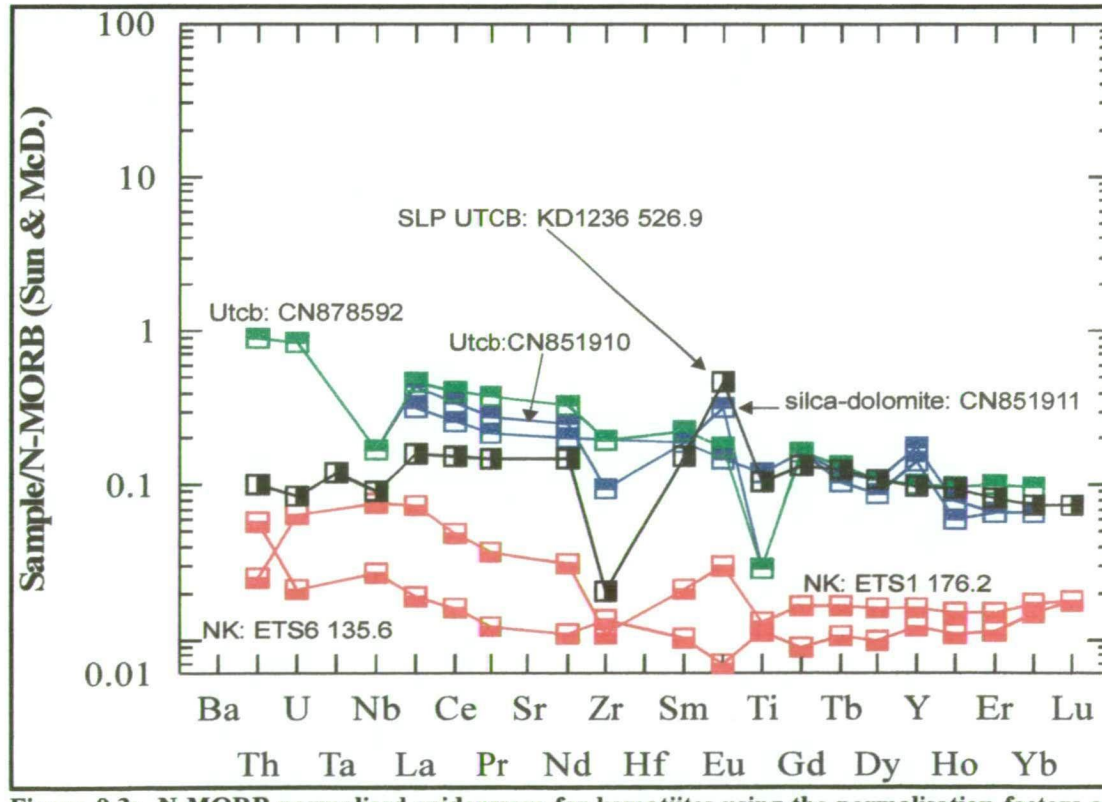

Figure 9.3: N-MORB normalised spidergram for komatiites using the normalisation factors of Sun & McDonough (1989). Samples shown are three komatiites from the Polar Bear Peninsula with two serpentinised dunite samples from the Norseman komatiite (NK) and a talc-carbonate (Utcb) altered sample of the Silver Lake Peridotite member (SLP) of the Kambalda Komatiite for comparison (Comparison samples from Ghaderi, 1998). The two Batch #2 Polar Bear samples had Y analysed by XRF and the anomalously high results probably result from analytical imprecision at these very low abundances (<5 ppm). Batch #1 used ICP-MS, which has greater precision.

9.4 INTERPRETATION AND DISCUSSION

Two of the komatiite samples are talc-carbonate altered, whereas the third (CN851911) is the quartz-carbonate (largely carbonate) sample described in section 3.3.4.2. The latter sample was collected 1 m downhole from talc-carbonate sample CN851910. It was sampled to determine the geochemical changes that take place in the transition from talc-carbonate to quartz-carbonate compositions, based on the assumption that samples from close together in a komatiite flow should have similar chemistry.

The geochemical parameters of Donaldson & others (1986) suggest that the talc-carbonate samples were originally olivine (ortho)cumulates. These samples have MgO abundances (calculated as volatile-free) of 40.5 and 43.7 wt%, within the cumulate range of 34 and 48 wt% MgO. This range also overlaps the compositional range of komatiitic dunites (olivine mesocumulates to adcumulates), but the dunites have lower levels of olivine-incompatible elements. The latter relationship is shown in figures 9.2 and 9.3 where two samples of serpentinised dunite from the Norseman komatiite are plotted for comparison.

The olivine (ortho)cumulate origin of the talc-carbonate samples is clearly shown by the M/Si ratios of 1.7 and 1.6 (see Table 4.1 for definition of the ratio). Non-cumulate komatiites have M/Si ratios less than 1.6, cumulate komatiites between 1.6 and 1.8, and komatiitic dunites greater than 1.9 (Donaldson & others, 1986). The latter value is derived from the M/Si for olivine which is 2.0 and the definition of a dunite as a rock containing greater than 90% olivine. In practice, Archaean komatiitic dunites typically have M/Si values greater than 1.95. Using this relationship, the M/Si ratios suggest that the Polar Bear talc-carbonate samples were composed of 85% and 79% olivine. The presence of cumulate komatiites may signify the presence of komatiite lava channels that are widely considered to be the host environment for the type I komatiite-associated nickel sulfide deposits of Lesher (1989).

Nesbitt & others (1979) defined aluminium-depleted komatiites (ADK) as having Al_2O_3/TiO_2 in the range of 9-13 and aluminium-undepleted komatiite (AUK) having ratios of 18-20. The talc-carbonate samples from the Polar Bear Peninsula possess Al_2O_3/TiO_2 of 5.9 and 9.5, outside typical ranges but closer to the ADK group. AUK is more common than ADK in the Eastern Goldfields and includes the Norseman komatiite and Kambalda Komatiite. The Polar Bear komatiites are actually Ti-enriched rather than Al–depleted. They have typical cumulate komatiite Al_2O_3 contents of about 2 wt%, but have TiO_2 abundances greater than the typical 0.1 wt% (Donaldson & others, 1986). This suggests that the standard model for petrogenesis

of ADK, involving the magma leaving residual aluminous garnet in the mantle source, is probably not appropriate for the Polar Bear samples. Instead, the mantle source may have been slightly less depleted than usual, which is supported by the flat rather than depleted LREE abundances (figure 9.2).

Komatiites typically have CaO/Al_2O_3 of 1. Talc-carbonate sample CN851910 has CaO of 1.55 wt% and CaO/Al_2O_3 of 1.0, suggesting that calcium, which is generally considered to be a mobile element, has been immobile in this sample. The other talc-carbonate sample, CN878592, has CaO of 0.36 wt% and CaO/Al_2O_3 of 0.2, indicating mobile calcium, probably during carbonation. The major element chemistry of the quartz-carbonate sample CN851911 has been heavily altered from its former abundances. As pointed out in section 3.2.5, the sample is now essentially ankerite with some small quartz veinlets, and its major element chemistry reflects this mineralogy.

These samples exemplify the remarkable immobility of REE. Despite the substantial mineralogical and major element chemical changes in CN851911, which were interpreted in section 3..2.5 as being the result of an intense flux of CO_2, the REE patterns of this sample are very similar to that of CN851910 (figure 9.2). The major difference is a slight depletion in Ho and a strong enrichment in Eu. The Eu anomaly could even be a primary feature as Ghaderi (1998) presented REE patterns for komatiites at Kambalda and Norseman with Eu varying from strongly negative anomalies, through flat to positive (figure 9.2). The immobility of the REE is all the more significant as the fluids altering the komatiite are interpreted to have been CO_2-rich, one of the factors considered by Humphries (1984) to be important in mobilising REE.

All three of the komatiites have spoon-shaped REE patterns. An analysis of a talc-carbonate altered Silver Lake Peridotite sample from Kambalda was also noted by Ghaderi (1998) as being spoon-shaped. These patterns were described and considered in some detail for basalts in section 6.5.3. It was concluded that they were probably contaminated by crust with a ladle-shaped chondrite-normalised REE pattern similar to the Dinky Buoys Porphyry. The komatiites may have a similar origin.

9.5 CONCLUSION

The aims outlined in section 9.1 can now be addressed.

- The two talc-carbonate komatiites have compositions that suggest they were originally olivine (ortho)cumulates. They have MgO abundances (calculated as volatile free) of 40.5 and 43.7 wt% and M/Si ratios suggest the samples were

composed of 85% and 79% olivine. The presence of cumulate komatiites may indicate the presence of komatiite lava channels that are widely considered to be the host environment for the type I komatiite-associated nickel sulfide deposits of Lesher (1989).

- The major element chemistry of the quartz-carbonate sample CN851911 is strongly altered, and reflects its mineralogy, which is now essentially ankerite with some small quartz veinlets. Despite the substantial mineralogical and major element chemical changes, the REE pattern of this sample is very similar to that of CN851910. The immobility of the REE is remarkable, particularly considering the interpreted CO_2-rich nature of the altering fluids, one of the factors thought to be important in mobilizing REE.

- The Polar Bear talc-carbonate samples have Al_2O_3/TiO_2 of 5.9 and 7.5, outside the typical ranges of both Aluminium-Depleted Komatiite (ADK) and Aluminium Undepleted Komatiite (AUK). The samples appear to be Ti-enriched rather than Al–depleted and the ADK petrogenetic model of aluminous garnet left in the mantle source is inappropriate. Instead, the mantle source may have been slightly less depleted in incompatible elements than usual.

CHAPTER TEN

Structural architecture of the Norseman Terrane and southern Coolgardie Domain

10.1 INTRODUCTION

Upright folding in the greenstone belts is evident throughout the Eastern Goldfields and was recognised by early workers. Details of other structures developed over time with increased regional mapping and a better understanding of the regional stratigraphy through U-Pb dating of zircons using the SHRIMP. A particularly strong contribution was made by the GSWA through its 1:100 000-scale mapping program in the 1980's and 1990's, which provided a broad view of structures extending for up to hundreds of kilometres. Most recently deep seismic surveys, undertaken by the Australian Geodynamics Cooperative Research Centre (AGCRC), have imaged major structures at depth.

Contributions to the structural understanding of the Norseman Terrane and southern Coolgardie Domain resulting from this study developed primarily through clarification of the stratigraphy and through detailed mapping at the Polar Bear Peninsula and at the Woodcutters prospect. The structural understanding allows a comparison of the tectonic history of the Norseman Terrane with other terranes to establish relationships, and provides constraints on tectonic models for greenstone formation. Another interest in structures for this study is to investigate the source and controls localizing gold mineralisation, which is discussed in Chapter 10.

Layout of the chapter

This study largely follows the structural scheme of Holcombe (1997), except where the conclusions differ, or the new work allows an elaboration about the structures. A structural nomenclature modified from Williams (1993) is used, as this is the most widely recognised for the major deformation events. A brief review of previous studies in the Norseman area 'sets the scene'. A structural overview follows, to provide an outline of the deformation events recognised in this study. The deformation events are then reviewed in more detail, providing references, and evidence and observations from this study.

10.1.2 Methods

The structures described in this study have been observed directly in the field, remotely from geophysical datasets and inferred from the sediment facies and juxtaposition of stratigraphic units out of sequence. Detailed mapping clarified the local structural deformation in the Polar Bear area, which assisted the elucidation of

the stratigraphic sequence for the Polar Bear Peninsula from basalt through to rhyolite. By comparing this stratigraphy to other areas, major repetitions within the Norseman Terrane were recognised.

The stratigraphy of the southern Coolgardie Domain was outlined in Chapter 6. Recognition of stratigraphic repetitions allowed thrust faults to be proposed in a similar manner to the Norseman Terrane. Detailed mapping of one area with a stratigraphic repetition, the Woodcutters prospect, established the presence of a fault. Major structures are also proposed for the lower Norseman Terrane, based on the stratigraphic problems described in Chapter 7.

The basis for many of the proposed D_2 thrust faults is the behaviour of the ultramafic units, visible in aeromagnetic images by their high magnetic intensity. In the Norseman area, aeromagnetic images and mapping show that there are multiple strands of komatiite. As komatiite is now regarded as a 2710-2700 Ma time marker for the entire Eastern Goldfields (Swager, 1997; Nelson, 1997), these multiple strands must be caused by major structural repetitions.

It is not within the scope of this study to provide an exhaustive examination of the structural geology of the Norseman Terrane. However, by establishing the stratigraphy and through detailed mapping, major structures have been defined by stratigraphic repetitions and deviations from the units expected. Major structures have been included in regional geological map provided in this chapter (figure 10.1; 10.4) to reconcile the stratigraphic column with the pattern of units observed.

10.2 PREVIOUS STUDIES

10.2.1 Introduction

Early work on the greenstones in the Eastern Goldfields Province comprised regional geological mapping, which identified upright folding and repetitions of mafic and ultramafic stratigraphy. The model of the stratigraphic architecture developed from this work incorporated repeated cycles of mafic and ultramafic volcanism. The stratigraphy was considered to be tightly folded within a greenstone belt that resembled a deep synclinal keel within surrounding granite. The idea of cycles of volcanism was refuted by two independent streams of work. Firstly, geological mapping by the GSWA for the 1:100 000 sheets interpreted thrust duplication of some of the supposed cycles (Griffin, 1988; Griffin 1990; Swager & Griffin, 1990). Secondly, SHRIMP zircon dating from the mid-1980's onwards, demonstrated that the mafic-ultramafic stratigraphy has a similar age province-wide. This conceptual

change led to a reinterpretation of volcanic repetitions, from cycles of volcanism to structural repetitions, in particular, thrust faults.

Since the mid-1980's, structures within the southern part of the Eastern Goldfields have been attributed to two main stages of compressional deformation: N-S compression developing thrusting and recumbent folding; and east-west compression developing NNW trending upright folds and NNW-trending sinistral strike-slip faults (Griffin 1990b). More recent studies have highlighted extensional structures, (Williams & Currie, 1993; Hammond & Nisbet, 1993) although unequivocal evidence for early extension is not recognised by many workers in the southern part of the Eastern Goldfields (Swager, 1997). The deformation events that are widely recognised in the Eastern Goldfields are described in section 2.2.4.2 Studies specific to the Norseman area are described in more detail below.

10.2.2 The Norseman Area

Archibald (1979) recognised multiple generations of folding, commencing with D_1 isoclinal folds, however his scheme is now largely superseded by later studies.

Keele (1984) recognised D_1 isoclinal folding in the Noganyer Formation from facing indicators observed in drill core, which showed that some of the repetitive jaspilite units are overturned. D_2 was also recognised in the Noganyer Formation as upright folding forming the Penneshaw Anticline. Keele (1984) attributed the regional upright cleavage and a subhorizontal N S stretching lineation of conglomerate pebbles at the base of the Noganyer Formation to D_2. The NNW shears such as the Princess Royal Fault were included in D_3 which is mainly a domainal foliation varying in orientation. D_3 was considered to be the peak of metamorphism, based on high temperature mineral overgrowths on S_2. D_4 and D_5 are subtle retrograde events detected in a few locations.

Spray (1986) also studied the Norseman area and recognised the early, high metamorphic grade, high-strain, low angle, layer-parallel mylonites that juxtapose gneiss of the Buldania Granodiorite and greenstone of the western Penneshaw Formation. The juxtaposition was attributed to thrust faulting and recorded as the first deformation event. Spray (1986) listed the Penneshaw Anticline as D_2 but attributed the prominent upright cleavage to D_3. Under Spray's scheme, D_3 was the major folding event, forming a NNW trending fold axis which refolded the Penneshaw anticline. The D_3 antiform was conceived by suggesting diverse mafics, ultramafics and felsics of the Buldania area in the west are equivalent to similar rocks in the Mount Thirsty area to the east. With the advent of detailed mapping and aeromagnetic images, this idea is no longer tenable and the antiform envisaged by

Widgiemooltha-Cowan	Norseman	Norseman	Kambalda-Lake Cowan	Northeastern Goldfields.	Southern Eastern Goldfields.	Norseman	Norseman
Archibald, 1979	**Keele, 1984**	**Spray, 1986**	**Griffin, 1990**	**Williams, 1993**	**Swager, 1997**	**Holcolme, 1997**	**This study**
	S_5: NW-WNW narrow domains foliated rock; 2nd pulse metamorph.						
D_4: N-S trending, N & S plunging open folds directly related to granite dome emplacement. S_4: N-S steep.	S_4: retrograde fracture cleavage and mineral lineation parallel to S_3; syn-Buldania Graniodiorite	D_4: late, open cross-folds with egg-box interference. S4: ENE-trending fracture cleavage	D_4: Localized folding related to faulting.		D_4: Regional shortening (E-W). Oblique dextral reverse faults.		
					D_{E4}: E-W extension restricted to Ida Fault, 5km displacement; min. age 2640±8 Ma.		
D_3: N-S trending, open to close folds with variable plunges. Polar Bear folds. S_3: developed in micaceous units.	D_3: syn-metamorphic foliation & NNW shearing S_3: high T mineral overgrowths on S_2; steep but domainal	D_3: NNW, major regional fold event. Refolds D_2 folds. S_3: steep NNW trending fabric	D3: NNW(N, NW) upright open to tight folds. S_3: major regional fabric	D_3: NW-NNW sinistral faults and shears; NE faults.	D_3: E-W Regional shortening; strike and reverse slip faults & en echelon folds	D_4: 330°-trending shears and localized folds. A weak local reflection of the major structural grain forming event occurring to the north of Norseman. Gold mineralisation.	D_3: (E-W) compression: Post-folding reverse faults including those hosting mineralisation. Sinistral offset on NNW trending shears such as Princess Royal Fault
					D_{E3}: emplacement of high-grade granite gneiss complexes into low grade greenstones across extensional shear zones. Coincident with *ca.* 2660 Ma granite; peak metamorphism.	D_E: cryptic interval of E-W? extension. Dip slip faults & dolerite sills splitting layers in Noganyer. Microgranite & porphyry intrusion.	D_{E2}: extension forming NNW trending block faults, some filled with dolerite.

D_2: N-NNW-trending open to tight folds; variable plunge due to D_1. S_2: N-NNW-trending slaty cleavage	D_2: NNE Penneshaw anticline, N plunge. S_2: schistosity, flat N pitching stretching lineation in conglomerate.	D_2: NNE trending, upright folds e.g. Penneshaw anticline. D_2:E, NE open upright folds. Refolded by D_3.	D_2: ENE-WSW shortening, upright folds, S_2: regional cleavage.	D_2: regional shortening (ENE-WSW). Upright doubly plunging NNW-trending folds & foliation; domain-scale thrusting; D_{E2} inversion.	D_3: dextral transpressive deformation producing N-trending folds, regional cleavage, reverse faults & dextral shears. Subhorizontal N-S stretching lineation.	D_3: Dextral-transpressive E-W deformation.	D_2: Pre-folding, layer-parallel thrusts; cleavage; stretching lineations; folding including Norseman Anticline.
				D_{E2}: Roll-over structures and stratigraphic cutouts on basal detachment. Core complex emplacement	D_{E2}: E-W extension-rollover anticlines with truncation of fold limbs at basal detachment; synclinal basins with clastic infill cover F_1 and have S_2.		
D_1: isoclinal folds refolded by D2.	D_1: Large isoclinal folds in jaspilite. Block faulting of Mararoa Pillow Lava. S_1 not developed.	D_1: high grade, high strain, low angle shear zones subparallel to bedding. Juxtapose greenstone against gneiss. Thrusts	D_1:tight to isoclinal recumbent folds and thrusts.	D_1: thrust faults and sequence repetitions; Basal shear to greenstone. Emplacement of granite magmas; *ca* 2680 Ma.	D_1: thrust stacking, recumbent folds; involves upper felsic unit in Kalgoorlie T. (min BFB age: ~2660 Ma , Barley & others 1998)	D_2: top to N ductile low angle thrust at base of Noganyer Fm. Causes overturning and duplication of jaspilite.	D_1: top to due north, low angle thrust. At base of and within Noganyer Fm; Hill Island thrust at top of the Norseman komatiite, stacking stratigraphy; within Penneshaw Formation.
				D_{E1}: Asymmetrical rifting and uplift of rocks west of EGP on shallowly dipping detachment.	D_{E1}: low angle shearing along granite-greenstone contact (north-south movement); syn-volcanic granite plutonism (2685-2675 Ma); synvolcanic domes	D_1: top to south? extension. Low-angle, detachment fault juxtaposes amphib facies against greenstone; forms core complexes. Syn-tectonic granites eastern edge of Pioneer Dome. *ca.* 2685 Ma; felsic & sed filled basins form. D_1 obliterated by D_2 on west side of Pen Penneshaw..	D_{E1}: Extension as defined by Holcolme (1997). Formation of Kalgoorlie Basin & deposition of BFB.

Spray (1986) is invalid. Open, cross-folding on ENE trending axes to generate egg-box interference patterns with earlier northerly trending folds was proposed as D_4. There is some support for the latter structure as north-south trending fold axes do appear to be doubly plunging in many areas, including the Polar Bear Peninsula.

Holcolme (1996; 1997) undertook studies of the Norseman area to update the understanding of the structural framework of the area for CNGC. His work involved field observations at spot locations over about four weeks, a review of previous studies and supervision of two small research projects on the Noganyer Formation. Holcombe (1997) examined the features noted by Spray (1986) and Keele (1985) and synthesized them with advances in the understanding of deformation throughout the Eastern Goldfields. Deformation events in the Norseman area were matched with similar regional events to the north, but anomalous features of the Norseman area were also highlighted.

In brief, Holcombe (1997) noted five main periods of deformation, D_1 to D_4 with one extensional event between D_3 and D_4 not given a "D" notation. D_1 was a major extensional event which resulted in upper amphibolite grade, metamorphic terranes being juxtaposed against lower grade greenstones by an originally low angle detachment zone, the D_1 of Spray (1986), with the sense of displacement reversed. Granites were emplaced during this event. D_2 was the north-south thrusting event widely recognised to the north of Norseman by Swager & Griffin (1990) that Holcombe found in the Noganyer Formation. D_3 involved east-west shortening, resulting in north-trending folds, cleavage and reverse faults. It is characterised by a subhorizontal, stretching in a north-south direction, consistent with partitioned, wrench-dominated transpression. A cryptic period of extension followed D_3 during which gabbros were intruded into the Noganyer Formation. D_4 was the final Archaean deformation event producing approximately 330° trending, reverse, dextral shears and localised folds. It was a weak reflection of the major, structural, grain-forming event that occurred to the north.

10.3 STRUCTURAL OVERVIEW

In this study, structures in the Norseman area have been divided into six phases of deformation, four of which, are consistent with the widely recognised schemes used for the Eastern Goldfields as described in Chapter 2:

- Local uplift within the Norseman Terrane, causing erosion of the submarine basalts;

- D_{E1}: Extension following mafic volcanism, coincident with emplacement of internal granitoids and formation of the basin hosting the felsic and sedimentary Black Flag Beds;
- D_1: N-S directed shortening causing regional-scale thrust faults;
- D_2: E-W shortening causing thrust faults and large-scale upright folds with N-S axes;
- D_{E2}: Extensional resulting in steep, NNW-trending block faults; and
- D_3: Continued E-W shortening causing movement on N-S to NNW-trending faults.

The earliest phase of deformation recognised in this study, considered to be responsible for uplift and erosion of basalts, is not given a "D" notation as it appears to be a local event.

The interpreted structures within the Norseman area are shown in figures 10.1 and 10.4.

D_{E1} structures have not directly observed in this study, but the event is considered to have caused the development of basins, which submerged previously exposed mafic volcanics in the Norseman Terrane. D_{E1} had a pronounced effect in the Kalgoorlie Terrane, producing the Kalgoorlie Basin that hosts the 2-3 km thick BFB. It is coeval with granitoids such as the Buldania Granodiorite, aged ca. 2686 Ma.

D_1, north-south directed compression caused at least two major thrust faults that repeat stratigraphy in the Norseman Terrane. The sequence of Chinaman's Well basalts through to Polar Bear rhyolite at the northern part of the terrane was thrust over the Norseman komatiite, repeating the basalts and komatiites of the Woolyeenyer Formation. The structure is partially exposed at Hill Island, south of the Norseman-Coolgardie Highway, where layer-parallel, due south to north-directed thrusting is evident with pre-peak metamorphism timing. This fault has a minimum displacement of approximately 6 km, the thickness of the basalt. The lower mafic portion of the Penneshaw Formation is probably a repetition of the Woolyeenyer Formation (see section 7.4), due to a D_1 thrust.

Swager (1997) originally suggested that the Kalgoorlie Domain bounding faults may be initiated as D_1 thrust transfers, given that no D_1 thrust faults are recognized in the Ora Banda Domain. A similar reasoning is used here to suggest that the Mission Fault was initiated as a D_1 transfer fault to the Hill Island thrust as the southern Coolgardie Domain does not display the effects of D_1. It is suggested that the

Mission Fault and Zuleika Shear have displacements of tens of kilometres having juxtaposed different terranes.

D_1 may also be responsible for broad, open folds with east-west axes in the Norseman Terrane. This folding causes egg box style interference patterns in some areas, and is responsible for the northerly plunge of the Norseman Anticline.

D_2 was east-west directed compression that shortened the Norseman Terrane in an east-west direction and stretched it in the north-south direction. The structures formed include thrust faults, particularly in the Coolgardie Domain and prominent upright folds in both the Norseman Terrane and Coolgardie Domain. D_2 thrust faults have displacements of hundreds of metres to a kilometre. The Norseman Anticline is a north-plunging D_2 structure that causes the major bend in the Woolyeenyer Formation and Norseman komatiite apparent in regional maps and aeromagnetic images.

D_{E2} is an extensional event that resulted in steep, NNW-trending, block faults. One D_{E2} fault, the Princess Royal Fault, has an apparent dextral offset where it passes through the jaspilite in the Norseman Terrane, due to the dip of the jaspilite. It is considered that these NNW block faults may be the result of dilation caused by a sinistral wrench strain on the bounding structures to the Norseman Terrane, caused by the east-west compression.

D_3 is a roughly east-west or ENE-directed compression that was active during gold mineralisation. It formed structures that are reverse faults in their current orientation (post-folding) and activated faults in weak lithologies which were at favourable orientations, particularly within the NNE-striking segment of Norseman komatiite. D_{E2} NNW-oriented faults were reactivated with a minor sinistral movement. These structures have displacements of metres to about 100 metres.

10.4 DEFORMATION OF THE NORSEMAN AREA

10.4.1 Introduction

This section will detail deformation events accepted to have operated in the Norseman Terrane and southern Coolgardie Domain. The concepts presented here have been derived from previous research and from work undertaken for this study. The structures identified, best explain the lithological pattern and aeromagnetic lineaments. The structures are integrated into the regional structural and stratigraphic map presented in this chapter.

10.4.2 First deformation – uplift and tilting

The first deformation event is interpreted to be uplift and tilting of the mafic succession as alluded to in section 5.2. This uplift and tilting is recognised by the exposure of submarine basalts, indicated by the presence of mafic conglomerate at the Polar Bear Peninsula as described in section 3.2.6, and the angular unconformity at the contact between the basalts and the overlying Abbotshall Beds as described in section 3.2.4. As similar early conglomerates and angular unconformities at the top of the basalt sequence have not been described from any other areas in the southern part of the Eastern Goldfields, the deformation event may have been a local event. Given the event appears to be a relatively minor local deformation, it has not been given a "D" notation to avoid confusion with more widely used regional structural nomenclature schemes.

10.4.3 D_{E1} extension

Holcolme (1997) noted several domains of amphibolite facies juxtaposed against lower metamorphic grade greenstones. In the Norseman Terrane, the eastern Penneshaw Formation and Buldania Granodiorite were listed as examples while to the west in the Coolgardie Domain, examples include the margins of the granitoids of the Widgiemooltha, Pioneer and Goodia Domes. (Following the compilation of previous petrographic studies presented in Chapter 7, the eastern Penneshaw is not accepted as being one of the high metamorphic grade domains in this study). Holcolme (1997) noted a strong syntectonic signature in the high strain margins of the Pioneer and Goodia Domes, with successive magma phases being less deformed. High strain sills of mylonitic and/or gneissic granite form a carapace to the granitoid domes and are more highly deformed than the amphibolite host. All high metamorphic grade units, the granite, gneiss and amphibolite, possess a layer-parallel foliation and strong, subhorizontal, N-S stretching lineation, which was tentatively suggested to have a top-to-the-south sense of shear. The layer-parallel foliation within the amphibolite wraps concordantly over the domes, the northern end of the Widgiemooltha Dome being the best exposed example.

The granites, with ages of *ca.* 2686 Ma, are distinctly younger than the mafic greenstones, but a strong, layer-parallel deformation is rare in the lower grade greenstones. Holcolme (1997) suggested the juxtaposition of low metamorphic grade against high grade and the strong, layer-parallel deformation implies a considerable displacement on an extensional detachment fault with the high grade domains and granites exposed as core complexes. Within the Norseman Terrane, a D_2 thrust along the margin of the Buldania Granodiorite has obliterated the early detachment fault.

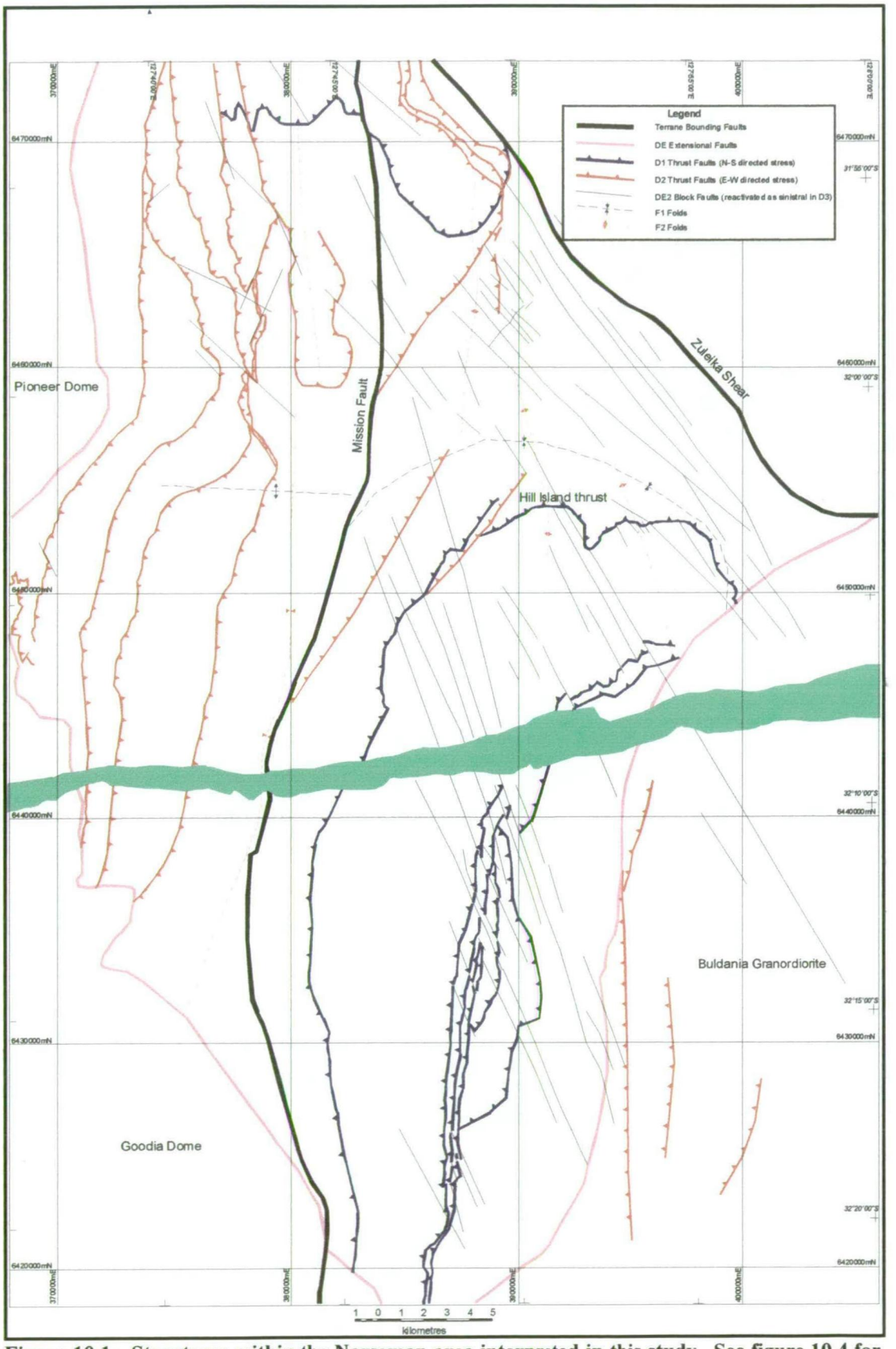

Figure 10.1: Structures within the Norseman area interpreted in this study. See figure 10.4 for full geology.

Holcombe (1997) suggested that early extension involving the introduction of granites may have been linked to the opening of felsic and sediment-filled basins, which is supported by the studies of Barley & others (1997). In the latter study, sedimentological and tectonostratigraphic concepts were used to suggest that the BFB were deposited in a rift basin named the "Kalgoorlie Basin". The volcanics within the BFB were dated and found to be coincident with the internal granitoid ages *ca.* 2686 Ma.

D_{E1} was not directly observed in this study but the effects of extension were observed in the stratigraphy. At the Polar Bear Peninsula, mafic conglomerate and sand, associated with erosion of the uplifted mafic substrate, are overlain by thin-bedded sandstone-shale and siltstone-shale turbidites and ultimately black shales. From being emergent and producing conglomerates, the substrate has been submerged to considerable depth, certainly below wave base, and distal from any source of terrigenous sediments. This submergence is recorded within the 25-50 metre thickness of the Abbotshall Beds, suggesting it was rapid.

10.4.4 D_1 north-south compression - thrust faults

10.4.4.1 Introduction

Identification of major thrust repetitions of the stratigraphy by major D_1 thrust faults has been a major outcome of this study. As described in sections 3.5, stratigraphic considerations, supported by geochemical testing (Chapter 4), indicate the Chinaman's Well basalts are thrust over the Norseman komatiite. The thrust is observed at Hill Island and in some diamond holes recently drilled into the Norseman komatiite. As Hill Island is the only location where the thrust is exposed at the surface, it is termed the "Hill Island thrust" in this thesis (figure 10.1 and sections 10.4.4.2 & 10.4.4.3).

A similar thrust repetition has subsequently been postulated by CNGC geologists for the lower Penneshaw Formation. The mafic succession of the lower Penneshaw is texturally very similar to the Woolyeenyer Formation and is suggested to be a thrust repetition. This structure is discussed in section 10.4.4.4.

Another D_1 structure, a thrust duplex, is suggested in this study to be associated with the Noganyer Formation. Holcolme (1997) previously located D_1 structures associated with the Noganyer Formation. These structures will be described in section 10.4.4.5 .

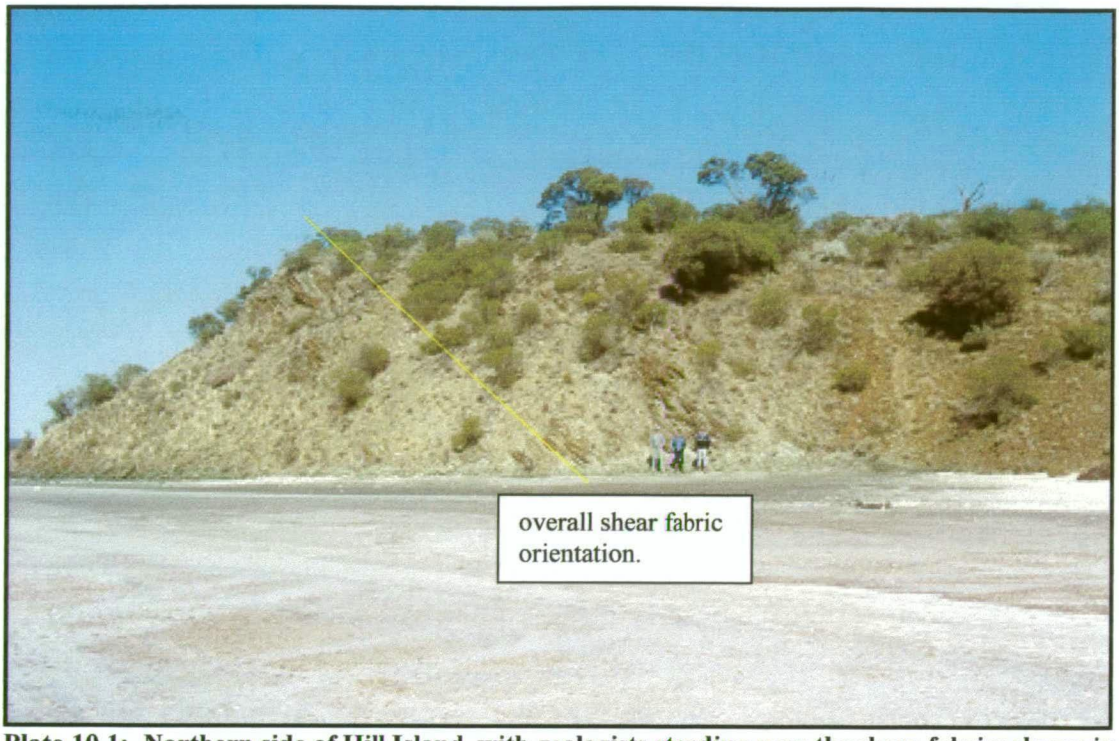

Plate 10.1: Northern side of Hill Island, with geologists standing near the shear fabrics shown in Plate 10.2.

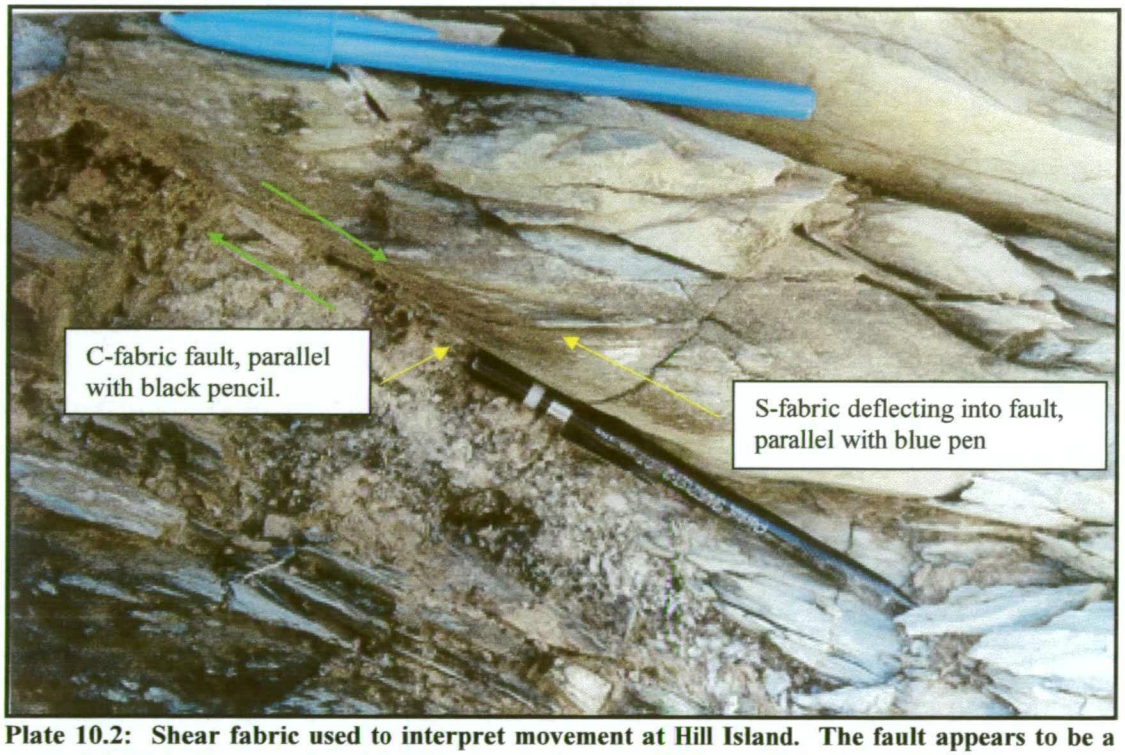

Plate 10.2: Shear fabric used to interpret movement at Hill Island. The fault appears to be a normal fault in its current orientation due to later F_2 folding. With the folding removed, the fault would be horizontal, with a top-to-the-due-north movement.

10.4.4.2 Hill Island thrust at Hill Island

Hill Island is located 1.7 km south of the causeway where the Coolgardie-Esperance Highway crosses Lake Cowan. It is about 125 metres west of the upper contact of the Norseman komatiite, which is well known at that location due to drilling at the Cobbler gold prospect. Hill Island exposes part of the major thrust fault which throws the lower Woolyeenyer Formation over the Norseman komatiite to form the Chinaman's Well basalts (Plate 10.1).

The presence of a fault at Hill Island has been noted by previous workers. Hodgkison (1995) described Hill Island as exposing talc-chlorite-amphibole ultramafics of the Norseman komatiite and the overlying Chinaman's Well basalt with a sheared contact between the two. McGoldrick (1993) illustrates Hill Island as comprising dolerite, pillow basalt and foliated, chloritic basalts.

Description

A reconnaissance of the shoreline in this study found highly variolitic and amygdaloidal basalt similar to the basalts at the causeway described in Chapter 4. Acicular metamorphic amphiboles are common within both massive and foliated basalts, randomly oriented in the plane of the foliation for the latter. The amphiboles are typically 2 mm in length, but reach a maximum of 1 cm. The amphiboles may give the impression of a medium to coarse doleritic grain size, but the ubiquitous amygdales suggest the island is composed entirely of extrusive basalt.

The basalt is foliated with the fabric becoming less prominent to the west along the eastern side of the island. McGoldrick (1993) noted igneous layering which dips 36° to the west, similar to his measurement for the foliation, suggesting the foliation is layer-parallel. Dragging of the foliation into the shear plane indicates a top to the north sense of movement (Plate 10.2). Stretched amygdales on the eastern shore of the island provide an azimuth to the shear movement (Plate 10.3), which is almost due north-south when the lineations are rotated with the layering to horizontal.

Discussion and interpretation

The foliation in the basalts at Hill Island is caused by a layer-parallel shear with a top-to-the-due-north sense of movement. This exposure of the shear is approximately 125 metres above the top of the Norseman komatiite and is considered to be part of the D_1 thrust that throws the mafic Woolyeenyer Formation over the Norseman komatiite. The acicular metamorphic amphiboles are not aligned with the stretching lineation in foliated basalts, indicating that the amphiboles post-date the

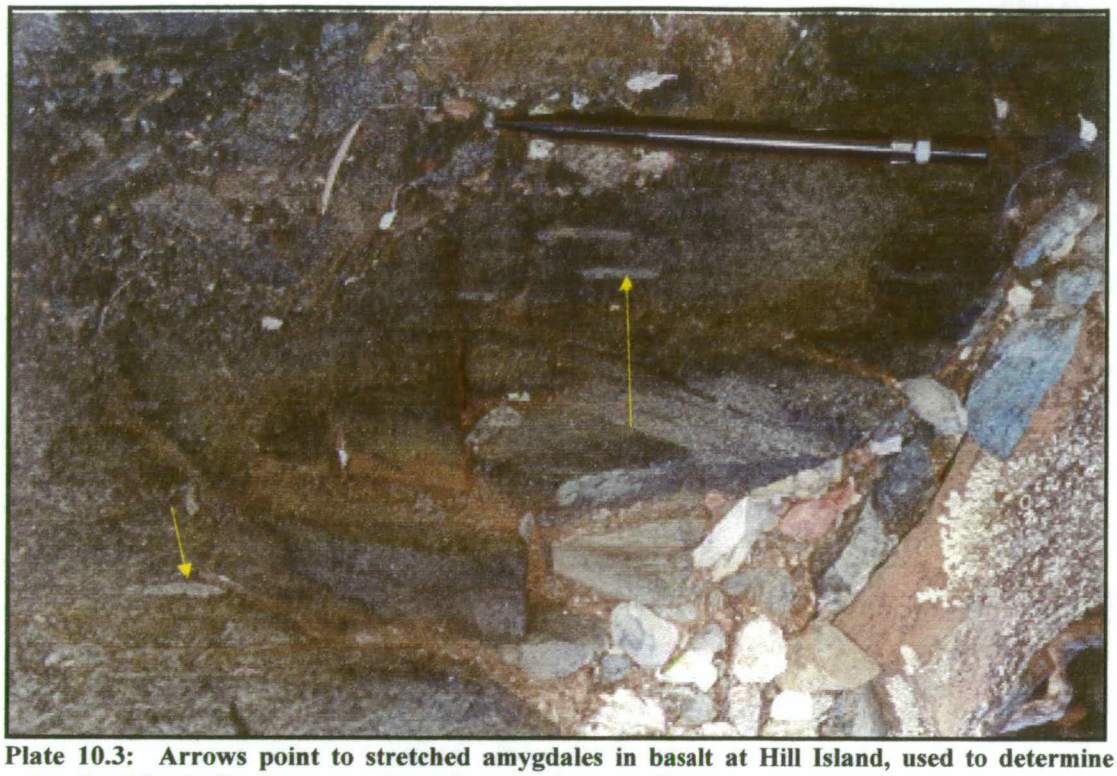

Plate 10.3: Arrows point to stretched amygdales in basalt at Hill Island, used to determine azimuth of the fault movement. Stretch parallel to pencil.

Plate 10.4: Hill Island Shear in ETS18

foliation. This implies the shear predates peak metamorphism, providing further support for the inference that it is an early D_1 structure.

The preservation of the D_1 fabric at Hill Island may be due to its location above the komatiite. The original D_1 fabric would not be preserved in the thrust at the margin of the komatiite as the komatiite has been altered to a weak talc-carbonate mineralogy leaving it highly susceptible to deformation. The komatiite hosts gold mineralisation in mafic enclaves at the Cobbler prospect, close to Hill Island, and therefore has been remobilised during D_3 deformation when the gold mineralisation was formed.

10.4.4.3 Hill Island thrust north of the Royal Peninsula

The D_1 thrust over the Norseman komatiite is also observed in a pair of diamond holes into the komatiite north of the Royal Peninsula and closer to the Norseman Anticline fold closure.

Description

ETS16 has moderate to strong shearing from the start of the hole to the end. The hole was drilled vertically and commenced in mafic rocks of the hanging-wall to the fault with a few sheared enclaves of talc-carbonate ultramafic before entering the Norseman komatiite at 84 metres. The shear planes have down-dip stretching lineations consistent with a north-south azimuth of movement.

ETS18 was collared in ultramafic and drilled to the southeast so missed the main section of the thrust at the top of the ultramafic. Nevertheless, the drill core intersects a broad shear and, from 151-195 metres depth, preserves a strong shear fabric with a shear plane orientation dipping at 54° towards 287° azimuth (Plate 10.4). As the komatiite strikes northeast at this locality, the shear foliation is consistent with a layer-parallel fault. At 173 metres depth, the shear has bands of biotite aligned with it, with the biotite bands themselves having an internal fine-scale striped pattern of S-bands at an angle of about 50° to the main band, the C-fabric. Thus the c-bands dip at 54° towards 287° azimuth, and the s-bands at 86° towards 107° azimuth. These S-C fabrics give a top-of-the-hole-to-the-north sense of movement.

Discussion and interpretation

The preservation of D_1 fabrics in these drill cores is considered to be the result of the drill holes being sited near the closure of the D_2 Norseman Anticline. The Norseman komatiite at this location trends approximately east-west, parallel to the D_2 and D_3

stress direction. As the komatiite is in a tensional orientation with respect to the D_2 and D_3 stress, it is less susceptible to remobilisation than komatiite with a strike at a larger angle to the stress.

10.4.4.4 D_1 thrust for the lower Penneshaw Formation

The lower Penneshaw Formation (eastern and central domains) comprises a thick mafic succession. During extensive drilling in this area in 1998 to 2000, it was found the igneous and volcanic textures such as pillow margins and chill zones at the margins of dolerite dykes, which are well preserved within the Woolyeenyer Formation, are identifiable within this area. The metamorphic grade of the lower Penneshaw Formation does not appear to be appreciably higher than the Woolyeenyer Formation. Following the recognition of the Hill Island thrust (figure 10.1), CNGC geologists working on the Penneshaw Formation proposed that the lower Penneshaw Formation could also be a repetition of the Woolyeenyer Formation. This proposal was assembled into a structural model by Connors (2000).

As there is little surficial exposure of the bedrock geology in the Penneshaw area, the location of the proposed thrust is inferred from aircore drilling to be where the bedrock geology changes from dominantly mafic, to dominantly felsic.

It appears that the western felsic domain of the Penneshaw Formation, the Noganyer Formation, and the Norseman Terrane greenstone stratigraphy, from the Woolyeenyer Formation to the rhyolite, has been thrust over the mafic succession in the lower Penneshaw Formation. The mafic Woolyeenyer Formation to the rhyolite has then been thrust over the Norseman komatiite by the Hill Island thrust. Thus the Hill Island thrust and the Penneshaw D_1 thrust are part of the same thrust sequence and stack the stratigraphy in the Norseman Terrane.

10.4.4.5. D_1 structures in the Noganyer Formation

Holcolme (1997) noted many D_1 characteristics within the Noganyer Formation. Thin section studies identified younging reversals, which define fold repetitions near the Jimberlana Dyke. At least one large synform-antiform pair was recognised with the eastern-most limb overturned. Further south, the Bon Accord jaspilite (which is the eastern-most jaspilite in that area) is also overturned. The folds are isoclinal with no axial plane cleavage.

Holcolme (1997) described a very ductile shear zone at the base of the Noganyer Formation north of the Jimberlana Dyke. It has a width of at least 50 metres and the rocks become platy and lineated. Minor isoclinal folds and transposed quartz veining are common. The north plunging lineation is coincidentally subparallel with the

stretching direction of D_2 so a very strong rodding is formed by the combination of the stretching and the intersection lineations. Asymmetric fabrics indicate a top-to-the-north dip-slip sense of shear. Holcolme (1997) considered the overturned folds in the Noganyer to be associated with the shear, which was suggested to be a very shallowly dipping thrust formed in D_1 that has subsequently been reoriented into its current dip-slip attitude by later folding. Smaller, parallel shear zones have also been noted higher in the Noganyer Formation.

The age of the western felsic domain of the Penneshaw Formation and the abundant dolerite dykes that cross-cut it, indicate that the felsic domain of the Penneshaw Formation predates the Woolyeenyer Formation and may be a fragment of the felsic basement that geophysical studies indicate lies beneath the greenstones of the Eastern Goldfields (see Chapter 7). The findings of Holcolme (1997) indicate that the Noganyer Formation was highly mobile in D_1, with a shallow top-to-the-north thrust movement. The location of the major shear zone, separating the eastern-most overturned jaspilite unit from the felsic domain of the Penneshaw Formation, indicates the Noganyer Formation is detached from the felsic Penneshaw. In the regional seismic reflection lines run north of Kalgoorlie, where the base of the basalt succession is not observed, regional seismic reflection lines have been interpreted as showing a detachment zone at the base of the greenstone, above the basement. It is possible that the shear zone at the base of the Noganyer Formation is an exposure of the detachment zone interpreted in seismic data.

Holcolme (1997) noted smaller parallel shears higher in the Noganyer Formation. These shears support the interpretation presented in Chapter 7 that there was originally only one jaspilite unit, as observed to the south in the Scotia area, and it has been structurally duplicated east of the Norseman township area. The structural duplication has occurred by thrusting, and by isoclinal folding. The three consecutive jaspilite units within the centre of the Noganyer Formation east of the township are all west-facing, and are not overturned, indicating thrust rather than fold duplication.

Petrographic evidence (Green, 1997) discussed in Chapter 7 suggests the Holstein Jaspilite, the western-most jaspilite, which lies immediately below the Woolyeenyer Formation, faces east. If this observation is correct then the uppermost jaspilite of the Noganyer Formation is overturned and there must be a major shear between the Woolyeenyer Formation and the Noganyer Formation. The Holstein Jaspilite would be an overturned limb of an isoclinal fold, with the upper limb sheared off. If this is the case the entire Noganyer Formation must be displaced with respect to both the underlying felsic Penneshaw and the overlying Woolyeenyer Formation.

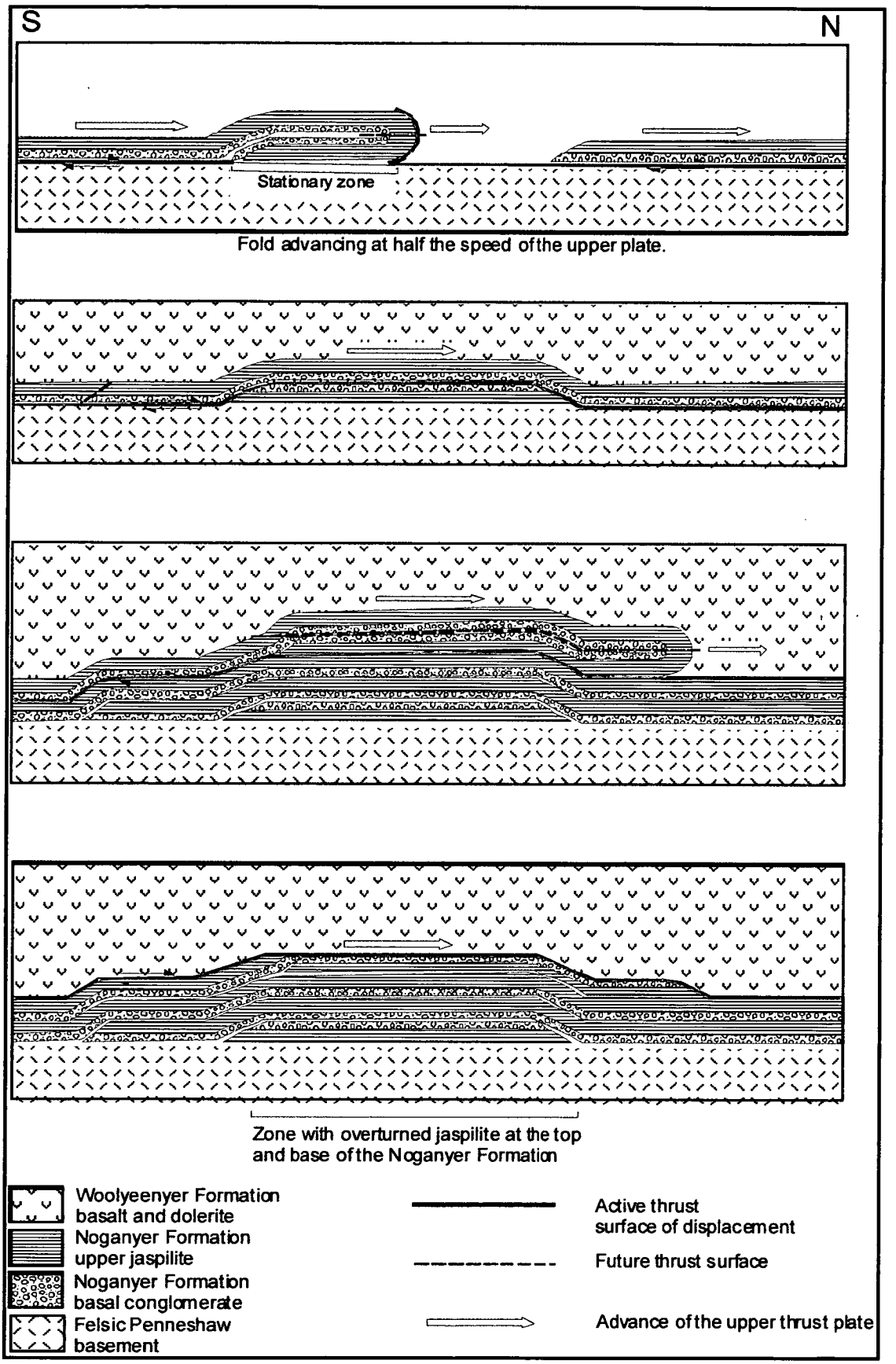

Figure 10.2: Cartoon cross-sections providing one possibility for the progressive D_1 fold and thrust development of the Noganyer Formation. Top cartoon shows initial thrusting and folding. Bottom cartoon shows ultimate development, with overturned jaspilite at the base (Bon Accord Jaspilite) and the top (Holstein Jaspilite). Woolyeenyer Formation is detached from Noganyer Formation where the latter folds over, and in the lower cartoon, where a fault movement between the Woolyeenyer Formation and the Noganyer Formation has removed the upper limb of a fold.

Green's observation about the facing of the Holstein Jaspilite remains tentative as it is based on limited petrographic studies. However, as reported in Chapter 7, the lack of abundant dolerite dykes within the Noganyer Formation, similar to those observed in drill core from the felsic Penneshaw, would support the displacement of the Noganyer Formation with respect to the Woolyeenyer Formation. The abundant dolerite dykes within the felsic Penneshaw and the lower Woolyeenyer Formation are considered to be feeders for the ascending basaltic magmas that formed the Woolyeenyer Formation. If they are present both below and above the Noganyer, then they should be observed within the Noganyer Formation if it was in its current location during the eruption of the Woolyeenyer Formation.

If the Noganyer Formation is detached and displaced with respect to the underlying and overlying formations, then there are major D_1 shear zones at the top and base of the Noganyer Formation. Other D_1 thrust faults within the formation, repeat the jaspilite zones. The Noganyer Formation would thus form a duplex system that has been thrust into its current location during D_1. One method that such a duplex with overturned jaspilites could be formed is presented in figure 10.2 as a series of cartoons showing progressive development.

There is another occurrence of jaspilite east of the Penneshaw Formation. These occur as isolated jaspilite enclaves in the highly tectonised zone along the western margin of the Buldania Granodiorite and at the base of the mafic part of the Penneshaw Formation (figures 1.3 & 10.4,). These jaspilite enclaves are considered to be equivalent to the Noganyer Formation.

10.4.4.6 Conclusion

Swager and Griffin (1990) provided the only previous description of a major D_1 thrust in the southern part of the Eastern Goldfields, being a duplex in the Kalgoorlie Terrane with the movement on the structure interpreted to be from south to north, based only on the geometry of the fault. The movement sense was not demonstrated with any certainty due to destruction of D_1 fabrics during later reactivation of the fault. The preserved D_1 thrust fabrics described in this section from the Norseman Terrane are therefore important as they confirm the movement of the D_1 thrust faults was top-to-the-north.

Given that D_1 thrust faults have not been identified in any localities other than in the Norseman Terrane, as described in this section, and the single duplex described by Swager and Griffin (1990), it appears that the Norseman Terrane may have a greater number of D_1 thrust faults than any other terrane in the southern part of the Eastern Goldfields.

10.4.5 N-S folding

Spray (1986) identified a folding event in the Norseman Terrane that he considered to have ENE trending fold axes. The event was considered to be late and to generate egg-box interference patterns with earlier NNW-tending folds.

ENE to east-west trending folds are recognised in this study, as plunge reversals are common for N-S trending F_2 faults at the Polar Bear Peninsula, and are also visible in aeromagnetic images.

A prominent example of a plunge reversal in aeromagnetic images is related to the Mission Sill. The serpentinised units of the Mission Sill are visible as a closure related to a south plunging syncline. Seven kilometres to the north, the same units reappear but as a hook-shaped closure with the opposite sense, plunging north (see figure 10.4).

Another example of a plunge reversal is provided by the geometry of the komatiite at the Polar Bear Peninsula. The east-west trending part of the komatiite at the Polar Bear Peninsula may be a reflection of the east-west portion of the Norseman komatiite, and the north-south trending section may be a reflection of the western limb of the Norseman komatiite.

Cross folds that cause such plunge reversals are broad, open folds with an approximately east-west trend, although the precise direction of their axes cannot be determined (figure 10.1). As the axes trend approximately east-west, they must be caused by N-S compression. As such a compressional event occurred in D_1, these folds are ascribed to D_1. Another suggestion, that the folds are late and related to the Albany-Fraser Orogeny cannot be dismissed, but is not the preferred explanation because the Albany-Fraser Orogeny post-dates the intrusion of the Proterozoic Dykes, and no deformation of theses dykes is apparent.

One result of the F_1 folding event that is important for this study is that it caused a northerly plunge to the stratigraphy in the Norseman township area. Following F_2 folding, which developed the Norseman Anticline, the northerly plunge of the anticline exposed the full 6 km thickness of the mafic succession and exposed the underlying units, the Noganyer Formation and felsic upper Penneshaw Formation. This section of the stratigraphy is not revealed anywhere else in the southern part of the Eastern Goldfields.

10.4.6 D2 east-west compression - thrust faults

10.4.6.1 Introduction

D_2 thrust faults are widely recognised in the Kalgoorlie region, particularly around granitoid domes. However, D_2 faults have only recently been recognised further south in the vicinity of Norseman (e.g. Connor 2000). As the fault surfaces are rarely exposed, the D_2 age of the thrust faults and the direction of movement is largely interpreted.

In this study, interpreted D_2 thrust faults are considered to have formed in response to east-west compression prior to regional folding, when the stratigraphy remained roughly horizontal. Thrusting is considered to have been east-west directed and typically focussed along ultramafic units. There is no evidence as to whether the thrusting involved movement of the hanging wall unit from east to west, or from west to east.

In the southern Coolgardie Domain, there are numerous approximately north-south trending thrust faults that may be related to D_2 east-west compression. These thrusts are revealed by repetitions of the komatiite, evident in aeromagnetic images, and also by out-of-sequence, juxtaposed stratigraphy, revealed by mapping and drilling. Examples of the latter are the BFB sediments lying beneath the komatiite below the Mount Thirsty Sill, and BFB sediments lying beneath the Woodcutters sill.

Although the majority of D_2 thrust faults occur in the southern Coolgardie Domain, a segment of Norseman komatiite was faulted during D_2 as indicated by a slice of imbricated komatiite close to the Tuna prospect, evident in aeromagnetic images of the Norseman Terrane.

In addition to having a movement sense orthogonal to D_1 thrust faults, D_2 thrust faults are an order of magnitude smaller. Stratigraphic offsets on D_2 thrust faults are typically hundreds of metres to a kilometre, whereas D_1 structures such as the Hill Island thrust have stratigraphic offsets in excess of 6 km, and possibly up to 10's of kilometres.

The numerous D_2 thrust faults within the Coolgardie Domain, contrasts with the Norseman Terrane where few are identified. This difference is considered to be due to the Norseman Terrane responding to D_2 compression mainly by folding and by the great thickness of competent basalts folded by the Norseman Anticline. Once formed, the east-west closure of the Norseman Anticline was not responsive to further east-west compression, and the competent basalts were not as susceptible to thrust failure as the ultramafics and sediments of the southern Coolgardie Domain. It

appears that further D_2 compression may have been taken up by a sinistral wrench motion on the terrane bounding faults (see section 10.4.8), perhaps due to the incompressibility of the Norseman Terrane following the formation of the Norseman Anticline.

10.4.6.2 Woodcutters Prospect description

A fault interpreted as a D_2 thrust is partially exposed and was mapped at the Woodcutters prospect within the southern Coolgardie Domain. The fault truncates the base of an altered komatiite layer and throws it against sandstone-shale turbidites of the younger BFB. The facing of the stratigraphy is known from differentiated layering in the Woodcutters sill. The geology of this prospect was described in section 6.3.6 and illustrated in figure 6.4.

The presence of a fault at this prospect is indicated by successive wedging out of komatiite flows. In the centre of the mapped area, there are at least four individual komatiite flows separated by interflow sedimentary bands. Within a distance of 400 metres to the north, three of the komatiite flows are truncated by a strike discordant NNE-trending fault.

The fault zone is marked on the ground by abundant quartz vein float in an area of poor outcrop. The best exposure was obtained from spoil next to a 1960's-vintage costean (now backfilled). This had schistose sedimentary rock of the BFB cut by a stockwork of blue-grey quartz veins.

As discussed in section 6.3.7, the fault can be traced 11 km to the NNE to the Pioneer prospect. At Pioneer, RC drilling provided evidence of a similar stratigraphy to that at Woodcutters, and shearing was identified at the base of the ultramafic rock.

Interpretation & discussion

The fault has significant extent and can be traced in aeromagnetic images to the NNE, curving around the corner of the Pioneer Dome, and then deflecting back to a N-S orientation through the Pioneer prospect, remaining at the base of the komatiite. This komatiite band continues north past the Pioneer Dome for about 40 km. The position of the fault, consistently at the base of the komatiite, suggests a dominantly layer-parallel fault. In the Woodcutters area the fault places ultramafic over younger BFB sediments. This juxtaposition, of older units overlying younger, and the layer-parallel nature of the fault, are consistent with a thrust. The local truncation of the ultramafic units overlying the thrust at Woodcutters prospect is unusual, suggesting that the Woodcutters area preserves a lateral ramp.

Over the extensive north-south length of the thrust, ultramafic is always thrown over the BFB indicating a largely east-west movement. The alternative, north-south directed thrusting is unlikely as it would require the offset of the fault to be equal to the N-S distance that the ultramafic rock lies above the BFB, i.e. in excess of 40 km. East-west thrusting suggests E-W compression, consistent with D_2.

10.4.7 D2 east-west compression – folding and fracturing

10.4.7.1 Introduction

D_2 is the most prominent deformation event in the area, forming upright folds with north-south trending axes and a prominent sub vertical cleavage. The largest of these folds is the north-plunging Norseman anticline, which is well defined by the Norseman komatiite in aeromagnetic images.

Holcolme (1997) noted that the S_2 cleavage has an unusual N-S trending, subhorizontal, stretching lineation. The lineation is particularly strong in the Polar Bear area, where pyrite nodules in sulfidic shales have quartz fringes. Keele (1984) previously noted the lineation in pebbles at the base of the Noganyer Formation. The lineation is unusual because contractional deformation systems generally have a steep stretching lineation, reflecting coincident crustal thickening. However, in the Norseman Terrane, the subhorizontal lineation shows that within the east-west compression, the crust was stretched in a north-south direction.

Holcolme (1997) also noted that north-south trending dextral shears and faults are commonly associated with D_2, particularly in the Noganyer Formation. The ENE bend in the Noganyer Formation is formed by north-south dextral faults offsetting the jaspilite units that actually have a NNE strike to their bedding. Holcolme (1997) suggested that the north-south striking dextral faults and east-west flattening with a north-south stretch could be the result of wrench-dominated transpressional deformation, which has decomposed into its simple shear and pure shear end members. The pure shear produces folds and cleavage whereas the simple shear component is partitioned into north-south striking shear zones that are almost parallel to the cleavage. Because the bulk deformation is wrench-dominated, the principal stretch deformation remains horizontal.

Other structural features attributed to D_2 in the Norseman Terrane include NE and NW trending lineaments, evident in large scale aeromagnetic images. These lineaments are abundant, but have very little apparent offset. It is considered that these lineaments are conjugate shear fractures, which formed in response to the east-west stress.

10.4.7.2 Norseman Anticline

Previous workers including Keele (1984) and Spray (1986) have used the presence of a fold known as the "Penneshaw Anticline" as evidence of the broadly east-west compression. The "Penneshaw Anticline" was defined by the deflection of the outcropping jaspilites of the Noganyer Formation from a north-south trend to the ENE in the vicinity of the Jimberlana Dyke. Sporadic north-south outcrops of jaspilite in a poorly outcropping area of granite and mylonite further west were considered to be the eastern limb of the fold, deformed by the Buldania Granodiorite.

McGoldrick (1993) and Holcombe (1997) mapped these outcrops north of the Jimberlana Dyke but found no fold closure. The jaspilites maintain a NNE strike but are segmented and offset by a swarm of dextral faults which leads to an apparent ENE trend. Holcolme noted that the isolated north-south striking segments of jaspilite in the Buldania Granodiorite are poorly understood, but appear to be caught up in a major shear zone with a sinistral sense of movement. The jaspilite segments may be a repetition of the Noganyer Formation at the base of the mafic lower Penneshaw, which is considered to be a repetition of the Woolyeenyer Formation. In any event, it appears that the jaspilite of the Noganyer Formation does not define a fold. The attitude of the Penneshaw Formation itself is unknown due to poor exposure so the "Penneshaw Anticline" is considered to have been based on erroneous data and is no longer valid.

Nevertheless, there is a major fold with a north-south fold axis in the Woolyeenyer Formation as shown by the Abbotshall Beds and Norseman komatiite, which in aeromagnetics define fold closures. This closure was called the "Norseman Anticline" by Keele (1984) with the axial trace passing through the north end of the Royal Peninsula and then across Lake Cowan through the area of the closure defined by komatiite. This anticline is a major structure which folds the majority of the greenstone. It has a northerly plunge due to the D_1 cross folds. Spray (1986) used the name "Norseman Anticline" for another structure defined further east, but that fold was based on erroneous stratigraphic correlations and is not accepted as valid.

10.4.7.3 Polar Bear

F_2 folds are prominent at the Polar Bear Peninsula and the S_2 cleavage is particularly intense ranging from fracture cleavage to schist. The F_2 folds have a wavelength of 500-600 m and repeat the stratigraphy in an east-west direction. Mafic rocks are exposed in the anticlines while the rhyolite is exposed in synclines. The plunge on the folds varies from north to south along strike due to the interference with F_1 cross folds. The shortest wavelength F_2 folds are in areas with rhyolite and sediment. This is considered to be due to the relative incompetence of these units. In contrast, the

basalt forms large competent blocks, less amenable to folding. The F_2 north-south stretching lineation is very strong at the Polar Bear Peninsula, defined by fringes on the pyrite nodules in black shale of the Abbotshall Beds.

The stretching has shortened the east-west axis of the rhyolite and stretched it in the north-south direction so it now has dimensions of 300 m by 3.3 km. Flow-banded rhyolite is commonly strongly lineated. The D_2 deformation has folded the rhyolite such that the original flow banding is now typically found as an upright foliation. The flow banding divides the rhyolite into thin sheets ranging from less than 1 mm to a few millimetres apart with the contact between the sheets forming a plane of weakness. The upright S_2 cleavage is subparallel to the flow banding and tends to follow the plane of weakness between thicker bands, enhancing the foliation related to the primary flow banding. The S_2 foliation follows flow bands oriented up to 14° away from the preferred cleavage orientation. The effect of the subparallel flow banding and cleavage is to form a strong foliation with a very strong intersection lineation.

10.4.8 D_{E2} extensional block faults

Holcolme (1997) suggested a cryptic interval of extension followed the east-west compression, evidenced by dip-slip shears in the Noganyer Formation. The Lady Mary Gabbro sill splits the stratigraphy within the Noganyer and was inferred to have been emplaced during this event, as were gabbros that cut the Noganyer Formation at a trend of 300°-330° in the Bon Accord area and fill NNW-trending faults. Holcolme (1997) was uncertain about the orientation of the extension, but suggested it may be broadly east-west. Another suggestion, that the microgranitoids and felsic porphyries intruded the stratigraphy during this event is not accepted in this study.

Keele (1984) noted block faulting with an east-block-down extensional sense of movement on the NNW trending Princess Royal Fault. This sense of movement was interpreted from the apparent dextral offset of the Bluebird Gabbro across the Princess Royal Fault at the North Royal. Keele considered the offset to be caused by the westerly dip of the Bluebird Gabbro and an east-block-down movement. This proposed east-block-down movement would explain the apparent dextral offset of the Noganyer Formation, where it is cut by the Princess Royal Fault as Keele mapped the jaspilite in this locality as having a moderate dip to the northwest.

Other large NNW faults such as the Wheel and Mount Barker Faults lie to the south of the Princess Royal Fault, but aeromagnetic images display only minor apparent dextral offset of the north-south trending section of the Noganyer Formation where it is cut by these faults. This is consistent with the block fault theory, as the north-south section of the Noganyer Formation dips almost vertically.

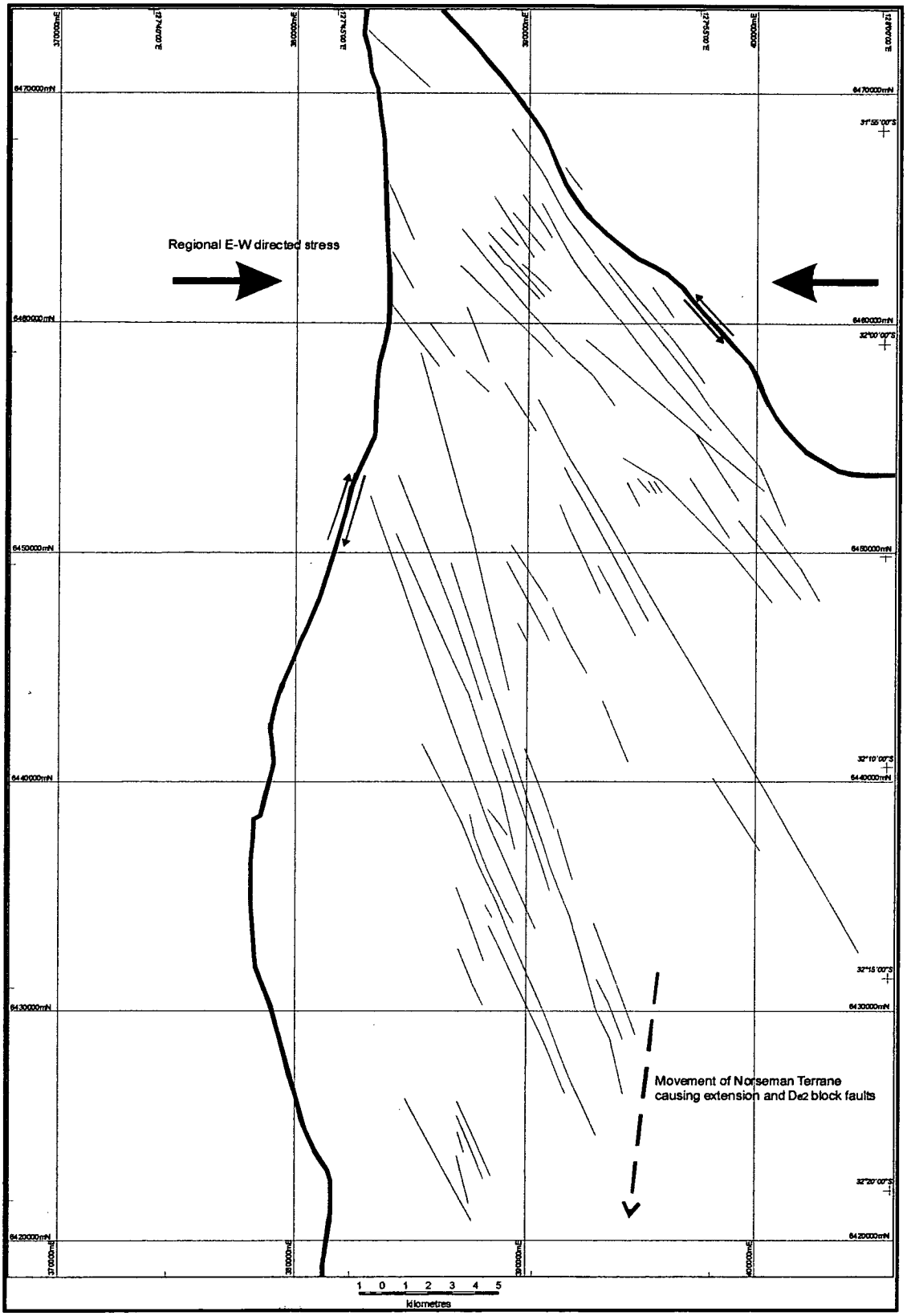

Figure 10.3: Interpreted movement on Terrane bounding structures (Mission Fault and Zuleika Shear) under E-W directed stress, causing an overall southerly movement of the Norseman Terrane and the release of compression, leading to formation of NNW-striking D_{E2} block faults.

Although the D_{E2} event is characterised in the Norseman Terrane by the formation of NNW trending extension faults, such extensional block faults have not been previously described in the Kalgoorlie Terrane. In this study, one possible extensional fault was noted within the southern Coolgardie Domain at the Woodcutters Prospect (section 6.3.6). This structure was recognised in aeromagnetics with a WNW trend, and its effect identified by geological mapping. The fault offsets BFB and komatiite, and a D_2 thrust at the base of the komatiite, but causes no offset of a pyroxenite layer (figure 6.4). Such a differential offset would be consistent with a post-D_2 block fault cutting layers with varying dips.

Therefore, block faults can be identified within the Kalgoorlie Terrane, but on current evidence, it appears they are rare and have a WNW to NW trend. In contrast block faults with a NNW trend characterise the Norseman Terrane.

The reason for the extensional block faults forming between the two east-west compressional events (D_2 and D_3) within the Norseman Terrane may be sinistral movement on the Zuleika Shear and dextral movement on the Mission Fault in response to E-W compression. This would result in overall southward movement of the Norseman Terrane and allow the formation of extensional structures (figure 10.3). The extension would thus occur within the regional E-W compression, but with the terrane bounding faults absorbing the compression and the resultant movement causing local extension.

10.4.9 D3 compression

10.4.9.1 Introduction

D_3 is coincident with gold mineralisation. In the Kalgoorlie Terrane, the most widely recognised structural schemes argue for an ENE directed compression in this event compared to due E-W for D_2. Large NNW-striking sinistral strike slip faults with associated with gold mineralisation such as the Boulder Lefroy Fault are commonly attributed to this event.

10.4.9.2 Movement on NNW structures in the Norseman Terrane

As pointed out in section 10.4.8, NNW faults in the Norseman Terrane are considered to have formed as block faults. However, Keele (1984) observed the effect of the Princess Royal Fault in the North Royal open cuts and showed that the latest deformation on it was sinistral. This observation was based on the offset caused to late porphyry intrusions. Such a sinistral movement would be consistent with the sinistral movement of the NNW trending faults at Kambalda. A sinistral deformation during D_3 for the NNW trending faults would imply an ENE-WSW

compression during this event. Like the NNW trending D_3 faults at Kambalda, the NNW faults in the Norseman Terrane are considered to have had a role in the gold mineralisation, which is considered further in Chapter 11. Thus, there are structural similarities for these deformational events in the Norseman and Kalgoorlie Terranes.

In contrast, Holcolme (1997) suggested a dextral movement on the faults, possibly based on the offset in evident aeromagnetic images. Holcolme sought to explain his inferred dextral movement by suggesting that it was caused by a pure shear contraction oriented at 45°. The explanation was that the Norseman Terrane lies within the strain shadow of regional NNW structures, such as the Zuleika Shear and Boulder-Lefroy Fault, which produce the dominant 315-330° trending structural grain in the Kambalda area to the north of Norseman. Holcolme suggested these structures may be in a bulk transpressional sinistral shear regime, but the effect of this shear regime on the low strain Norseman Terrane could be modelled by a pure shear contraction with the maximum shortening direction oriented at approximately 45°. The superposition of such a strain on pre-existing D_2 structures would reactivate steeply dipping N-S shears as dextral shears; 320-340° dilation zones are oriented such that they would be reoriented in contraction as reverse faults, perhaps with a minor component of dextral displacement.

Although the observation of Holcolme (1997), that Norseman lies in a strain shadow, without the dominant 315-330° structural grain is valid, the explanation for the movement on the faults is not accepted. Little explanation is provided for the reorientation of the stress to 45°. The explanation appears to assume the apparent dextral offset on the Princess Royal Fault is real. However, as noted in section 10.4.8, the apparent dextral offset on these faults can be explained using the findings of Keele (1984), that the faults have an earlier east–block–down dip-slip movement.

10.4.9.3 Mineralised D_3 structures

D_3 reflects a broadly east–west directed stress, and is the mineralisation event. Some authors consider D_3 to be distinguished from D_2 largely by a slight reorientation of the stress to an ESE-WSW orientation and activation of sinistral NNW-trending shears, rather than folding. The results of this study suggest D_3 and D_2 were part of a large scale compressional tectonic continuum, but that locally within the Norseman Terrane, the events can be distinguished by the effects of the strain. The differences include the separation of D_3 and D_2 by an extensional event, D_{E2}, and the smaller size and their post-folding timing and orientation of the D_3 faults.

Mineralisation occurred very late in the tectonometamorphic history of the greenstone domains and is typically the last event affecting long-lived faults (Groves

& others, 1995) In the southern part of the Eastern Goldfields, mineralisation developed under E-W to ENE-WSW directed compression.

The classic Norseman mineralisation is hosted in broadly N-S to NNE-striking quartz veins ("reefs"). These have a moderate dip to the east, typically varying between 30° and 60°. The characteristics of these mines have been extensively documented (Campbell, 1990; Thomas & others, 1990; McCuaig, 1996). The Norseman ore deposits are considered to have formed broadly syn-late deformation and syn-post peak metamorphism based on overprinting characteristics of alteration assemblages (McCuaig, 1990).

The north striking reefs are faults with a dextral-reverse offset (McCuaig, 1990). The reefs formed under ESE-WSW compression, but differ from the D_2 thrust faults also formed under broadly east-west deformation in the magnitude and timing of the offset. D_3 north-south striking ore-hosting structures have a reverse movement of less than 100 metres, while D_2 thrust faults typically have an offset of hundreds of metres to a kilometre. The different timing is shown by the orientation of the faults and is the most reliable distinguishing characteristic. D_3 structures are reverse faults in their current orientation whereas D_2 thrust faults formed as layer-parallel thrust faults prior to D_2 folding, and are now steeply dipping and typically layer-parallel. D_3 ore-hosting faults are too small to show on the regional structural map (figure 10.1).

10.4.9.4 Polar Bear Peninsula

A number of fault orientations are present in the mapped area at the Polar Bear Peninsula. The most common are north-south trending, typically with an apparent west-side-down sense of offset, based on stratigraphic juxtapositions. These faults are essentially parallel to stratigraphy and near parallel to the F_2 fold axes.

The Hinemoa Fault is one such north-south oriented fault, which can be traced for approximately 5 km. It hosts the abandoned Hinemoa Mine, a gold-bearing quartz reef, similar in style to the veins in the Norseman field. The expression of the fault in the vicinity of the Hinemoa Mine is a steeply east-dipping, faulted contact between talc-carbonate ultramafic rocks to the east and sandstone-shale turbidite to the west, suggesting a component of reverse movement consistent with east-west compression. Based on the layer-parallel movement and the divergence between mineralisation and the thrusting discussed in section 11.5.4, the Hinemoa Fault is considered to have initiated in D_2 but to have been reactivated in D_3. The D_2 section remains a steep thrust, whereas mineralisation within D_3 faulting attempts to attain a reverse fault orientation.

The Hinemoa fault can be traced in the vicinity of the Hinemoa Mine using the exposures in mine workings and by outcrop patterns as the fault throws black shales against ultramafic rocks. Further south, the Hinemoa Fault usually has black shale on both sides for most of its length. Its effect on the outcrop pattern is to broaden the black shale by structural repetition.

10.4.10 Terrane Bounding Structures

The structures which bound the Norseman Terrane are the Zuleika Shear to the east and the Mission Shear to the west. In section 10.3, it was noted that Swager (1997) suggested that the Kambalda Domain bounding faults may be initiated as D_1 thrust transfers, given that no D_1 thrust faults in the Kambalda Domain are recognized to continue into the Ora Banda Domain. Using a similar logic, the Mission Fault may have acted as a D_1 transfer fault to because the Hill Island D_1 thrust does not extend into the Coolgardie Domain.

However, the movement on the bounding faults to the Norseman Terrane is considered to be greater than the action of D_1 transfers. In Chapter 12, following a synthesis of all the results of the study and a consideration of the possible tectonic environment, it is proposed that the entire Norseman Terrane has moved northwards relative to the Kalgoorlie Terrane, closing the Kalgoorlie Basin and causing it to wrap around the Norseman Terrane. Such a movement is likely to have occurred on a basal detachment at the contact between the greenstone and the basement and by strike-slip movement along the terrane bounding faults. If this is the case, the terrane bounding faults must have an offset of tens of kilometres. Thus the bounding shears are suggested to be steep faults with a major strike slip movement that extend in depth to the basement but not into the basement.

D_1 folds with approximately E-W axes cross the terrane bounding faults, with interference patterns being apparent in southern Coolgardie Terrane and in the Norseman Terrane. This would suggest that the folding occurred at the cessation of the northward movement of the Norseman Terrane.

Although both the Norseman Terrane and southern Coolgardie Terrane have experienced F_2 folding, the physical expression of the folding appears to be individual to each terrane, as structures such as the Norseman Anticline do not extend across the terrane bounding faults. Thus the terrane bounding faults have taken up some of the strain in response to D_2 and partitioning it separately within the terranes.

10.5 NOTES ABOUT THE SOLID GEOLOGY MAP IN FIGURE 10.4

- The solid geology map provided as figure 10.4 was compiled using GSWA 1:100 000-scale geological maps, CNGC aircore drillhole data, aeromagnetic images, and mapping completed for this study, all interpreted by the findings of this study.

- The D_{E1} extensional faults at the margins of the granites are mapped using the findings of Holcolme (1997) for the Pioneer and Goodia areas on the western margin of the map. On the eastern margin of the map adjacent to the Buldania Granodiorite, Holcolme noted that a D_{E1} structure had been obliterated by later D_2 thrust faults and only traces of an early gneissic texture were preserved. In this area, D_2 thrust commonly occur as mylonite in granitoid dykes and sills. Nevertheless, the solid geology map shows a D_E fault adjacent to the Buldania Granodiorite as this is considered critical in the emplacement of the granite at its current crustal level. D_2 thrust are not shown in this area as they cannot be mapped with the data available.

- The Buldania Granodiorite was mapped using its distinctive texture in aeromagnetic images. The D_e fault was placed at the boundary of the granite. Basalt and sediment outcrops within the granodiorite north of the Jimberlana Dyke are probably represent roof pendants, as the aeromagnetics and outcrop geology indicates Granodiorite occupying this area. Granodiorite west of the D_E fault is considered to represent dykes and sills.

- Aircore drillhole data and aeromagnetic images indicate some minor ultramafic rocks within the Penneshaw Formation, east of the Noganyer Formation. It is unclear whether the ultramafic is extrusive komatiite, or intrusive dykes or sills. No specific interpretation is placed on the ultramafic.

- The western felsic domain of the Penneshaw Formation is mapped using the geology indicated in aircore drilling. The aircore holes indicate the area has approximately 30-50% felsic lithologies. The remainder of the area is dolerite and lesser basalt. These lithologies are considered to be consistent with the geology logged in PE1 (Chapter 7), with the mafic rocks representing dolerite dykes.

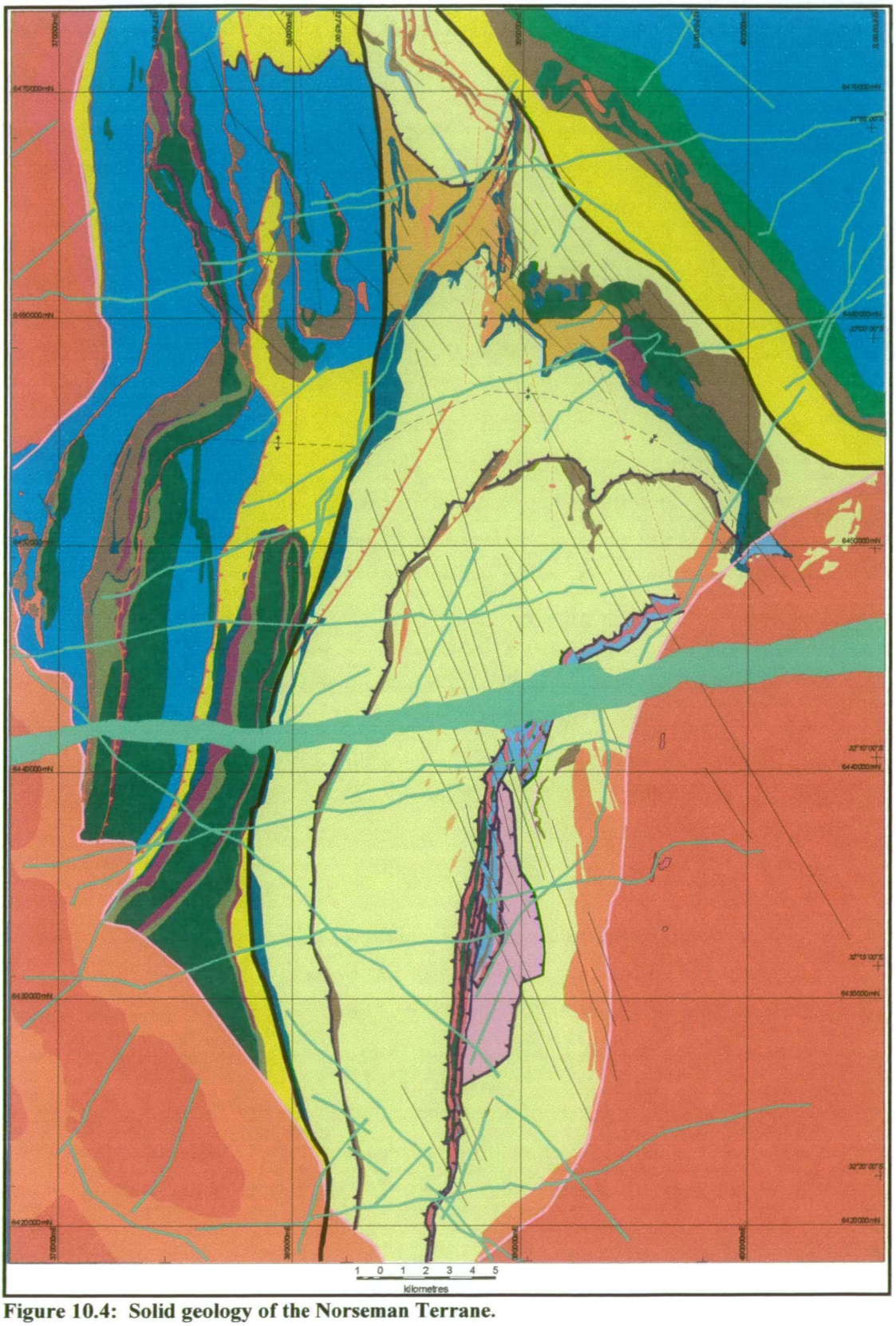

Figure 10.4: Solid geology of the Norseman Terrane.

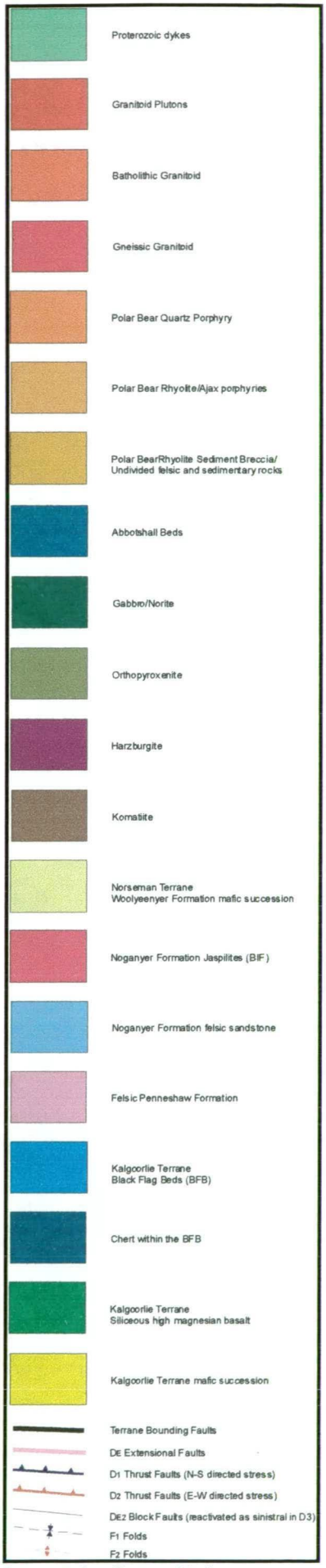

Legend for figure 10.4

- The extensive komatiite, layered mafic dykes and basalt within the part of the Coolgardie Domain shown, are interpreted from aeromagnetic images (komatiite and harzburgite units are typically highly magnetic) and outcrop mapping completed in this study or by the GSWA. Where these mafic and ultramafic units are surrounded by felsic and sedimentary rocks of the Black Flag Beds, they are interpreted to be emplaced by D_2 thrust faults.

- At the far north of the map in the Coolgardie Domain and Norseman Terrane, the rocks are covered by lake sediments and there are few aircore holes. The interpreted geology in this area is considered less accurate than the rest of the map. Mafic domains are shown as emplaced with D_1 thrust faults.

- As discussed in section 10.4.4, mafic stratigraphy in the Norseman Terrane is interpreted to comprise structural repetitions of the Woolyeenyer Formation, caused by D_1 thrust faults. The Chinaman's Well basalts overlying the Norseman komatiite are directly overlain by the Abbotshall Beds due to a pinch out of the komatiite, which would otherwise overlie the basalt. Such pinch-outs are recognised in the Kambalda region (section 2.4.2).

10.6 CONCLUSION

A complex sequence of deformational events has affected the Norseman region. Although many of the deformational events are recognised in other terranes, the Norseman Terrane also exhibits a number of unusual structural features that are not recognised elsewhere. These include early local uplift, stretching in the north-south direction accompanying east-west compression in D_2, and an extensional event causing block faults between D_2 and D_3. These deformational events indicate that Norseman has experienced different strain to the Kalgoorlie Terrane, probably due to the terrane bounding structures accommodating some of the regional stress and causing a different partitioning of strain within the Norseman Terrane. Some kinematic solutions have been proposed by previous workers to explain these unique deformational features, but a comprehensive, overall tectonic framework is not yet available to explain the complete deformational history of the Norseman Terrane.

A major contribution from this study is the recognition of major D_1 thrust faults, stacking the stratigraphy within the Norseman Terrane. The major structure recognised is the Hill Island thrust, for which an exposure was located. The structural fabrics within the Hill Island thrust demonstrate a top-to-the-due-north offset. It is also speculated that the Noganyer Formation may have been emplaced beneath the Woolyeenyer Formation in D_1 as a thrust duplex.

This study also recognised D_2 thrust faults affecting the southern Coolgardie Domain. An example of such a thrust was mapped at the Woodcutters prospect, and traced north in aeromagnetics to the Pioneer prospect, where it was located by drilling. These thrust faults are typically layer-parallel and throw komatiite above the BFB. These thrust faults are common within the southern Coolgardie Domain, but rare in the Norseman Terrane.

The Norseman Terrane has responded to D_2 E-W compression by folding into the Norseman Anticline. It is suggested that few D_2 thrust faults are found in the Norseman Terrane because the broad closure of the Norseman Anticline was unresponsive to further east-west compression and the great thickness of basalts in the fold are competent and non-susceptible to thrust failure. In addition, it is suggested that further east-west compression may have been accommodated by strike-slip motion on the terrane bounding shears, leading to the entire Norseman Terrane moving south. Such a motion would cause extension in the Norseman Terrane and would therefore explain the unique extensional event that occurred within the Norseman Terrane between the D_2 and D_3 E-W compressional events. The extensional deformation generated NNW-striking block faults such as the Princess Royal Fault that are prominent within the Norseman main gold field.

The final compression event, D_3, is considered to have been formed under E-W to ENE directed compression and was concurrent with gold mineralisation. It remobilised the NNW block faults formed in D_{E2} with a sinistral movement. As these NNW-striking faults were formed as block faults, they are straight and parallel, contrasting with the long and sinuous, sinistral strike-slip shears such as the Boulder-Lefroy Fault, which are associated with gold mineralisation within the Kalgoorlie Terrane. Under D_3, the reefs that host the major gold lodes at Norseman were also formed, being north-south striking, reverse faults with a component of dextral motion, and south-dipping, ENE-striking fractures in a tensional orientation. North-south striking D_3 faults can be separated from D_2 thrust faults by their post-folding orientation, such that they remain moderately-dipping reverse faults in their current orientation, rather than the steeply dipping layer-parallel D_2 thrust faults.

CHAPTER ELEVEN

Mineralisation and Targeting

11.1 INTRODUCTION

Approximately 5 Moz of gold has been won from the ore bodies at Norseman with the metal coming predominantly from quartz reefs hosted within the lower section of the Woolyeenyer Formation. The area in which the major orebodies occur, close to Norseman and on the Royal Peninsula, is known as the "main field". The major historic production has come from three reefs, the Mararoa, Crown and Princess Royal reefs with the latter structure providing nearly 2 Moz, almost as much as the other two combined. These reefs have a N to NNE strike and dip moderately to the west but at a high angle to the mafic stratigraphy. The reefs lie within shear zones and the orebodies are dominantly developed where the reefs are hosted by dolerite or ultramafic dykes. More recently, production has been sourced largely from reefs known as crosslinks, striking ENE to E and with a dip varying from shallow to steep towards the SSE.

The orebodies at Norseman have been comprehensively studied over a long period, with the most recent and relevant studies including Campbell (1990), Keele (1984) and McCuaig (1996). However, the focus of these studies was largely at ore shoot scale, stope scale and larger, seeking to determine the controls on the development of orebodies, the development of reefs and the controls on the deposition of gold. No studies have worked at a smaller scale and examined the regional controls on the gold mineralisation. This chapter develops a model to explain the location of gold mineralisation at the scale of shear zone networks such as the main field adjacent to Norseman township (figure 1.3) (Norseman, Mararoa, Crown, Bluebird Link, OK reefs). A well documented example of such a shear zone network is displayed by the Harlequin prospect (figure 3.3, 3.4). The chapter defines controls that can be identified at a regional scale and thereby develops a predictive capability for targeting further networks.

Format of the chapter

The first part of the chapter discusses a history of exploration targeting at Norseman and general models for Archaean lode gold mineralisation. The second part of the chapter examines mineralisation in the Norseman area in grater detail. Classic Norseman reef-hosted mineralisation is discussed first, with reviews of relevant studies culminating in the proposal of a model to explain the locations of gold-bearing shear networks or complexes, areas of approximately 2 to 4 km^2. The third part of the chapter examines gold mineralisation at the Polar Bear Peninsula, which

exhibits significant differences to the classic Norseman reefs. Features of the mineralisation are described and the implications for its formation proposed.

11.2 TARGETING HISTORY

Gold was discovered at Norseman in 1894, reputedly when a prospector's horse named Norseman unearthed a gold nugget. The field contains little gold in the regolith and underground workings quickly developed. The history of the targeting and discovery of orebodies at Norseman from WMC's entry into the field in 1933 through to the 1980's has been comprehensively documented by Campbell (1990). In essence, the targets at this time were new blind ore shoots on known N-S striking quartz reefs. Exploration consisted of limited diamond drilling and extensive driving along strike using interpreted shoot plunges and hypotheses such as the favourable beds concept. Although highly successful, the utility of these methods were exhausted by the 1980's when all the major known N-S reefs and many of the minor E-W reefs in the main field had received some form of testing. With little recent success in the main field, access to new exploration acreage was required for new discoveries. However, a major problem was that away from the main field, the bedrock is largely buried by unconsolidated transported cover, so the presence of reefs that might be prospective for new orebodies was unknown and the old targeting methods were not appropriate.

With improvements in drilling technology, in the mid-1980's to early 1990's, RAB and aircore drilling, were used to test for gold in regolith beneath cover in land areas, searching for near surface ore. Targets were largely empirical, being along-strike extrapolations of known mineralisation and gold or arsenic in soil anomalies. The Scotia Mine approximately 30 km south of Norseman was found in this period.

The real impetus to remote targeting took place between 1990 and 1993. By 1990, the North Royal pits were exhausted and underground mining was working orebodies with short lives or taking remnants from mined-out positions at Scotia, the Royal Tiara, the Regent, OK and Viking Mines. It was apparent that new orebodies were needed urgently for the survival of CNGC. The most attractive new exploration acreage was offshore of the Royal Peninsula, near the North Royal Mine, the best ore body in the field. To work on Lake Cowan would require a technological advance to develop a drilling rig that was mobile on the muddy surface of Lake Cowan, and would also require new targeting and exploration procedures. Ultimately, a custom designed drilling rig was successfully developed, mounted on Norwegian Hagglunds, which are designed to travel over snow.

Concomitant with the lake drilling developments, in 1991, the Bluebird Link orebody was discovered in the main field. This was a classic old-style Norseman success, a

blind orebody in the heart of the main field. However, this orebody occurs on a reef with an ENE strike, considered to be a tensional orientation and termed a "crosslink". Although crosslinks were previously known from the goldfield, they had received little consideration as targets as no significant mineralisation had previously been discovered in them. Therefore, the discovery highlighted crosslinks as prospective targets for exploration in the main field.

The lake targeting methods were largely developed by the exploration geologists at the time. Considerable work was undertaken documenting what the regolith expression of near surface Norseman orebodies was and what drilling grid would be required to find them, using Scotia and the North Royal as examples.

A principal concept of the early lake targeting was that NNW corridors control the metallogenic plumbing system in the Norseman area (Peters & others, 1991). This concept followed the ideas of Thomas & others (1990), who noted that ore zones in the N-S reefs were associated with major NNW-striking fault corridors and suggested that "the Princess Royal Fault and associated splays may have a direct and fundamental control on the distribution of gold mineralisation". It was considered likely that such a NNW corridor may lie between North Royal Mine and the Higginsville Mine to the northwest of Lake Cowan. Specifically, the Princess Royal Fault was projected towards Higginsville.

Targeting concepts were further developed by Archer (1990), who considered that the Princess Royal Fault and other NNW-striking shear zones were important controlling structures in the emplacement of the Norseman ore bodies. Archer (1990) also pointed out that NNE-striking lineaments may be important based on the observation that the Dragon Lineament passes through the Golden Dragon open cut and is associated with brittle west-dipping shearing. With further refinement, a targeting model using aeromagnetic remote sensing was developed, based on intersections between N-S and NNW-trending lineaments.

Using multiclient aeromagnetics with 200 metre spaced flight lines, the intersection between a N-S and NNW-trending lineament just offshore of the Royal Peninsula was targeted. The target, named "Harlequin" was tested by the new Hagglund-mounted drill rigs in December 1992. One of the aircore holes intersected reef quartz with visible gold. Subsequent diamond drill testing from gypsum causeways revealed a major gold deposit in a crosslink orientation (figure 3.3). This was ultimately opened up as the HV1 orebody at the Harlequin Mine. Subsequent testing has revealed an array of further gold-bearing reefs and exploration is ongoing (figure 3.3, 3.4). Of the original target elements, the NNW-trending lineament is the

Wheel Fault and the N-trending lineament was found to be a magnetic low over the elongated Harlequin Granodiorite.

11.3 LODE GOLD MINERALISATION

Groves & others (1995) reviewed lode gold deposits in the Yilgarn Craton and pointed out features which suggest that Archaean lode gold deposits are a coherent genetic group that formed approximately contemporaneously at the full spectrum of crustal depths at about 2635±10 Ma. Most deposits appear to be syn-peak to post-peak metamorphism. Differences in age of up to 20-30 Ma cannot be discounted with available dating and deposit styles overprinting each other may be present in the same field (e.g. Mt Charlotte in the Kalgoorlie Goldfield).

Collectively available data for lode gold deposits suggest that the P-T conditions range from 180°C at <1 kbar to 700°C at 5 kbar. A deeply sourced, low salinity, H_2O-CO_2-CH_4 bearing fluid, which has been equilibrated with granitic rock and has moved up vertically extensive fluid conduits is implicated. Over-pressured fluids are indicated by hydraulic breccias, which imply that fluid flow will be outward, away from source and there will be an upward directed hydraulic gradient.

The mineralisation occurred very late in the tectonometamorphic history of the greenstone domains and is commonly the last event affecting long-lived faults. The lack of evidence of mineralisation in major craton and greenstone-scale faults suggests they these large faults were never major fluid conduits. Most deposits are related to second, third or lower order faults. In some instances there is no obvious shear control on the mineralisation and it has moved up pipe-like fracture zones in competent units (e.g. Mt Charlotte). Thus, it is difficult to define a structural model for fluid focussing that is applicable to all lode gold deposits in the Yilgarn Craton. The concept that fluid was focussed into low mean stress sites may be the most universal application. On a more regional scale, most gold deposits are focussed in competent units or at the contacts between units of contrasting competency in greenstone belts that are sub-perpendicular to the inferred east-west compression. Incompetent units are rarely mineralised, except in fold hinges where layering is locally sub-parallel to far field compressive stress.

As discussed in section 2.2.4.3, Drummond & Goleby (1998) noted that a possible source of the Au-bearing hydrothermal fluids has been interpreted in seismic reflection images from north of Kalgoorlie. The interpreted source is an anomalously non-reflective section of middle crust adjacent to the intersection of the Ida fault and the Bardoc Shear at about 15 km depth. The lack of reflectors in this zone is of interest as it may result from homogenisation of crustal densities due to either

dehydration or hydrothermal alteration. The area of this non-reflective crust measures approximately 40 km wide by 15 km thick.

11.4 MINERALISATION IN NORSEMAN DEPOSITS

11.4.1 Formation of Norseman vein-hosted mineralisation

Classic Norseman quartz reefs have relatively minor wall rock alteration and there is insignificant gold mineralisation within the wall rock in comparison to the quantity of gold in the quartz veins. These features are considered to indicate that gold deposition is controlled by pressure change rather than chemical changes related to wall rock interaction.

Incremental opening of the veins caused an influx of fluid into the low pressure site and devolatilisation of the fluid. The loss of volatiles, including H_2S, drove a chemical reaction that destabilised gold complexes and caused the precipitation of gold. McCuaig (1996) considers that the "ubiquitous occurrence of native gold in quartz vein, and the location of gold orebodies in dilation sites on the quartz vein systems, suggests that phase immiscibility may have been the dominant mechanism for gold deposition".

The lateral zonation of alteration assemblages reflects the progressive addition of LILE (K_2O, Cs, Rb, Ba) and volatiles (H_2O, CO_2, H_2S) to the wall rock. REE, HFSE, P, V, Sc and Al are relatively unaffected by even the most intense alteration (McCuaig, 1996). Galena is characteristic in gold-bearing reefs in the main field, whereas arsenopyrite is common at Harlequin.

McCuaig (1996) used various geothermometers to calculate hydrothermal alteration temperatures of 420°-475°C for northern deposits (North Royal), 470°-500°C for central deposits (Mararoa and Crown), and 490°-540°C for the southern deposits at Scotia.

Variably deformed veins and contiguous alteration assemblages indicate that all deposits formed during deformation.

11.4.2 Norseman Pb Isotopes and ore fluid sources

Pb isotopic data from lode gold deposits in the Eastern Goldfields tends to form linear arrays interpreted as a mixture of two Pb sources in the ore fluid. The sources are considered to be the mantle-derived greenstones and a more radiogenic component derived from granitic crust. Deposits lying in extensive mafic greenstone successions tend to have a greater proportion of greenstone-derived Pb.

Browning & others (1987) showed that Norseman galenas had an unusually radiogenic Pb-isotopic composition. Perring (1989) undertook further sampling of ore galenas and confirmed the work of Browning & others. Petrographic work suggested the most radiogenic galenas formed late in the ore mineral petrogenesis. Perring concluded the radiogenic nature of the Norseman ore galenas as compared to other gold-related galenas in the eastern Goldfields is probably due to the unusual abundance of granitic rocks with respect to mafic ones in the Norseman district.

McCuaig (1996) found that galena and altaite compositions in the Norseman deposits become more radiogenic to the south, to the east and with increasing depth. Together, these variations reflect increasing proximity to the felsic Penneshaw or the Buldania Granodiorite at the eastern margin of the Norseman Terrane.

Although the external granitoids that bound the greenstone belt in the Norseman district have appropriate compositions to explain the radiogenic Pb within galenas (McCuaig, 1996), a more likely source is felsic basement. As the base of the mafic succession is exposed at Norseman, it is suggested that the basement is relatively close to the surface. Indeed, the felsic domain of the Penneshaw Formation is considered to be a fragment of the basement (*cf.* Chapter 7). Similarly, basement is considered to be close to the margin between the mafic eastern Penneshaw and the Buldania Granodiorite due to the presence of Noganyer Formation-style BIF outcrops in that area.

As suggested in section 11.3, ore fluids appear to be deeply sourced and have equilibrated to granitic rock and moved vertically up extensive fluid conduits. This is consistent with the identification in seismic images of a possible ore fluid source in the basement (section 2.2.4.3). This evidence suggests that the basement is more likely to be the source of ore fluids than the external granitoids.

The felsic Penneshaw is likely to have extremely radiogenic Pb as the one trace element analysis available of granitoid in the felsic Penneshaw, indicates exceptionally high abundances of U and Th. (The analysis is provided by Ghaderi (1998) from drillhole PE1-*cf.* Chapter 7).

Thus, the highly radiogenic nature of the Pb in galenas at Norseman is considered to reflect the greater proximity of the orebodies to the felsic basement, compared to any other deposit in the Kalgoorlie region.

11.4.3 Norseman NNW-striking fault control

As noted in section 11.2, Thomas & others (1990), noted the association of ore zones with major NNW-striking fault corridors and suggested that the Princess Royal Fault may have a direct control on the distribution of gold mineralisation.

Archer (1990) considered that the Princess Royal Fault and other NNW-striking shear zones were important controlling structures in the emplacement of the Norseman ore bodies based on three lines of evidence:

- The observation that Norseman ore bodies can occur juxtaposed against the western side of NNW-striking faults (eg. North Royal against Princess Royal Fault; Crown against "B-Fault"; Golden Dragon against "GD-Fault"), and that the highest grades at the North Royal occur close to the Princess Royal Fault.

- The poles to planes of faults, reefs, shears and quartz veins plot on a common great circle on a stereonet which can be inferred to suggest the NNW-striking faults are part of the structural regime which has given rise to the reefs.

- Work by McCuaig showed that a similar suite of chemical elements are enriched within the NNW-striking faults and the reef shears, suggesting that the same fluids had passed through both types of structures. The latter point is described in more detail below.

McCuaig (1996) described the Princess Royal Fault close to the North Royal Mine as a greater than 100 m wide zone of planar to anastomosing ductile fabric varying in intensity such that weakly deformed blocks are surrounded by zones of intense fabric development. The metamorphic mineralogy of the host rocks is destroyed and replaced by chlorite + carbonate + quartz ± plagioclase with biotite abundant in discreet zones. The shear fabric is defined by alignment of chlorite, biotite and quartz-carbonate veins that have been transposed subparallel to the shear zone margins.

McCuaig (1996) also described B-Fault, a NNW striking, brittle-ductile shear zone that transects the Regent Mine stratigraphy and deforms the Mararoa and Crown vein systems. Mineral assemblages comprise amphibole + quartz + ilmenite ± chlorite ± plagioclase ± biotite. A ductile fabric is well developed defined by the alignment of amphibole + chlorite and the rodding of quartz. The similarities between the hydrothermal alteration surrounding folded gold-bearing quartz veins in B-Fault and that surrounding the Mararoa and Crown reefs indicates that B-Fault was active during mineralisation and acted as a conduit for ore fluids.

McCuaig's observations were made in close proximity to the mines, so it is not possible to be certain that mineralised fluids from the reef shear did not permeated and alter the NNW-striking shears rather than vice versa. However, observations from regional exploration drillholes, distal from the mines supports his contention that the NNW-striking faults were conduits for fluids. A drill hole at approximately 6452500mN, 397550mE MGA, NE of Norseman, intersected alteration associated

with a NNW-trending aeromagnetic lineament that lies along the footwall of a section of the Norseman komatiite. Percussion drill spoil at this location comprises reef quartz with strong biotite-carbonate alteration. The samples were assayed for gold but returned no significant result. Further drill holes in the area did not detect any gold in regolith and it was concluded that the quartz and alteration was not associated with any near surface gold resource.

From this intersection two inferences can be made:

- prominent NNW-striking faults have been altered by mineralisation-style hydrothermal alteration, distal from any known gold mineralisation, suggesting they are ore fluid conduits as proposed by McCuaig (1996); and

- gold entering the ore fluid was a discreet event, occurring during a narrow time interval. Outside of that period, fluid was produced and produced appropriate alteration, but no gold was present.

Subsequent to the work of the previous authors who noted a link between gold mineralisation and NNW-striking faults, further empirical evidence has been gathered from new discoveries of mineralisation that NNW-striking faults are important in the localisation of gold deposits. The Wheel Fault, a prominent NNW lineament, projects through the Harlequin prospect, very close to the orebodies. It was in fact the linear that was targeted and resulted in the discovery of HV1. The Wheel Fault also projects into the Jewfish prospect, an area with regolith and bedrock gold mineralisation.

11.4.4 Norseman ore-hosting structures

The dominant ore-hosting structures at Norseman are north-south striking reefs with a reverse-dextral movement as documented by Keele (1984), and crosslink structures with an ENE strike and a southerly dip. These orientations support an ENE-directed compression during the mineralisation event, which occurred during D_3.

On N-S reefs, the character of the mineralisation has been comprehensively documented by Campbell (1990). Ore shoots tend to be better developed on flatter sections of the reefs where there is greater dilation. Steeper sections are generally not significantly mineralised. Mineralisation on crosslink structures is not well confined to flatter sections as these reefs are not reverse faults. The controls on the ore shoots are not clear.

Rather than being viewed in isolation, Norseman ore bodies can be considered to occur within integrated shear systems. The Harlequin prospect is a particularly well documented shear system with mineralisation having been located on numerous

interconnecting structures including HV1, HV6, HV5A, HV5B, HV5C and HV5F (figure 1.3; 3.3, 3.4). Further discoveries at Harlequin are being made as exploration expands outwards from HV1. The Mararoa, Crown, Bluebird Link (Bullen Mine) and Norseman Reefs as well as other local shears and structures adjacent to the Norseman township can also be considered to be an interconnected mineralised complex, hosting over 2 Moz of gold. The Princess Royal and North Royal Mines form another complex vein system that hosted approximately 2 Moz.

11.4.5 Host Rock Control at Norseman

Campbell (1990) described an idea that was developed at Norseman during the course of exploration in the 1940's, of certain stratigraphic units being favourable for the development of ore shoots and hosting all the significant gold deposits. This concept was used to guide exploration which ultimately discovered the North Royal Mine. The favourable stratigraphy concept was re-evaluated by an extensive stratigraphic study of the main field using drill core during the 1980's. The outcome of this work, described by Thomas (1991), was to draw attention to the ubiquitous development of all major reefs within a pre-existing mafic or ultramafic intrusive dyke. The apparent restriction of major ore positions to a particular part of the stratigraphy was concluded to actually reflect the occurrence of dykes favourable for reef development.

Subsequently, more recent ore discoveries, such as Harlequin, in new stratigraphic units such as the Desirable Pillow Lava, have supported the conclusions of Thomas (1991), as the ore shoots are largely hosted by medium-grained dolerite dykes. There appears to be a strong rheological control on the development of structures favourable for ore shoots, with medium-grained rocks being important. The rheological control may act by providing a brittle host rock, initiating failure or causing refraction of the host structure.

As described in section 11.4.1, pressure release through dilation appears to be the primary control on the deposition of gold in the Norseman orebodies. Accordingly, brittleness, allowing the development of veins appears critical in the development of economic mineralisation. It appears that dolerite dykes are more competent than basalts and form better dilational sites.

Empirical observations of the importance of medium grained rocks have been reported by Campbell, (1990) for the main field. Another example is the Sailfish prospect, which hosts high grade gold mineralisation only within the Bluebird Gabbro. Conversely, mineralisation discovered to date at the Jewfish prospect is insufficiently rich to form an economic proposition, being hosted in thinly-veined

and altered basalt, perhaps because the absence of dolerite dykes at the prospect prevented the formation of a quartz reef.

The refraction control exerted by medium grained rocks is shown by the HV6 shear where it flattens as it exits the western side of the Harlequin granodiorite (figure 3.4). The HV6 ore shoot is developed at the contact with the granodiorite where the shear flattens.

11.4.6 Model for fluid conduits at Norseman

A model is proposed here for controls on gold mineralisation at a shear network or prospect scale, built upon the observations described above. The model is necessarily speculative as data is not comprehensive or conclusive. It is proposed that NNW faults connect to a deep structure that is tapping the ore fluid source. The NNW faults have this role as conduits because they were active during D_3, the time of mineralisation, and because (having originated as block faults), they are relatively steep and cut down through the stratigraphy to the basement. In contrast, earlier major faults such as the thrusts developed during D1 and D2, were not active at the time of mineralisation, and are largely layer parallel, so they fold with greenstone stratigraphy rather than cut through it. The fluid is assumed to have been sourced from deep in the basement, therefore the conduit feeding fluid from the source to the gold lode must cut through the greenstone and reach a conduit in the basement. As the base of the greenstone is proximal at Norseman, it appears the basement is not far beneath the main field, which is supported by the highly radiogenic Pb compositions of ore galenas. Accordingly, it appears that the NNW faults should be sufficiently penetrative to reach the basement.

A corollary of this model is that larger NNW faults are more prospective than smaller faults. Detailed large-scale examination of aeromagnetic images of the Noganyer Formation reveals numerous NNW lineaments cutting the BIFs. However, most of these faults are very small and are not visible in smaller scale images. Such small NNW-striking faults are considered less prospective as they may not be large enough to reach the basement and tap into fluid source. Therefore the most prospective faults are obviously the larger ones such as the Princess Royal Fault, the Wheel Fault, the Mt Barker Fault and other unnamed lineaments between the Wheel Fault and the Princess Royal Fault.

However, the model does not suggest the NNW-striking faults carry anomalous gold grades all along their length. Rather, it is assumed that the NNW-striking faults were subject to fluid pressure and had the potential to transmit fluid provided a low pressure site was generated to attract the fluid. During D_3, failure occurred on the ore hosting structures at Norseman, generating dilational sites. The formation of the low

pressure site provided the ore fluid with a destination so it rapidly moved through the NNW-striking faults and into the dilational sites.

In the periods between shear failures, there was no movement of fluid along NNW-striking faults because there was no low pressure site attracting fluid. Given the NNW-striking faults and reef shears were subject to similar degrees and orientations of stress and may have experienced similar fluid pressures, they are likely to have failed synchronously, aiding the transport of fluid from the basement. Fluid would tend to travel up the most convenient route from the basement source to the low pressure site, rather than all along the NNW-striking shear zone. Where fluid has moved along the NNW-striking faults, into the reef shear, the NNW-striking faults carry substantial wall rock alteration.

As noted in section 11.4.1, a pressure drop appears to control deposition of gold in the orebodies at Norseman, so a dilational site is needed to form an economic ore position. No mineralisation has yet been located in NNW-striking faults, possibly because no dilational sites have been located. Perhaps dilational sites do not exist within NNW-striking faults, but the structures have not been comprehensively explored. Mineralisation within the NNW-striking faults cannot be ruled out.

The critical factor for an ore hosting structure is to be active and dilational during D_3, when ore fluids are available. The shear system must also intersect a NNW-striking fluid conduit at some point, to feed fluid into the system.

To generate a reef, a medium to coarse grained the host rock is important. Within the lower part of the Woolyeenyer Formation, dolerites are ubiquitous, so suitable sites are likely to occur. Other suitable rocks are substantial felsic bodies that can act as discontinuities causing the reef shear to refract.

11.4.7 Prospectivity

The major NNW-striking faults are considered to be critical in feeding ore fluids into the shear zone networks, and can be used in exploration for new gold deposits in the Norseman field. The NNW-striking faults are most prominent where they cut the Noganyer Formation. The most prospective faults appear cut the Noganyer from the Princess Royal Fault in the north, to the end of the Bon Accord BIF in the south. A number of un-named NNW-striking faults, south of the Mount Barker Fault, project through the main field, close to Norseman.

In terms of finding new gold deposits, ore hosting structures must also be considered. Ore hosting structures have not been detected remotely in aeromagnetic datasets as they are narrow, do not have a substantial offset or alteration and the N-S striking structures in particular are parallel to stratigraphy in the main field. However, some

areas can be predicted to be more likely to slip under ENE compression. The N-S to NE-striking sections of the Norseman komatiite are likely to slip with a dextral movement as this is a weak lithology. However, a brittle host rock such as a late dolerite cutting the komatiite would need to be located. Such dolerites do exist, having previously been intersected within the Norseman komatiite.

In terms of host rocks, the importance of dolerites suggests the lower parts of the Woolyeenyer are likely to be more prospective than the upper sections. This is because there is a greater quantity of dolerite dykes lower in the Woolyeenyer Formation. Basalts close to the top of sequence are cut by fewer dolerite dykes. Empirically, this model is supported by the Jewfish prospect. Bedrock gold mineralisation has been found at Jewfish, hosted in basalt primarily as zones of alteration, but the grades and continuity of the mineralisation is not sufficient to be economic. The lack of a quartz reef to host the gold is considered to be due to the absence of dolerite dykes. Only basalt is found at the Jewfish prospect, because it lies close to the Abbotshall Beds, which mark the top of the basalt sequence.

Due to the Hill Island thrust, lower, dolerite-bearing sections of the Woolyeenyer Formation should occur in the Chinaman's Well basalt above the Norseman komatiite as well as in the main field. The lower sections of the Desirable Pillow Lava below the Norseman komatiite contain plentiful dolerites, but these are expected to become scarce closer to the Norseman komatiite. Similarly the upper sections of the Chinaman's Well basalt are likely to be less favourable for Norseman style ore deposits.

Iron oxide bearing, granophyric layers of differentiated tholeiitic dykes are important hosts for gold deposits in the Kambalda region and at Kalgoorlie. As discussed in Chapter 7, these late-stage sills, which typically lie at the base of the BFB, are rare at Norseman. However, minor magnetite-bearing examples have been intersected within drillholes in the Norseman komatiite. The major late stage sills within the southern Coolgardie Domain are high magnesium varieties and do not contain iron oxide-bearing zones and do not appear to host epigenetic gold mineralisation.

The magnetite within the BIF of the Noganyer Formation should be an excellent chemical host rock to form gold deposits through sulfidation reactions. (It appears that the iron oxide alteration to form the BIF predated the gold mineralisation event because when gold intersections are made in the BIF, they appear to be in gossanous, sulfidised BIF). An additional positive factor is that the BIFs are cut by the NNW-striking faults providing conduits for the ore fluids. However, no significant gold deposits have been located within the BIF. Two explanations can be provided for this conundrum:

- Firstly, dilational sites probably did not occur within the Noganyer. The layers within the formation are sub-perpendicular to the inferred stress direction during D_3 and are steeply dipping. Failure within the Noganyer would be most likely to occur as slippage between layers rather than as reverse faults. These movements are unlikely to have provided dilational sites to attract ore fluids. As noted in section 11.3, Groves & others (1995) pointed out that incompetent units are rarely mineralised except in fold hinges.

- As argued in section 11.4.3, there appears to have been a delay in gold entering the potassic and carbonated fluids. Hence, quartz veins can be found, associated with extensively biotite-carbonate-pyrite altered shears, but no gold. The introduction of gold into these fluids appears to have occurred as a later discreet event. The result of this delay is that early fluids have altered the BIF prior to the arrival of gold-bearing fluids. By the time the gold enters the system, the wall rocks to the conduits have been altered and are in equilibrium with the fluids. Hence the fluid does not contact the wall rocks and no sulfidation reactions occur to destabilise gold complexes. Gold mineralisation typically occurs only in fractures where gold-bearing fluids leak out into unaltered BIF.

As a result of perhaps one or both of these reasons, despite extensive exploration, no bulk, BIF-hosted gold mineralisation of the Hill 50-style (Mount Magnet) has been located within the Noganyer. Instead, the Noganyer Formation hosts a large quantity of gold in insignificant fractures which cannot be aggregated into commercial orebodies. No significant structured ore bodies have been located within the Noganyer.

To date, all mineralisation discovered in the vicinity of Norseman is located in the Norseman Terrane. Extensive aircore drilling west of the Mission Fault in the White Butt, Heliopolis, Pioneer, Petersen's Gossan and Mt Thirsty project areas did not locate any significant mineralisation. The reason for this relationship is not clear. The closest mineralisation that has been located in the Coolgardie Domain is at Higginsville, 50 km to the NNW.

11.5 MINERALISATION AT THE POLAR BEAR PENINSULA

11.5.1 Introduction

The Polar Bear Peninsula has been poorly explored in contrast to the Norseman region. The reason for this may be the isolation of the area, and the lack of immediate success of the exploration efforts. As a consequence, mineralisation at the Polar Bear Peninsula is poorly known in contrast to the Norseman area.

The detailed mapping work for this study located several prospective zones for gold mineralisation which were tested with drilling. Gold mineralisation was located at two of these prospects. These occurrences are significantly different to typical Norseman reefs discussed in section 11.4. This section will document the preliminary observations about the Polar Bear Peninsula mineralisation.

11.5.2 Exploration History

Historic gold mining at the Polar Bear Peninsula has been centred around the Hinemoa or Day dawn Mine, located on the eastern side of the peninsula. Ore was won from a quartz reef which trends north-south with a dip varying from vertical to 77° east. The surface workings follow the faulted contact between talc-carbonate ultramafic and argillaceous sedimentary rocks. Maps of the workings suggest that the ore shoot is either horizontal or pitches gently to the north.

11.5.2.1 Prospecting at the Hinemoa Mine

The early history of the Hinemoa Mine was described by Catling (1899). The Hinemoa Mine was initially named "Day Dawn" and prospected by a Mr McGonigal probably in the year or two following the discovery of gold at Norseman in 1894. Ownership of the lease passed to Central Wealth Consolidated Goldfields Limited who developed the mine "vigorously" then lost confidence. The loss of confidence may have been due to the presence of copper mineralisation in the form of attacamite ($Cu_4Cl_2(OH)_6$) within the reef. The Scottish Westralia Company bought the mine in May 1898 on the recommendation of a Mr J.W. Tank, who recognised that the copper was not in metallic form and would not affect gold amalgamation.

The Scottish Westralia Company equipped the mine and floated it and the surrounding 42 acres (17 ha) in London under the name "Hinemoa Mine". Five shafts were sunk, proving the continuation of the reef from one end of the ground to the other, a distance of about 650 m. Total production to March 1899 was 2041 tonnes at 27.2 g/t for 1783 ounces. The subsequent history of the company is not documented.

The main shaft is vertical, following the reef for the first 76 feet (23 m), then moving into the footwall as the reef flattened in dip to about 77° east. The country rock is "felstone" (ultramafic?). The reef is ferruginous at the surface, but changes to a dark amber colour with depth. At the 150 foot level (46 m), the reef is "impregnated with copper", about 3 foot (0.9 m) in width and 640 foot (195 m) of driving located two "splendid chutes" (shoots) 400 foot (122 m) and 40 foot (12 m) in length. Maps of the ore suggest the larger shoot has a gentle pitch to the north. At the 200 foot level

(61 m), the reef occurs 2 foot (0.6 m) inside a body of slate. The crosscut extended another 10 foot (3 m) in slate before "felstone" was again encountered.

Stanley Leeders, a Norseman-based prospector, acquired a small gold mining lease (GML) surrounding the Hinemoa Mine, opened the mine and stoped minor quantities of ore in the late 1970's and early 1980's. CNGC acquired an option in 1980 and explored the GML with detailed mapping and extensive drilling. Some mineralisation was encountered and a resource estimated of 30,300 tonnes at 11.3 g/t in two separate blocks. This was not considered adequate to exercise the option and it was allowed to expire.

11.5.3 Mineralisation Characteristics

A number of mineralised prospects have been located in the belt of rocks exposed along the eastern side of the Peninsula (figure 11.1). These rocks include ultramafic rocks, fine-grained sedimentary rocks and felsic rocks, which are atypical compared with those hosting the gold-bearing reefs within the Norseman main field.

11.5.3.1 Hinemoa Fault

Description

Mineralisation associated with the Hinemoa Mine is hosted by the Hinemoa Fault that trends north-south along the contact between the Abbotshall Beds and the komatiite (figure 3.2). The komatiite is exposed in the core of a tight anticline (section 3.2.5). The western contact of the komatiite with sedimentary rock is the Hinemoa Fault. Mapping the fault to the north and south reveals repeated enclaves of ultramafic rocks in shale associated with small workings and shearing, suggesting there is some thrusting associated with the contact. In addition, drilling around the Hinemoa Mine has found ultramafic units around the contact separated by as much as 15 m of black shale, an unreasonably thick unit to represent interflow sedimentary rocks. It is likely that this indicates thrusting of ultramafic slivers into the Abbotshall Beds.

Near surface, the Hinemoa Fault appears to be near vertical based on mine inspection reports (Catling, 1899) and observations of the old workings. At about 20 m depth, Catling reported that the reef in the Hinemoa Mine deviates to a flatter dip of approximately 80°E. Drilling data at the Hinemoa Mine suggests further flattening of the mineralisation to 65°E and to about 30°E immediately north of Leeders GML.

The Abbotshall Beds-ultramafic rock contact remains steep which implies the flatter dipping mineralisation migrates away from the contact. The mineralisation appears to jump to contacts between faulted slivers of ultramafic rock and sedimentary rock

horizons. Beyond about 30 m from the western ultramafic contact, there are no further interflow sedimentary rocks and the mineralisation again becomes steep, following the interflow sedimentary rock and dying away between 90 and 120 m depth.

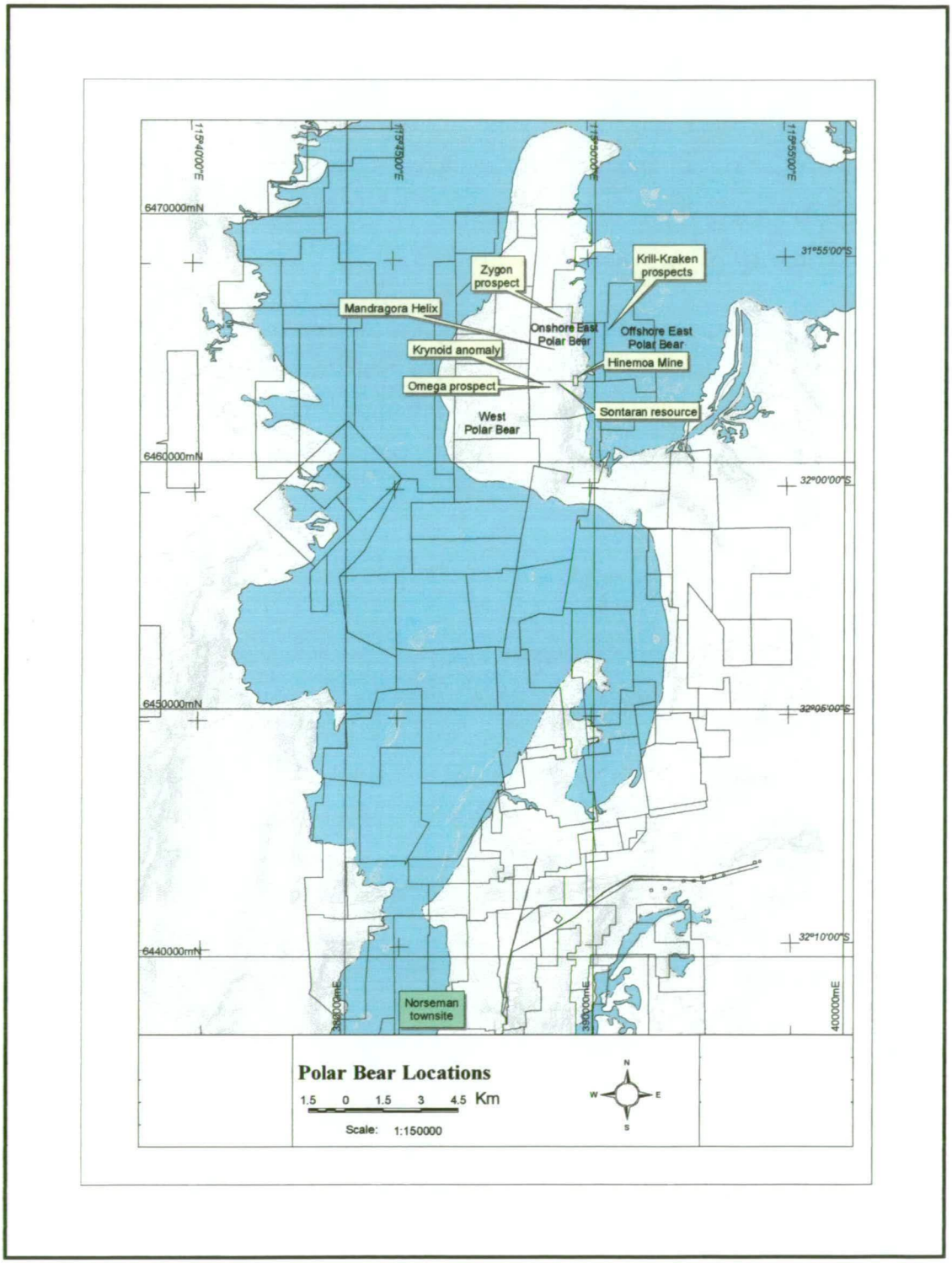

Figure 11.1: Location plan of the Polar Bear Peninsula and some of the major prospects.

Thick quartz reefs with a true width of up to 8 m are common in the drill holes around Hinemoa Mine, but do not appear to be a major host for gold mineralisation. Some veins are mineralized along their contacts, others are barren. Mineralisation appears to favour less prominent laminated veining.

Intense carbonation is a feature of the ultramafic rocks in the Polar Bear area resulting in recrystallised carbonate rocks with fine quartz veinlets. In drill core from Hinemoa Mine these zones are interlayered with talc-carbonate rocks and are probably the result of an intense CO_2 flux along fluid conduits. Mineralised quartz veins have euhedral carbonate growth in the vein indicating the carbonate introduction predated or was synchronous with the mineralisation.

Interpretation & discussion

Hinemoa Mine mineralisation can be characterised as quartz vein-hosted, localised in shear zones which follow ultramafic-shale contacts. The shear zones attempt to attain a moderate easterly dip but are strongly controlled by lithological contacts and die out away from these.

The steep dip of lithologies is probably the result of east-west D_2 compression, which caused thrusting of ultramafic enclaves into shales of the Abbotshall Beds and folding to steep dips. Mineralisation was introduced during D_3 compression that was also approximately east-west directed, but differed from D_2 in that the rock package had already been folded into a steep orientation. Thus, D_3 resulted in faults that are reverse in their current orientation. D_2 layer-parallel thrusting generated platy hydrous minerals along slip surfaces. D_3 faults attempted to follow these layers as they are the lowest friction surfaces.

11.5.3.2 Sontaran Prospect

Description

The Sontaran prospect lies near the top of the basalt succession exposed in a large scale anticline. Komatiite is absent, probably due to a stratigraphic pinch out, so basalt is directly overlain by the Abbotshall Beds (figure A1.2.3, Appendix 1). The basalt is pillowed, very fine-grained, highly amygdaloidal and aphyric with altered feldspar microlites being the only visible crystals. Interflow sedimentary bands within the basalt succession are frequent and range in thickness from <1 to 6 m thick. These sedimentary rocks typically have the appearance of laminated chert at the surface, but below the base of weathering, they are generally found to be black shales or siltstones although lesser sulfidic chert has also been intersected.

Plate 11.1. Stockwork veining in outcropping interflow sedimentary rock along the main lode at Sontaran.

Plate 11.2. PEN1206 sedimentary rock & basalt drill core from approximately 58.8-68.0 metres depth. The white material is vein quartz; the orange is limonite staining from weathered sulfide.

The main lode at Sontaran is exposed at the surface as an interflow sedimentary rock approximately one metre wide with stockwork quartz veining (Plate 11.1). The mineralisation follows the interflow sedimentary band, which strikes at 35° and has a steep dip of 85°SE (figure 3.4; 3.5). To the NE, the interflow sediment band is truncated at the base of the Abbotshall Beds along an angular unconformity. At this location, the mineralisation deviates to follow the Abbotshall Beds-basalt contact, which strikes north and dips 50°E (figure 3.5). The grade of the mineralisation diminishes as it changes direction.

The most reliable data about the Sontaran mineralisation was obtained from a single diamond hole, PEN1206. At 65.0 m depth, the mineralisation is hosted by bleached basalt just below the contact with laminated sediment (Plate 11.2). In the partly weathered core hole, the sedimentary rock appears to be cherty with iron oxide staining after sulphide. However, in an RC hole drilled beneath PEN1206, the sedimentary rock is black shale, suggesting that the shale is silicified near surface.

The mineralised structure at Sontaran differs from the typical Norseman-style reefs as it comprises quartz veins between brecciated basalt clasts rather than laminated reefs and sulfide (dominated by fine-grained arsenopyrite) is more abundant. The core of the structure in PEN1206 is a zone approximately 2 m wide with abundant altered basalt clasts hosted in a quartz matrix with arsenopyrite. This extends outwards into crackle-veined basalt and finally fragments of brecciated vein quartz hosted by chloritised and sulfidised wall rock. Minor sulfide in fractures continues approximately 2 m beyond these quartz-bearing zones. Traces of galena are present in the quartz-rich core of the mineralisation but visible gold has not been observed. Correlation of analytical results with logging from the RC holes suggests that the highest grades are associated with the most abundant arsenopyrite and the quantity of vein quartz is unimportant.

Although all the rocks in the Polar Bear area are moderately cleaved, there is a subtle increase in the foliation extending about one metre away from the main lode in the basalt, suggesting a discreet shear zone. Overall, however, the mineralisation does not appear to be heavily influenced by structural fabrics.

Interpretation & Discussion

The brecciation around the mineralisation appears to be hydraulic, implying over-pressured fluids. The hydraulic failure has been localised in a small discreet shear. The shear was initiated along a lithological contact, probably due to the interflow sedimentary rock being a discontinuity in the basalt package, forming a plane of weakness during regional compression. The NNE orientation of the interflow

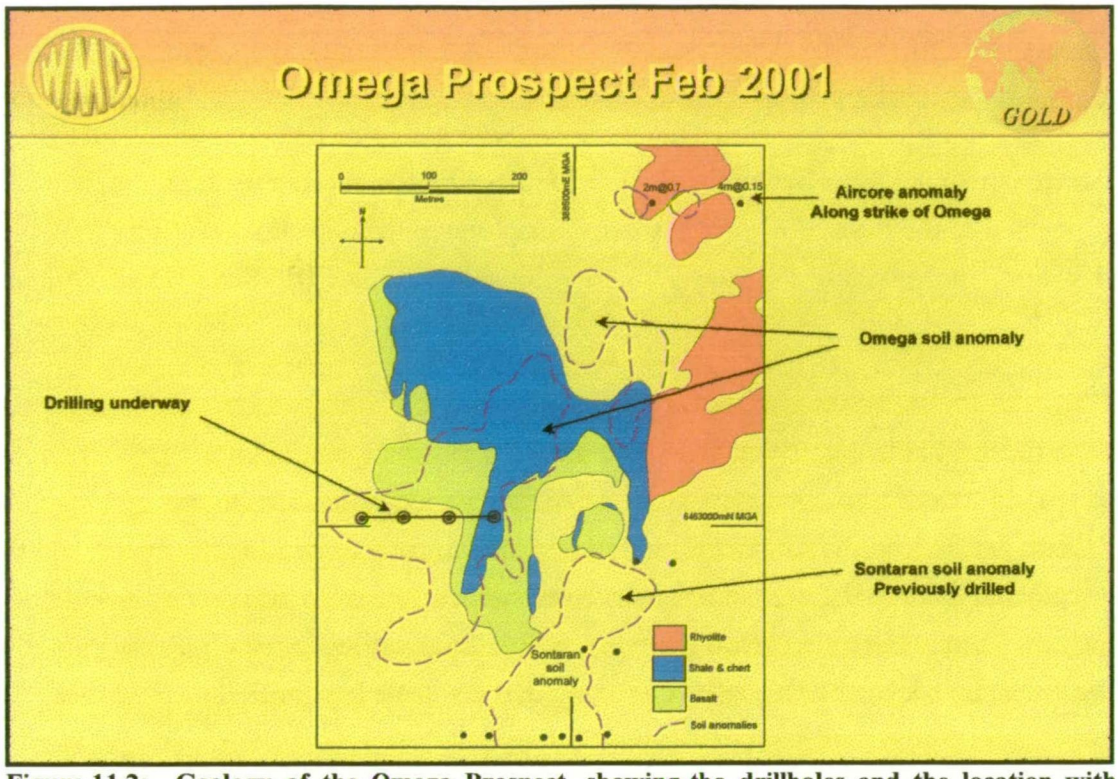

Figure 11.2: Geology of the Omega Prospect, showing the drillholes and the location with respect to the Sontaran Prospect.

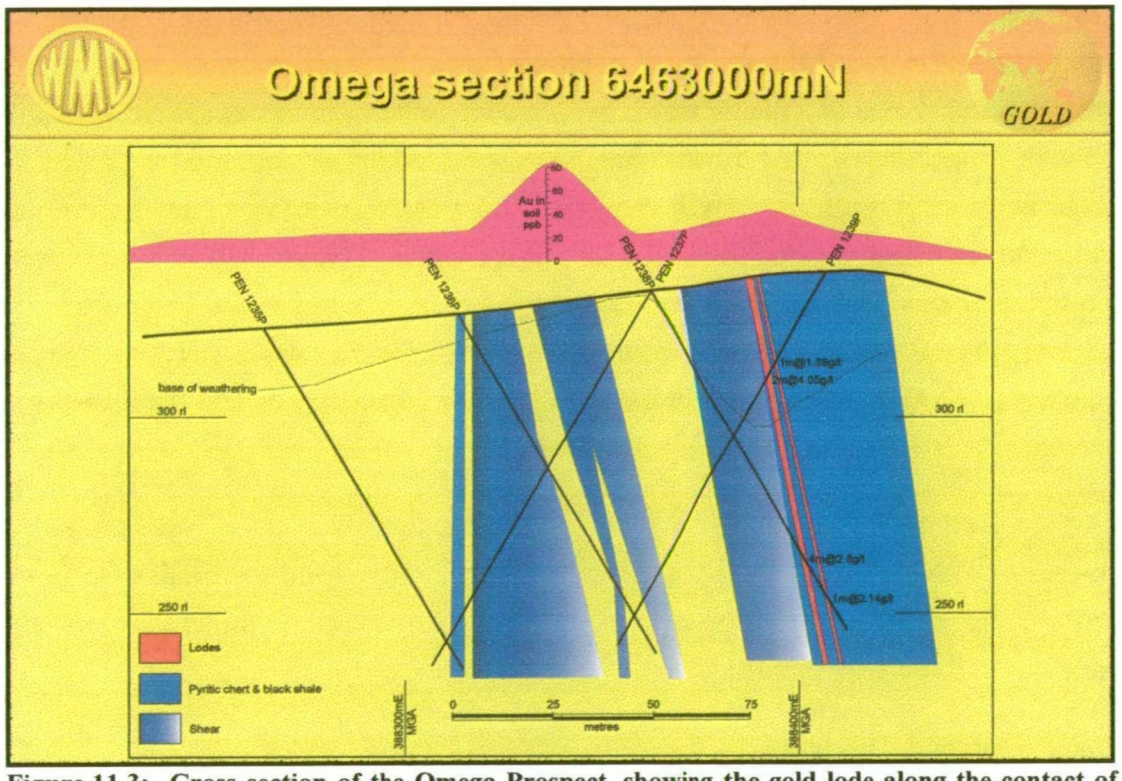

Figure 11.3: Cross section of the Omega Prospect, showing the gold lode along the contact of the sedimentary rock, and the shear zones. At the top is a graphical representation of the Au in soil values.

sedimentary band was also a near-optimal orientation for dextral slip during east west compression.11.5.3.3 Omega Prospect.

Omega prospect occurs about 150 m northwest of Sontaran (figure 11.2)

Description

The geology is similar to the Sontaran prospect. Basalts are exposed in the large anticline adjacent to chert of the Abbotshall Beds. An unusual geometrical feature of the geology is a 170 metre long tongue of chert extending SSW along a ridge top from the main belt of sedimentary rock that trends east-west at the anticlinal closure (figure 11.2). In fresh rock, the chert is found to consist of laminated pyritic chert and lesser sulfidic black shale.

Drilling at the Omega prospect showed that the NNE-trending tongue of chert is fault controlled. A moderate to strong shear zone approximately 15 m in width, lies in basalt immediately adjacent to the chert. Two thin gold lodes are hosted within the sedimentary rock, close to the contact with the sheared basalt (figure 11.3). The orientation of the lodes is similar to the Sontaran prospect, NNE striking and steeply dipping to the east at about 80°, subparallel to the chert contact. The lodes were drilled with reverse circulation holes, therefore, little is known about the textural characteristics of the mineralisation except that some vein quartz is associated with the intersections.

Interpretation & Discussion

Absence of diamond drilling limits the understanding of the gold lodes at the Omega prospect. Nevertheless, it appears to bear a striking resemblance to Sontaran prospect. The important control on mineralisation would appear to be the basalt-sedimentary rock contact, which in turn was caused by a fault.

11.5.4 Common features of the mineralisation at the Polar Bear Peninsula

There are two common themes that can be recognised for the mineralisation at the Polar Bear Peninsula. One is that all resources with multiple intersections so far have been found in anticlines. Anticlines are generally considered to be favourable for lode gold deposits, but it is not clear whether they are important at the Polar Bear Peninsula. The apparent anticline association may be a host rock control as anticlines tend to expose mafic and ultramafic rocks, whereas synclines tend to be filled with rhyolite.

Another common theme of the known mineralisation at the Polar Bear Peninsula is its localisation against sedimentary rock contacts. However, it is not clear whether

the sedimentary rock relationship is a cause or effect of the structure initiating the mineralisation. The less intense structures such as Sontaran appear to follow the sedimentary rock contacts. Strong structures such Omega, appear to cause the juxtaposition of the sedimentary rock and basalt rather than following a stratigraphic contact. The Hinemoa Fault appears to involve both themes; the fault is strong and exhibits enclaves of ultramafic rock thrust into the black shale. However, it also appears to be close to the position where the stratigraphic contact is expected. Adjacent to the Hinemoa Mine, shearing occurs along the contacts of thin ultramafic and sedimentary bands and mineralisation appears to migrate east across to these sedimentary bands to achieve a moderate dip while following planes of weakness caused by existing shearing.

It is likely that the current structural regime observed for the mineralisation at the Polar Bear Peninsula was generated by two stages of deformation. The main stage of orogenic east-west deformation, D_2, initially generated thrusts with a north-south strike (Hinemoa Fault) and small dextral strike-slip faults with a NE orientation (Omega). Thrusts initiated at a shallow angle were steepened by subsequent north-south trending, tight to isoclinal folds. Dilational jogs in the reverse faults were infilled with massive quartz, but no mineralising fluids were involved at that time.

By D_3 the folds had achieved their current shape and locked up. Continued moderate east-west to ENE-WSW directed deformation was accommodated by faulting, which was enhanced by the introduction of over pressured mineralising fluids. Structures generated under this deformation regime were primarily steep NE dextral or moderately dipping north-south reverse faults. The rheological contrast of sedimentary rock-basalt or ultramafic rocks was vital discontinuities exploited by the deformation. The sedimentary rock contacts used were both pre-existing D_2 structures, which were reactivated during D_3, and interflow sedimentary rock contacts which had not previously been deformed. Thus the Sontaran prospect exhibits little tectonic deformation but strong evidence for control by over pressured fluids, whereas reactivated structures such as the Omega prospect shows strong tectonism. The Hinemoa Fault has strong shearing, but mineralisation migrates east jumping to D_2 thrusted ultramafic-sedimentary rock layers as it follows attempts to achieve a moderate dip.

11.5.5 Conclusion

Mineralisation at the Polar Bear Peninsula occurs at orientations which are favourable for fault activation under broadly east west compression. N-S and NE trending structures are known to be favourable. NW structures may also be important as the conjugate partner to the NE structures. Sedimentary rock contacts, as discontinuities, appear to be important in localising shears.

Despite the differences in geometry and host rock between the Hinemoa Mine and classic Norseman Reefs such as the Mararoa, there are some similarities. Both systems are hosted by north-south trending reverse fault systems. Rheological contrasts appear to be important in the generation of the fault system. The Mararoa follows the ultramafic Butterfly Dyke, whereas the Hinemoa Fault follows ultramafic-sedimentary rock contacts. The Hinemoa Mine also appears to have a shallow northerly ore shoot plunge similar to the Mararoa. Therefore blind orebodies may occur that do not project to the surface, but have significant subsurface strike extent, similar to the Mararoa. Detailed mapping at the Polar Bear Peninsula has extended the known length of the structure from 1 km to 4.5 km, but testing for deeper orebodies on the Hinemoa Fault has not been undertaken.

CHAPTER TWELVE

Synthesis: Formation of the Norseman Terrane and its relation to surrounding domains

12.1 INTRODUCTION

There has been extensive speculation about the evolution of the Yilgarn Craton and the Eastern Goldfields in particular for the last 35 years. Models for granite greenstone evolution generally fall into one of three categories:

- ensialic rift models;
- plate tectonic island arc/backarc basin models; and
- Mantle plumes rising from the core-mantle boundary.

The latter model has generally fallen out of favour, primarily because it fails to explain the regional shortening. Variations on the former two models are most commonly invoked.

Earlier models tended to concentrate largely on explaining the mafic and ultramafic rocks, the compressional structures and the granites, as these are the features which were the most widely known at the completion of the GSWA 1:100,000 scale mapping between Norseman and Menzies. For instance, Swager (1997) suggested deposition of the greenstones in an original east-west, ensialic extensional basin, formed as a failed rift above an aborted spreading centre. The basin closed in response to far-field stresses controlled by convergence and/or collision at a distant plate boundary. More recently, results of the AMIRA Project 437 study have become available, providing data about the felsic and sedimentary successions that were previously largely neglected. The felsic and intermediate rocks have a strong subduction signature, suggesting that plate tectonic models are the most appropriate for at least the latter stages of the greenstone history. Barley and others (1998), and Hand (1998) used this information to formulate a detailed plate tectonic model, using the Solomon Islands area of the southwest Pacific as an analogue.

This study does not propose a comprehensive tectonic model because it would be presumptuous to use a study of the Norseman Terrane to explain the genesis of the entire Eastern Goldfields. However, the findings of this study do place constraints on the models and some new ideas that will be pointed out. In addition this is one of the most detailed multidisciplinary studies undertaken on the difference between terranes and large scale tectonic information can be gleaned from the results, which must be fed into any models.

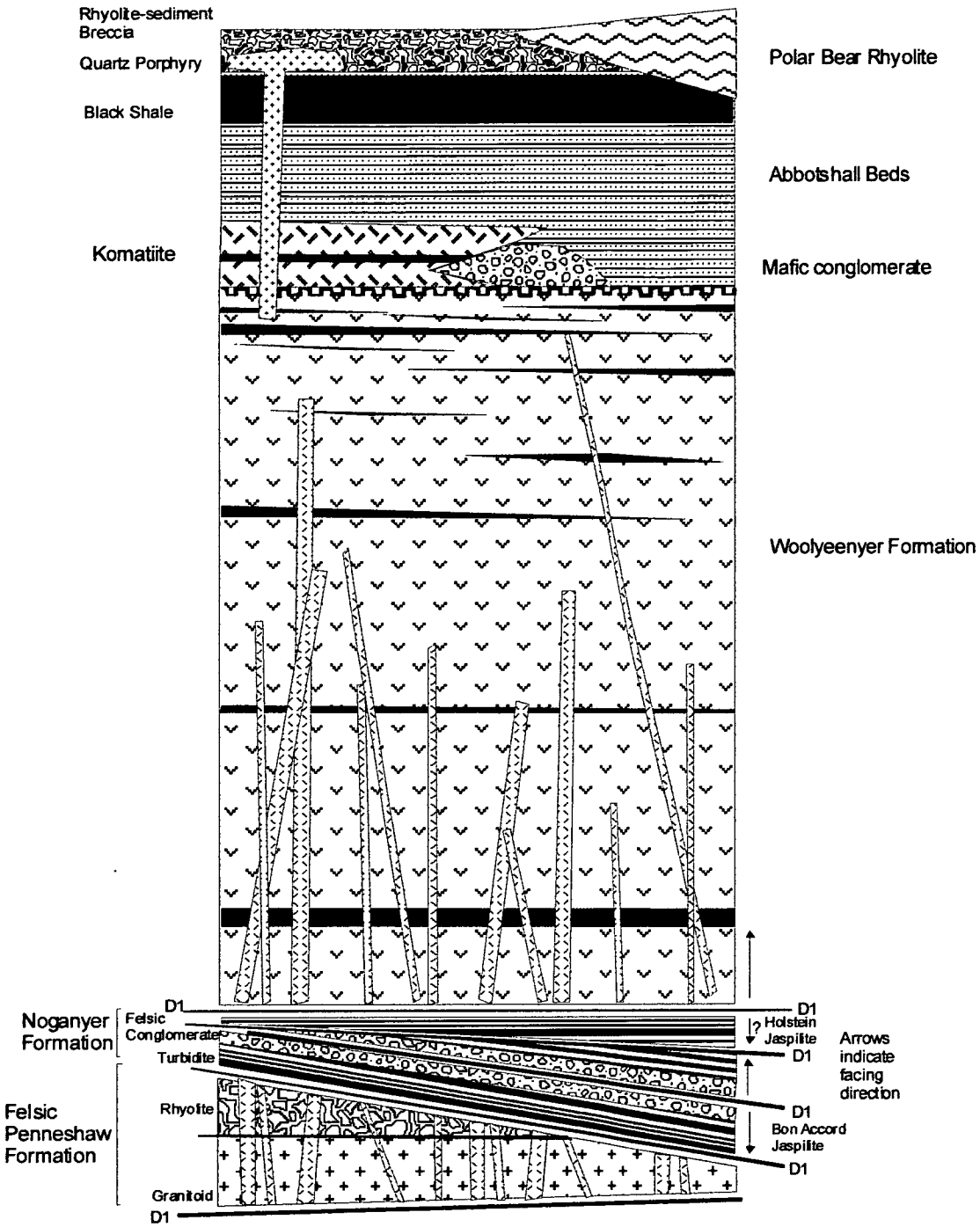

Figure 12.1: Complete stratigraphic column for the Norseman Terrane. The Noganyer Formation is included, but may be thrust in. Other thrusts repeating the Woolyeenyer Formation have been removed. The stratigraphy from the komatiite to the rhyolite is derived from the Polar Bear Peninsula, the only location in the Norseman Terrane that exposes these units.

Format of the chapter

This synthesis assumes familiarity with the conclusions of the preceding chapters. The geological history will initially pull together all the findings of the individual chapters into a coherent story for the evolution of the Norseman Terrane and southern Coolgardie Domain. The detailed tectonic implications will then be discussed and finally, the evolution of the southern part of the Eastern Goldfields will be discussed.

12.2 EVOLUTION OF THE NORSEMAN TERRANE

The stratigraphy of the Norseman Terrane as elucidated by this study is presented in figure 12.1.

12.2.1 Crustal basement

The greenstone terranes of the Eastern Goldfields are widely accepted as ensialic, having been formed on pre-existing crustal basement. The lines of evidence that suggest this are:

- ancient zircons inherited by basalts at Kambalda; and
- the composition of siliceous high-MgO lava overlying the komatiite at Kambalda, which is modelled as komatiite contaminated with crust during its ascent.

Similar geochemical modelling for basalts in Chapter 4 of this study indicates continental crust lay beneath the Norseman Terrane during the eruption of the Woolyeenyer Formation.

Seismic lines have established that the greenstones currently overlie continental crust, but a strong flat-lying reflector at the base of the greenstone is widely considered to be a detachment surface, so the location of the basement relative to the greenstone at the time of its formation is unknown.

12.2.2 Felsic domain of the Penneshaw Formation

Felsic rocks within the Penneshaw Formation are the oldest rocks found in the Eastern Goldfields and may be examples of the continental basement beneath the greenstone. Zircon ages of *ca.* 2930 Ma have been obtained from the felsic domain of the Penneshaw Formation. The samples from the drill core that were dated are considered to be granite rather than rhyolite as originally described.

In one drill core of the felsic domain of the Penneshaw Formation that was examined, very fine-grained rhyolite occurs at the top of the core hole, separated from the

granite by a major shear zone and numerous mafic dykes. Insufficient textures are present to determine whether the rhyolite is extrusive, or a high level intrusive. The rhyolite and the granite are both of lower amphibolite facies grade metamorphism, similar to the main field segment of the Norseman Terrane. Neither the rhyolite nor the granites possesses obvious structural fabrics that are not found in other rocks.

From the available evidence, it is not clear whether the rhyolite is related to the granite, whether the rhyolite may actually be much younger than the granite and in fact be the source of the felsic conglomerate at the base of the Noganyer Formation, or whether the rhyolite is unrelated to either the granite or the conglomerate.

One geochemical analysis of the granite is available, indicating it is high silica granite, which is enriched in U and Th, but has affinities to the High-Al TTD suite. The granite has the subduction signature of depleted Nb, Ta and Ti, but also a depletion of Eu indicating the involvement of feldspar fractionation.

Both the rhyolite and the granite are heavily intruded with dolerite dykes that are correlated with extrusion of the Woolyeenyer Formation. The dykes are precisely what would be expected for the footwall of the Woolyeenyer Formation following the mafic volcanism. The dykes are convincing evidence that both the rhyolite and the granite in the felsic domain of the Penneshaw Formation predate the main phase of mafic magmatism, which is represented in the Norseman Terrane by the Woolyeenyer Formation.

If the felsic domain of the Penneshaw Formation is indeed a fragment of the continental basement, then the overlying structures may correlate with the detachment surface postulated from the evidence of seismic reflection lines, to occur at the base of the greenstones. This is discussed further in section 12.2.3.

12.2.3 Noganyer Formation

The multiple repetitions of jaspilite within the Noganyer Formation are structural repetitions. Prior to structural reorganization, the Noganyer Formation consisted of one fining upwards, depositional sequence, from felsic conglomerate to thin bedded turbidites The turbidites have subsequently been altered with iron oxide to resemble banded iron formation and are conventionally termed jaspilites or BIF. A zircon U-Pb age of 2706±5 Ma for the jaspilite is considered to be a maximum age as the zircon, like the jaspilite, is likely to be clastic.

It is uncertain whether the monomict felsic conglomerate and sandstone within the Noganyer Formation belongs to the Association 1 felsic to intermediate volcanic rocks aged *ca.* 2710 Ma of Barley & others (1998) as the age dating does not provide sufficient resolution to be conclusive.

Ultramafic rock is found within the Noganyer Formation, but the poor preservation of textures and contacts in the existing drill core precludes the determination of whether the ultramafic rock is intrusive or extrusive.

The mafic intrusions within the Noganyer Formation comprise the Gabbroic Lady Mary Member, and a sequence of mafic dykes that are associated with 340°-trending faults that cross-cut the Noganyer Formation. The association of these dykes with faults suggests they are late stage. There is an absence of widespread mafic dykes which can be correlated with extrusion of the Woolyeenyer Formation. The absence of such dykes in the Noganyer Formation contrasts with the felsic domain of the Penneshaw Formation.

The absence in the Noganyer Formation, of dykes correlating with the Woolyeenyer Formation, suggests that the Noganyer Formation may not have underlain the Woolyeenyer Formation during the main phase of mafic volcanism. This theory is supported by an easterly facing direction that Green (1997) determined for the westernmost jaspilite unit immediately below the Woolyeenyer Formation, indicating that the jaspilite unit is upside down. These lines of evidence suggest that the entire Noganyer Formation was structurally emplaced by thrust duplexes into its current location. This theory is consistent with the structural evidence from the lowermost units in the Noganyer Formation, which are well established as having a structural contact with the Penneshaw Formation. The shear has been observed north of the Jimberlana Dyke and the Bon Accord BIF at the base of the Noganyer Formation, is upside down (faces east).

As pointed out in section 12.2.2, the possibility that the felsic domain of the Penneshaw Formation may be a fragment of the continental basement, would imply that the detachment surface, postulated from seismic reflection lines to lie between the greenstone and the basement, may be preserved at the top of the Penneshaw Formation. In Chapter 10, based on the evidence summarised above and structural data, it was proposed that the entire Noganyer Formation represents a D_1 thrust duplex, inserted into the stratigraphy from the south. If this proposal is correct, a mobile Noganyer Formation would seem to accord with the proposed detachment zone. However, at least in the Norseman region, it would suggest that rather than the seismic reflector marking a surface where the greenstone has moved over the basement, the seismic reflector would mark the Noganyer formation, which has moved between the greenstone and the basement.

12.2.4 Basalts & Dolerites

The basalts and dolerites that dominate greenstone units in the Eastern Goldfields are represented in the Norseman Terrane by the Woolyeenyer Formation. The formation is unique in the Eastern Goldfields as the full mafic stratigraphy is exposed, showing that the Woolyeenyer Formation has a thickness of about 6 km thick. Barley & others, (1998) suggest that the Woolyeenyer Formation was thickened by intrafolial folding, but provide no evidence to support this claim.

At the base of the succession around the major goldmines close to the town of Norseman, the basalts are extensively intruded with dolerite dykes. Towards the top of the sequence, observed at the Jewfish prospect, dolerite dykes are rare. The greater proportion of dykes within the Woolyeenyer Formation at the base and lesser proportion near the top supports the contention that the dykes were local feeders to basalt eruptive centres.

The age of the Woolyeenyer Formation is commonly taken to be 2714±5 Ma, based on a zircon from a differentiated phase of the Crown Main dyke (Campbell, 1989). However, it is possible that this zircon was inherited from an underlying felsic rock that the mafic magma passed through.

The mafic formations in the Norseman and Kambalda areas do not represent oceanic crust as the results of geochemical modelling provide evidence that the basalts have assimilated continental crust. In addition, the mafic formations do not possess the typical features of oceanic crust as revealed by ophiolites and deep ocean drilling. Typical oceanic crust includes sheeted dykes underlain by large gabbroic and ultramafic intrusions. However, the Woolyeenyer Formation at Norseman comprises a pile of basalts almost as thick as an entire section of oceanic crust, but shows none of the deeper mafic and ultramafic magma chambers found in oceanic crust. The formation comprises a monotonous sequence of basalts and dolerite feeders with interflow sedimentary rocks laid down in quiescent phases.

Although dykes are common, they do not comprise the distinctive sheeted dykes of oceanic crust. Sheeted dykes are formed directly as a response to extension in oceanic crust, with basalt produced by adiabatic melting intruding extension fractures. The absence of such dykes precludes direct evidence for extension fractures and therefore the processes that form oceanic crust.

Another typical feature of mid-ocean ridges and back-arc basins is the eruption of basalts from a longitudinal centre, with basalts becoming older laterally away from the eruptive centre. Such a temporal difference in basalts would be difficult to recognise in basaltic terranes following the deformation periods. However, within

the Woolyeenyer Formation, there is a recognisable temporal transition upwards through the basaltic successions. Interflow sediment bands are common, representing extended hiatuses in basaltic volcanism, overlain by basalts representing renewed volcanism.

A stratigraphic drilling program undertaken around the main field at Norseman in 1983 succeeded in defining a basaltic stratigraphy for an area of about 14 km north to south and 4 km east to west. This stratigraphy includes four slate members which are regionally extensive across this area, indicating that the hiatuses in volcanism are also regionally extensive. The renewal of volcanism throughout the Woolyeenyer Formation after deposition of the interflow sediment bands, suggests that numerous volcanic vents were active over a large areal extent, without a central focus to the volcanic activity. Over time the mafic pile built upwards over a large area rather than moving away from an eruptive spreading centre.

Near the top of the basalt succession in the Polar Bear region, interflow sediment bands are common and basalt units may be as little as 10 m thick. This suggests waning of the volcanic activity with longer time periods between eruptions.

The geochemistry of the basalts contradicts the geological features described above. The basalts have an N-MORB style signature, similar to mid-ocean ridge basalts that are thought to be derived by decompression melting as depleted mantle rises up beneath spreading centres. A similar depleted mantle must have undergone a similar process beneath the crust in the Eastern Goldfields to produce such basaltic magma. However, the geological features indicate the decompression was not focussed beneath a spreading centre. The required decompression melting must have taken place across a wide area over an extended time period. This might indicate widespread extension causing thinning of the entire continental crust.

The plume model of Campbell & Hill (1988) explains the widespread basaltic volcanism as melting of a plume head, but the model envisages the plume head to consist of deep mantle mixed with upper depleted mantle. An incompatible element-depleted, upper mantle signature would not be expected but rather, a P-MORB-style, incompatible element-enriched geochemistry from the deep mantle that comprises the dominant component of the plume head. McCuaig (1998) notes that some samples from one drillhole at Norseman have incompatible element-enriched geochemistry of this style, but overall, such examples are too rare to provide support for the plume model of Campbell & Hill. Mafic magmatism models are considered further in section 12.5.

The geochemical study of the basalts in the Woolyeenyer Formation provides some information as to the nature of the crustal basement during the basalt intrusion. In

Chapter 4, spoon-shaped REE patterns found for some basalts high in the mafic package were modelled as high-magnesium tholeiitic basalt contaminated with crust possessing a ladle-shaped, REE pattern similar to the Dinky Buoys Porphyry at the North Royal Mine. Ladle-shaped patterns such as that possessed by the Dinky Buoys Porphyry are characteristic of some trondhjemites that must involve substantial amphibole subtraction during their formation. Therefore, the modelling suggests that at least some of the basement must have a trondhjemitic composition.

In the Norseman Terrane, there is no upper high magnesian basalt succession, overlying the komatiite. Such magmas, which are derived from crustal contamination of komatiite, are restricted to the Kambalda and Ora Banda Domains of the Kalgoorlie Terrane. Basalts overlying the komatiite in the Norseman Terrane are structural repetitions of the Woolyeenyer Formation.

12.2.5 Mafic conglomerate

The mafic conglomerate found at the Polar Bear Peninsula and Cyprus Hill indicates that the submarine basaltic substrate became exposed after the cessation of volcanism. The conglomerate cannot be the result of shield volcanoes becoming emergent as it contains minor chert clasts, indicating the erosion of interflow sediment bands that were deposited below wave base. A drop in sea level or tectonic uplift may explain such exposure of chert. Tectonic uplift is the favoured explanation as the geometry of the interflow sediment bands with respect to the overlying sediment units suggests an angular unconformity at the top of the basalt. The angular unconformity demonstrates the strata have been tilted, indicating tectonic activity. No other descriptions of such early-stage erosion of the mafic substrate and deposition of mafic conglomerate have been published for the Eastern Goldfields, so the interpreted uplift may be a local tectonic event.

The conglomerate was likely rounded in an alluvial fan system or possibly on a beach. Ultimately it was fed into a small submarine fan system and deposited as channel facies. The conglomerate is invariably found beneath the Abbotshall Beds, occasionally with overlying or laterally equivalent thin-bedded turbidites.

One locality at the Polar Bear Peninsula, with strongly deformed mafic conglomerate, suggests the conglomerate was locally deposited above the earliest komatiite units but below the majority of the komatiite. If this is the case, it would indicate near shore sequestering of the conglomerate, with later movement offshore and into the channel system, concomitant with the komatiite eruption.

12.2.6 Komatiite

The komatiite at the Polar Bear Peninsula has abundant spinifex textures and interflow sediment bands. Using the conventional interpretation, it is considered to be lava. Some dunitic sequences, representing cumulate that may have formed as channel facies are present and have been the subject of an MSc study (Cherry, 2002). However, overall, the entire komatiite package is rather thin and it pinches out laterally. The komatiite pinchout is critical in the interpretation of the stratigraphy in the Norseman area as it explains the absence of komatiite between the top of the Chinaman's Well basalts and the overlying Abbotshall Beds where it would otherwise be expected for the basalts to be a repetition of the lower Woolyeenyer Formation.

The traditional view of komatiite is that it represents ultramafic lava with an original MgO content of up to 30 wt% and an anhydrous liquidus temperature of 1500-1650°C. Even in the Archaean, such a temperature could only have been derived from deep within the mantle. Campbell & Hill (1988) explained such a temperature for komatiites by suggesting that it represents melting of mantle that originated from the core-mantle boundary and arose via a plume. However, more recently, Grove and others (1996) have suggested that komatiite magmas may have been hydrous, potentially lowering the emplacement temperature to 1300-1350°C, a temperature, which may have been attained in the upper mantle in the Archaean. Grove and others (1996, 1999) suggest a hydrous melt may indicate subduction processes were involved in the genesis of komatiite. There is also controversy over whether the komatiite was emplaced following a cataclysmic eruption from a vent somewhere in the northern Goldfields and flowed south for hundreds of kilometres, or whether it was erupted from many vents simultaneously.

Irrespective of the ongoing controversies in interpreting the genesis of the komatiite, it is useful in establishing the stratigraphy in the Eastern Goldfields as regional studies and age dating suggests there was only one komatiitic volcanic event at approximately *ca.* 2705 Ma.

12.2.7 Abbotshall Beds

Turbidites that are laterally equivalent to the mafic conglomerate belong to the Abbotshall Beds and pass upwards into shales. The exact sequence of units within the Abbotshall Beds has not been defined but the lowermost unit consists of thin-bedded turbidites and the uppermost unit is sulfidic black shale. Between these units, the lithology alternates between thin-bedded turbidite, sulfidic shale and sulfidic chert. The total thickness of the Abbotshall Beds is 25 to 50 m.

The sulfidic black shales are formed by ambient sedimentation in anoxic conditions and represent condensed sections of stratigraphy. The shales possess a geochemical signature similar to the high-Al TTD suites in the Kalgoorlie Terrane, suggesting the grains have been sourced from that terrane by erosion or more likely, by pyroclastic deposition.

The sequence of mafic conglomerate to thin-bedded turbidites and ultimately to shales represents starvation of a submarine fan. The conglomerate was derived by erosion of a subaerial source which was eroded away or drowned by rising sea levels so the sedimentary rocks rapidly become increasingly fine. The black shales are dominated by ambient sedimentation in an anoxic environment with terrigenous input limited to pyroclastic transport of fine ash.

12.2.8 Rhyolite

The uppermost greenstone units within the Norseman Terrane are rhyolite lava. The rhyolite is present at the Polar Bear Peninsula, which is the only location within the Norseman Terrane that exposes the upper stratigraphy. The rhyolite overlies the Abbotshall Beds with a peperitic contact. The lava is currently exposed over an area almost 4 km in length and 500 m wide. It represents a lava dome that is distorted from its original shape by east-west shortening and north-south extension. At the northern and southern ends, the rhyolite pinches out and breccias fill the equivalent stratigraphic position. The most common breccias contain both rhyolite and sediment clasts. They have features indicative of deposition from high density turbidity currents. The turbidites may have been formed through collapse of sections of the rhyolite dome due to gravitational instability, which transformed into high density turbidite currents transporting rhyolite fragments. Evidence remains of previously deposited beds of shale having been scoured by the turbidites. The sediment clasts within the basalt are considered to have been incorporated by rip-up of such suspension sedimentary rocks.

The peperite and hyaloclastite exposures and the sediment horizons associated with the breccias indicate that the rhyolite was erupted in a submarine setting. The setting is interpreted to represent deep water on the basis of the black shale substrate and by the absence of pumice fragments. However, it is acknowledged that the absence of pumice could be the result of a rhyolite with low volatile contents rather than deep water.

Geochemical features indicate that the Polar Bear rhyolite is similar to the intrusive rhyolitic porphyry near the Harlequin Mine, the Ajax suite of rhyolite dykes from the mining centre at Norseman and possibly the Dundas Granite. These rhyolites and granite are volumetrically the dominant form of felsic magmatism within the

Norseman Terrane. They are considered to be derived by crustal melting based on the work of Perring (1989), who found Pb-isotopes in the Ajax suite indicating a highly radiogenic source that could not be the mantle. A crustal source is also consistent with some of the subtle oddities of the geochemistry such as the small Ta-Nb depletion. In Chapter 8, it was suggested that the Penneshaw granitoid in drillcore PE1 has appropriate characteristics for the source. In addition to being highly radiogenic, the source rock was highly siliceous, and had a subduction signature that the rhyolite inherited.

The trace element geochemical patterns indicate that during the rhyolite magmatism, feldspar was left in the residuum. There appears to be a transition from the Polar Bear rhyolite to the Harlequin rhyolitic porphyry to the Ajax rhyolite suite in which the proportion of plagioclase subtraction increases and the apparent calc-alkaline characteristics decrease. It is likely that the original magma was derived from fusion of a calc-alkaline or high-Al TTD crustal source, but that progressive low pressure plagioclase fractionation has caused the geochemical characteristics to become increasingly similar to the tholeiite series.

The Dundas Granite is the only granitoid present within the Norseman Terrane and it has a REE pattern similar to the rhyolites. The similarity of the REE patterns suggests the granites and the rhyolites are related.

12.2.9 Other felsic rocks & late-stage mafic sills

High-Al TTD felsic rocks such as those found in the BFB in the Coolgardie Domain are very minor in the Norseman Terrane. The Harlequin Granodiorite and the Polar Bear quartz porphyry are suggested to belong to the high-Al TTD suite, but were trapped in magma chambers and modified by plagioclase fractionation.

12.3 EVOLUTION OF THE UPPER COOLGARDIE DOMAIN

The lower greenstone sequence of the southern Coolgardie Domain is similar to the Norseman Terrane in that there is no upper basalt overlying the komatiite. However, the felsic and sedimentary sequences in the southern Coolgardie Domain are substantially different from those in the Norseman Terrane. In addition, unlike the Norseman Terrane, the southern Coolgardie Domain is extensively intruded by large, late stage, mafic sills that tend to occupy the base of the felsic and sedimentary sequence.

The felsic volcanic sequence in the southern Coolgardie Domain is represented by a thick sequence of epiclastic volcanic rocks deposited predominantly by low-density and high-density turbidites. These epiclastic sequences are similar and directly equivalent to the Black Flag Beds (BFB) at Kalgoorlie. The stratigraphy within the

BFB equivalents in the southern Coolgardie Domain is poorly defined due to inadequate exposures, and probably by lack of regional continuity, but felsic conglomerate, felsic sandstone, siltstones and mafic–derived, quartz-amphibole-biotite sedimentary rocks have been observed. Fragmented clasts observed within siltstones may indicate explosive volcanism, and the conglomerates indicate reworking in a subaerial environment, suggesting erosion of an emergent volcanic cone. The BFB package is estimated by Barley & others (1998) to have a thickness of 2-3 km, and was deposited in a basin termed the Kalgoorlie Basin.

A feldspar porphyry intrusive collected from "Fram Island" off the western shore of Lake Cowan has a geochemical trace element pattern almost identical to the epiclastic felsic volcanic rocks of the BFB. It may represent a subvolcanic feeder.

The felsic volcanic rocks comprising the sedimentary rocks of the BFB in the southern Coolgardie Domain are dacitic high-Al TTD compositions. The results are consistent with the findings of Hand (1998) for the Coolgardie Domain 80 km to the north. High Al-TTD suites have the subduction signature of Ta, Nb and Ti depletion, and are thought to have been have formed as partial melts of subducted, young, hot, oceanic crust. The trace element characteristics of the high Al-TTD volcanic rocks of the BFB suggest the magmas have been little modified by low pressure fractionation.

The southern Coolgardie Domain also differs structurally from the Norseman Terrane. The Norseman Terrane is broadly folded into a large, north-plunging antiform with associated smaller parasitic folds. The Coolgardie Domain is juxtaposed against the western limb of the antiform and has an opposite facing (to the east). The units within the southern Coolgardie Domain broadly strike north-south except around granite domes. The Coolgardie Domain and Norseman Terrane are separated by the Mission Fault.

12.4 STRUCTURAL EVOLUTION

The earliest deformation recognised in this study is the compression that caused the uplift and tilting of the mafic succession, giving rise to the mafic conglomerate and the angular unconformity at the Polar Bear Peninsula. This event is interpreted to be a local deformation as it has not been recognised elsewhere in the Eastern Goldfields. A highly speculative origin for this deformation may be uplift in response to the subduction of a shallowly dipping plate.

Under this speculative model, the reason this uplift is not experienced by other terranes is that Norseman is interpreted to be closer to the interpreted subduction

zone in the south and thereby closer to the fore-arc region. In contrast, the Kalgoorlie Terrane was the location of the main volcanic arc.

The earliest regional structural event proposed by some authors is extension correlating with eruption of the basaltic sequence. If this event did occur, the evidence is now obliterated by the volcanism and subsequent compressive deformations.

In the Norseman Terrane, the structural transition from the potentially minor uplift event which exposed basalt, to the drowning of the sediment source and the dominance of ambient sedimentation of the Abbotshall Beds seems to be consistent with the extension which formed the Kalgoorlie Basin in the Kalgoorlie Terrane. This would suggest that the sedimentary rocks and felsic rocks in the Norseman Terrane are the time equivalents of the BFB in the Kalgoorlie Terrane. This deformation event is known as D_{E1}.

The Buldania Granodiorite and the other granodiorite domes are geochemically similar to the high-Al TTD suite, like the BFB. Likewise, the Dundas Rocks Granite within the Norseman Terrane is geochemically similar to the rhyolites that form the dominant suite of felsic rocks within the Norseman Terrane. Furthermore, as noted in section 2.4.3, the Buldania Granodiorite has been dated at 2686±6 Ma which is not resolvable from the date of 2687±3 Ma for felsic rocks interpreted as BFB equivalents at the Abbotshall Mine, and within the age range of 2698-2675 Ma determined by Barley & others (1998) for the BFB. Thus it appears that the internal granitoids were part of the overall felsic magmatic event, formed from a similar magma at a similar time.

The effect of the D_{E1} extensional deformation is pronounced around the granitoid domes. Along the margins of granitoids such as the Pioneer and Goodia Domes, layer parallel deformation interpreted as extensional detachment faults has juxtaposed high metamorphic grade rocks from depth against lower grade greenstones. The granitoid domes are exposed as core complexes. Holcolme (1997) suggested a top to the south sense of movement on the layer parallel shears.

The first regional compressional deformation is D_1, the north-south compression that has a pronounced effect in the Norseman Terrane. Holcolme (1997) identified overturned folds in the Noganyer Formation and the strong shear at the base of the formation as being D_1. In this study, it is suggested that the entire Noganyer Formation was emplaced beneath the Woolyeenyer Formation as a major D_1 thrust duplex. A second major D_1 structure, the Hill Island thrust has also been identified, which has thrown basalts of the Woolyeenyer Formation over the Norseman komatiite such that the entire succession from the Chinaman's Well basalts to the

Polar Bear Peninsula comprises a structural repetition. Kinematic textures within the exposure of the structure at Hill Island confirm a top to the north sense of movement. As the Hill Island thrust is not identified in the Coolgardie Domain, it is suggested that the Mission Fault has acted as a D_1 thrust transfer fault. D_1 is also thought to be responsible for a broad and gentle folding with east-west axes in the Norseman Terrane.

In the Norseman Terrane, D_2 is the most obvious structural event. It comprised an east-west compression that has folded the Terrane. The combination of the folding along north-south axes in D_2, combined with the broad buckling with east-west axes formed by D_1, has formed the north plunging Norseman Anticline that is unique in the Eastern Goldfields in exposing the full thickness of the basalt succession and the units which underlie it.

A curiosity of the D_2 deformation is that the east-west shortening was accompanied by a north-south stretching, which is particularly prominent at the Polar Bear Peninsula. Holcolme (1997) suggested it may indicate transpressional deformation caused by a wrench-dominated environment. D_2 also formed thrusts in the Norseman Terrane, particularly associated with the Norseman komatiite.

D_2 is seen in the Coolgardie Domain as an array of broadly north-south striking thrust faults, related to the east-west compression. These faults are apparent in aeromagnetic images which show several strands of magnetic ultramafic rock, a number of which are known to be komatiite.

A period of moderate extension followed D_2 and is known as D_{E2}. The extension is visible as an east block down movement for structures such as the Princess Royal Fault. The gabbro dykes that split some stratigraphic units and fill 330°-trending extension fractures in the Noganyer Formation may have been intruded during this extension period.

D_3 is the mineralization event. It is widely accepted that that the mineralization occurred under E-W to ENE-WSW directed compression in the south eastern Goldfields. 330°-trending shears such as the Princess Royal Fault and Wheel Fault were activated with a sinistral movement during D_3. The classic vein-hosted mineralization at Norseman is hosted in broadly N-S trending reverse faults that were formed under D_3. The latter structures can be distinguished from D_2 thrusts by the smaller magnitude of offset being tens of metres only, and by their dip, which is moderate in the current orientation of the folded stratigraphy. In contrast, D_2 thrusts are typically steep, layer-parallel structures in the current folded stratigraphy, with interpreted offsets of hundreds of metres.

The final structural event which can be recognised is the widespread emplacement of mafic dykes in E-W, NW and NE trending orientations during the Proterozoic. The Jimberlana Dyke at Norseman is the largest of these dykes with a strike extent of hundreds of kilometres. It is considered that these dykes were emplaced in an extensional regime.

12.5 CONCLUSIONS ABOUT THE NORSEMAN TERRANE

The features of the southern Coolgardie Domain, which are consistent with the Kalgoorlie Terrane as a whole, indicate that at a late stage in the formation of the Terrane, it underwent substantial extension. The extension allowed high-Al TTD felsic to intermediate magmas, generated at depth in a subduction setting, to rise to the surface and erupt without pooling in the crust and undergoing significant low pressure fractionation. The extension also generated the Kalgoorlie Basin, which acted as a repository for the epiclastic sedimentary rocks generated by the felsic to intermediate volcanism. Studies of the Kalgoorlie Terrane by Barley & others (1998) indicate that in sequence stratigraphic terms, throughout the temporal period covered by the 2 to 3 km of exposed sedimentary rocks, the Kalgoorlie Basin remained underfilled in that the basin subsidence kept pace with sediment supply preventing progradation of sedimentary facies.

At a still later stage, the extension within the Kalgoorlie Terrane allowed major bodies of mafic magma to rise to a high level and form sills close to the base of the Black Flag Beds, which presumably is where the magmas reached neutral buoyancy. In the absence of trace element geochemistry, it may be speculated that the generation of these mafic bodies may be caused by thinning of the crust during extension, allowing adiabatic melting to occur. Alternatively, they may represent mafic subduction zone melts.

In contrast with the Kalgoorlie Terrane, the features of the Norseman Terrane suggest it underwent little extension during the felsic magmatic event. In the Norseman Terrane, high-Al TTD rocks are volumetrically insignificant, whereas intrusives, such as the Harlequin "granodiorite", considered to have formed through plagioclase fractionation of high-Al TTD within a crustal magma chamber, are prominent. The pooling of magmas within a magma chamber rather than rapid ascent to the surface, indicates a lack of extension-derived conduits.

The major felsic magmatic event in the Norseman Terrane is a suite of rhyolitic volcanic rocks and intrusives. The suite shows progressively higher degrees of feldspar fractionation, imposed upon a magma which was derived by melting of continental crust. The crust itself had a calc-alkaline or high-Al TTD chemistry. It is

considered that fusion of the crust resulted from heating by subduction-related mafic melts underplated at the base of the crust.

More supporting evidence for this lack of extension within the Norseman Terrane is the lack of the late-stage mafic sills that are so prevalent in the Kalgoorlie Terrane. The only definitive example in the Norseman Terrane is a small magnetite bearing intrusion intersected by drill hole ETS18 in the Norseman komatiite. The gabbroic Lady Mary Member in the Noganyer Formation may be another example. In contrast, the Kalgoorlie Terrane has abundant thick, mafic sills.

Based on the conclusions above, it appears that the Mission Fault, which is the bounding structure separating the Norseman Terrane from the Coolgardie Domain, divides terranes that developed under differing tectonic conditions.

Having considered the differences in magmatism in the terranes and the implications for extensional tectonism, the overall geometry of the terranes should be considered. The Norseman Terrane is wedge shaped with the apex to the north between the bounding structures of the Mission Fault and the Zuleika Shear (figure 10.4). To the west is the southern Coolgardie Domain, to the east, the Kambalda Domain of the Kalgoorlie Terrane. Both these domains have thick sequences of BFB. The Norseman Terrane lying between the domains has no BFB exposed and judging from the composition of the high-level intrusives, it is unlikely that BFB-style high-Al TTD magmas were ever erupted. Unlike the Kalgoorlie Terrane, intrusives with high-Al TTD chemistry are volumetrically insignificant in the Norseman Terrane.

Within the Norseman Terrane the uppermost rhyolite was erupted into water which is inferred to be deep, and certainly below wave base. It is inconceivable that extensive successions of BFB epiclastic volcanic rocks could be deposited to the east and west, but not in the Norseman Terrane as the present geometrical configuration would suggest. Accordingly, it is suggested that the current geometry of the terranes does not reflect the geometry during eruption and deposition of the BFB. Instead, it is likely that the Norseman Terrane is allochthonous and has been moved into its current location, splitting the Kalgoorlie Terrane and the Kalgoorlie Basin into eastern and western strands with the Norseman Terrane in between. Thus, there was probably a large component of movement along the bounding structures to the Norseman Terrane.

As the Kalgoorlie Basin was formed in D_E and it was split into eastern and western strands around the Norseman Terrane, emplacement of the Norseman Terrane must be post-D_E. The orientation of the Norseman Terrane splitting the Kalgoorlie Terrane would be consistent with its emplacement with a south to north movement.

It is considered to have been emplaced during D_1 and the Mission Fault is thereby a major D_1 transfer fault.

Although it is allochthonous, the Norseman Terrane is not considered to be an unrelated piece of crust accreted to the Kalgoorlie Terrane through subduction-related collision. The Norseman Terrane and Kalgoorlie Terrane share similar geological histories with only the felsic volcanism differing. As outlined above, much of the difference in the felsic magmas can be explained as varying amounts of extension under D_E. In addition, the top to the north movement of the thrust faults in the Norseman Terrane would be inappropriate if the Norseman Terrane had collided with the Kalgoorlie Terrane as the opposite sense of movement would be expected within the Norseman Terrane. As result of this study, it is proposed that the Norseman Terrane was originally contiguous with the crust that is now the Kalgoorlie Terrane. However, the Norseman Terrane has developed from the segment of crust that bordered the Kalgoorlie Basin to the south and was not itself heavily extended during the felsic magmatic event. During D_1, a massive north-directed stress emanating from the south caused that segment of unextended crust to be shunted north, closing the Kalgoorlie Basin, driving it like a wedge and splitting it. One of the tear faults that allowed the crust to be shunted north was the Mission Fault. In this way the Norseman Terrane was born.

The origin of the north directed stress is now unknown, as the evidence would lie far to the south of Norseman towards Esperance in the area that was subsequently influenced by the Proterozoic Fraser Orogeny. However, it can be speculated that there may have been a broadly north-dipping subduction zone in this region that generated the high-Al TTD arc magmas which erupted in the Kalgoorlie Basin. Ultimately, another slice of continental crust may have collided with the continental margin south of Norseman, causing the north directed stress of D_1 and closing the Kalgoorlie Basin.

With multiple, large D_1 structures, the Norseman Terrane has the largest degree of D_1 deformation of any terrane in the Eastern Goldfields. In addition to the Hill Island thrust that has stacked the entire greenstone stratigraphy over the Norseman komatiite, the entire Noganyer Formation may be structurally emplaced through a D_1 thrust duplex. Certainly the eastern margin of the Noganyer Formation is a D_1 thrust involving overturned stratigraphy such as the Bon Accord BIF. Further, the eastern mafic portion of the Penneshaw Formation is considered to be a structural repetition of the Woolyeenyer Formation, caused by a D_1 fault. In addition, the Norseman Terrane has been buckled along east-west axes. In the Kalgoorlie Terrane, Swager and Griffin (1990) described an extremely large D_1 thrust duplex, arising just north of the Norseman Terrane in the Republican area. Apart from these examples,

descriptions of D_1 thrusts are sparse. Norseman may have particularly strong D_1 deformation as it is the closest terrane to the postulated site of crustal collision.

12.6 EVOLUTION OF THE EASTERN GOLDFIELDS

The tectonic evolution of the southern part of the Eastern Goldfields is now considered, using the results of this study combined with the work of previous authors' studies.

The earliest units of the current greenstone sequence in the Eastern Goldfields Province are assumed to have been emplaced on crustal basement. Studies by Compston & others (1986), Arndt and Jenner (1986) and Sun & others (1989) have indicated the presence of sialic basement with a composition similar to average modern crust beneath Kambalda during the eruption of the basalts and komatiite of the greenstone (see section 4.8.2). Similar research has been extended to the Norseman area in this study (section 4.10.3), which demonstrates that some unusual (spoon-shaped) trace element geochemical patterns in basalts can be explained by contamination of a high MgO tholeiitic basalt with trondhjemitic crust, suggesting that crustal basement was present during the eruption of the basalts at Norseman.

Direct evidence of crustal basement is provided by granitoid with a high-Al TTD composition from the eastern Penneshaw Formation in the Norseman Terrane, which has been dated at *ca.* 2930 Ma. The granitoid is heavily intruded by dolerite dykes, suggesting the Woolyeenyer Formation mafic magmas passed through the granitoid during their ascent to erupt at the surface. Little information is available about this granitoid basement other than the age date and one geochemical sample that has characteristics of high-Al TTD. The structural and stratigraphic relationship of the granitoid with the overlying sequences is unclear.

The earliest greenstone units in the Eastern Goldfields are calc-alkaline andesite-dominated lavas, shallow intrusives and volcaniclastics dated at *ca.* 2710 Ma. The andesite complexes form discreet centres that are interpreted to represent emergent stratovolcanoes with high relief which were rapidly eroded to produce voluminous debris. The interfingering of basalt and andesitic epiclastic sedimentary rocks indicates that andesitic and basaltic volcanism was coeval. These early units were termed Association 1 by Barley & other (1998) and are chiefly known in the Laverton area, but also extend north into the Duketon Greenstone Belt and south into the Edjudina, Mulgabbie and Pinjin Terranes of Swager (1995). The Bore Well, Welcome Well and Ida Hill complexes are included in Association 1.

The geochemical characteristics of these Association 1 complexes indicate they are subduction related. Barley & others (1998) suggested an island arc tectonic setting

for the complexes based on their composition and stratigraphic relationships. Association 1 was not encountered in this study so nothing can be added to this interpretation. As these complexes are the earliest rocks of the greenstone succession, they occur at the surface only in rare localities where the base of the greenstone is exposed so no comment can be made as to their original distribution. It can be assumed that subduction of oceanic crust was taking place at this time, but the geometry of the subduction is unknown due to patchy data.

The next major event in the evolution of the greenstone was eruption of the basalts. The Woolyeenyer Formation at Norseman is particularly informative about this event as the entire basalt package is exposed across the Norseman Anticline. At Norseman the mafic sequence is approximately 6 km thick but possesses none of the characteristic features of oceanic crust such as an upper sheeted dyke sequence underlain by mafic and ultramafic bodies. The geological features of the basalts indicate a temporal progression upwards rather than the lateral progression that would be expected by mafic magmas erupting at a spreading centre. The lower portion of the Woolyeenyer Formation has more dykes than the top, which is consistent with progressive volcanism from multiple vents such that later magmas ascending to the surface pass through earlier basalts. Such an upward temporal progression is also indicated by interflow slate units, which can be identified over a widespread area.

The basalts of the Eastern Goldfields are dominantly tholeiites with an N-MORB style geochemical signature. Magmas of this type are thought to be derived by decompression melting of depleted upper mantle. A similar mechanism must have operated in the Archaean upper mantle to derive these basalts. It is suggested that the upper mantle welled upward beneath the continental crust causing it to rise and extend. The cause of the upwelling of the upper mantle is unclear, but it may be some form of plume. The uplift of the crust caused it to thin due to lithospheric stretching and gravity driven processes. The thinning of the crust reduced pressure on the upper mantle such that adiabatic melting occurred and basaltic magmas were generated which ascended through the crust aided by widespread extension. The geological features of the Woolyeenyer Formation are not consistent with a spreading centre, so the crust did not split. Instead basalt magmas rose through the crust across the entire Eastern Goldfields using pervasive extension fractures and giving rise to innumerable small volcanic vents. There was no focus to the volcanism.

Throughout the entire 6 km thickness of the Woolyeenyer Formation, the basalts were erupted in a submarine environment. The ability to maintain this thickness of basalt in a submarine environment suggests that the basalt was hosted in a basin that

continued to subside throughout the mafic magmatic period. Basin subsidence is consistent with crustal extension.

Towards the top of the Woolyeenyer Formation, there is evidence of a waning magmatic flux indicated by interflow shale bands separating basalt units as thin as 10 m. Brief eruptions were interspersed with long periods of ambient sedimentation.

The basalts of the Archaean resemble Continental Flood Basalts (CFB) in that they involve vast thicknesses of laterally extensive basalt lava flows. Most CFB are associated with extensional tectonics, apparently as a consequence of lithospheric stretching associated with the upwelling of deeper hotter mantle (Wilson, 1989). Despite the great thicknesses of lava, CFB provinces seem never to have developed much relief. As the basalt poured out, the underlying crust subsided to form a basin of almost the same size and extent as the lavas that filled it (McBirney, 1984). However, a difference between the Archaean basalts and CFB is that Archaean basalts are geochemically similar to N-MORB, whereas CFB are more akin to enriched MORB and ocean-island tholeiites.

In the Norseman area, the conclusion of the basaltic volcanism was followed by a local tectonic event which uplifted the basaltic terrane. The Woolyeenyer Formation at the Polar Bear Peninsula is locally overlain by basaltic conglomerate with minor chert cobbles indicating subaerial exposure and erosion of the basaltic succession. There is also an erosional unconformity at the top of the basaltic succession at the Polar Bear Peninsula. As similar conglomerates of this age have not been described elsewhere in the Eastern Goldfields, it is concluded that the Woolyeenyer Formation was exposed through local tectonic uplift. The clasts were rounded in an alluvial fan, and then fed into a small submarine fan that ultimately deposited the clasts.

In the southern Eastern Goldfields, the basalt is overlain by shale, indicating a period of ambient sedimentation prior to the next volcanic event, the eruption of komatiite.

This study does not provide any additional data to assist with the major controversies in the genesis of komatiite, and no particular model is favoured. The Campbell & Hill (1988) plume model, which involves upwelling of the upper mantle, would be consistent with the interpreted genesis of the basalts. Alternatively, the hydrous komatiite model of Grove & others (1996, 1999), would be consistent with the subsequent felsic magmatism, which involved subduction processes.

The komatiite is overlain by fine-grained sedimentary rocks, indicating ambient sedimentation below wave base. This sedimentary unit is known variously as the Kapai Slate in the Kambalda Domain, the Widgie chert in the Coolgardie Domain and the Abbotshall Beds in the Norseman Terrane. All these units include black

shales and sections that are sulfidic with pyrite and pyrrhotite. The Abbotshall Beds differs from the other units in that it is thicker, typically 25 to 50 m, and comprises sandstone-shale and siltstone-shale turbidites at the base. The Abbotshall Beds appears to form a fining upward sequence from the mafic conglomerate, suggesting drowning of the terrigenous sediment source. The upward fining sequence was not interrupted by the geologically instantaneous emplacement of komatiitic lavas.

In the Ora Banda and Kambalda Domains of the Kalgoorlie Terrane, the Kapai Slate is overlain by siliceous high-MgO basalts. These basalts represent komatiite that has been contaminated with continental crust, presumably while stored in a magma chamber within the crust. Other domains and terranes including the Coolgardie Domain and the Norseman Terrane do not have the upper basalt.

Felsic volcanism commenced after 2698 Ma and extended until about 2675 Ma. The character of the felsic volcanism varies with location. Calc-alkaline andesites and rhyolites from a submarine volcanic complex are exposed at Spring Hill in the Duketon Greenstone Belt. Barley & others (1998) consider these rocks to represent subduction volcanic rocks, with the silicic character possibly indicating a continental margin setting.

Further south, from Teutonic Bore to Melita and Jeedamaya, bimodal volcanic rocks are exposed, comprised of interfingering pillow basalt and rhyolite to dacite lavas that were emplaced in shallow water. Geochemistry indicates that the felsic magmas were derived by crustal melting. Barley and other (1998) suggested that the bimodal volcanic rocks represent an extensional setting, possibly rifting of arc crust. However, extension at Melita is difficult to reconcile with the sedimentary and volcanic facies, which indicate shallow water and subaerial volcanism. Analogous volcanic rocks, which do not involve extension, are the bimodal basalt-rhyolite volcanic rocks at the Snake River Plain – Yellowstone Park region, which are thought to be related to the passage of the North American plate over a mantle hot spot (Wilson, 1989).

Within the Kalgoorlie Terrane, the felsic volcaniclastics of the Black Flag Beds have a high-Al TTD geochemical signature. The volcanoes erupting the BFB grew to become emergent, indicated by felsic volcanic conglomerate units. The most voluminous products of the BFB are felsic volcanic-derived sandstone and mudrock that were deposited by turbidity currents within a depositional entity named the Kalgoorlie Basin. The BFB volcanic rocks are also considered to be related to subduction, and the presence of the Kalgoorlie Basin, which holds a 2 to 3 km thickness of volcanic-derived sediment, indicates that extension was occurring.

Barley & others (1998) noted that the BFB shows no coarsening upwards sequences, and interpreted it as a rift basin.

In the Norseman Terrane, rhyolites derived from melting of crust comprise the most voluminous suite of felsic rocks, which includes the submarine rhyolite dome at the Polar Bear Peninsula and the Ajax suite of rhyolitic intrusives. High-Al TTD suites are also found that have been modified by fractionation of feldspar. High-Al TTD volcanic rocks unaffected by fractionation similar to the dacites of the BFB are extremely rare in the Norseman Terrane. Extension is considered to have been minor in the Norseman Terrane.

Granites typically have a similar geochemistry to the felsic volcanic rocks of the region. A-type granites are found associated with the bimodal volcanic suite in the Melita area. Internal granitoids within the Kalgoorlie Terrane such as the Pioneer Dome are typically high-Al trondhjemites. The Dundas Granite within the Norseman Terrane has geochemical similarities to the rhyolites derived from melting of crust. The granites also have a similar age to the volcanic rocks and are considered to represent batches of the same magma that did not reach the surface. Holcolme (1997) found that textures in the granitoid domes in the Kalgoorlie Terrane are suggestive of syn-tectonic granitoids with extension accompanying intrusion. Therefore, granite studies confirm that extension accompanied eruption of the BFB felsic volcanic rocks and intrusion of the granites, ultimately exposing the granitoids as core complexes and providing a basin for the deposition of the volcanic rocks in the Kalgoorlie Terrane.

As the granites are exposed as core complexes, bounded against the greenstones by extensional faults that were not present when the greenstones were erupted, the current boundaries of the greenstone belts do not represent the original greenstone distribution. Hence, arguably the mafic stratigraphy was originally far more extensive, potentially extending right across the Yilgarn Craton prior to being dissected by extensional faults controlling the emplacement of the first granitoids.

Thus, the post-2710 Ma greenstones are interpreted as being downthrown, preserved blocks of a volcanic and sedimentary succession which originally extended right across the Eastern Goldfields and potentially, right across the Yilgarn Craton. It is noted that there is no evidence preserved of post-2710 Ma greenstones in the older Southern Cross Province, but this may be the result of erosion of the bulk of the proposed younger greenstones, combined with a lack of detailed geochronological sampling in areas where structurally downthrown remnants of younger greenstone could be preserved. The Ida Fault, which forms the boundary between the Eastern Goldfields and the Southern Cross Province, shows a normal movement,

downthrowing the Eastern Goldfields by about 5 km compared to the Southern Cross Province. Thus up to 5 km more rock may have been removed from the Southern Cross Province compared to the Eastern Goldfields Province.

Further to this argument, there is no reason to suppose that the current distribution of exposed felsic volcanic rocks resembles the original distribution. Thus, tectonic models based on perceived patterns of felsic volcanic rocks from maps such as that shown in figure 2.3 are questionable.

All the later felsic volcanic rocks appear to involve subduction magmatism in some form. It was argued in section 12.5 that the Kalgoorlie Terrane underwent extension over a subduction setting that allowed ready access to the surface of high-Al TTD dacites and later emplacement of late mafic sills at high levels. The extension is now physically represented by the BFB sedimentary rocks filling the Kalgoorlie Basin. It was also argued that the Norseman Terrane did not undergo this extension and was originally situated along the outer margin of the Kalgoorlie Basin.

Two positions commonly experience extension in arc environments: marginal or backarc basins that may cause rifting of the arc; and forearcs if the subducted plate sinks at a steeper vector than it dips. The Kalgoorlie Basin is considered unlikely to represent a forearc basin for two reasons. Firstly, the presence of high level intrusives of similar composition to the epiclastic volcanic rocks as seen in this study for the southern Coolgardie Domain indicates it lay within the volcanic arc. Secondly, forearc basins tend to close by direct collision with continental crust (*cf.* figure 9.4 *in:* Molnar, 1990). However, it is argued here that the collision occurred south of the Norseman Terrane and south of the basin. Thus the preferred setting of the Kalgoorlie Basin is an island arc undergoing extension and perhaps rifting, which failed to split completely due to the thickness of pre-existing continental crust and due to collision closing the basin.

The Norseman Terrane was located within the zone of arc magmatism but lacked the extension to allow easy access of these magmas to the surface. High Al TTD magmas were trapped within crustal magma chambers and underwent low pressure fractionation that included feldspar. The rhyolites that comprise the most voluminous volcanic rocks in the Norseman Terrane were generated through melting of continental crust. The melting may have been caused by intrusion and crustal underplating of arc-derived magmas.

As felsic volcanism continued for about 25 Ma, it is assumed that the tectonic environment over this time span involved change and therefore is complex. There may have been subduction of oceanic crust in a northerly direction from south of the Norseman Terrane. Following collision of continental crust with what is now the

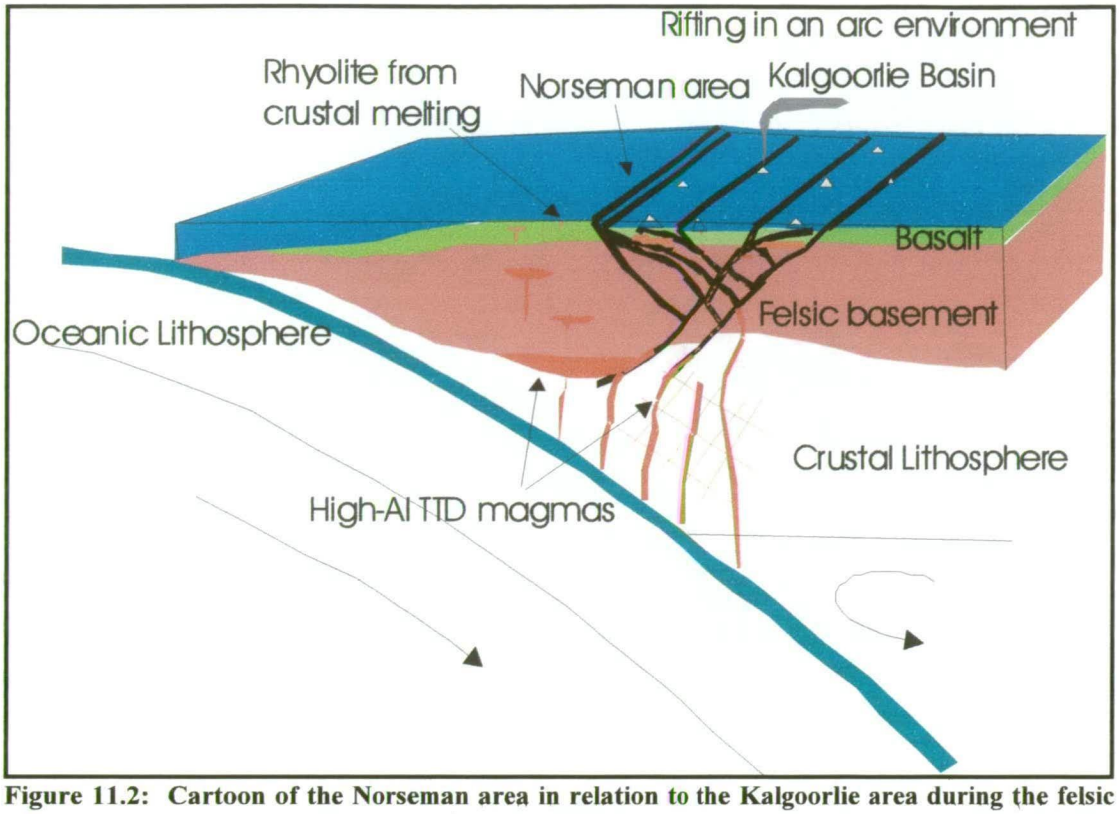

Figure 11.2: Cartoon of the Norseman area in relation to the Kalgoorlie area during the felsic magmatic event.

southern Eastern Goldfields, the Norseman Terrane was shunted to the north, splitting the Kalgoorlie Basin and generating the major D_1 thrusts in the southern Goldfields, which are younger than 2665 Ma. If the collision was somewhat oblique rather than due north-south, it may have caused rotation of the greenstone, such that continued compression ultimately became the east-west directed D_2. Alternatively, a second collision may have occurred from the east-west due to another subduction zone.

For reasons that are unclear, the east-west compression caused N-S stretching associated with the E-W compression in D_2. Holcolme (1997) suggested that this was due to transpression, caused by the bulk deformation in the Norseman Terrane during D_2 being wrench-dominated. The transpression decomposed to pure shear and simple shear members, the latter being N-S striking dextral faults. It is unknown why the deformation in the Norseman Terrane would be dominated by dextral wrench during D_2.

The period of compression that followed the felsic volcanism closed the Kalgoorlie Basin, which is reflected in isolated remnants of regressive sediment cycles. Coarsening upwards, channel-facies turbidites are exposed in the Kurrawang Conglomerate and Penny Dam west and east of Kalgoorlie respectively. The clasts within these units comprise all greenstone rock types and minor granite, indicating uplift and erosion of the terranes. These differ from the BFB where no coarsening upward sequences are known

Further progression of basin closure is indicated by the fluvial Merougil Beds at Kambalda. Granite clasts predominate indicating further unroofing of the granite intrusions. The contact between turbidites in the BFB and Merougil Beds at Kambalda is a slight angular unconformity indicating uplift and erosion prior to the Merougil Beds deposition. The Kurrawang Conglomerate and Merougil Beds were deposited before and approximately synchronously with D_2, (2660±3 Ma). These clastic sequences survive only in isolated fault blocks as the fate of such compressional sediment sequences is ultimately uplift and erosion.

East-west compressional tectonics formed upright folds and thrusts, the latter particularly around internal granite domes. Gold deposition, normal faulting along the Ida Fault and post-deformation granitoids are the final events that marked the cratonisation of the Yilgarn. Extension in the Proterozoic allowed intrusion of the mafic dykes.

CHAPTER THIRTEEN

Conclusion

13.1 INTRODUCTION

As outlined in Chapter 1, at the commencement of the study, the understanding of the stratigraphy within the Norseman Terrane had not progressed far beyond the compilation of Doepel (1973). In particular, the felsic and sedimentary successions were essentially unknown due largely to poor exposure. However, the drilling that took place across Lake Cowan and the eastern Penneshaw region during the 1990's has provided new data. In addition, regional studies across the Eastern Goldfields have provided background information useful for understanding the stratigraphy in the Norseman Terrane.

This study has used detailed mapping, drill core logging, petrography, trace element geochemistry and compilation of previous work to clarify the stratigraphy of the Norseman Terrane and its tectonic relationship to the Kalgoorlie Terrane. The results of this study include one of the most comprehensive documentations of the differences between terranes in the Yilgarn, and an interpretation of the tectonic relationships between the terranes.

The Norseman Terrane is particularly suited to a detailed terrane study. It is relatively small, such that a single geologist can, over a reasonable period of time, see a large proportion of it. It has a unique aspect in that the full extent of the basalt stratigraphy is exposed and the units under the basalt are exposed. Due to the importance of the mineralisation and ownership by CNGC for 68 years from 1933 to 2001, there is a significant body of research into a variety of factors about the geology around the mine site.

The difficulty that has previously prevented comprehensive studies of the terrane is primarily the absence of a well defined stratigraphy due to the unconsolidated cover across Lake Cowan. The cover precluded direct studies of the areas north of the Royal Peninsula until 1991, when the first lake drilling rig was developed. Furthermore, the one area where the felsic rocks are well exposed, the Polar Bear Peninsula, lies isolated within Lake Cowan on the Cowan 100 000 map sheet rather than the Norseman sheet. Therefore, individual GSWA geologists did not see both areas and tie the stratigraphy together to any significant degree. However, the GSWA did clarify the geology of the Kambalda Terrane and develop the terrane model for the Yilgarn, which greatly benefited geological studies by clarifying which regions are related in terranes and domains, and which areas should be studied in isolation.

Since 1991, extensive drilling by CNGC, across the previously inaccessible Lake Cowan, has resulted in a substantial database about the geology beneath the lake cover. Additional information available to this study was aeromagnetic data from both propriety and multiclient surveys that were flown across the region. Combining these new data, with detailed mapping and geochemistry, and with the new understanding of felsic and sedimentary successions, geochronology and terranes from the Eastern Goldfields as a whole, provided suitable information for significant findings about the Norseman Terrane and parts of the Coolgardie Domain of the Kalgoorlie Terrane.

The study was particularly wide ranging, covering field mapping, stratigraphy, petrography, geochemistry of mafic and felsic rocks, facies analysis of felsic and sedimentary rocks; structural geology and mineralisation. It also operated at different scales, from thin section, to detailed outcrop mapping, to entire terrane scale. Accordingly the outcomes and findings were correspondingly wide ranging and numerous. The individual outcomes and conclusions resulting from this study are listed below.

13.2 OUTCOMES AND CONCLUSIONS OF THE STUDY

- **Detailed maps of the Polar Bear Peninsula at 1:2500-scale.**

  Mapping had previously been completed at scales of up to 1:5000-scale by Anaconda Inc, but this work was undertaken in the 1970's for mineral prospecting purposes and was not integrated with regional studies. No previous detailed mapping had been completed with the objective of comparing with the stratigraphy in the Norseman Terrane with other terranes. The rock units at the Polar Bear Peninsula are tightly folded and geometrically complex such that the stratigraphy cannot be sufficiently unravelled with regional scale mapping.

- **Definition of the stratigraphy in the Norseman Terrane and correction of the stratigraphic synthesis of Doepel (1973), by recognising that his synthesis includes rock units from two separate terranes.**

  The detailed mapping succeeded in defining the stratigraphy of the Polar Bear Peninsula. As the Polar Bear Peninsula is within the Norseman Terrane, this stratigraphy was recognised as being the upper stratigraphy of the terrane. The stratigraphy at the Polar Bear Peninsula extends from mafic rocks equivalent to the Woolyeenyer Formation, through komatiite, to rhyolite at the top of the succession.

The conventional understanding of the stratigraphy as compiled by Doepel (1973) (figure 1.2, 1.3) is incorrect because it includes rock units from two separate terranes. The Penneshaw, Noganyer and Woolyeenyer Formations belong to the Norseman Terrane, as do the shales in the Abbotshall Beds, but the Mount Kirk Formation belongs to the Coolgardie Domain of the Kalgoorlie Terrane. The Mount Thirsty Beds (figure 1.2) in Doepel's Mount Kirk Formation are equivalent to the Black Flag Beds in the Kalgoorlie Terrane.

- **Recognition of D_1 thrust faults repeating the stratigraphy within the Norseman Terrane.**

  In this study, it was noted that geochronological studies by Nelson (1997), found there is only one komatiitic unit in the Eastern Goldfields. If this is the case then the komatiite at the Polar Bear Peninsula is stratigraphically equivalent to the Norseman komatiite and the basalt below the komatiite at the Polar Bear Peninsula is stratigraphically equivalent to the lower Woolyeenyer Formation at Norseman. As this basalt sequence (known locally as the Chinaman's Well basalts) overlies the Norseman komatiite, then it must have been thrust into that position. By this logic, the first major repetitions of the Norseman stratigraphy were recognised.

- **Recognition of other D_1 thrust faults within the Norseman Terrane.** Holcolme (1997) recognised a D_1 shear beneath the Noganyer Formation. Following recognition of the thrust repeating mafic strata above the Norseman komatiite, CNGC geologist working in the Penneshaw Formation postulated that the lower portion (eastern side) of the Penneshaw Formation may also be a thrust repetition of the Woolyeenyer Formation. This study has also recognised further D_1 thrusts associated with the Noganyer Formation.

- **The results of trace element geochemistry that tested the D_1 thrust repetition theory for the mafic stratigraphy.**

  22 basalts from the Chinaman's Well basalts from Lake Cowan and the Polar Bear Peninsula, and 5 basalts from the Penneshaw Formation were analysed for a suite of major trace elements. In addition, a number of these samples were examined petrographically. The basalts are dominantly low magnesian tholeiites and are comparable to the lower Woolyeenyer Formation. Importantly, no basalts were found with the distinctive petrographic or trace element characteristics of the siliceous high magnesian basalts (Paringa Basalt) that overlies the komatiite within the Kambalda and Ora Banda Domains of the Kalgoorlie Domain. These findings support the theory that the Chinaman's Well basalts are a thrust repetition of the lower Woolyeenyer Formation.

- **Discovery of an exposure of the D_1 thrust that throws the Chinaman's Well basalts over the Norseman komatiite and documentation of the sense of movement.**

  An exposure of the D_1 thrust that throws the Chinaman's Well basalts over the Norseman komatiite was discovered at Hill Island. The island exposes basalts with a bedding-parallel shear fabric. Deflection of the fabrics indicates a top to the north movement. Stretching of amygdales indicates a due north direction of movement. The Hill Island thrust was also exposed within oriented drill core from drill holes ETS16 and ETS18. Stretching lineations and S-C fabrics indicated a top to the north and N-S movement.

- **Documentation of the geochemical characteristics of the Chinaman's Well basalts.**

  A previous study documented a number of different petrogenetic varieties of basalt within the lower Woolyeenyer Formation near Norseman. The geochemical samples collected for this study were geochemically matched with these groups. The most abundant samples are tholeiites with N-MORB trace element characteristics. However, one sample is a high MgO tholeiite, one is a high Fe tholeiite, and one may have been derived through fractional crystallisation of olivine and pyroxene from a petrogenetic group termed the enriched high magnesium tholeiites. An additional nine samples have unusual spoon-shaped chondrite normalised REE patterns.

- **An indication from geochemical modelling that basement was present beneath the Norseman Terrane when the basalts were erupted.**

  The basalts with the unusual spoon-shaped REE patterns were successfully modelled through AFC processes using 10 to 20% assimilation of crust with a composition similar to the Dinky Buoys Porphyry at Norseman, and 15 to 25% clinopyroxene fractional crystallisation. No other combination of assimilation or fractional crystallisation was found that would produce the spoon-shaped REE patterns. Therefore, the results suggest that crust with a REE pattern similar to the Dinky Buoys porphyry was present beneath the Norseman Terrane and was assimilated by the ascending basaltic magma.

- **Recognition that the full basalt stratigraphy is exposed across the Woolyeenyer Formation at Norseman and it does not represent oceanic crust.**

The mafic stratigraphy comprises a succession of submarine basalts cut by numerous dykes that presumably acted as feeders for the overlying vents. The typical features of oceanic crust such as sheeted dykes underlain by mafic and ultramafic sills are not present. The laterally extensive interflow sedimentary units within the Woolyeenyer Formation indicate a temporal succession upwards rather than laterally away from a spreading centre.

- **The first documentation from the southern Goldfields, of basaltic conglomerate, immediately above the mafic stratigraphy and below the sedimentary rocks and felsic stratigraphy.**

  Isolated exposures of basaltic conglomerate are located just above the basaltic sequence and below the Abbotshall Beds at the Polar Bear Peninsula. The conglomerate includes sand layers and appears consistent with deposition from a high density turbidite. It was interpreted as the channel facies of a submarine fan. In addition to basaltic clasts, there are rare chert clasts indicating derivation by erosion of submarine basalts with interflow sedimentary rocks, rather than an emergent volcano. Basalt clasts have been previously found in the BFB, but for the southern part of the Eastern Goldfields, this is the first evidence for early exposure and erosion of the basaltic stratigraphy, prior to deposition of the sedimentary rocks and felsic sequences.

- **Recognition of an erosional unconformity at the top of the basalt at the Polar Bear Peninsula.**

  The unconformity was recognised near the Sontaran prospect at the Polar Bear Peninsula through discordance between interflow sedimentary bands and the overlying Abbotshall Beds. It is considered that the basalt in the Polar Bear area was exposed through early tectonic uplift, eroded and the resultant cobbles transported into a submarine fan. Subsequent drowning and starvation of the submarine fan is recorded by the thin-bedded turbidites and black shales of the Abbotshall Beds.

- **Recognition, mapping and facies documentation of a new proximal felsic volcanic centre in the Eastern Goldfields at the Polar Bear Peninsula, not previously described.**

  In line with the original intentions of this study, the felsic rocks of the Norseman Terrane were documented. In addition to clarifying the stratigraphy, the detailed mapping at the Polar Bear Peninsula also located a submarine rhyolite dome with excellent textural preservation. The dome is now about 4 km in length and 250 m wide, but this follows E-W shortening and N-S stretching. Originally, the

dimensions would have been more equant. The rhyolite lava has strong flow banding and there are excellent exposures of hyaloclastite and peperite, indicating the rhyolite was erupted in a submarine environment, on wet sediment. Where the rhyolite dome pinches out of the stratigraphy, proximal breccias take that stratigraphic position.

- **Documentation and facies interpretation of unusual rhyolite-sediment breccias associated with the rhyolite dome at the Polar Bear Peninsula.**

  The most voluminous breccia replacing the rhyolite lava is an unusual rhyolite-sediment breccia. Detailed facies studies were undertaken on the best exposures to determine the origin of the breccia. The facies within the breccia support deposition from high density turbidity currents. Many of the rhyolite clasts have curviplanar margins indicative of quench fragmentation. The best exposures have shale layers between breccia turbidites. The rhyolite clasts were probably derived by partial collapse of the dome due to gravitational instability. The collapse events transformed into high density turbidity currents that ripped up shale substrate immediately prior to the coarse fractions being deposited.

- **Recognition of Black Flag Beds (BFB) in the southern Coolgardie Domain near Mt Thirsty.**

  The geology the southern Coolgardie Domain was examined through reconnaissance mapping of a number of areas, re-examination of end-of-hole samples from aircore drill holes into covered areas and detailed facies analysis of one area, combined with petrography and geochemistry. The felsic volcanics that Doepel (1973) called the Mount Thirsty Beds (figure 1.2) were found to be epiclastic; conglomerates, sandstones and siltstones deposited in units indicative of deposition from high density turbidite flows. The feldspar–phyric nature of the volcanics indicates a dacitic composition and the presence of conglomerates indicates emergent volcanic centres. The nature of the felsic rocks closely matches descriptions of the BFB for the Kalgoorlie Terrane and in particular, for the Widgiemooltha area 80 km to the north within the Coolgardie Domain.

- **Recognition of where the late-stage layered mafic sills in the southern Coolgardie Domain lie in the stratigraphy.**

  It was recognised that the late stage mafic sills within the southern Coolgardie Domain typically lie immediately above the komatiite and may even split the chert layer above the komatiite. This is interpreted to be due to the mafic magma rising to the level of neutral buoyancy, which is above the solidified mafic rocks and ultramafic rocks, but below the felsic epiclastic rock layers of the BFB.

- **Recognition that numerous D_2 thrust faults repeat stratigraphy throughout the southern Coolgardie Domain by thrusting ultramafic over BFB.**

  Field studies in a number of areas in the southern Coolgardie Domain indicate that the komatiite layer commonly overlies felsic and mafic-derived sedimentary rocks. The sedimentary rocks are interpreted as BFB. A faulted contact between the komatiite and BFB was recognised where exposure or drilling was sufficient at Woodcutters north and Pioneer. As there is only one komatiite unit further north at Widgiemooltha where it overlies mafic substrate, the komatiite was interpreted as being thrust over the BFB. These D_2 thrusts may also repeat the mafic sills. The Mission, Mt Thirsty and Woodcutters sills are probably the same sill, repeated by D_2 thrusts.

- **Recognition of distinct petrogenetic suites of felsic volcanics, intrusive porphyries and granitoids associated with the different terranes.**

  The dominant felsic magma in the Coolgardie Domain, like the entire Kalgoorlie Terrane, comprises high-Al TTD dacites. The trace element geochemical pattern of this suite indicates amphibole subtraction, likely from a wet source at high pressure below the crust. Some granitoids, such as the Buldania Granodiorite have a similar pattern. The geochemical pattern shows no evidence for low pressure feldspar fractionation within the crust.

  Within the Norseman Terrane, a rhyolite suite is volumetrically the dominant felsic suite. The suite includes the rhyolite lava dome at the Polar Bear Peninsula, the Harlequin porphyry intrusive and the Ajax suite of rhyolite dykes. The Dundas Granite within the Norseman Terrane has a similar REE pattern to the rhyolites and is also considered to be a member of the suite. Although the members of the suite have variable trace element patterns, it is considered that the various members were derived by increasing degrees of fractional crystallisation of feldspar from a similar magma. The magma is interpreted to have been derived from fusion of continental crust that had a geochemical subduction signature.

  High-Al TTD magmas similar to the Coolgardie Domain are rare within the Norseman Terrane. However, the Harlequin "Granodiorite" and the quartz porphyry intrusive at the Polar Bear Peninsula are interpreted to represent such magmas that underwent feldspar fractionation within the crust.

- **Recognition that the Abbotshall Beds within the Norseman Terrane record eruption of emergent volcanic centres in the Kalgoorlie Terrane.**

  It was found that the Abbotshall Beds within the Norseman Terrane have a high-Al TTD geochemical signature, interpreted to be due to deposition of fine grained ash following pyroclastic eruptions of emergent centres within the Kalgoorlie Terrane. It also indicates that felsic volcanism within the Kalgoorlie Terrane pre-dates extrusion of the rhyolite dome at the Polar Bear Peninsula.

- **Interpretation of the differing compositions of the felsic magma suites between the terranes as being controlled by tectonics.**

  The high-Al TTD dacites of the BFB are interpreted as having been emplaced in the Kalgoorlie Terrane under an extensional regime that aided the formation of efficient magma conduits to the surface. Thus, the magmas did not undergo low pressure feldspar fractionation. In contrast, the feldspar fractional crystallisation controlling the REE patterns of felsic rocks within the Norseman Terrane suggests the magmas were trapped in magma chambers within the crust. This is interpreted as being due to a lack of significant extension to aid the ascent of the magmas.

- **Synthesis of the interpreted tectonic controls of felsic petrogenetic suites with the results of previous stratigraphic studies of the BFB**

  The interpretation from the felsic petrogenetic considerations, of significant extension within the Kalgoorlie Terrane accords with previous studies of the BFB that suggested the 2-3 km thickness was deposited within a rift basin. The interpreted extension can also be used to explain the abundance of late-stage, differentiated mafic sills at the base of the BFB in the Kalgoorlie Terrane, in comparison to the other terranes.

- **A new compilation of the structural history of the Norseman Terrane and the southern Coolgardie Domain, by updating previous work with the structural findings of this study.**

  The earliest periods of deformation recognised within the Norseman Terrane may be minor events of local significance only. Volcanic conglomerates and an angular unconformity at the top of the basalt at the Polar Bear Peninsula suggest a compressional deformation event. The basalts were subsequently resubmerged by the major regional extensional event D_{E1}.

  Previous studies have recognised D_{E1} faults near granite-greenstone margins, juxtaposing high-metamorphic grade rocks against low metamorphic grade. D_{E1}

is considered responsible for exposing the granitoids as core complexes. In the Kalgoorlie Terrane, D_{E1} formed the Kalgoorlie Basin that hosts the BFB.

The first widely recognised compressive deformational event is D_1. It is suggested that the Norseman Terrane displays a greater amount of strain from D_1 than any other terrane. In this study, three major D_1 thrust faults with a N-S movement are recognised within the Norseman Terrane. In addition, the open folds with E-W axes that cause the northerly plunge of the Norseman anticline in the Norseman Terrane are attributed to D_1.

The next compressional deformation is D_2 with an E-W directed compression. D_2 thrust faults are an order of magnitude smaller than the D_1. These thrusts are most prevalent within the southern Coolgardie Domain where they thrust komatiite over the BFB. Within the Norseman Terrane, D_2 causes folding with N-S axes such as the Norseman Anticline and the tight folds at the Polar Bear Peninsula.

Following D_2, within the Norseman Terrane, there is a cryptic period of extension D_{E2} that gives rise to NNW-trending block faults.

Compression in D_3 is ENE-WSW directed and reactivates the NNW block faults with a small sinistral movement. However, the major expression of D_3 within the Norseman Terrane is reverse faults that are an order of magnitude smaller than D_2 thrusts. They can be recognised as they remain in a reverse fault orientation, being younger than the folding. The mineralised structures within the Norseman Terrane are related to D_3.

- **The structural deformation events have been related to interpreted tectonic events.**

Following the mafic volcanic event, the entire southern Goldfields area is interpreted to have been influenced by subduction, with the BFB being the primary expression of the volcanic arc. It is speculated that the first interpreted compressional deformation, uplift and erosion of the basalts, may mark the earliest effects of subduction, with compression due to a shallow subduction angle. This might explain the limited areal extent of the deformation as it is only recognised in the Norseman Terrane. D_E is interpreted to be related to rifting of a volcanic arc due to back-arc processes. D_1 is interpreted to be due to collision of continental crust with the Eastern Goldfields in an area far to the south. The Norseman Terrane, being closer to the collision zone than other terranes experienced greater D_1 deformation than the other terranes. The Norseman Terrane was driven north into the Kalgoorlie Terrane, closing the Kalgoorlie

Basin and causing it to wrap around the Norseman Terrane. D_2 is suggested to be the result of either rotation of the Eastern Goldfields under the southern continental collision, or a new collision in another subduction zone. D_{E2}, the block faulting event in the Norseman Terrane is poorly understood, but would be best explained as the result of dilation caused by a wrench deformation along the bounding faults to the Norseman Terrane, under the influence of the E-W compression. D_3 is probably a continuation of the D_2 east-west compression, experienced within the Norseman Terrane following a cessation of the wrench movement on the bounding faults.

- **A new documentation of the felsic domain of the Penneshaw Formation.**

  The Penneshaw Formation is widely recognised as having the oldest known radiometric age of any unit in the Eastern Goldfields. However, the nature of the dated material was unclear, documented as being felsic volcanic. This study re-examined and relogged the dated core and reinterpreted the dated rock as sheared granitoid. The relationship of the granitoid to rhyolite higher in the drill core is unclear due to extensive shearing and intrusion of mafic dykes.

- **Recognition that geological factors indicate the felsic domain of the Penneshaw Formation is basement to the mafic Woolyeenyer Formation.**

  The swarms of mafic dykes cutting the felsic domain of the Penneshaw Formation are consistent with the domain being basement to the Woolyeenyer Formation.

- **A new interpretation for origin of the Noganyer Formation.**

  Aspects of the Noganyer Formation were examined and the origin of the unit reinterpreted. It is now widely recognised that the "BIF" units are not chemical sedimentary rocks, but fine-grained clastic sedimentary rocks (turbidites) that have been altered by magnetite. It is also widely recognised that BIF units have been repeated within the stratigraphy as they increase in number from south to north. This study examined the felsic conglomerate beneath the BIF and reinterpreted the Noganyer as originally consisting of one fining up unit, from felsic conglomerate to thin-bedded turbidite. The zircon U-Pb age of 2706±5 Ma was reinterpreted as the maximum age of the unit, considering the clastic origin. The felsic clastic material within the Noganyer Formation and the zircon age suggest the clastic source may have been an association 1 early felsic volcanic centre (eg. Welcome Well and Bore Well in the Northern Goldfields) that pre-date the deposition of the komatiite. Ultramafic rock is present within the

Noganyer Formation, but textures are not sufficiently preserved to determine whether it represents komatiite or an intrusive body.

- **A new structural interpretation for the Noganyer as a thrust duplex inserted into the stratigraphy.**

  The Bon Accord Jaspilite at the base of the Noganyer Formation is overturned, suggesting an origin as a recumbent fold which has subsequently been thrust out. Previous studies have also recognised a major D_1 shear at the base of the Noganyer Formation. These data indicates that the Noganyer Formation is thrust over the felsic Penneshaw Formation. A previous study of facing directions in the Noganyer indicated the upper BIF unit is also overturned implying that the upper BIF is the lower limb of a recumbent fold and a thrust fault lies between the Noganyer Formation and the Woolyeenyer Formation.

  These findings suggest the entire Noganyer forms a thrust duplex inserted into the stratigraphy. The absence of swarms of mafic dykes through the Noganyer Formation, as seen in the underlying felsic Penneshaw Formation, supports the contention that the Noganyer Formation was not below the Woolyeenyer Formation during the greenstone magmatic event and was later thrust into the stratigraphy. The depositional age of the Noganyer Formation is unknown, but is less than 2706±5 Ma. If the ultramafic units within the Noganyer Formation represent komatiite, then the Noganyer Formation would be younger than the mafic greenstones.

- **Recognition that the Noganyer Formation may represent the basal greenstone detachment.**

  Seismic studies across the Eastern Goldfields have interpreted a detachment structure at the base of the greenstones. If the felsic domain of the Penneshaw Formation is basement as the zircon age and the mafic dyke swarms suggest, then the detachment surface may be represented in the Norseman Terrane by the Noganyer thrust duplex.

- **A new regional geological map and geological interpretation.**

  The improved understanding of the stratigraphy, structural history and tectonics, and geochemistry resulting from this study allowed production of a new regional solid geological map, with interpreted major structures.

- **A new understanding of the controls that localise mineralisation.**

  Proximity to major NNW-striking faults such as the Princess Royal Fault has long been empirically recognised at CNGC as important for mineralisation at Norseman. In this study, it is suggested that these shears are important as they are steep and cut down through the stratigraphy, therefore they may intersect deep fluid bearing structures in the basement. Earlier thrusts and extensional faults are largely layer parallel and therefore do not cut down through stratigraphy to reach the basement.

  Alteration within the NNW-striking faults indicates that they were active during the mineralisation event. It is suggested there was a high fluid pressure along these shears, but they were not in a dilational orientation during mineralisation. When failure of a D_3 reverse fault occurred, causing dilation, fluid rushed out of the NNW-striking fault into the low pressure site and decompression caused devolatilization and destabilisation of gold complexes. However, the gold event was restricted in time relative to the potassic-carbonate fluid, so that prospective alteration can be found with no gold. This may explain why the Noganyer Formation does not contain substantial economic gold deposits (>100 000 ounces).

  Medium-grained dykes appear to be important for generating dilational sites. There are a greater number of dolerites in the lower Woolyeenyer Formation in comparison to the upper sections near the Norseman komatiite and at the Polar Bear Peninsula as the dykes acted as feeders to overlying basalts.

- **Recognition of the differences in geology between the Norseman and Kalgoorlie Terranes.**

  This study has revealed that the differences between the Kalgoorlie Terrane and the Norseman Terrane are largely in the upper felsic and sedimentary units. The interpretation of this study is that these differences are the result of the different tectonic conditions due to the differing localities of the terranes in respect to a rifting volcanic arc. The Kalgoorlie Terrane was the centre of the arc and had prolific volcanism with emergent volcanic centres. As subduction continued, the arc rifted, enabling ready passage to the surface of subduction magmas.

  In contrast, the Norseman Terrane was away from the central magmatic axis and outside the rift basin. Arc-derived felsic magmatism was restricted and the magmas typically were trapped within the crust. The most prolific felsic magmas in the Norseman Terrane are rhyolites derived by crustal melting,

In D_1, collision of continental crust with the subduction zone is interpreted to have occurred, causing N-S compression. The Norseman region was pushed north, forming the Mission Fault and Zuleika Shears and creating the Norseman Terrane.

- **Recognition that the Norseman Terrane is indeed a terrane, rather than a domain, but not for the reasons ascribed by Swager and others (1995) (See Chapter 1).**

The Norseman Terrane has considerable quantities of komatiite within it and cannot be differentiated from the Kalgoorlie Terrane on that basis. It also cannot be distinguished by the presence of the Noganyer Formation or the felsic Penneshaw Formation as the presence or absence of these units cannot be readily ascertained in the Kalgoorlie Terrane due to the lack of exposures of the base of the mafic greenstone. In fact, seismic studies actually indicate a felsic basement beneath the greenstones in the Kalgoorlie Terrane, which may be equivalent to the felsic Penneshaw. The absence, within the Norseman Terrane, of the upper siliceous high magnesian basalts that overlies the komatiite at Kambalda is of no particular consequence, as these units are restricted to the Ora Banda and Kambalda Domains of the Kalgoorlie Terrane and are not present within the other domains such as the Coolgardie Domain.

The difference between the Norseman Terrane and the Kalgoorlie Terrane lies primarily in the felsic successions and is sufficient to qualify the Norseman Terrane as distinct greenstone stratigraphy. In addition, the uplift causing early erosion of the basalts, the NNW-trending block faults, and the N-S extension concomitant with D_2 compression in the Norseman Terrane are not recognised within other areas of the Eastern Goldfields and therefore, provide evidence of a distinct deformation history. Following the northward movement of the Norseman region, bounding structures to the Norseman area were formed. On the basis of a distinct greenstone stratigraphy and deformation history within an area delineated by bounding structures, the Norseman region may be considered a terrane under the criteria of Swager & others (1995).

References

Archer, N.R., 1990, Preliminary exploration strategy – North Royal deeps. Internal CNGC memorandum (dated 30 Aug. 1990).

Archibald, N.J., 1979, Tectonic - Metamorphic Evolution of an Archean Terrain. Phd thesis Uni. West. Aust (Unpublished).

Archibald, N., 1998a, An allochthonous model for greenstone belt evolution in the Menzies-Norseman area, Eastern Goldfields Province: Implications for gold mineralisation. *In:* Extended Abstracts from Geodynamics & Gold Exploration in the Yilgarn. *Australian Geodynamics Cooperative Research Centre Workshop.*

Archibald, N., 1998b, 3D Geology and Tectonic Synthesis of the Kalgoorlie Terrane. *In:* Extended Abstracts from Geodynamics & Gold Exploration in the Yilgarn. *Australian Geodynamics Cooperative Research Centre Workshop.*

Arndt, N.T. & Brooks, C., 1980, Komatiites. *Geology, 8, pp155-156.*

Arndt, N.T. & Nisbett, E.G., 1982, What is a komatiite?, *In:* Arndt, N.T. & Nisbett, E.G., (Eds.) Komatiites, *George Allen & Unwin, London, pp19-28.*

Arndt, N.T. & Jenner, G.A., 1986, Crustally contaminated komatiites and basalts from Kambalda, Western Australia. *Chemical Geology, 56, pp229-255*

Arth, J.G., 1976, Behaviour of trace elements during magmatic processes – a summary of theoretical models and their applications. *Jour. Res. U.S. Geol. Surv., 4, pp41-47.*

Barker, F., 1979, Trondhjemite: Definition, environment and hypotheses of origin. *In:* Barker, F., (Ed.) Trondhjemites, dacites and related rocks. *Elsevier, Amsterdam, pp1-12.*

Barker, F., & Arth, J.G., 1976, Generation of trondhjemitic-tonalitic liquids and Archean bimodal trondhjemitic-basalt suites. *Geology, 4, pp596-600.*

Barley, M.E., & McNaughton, N.J., 1988, The tectonic evolution of greenstone belts and setting of Archean gold mineralization in Western Australia geochronological constraints on conceptual models. *In:* Ho, S.E. & Groves, D.I., (Eds.) Advances in Understanding Precambrian Gold Deposits, Vol. II. *Geology Department & University Extension, The University of Western Australia, Publication 12, pp23-40.*

Barley, M.E., Eisenlohr, B.N., Groves, D.I., Perring, C.S., & Vearncombe, J,R., 1989, Late Archaean convergent margin tectonics and gold mineralisation: a new look at the Norseman-Wiluna Belt, Western Australia, *Geology, 17, pp826-829.*

Barley, M.E., Krapez, B., Brown, S.J.A., Hand, J., Cas, R.A.F., 1998, Mineralised volcanic and sedimentary successions in the Eastern Goldfields Province, Western Australia. *AMIRA Project P437, Final report.*

Bevins, R.E., Kokelaar, B.P., & Dunkley, P.N., 1984, Petrology and geochemistry of lower to middle Ordovician igneous rocks in Wales: a volcanic arc to marginal basin transition. *Proc. Geol. Ass. 95, pp337-347.*

Binns, R.A., Gunthorpe, R.J., & Groves, D.I., 1976, Metamorphic patterns and development of greenstone belts in the eastern Yilgarn Block, Western Australia. *In:* Windley, B.F., (Ed.) The Early History of the Earth. *London, John Wiley and Sons, pp303-313.*

Borg, L.E., & Clynne, M.A., 1998, The petrogenesis of felsic calc-alkaline magmas from the southernmost Cascades, California: origin by partial melting of basaltic lower crust. *Journal Petrology39 no.6 pp1197-1222.*

Briggs, M.S., 1997, Structural Geology of the Eyre prospect, Norseman district, Western Australia. BSc. (Hons.) thesis, Univ. of Queensland (Unpublished).

Browning, P., Groves, D.I., Blockely, J.G., & Rosman, K.J.R., 1987, Lead isotope constraints on the age and source of gold mineralisation in the Archaean Yilgarn Block, Western Australia. Econ. Geol., 82, pp971-986.

Campbell, I.H., 1989, Final report for the ion probe project, 1988. *Report to WMC Ltd 1 February 1989. (Unpubl).*

Campbell, I.H., & Hill, R.I., 1988, A two stage model for the formation of the granite-greenstone terrains of the Kalgoorlie-Norseman area, Western Australia. *Earth and Planetary Science Letters, 90, pp11-25.*

Campbell, J.D., 1990, Hidden gold, the Central Norseman story. An account of the structural geological studies and ore-search at Norseman, Western Australia. *AusIMM, Monograph 16.*

Cas, R., Brauns, K., Clifford, B., & Squire, R., 1993, Submarine volcanism: concepts, problems and significance. *In:* Williams, P.R., Haldane, J.A., (Eds.) An International Conference on Crustal Evolution, Metallogeny and Exploration of the Eastern Goldfields. *Extended Abstracts Record 1993/54 Australian Geological Survey Organisation pp1-2.*

Catling, A., 1899, The Norseman Gold Belt, Dundas Goldfield. *Sands & McDougal Publishers Ltd*

Champion, D.C., 1997, Granitoids in the Eastern Goldfields. *In:* Cassidy, K.F., Whitacker, A.J. & Liu, S.F. (Eds.) Kalgoorlie '97: Crustal Evolution, Metallogeny and Exploration of the Yilgarn Craton- An Update. *Extended Abstracts Record 1997/41 Australian Geological Survey Organisation pp7-9.*

Chappell, B.W. & White, A.J.R., 1974, Two contrasting granite types. *Pacific Geology 8, pp173-174.*

Chapman, J.S., 1989, Petrography for Penneshaw PE260. Internal WMC memorandum GL-12.

Cherry, J.L., 2002, The volcanology of the Norseman komatiite and the evolution of the Norseman greenstone sequence, Norseman, Western Australia. MSc thesis Monash Univ. (Unpublished).

Claoue-Long, J.C., 1990, High resoluton timing constraints on the evolution of the Kalgoorlie-Kambalda mineral belt. *In: Glover, J.E. &Ho, S.E.,* (Eds.) Third International Archaean Symposium, Perth, 1990. *Extended Abstracts Volume. Geoconferences (W.A.) Inc, Perth.*

Clark, M.E., 1987, The geology of the Victory Gold Mine, Kambalda, Western Australia. Unpublished Ph.D. thesis Queens University, Kingston Ontario, Canada.

Compston, W., Williams, I.S., Campbell, I.H. & Gresham, J.J., 1986, Zircon xenocrysts from the Kambalda volcanics: age constraints and direct evidence for older continental crust below the Kambalda-Norseman greenstones. *Earth and Planetary Science Letters 76: pp299-311.*

Connors, K.A., 2000, reinterpretation of the surface geology for the CNGC lease area at 1:50 000. Unpublished Central Norseman Gold Corp internal technical report CNG/T/044. 12p

Conybeare, C.E.B., 1980, Oil search in Australia. *Australian National University Press, Canberra.*

Cowden, A., & Archibald, N.J., 1989. Stratigraphy of the Kambalda-Kalgoorlie Archaean greenstone terrain, Western Australia. (WMC) Report (Unpublished).

Craske, T.E., 1997, Granites. *The Geoscientific Legend, Part III, Rock and geological structure classification and depiction schemes. Unpublished internal WMC document.*

Crozier, S. 1999. Paleovolcanology of the Archaean Spring Well Volcanic Complex. BSc. Hons. thesis, Monash Univ. (Unpublished).

DePaolo, D.J., 1981, Trace element and isotopic effects of combined wallrock assimilation and fractional crystallisation. *Earth Planet. Sci. Lett., 53, pp189-202.*

Doepel, J.J.G., 1973, Norseman Western Australia. 1:250,000 geological series-explanatory notes; Norseman Western Australia. *Bureau of Mineral Resources, Geology and Geophysics Publication.*

Donaldson, M.J., Lesher, C.M., Groves, D.I., & Gresham, J.J., 1986, Comparison of Archean Dunites and komatiites associated with nickel mineralisation in Western Australia: implications for dunite genesis. *Mineral. Deposits 21, pp296-305.*

Drummond, B.J., & Goleby, B.R., 1998, Yilgarn crustal structure revealed in five seismic profiles. *In:* Wood, S.E. (Ed.) Geodynamics & gold exploration in the Yilgarn. Workshop extended Abstracts. Australian Geodynamics Cooperative Research Centre.

Drummond, M.S., & Defant, M.J., 1990, A model for trndhjemite-tonalite-dacite genesis and crustal growth via slab melting: Archean to modern comparisons. *JournalGeophysical Research 95,(B13), pp21503-21521.*

Eggins, S.M., Woodhead, J.D., Kinsley, L.P.J., Mortimer, G.E., Sylvester, P., McCulloch, M.T., Hergt, J.M., and Handler, M.R., 1997. A simple method for the precise determination of ≥ 40 trace elements in geological samples by ICPMS using enriched isotope internal standardisation. *Chemical geology 134, pp311-326.*

Gee, R.D., Baxter, J.L., Wilde, S.A. & Williams, I.R., 1981, Crustal Development in the Archaean Yilgarn Block, Western Australia. *In:* Glover, J.E. & Groves, D.I., (Eds.) Archaean Geology: Second International Symposium, Perth, 1980. *Spec. Publs. Geol. Soc. Aust., 7, pp43-56.*

Gemuts, B, 1968, Geological map showing outcrop, inferred geology and major structure, Mt thirsty area, 1000' to 1 inch. *In:* Mackay, N.J., Annual report, 1968 on Temporary reserve No. 3508, Anaconda Australia Inc. Western Division. 12p. *DME(WA) item A351.*

Geological Survey of Western Australia, 1990, Geology and mineral resources of Western Australia: *Western Australia Geological Survey, Memoir 3, 827p.*

Ghaderi, M., 1998, Sources of Archaean gold mineralisation in the Kalgoorlie-Norseman region of Western Australia, determined from Strontium-Neodymium isotopes and trace elements in scheelite and host rocks. Ph.D. thesis Australian National Univ. (Unpublished).

Goleby, B.R., & Drummond, B.J., 2000, The 1991 deep seismic survey, Eastern Goldfields, W.A. *In:* Crustal structure and fluid flow in the Eastern Goldfields, Western Australia: results from the Australian Geodynamics Cooperative research Centre's (AGCRC) Yilgarn deep seismic reflection survey and fluid flow modelling projects. *Australian Geological Survey Organisation record 2000/34. pp46-52.*

Green, T.A., 1997, A geological investigation of the stratigraphy and structure of the Noganyer Formation Norseman , Western Australia. MSc thesis, Univer. Exeter. (Unpublished).

Green, T.H., & Pearson, N.J., 1987, An experimental study of Nb and Ta partitioning between Ti-rich minerals and silicate liquids at high pressure and temperature. *Geochim. Cosmochim. Acta, 51, pp55-62.*

Griffin; T.J., 1988, Cowan, West. Aust. Geol. Survey 1:100 000 Geol. Ser., sheet SH51-14-3234

Griffin, T.J., 1990a, Eastern Goldfields Province. *In:* Geology and Mineral Resources of Western Australia: *Western Australia Geological Survey, Memoir 3, pp77-119.*

Griffin, T.J., 1990b, Geology of the granite-greenstone terrane of the Lake Lefroy and Cowan 1:100 000 sheets, Western Australia. *Western Australia Geological Survey, Report 32, 53p*

Grove, T.L., de Witt, M.J. & Dann, J.C., 1996, Komatiites from the Komati type section, Barberton South Africa. *In*: M.J. deWit and L.D. Ashwal, (Eds) Tectonic Evolution of Greenstone Belts. *Oxford Univ. Press, pp. 438-453.*

Grove, T.L., Parman, S.W., and Dann, J.C.,1999, Melt generation conditions for hydrous Barberton komatiite magmas: Subduction zone versus deep mantle plumes. *Trans. Amer. Geophys. Union, 80, S370.*

Groves, D.I, Ridley, J.R., Bloem, E.M.J., Gebre-Mariam, M., Hagemann, S.G., Hronsky, J.M.A., Knight, J.T., McNaughton, N.J., Ojala, J., Vielreicher, R.M., McCuaig, T.C. & Holyland, P.W., 1995, Lode-gold deposits of the Yilgarn block: products of Late Archaean crustal-scale overpressured hydrothermal systems. *In:* Coward, M.P. & Ries, A.C. (Eds.) Early Precambrian Processes. *Geol. Soc. (London) Spec. Publ., 95, pp155-172.*

Hall, H.I.E. & Bekker, C., 1965, Gold deposits of Norseman. *In:* HcAndrew, J., (Ed.) Geology of Australian ore deposits (2nd edition). Melbourne, 8th Commonwealth Mining and Metallurgical Congress pp101-107.

Hallberg, J.A., 1970, The petrology and geochemistry of metamorphosed Archaean basic volcanic and associated rocks between Coolgardie and Norseman, Western Australia. Ph.D. thesis Univ. West. Australia. (Unpublished)

Hallberg, J.A., Ahmat, A.H., Morris, P.A., & Witt, W.K., 1993, An overview of felsic volcanism within the Eastern Goldfields Province, Western Australia. *In:* Williams, P.R., Haldane, J.A., (Eds.) Crustal Evolution, Metallogeny and Exploration of the Eastern Goldfields. *Extended Abstracts Record 1993/54 Australian Geological Survey Organisation pp2-32.*

Hallberg, J.A., & Giles, C.W., 1986. Archaean felsic volcanism in the northeastern Yilgarn Block Western Australia. *Precambrian Research 33, pp423-427.*

Hammond, R.L. & Nisbet, B.W., 1993, Archaean crustal processes as indicated by the structural geology, Eastern Goldfields Province of Western Australia. *In:* Williams, P.R., Haldane, J.A., (Eds.) Crustal Evolution, Metallogeny and Exploration of the Eastern Goldfields. *Extended Abstracts Record 1993/54 Australian Geological Survey Organisation pp105-114.*

Hand, J.L., 1998, The sedimentological and stratigraphic evolution of the Archaean Black Flag Beds, Kalgoorlie, Western Australia: Implications for regional stratigraphy and basin setting of the Kalgoorlie Terrane. Phd thesis Monash Univ. (Unpublished).

Hill, R., 1987. Norseman greenstone stratigraphy. *Correspondence to Arthur Thomas, CNGC (dated 16 July 1987).*

Hill, R.E.T., Barnes, S.J., Gole, M.J. & Dowling, S.E., 1990, Physical volcanology of komatiites. *Geol. Soc. Aust.(W.A. Division) Excursion Guide Book no. 1*

Hill, R.E.T., Barnes, S.J., Gole, M.J. & Dowling, S.E., 1993, Recent advances in the understanding of Komatiite Volcanology in the Norseman-Wiluna Greenstone Belt. *In:* Williams, P.R., Haldane, J.A., (Eds.) Crustal Evolution, Metallogeny and Exploration of the Eastern Goldfields. *Extended Abstracts Record 1993/54 Australian Geological Survey Organisation pp7-13.*

Hill, R.I., Campbell, I.H., Chappell, B.W., & Johnson, K., 1990, Crustal growth, crustal reworking and granite genesis in the southeast Yilgarn Block, Western Australia. *In:* The Australian National University research School of Earth Sciences annual report, 1990 *pp2-4.*

Hill, R.I., Campbell, I.H. & Chappell, B.W., 1992a, Crustal growth, crustal reworking and granite genesis in the southeastern Yilgarn Block, Western Australia. *In:* Glover, J.E. & Ho, S.E. (Eds.) The Archaean: terrains, processes and metallogeny. Proceedings Volume for the Third International Archaean Symposium, Perth, Western Australia, *Geology Dept (Key Centre) & University Extension, University of Western Australia Publication, 22, pp203-212.*

Hill, R.I., Chappell, B.W. and Campbell, I.H., 1992b, Late Archaean granites of the southeast Yilgarn Block, Western Australia: age, geochemistry, and origin. *Transactions of the Royal Society of Edinburgh: Earth Sciences, 83, pp211-226.*

Hodgkison, J., !995, A geological investigation of the Archaean Golden Rainbow area, Lake Cowan, Western Australia. Geology Project 427. B.Sc (Hons.) thesis WA School. Mines, Kalgoorlie. (unpublished).

Hofmann, A.W., Jochum, K.P., Seufert, M. & White, W.M., 1986, Nb and Pb in oceanic basalts: new constraints on mantle evolution. *Earth and Planetary Science Letters 79, pp33-45.*

Holcolme, R.J., 1996, Structural framework of the Norseman area. Unpublished Central Norseman Gold Corp. internal technical report. *7p*

Holcolme, R.J., 1997, Structural framework of the Norseman area; Summary of observations to June 1997. Unpublished Central Norseman Gold Corp. internal technical report *10p.*

Hudson, G.R., 1966, The geology of part of the Norseman succession west of the mining area, Norseman, Western Australia. B.Sc. (Hons.) thesis Univ. West. Australia. (Unpublished).

Humphries, S.E., 1984, The mobility of rare earth elements in the crust. *In:* Henderson P. (Ed.) Rare earth element geochemistry. *Elsevier, Amsterdam, pp315-341.*

Keele, R.A., 1984, Emplacement and deformation of Archaean gold-quartz veins, Norseman Western Australia. Unpublished Phd thesis, Univer. Leeds.

Le Maitre, R.W., Bateman, P., Dudek, A., Keller, J., Lameyre Le Bas, M.J., Sabine, P.A., Schmid, R., Sorensen, H., Streckeisen, A., Wooley, A.R., & Zanettin, B., 1989, A classification of igneous rocks and glossary of terms. *Blackwell, Oxford.*

Lentz, D.R., 1998, Petrogenetic evolution of felsic volcanic sequences associated with phanerozoic volcanic-hosted massive sulphide systems: the role of extensional geodynamics. *Ore Geology Reviews 12, pp289-327.*

Lesher, C.M., Goodwin, A.M., Campbell, I.H., & Gorton, M.P., 1986, Trace-element geochemistry of ore-associated and barren, felsic metavolcanic rocks in the Superior Province Canada. *Can. J. Earth Sci. 23 pp222-237.*

Lesher, C. M., 1989, Komatiite-associated nickel sulfide deposits. *In:* Whitney, J.A., Naldrett, A.J., (Eds.) Ore Associated with magmas. *Reviews in Economic Geology Vol. 4, Society of Economic Geologists. pp45-101.*

Lowe, D.R., 1982, Sediment gravity flows: II. Depositional models with special reference to deposits of high density turbidity currents. *J. Sediment Petrol 52:pp279-297.*

McBirney, A.R., 1984, igneous Petrology. *Oxford University Press.*

MacGeehan, P.J., 1986, Exploration Potential – Penneshaw Beds. Unpublished internal WMC memorandum XK 24/86.

McCall, G.J.H., 1970, The Norseman area: *Geol. Soc. Australia Symposium,* The Archaean rocks, *Perth/Kalgoorlie, May, 1970, Field Excursion Guide Book, pp24-38.*

McCall, G.J.H., 1973, Geochemical characteristics of some Archaean greenstone suites of the Yilgarn Structural province, Australia. *Chemical Geology11, pp243-269.*

McCuaig, T.C., 1991, Relative age of the Dinky Buoys Porphyry and mineralization. *Internal CNGC memorandum (dated 13 February1991).*

McCuaig, T.C., 1996, The genesis and evolution of lode gold mineralization and mafic host lithologies in the late-Archean Norseman Terrane, Yilgarn Block, Western Australia. PhD thesis Uni. Saskatchewan (Unpublished).

McGoldrick, P.J., 1993, Norseman, West. Aust. Geol. Survey 1:100 000 Geol. Series, sheet

McPhie, J., Doyle, M., & Allen, R., 1993, Volcanic textures, a guide to the interpretation of textures in volcanic rocks. *Centre for ore deposits and exploration studies, Univ. Tasmania.*

McPhie, J., & Gemmell, B., 1998, Facies interpretation of ancient volcanic successions. Field Guide II. Mount Read Volcanics, western Tasmania. *Master of Economic Geology Course Work Manual 9, fifth Edition. Centre for Ore Deposit Research, Univ. Tasmania*

Molnar, P., 1990, The structure of mountain ranges. *In:* Moores, E.M., (Ed.), Shaping the earth: tectonics of continents and oceans. Readings from Scientific American Magazine. *Freeman, New York.pp125-138.*

Morris, P.A., Pescud, L., Thomas, A., Gamble, J., Tovey, E., Marsh, N. & Everett, R., 1991, Geochemical analyses of Archaean and ultramafic volcanics, Eastern Yilgarn Craton, Western Australia. *Geological Survey of Western Australia record 1991/8.*

Morris, P.A., 1993a, Comparative geochemistry of stratigraphically equivalent volcanic units in the Eastern Goldfields. *In:* Williams, P.R., Haldane, J.A., (Eds.) Crustal Evolution, Metallogeny and Exploration of the Eastern Goldfields. *Extended Abstracts Record 1993/54 Australian Geological Survey Organisation pp15-21.*

Morris, P.A., 1993b, Archaean mafic and ultramafic volcanic rocks, Menzies to Norseman, Western Australia. *Geological Survey of Western Australia Report no. 36.*

Murphy, G.C., 1988, Report about the Norseman Project. Unpublished report by BHP-Utah Mine3rlas International.

Myers, J.S., 1997, Tectonic evolution of the Yigarn Craton. *In:* Cassidy, K.F., Whitacker, A.J. & Liu, S.F. (Eds.) Kalgoorlie '97: Crustal Evolution, Metallogeny and Exploration of the Yilgarn Craton- An Update. *Extended Abstracts Record 1997/41 Australian Geological Survey Organisation pp7-9.*

Myers, J.S., 1993, Precambrian history of the West Australian Craton and adjacent Orogens. *Annu. Rev. Earth Planet. Sci. 21, pp453-485*

Nelson, D.R., 1995, Compilation of SHRIMP U-Pb zircon geochronology data, 1994. *Geological Survey of Western Australia record 1995/3.*

Nelson, D.R., 1997, SHRIMP U-Pb zircon chronolgical constraints on the evolution of the Eastern Goldfields granite-greenstone terranes. *In:* Cassidy, K.F., Whitacker, A.J. & Liu, S.F. (Eds.) Kalgoorlie '97: Crustal Evolution, Metallogeny and Exploration of the Yilgarn Craton- An Update. *Extended Abstracts Record 1997/41 Australian Geological Survey Organisation pp11-14.*

Nesbitt, R.W., Sun, S.-S., & Purvis, A.C., 1979, Komatiites: Geochemistry and genesis. *Canadian Mineralogist, V.17, pp.165-186.*

Offe, L.A., 1994, Dot and Eve VMS Prospects, Polar Bear Peninsula, Western Australia. Unpublished Central Norseman Gold Corp. internal technical report CNG/T/018.

Pearce, J.A., Harris, N.B.W., & Tindle, A.G., 1984, Trace element discrimination diagrams for the tectonic interpretation of granitic rocks. *J. Petrol., 25,pp 956-983.*

Perring, C.S., 1989, The significance of 'porphyry' intrusions to Archaean gold mineralization in the Norseman-Wiluna belt of Western Australia. Phd thesis Univ. West. Australia (Unpublished).

Peters. S.G., Archer, N.R., Offe, L.A., Pilapil, L. & Johnson, K., 1991, CNGC Lake exploration programme. Pre-implementation summary, 1991. Internal CNGC memorandum (dated 14 August 1990).

Powell, R., 1984, Inversion of the assimilation and fractional crystallisation (AFC) equations; characterisation of contaminants from isotope and trace element relationships in volcanic suites. *Journal Geol. Soc. Lond., 141, pp447-452.*

Redman, B.A., 1982, Petrography, petrology and geochemistry of Archaean basic volcanism in the Eastern Goldfields Province, Western Australia : stratigraphic control of gold mineralization. MSc Thesis. Univ. of Melbourne (Unpublished), 304p.

Redman, B.A. & Keays, R.R., 1985. Archaean basic volcanism in the Eastern Goldfields Province, Yilgarn Block, Western Australia. *Precambrian Research, 30, pp113-152.*

Rollinson, H.R., 1993, Using geochemical data: evaluation, presentation, interpretation. *Longman Scientific and Technical, New York, 352p.*

Rudnick, R.L., & Fountain, D.M., 1995, Nature and composition of the continental crust: a lower crustal perspective. *Review of Geophysics, 33, pp267-309.*

Smith, I.E.M., Worthington, T.J., Price, R.C., & Gamble, J.A., 1997, Primative magmas in arc-type volcanic associations: examples from the southwest Pacific. *Canadian Mineralogist 35 pp257-273.*

Squire, R.J., Cas, R.A.F., Clout, J.M.F. & Behets, R., 1998, Volcanology of the Archaean Lunnon Basalt and its relevance to nickel sulfide-bearing trough structures at Kambalda, Western Australian. *Aust. J. Earth Sci. 45, pp695-715.*

Sofoulis, J., 1963. Boorabbin. West. Aust. Geol. Surv. 1:250,000 geological series-explanatory notes.

Spray, J.G., 1986, Geological setting of Archaean vein-type gold deposits within the Norseman greenstone sequence, Western Australia. *In:* Gallagher, M.J., Ixer, R.A., Neary, C.R. & Prichard, H.M. (Eds.) metallogeny of basic and ultrabasic rocks, *Inst. Min. Metall., London pp133-150.*

Sun, S-s., & McDonough, W.F. 1989, Chemical and isotopic systematics of oceanic basalts: implications for mantle compositions and processes, *In:* Saunders, A.D. & Norry, M.J. (Eds.) Magmatism in the ocean basins, *Geological Society Special Publication 42, pp313-345.*

Sun, S-s, Nesbitt, R.W., & McCulloch, M.T., 1989, Geochemistry andpetrogenesis of Archean and early Proterozoic siliceous high-magnesian basalts, *In:* Crawford, A.J. (Ed.) Boninites and related rocks, *Allen & Unwin, pp148-173.*

Swager C.P. 1995. Geology of the greenstone terranes in the Kurnalpi-Edjudina region, Southeast Yilgarn Craton. *Western Australia Geological Survey, Report 47, 31p.*

Swager, C.P., 1997, Structural Evolution of Greenstone Terranes in the Southern Eastern Goldfields, Western Australia. *In:* Cassidy, K.F., Whitacker, A.J. & Liu, S.F. (Eds.) Kalgoorlie '97: Crustal Evolution, Metallogeny and Exploration of the Yilgarn Craton- An Update. *Extended Abstracts Record 1997/41 Australian Geological Survey Organisation pp49-53.*

Swager, C.P., Goleby, B.R., Drummond, B.J., Rattenbury, M.S. & Williams, P.R., 1997, Crustal structure of granite-greenstone terranes in the Eastern Goldfields, Yilgarn Craton, as revealed by seismic reflection profiling. *Precambrian Research, 8, pp43-56.*

Swager, C.P., & Griffin, T.J., 1990, An early thrust duplex in the Kalgoorlie-Kambalda greenstone belt, Eastern Goldfields Province, western Australia. *Preecambrian Research 48 pp63-73.*

Swager, C.P., Griffin, T.J., Witt, W.K., Wyche, S., Ahmat, A.L., Hunter, W.M. & McGoldrick, P.J., 1995, Geology of the Archaean Kalgoorlie Terrane - an explanatory note: *Western Australia Geological Survey, Report 48, 26p. (Reprint of Record 1990/12).*

Sylvester, P.J., Campbell, I.H. & Bowyer, D.A., 1997, Niobium/uranium evidence for early formation of continental crust. *Science 275, pp521-523.*

Taylor, S.R., & McLennan, S.M., 1985, The continental crust: its composition and evolution. *Blackwell, Oxford.*

Tepper, J.H., Nelson. B.K., Bergantz, G.W., & Irving, A.J., 1993, Petrology of the Chilliwack Batholith, North Cascades, Washington; generation of calc-alkaline granitoids by melting of mafic lower crust with variable water fugacity. *Contributions to Mineralogy & Petrology 113, pp333-351.*

Thomas, A., Johnson, K. & MacGeehan, P.J., 1990. Norseman gold deposits, *In:* Hughes, F.E. (Ed.) Geology of the Mineral Deposits of Australia and Papua New Guinea. *The Australian institute of Mining and Metallurgy, monograph 14, pp493-504.*

Thomas, 1991. The stratigraphic project, 1983. Internal CNGC report (Unpublished).

Thompson, R.N., Morrison, M.A., Dickin, A.P. & Hendry, G.L., 1983, Continental flood basalts... Arachnids rule OK? *In:* Hawkesworth, C.J. & Norry, M.J. (Eds.) Continental basalts and mantle xenoliths. *Shiva, Cheshire. pp158-185.*

Trendall, A.F., 1990, Cratons - Introduction. *In:* Geology and Mineral Resources of Western Australia: *Western Australia Geological Survey, Memoir 3, p11.*

Walker, R.G., 1984, Turbidites and associated coarse clastic deposits. *In:*Walker, R.G. (Ed.) Facies Models, second edition. *Geoscience canada, Reprint series 1 pp171-185.*

Whalen, J.B., Currie, K.L. & Chappell, B.W., 1987, A-type granites: geochemical characteristics, discrimination and petrogenesis. *Contrib. Mineral. Petrol., 95, pp407-419.*

Williams, P.R., (1993), A new hypothesis for the evolution of the Eastern Goldfields Province. *In:* Williams, P.R., Haldane, J.A., (Eds.) An International Conference on Crustal Evolution, Metallogeny and Exploration of the Eastern Goldfields. *Extended Abstracts Record 1993/54 Australian Geological Survey Organisation pp77-83.*

Williams, P.R. & Currie, K.L., 1993, Character and regional implications of the sheared Archaean granite-greenstone contact near Leonora, Western Australia. *Precambrian research, 62, pp343-365.*

Williams, D.A.C. & Hallberg, J.A., 1973, Archaean layered intrusions of the Eastern Goldfields , Western Australia. *Contributions to mineralogy and Petrology 38, pp 45-70.*

Wilson, M., 1989, Igneous petrogenesis. *Unwin Hyman. 466p*

Winchester , J.A. & Floyd, P.A., 1976, Geochemical magma type discrimination; application to altered and metamorphosed basic igneous rocks. *Earth Planet. Sci. Lett., 28, pp459-469.*

Winkler, H.G.F., 1979, Petrogenesis of metamorphic rocks. *Springer Study Edition. 348p.*

Witt, W.K., 1995, Tholeiitic and high-Mg mafic/ultramafic sills in the eastern Goldfields Province, Western Australia: implications for tectonic settings. *Australia Journal earth Sciences 42, pp407-422.*

Witt, W.K. & Davy, R., 1993, Pre- and post-regional folding, I-type granitoid suites in the southwest Eastern Goldfields Province: an Archaean syn-collisional plutonic event? *In:* Williams, P.R., Haldane, J.A., (Eds.) An International Conference on Crustal Evolution, Metallogeny and Exploration of the Eastern Goldfields. *Extended Abstracts Record 1993/54 Australian Geological Survey Organisation pp33-37.*

Wood, B.J., & Fraser, D.G., 1976, Elementary thermodynamics for geologists. *Oxford: Oxford University Press.*

Wyche, S., 2000, Structure and stratigraphy in the southern part of the Eastern Goldfields. *In:*, Crustal structure and fluid flow in the Eastern Goldfields, Western Australia: results from the Australian Geodynamics Cooperative research Centre's (AGCRC) Yilgarn deep seismic reflection survey and fluid flow modelling projects. *Australian Geological Survey Organisation record 2000/34. pp35-42.*

Yeats, C.J. & McNaughton, N.J., 1997, Significance of SHRIMP II U-Pb geochronology on lode-gold deposits of the Yilgarn Craton. *In:* Cassidy, K.F., Whitacker, A.J. & Liu, S.F. (Eds.) Kalgoorlie '97:

Crustal Evolution, Metallogeny and Exploration of the Yilgarn Craton- An Update. *Extended Abstracts Record 1997/41 Australian Geological Survey Organisation pp125-130.*

APPENDIX 1

Polar Bear Key Area Descriptions

A1.1 Introduction

The geology of the Polar Bear Peninsula is complex due to lateral facies changes in addition to folding and faulting. A number of areas were crucial in advancing the geological understanding. These areas are unusually well-preserved such that way-up indicators can be found that allow the stratigraphy to be pieced together and structures defined, or contacts are exposed that allow the relationship between units to be elucidated. These key areas are described below to present the evidence used for the interpretation of the geology of the Polar Bear Peninsula.

A1.2 Key areas defining stratigraphy and structure

The key areas described below are the locations which preserve textures or sequences which reveal the stratigraphy and structure.

A1.2.1 Hinemoa Shore - stratigraphy

Key elements of the stratigraphy are exposed along the shoreline southeast of the Hinemoa Mine at 6462745mN, 389515mE MGA. Offshore, aircore drilling has identified an extensive mafic rock package. On the lake close to the shoreline, lumps of weathered talc-carbonate ultramafic rock are exposed over a backfilled costean (Plate A1.1). A steep slope runs along the shoreline into which a short adit has been driven several metres. Black shales and siltstones are exposed in the adit with graded bedding indicating a westward facing. The shales are brecciated at the end of the adit adjacent to a northwest striking shear zone. Above the shales on the slope, quartz porphyry caps the hill. 500 m further north along this shoreline, the shear zone is not present but quartz porphyry remains stratigraphically above the shale.

Thus the stratigraphic sequence at this location from bottom to top is mafic rocks, ultramafic rock, black shale, and quartz porphyry. Along strike to the north, spinifex textures are common in the ultramafic rock, confirming it to be komatiite. As there is only one komatiitic event in the Eastern Goldfields Nelson (1997), the Polar Bear komatiite must correlate with the Norseman komatiite, and the mafic rocks underlying the Polar Bear komatiite offshore of East Polar Bear must correlate with the Woolyeenyer Formation.

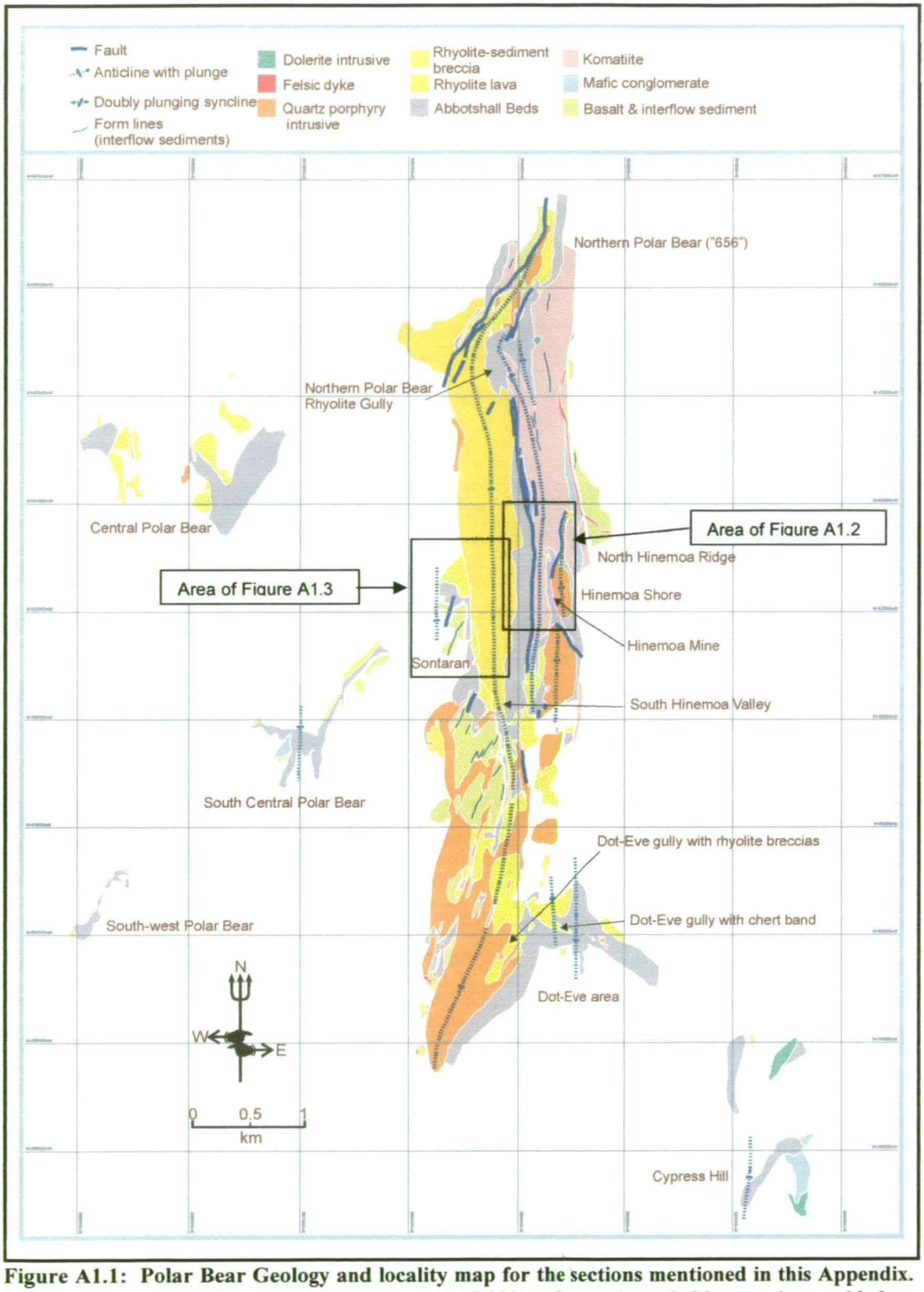

Figure A1.1: Polar Bear Geology and locality map for the sections mentioned in this Appendix. Solid geology shown for exposed areas. A 1:10 000-scale version of this map is provided as map 9 in Appendix 4. The solid geology was developed by consolidating and interpreting 1:2500-scale geological maps 1 to 8 in Appendix 4. Figure 3.2 in Chapter 3 is a version of this map showing the locations of the map sheets in Appendix 4, and the outline of the Polar Bear Peninsula shoreline.

Plate A1.1: Hinemoa Shore. Spoil on backfilled costeans in foreground exposes talc-carbonate ultramafic rock. A thin sequence of shales is exposed at the base of the hill. Outcrop on the hill is quartz porphyry.

A1.2.2 Hinemoa Mine sequence - stratigraphy & structure

Extensive diamond drilling was carried out at the Hinemoa Mine by CNGC in 1980. The logs for this drilling can be combined with mapping the excellent outcrop (figure A1.2) to gain a useful understanding of the stratigraphy and the structure affecting the rocks.

A surface width of approximately 120 m of talc-carbonate ultramafic rock is exposed immediately east of the Hinemoa Mine workings, terminated on its western contact by the Hinemoa Fault. Spinifex textures are found in rare occurrences along the eastern contact of the ultramafic rock, indicating an eastward facing. A surface width of approximately 50 m of chert and sulfidic black shale correlated with the Abbotshall Beds overlies the ultramafic rock to the east and the sequence then passes into quartz porphyry at the top of the hill (figure A1.2). This stratigraphic sequence of ultramafic rock to sedimentary rock to quartz porphyry shows the same transitions as the Hinemoa shore sequence described above, but with an opposite easterly facing.

Further north, the Hinemoa Mine ultramafic rock merges with the northern extension of the komatiite along the lake shore described in section A1.2.1, demonstrating that they comprise the same unit (figure A1.1; map 9 & map 2; Appendix 4). The division of the ultramafic rock into two strands separated by sedimentary rocks of the Abbotshall Beds and quartz porphyry is the result of complex doubly plunging folds. The opposite facings of the Hinemoa shore sequence (section A1.2.1) and eastern Hinemoa Mine sequences define a syncline, the core of which is occupied by quartz

porphyry. The quartz porphyry possesses the S_2 cleavage indicating it is folded and its consistent stratigraphic position above the shale suggests it is conformable with stratigraphy.

Additional information is provided by a diamond drill hole, PEN6, which was collared in ultramafic rock, approximately 90 m west of the quartz porphyry contact and drilled east plunging at 55° to a final depth of 259.2 m. Comparing the depth at which the sedimentary rocks were intersected with their surface contact suggests an average dip of about 75°E. The hole ended without entering quartz porphyry, therefore, the porphyry margin must have a dip of less than 75°E but may still have a shape roughly conformable with the stratigraphy. Peperitic contacts are not present at the surface along the quartz porphyry-sediment contact indicating the porphyry was emplaced into compacted shales. It is considered to be a sill.

The sedimentary rocks of the Abbotshall Beds are also exposed along the faulted western contact of the ultramafic rock at the Hinemoa Mine (figure A1.2). At the surface, the majority of the sedimentary rocks appear to be siltstone-shale turbidites in which the shale units are sulfidic, having cavities after pyrite nodules. In drill core, the sedimentary rocks are dominated by sulfidic black shale with common pyrite nodules. Siltstone or very fine sandstone layers a couple of centimetres thick are lesser components interbedded with the shale. Locally, siltstone may occur as units up to 2 m thick. The dip of the Abbotshall Beds west of the ultramafic rock varies, but compilation of drilling data shows the overall dip is subvertical to steeply west dipping and the sediment package varies in thickness between 120 and 180 m.

To the west, the sediment passes into flow-banded rhyolite along a rhyolite-sediment breccia contact interpreted as peperite (figure A1.2). The peperite contact indicates the sediment predates the rhyolite and therefore the sequence west of the Hinemoa Mine faces west. Thus the stratigraphic position above the Abbotshall Beds is occupied by a quartz porphyry sill along the lake shore and by an extrusive rhyolite flow west of the Hinemoa Mine (figure A1.2). The Abbotshall Beds west of the Hinemoa Mine have a greater thickness than those intruded by the quartz porphyry sill, which may indicate stoping out, or splitting of the sedimentary rocks by the intrusive.

Based on the stratigraphy further north (figure A1.1; map 9, Appendix 4) and the sequence described in section A1.2.1, the Abbotshall Beds west of the Hinemoa Mine should be underlain by komatiite. Ultramafic rock does underlay the sedimentary rocks, but with the structural contact of the Hinemoa Fault.

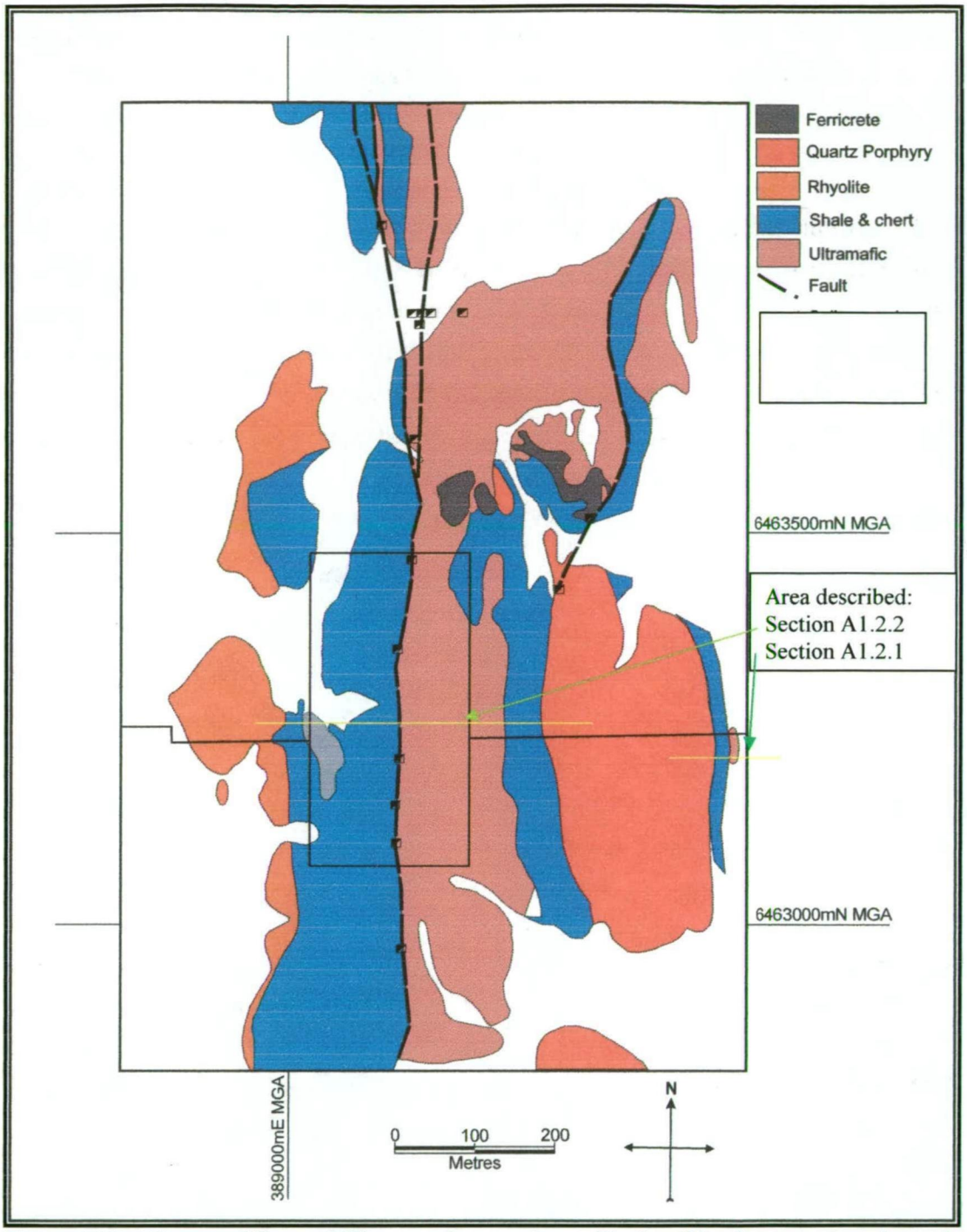

Figure A1.2: Hinemoa Mine and Hinemoa shore geology. The localities for sequences shown in section A1.2.1 and section A1.2.2 are shown.

The Hinemoa Fault, which is exposed by mine openings, lies along the western contact of the ultramafic rock, separating the latter from siltstone-shale turbidites. It is subvertical at the surface but according to mine sections, rolls to a dip of 70°E at 20 m depth. The movement on the fault cannot be directly measured, but in section 10.5.2.1 and 10.5.5, from compilation of drillhole data, it is proposed that the Hinemoa Fault is a D_2 thrust. As no stratigraphic units are missing, the Hinemoa Fault may be layer parallel in this area (thrust flat) and occupy the position behind the thrust ramp, where the units have not been thrown over higher units. In addition, the

west facing of the sequence west of the fault and the east facing of the sequence east of the fault, combined with the absence of missing units at the fault, indicates that the ultramafic rock adjacent to the Hinemoa Fault may occupy the core of an anticline. This structural interpretation is shown on the maps in Appendix 4, and figure A1.1.

The interpretation of the ultramafic rock as occupying the core of an anticline is supported by the geometry of the geology 400 m south of the Hinemoa main shaft. In this area (6462720mN, 389200mE MGA), the ultramafic rock exposure disappears beneath cover along a creek. Further to the south where outcrop reappears, brecciated black shales from east and west of the ultramafic rock merge and occupy the position formerly held by the ultramafic rock (figure A1.1; map 9, Appendix 4). This transition from ultramafic rock to black shale to the south, is interpreted to be due to a gentle southerly plunge of an anticline.

A1.2.3 Sontaran Prospect (West of Hinemoa Mine) – stratigraphy & structure

At the Sontaran prospect, 700 m southwest of the Hinemoa Mine main shaft, the ultramafic unit is absent as a result of stratigraphic pinchout. Basalt with interflow sediment bands is directly in contact with the Abbotshall Beds sediment package (figure A1.3). The Abbotshall Beds strike north-south with the basalt on the western contact and rhyolite to the east. There are no younging indicators, but the sequence can be interpreted to face east from the stratigraphy that resembles that described above for the Hinemoa shore and Hinemoa Mine.

The Sontaran prospect lies close to the top of the basalt package. A diamond drill hole has revealed the character of this basalt sequence. Interflow sediment horizons are abundant and the basalt packages between the sedimentary rocks vary in thickness from 1 to 30 m. The basalts are pillowed and highly amygdaloidal with altered feldspar microlites.

The Abbotshall Beds at Sontaran were drilled with reverse circulation percussion holes on several sections including two that intersected the full width of the sediment package (figure A1.4). The true width of the Abbotshall Beds varies from 26 to 50 m. Sulfidic black shale with laminations of siltstone dominates the base whereas pyritic chert is more prevalent at the top. Along strike, the pyritic chert grades into pyritic massive sulfide. Felsic rock layers from <1 to 5 m thick are common within the Abbotshall Chert at Sontaran. The lack of continuity of these layers along strike suggests they are more likely to be intrusive than felsic volcanic sedimentary rocks.

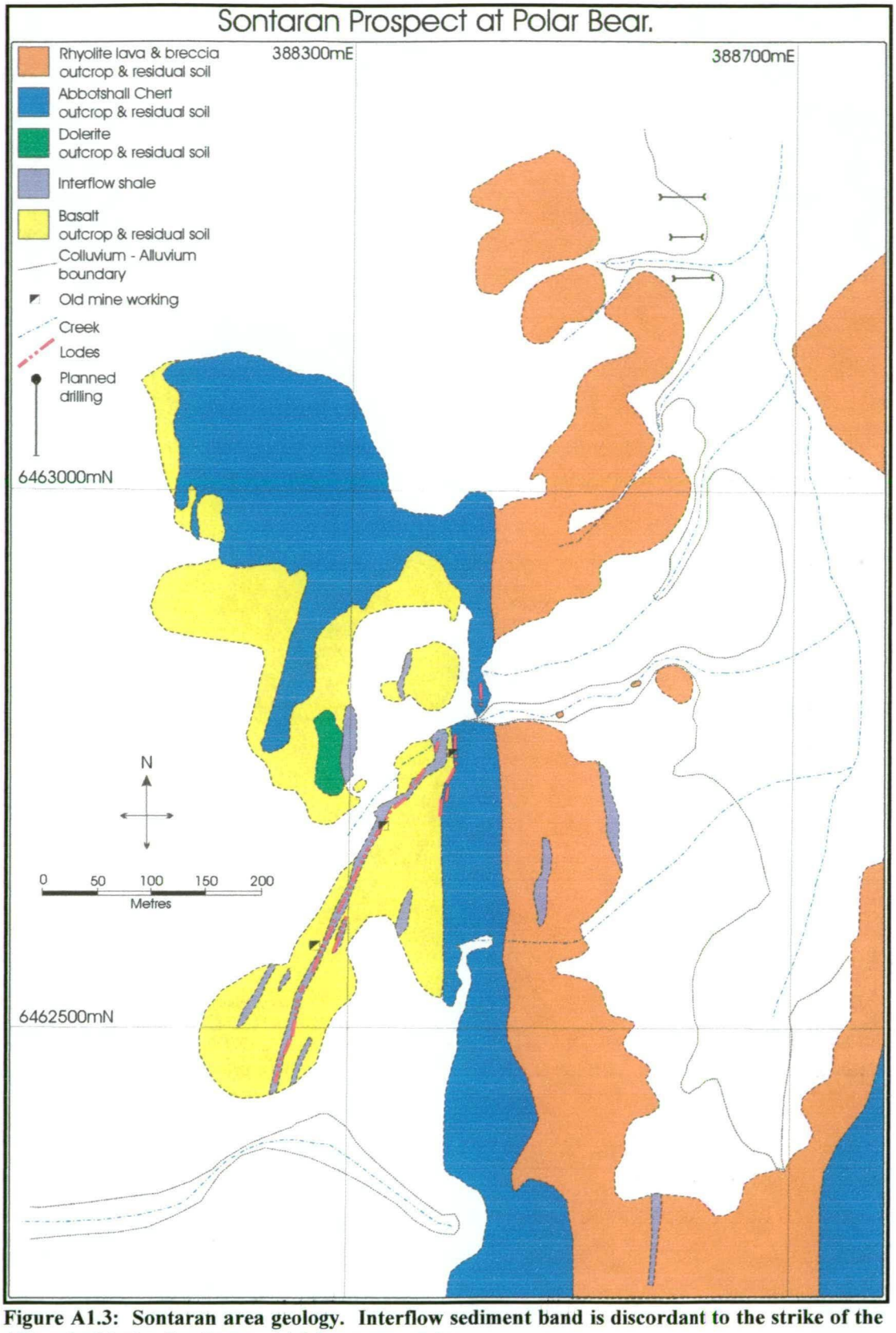

Figure A1.3: Sontaran area geology. Interflow sediment band is discordant to the strike of the Abbotshall beds. See figure A1.3 for cross section.

Within the basalt package at Sontaran there are a number of interflow sediment bands, one of which has been traced striking NNE and converging upon the N-S striking Abbotshall Beds (figure A1.3). This discordance indicates an angular unconformity at the top of the basalt sequence. Reverse circulation drilling has confirmed the angular discordance in vertical cross section (figure A1.4). The Abbotshall beds dip at 50-60° to the east whereas the interflow sediment bands within the basalt dip at 80-85°E.

The angular unconformity indicates that the basaltic succession was deformed and eroded prior to the deposition of the Abbotshall Beds. If the latter Beds are rotated back to the horizontal, the interflow sediment bands have a dip of about 40° towards the southeast, presumably their attitude when the Abbotshall Beds were deposited.

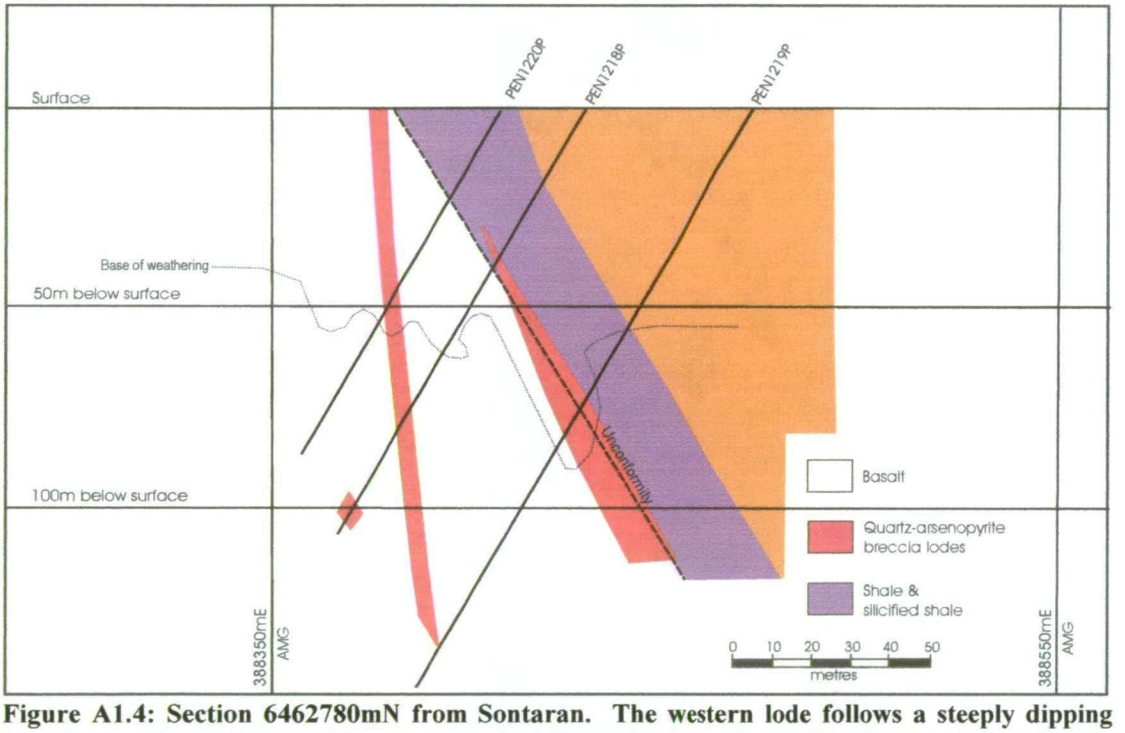

Figure A1.4: Section 6462780mN from Sontaran. The western lode follows a steeply dipping interflow sediment band. The eastern lode follows the unconformable Abbotshall Beds-basalt contact.

A1.2.4 South-central Polar Bear - stratigraphy

Mafic conglomerate with cobble-sized clasts of basalt and chert is exposed in a creek at location 6461655mN, 386765mE MGA, overlain by laminated chert of the Abbotshall Beds (figure A1.1; map 9, map 7, Appendix 4). The conglomerate is bounded along one side by coherent basalt, a contact that is not parallel with the overlying laminated chert. The basalt-conglomerate contact may represent the margin of an eroded ravine in the basalt substrate which has subsequently been used as a submarine fan channel and filled with channel facies. Cover prevents examination of the opposite basalt-conglomerate contact.

Further up the same creek, just below the laminated chert, but stratigraphically above the mafic conglomerate, there are excellent exposures of low-density turbidites at 6461855mN, 386895mE MGA. Individual turbidites are less than 10 cm thick and range from basal coarse sandstone or gravel to mudstone. Several rounded chert pebbles were noted within gravel units indicating the same sediment source as the underlying mafic conglomerate.

Overall, the succession shows a fining up sequence from mafic cobble and boulder conglomerate, through low-density, gravel/sandstone-shale turbidites, to laminated chert interpreted to represent surficial silicification of siltstone and shale. The conglomerate is submarine fan channel facies with the gravel/sandstone-shale turbidites capping the channel-fill. This thinning upwards sequence may represent filling and abandonment of the channel. The laminated chert is not channelised and is the part of the widespread Abbotshall Beds. This fine-grained sediment package consists of distal and ambient sedimentation that indicates starvation of the submarine fan. Starvation of the fan is most likely to have occurred through drowning of the source due to either sea-level rise or subsidence.

A1.2.5 Cyprus Hill - stratigraphy

Cypress Hill shows a similar sequence to south-central Polar Bear, with mafic conglomerate overlain by chert (figure A1.1; map 9, map 4 Appendix 4). The mafic conglomerate contains pebble-sized clasts and chert clasts are only present at the base of the hill. Similar to south-central Polar Bear, the outline of the conglomerate package is not parallel to the overlying chert and it appears to delineate a channel incised into the basalt substrate. This outcrop of mafic conglomerate was noted by Doepel (1973).

A1.2.6 North Hinemoa ridge - stratigraphy

Along a low ridge at North Hinemoa between approximately 6463550mN-6464650mN, 389550mE MGA, mafic pebble-conglomerate is preserved in an area that also contains komatiite (figure A1.1; map 9, map 2, Appendix 4). The lithologies in this area are heavily obscured due to strong flattening and brecciation associated with a fault, nevertheless, the mafic conglomerate can be discerned locally, particularly where small chert clasts are present (Plate A1.2, & A1.3). Basalt and chert clasts are also visible in thin section (Plate A1.4 & A1.5). Mafic sandstones associated with the conglomerate become predominant to the north. The importance of this key area is that it appears to show how the mafic conglomerates fit in the stratigraphy relative to the komatiite, although it would be more convincing if the textures were not so heavily obscured.

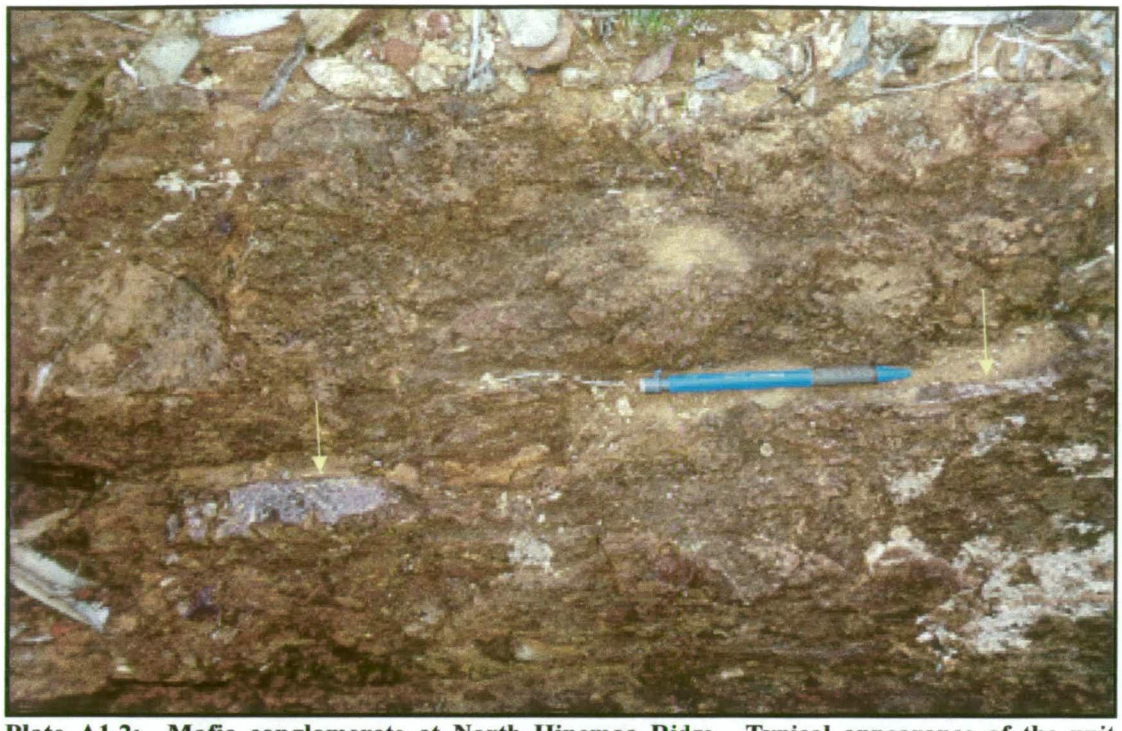

Plate A1.2: Mafic conglomerate at North Hinemoa Ridge. Typical appearance of the unit except for the stretched chert clasts (yellow arrows) which are rare. S2 cleavage parallel to pencil.

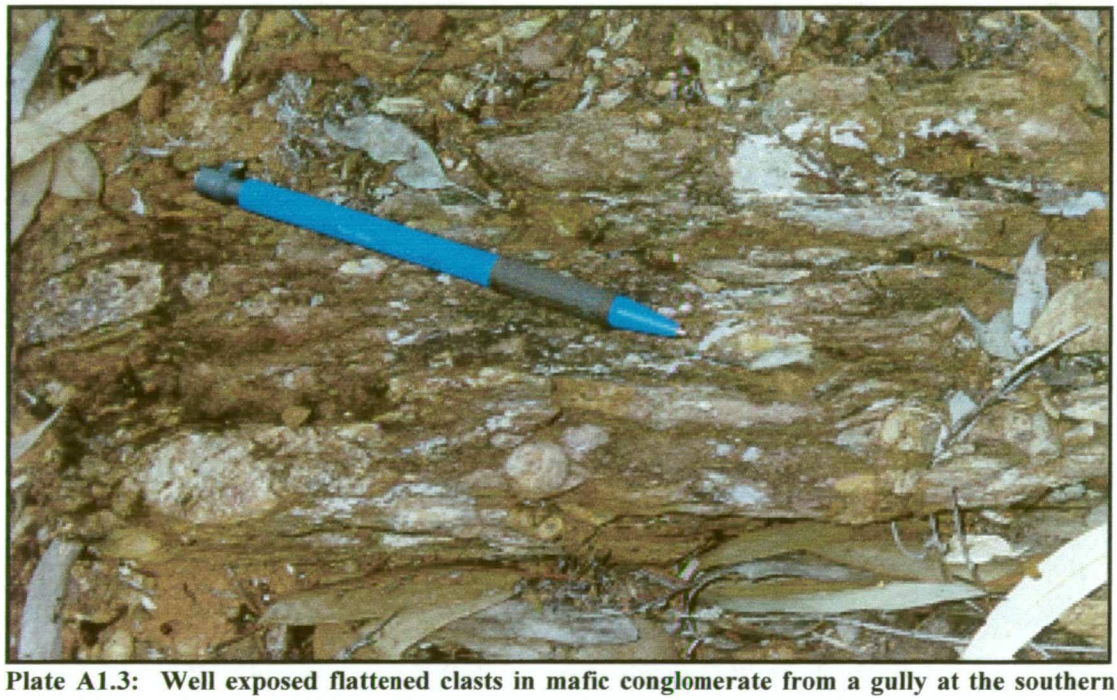

Plate A1.3: Well exposed flattened clasts in mafic conglomerate from a gully at the southern end of North Hinemoa Ridge. This is an atypical exposure as the clasts are usually poorly defined.

The sequence youngs to the west and mafic rocks, particularly basalt but also dolerite, are the easternmost, and therefore oldest lithologies exposed. These rocks are tectonically crackled and disrupted, particularly to the north where a shearing and fault breccia has been mapped (map 2, Appendix 4). Thin interflow sediment bands can be traced for short distances through the mafic rocks and typically show a NNE strike, discordant to the general north-south strike of the overlying ultramafic rock

and sedimentary sequence. This is consistent with the interpretation provided in section A1.2.3, of an angular unconformity at the top of the mafic sequence. However, this area provides additional information, indicating that the unconformity predates the komatiite that overlies it.

A thin band of shale, approximately one metre thick, separates the top of the mafic succession from talc-carbonate altered and type 1 silicified komatiite. The shale band is parallel to interflow sedimentary rocks within the komatiite sequence rather than the interflow sedimentary rocks within the mafic succession and is considered to be part of the former package. In the southern area, the ultramafic sequence has a surface width varying from 60 m to 10 m.

Mafic conglomerate has a surface width of approximately 50 m in the southern area, reaching a maximum of 70 m then gradually thinning out of the sequence to the north where sandstones become predominant. At the south end, the sequence is somewhat disrupted by faults. Nevertheless, it appears the conglomerate has thinned to just 10 m adjacent to the lake shore where the exposure ends. A black shale band is present within the conglomerate sequence, but changes stratigraphic position from the base of the conglomerate in the southern part of the exposure, to the middle of the conglomerate package at 6464000mN MGA (figure A1.5, map 2, Appendix 4). This change in the stratigraphic position of the black shale relative to the conglomerate is interpreted as being the result of the conglomerate outcrops as they now exist, having been built up over time as an amalgamation of submarine fan channel facies deposits. The axes of the channels alternated over the time, so that conglomerate commenced deposition later in the area with the shale at the base of the sequence.

In addition to underlying the conglomerate, the talc-carbonate ultramafic rock also overlies the conglomerate at its western margin. This ultramafic rock extends for a surficial width of about 350 m although this is considered to be broadened by folding. Spinifex textures through the ultramafic rock show it consists of multiple flows.

These outcrops indicate that the mafic conglomerate was deposited between komatiite flows and consists of at least two high-density turbidites (interpreted as channel facies), separated by a black shale band representing an extended period of ambient sedimentation. The komatiite has also erupted over an extended period as evidenced by the abundant interflow sediment horizons.

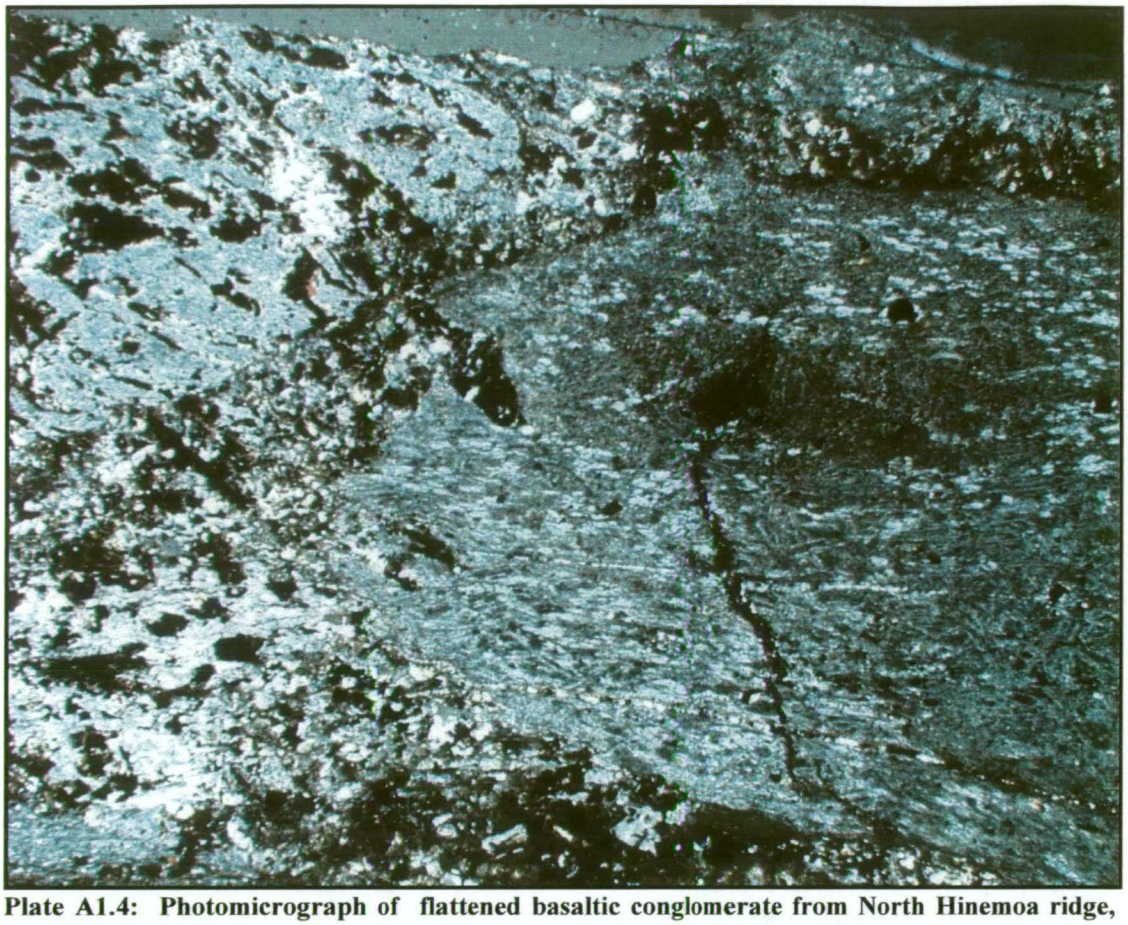

Plate A1.4: Photomicrograph of flattened basaltic conglomerate from North Hinemoa ridge, sample CN851955. Two large basalt clasts prominent. In top left quadrant, basalt is composed of fine-grained carbonate-chlorite mosaic. Centre right, basalt is chlorite carbonate but also has clear patches which are acicular feldspar. Field of view 8 mm. Cross polarised light.

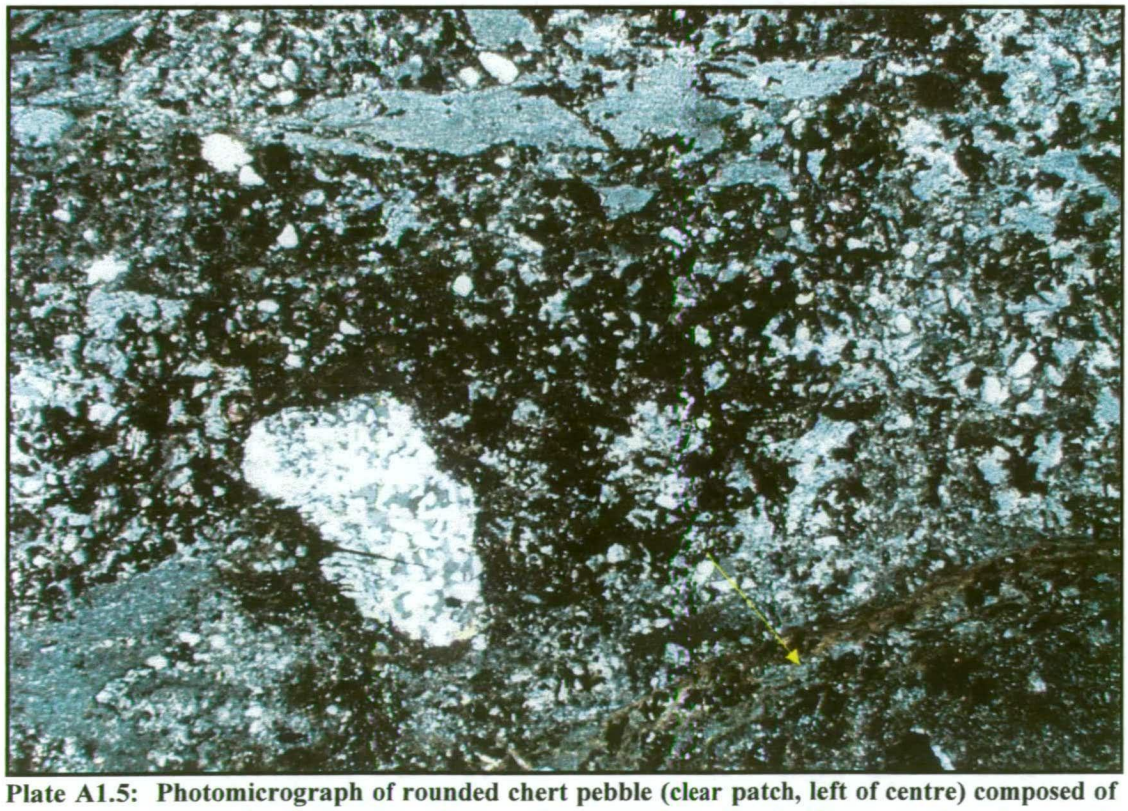

Plate A1.5: Photomicrograph of rounded chert pebble (clear patch, left of centre) composed of polygonal quartz in flattened mafic conglomerate from North Hinemoa ridge in sample CN851955. Edge of a basalt pebble in lower left quadrant (arrow). Field of view 8 mm. Cross polarised light

A1.2.7 Northern Polar Bear ("656 area") rhyolite gully - stratigraphy

At location 6465325mN, 388635mE MGA, a steep, almost cliff-like outcrop along the eastern margin to a N-S trending alluvial valley has excellent exposures of in situ hyaloclastite rhyolite adjacent to flow-banded rhyolite (Plate 3.14). Further details of the rhyolite are exposed along a gully at this location, which has incised the rhyolite outcrop.

The rhyolite along the gully has many small dark clasts that appear to be sediment fragments. At various locations, autobrecciated rhyolite is juxtaposed against flow-banded rhyolite (Plate 3.15). At the eastern end of the gully at location 6465355mN, 388685mE MGA, there are exceptional exposures of peperite at the contact between rhyolite lava and sulfidic black shale (Plates A1.6, A1.7, 3.21, 3.22). The peperite largely comprises peperitic hyaloclastite, particularly around to the margins of large lobes of rhyolite that have foundered into the shale. As the peperite shows the rhyolite was emplaced on wet unconsolidated sediment, the rhyolite is conformable with the sediment.

A1.2.8 Northern Polar Bear ("656 area") top of rhyolite - stratigraphy

250 m due west of the locality described in section A1.2.7, at the western side of the valley, another rhyolite sediment contact is preserved. Although this contact is less clear than the locality described in section A1.2.7, there appears to be a complex interfingering relationship between the rhyolite and the sediment suggesting that this margin is also peperitic.

One interpretation of the geometry of the rhyolite in this area is that it occupies the core of a north-south trending syncline, as both the eastern and western margins have peperitic relationships with the sediment and may be considered as side or basal contacts. Such a syncline would also be consistent with the stratigraphy due south between Sontaran and the Hinemoa Mine

However, a large thrust fault passes through this location adding further complexity to the interpretation (figure A1.1; map 1, Appendix 4). Although there are some large quartz blows that may be related to the fault within the valley occupied by the rhyolite, the major effect of the fault is to cut the sediment out of the stratigraphy just to the west of the peperite exposure. It appears there is little offset within the rhyolite and it is interpreted to occupy the core of a syncline.

Plate A1.6: wide view of the excellent peperite exposure in the gully at North Polar Bear. The hammer lies on the weathered and bleached shale substrate. To the left of the hammer, peperitic breccias are exposed. The black rock at the far left of the photo is shown in more detail in Plate A1.7.

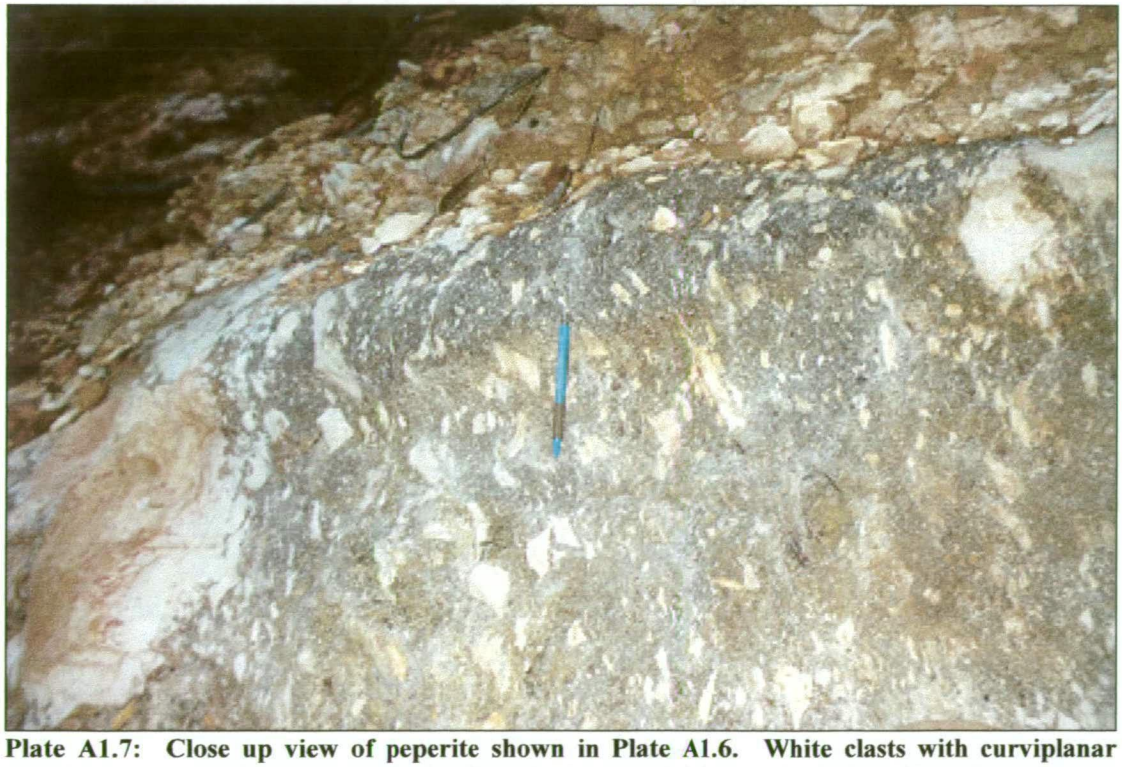

Plate A1.7: Close up view of peperite shown in Plate A1.6. White clasts with curviplanar margins are quench fragmented rhyolite, dark material is black shale. Note the coherent rhyolite lobe with the fragmented margin at the left side of the photo. A closer view of the rhyolite clast textures is provided in Plate 3.21.

A1.2.9 Northern Polar Bear valley("656 area") - stratigraphy

A number of outcrops expose the margins of the widespread quartz porphyry and none show evidence of peperite. The most convincing exposure is at location 6465595mN, 388675mE MGA along the eastern margin of an alluvial valley where a knife sharp quartz porphyry-shale contact is exposed (figure A1.1; Plate 3.16). This contact is the basis for suggesting that the shales were compacted when the quartz porphyry was emplaced.

A1.2.10 South Hinemoa valley - stratigraphy

The rhyolite is well exposed southwest of the Hinemoa Mine where a sharp valley is incised into rhyolite and sediment cover is not significant (figureA1.1; map 3, Appendix 4). Exposures up numerous gullies allow portions of the rhyolite to be examined.

The centre of the valley along the creek axis is occupied by coherent rhyolite lava. Best exposures on the eastern margin of the rhyolite have good examples of peperite which becomes increasingly sediment-rich to a gradational contact with shaly turbidites. On the western margin of the rhyolite, rhyolite-sediment breccia with incorporated lenses of sandstone is present. The rhyolite is flanked to the east and west by sedimentary rocks interpreted as the Abbotshall Beds and is believed to occupy the core of a N-S trending syncline. In this case, both the east and west margins show the base of the rhyolite, despite the differing facies.

The pinchout of the rhyolite at 6462000mN, 388900mE defines the edge of the rhyolite dome. The rhyolite lava is replaced along strike by a band of rhyolite-sediment breccia interpreted to be debris from the rhyolite dome (figure A1.1, map 9, map 2, Appendix 4). This pinchout and replacement illustrates the non-layer cake stratigraphy in this volcanic terrain. The same stratigraphic horizon has rapid changes in thickness due to a change in the facies.

APPENDIX 2

Details of Geochemical Procedures

Samples were submitted to Analabs Pty Ltd in Perth for analysis in two batches five months apart. The first batch consisted of 24 samples which included three analytical quality control samples. The second batch was the main run and consisted of 43 samples including two quality controls.

Samples were dried, jaw crushed to 6mm and pulverised to a nominal 75 μm in a Cr-steel ringmill. For batch #1, the mill was flushed before and after the batch with barren feldspar. Elements expected to be unreliable due to the contamination from the mill are FeO*, MnO and Cr_2O_3. Major elements were analysed by XRF on a fused glass disc and the volatile loss on ignition (LOI) at 1000°C was measured. 33 trace elements, including the REE, were analysed by ICP-MS of a 0.2 g split digested in hydrofluoric, perchloric, hydrochloric and nitric acid. Elements with abundances at levels greater than the upper detection limit of ICP-MS were analysed with ICP-OES using the same solution.

The quoted ICP-MS detection limits are listed in Table A2.1 and range from 0.05 to 10 ppm. However, the Analabs laboratory manager (R. Bowen, pers. comm.) suggested that these limits are only applicable in ideal test conditions. In practice, because of interference from other elements and short-lived, exotic compounds formed in the plasma, the accuracy of abundances less than five to ten times the quoted detection limit should be regarded as dubious.

For the first batch of samples, major elements, REE and some trace elements analyses for the three quality control samples compared favourably with the results achieved by Ghaderi (1998). However, Th, U, Nb, Ta and Hf correlated poorly with values up to 30 times greater than expected. These problems were not detected at the laboratory due to the internal standards being set for base metals rather than research quality whole rock analyses. Following check analyses, it was established that the solutions had been contaminated by columbite from Greenland, which was being analysed at the same time.

Subsequently, new solutions were prepared from residue splits and all trace elements with the exception of Lu and Cr were analysed in an ICP-MS batch in which the laboratory included four certified silicate standards with trace element levels comparable to those expected for the Norseman rocks. Analytical results for the standards compare well with the certified values for the majority of the standards. However, Zr, and Hf values measured for one standard compared unfavourably with the certified levels, probably due to a mineral phase resistant to the acid solvent, thereby reducing the values.

A comparison of the reanalyses of the quality control samples with the values obtained from adjacent samples by Ghaderi (1998), indicated that although Ta values were lower in the reanalyses, they remained too high. Ghaderi's analyses indicated that Ta should be present at abundances below the detection limits. The Ta analyses are regarded as inaccurate and have been removed from mafic batch #1 analyses. It is probable that contamination by columbite must have been introduced early in the sample preparation procedure. Nb values are also elevated above the abundances measured by Ghaderi in basalts, where absolute limits are very low. However, the certified standards idsicate that Nb levels are accurate at the higher levels present in felsic rocks.

Zr and Hf are slightly depleted, but that is thought to be due to incomplete dissolution of resistant minerals. Ghaderi (1998) addressed a similar problem by conducting laser ablation on his samples with anomalously low Zr and Hf and demonstrated that these elements were reading too low by ICP-MS. The batch #1 sample pulps were subsequently reanalysed for Zr and Ti using XRF on pressed powder pellets, to combat incomplete dissolution of zircons. The results are regarded as accurate with the exception of a few samples with very low Zr abundances, close to the detection limits of XRF, which read too high. Samples where this is a problem are noted in the text. Hf is present in abundances too low to be measured using XRF, so remains anomalously depleted.

Following the problems encountered in batch #1, changes in the analytical procedure were introduced for batch #2. To combat the low Zr readings, Zr, Ba, Rb, Sr, Y, Zn, Cr and Ti were analysed using XRF on pressed powder pellets. (Elements other than Zr were measured with XRF to obtain economies of scale). Bi did not register above detection in batch #1, so this element was removed from the analytical suite.

To ensure care in preparation and analysis of the elements, Analabs was notified that the samples were for research. Mills were flushed with barren feldspar between samples and the internal standards were switched to the appropriate silicate rocks. These changes were entirely successful. All results for batch #2 are considered to be accurate with the exception of Hf, which is present in minerals resistant to dissolution at abundances too low to be measured with XRF.

As anticipated, Ta and Nb were at very low levels in the basalts, whereas Zr abundances increased to expected levels.

Table A2.1: Detection Limits of elements measured using XRF and ICP-MS.

Element	**SiO_2**	**Al_2O_3**	**TiO_2**	**Fe_2O_3**	**MnO**	**CaO**	**K_2O**	**MgO**	**P_2O_5**	**Na_2O_3**	**LOI**
Detection limit (%)	0.05	0.05	0.01	0.01	0.01	0.01	0.01	0.01	0.01	0.05	0.01
Element	**Ba**	**Rb**	**Sr**	**Y**	**Zr**	**Zn**	**Cr**	**Ti**			**La**
Detection Limit (ppm)	10	5	5	3	5	10	5	100			0.05
Element	**Ce**	**Pr**	**Nd**	**Sm**	**Eu**	**Gd**	**Tb**	**Dy**	**Ho**	**Er**	**Yb**
Detection Limit (ppm)	0.05	0.05	0.1	0.1	0.05	0.1	0.05	0.1	0.05	0.1	0.1
Element	**Lu**	**U**	**Th**	**Hf**	**Pb**	**Cu**	**Ni**	**Co**	**As**	**Ta**	**Nb**
Detection Limit (ppm)	0.1	0.05	0.05	0.1	1	2	2	0.2	1	0.1	0.2

Sample_no	MGA north	MGA east	rl	Drill hole	Area	field description of rock type	Geochem	T/S	XRD	Batch #
quality control										1
CN851596	6433266.066	386668.087	333.54	S177 217.5-217.63		Dolerite	X			1
CN851603	6445226.244	383272.394	261	CWS51 274.0-274.5		Dolerite: bladed amphibole. Leucoxene	X			1
CN851604	6441488.141	386608.246	290.88	S577 67.2-67.3	main field	Basalt: Small feldspar phenocrysts and very small carbonate crackle veins.	X			1
mafic and ultramafic										1
CN793733	6438456.177	392637.613	260	EYP1614 103.5-103.6	mafic Penneshaw	Basalt: Black acicular minerals. Very fresh.	X			1
CN793734	6439381.135	391277.204	259	EYP1428 214.6-214.8	mafic Penneshaw	Basalt: minor carbonate crackle veins	X			1
CN793735	6439056.139	391462.236	259	EYP1426 131.2-131.3	mafic Penneshaw	Basalt: Black acicular minerals. Minor carbonate crackle veins.	X			1
CN793736	6438454.789	392438.087	257.75	EYP1565 99.3-99.5	mafic Penneshaw	Basalt: Black acicular minerals. Minor carbonate crackle veins.	X			1
CN793737	6439696.129	391307.118	259	EYP1433 228.4-228.6	mafic Penneshaw	Basalt: Black acicular minerals. Minor carbonate crackle veins.	X			1
CN851339	6462756.945	388509.055	322.892	PEN1205P 154-155	Polar Bear	Basalt: clear-coloured acicular minerals	X			1
CN851595	6451512.292	383939.643	263.247	JEW18 291.6-291.8	Jewfish	Basalt	X			1
CN851597	6451408.294	383938.239	263.278	JEW17 229.55-229.7	Jewfish	Basalt:very minor carbonate crackle veins	X			1
CN851598	6463104.264	389226.168	290.28	PENS12 94.9-95.05	Polar Bear	Basalt: clear-coloured acicular minerals	X			1
CN851599	6463160.025	389245.968	298.86	PENS5 188.35-188.5	Polar Bear	Basalt/dolerite with leucoxene	X			1
CN851600	6456756.332	385687.355	260	ETS13 120.95-121.10	Snapper	Basalt: slight carbonation	X			1
CN851601	6456756.339	385887.352	260	ETS14 140.95-141.1	Snapper	Basalt: black acicular minerals. Minor carbonation	X			1
CN851602	6456756.333	385727.355	260	ETS15 114.05-114.2	Snapper	Basalt: black acicular minerals and feldspar phenocrysts	X			1
CN851901	6463641.102	389699.986	0		North Leeders shore	Dolerite	X	X	X	2
CN851902	6442705.985	381834.933	0		Causeway	Basalt	X	X	X	2
CN851904	6466504.119	389219.985	0		656 area	Basalt	X	X	X	2
CN851905	6460002.083	384929.958	0		SW Polar Bear	Basalt	X	X	X	2
CN851906	6463846.103	389734.987	0		North Leeders shore	Basalt	X	X	X	2
CN851907	6457881.068	391674.995	0		Cypress Hill	Basaltic sand	X	X	X	2
CN851909	6462754.839	388485.393	322.848	PEN1206 95.6-95.75	Sontaran	Basalt	X	X	X	2
CN851910	6463681.116	389126.173	281.42	PEN82 86.8-87.05	Hinemoa Mine	Ultramafic: talc-carbonate	X	X	X	2
CN851911	6463681.116	389126.173	281.42	PEN82 85.3-85.6	Hinemoa Mine	Qz-dolom ultramafic	X	X	X	2
CN851913	6463104.264	389226.168	290.28	PENS12 81.65-81.80m	Offshore Polar Bear	Basalt	X	X	X	2
CN851914	6451459.272	383471.079	263.065	JEW9 227.65-227.8m	Jewfish	Basalt	X	X	X	2
CN851915	6451460.312	384386.804	263.306	JEW4 116.85-117.0	Jewfish	Basalt	X	X	X	2
CN851916	6451408.294	383938.239	263.278	JEW17 204.35-204.5	Jewfish	Basalt	X	X	X	2
CN851917	6456756.332	385687.355	260	ETS13 110.05-110.15	Snapper	Basalt	X	X	X	2
CN851918	6453856.277	393687.391	269	LB2618R 96-99m	Davros	Basalt	X	X	X	2
CN851919	6454056.279	393687.391	268.6	LB2545R 79-81m	Davros	Basalt	X	X	X	2
CN851948	6453786.35	390237.377	260	TNA5 43.9-44.05	Tuna	Komatiitic basalt. Spinifex textures	X	X	X	2
CN878592	6464056.328	389242.374	274	PEN1198P 101-102		Ultramafic: talc-carbonate	X			1
CWS51 150	6445226.2	383272.4	261		Swordfish		X			1
CWS51 265.5	6445226.2	383272.4	261		Swordfish		X			
CWS51 274	6445226.2	383272.4	261		Swordfish		X			
CWS51 308.6	6445226.2	383272.4	261		Swordfish		X			
felsic										
CN851605	6464556.332	389032.375	274	PEN1199 96.4-96.6		Rhyolite: One small quartzite clast included.	X			1
CN851908	6462754.839	388485.393	322.848	PEN1206 51.7-51.9	Sontaran	Felsic, fresh acicular minerals	X	X	X	2
CN851920	6448496.021	376294.904	0		Hwy, Mt Thirsty	Felsic sandstone, coarse-grained, laminated	X	X	X	2
CN851921	6448426.02	376324.904	0		Hwy, Mt Thirsty	Felsic sandstone, fine-grained	X	X	X	2
CN851922	6466474.119	389232.985	0		656 area	Quartz Porphyry, minor cleavage	X	X	X	2
CN851923	6461952.093	388620.98	0		South Leeders	Quartz Porphyry, cleavage, sericitised	X	X	X	2
CN851924	6464842.109	388688.981	0		North Leeders	Rhyolite, black, fresh	X	X	X	2
CN851925	6462170.094	388818.981	0		Hinemoa south gully	Rhyolite, pale green, cleaved	X	X	X	2
CN851926	6463852.103	389696.987	0		North Leeders shore	Granodiorite, moderate freshness	X	X	X	2
CN851927	6462006.093	388759.98	0		South Leeders	Quartz Porphyry, strong cleavage, strongly ericitised	X	X	X	2

Sample_no	MGA north	MGA east	rl	Drill hole	Area	field description of rock type	Geochem	T/S	XRD	Batch #
CN851928	6448426.02	376314.904	0		Hwy, Mt Thirsty	Felsic conglomerate, fresh	X	X	X	2
CN851929	6464826.109	388904.982	0		North Leeders	Rhyolite, spherulitic, fresh	X	X	X	2
CN851930	6462129.094	388842.981	0		Hinemoa sheet	Feldspar porphyry, fresh, black	X	X	X	2
CN851931	6464576.109	386189.967	0		Central Polar Bear	Rhyolite (breccia), black with grey inclusions	X	X	X	2
CN851936	6445881.499	384738.357	264.04	HAR460 57.6-57.75	Greater Harlequin	Granodiorite	X	X	X	2
CN851937	6445855.189	385285.922	264	HAR450 180.75-180.9	Greater Harlequin	Felsic Porphyry, fresh, rare qz phenocrysts	X	X	X	2
CN851938	6445800.232	384900.488	264	HAR475 173.35-173.55	Greater Harlequin	Felsic Porphyry, adjacent to granodiorite, feldspar phenes	X	X	X	2
CN851939	6445800.672	384899.658	264	HAR476 121.55-122.05	Greater Harlequin	Granodiorite, trace of shear	X	X	X	2
CN851940	6445800.672	384899.658	264	HAR476 161.3-161.6	Greater Harlequin	Granodiorite	X	X	X	2
CN851941	6459366.409	380872.307	260	WT956 87.9-88.20	Fram Island	Feldspar Porphyry, fresh, glomeroporphyritic feldspars	X	X	X	2
CN851942	CN851942	6461120.09	389130	0	South Leeders	Rhyolite, greenish	X	X	X	2
CN851943	CN851943	6462126.09	389315	0	Hinemoa Mine shore	Quartz Porphyry, green-white	X	X	X	2
CN851944	CN851944	6463301.1	388935	0	West Hinemoa Mine	Rhyolite, black but partly weathered	X	X	X	2
CN851946	6445605.899	384938.618	264.2	HAR448 171.75-172.05	Greater Harlequin	Felsic Porphyry, eastern margin to granodiorite	X	X	X	2
CN851947	6445605.899	384938.618	264.2	HAR448 351.2-351.5	Greater Harlequin	Granodiorite	X	X	X	2
CN877215	6464856.337	388787.374	274	PEN1202P 64-65		Dark rhyolite	X			1
CN878735	6464556.332	389032.375	274	PEN1199P 84-85		Dark rhyolite	X			1
CN879476	6461056.305	389122.355	274	PEN1182P 75-76		Quartz Porphyry with abundant phenocrysts	X			1
CN879584	6461056.305	389162.355	274	PEN1183P 93-94		Quartz Porphyry	X			1
CN851496						Weathered shale	X			1

					All iron converted to FeO* and majors recalculated to 100%													
Sample	Description	SiO2	TiO2	Al2O3	Fe2O3	FeOt	MnO	MgO	CaO	Na2O	K2O	P2O5	old totals	new totals	Ti	Cr	Co
CN851901	N. Leed. dolerite	53.22	2.01	14.76	*	18.50	0.35	2.87	5.22	2.82	0.05	0.20	91.17	100	11000	123	56
CN851902	Causeway basalt	61.84	0.62	14.86	*	7.90	0.17	4.06	8.38	2.06	0.08	0.04	98.13	100	3400	369	66.9
CN851903	S577 qual contr.	52.22	0.96	15.07	*	10.67	0.21	7.67	10.02	2.64	0.46	0.07	97.76	100	5240	226	68.8
CN851904	656 Basalt	58.68	0.76	16.29	*	5.70	0.12	4.59	9.76	3.15	0.87	0.06	98.43	100	3850	495	54.2
CN851905	SW PB, hi Mg	53.19	0.97	15.97	*	10.18	0.28	7.22	9.07	2.92	0.12	0.08	90.48	100	4720	171	21.8
CN851906	N Leeders shore	61.75	1.89	15.08	*	13.79	0.28	2.84	0.37	3.56	0.34	0.11	94.83	100	10700	124	44.9
CN851907	basaltic sand	52.65	0.96	10.63	*	18.88	0.70	4.38	11.57	0.13	0.05	0.06	85.82	100	5030	271	61.8
CN851908	sontaran felsic	69.41	0.44	15.72	*	3.40	0.07	1.85	1.96	5.45	1.60	0.09	96.27	100	2430	7	7
CN851909	sontaran basalt	58.54	0.97	16.56	*	7.71	0.22	3.50	9.22	2.74	0.46	0.09	89.92	100	5090	212	62.1
CN851910	UTCB	44.59	0.21	1.58	*	11.34	0.13	40.46	1.55	0.12	0.01	0.01	76.03	100	920	1055	117
CN851911	qz-dol	3.55	0.04	0.32	*	17.80	0.74	26.69	50.81	0.00	0.02	0.04	55.56	100	220	89	11.2
CN851912	main field	50.62	0.81	14.57	*	11.11	0.20	8.30	12.47	1.74	0.11	0.06	97.43	100	4360	276	58.9
CN851913	PENS12	49.72	1.17	18.34	*	11.70	0.39	3.77	12.14	2.30	0.37	0.09	87.20	100	6620	301	39.5
CN851914	JEW9	57.52	0.72	16.93	*	9.56	0.29	4.22	7.06	2.97	0.67	0.05	92.18	100	4120	418	58.3
CN851915	JEW4 HI Mg	52.22	0.68	14.97	*	11.79	0.26	8.40	10.05	1.54	0.04	0.05	94.81	100	3750	445	59.6
CN851916	JEW17	52.01	1.27	15.72	*	12.26	0.27	4.20	11.50	2.62	0.06	0.10	89.72	100	6930	202	56.2
CN851917	Snapper ETS13	50.48	1.43	17.20	*	11.50	0.33	4.23	9.90	4.23	0.59	0.12	89.70	100	7080	213	57.8
CN851918	Davros	55.40	0.69	16.37	*	12.68	0.34	7.29	5.02	2.03	0.13	0.05	92.29	100	3810	413	73.5
CN851919	Davros	57.58	0.73	16.81	*	11.22	0.37	7.79	2.22	2.92	0.31	0.05	92.26	100	3810	464	60.8
CN851948	TNA5 spinifex	51.57	0.50	15.27	*	10.83	0.18	10.43	8.92	2.17	0.10	0.03	94.15	100	2710	1055	56.8
CN851339	PEN1205P basalt	57.68	1.00	15.75	*	8.62	0.35	3.82	9.66	1.62	1.42	0.08	90.81	100	4700	225	67.4
CN878592	PEN1198P tal-carb	43.27	0.33	1.96	*	10.02	0.24	43.66	0.36	0.12	0.01	0.03	75.50	100	220	415	118.5
CN851595	JEW18 basalt	50.37	1.31	15.93	*	12.41	0.43	4.58	11.17	2.87	0.80	0.14	88.72	100	7090	160	59.6
CN851596	S177 qual contr.	51.52	0.79	15.02	*	10.83	0.18	7.82	11.93	1.72	0.12	0.06	97.52	100	4430	255	57.1
CN851597	JEW17 basalt	50.46	1.38	16.46	*	12.73	0.18	7.53	8.01	3.10	0.04	0.11	89.88	100	7400	160	58.7
CN851598	PENS12 basalt	53.11	1.08	17.23	*	10.43	0.32	3.82	10.95	2.61	0.35	0.09	87.67	100	6040	205	64.9
CN851599	PENS5	51.03	1.81	17.67	*	12.79	0.15	4.99	7.26	3.37	0.71	0.21	91.02	100	8530	96	47.9
CN851600	Snapper ETS13	48.15	1.38	17.02	*	13.60	0.41	4.38	10.98	3.28	0.70	0.11	87.27	100	6840	160	57.4
CN851601	Snapper ETS14	53.86	3.05	14.70	*	11.02	0.33	3.94	8.87	3.16	0.78	0.30	89.96	100	14800	24	41
CN851602	Snapper ETS15	51.89	1.59	13.76	*	14.98	0.20	4.69	9.68	3.03	0.02	0.15	88.49	100	8310	52	60.1
CN851603	CWS51 qual contr.	48.31	0.38	9.77	*	12.35	0.20	19.14	9.41	0.34	0.06	0.03	92.81	100	2530	315	75.7
CN851604	S577 qual contr.	51.43	1.07	14.19	*	11.30	0.27	7.58	11.36	2.35	0.35	0.10	96.22	100	7530	180	55.4
CN793733	Penneshaw	52.35	0.92	15.07	*	10.14	0.21	8.16	10.50	2.28	0.29	0.08	96.75	100	5490	255	57.4
CN793734	Penneshaw	54.65	1.09	14.82	*	10.58	0.25	6.27	6.65	5.11	0.50	0.08	97.96	100	6190	240	57.4
CN793735	Penneshaw	50.49	1.21	14.74	*	12.82	0.22	7.33	9.94	2.99	0.15	0.10	97.46	100	6800	170	64.8
CN793736	Penneshaw	51.65	0.73	14.86	*	9.77	0.17	8.79	12.30	1.57	0.10	0.06	98.32	100	4200	330	53.2
CN793737	Penneshaw	50.93	1.13	15.15	*	12.65	0.21	7.79	8.73	3.00	0.34	0.08	97.18	100	6160	235	62.8
CN851920	Mt Thirsty sst	72.90	0.58	17.03	*	0.70	0.00	0.13	3.49	4.61	0.52	0.04	98.60	100	3180	5	19.8
CN851921	Mt Thirsty sst	76.08	0.41	14.00	*	1.20	0.00	0.48	2.71	4.29	0.80	0.03	97.99	100	2350	6	4.7
CN851922	656 QP	77.90	0.16	13.19	*	2.26	0.00	0.46	0.06	1.68	4.27	0.02	97.90	100	980	6	0.9
CN851923	S. Leed. QP	79.18	0.39	15.79	*	0.56	0.00	0.06	0.02	1.36	2.63	0.01	97.34	100	1980	5	0.5
CN851924	N. Leed. rhyolite	77.05	0.04	12.05	*	0.39	0.00	0.02	0.09	0.14	10.21	0.01	99.82	100	220	20	0.6
CN851925	H'moa gully rhyolite	76.83	0.04	14.69	*	0.63	0.00	0.18	0.03	3.47	4.12	0.00	98.34	100	300	7	0.5
CN851926	N. Leed. granodio	73.80	0.20	16.24	*	1.30	0.00	0.32	0.19	6.04	1.91	0.00	98.12	100	1310	17	3.3
CN851927	S. Leed. QP	77.76	0.37	16.70	*	0.55	0.00	0.09	0.00	0.54	3.97	0.03	95.22	100	1770	0	0.4
CN851928	Mt Thirsty conglom.	73.89	0.61	16.05	*	1.08	0.00	0.17	2.02	6.00	0.16	0.02	98.38	100	3190	37	0.9

					All iron converted to FeO* and majors recalculated to 100%												
Sample	**Description**	**SIO2**	**TIO2**	**AI2O3**	**Fe2O3**	**FeOt**	**MnO**	**MgO**	**CaO**	**Na2O**	**K2O**	**P2O5**	**old totals**	**new totals**	**Ti**	**Cr**	**Co**
CN851929	N. Leed. rhyolite	80.07	0.06	11.77	*	0.45	0.00	0.07	0.11	3.49	3.97	0.01	98.90	100	330	13	0.4
CN851930	H'moa Fspr porph.	79.91	0.35	12.86	*	1.97	0.00	0.48	0.19	2.10	2.10	0.04	94.23	100	1810	95	2.7
CN851931	Central PB grit	84.53	0.09	7.04	*	5.47	0.00	0.39	0.13	0.00	2.32	0.02	97.21	100	590	124	0.9
CN851936	G.Har granodior	71.57	0.38	14.78	*	3.84	0.05	0.65	1.92	5.63	1.10	0.08	98.25	100	2290	7	6.7
CN851937	G.Har porphyry	77.52	0.04	12.95	*	1.31	0.02	0.11	2.51	2.94	2.61	0.00	98.11	100	330	0	0.5
CN851938	G.Har porphyry	77.75	0.04	13.36	*	1.09	0.02	0.05	1.05	4.85	1.78	0.00	98.63	100	280	0	0.4
CN851939	G.Har granodior	75.80	0.14	13.18	*	1.94	0.03	0.45	1.91	4.81	1.70	0.03	97.74	100	910	8	2.5
CN851940	G.Har granodior	70.46	0.42	14.76	*	3.97	0.07	0.76	2.78	4.89	1.79	0.08	97.67	100	2490	6	7.3
CN851941	Fram Is. fspr porph	66.71	0.65	16.40	*	4.87	0.07	2.49	0.96	7.48	0.28	0.09	97.47	100	3480	16	8.7
CN851942	S. leed. rhyolite	80.23	0.04	14.30	*	0.75	0.00	0.27	0.00	0.37	4.03	0.01	98.38	100	280	5	0.2
CN851943	H'moa mine QP	81.34	0.13	13.93	*	0.36	0.00	0.19	0.00	0.24	3.79	0.02	98.43	100	810	7	0.5
CN851944	H'moa mine rhyolite	77.54	0.06	13.28	*	2.45	0.00	0.12	0.06	3.47	3.01	0.01	98.30	100	400	17	1.1
CN851946	G.Har porphyry	76.48	0.06	13.12	*	1.29	0.01	0.08	1.04	4.03	3.89	0.00	98.72	100	330	0	0.6
CN851947	G.Har granodior	71.33	0.35	14.62	*	3.71	0.06	0.65	2.97	4.68	1.55	0.08	98.72	100	2220	6	6.4
CN851605	PEN1199 rhyolite	75.49	0.06	14.47	*	1.23	0.01	0.34	0.19	4.21	3.97	0.02	98.88	100	400	92	3.9
CN878735	PEN1199P rhyol	77.24	0.05	12.41	*	2.38	0.05	0.22	0.07	4.12	3.43	0.02	98.23	100	390	35	6.9
CN879584	PEN1183P QP	78.81	0.04	12.31	*	1.47	0.04	2.31	3.83	0.36	0.82	0.01	95.13	100	250	18	0.8
CN879476	PEN1182P QP fsp	77.24	0.34	14.04	*	2.08	0.03	2.00	2.44	0.39	1.36	0.07	96.53	100	1670	17	5.4
CN877215	PEN1202P rhyolite	76.74	0.04	13.77	*	2.13	0.06	0.38	0.05	2.32	4.49	0.02	97.11	100	260	145	10.8
Data of Ghaderi (1998)																	
86-222 (PE1)	P'shaw felsic	74.84	0.16	15.74	0.80	0.16	0.01	0.51	0.43	4.00	3.04	0.05		98.94	1092.863	6.513	35.394
CWS51 150.0	Swordfish	49.12	0.59	14.46	*	11.11	0.46	11.29	12.08	0.22	0.61	0.05		99.99	2827.34	490.194	66.071
CWS51 265.5	Swordfish	52.86	0.63	14.95	*	10.46	0.21	9.44	8.71	2.27	0.41	0.04		99.98	3229.174	579.114	37.576
CWS51 274.0	Swordfish	46.35	0.43	10.23	*	14.15	0.20	19.90	8.40	0.24	0.06	0.04		100	2422.167	571.166	67.012
CWS51 308.6	Swordfish	54.22	0.64	14.79	*	10.08	0.22	9.10	8.79	1.90	0.23	0.04		100.01	3480.281	380.294	28.707

Sample	Description	Ni	Cu	Zn	Rb	Sr	Y	Zr	Nb	Ta	Ba	La	Ce	Pr	Nd	Sm	Eu
CN851901	N. Leed. dolerite	128	49	115	0	80	42	129	4.7	0.3	42	10.5	25.9	3.7	18.1	4.9	1.5
CN851902	Causeway basalt	200	160	89	0	108	16	36	1.5	0.2	45	2.8	7.05	1.04	5.2	1.6	0.65
CN851903	S577 qual contr.	172	130	94	17	104	27	46	2	0.2	88	3.4	8.9	1.34	7	2.3	0.9
CN851904	656 Basalt	147	23	100	26	159	19	47	1.8	0.2	150	2.95	7.4	1.12	5.7	1.8	0.74
CN851905	SW PB, hi Mg	134	40	97	0	109	17	43	2	0.2	59	3.95	9.9	1.45	7.2	2.3	1
CN851906	N Leeders shore	120	55	200	8	67	41	131	1.5	0.08	100	7.6	15.2	2.6	12.8	3.7	1.22
CN851907	basaltic sand	103	59	115	0	42	23	38	1.4	0.1	29	5.2	11.6	1.62	7.9	2.3	0.89
CN851908	sontaran felsic	40	13	35	41	79	12	176	3.9	0.4	660	21.4	37.3	3.95	14.1	2.6	0.77
CN851909	sontaran basalt	127	99	70	9	97	18	65	2	0.2	155	6.75	14.3	1.83	8.2	2.2	0.8
CN851910	UTCB	1500	15	105	0	12	5	7	0.4	0	13	1.1	2.55	0.37	1.8	0.5	0.15
CN851911	qz-dol	186	0	49	0	196	4	0	0	0	23	0.8	1.94	0.29	1.5	0.5	0.33
CN851912	main field	145	127	81	0	85	25	55	2.1	0.2	52	3.65	9.25	1.36	7	2.2	0.85
CN851913	PENS12	161	86	99	8	92	22	59	1.4	0.1	87	5.35	13.4	1.97	9.7	2.8	0.88
CN851914	JEW9	124	87	68	23	78	13	33	1.4	0.1	91	3.05	7.65	1.13	5.5	1.6	0.66
CN851915	JEW4 Hi Mg	148	57	81	0	85	17	42	1.6	0.2	30	2.95	7.4	1.08	5.4	1.7	0.7
CN851916	JEW17	113	99	110	0	178	26	65	2.4	0.2	43	5.2	12.9	1.85	9.3	2.9	1.15
CN851917	Snapper ETS13	108	99	95	16	67	29	81	3.2	0.3	220	5.35	13.7	2	10	3.2	1.21
CN851918	Davros	136	68	99	0	66	19	34	1.5	0.1	38	2.9	7.2	1.07	5.5	1.8	0.69
CN851919	Davros	128	28	75	7	40	12	40	1.6	0.2	94	2.6	6.65	0.97	4.9	1.5	0.59
CN851948	TNA5 spinifex	157	60	66	0	116	14	21	1	0.1	46	1.65	3.95	0.57	2.9	1	0.43
CN851339	PEN1205P basalt	129	125	105	53.4	44.7	22.3	61	3.7	0.8	289	4.55	10.4	1.61	7.9	2.4	1.16
CN878592	PEN1198P tal-carb	>2000	85	62	0.36	2.9	2.85	72	0.4	<0.1	3	1.18	3.1	0.5	2.4	0.6	0.18
CN851595	JEW18 basalt	93	38	114	31.6	185	20.8	49	5.9	.	83	4.55	11.3	1.79	9.1	2.6	1.08
CN851596	S177 qual contr.	129	129	88	2.55	80.3	21.7	83	5.4	1.5	41	3.6	8.35	1.33	6.6	2	0.78
CN851597	JEW17 basalt	98	119	104	2.1	183	29.1	63	3.8	0.9	17	4.15	10.9	1.76	9.1	2.8	1.14
CN851598	PENS12 basalt	174	120	94	10.8	87.3	10.9	138	3.3	0.9	96	3	7.8	1.27	6.6	2	0.76
CN851599	PENS5	81	42	131	15.3	102.5	40.4	76	4.4	0.9	145	7.1	18.2	2.9	14.7	4.4	1.62
CN851600	Snapper ETS13	93	27	137	21.6	59.5	14.5	228	3.2	0.8	72	4.2	10.6	1.7	8.7	2.6	0.91
CN851601	Snapper ETS14	30	79	111	26.6	216	31.6	104	13.2	1.1	494	21.6	49.6	7.05	31.5	7.7	2.45
CN851602	Snapper ETS15	50	84	125	0.65	100	16.5	63.9	3.8	0.6	17	8.1	19.2	2.8	13.1	3.4	1.14
CN851603	CWS51 qual contr.	709	<2	199	3.1	18.4	10.5	19.8	2.7	0.7	2	1.25	3.1	0.52	2.6	0.9	0.27
CN851604	S577 qual contr.	114	80	128	16.3	99	30.8	56.4	4.6	1	76	3.95	10.2	1.63	8.4	2.6	1.01
CN793733	Penneshaw	134	101	93	9.6	94.3	21.8	64	4.6	0.9	103	4.9	11.8	1.8	8.7	2.5	0.89
CN793734	Penneshaw	117	85	96	14.3	73.2	26	67	3.8	0.7	127	3.15	8.35	1.34	6.9	2.4	0.98
CN793735	Penneshaw	143	106	119	0.96	94.9	32.9	84	4.1	0.7	26	4.6	12	1.95	9.8	3.1	1.17
CN793736	Penneshaw	152	109	84	0.64	77.8	19.2	44	3.9	1	19	2.95	7.3	1.17	5.9	1.9	0.72
CN793737	Penneshaw	121	105	114	9.75	116	27.5	66	4.1	0.8	99	4.25	10.8	1.7	8.7	2.7	1.07
CN851920	Mt Thirsty sst	16	183	0	6	394	11	135	2.7	0.4	320	12	22.2	2.3	8.3	1.8	0.47
CN851921	Mt Thirsty sst	13	19	14	11	302	9	176	3	0.4	1850	8.65	16	1.85	7.4	1.8	0.45
CN851922	656 QP	7	13	29	83	27	31	173	6.6	0.7	890	41	77.9	8.3	30.3	6.1	0.87
CN851923	S. Leed. QP	9	0	0	71	117	17	215	4.6	0.5	375	10.2	18.3	1.67	5.9	1.1	0.31
CN851924	N. Leed. rhyolite	8	3	0	213	33	15	58	5.8	1	1270	13.2	21.8	2.2	7.3	1.6	0.16
CN851925	H'moa gully rhyolite	9	3	14	121	62	22	72	6.8	1.2	595	19.5	33.7	3.4	12.1	2.9	0.37
CN851926	N. Leed. granodio	18	5	26	45	741	7	93	1.8	0.2	1040	4.45	9.4	1.09	4.2	0.9	0.16
CN851927	S. Leed. QP	16	12	0	96	134	22	205	4.8	0.5	425	46.1	69.1	6.35	19.5	3.4	0.8
CN851928	Mt Thirsty conglom.	15	6	0	0	257	8	134	2.8	0.4	160	7.2	13.5	1.48	5.5	1.1	0.48

Sample	Description	Ni	Cu	Zn	Rb	Sr	Y	Zr	Nb	Ta	Ba	La	Ce	Pr	Nd	Sm	Eu
CN851929	N. Leed. rhyolite	3	13	10	91	59	18	57	4.3	0.8	550	10.4	19.7	2.1	7.3	1.7	0.29
CN851930	H'moa Fspr porph.	14	76	11	53	198	24	184	5.1	0.6	455	44.6	82.4	8.7	30.9	5.1	1.1
CN851931	Central PB grit	14	5	0	86	24	33	135	10.1	1.4	515	14.5	24.6	2.55	8.9	2.4	0.35
CN851936	G.Har granodior	18	6	53	40	156	25	187	6.1	0.6	360	50.8	88.1	9.2	32.3	5.6	0.95
CN851937	G.Har porphyry	20	2	35	78	48	35	101	7.7	0.9	280	16.5	34.9	3.95	15.5	4.4	0.59
CN851938	G.Har porphyry	16	4	32	67	49	49	93	10.1	1.2	530	11.2	25.6	3.3	14.2	4.7	0.46
CN851939	G.Har granodior	28	4	42	65	95	37	148	7.1	0.8	400	34.9	66	7.2	26.9	5.6	0.83
CN851940	G.Har granodior	24	3	57	69	158	28	173	6.2	0.6	310	33.3	60.9	6.75	24.7	4.8	0.93
CN851941	Fram Is. fspr porph	38	0	42	6	112	20	169	4.5	0.5	135	11.1	20.3	2.3	8.7	1.7	0.45
CN851942	S. leed. rhyolite	23	0	11	111	54	17	75	6.3	1.2	625	6.85	10.8	1.24	4.1	1	0.15
CN851943	H'moa mine QP	30	0	0	90	35	24	147	6.3	0.8	510	38.3	68.9	7.2	25.1	4.8	0.68
CN851944	H'moa mine rhyolite	27	13	42	100	55	21	72	7	1.1	640	12.8	23.8	2.45	8.9	2.2	0.28
CN851946	G.Har porphyry	27	0	29	112	47	49	100	8.9	1.1	940	13.3	29.1	3.55	14.8	4.5	0.48
CN851947	G.Har granodior	31	6	56	50	191	26	173	5.9	0.6	535	38.3	69.4	7.35	26.8	5.1	1.1
CN851605	PEN1199 rhyolite	18	23	40	137	38.7	22.7	65.3	7.7	1.7	544	12.8	25.6	3	11.1	2.5	0.39
CN878735	PEN1199P rhyol	39	23	246	112	43.1	23.9	64	5.9	1.1	488	11.2	21.7	2.5	9.4	2.4	0.39
CN879584	PEN1183P QP	3	4	49	25.6	23.4	35.2	94	6.4	0.9	82	13.1	28.4	3.85	16.6	4.7	0.59
CN879476	PEN1182P QP fsp	22	25	173	40.4	34.4	28.7	199	5.4	0.7	179	35.1	66.7	7.85	29.5	5.6	0.98
CN877215	PEN1202P rhyolite	30	16	554	228	64.1	29.6	69	7	1.3	1495	13.3	25.7	2.95	10.9	2.8	0.47
Data of Ghaderi (1998)																	
86-222 (PE1)	P'shaw felsic	2.257	6.214	56.627	104.613	57.593	13.127	180.65	8.667	1.326	612.243	68.86	107.611	10.86	35.172	5.078	0.802
CWS51 150.0	Swordfish	376.552	2.027	220.812	22.477	22.99	12.473	30.036	1.364	0.091	71.946	1.693	4.838	0.772	4.098	1.344	0.467
CWS51 265.5	Swordfish	161.169	3.245	133.662	20.662	68.051	14.259	28.187	1.363	0.087	9.639	1.326	3.757	0.589	3.089	1.056	0.385
CWS51 274.0	Swordfish	694.992	1.941	201.372	2.766	11.621	9.982	23.094	0.982	0.073	0.675	1.171	3.334	0.525	2.788	0.915	0.225
CWS51 308.6	Swordfish	138.084	1.73	89.727	7.58	56.152	12.779	31.892	1.482	0.093	10.493	1.615	4.488	0.711	3.743	1.232	0.426

Sample	Description	Gd	Tb	Dy	Ho	Er	Tm	Yb	Lu	Hf	Pb	Bi	Th	U	As	M/Si	Mg#
CN851901	N. Leed. dolerite	4.7	0.65	3.9	0.72	2.2	0.23	2.4	0.4	3.3	3	*	0.65	0.18	27	0.38	21.7
CN851902	Causeway basalt	2.2	0.37	2.4	0.52	1.6	0.18	1.5	0.2	0.5	2	*	0.17	0.07	16	0.21	47.8
CN851903	S577 qual contr.	3.6	0.62	4.2	0.91	2.8	0.33	2.6	0.4	0.9	1	*	0.17	0	5	0.39	56.2
CN851904	656 Basalt	2.5	0.42	2.7	0.56	1.7	0.23	1.6	0.2	1	4	*	0.19	0.06	37	0.20	58.9
CN851905	SW PB, hi Mg	3.3	0.55	3.6	0.77	2.3	0.26	2.2	0.3	1.1	0	*	0.21	0.07	34	0.37	55.8
CN851906	N Leeders shore	4.3	0.63	3.5	0.68	2	0.29	2.3	0.4	2	4	*	0.59	0.29	139	0.26	26.8
CN851907	basaltic sand	2.9	0.45	2.9	0.59	1.9	0.22	2.2	0.3	1.3	1	*	0.17	0.11	25	0.44	29.3
CN851908	sontaran felsic	2.4	0.32	1.8	0.34	1	0.11	0.9	0.1	4.7	7	*	5.7	1.42	148	0.08	49.2
CN851909	sontaran basalt	2.4	0.33	1.9	0.35	1	0.11	1.1	0.2	1.5	4	*	0.92	0.25	25	0.20	44.8
CN851910	UTCB	0.6	0.08	0.5	0.08	0.2	0	0.2	0	0.2	1	*	0.11	0	118	1.57	86.4
CN851911	qz-dol	0.6	0.07	0.4	0.06	0.2	0	0	0	0	0	*	0	0	11	15.59	72.8
CN851912	main field	3.2	0.54	3.6	0.77	2.3	0.3	2.2	0.3	1	0	*	0.24	0.06	3	0.43	57.1
CN851913	PENS12	2.8	0.37	1.8	0.32	1	0.12	1.2	0.2	1.1	5	*	0.24	0.06	6	0.32	36.5
CN851914	JEW9	2	0.31	1.9	0.38	1.1	0.13	1.2	0.2	0.9	0	*	0.14	0	83	0.25	44.0
CN851915	JEW4 Hi Mg	2.4	0.41	2.7	0.58	1.8	0.23	1.7	0.2	0.6	0	*	0.16	0	28	0.43	55.9
CN851916	JEW17	4.1	0.66	4.4	0.92	2.8	0.32	2.5	0.3	0.7	2	*	0.26	0.06	76	0.32	37.9
CN851917	Snapper ETS13	4.5	0.73	4.7	0.96	2.8	0.35	2.7	0.4	1.8	0	*	0.29	0.06	6	0.32	39.6
CN851918	Davros	2.6	0.42	2.9	0.63	1.9	0.22	1.8	0.3	0.6	2	*	0.15	0.07	16	0.39	50.6
CN851919	Davros	2.2	0.35	2.4	0.49	1.5	0.18	1.4	0.2	0.4	0	*	0.16	0.11	16	0.37	55.3
CN851948	TNA5 spinifex	1.5	0.26	1.9	0.4	1.2	0.18	1.3	0.2	0.5	0	*	0.2	0.22	8	0.48	63.2
CN851339	PEN1205P basalt	3.3	0.51	3.5	0.73	2.2		2.1	0.3	1.4	2	<0.1	0.55	0.21	45	0.23	44.1
CN878592	PEN1198P tal-carb	0.6	0.09	0.5	0.1	0.3		0.3	<0.1	0.4	<1	<0.1	0.11	<0.05	4	1.70	88.6
CN851595	JEW18 basalt	3.8	0.47	3.3	0.64	1.9		2.4	0.3	2.1	16	<0.1	0.4	0.09	116	0.35	39.7
CN851596	S177 qual contr.	2.9	0.48	3.4	0.72	2.2		2.1	0.3	1	3	<0.1	0.52	0.1	6	0.41	56.3
CN851597	JEW17 basalt	4.1	0.67	4.6	0.97	2.9		2.8	0.4	1.2	2	<0.1	0.38	0.09	5	0.44	51.3
CN851598	PENS12 basalt	2.3	0.33	1.9	0.34	1		1.4	0.2	1.5	7	<0.1	0.26	0.08	5	0.28	39.5
CN851599	PENS5	6	0.99	6.6	1.36	4.1		3.8	0.5	3.4	3	<0.1	0.82	0.19	3	0.36	41.0
CN851600	Snapper ETS13	3	0.43	2.7	0.5	1.6		2	0.3	1.5	<1	<0.1	0.35	0.07	30	0.38	36.5
CN851601	Snapper ETS14	8.1	0.98	5.8	1.09	2.9		2.9	0.4	5.9	2	<0.1	2.25	0.45	14	0.29	38.9
CN851602	Snapper ETS15	3.6	0.48	3	0.58	1.7		1.9	0.3	2.1	<1	<0.1	0.79	0.17	15	0.38	35.8
CN851603	CWS51 qual contr.	1.3	0.22	1.6	0.34	1.1		1.1	0.2	0.7	<1	0.4	0.14	<0.05	89	0.81	73.4
CN851604	S577 qual contr.	3.9	0.66	4.7	0.97	3		3.1	0.4	1.7	4	<0.1	0.34	0.1	7	0.41	54.5
CN793733	Penneshaw	3.3	0.53	3.6	0.73	2.2		2.3	0.3	1.1	6	<0.1	0.71	0.16	5	0.40	58.9
CN793734	Penneshaw	3.6	0.6	4.1	0.86	2.6		2.4	0.3	1.2	4	<0.1	0.48	0.12	2	0.34	51.4
CN793735	Penneshaw	4.6	0.75	5.1	1.09	3.3		3.1	0.4	1.6	3	<0.1	0.43	0.1	3	0.43	50.5
CN793736	Penneshaw	2.7	0.44	3.1	0.65	2		1.9	0.2	0.6	2	<0.1	0.27	0.06	2	0.41	61.6
CN793737	Penneshaw	3.9	0.63	4.3	0.9	2.7		2.5	0.3	1.7	2	<0.1	0.44	0.1	3	0.44	52.3
CN851920	Mt Thirsty sst	1.7	0.25	1.4	0.27	0.8	0.12	0.9	0.1	3.6	9	*	7.15	2.95	2	0.01	25.1
CN851921	Mt Thirsty sst	1.8	0.25	1.4	0.27	0.8	0.12	1	0.2	4.7	10	*	9.35	3.15	4	0.02	41.5
CN851922	656 QP	5.5	0.74	4.2	0.8	2.4	0.35	2.6	0.4	5.2	10	*	12.7	3	229	0.03	26.6
CN851923	S. Leed. QP	1.4	0.24	1.7	0.37	1.2	0.19	1.3	0.2	5.6	10	*	8.15	1.41	10	0.01	16.3
CN851924	N. Leed. rhyolite	1.7	0.28	1.9	0.4	1.3	0.2	1.4	0.2	2.4	19	*	7.45	1.96	14	0.00	8.4
CN851925	H'moa gully rhyolite	3	0.47	3	0.59	1.8	0.27	1.9	0.3	3.2	13	*	10.2	3.35	6	0.01	34.1
CN851926	N. Leed. granodio	0.7	0.09	0.5	0.08	0.3	0	0.3	0	2.7	6	*	1.28	0.28	58	0.02	30.2
CN851927	S. Leed. QP	3	0.43	2.6	0.51	1.5	0.23	1.7	0.3	5.6	33	*	9.55	1.15	9	0.01	23.5
CN851928	Mt Thirsty conglom.	1	0.15	0.9	0.18	0.6	0.09	0.7	0.1	3.3	17	*	5.05	1.37	3	0.02	22.2

Sample	Description	Gd	Tb	Dy	Ho	Er	Tm	Yb	Lu	Hf	Pb	Bi	Th	U	As	M/Si	Mg#
CN851929	N. Leed. rhyolite	1.8	0.32	2.2	0.45	1.4	0.21	1.5	0.2	2.3	9	*	8.15	3.05	3	0.01	22.1
CN851930	H'moa Fspr porph.	3.6	0.39	2	0.35	1.1	0.18	1.3	0.2	4.9	37	*	9.05	1.31	28	0.03	30.2
CN851931	Central PB grit	2.6	0.4	2.6	0.49	1.4	0.23	1.6	0.2	4.6	23	*	9.95	4.85	32	0.06	11.3
CN851936	G.Har granodior	4.9	0.66	3.8	0.72	2.1	0.31	2	0.3	4.9	9	*	9.3	2.2	5	0.06	23.2
CN851937	G.Har porphyry	5.4	0.87	5.5	1.09	3.3	0.45	3.2	0.5	4	22	*	13.7	5.7	3	0.02	13.2
CN851938	G.Har porphyry	5.5	0.86	5.4	1.06	3.2	0.46	3.3	0.5	4.6	23	*	12.8	5.25	339	0.01	7.6
CN851939	G.Har granodior	5.3	0.74	4.1	0.75	2.1	0.28	2.1	0.3	5	21	*	12.6	3.7	37	0.03	29.2
CN851940	G.Har granodior	4.5	0.62	3.5	0.66	1.9	0.27	1.8	0.3	4.4	9	*	8.45	2.25	77	0.06	25.4
CN851941	Fram Is. fspr porph	1.7	0.24	1.4	0.27	0.8	0.12	0.8	0.1	4	4	*	2.55	0.49	6	0.12	47.7
CN851942	S. leed. rhyolite	1.4	0.26	1.7	0.36	1.2	0.19	1.4	0.2	3	11	*	9.3	2.6	2	0.01	39.5
CN851943	H'moa mine QP	3.7	0.5	2.9	0.56	1.7	0.25	1.8	0.3	4.6	36	*	14.1	2.1	2	0.01	49.1
CN851944	H'moa mine rhyolite	2.2	0.37	2.4	0.49	1.5	0.24	1.7	0.2	2.9	13	*	11.6	3.65	2	0.03	8.1
CN851946	G.Har porphyry	4.9	0.72	4.1	0.76	2.2	0.34	2.3	0.3	4.1	15	*	12.2	2.45	4	0.02	10.1
CN851947	G.Har granodior	5	0.7	4.1	0.81	2.4	0.33	2.3	0.3	4.8	12	*	9.7	2.55	4	0.06	23.8
CN851605	PEN1199 rhyolite	2.8	0.47	3.3	0.69	2.3		2.3	0.3	3.5	14	<0.1	10.9	4.75	31	0.02	33.3
CN878735	PEN1199P rhyol	3	0.51	3.4	0.71	2.1		2.2	0.3	2.9	16	<0.1	10.3	5	17	0.03	14.4
CN879584	PEN1183P QP	5.3	0.82	5.2	1.06	3.1		3.1	0.5	4.3	14	<0.1	15.1	6.45	2	0.06	73.8
CN879476	PEN1182P QP fsp	5.5	0.72	4.6	0.89	2.5		2.4	0.4	5.5	16	0.1	11.6	5.05	2	0.06	63.2
CN877215	PEN1202P rhyolite	3.5	0.58	3.8	0.85	2.5		2.4	0.4	3.2	32	0.5	11.6	5.4	18	0.03	24.2
Data of Ghaderi (1998)																	
86-222 (PE1)	P'shaw felsic	3.206	0.434	2.18	0.438	1.117		1.178	0.181	4.424	45.296	0.751	28.704	13.794	*	0.01	85.0
CWS51 150.0	Swordfish	1.726	0.298	1.974	0.444	1.242		1.315	0.193	0.758	4.421	0.186	0.139	0.036	*	0.54	64.4
CWS51 265.5	Swordfish	1.505	0.3	2.13	0.492	1.421		1.471	0.221	0.753	3.914	0.359	0.145	0.038	*	0.44	61.7
CWS51 274.0	Swordfish	1.223	0.228	1.513	0.347	0.987		1.052	0.163	0.626	0.037	0.438	0.109	0.028	*	0.90	71.5
CWS51 308.6	Swordfish	1.676	0.305	2.008	0.451	1.256		1.313	0.205	0.857	2.404	2.41	0.144	0.036	*	0.41	61.7

													Ti*=(Eu*.Gd)^0.5				
Sample	Description	CaO/Al2O3	Al2O3/TiO2	Ti/Zr	Zr/Y	LaN	(La/Yb)N	(La/Sm)N	(Gd/Yb)N	Eu/Eu*	Sr/Sr*	Ti/Ti*	Nb/Nb*	U/0.0235	Th/0.0853	UN/ThN %	Nb/Th
CN851901	N. Leed. dolerite	0.4	7.4	85.3	3.1	44.3	3.1	1.4	1.6	1.0	0.3	1.0	0.4	7.7	7.6	100.5	7.2
CN851902	Causeway basalt	0.6	23.9	94.4	2.3	11.8	1.3	1.1	1.2	1.1	1.4	0.7	0.5	3.0	2.0	149.5	8.8
CN851903	S577 qual contr.	0.7	15.7	113.9	1.7	14.3	0.9	1.0	1.1	1.0	1.1	0.7	0.6	0.0	2.0	0.0	11.8
CN851904	656 Basalt	0.6	21.4	81.9	2.5	12.4	1.3	1.1	1.3	1.1	1.9	0.7	0.5	2.6	2.2	114.6	9.5
CN851905	SW PB, hi Mg	0.6	16.4	109.8	2.5	16.7	1.3	1.1	1.2	1.1	1.0	0.7	0.5	3.0	2.5	121.0	9.5
CN851906	N Leeders shore	0.0	8.0	81.7	3.2	32.1	2.4	1.3	1.5	0.9	0.4	1.2	0.1	12.3	6.9	178.4	2.5
CN851907	basaltic sand	1.1	11.1	132.4	1.7	21.9	1.7	1.5	1.1	1.1	0.3	0.8	0.2	4.7	2.0	234.9	8.2
CN851908	sontaran felsic	0.1	36.0	13.8	14.7	90.3	17.1	5.3	2.2	0.9	0.2	0.4	0.1	60.4	66.8	90.4	0.7
CN851909	sontaran basalt	0.6	17.1	78.3	3.6	28.5	4.4	2.0	1.8	1.1	0.7	1.0	0.2	10.6	10.8	98.6	2.2
CN851910	UTCB	1.0	7.5	131.4	1.4	4.6	3.9	1.4	2.5	0.8	0.4	0.7	0.3	0.0	1.3	0.0	3.6
CN851911	qz-dol	156.8	9.0	#DIV/0!	0.0	3.4	*	1.0	*	1.8	9.1	0.2	0.0	0.0	0.0	*	*
CN851912	main field	0.9	18.0	79.3	2.2	15.4	1.2	1.1	1.2	1.0	0.8	0.7	0.5	2.6	2.8	90.7	8.8
CN851913	PENS12	0.7	15.7	112.2	2.7	22.6	3.2	1.2	1.9	1.0	0.6	1.1	0.2	2.6	2.8	90.7	5.8
CN851914	JEW9	0.4	23.7	124.8	2.5	12.9	1.8	1.2	1.4	1.1	0.9	1.0	0.4	0.0	1.6	0.0	10.0
CN851915	JEW4 Hi Mg	0.7	22.2	89.3	2.5	12.4	1.2	1.1	1.2	1.1	1.1	0.8	0.5	0.0	1.9	0.0	10.0
CN851916	JEW17	0.7	12.4	106.6	2.5	21.9	1.5	1.2	1.4	1.0	1.3	0.8	0.4	2.6	3.0	83.8	9.2
CN851917	Snapper ETS13	0.6	12.1	87.4	2.8	22.6	1.4	1.1	1.4	1.0	0.4	0.8	0.5	2.6	3.4	75.1	11.0
CN851918	Davros	0.3	23.6	112.1	1.8	12.2	1.2	1.0	1.2	1.0	0.8	0.7	0.5	3.0	1.8	169.4	10.0
CN851919	Davros	0.1	23.1	95.3	3.3	11.0	1.3	1.1	1.3	1.0	0.6	0.8	0.6	4.7	1.9	249.5	10.0
CN851948	TNA5 spinifex	0.6	30.6	129.0	1.5	7.0	0.9	1.1	1.0	1.1	2.7	0.9	0.2	9.4	2.3	399.3	2.0
CN851339	PEN1205P basalt	0.6	15.7	77.0	1.7	19.2	2.7	1.2	1.3	1.3	0.4	0.7	0.7	8.9	6.4	138.6	6.7
CN878592	PEN1198P tal-carb	0.2	5.9	15.2	5.1	5.0	5.1	1.3	1.7	0.9	0.1	0.2	0.3	#VALUE!	1.3	#VALUE!	3.6
CN851595	JEW18 basalt	0.7	12.2	98.5	2.9	19.2	3.5	1.1	1.3	1.1	1.4	0.9	1.2	3.8	4.7	81.7	14.8
CN851596	S177 qual contr.	0.8	19.0	90.4	1.3	15.2	2.3	1.2	1.1	1.0	0.8	0.7	1.2	4.3	6.1	69.8	10.4
CN851597	JEW17 basalt	0.5	11.9	89.2	1.5	17.5	2.9	1.0	1.2	1.0	1.5	0.9	0.9	3.8	4.5	86.0	10.0
CN851598	PENS12 basalt	0.6	15.9	95.9	4.0	12.7	5.8	1.0	1.4	1.1	1.0	1.2	1.0	3.4	3.0	111.7	12.7
CN851599	PENS5	0.4	9.7	61.8	2.6	30.0	3.4	1.0	1.3	1.0	0.5	0.7	0.6	8.1	9.6	84.1	5.4
CN851600	Snapper ETS13	0.6	12.4	90.0	2.9	17.7	5.2	1.0	1.2	1.0	0.5	1.1	0.7	3.0	4.1	72.6	9.1
CN851601	Snapper ETS14	0.6	4.8	64.9	5.7	91.1	7.2	1.8	2.3	0.9	0.4	0.8	0.5	19.1	26.4	72.6	5.9
CN851602	Snapper ETS15	0.7	8.6	79.9	3.9	34.2	6.3	1.5	1.6	1.0	0.5	1.0	0.4	7.2	9.3	78.1	4.8
CN851603	CWS51 qual contr.	1.0	25.9	127.8	1.9	5.3	1.9	0.9	1.0	0.8	0.5	0.9	1.9	*	1.6	*	19.3
CN851604	S577 qual contr.	0.8	13.3	133.5	1.8	16.7	1.8	1.0	1.0	1.0	0.8	1.0	1.1	4.3	4.0	106.8	13.5
CN793733	Penneshaw	0.7	16.4	85.8	1.6	20.7	2.9	1.3	1.2	0.9	0.7	0.8	0.8	6.8	8.3	81.8	6.5
CN793734	Penneshaw	0.4	13.6	92.4	1.4	13.3	2.6	0.8	1.2	1.0	0.8	0.8	1.1	5.1	5.6	90.7	7.9
CN793735	Penneshaw	0.7	12.2	81.0	1.5	19.4	2.6	1.0	1.2	0.9	0.7	0.7	0.8	4.3	5.0	84.4	9.5
CN793736	Penneshaw	0.8	20.3	95.5	0.8	12.4	2.3	1.0	1.2	1.0	0.9	0.8	1.2	2.6	3.2	80.7	14.4
CN793737	Penneshaw	0.6	13.4	93.3	1.0	17.9	2.4	1.0	1.3	1.0	0.9	0.8	0.9	4.3	5.2	82.5	9.3
CN851920	Mt Thirsty sst	0.2	29.5	23.6	12.3	50.6	9.6	4.3	1.6	0.8	1.9	0.8	0.1	125.5	83.8	149.8	0.4
CN851921	Mt Thirsty sst	0.2	34.3	13.4	19.6	36.5	6.2	3.1	1.5	0.8	1.9	0.6	0.2	134.0	109.6	122.3	0.3
CN851922	656 QP	0.0	80.7	5.7	5.6	173.0	11.3	4.3	1.7	0.5	0.0	0.1	0.1	127.7	148.9	85.7	0.5
CN851923	S. Leed. QP	0.0	40.4	9.2	12.6	43.0	5.6	6.0	0.9	0.8	0.7	0.7	0.3	60.0	95.5	62.8	0.6
CN851924	N. Leed. rhyolite	0.0	300.8	3.8	3.9	55.7	6.8	5.3	1.0	0.3	0.2	0.1	0.3	83.4	87.3	95.5	0.8
CN851925	H'moa gully rhyolite	0.0	361.3	4.2	3.3	82.3	7.4	4.3	1.3	0.4	0.2	0.0	0.2	142.6	119.6	119.2	0.7
CN851926	N. Leed. granodio	0.0	79.7	14.1	13.3	18.8	10.6	3.2	1.9	0.6	8.1	0.8	0.3	11.9	15.0	79.4	1.4
CN851927	S. Leed. QP	0.0	45.4	8.6	9.3	194.5	19.5	8.8	1.5	0.8	0.2	0.3	0.1	48.9	112.0	43.7	0.5
CN851928	Mt Thirsty conglom.	0.1	26.3	23.8	16.8	30.4	7.4	4.2	1.2	1.4	2.0	1.4	0.3	58.3	59.2	98.5	0.6

													Ti*=(Eu*.Gd)^0.5				
Sample	Description	CaO/Al2O3	Al2O3/TiO2	Ti/Zr	Zr/Y	LaN	(La/Yb)N	(La/Sm)N	(Gd/Yb)N	Eu/Eu*	Sr/Sr*	Ti/Ti*	Nb/Nb*	U/0.0235	Th/0.0853	UN/ThN %	Nb/Th
CN851929	N. Leed. rhyolite	0.0	194.0	5.8	3.2	43.9	5.0	3.9	1.0	0.5	0.3	0.1	0.3	129.8	95.5	135.8	0.5
CN851930	H'moa Fspr porph.	0.0	36.7	9.8	7.7	188.2	24.6	5.6	2.3	0.8	0.3	0.2	0.1	55.7	106.1	52.5	0.6
CN851931	Central PB grit	0.0	76.0	4.4	4.1	61.2	6.5	3.9	1.3	0.4	0.1	0.1	0.4	206.4	116.6	176.9	1.0
CN851936	G.Har granodior	0.1	39.2	12.2	7.5	214.3	18.2	5.9	2.0	0.6	0.2	0.2	0.1	93.6	109.0	85.9	0.7
CN851937	G.Har porphyry	0.2	317.5	3.3	2.9	69.6	3.7	2.4	1.4	0.4	0.1	0.0	0.4	242.6	160.6	151.0	0.6
CN851938	G.Har porphyry	0.1	329.5	3.0	1.9	47.3	2.4	1.5	1.4	0.3	0.2	0.0	0.7	223.4	150.1	148.9	0.8
CN851939	G.Har granodior	0.1	92.0	6.1	4.0	147.3	11.9	4.0	2.1	0.5	0.2	0.1	0.1	157.4	147.7	106.6	0.6
CN851940	G.Har granodior	0.2	35.2	14.4	6.2	140.5	13.3	4.5	2.1	0.6	0.3	0.2	0.1	95.7	99.1	96.7	0.7
CN851941	Fram Is. fspr porph	0.1	25.4	20.6	8.5	46.8	10.0	4.2	1.8	0.8	0.6	0.9	0.3	20.9	29.9	69.7	1.8
CN851942	S. leed. rhyolite	0.0	351.8	3.7	4.4	28.9	3.5	4.4	0.8	0.4	0.5	0.1	0.5	110.6	109.0	101.5	0.7
CN851943	H'moa mine QP	0.0	105.5	5.5	6.1	161.6	15.3	5.2	1.7	0.5	0.1	0.1	0.1	89.4	165.3	54.1	0.4
CN851944	H'moa mine rhyolite	0.0	217.5	5.6	3.4	54.0	5.4	3.8	1.1	0.4	0.3	0.1	0.4	155.3	136.0	114.2	0.6
CN851946	G.Har porphyry	0.1	215.8	3.3	2.0	56.1	4.1	1.9	1.8	0.3	0.2	0.0	0.5	104.3	143.0	72.9	0.7
CN851947	G.Har granodior	0.2	41.2	12.8	6.7	161.6	11.9	4.8	1.8	0.7	0.3	0.2	0.1	108.5	113.7	95.4	0.6
CN851605	PEN1199 rhyolite	0.0	238.5	6.1	2.9	54.0	4.0	3.3	1.0	0.5	0.2	0.1	0.4	202.1	127.8	158.2	0.7
CN878735	PEN1199P rhyol	0.0	243.8	6.1	2.7	47.3	3.7	3.0	1.1	0.4	0.2	0.1	0.4	212.8	120.8	176.2	0.6
CN879584	PEN1183P QP	0.3	292.8	2.7	2.7	55.3	3.0	1.8	1.4	0.4	0.1	0.0	0.4	274.5	177.0	155.0	0.4
CN879476	PEN1182P QP fsp	0.2	41.1	8.4	6.9	148.1	10.5	4.0	1.9	0.5	0.1	0.1	0.1	214.9	136.0	158.0	0.5
CN877215	PEN1202P rhyolite	0.0	334.3	3.8	2.3	56.1	4.0	3.1	1.2	0.5	0.3	0.0	0.4	229.8	136.0	169.0	0.6
Data of Ghaderi (1998)																	
86-222 (PE1)	P'shaw felsic	0.0	98.4	6.0	13.8	290.5	41.9	8.8	2.3	0.6	0.1	0.1	0.1	587.0	336.5	174.4	0.3
CWS51 150.0	Swordfish	0.8	24.5	94.1	2.4	7.1	0.9	0.8	1.1	0.9	0.4	0.8	0.8	1.5	1.6	94.0	9.8
CWS51 265.5	Swordfish	0.6	23.7	114.6	2.0	5.6	0.6	0.8	0.8	0.9	1.6	1.0	1.0	1.6	1.7	95.1	9.4
CWS51 274.0	Swordfish	0.8	23.8	104.9	2.3	4.9	0.8	0.8	1.0	0.7	0.3	0.9	0.9	1.2	1.3	93.2	9.0
CWS51 308.6	Swordfish	0.6	23.1	109.1	2.5	6.8	0.9	0.8	1.1	0.9	1.1	1.0	0.9	1.5	1.7	90.7	10.3

Sample	Description	Nb/U	U/Th		Sample		Na2O+K2O	Nb/Y	Th/Y	Th/Yb
CN851901	N. Leed. dolerite	26.1	0.277	107.752	CN851901		2.87	0.11	0.02	0.27
CN851902	Causeway basalt	21.4	0.412	160.220	CN851902		2.14	0.09	0.01	0.11
CN851903	S577 qual contr.	#DIV/0!	0.000	0.000	CN851903		3.10	0.07	0.01	0.07
CN851904	656 Basalt	30.0	0.316	122.875	CN851904		4.02	0.09	0.01	0.12
CN851905	SW PB, hi Mg	28.6	0.333	129.702	CN851905		3.04	0.12	0.01	0.10
CN851906	N Leeders shore	5.2	0.492	191.255	CN851906		3.90	0.04	0.01	0.26
CN851907	basaltic sand	12.7	0.647	251.774	CN851907		0.17	0.06	0.01	0.08
CN851908	sontaran felsic	2.7	0.249	96.935	CN851908		7.05	0.33	0.48	6.33
CN851909	sontaran basalt	8.0	0.272	105.735	CN851909		3.19	0.11	0.05	0.84
CN851910	UTCB	*	0.000	0.000	CN851910		0.13	0.08	0.02	0.55
CN851911	qz-dol	*	#DIV/0!	#DIV/0!	CN851911		0.02	0.00	0.00	#DIV/0!
CN851912	main field	35.0	0.250	97.276	CN851912		1.86	0.08	0.01	0.11
CN851913	PENS12	23.3	0.250	97.276	CN851913		2.67	0.06	0.01	0.20
CN851914	JEW9	*	0.000	0.000	CN851914		3.65	0.11	0.01	0.12
CN851915	JEW4 Hi Mg	*	0.000	0.000	CN851915		1.58	0.09	0.01	0.09
CN851916	JEW17	40.0	0.231	89.793	CN851916		2.68	0.09	0.01	0.10
CN851917	Snapper ETS13	53.3	0.207	80.504	CN851917		4.82	0.11	0.01	0.11
CN851918	Davros	21.4	0.467	181.582	CN851918		2.16	0.08	0.01	0.08
CN851919	Davros	14.5	0.688	267.510	CN851919		3.23	0.13	0.01	0.11
CN851948	TNA5 spinifex	1.8	1.100	428.016	CN851948		2.26	0.07	0.01	0.15
CN851339	PEN1205P basalt	17.6	0.382	148.567	CN851339		3.04	0.17	0.02	0.26
CN878592	PEN1198P tal-carb	#VALUE!	#VALUE!	#VALUE!	CN878592		0.13	0.14	0.04	0.37
CN851595	JEW18 basalt	65.6	0.225	87.549	CN851595		3.67	0.28	0.02	0.17
CN851596	S177 qual contr.	54.0	0.192	74.828	CN851596		1.85	0.25	0.02	0.25
CN851597	JEW17 basalt	42.2	0.237	92.156	CN851597		3.15	0.13	0.01	0.14
CN851598	PENS12 basalt	41.3	0.308	119.725	CN851598		2.97	0.30	0.02	0.19
CN851599	PENS5	23.2	0.232	90.158	CN851599		4.09	0.11	0.02	0.22
CN851600	Snapper ETS13	45.7	0.200	77.821	CN851600		3.98	0.22	0.02	0.18
CN851601	Snapper ETS14	29.3	0.200	77.821	CN851601		3.94	0.42	0.07	0.78
CN851602	Snapper ETS15	22.4	0.215	83.731	CN851602		3.05	0.23	0.05	0.42
CN851603	CWS51 qual contr.	*	#VALUE!	#VALUE!	CN851603		0.41	0.26	0.01	0.13
CN851604	S577 qual contr.	46.0	0.294	114.443	CN851604		2.70	0.15	0.01	0.11
CN793733	Penneshaw	28.8	0.225	87.686	CN793733		2.57	0.21	0.03	0.31
CN793734	Penneshaw	31.7	0.250	97.276	CN793734		5.61	0.15	0.02	0.20
CN793735	Penneshaw	41.0	0.233	90.490	CN793735		3.14	0.12	0.01	0.14
CN793736	Penneshaw	65.0	0.222	86.468	CN793736		1.67	0.20	0.01	0.14
CN793737	Penneshaw	41.0	0.227	88.433	CN793737		3.34	0.15	0.02	0.18
			#DIV/0!	#DIV/0!			0.00	#DIV/0!	#DIV/0!	#DIV/0!
CN851920	Mt Thirsty sst	0.9	0.413	160.540	CN851920		5.13	0.25	0.65	7.94
CN851921	Mt Thirsty sst	1.0	0.337	131.089	CN851921		5.08	0.33	1.04	9.35
CN851922	656 QP	2.2	0.236	91.915	CN851922		5.94	0.21	0.41	4.88
CN851923	S. Leed. QP	3.3	0.173	67.318	CN851923		3.99	0.27	0.48	6.27
CN851924	N. Leed. rhyolite	3.0	0.263	102.369	CN851924		10.35	0.39	0.50	5.32
CN851925	H'moa gully rhyolite	2.0	0.328	127.794	CN851925		7.59	0.31	0.46	5.37
CN851926	N. Leed. granodio	6.4	0.219	85.117	CN851926		7.95	0.26	0.18	4.27
CN851927	S. Leed. QP	4.2	0.120	46.856	CN851927		4.51	0.22	0.43	5.62
CN851928	Mt Thirsty conglom.	2.0	0.271	105.559	CN851928		6.16	0.35	0.63	7.21

Sample	Description	Nb/U	U/Th		Sample		Na2O+K2O	Nb/Y	Th/Y	Th/Yb
CN851929	N. Leed. rhyolite	1.4	0.374	145.616	CN851929		7.46	0.24	0.45	5.43
CN851930	H'moa Fspr porph.	3.9	0.145	56.323	CN851930		4.20	0.21	0.38	6.96
CN851931	Central PB grit	2.1	0.487	189.664	CN851931		2.32	0.31	0.30	6.22
CN851936	G.Har granodior	2.8	0.237	92.046	CN851936		6.73	0.24	0.37	4.65
CN851937	G.Har porphyry	1.4	0.416	161.890	CN851937		5.54	0.22	0.39	4.28
CN851938	G.Har porphyry	1.9	0.410	159.594	CN851938		6.63	0.21	0.26	3.88
CN851939	G.Har granodior	1.9	0.294	114.261	CN851939		6.51	0.19	0.34	6.00
CN851940	G.Har granodior	2.8	0.266	103.608	CN851940		6.69	0.22	0.30	4.69
CN851941	Fram Is. fspr porph	9.2	0.192	74.769	CN851941		7.76	0.23	0.13	3.19
CN851942	S. leed. rhyolite	2.4	0.280	108.782	CN851942		4.39	0.37	0.55	6.64
CN851943	H'moa mine QP	3.0	0.149	57.952	CN851943		4.03	0.26	0.59	7.83
CN851944	H'moa mine rhyolite	1.9	0.315	122.434	CN851944		6.48	0.33	0.55	6.82
CN851946	G.Har porphyry	3.6	0.201	78.140	CN851946		7.92	0.18	0.25	5.30
CN851947	G.Har granodior	2.3	0.263	102.291	CN851947		6.23	0.23	0.37	4.22
CN851605	PEN1199 rhyolite	1.6	0.436	169.564	CN851605		8.18	0.34	0.48	4.74
CN878735	PEN1199P rhyol	1.2	0.485	188.886	CN878735		7.55	0.25	0.43	4.68
CN879584	PEN1183P QP	1.0	0.427	166.207	CN879584		1.18	0.18	0.43	4.87
CN879476	PEN1182P QP fsp	1.1	0.435	169.395	CN879476		1.75	0.19	0.40	4.83
CN877215	PEN1202P rhyolite	1.3	0.466	181.135	CN877215		6.81	0.24	0.39	4.83
Data of Ghaderi (1998)			#DIV/0!	#DIV/0!			0.00	#DIV/0!	#DIV/0!	#DIV/0!
86-222 (PE1)	P'shaw felsic	0.6	0.481	186.988	86-222 (PE1)		7.04	0.66	2.19	24.37
			#DIV/0!	#DIV/0!			0.00	#DIV/0!	#DIV/0!	#DIV/0!
CWS51 150.0	Swordfish	37.9	0.259	100.775	CWS51 15	HMT	0.83	0.11	0.01	0.11
CWS51 265.5	Swordfish	35.9	0.262	101.972	CWS51 26	HMT	2.68	0.10	0.01	0.10
CWS51 274.0	Swordfish	35.1	0.257	99.954	CWS51 27	HMT	0.30	0.10	0.01	0.10
CWS51 308.6	Swordfish	41.2	0.250	97.276	CWS51 30	HMT	2.13	0.12	0.01	0.11
							0.00	#DIV/0!	#DIV/0!	#DIV/0!
			#DIV/0!	#DIV/0!			0.00	#DIV/0!	#DIV/0!	#DIV/0!

APPENDIX 3 Geochemical characteristics of reference groups from Lentz (1998); Barley & others 1998) and Perring (1989)

GROUP	Tholeiitic	Calc-alkal.	Alkalic	A-type	I/M-type	Assoc. 1 Bore Well	Assoc. 2 Spring Well	Assoc. 3 Melita	Assoc. 4 BFB	Dinky Buoys
Prospect area						Bore Well	Spring Well	Melita	Widgiemlth	Norseman
Classification						Rhy (only)	Dacite (only)	Rhy (only)	Dac. (only)	Qz kerato.
Series						Calc-alkaline	Calc-alkaline	A-type?	Hi-Al TTD	lo-Al TTD
SiO_2 wt%						~76 - 78	~73 - 76	~ 76 – 77.5	~67 - 72	71.6
Al_2O_3 wt%						~ 11.5	~13	~ 11.5	~15 – 18.5	14.3
Na_2O+K_2O	< 6	6 –8	> 8	7 – 11	5 – 8	~6.5 - 7	6.9 – 8.1	6.4 – 7.1	7.9 – 9.6	6
FeO_t/MgO	> 4-5	< 4 – 5	>> 5	>> 4	< 4	~3 – 4.5	3.4 – 5.7	9.4 – 9.8	3.1 – 4.0	5
Zr (ppm)	> 200	< 200	> 500	> 400	< 250	~285 - 300	245 – 300	365 - 485	205 – 232	152
Y (ppm)	> 30	< 30	> 50	>> 25	< 40	~38	40 – 41	80 – 165	11.0 – 14.0	23
Zr/Y	2 – 7	> 7	> 7	> 7	< 4	~ 7.5- 8.0	6 – 7.1	3.0 – 4.6	14.6 – 21.1	6.6
Nb (ppm)	>> 5	<< 40	>> 40	>> 10	<< 30	~ 11.5 – 12.0	10 – 20	5.8 – 31.3	4.9 – 10.0	9.0
Nb/Y	< 0.7	<< 0.7	>> 0.7	> 0.7	<< 0.7	0.3	0.2 – 0.5	0.1 – 0.2	0.4 – 0.7	0.4
La (ppm)	> 6	<< 60	>> 45	>> 30	10 – 30	32.0 – 34.0	16 – 25	42.5 – 48.2	24.1 – 26.2	23.4
Yb (ppm)	>> 1.5	<< 5	>> 5	>> 2	<< 3	3.5	2.5 – 3.2	7.9 – 10.4	0.9 – 1.2	3.5
Th (ppm)	< 3	< 20	> 10	> 10	> 4	7.0 – 7.5	3.4 – 4.0	8.7 – 12.3	5.7 – 8.7	12.0
Th/Yb	< 0.03	> 0.3	>> 0.3	1 - 15	> 0.3	2.0 – 2.1	1.2 – 1.4	0.8 – 1.6	5.0 – 9.4	3.5
Th/Y	< 0.003	> 0.03	> 0.1	0.2 – 1.2	> 0.1	0.2	0.1	0.1 – 0.2	0.4 – 0.8	0.5
Zn (ppm)	50-200	< 120	> 100	30 – 300	20 – 80	24 – 62	54 – 113	76 – 103	25 – 26	61
Cu (ppm)	5-20	< 40	1 – 30	1 – 10	5 – 50	14 – 15	0	0 – 71	0 – 10	23.4
Pb (ppm)	> 5	5 - 50	> 10	20 – 40	20 – 40	6 – 10	1 – 7	2 – 15	2 – 28	23
$(La/Yb)_N$	< 6	> 6	>> 6	2 - 15	< 6	6.6 – 6.8	4.8 – 5.5	3.3 – 3.9	16.3 – 18.6	4.8
$(La/Sm)_N$						3.3	3.0 – 3.3	2.5 – 2.7	3.2 – 5.4	2.3
$(Gd/Yb)_N$						1.4	1.1 – 1.4	1.1 – 1.3	2.1 – 2.6	1.7
Eu/Eu*						0.5	0.6	0.5	1.0 – 1.1	0.9
Ti/Ti*						0.09	0.3 – 0.4	0.08 – 0.3	0.4 – 0.5	0.02
Nb/Nb*						0.3	0.3 – 1.0	0.1 – 0.5	0.1 – 0.3	0.3